

Université de Montréal

**Design and Synthesis of Constrained Azacyclic Pyrrolidine  
Analogues of FTY720 as Anticancer Agents & Metal  
Coordination-Controlled and Bifunctional Catalysis  
Toward Tertiary  $\beta$ -Ketols**

par  
Bin Chen

Département de chimie  
Faculté des Arts et Sciences

Thèse présentée à la Faculté des études supérieures et postdoctorales  
en vue de l'obtention du grade de *Philosophiæ Doctor* (Ph. D.)  
en chimie

Août 2015

© Bin Chen, 2015

## Résumé

Cette thèse se compose en deux parties:

**Première Partie:** La conception et la synthèse d'analogues pyrrolidiniques, utilisés comme agents anticancéreux, dérivés du FTY720.

FTY720 est actuellement commercialisé comme médicament (Gilenya<sup>TM</sup>) pour le traitement de la sclérose en plaques rémittente-récurrente. Il agit comme immunosuppresseur en raison de son effet sur les récepteurs de la sphingosine-1-phosphate. A fortes doses, FTY720 présente un effet antinéoplasique. Cependant, à de telles doses, un des effets secondaires observé est la bradycardie dû à l'activation des récepteurs S1P<sub>1</sub> et S1P<sub>3</sub>. Ceci limite son potentiel d'utilisation lors de chimiothérapie.

Nos précédentes études ont montré que des analogues pyrrolidiniques dérivés du FTY720 présentaient une activité anticancéreuse mais aucune sur les récepteurs S1P<sub>1</sub> et S1P<sub>3</sub>. Nous avons soumis l'idée qu'une étude relation structure-activité (SARs) pourrait nous conduire à la découverte de nouveaux agents anti tumoraux. Ainsi, deux séries de composés pyrrolidiniques (*O*-arylmethyl substitué et *C*-arylmethyl substitué) ont pu être envisagés et synthétisés (Chapitre 1). Ces analogues ont montré d'excellentes activités cytotoxiques contre diverses cellules cancéreuses humaines (prostate, colon, sein, pancréas et leucémie), plus particulièrement les analogues actifs qui ne peuvent pas être phosphorylés par SphK, présentent un plus grand potentiel pour le traitement du cancer sans effet secondaire comme la bradycardie.

Les études mécanistiques suggèrent que ces analogues de déclencheurs de régulation négative sur les transporteurs de nutriments induisent une crise bioénergétique en affamant les cellules cancéreuses. Afin d'approfondir nos connaissances sur les récepteurs cibles, nous avons conçu et synthétisé des sondes diazirine basées sur le marquage d'affinité aux photons (méthode PAL: Photo-Affinity Labeling) (Chapitre 2). En s'appuyant sur la méthode PAL, il

est possible de récolter des informations sur les récepteurs cibles à travers l'analyse LC/MS/MS de la protéine. Ces tests sont en cours et les résultats sont prometteurs.

**Deuxième partie:** Coordination métallique et catalyse di fonctionnelle de dérivés  $\beta$ -hydroxy cétones tertiaires.

Les réactions de Barbier et de Grignard sont des méthodes classiques pour former des liaisons carbone-carbone, et généralement utilisées pour la préparation d'alcools secondaires et tertiaires. En vue d'améliorer la réaction de Grignard avec le 1-iodobutane dans les conditions « one-pot » de Barbier, nous avons obtenu comme produit majoritaire la  $\beta$ -hydroxy cétone provenant de l'auto aldolisation de la 5-hexen-2-one, plutôt que le produit attendu d'addition de l'alcool (Chapitre 3). La formation inattendue de la  $\beta$ -hydroxy cétone a également été observée en utilisant d'autres dérivés méthyl cétone. Étonnement dans la réaction intramoléculaire d'une tricétone, connue pour former la cétone Hajos-Parrish, le produit majoritaire est rarement la  $\beta$ -hydroxy cétone présentant la fonction alcool en position axiale. Intrigué par ces résultats et après l'étude systématique des conditions de réaction, nous avons développé deux nouvelles méthodes à travers la synthèse sélective et catalytique de  $\beta$ -hydroxy cétones spécifiques par cyclisation intramoléculaire avec des rendements élevés (Chapitre 4). La réaction peut être catalysée soit par une base adaptée et du bromure de lithium comme additif en passant par un état de transition coordonné au lithium, ou bien soit à l'aide d'un catalyseur TBD di fonctionnel, via un état de transition médiée par une coordination bidenté au TBD. Les mécanismes proposés ont été corroborés par calcul DFT. Ces réactions catalytiques ont également été appliquées à d'autres substrats comme les tricétones et les dicétones. Bien que les efforts préliminaires afin d'obtenir une enantioselectivité se sont révélés sans succès, la synthèse et la recherche de nouveaux catalyseurs chiraux sont en cours.

**Mots-clés:** FTY720, cancer, cycle rigide, pyrrolidine, sondes diazirine basées sur le marquage d'affinité aux photons (PAL), diazirine, réaction de Barbier, réaction de Grignard, réaction d'auto aldolisation,  $\beta$ -hydroxy cétone, catalyse.

## Abstract

This thesis consists of two parts:

**Part 1:** Design and synthesis of constrained azacyclic pyrrolidine analogues of FTY720 as anticancer agents

FTY720 is presently marketed as a drug (Gilenya<sup>TM</sup>) for the treatment of relapsing-remitting multiple sclerosis. It functions as an immunosuppressant due to its effect on sphingosine-1-phosphate (S1P) receptors. At higher doses, FTY720 also has antineoplastic actions. However, at such doses it induces bradycardia due to the activation of the S1P<sub>1</sub> and S1P<sub>3</sub> receptors. This limits its potential to be used as a cancer therapy in humans.

Our previous studies have shown that some constrained pyrrolidine analogues of FTY720 have anticancer activity but no activity toward S1P<sub>1</sub> and S1P<sub>3</sub> receptors. We reasoned that a study of the structure-activity relationships (SARs) could lead to the discovery of new effective antitumor agents. Thus, two series of constrained analogues (*O*-arylmethyl-substituted pyrrolidines and *C*-aryl-substituted pyrrolidines) were designed and synthesized (Chapter 1). These analogues showed excellent cytotoxic activity against various human cancer cells (prostate, colon, breast, pancreas and leukemia). Especially, several active analogues, which cannot be phosphorylated by SphK, have the potency to be further studied in the treatment of cancer without inducing bradycardia.

Mechanistic studies suggest that these constrained analogues trigger down-regulation of nutrient transporters, which induce a bioenergetic crisis and the cancer cells starve to death. To further investigate their target receptors, we have designed and synthesized diazirine based photo-affinity labeling (PAL) probes (Chapter 2). Aided by the PAL technique, information regarding the target receptor could be obtained through LC/MS/MS protein analysis. These tests are in progress and the preliminary results appear promising.

**Part 2:** Metal coordination-controlled and bifunctional catalysis toward tertiary  $\beta$ -ketols

The Barbier and Grignard reactions are classical methods to form carbon-carbon bonds, and generally used to prepare secondary or tertiary alcohols. In an attempt to perform a Grignard reaction with *n*-butyl iodide under Barbier one-pot conditions, we obtained major product  $\beta$ -hydroxyl ketol from the self-aldol reaction of 5-hexen-2-one, rather than the expected addition alcohol product (Chapter 3). The unusual  $\beta$ -ketol formation was also observed using other methyl ketone substrates. Interestingly, in an intramolecular reaction of a triketone substrate, which is well known to give the Hajos-Parrish ketone, the favored product was a rarely studied  $\beta$ -ketol with the hydroxyl group at axial position. Intrigued by these results, after systematic reaction condition studies, we developed two new methods toward the catalytic synthesis of specific  $\beta$ -ketols by intramolecular cyclization in high yield and selectivity (Chapter 4). The reaction can be catalyzed either by a suitable base and lithium bromide as the additive, through a lithium pre-organized transition state or by a bifunctional catalyst TBD (triazabicyclodecene), through a TBD mediated bidentate transition state. The proposed mechanisms were corroborated by DFT computation. These catalytic reactions were also extended to other triketone and diketone substrates. Although the initial efforts to achieve enantioselectivity were not successful, they merit further study of the synthesis and investigation of new chiral catalysts.

**Keywords:** FTY720, cancer, constrained analogue, pyrrolidine, photoaffinity labeling (PAL), diazirine, Barbier reaction, Grignard reaction, self-aldol reaction,  $\beta$ -ketols, catalysis.

# Table of Contents

Résumé.....	i
Abstract.....	iii
Table of Contents.....	v
List of Tables.....	xii
List of Figures.....	xiii
List of Schemes.....	xviii
Abbreviations.....	xxi
Acknowledgments.....	xxvii
Chapter 1: Design and Synthesis of Constrained Azacyclic Pyrrolidine Analogues of FTY720 as Anticancer Agents.....	1
1-1 Introduction.....	1
1-1-1 Discovery of FTY720.....	i
1-1-2 FTY720 in immunosuppression.....	4
1-1-2-1 Mechanism of FTY720 in immunosuppression.....	4
1-1-2-2 FTY720 in the treatment of multiple sclerosis (MS).....	9
1-1-3 FTY720 in cancer therapy.....	12
1-1-4 Constrained analogues of FTY720 in S1P receptors studies.....	15
1-1-5 Design of new constrained pyrrolidine analogues of FTY720.....	19
1-2 Results and Discussion.....	20
1-2-1 Synthesis of constrained <i>O</i> -arylmethyl-substituted pyrrolidine analogues.....	20
1-2-1-1 Synthesis of 2-hydroxymethyl-3- <i>O</i> -arylmethylpyrrolidine analogues.....	21
1-2-1-1-1 Synthesis of <i>trans</i> -2-hydroxymethyl-3- <i>O</i> -arylmethylpyrrolidine analogues.....	21
1-2-1-1-2 Synthesis of <i>cis</i> -2-hydroxymethyl-3- <i>O</i> -arylmethylpyrrolidine analogues.....	23
1-2-1-2 Synthesis of 2-hydroxymethyl-4- <i>O</i> -arylmethylpyrrolidine analogues.....	25

1-2-1-2-1 Synthesis of <i>trans</i> -2-hydroxymethyl-4-O-arylmethylpyrrolidine analogues .....	25
1-2-1-2-2 Synthesis of <i>cis</i> -2-hydroxymethyl-4-O-arylmethylpyrrolidine analogues .....	30
1-2-1-3 Synthesis of 3- <i>O</i> -arylmethylpyrrolidine analogues .....	32
1-2-2 Synthesis of constrained <i>C</i> -aryl substituted pyrrolidine analogues .....	35
1-2-2-1 Synthesis of 2,5-bis(hydroxymethyl)-3-arylpyrrolidine analogues .....	35
1-2-2-2 Synthesis of 2,3-substituted <i>C</i> -aryl analogues .....	37
1-2-2-2-1 Synthesis of 2-hydroxymethyl-3-arylpyrrolidine analogues .....	37
1-2-2-2-2 Synthesis of 2-hydroxymethyl-3-aryl-substituted lactam analogues .....	38
1-2-2-2-3 Synthesis of 2-methoxymethyl- and 2-methyl-3-arylpyrrolidine analogues .....	39
1-2-2-2-4 Synthesis of phosphates of 2-hydroxymethyl-3-arylpyrrolidine analogues. ....	40
1-2-2-3 Synthesis of 2-hydroxymethyl-4-arylpyrrolidine analogues .....	41
1-2-2-3-1 Synthesis of <i>cis</i> -2-hydroxymethyl-4-arylpyrrolidine analogues .....	42
1-2-2-3-2 Synthesis of <i>trans</i> -2-hydroxymethyl-4-arylpyrrolidine analogues.....	46
1-2-2-4 Synthesis of 3-arylpyrrolidine analogues.....	47
1-2-3 Biological evaluations of constrained <i>O</i> -arylmethyl substituted pyrrolidine analogues.....	52
1-2-4 Biological evaluations of constrained <i>C</i> -aryl substituted pyrrolidine analogues ....	58
1-2-5 Discussion .....	64
1-3 Conclusion .....	65
1-4 Experimental.....	66
1-5 References .....	127
Chapter 2: Design and Synthesis of Photoaffinity Labeling Probe of Amino Alcohol <b>1.57</b> and <b>1.65</b> .....	137
2-1 Introduction .....	137
2-1-1 General mechanism of photoaffinity labeling (PAL).....	137
2-1-2 Photoaffinity probe (PAP).....	138

2-1-2-1 Photoreactive groups.....	139
2-1-2-2 Reporter groups.....	141
2-1-3 Design of photoaffinity labeling probes from <b>1.57</b> and <b>1.65</b> .....	147
2-2 Results and Discussion .....	149
2-2-1 Screening of the position of diazirine .....	149
2-2-1-1 Synthesis of ketone <b>2.1</b> .....	149
2-2-1-2 Synthesis of ketone <b>2.2</b> .....	152
2-2-1-3 Synthesis of ketone <b>2.3</b> .....	154
2-2-1-4 Synthesis of ketone <b>2.4</b> .....	155
2-2-1-5 Biological evaluation of ketones <b>2.1</b> , <b>2.2</b> , <b>2.3</b> and <b>2.4</b> .....	156
2-2-1-6 Synthesis of diazirines <b>2.21</b> and <b>2.22</b> .....	158
2-2-1-7 Biological evaluation of diazirines <b>2.21</b> and <b>2.22</b> .....	160
2-2-2 Screening of the reporter group.....	162
2-2-3 Synthesis of the photoaffinity probes <b>2.31</b> and <b>2.39</b> .....	164
2-2-4 Biological evaluations of photoaffinity probes <b>2.31</b> and <b>2.39</b> .....	167
2-3 Conclusion .....	170
2-4 Experimental.....	170
2-5 References .....	190
Chapter 3: Studies of Unusual Barbier-Grignard Type Reactions.....	196
3-1 Introduction .....	196
3-1-1 Barbier reaction.....	196
3-1-2 Grignard reaction.....	199
3-1-3 An unsuccessful Barbier-Grignard type intramolecular cyclization.....	208
3-2 Results .....	211
3-2-1 Intermolecular reactions.....	211
3-2-2 Intramolecular reaction .....	213
3-3 Discussion.....	215
3-4 Conclusion .....	218
3-5 Experimental.....	219
3-6 References .....	225



Chapter 4: From Synthetic Study of 2-hydroxy-2,5-dimethylbicyclo[3.2.1]octane-6,8-dione (a constitutional isomer of the Hajos-Parrish ketone), to Catalytic Synthesis of Tertiary $\beta$ -Ketols .....	230
4-1 Introduction .....	230
4-1-1 $\beta$ -Ketols from Aldol reaction .....	230
4-1-2 Synthetic background of $\beta$ -ketol <b>3.20</b> from triketone <b>3.18</b> .....	234
4-2 Results .....	236
4-2-1 Screening of reaction conditions for the synthesis of $\beta$ -ketol <b>3.20</b> .....	236
4-2-1-1 Temperature and catalysts loading .....	236
4-2-1-2 Solvents .....	237
4-2-1-3 Additives .....	238
4-2-1-4 Achiral bases .....	239
4-2-2 Studies toward an enantioselective synthesis of <b>3.20</b> .....	243
4-3 Discussion .....	245
4-3-1 Proposed mechanisms for catalytic synthesis of <b>3.20</b> .....	245
4-3-1-1 Mechanism involving LiBr .....	245
4-3-1-2 Bifunctional H-bonded mechanism .....	249
4-3-2 Studies toward the symmetric syntheses of $\beta$ -ketols from benzyl triketone <b>4.6</b> ..	253
4-3-3 $\beta$ -Ketol formation from a benzyl diketone <b>4.10</b> .....	258
4-4 Conclusion .....	260
4-5 Experimental .....	262
4-6 References .....	274
Annex 1: $^1\text{H}$ and $^{13}\text{C}$ NMR Spectra of Compound <b>1.32</b> .....	280
Annex 2: $^1\text{H}$ and $^{13}\text{C}$ NMR Spectra of Compound <b>1.39</b> .....	282
Annex 3: $^1\text{H}$ and $^{13}\text{C}$ NMR Spectra of Compound <b>1.44</b> .....	284
Annex 4: $^1\text{H}$ and $^{13}\text{C}$ NMR Spectra of Compound <b>1.49</b> .....	286
Annex 5: $^1\text{H}$ and $^{13}\text{C}$ NMR Spectra of Compound <b>1.65</b> .....	288
Annex 6: $^1\text{H}$ and $^{13}\text{C}$ NMR Spectra of Compound <b>1.70</b> .....	290
Annex 7: $^1\text{H}$ , $^{13}\text{C}$ and $^{31}\text{P}$ NMR Spectra of Compound <b>1.77</b> .....	292

Annex 8: $^1\text{H}$ and $^{13}\text{C}$ NMR Spectra of Compound <b>1.100</b> .....	295
Annex 10: $^1\text{H}$ and $^{13}\text{C}$ NMR Spectra of Compound <b>1.114</b> .....	299
Annex 11: $^1\text{H}$ and $^{13}\text{C}$ NMR Spectra of Compound <b>1.117</b> .....	301
Annex 12: $^1\text{H}$ and $^{13}\text{C}$ NMR Spectra of Compound <b>1.120</b> .....	303
Annex 13: $^1\text{H}$ and $^{13}\text{C}$ NMR Spectra of Compound <b>1.123</b> .....	305
Annex 14: $^1\text{H}$ and $^{13}\text{C}$ NMR Spectra of Compound <b>1.124</b> .....	307
Annex 15: $^1\text{H}$ and $^{13}\text{C}$ NMR Spectra of Compound <b>1.125</b> .....	309
Annex 16: $^1\text{H}$ and $^{13}\text{C}$ NMR Spectra of Compound <b>1.126</b> .....	311
Annex 17: $^1\text{H}$ and $^{13}\text{C}$ NMR Spectra of Compound <b>1.127</b> .....	314
Annex 18: $^1\text{H}$ and $^{13}\text{C}$ NMR Spectra of Compound <b>1.129</b> .....	317
Annex 19: $^1\text{H}$ and $^{13}\text{C}$ NMR Spectra of Compound <b>1.131</b> .....	319
Annex 20: $^1\text{H}$ and $^{13}\text{C}$ NMR Spectra of Compound <b>1.134</b> .....	321
Annex 21: $^1\text{H}$ and $^{13}\text{C}$ NMR Spectra of Compound <b>1.137</b> .....	323
Annex 22: $^1\text{H}$ , $^{13}\text{C}$ and $^{31}\text{P}$ NMR Spectra of Compound <b>1.139</b> .....	325
Annex 23: $^1\text{H}$ , $^{13}\text{C}$ and $^{31}\text{P}$ NMR Spectra of Compound <b>1.141</b> .....	328
Annex 24: $^1\text{H}$ and $^{13}\text{C}$ NMR Spectra of Compound <b>1.150</b> .....	331
Annex 25: $^1\text{H}$ and $^{13}\text{C}$ NMR Spectra of Compound <b>1.157</b> .....	333
Annex 26: $^1\text{H}$ and $^{13}\text{C}$ NMR Spectra of Compound <b>1.161</b> .....	335
Annex 27: $^1\text{H}$ and $^{13}\text{C}$ NMR Spectra of Compound <b>1.164</b> .....	337
Annex 28: $^1\text{H}$ and $^{13}\text{C}$ NMR Spectra of Compound <b>1.170</b> .....	339
Annex 29: $^1\text{H}$ and $^{13}\text{C}$ NMR Spectra of Compound <b>1.175</b> .....	341
Annex 30: $^1\text{H}$ and $^{13}\text{C}$ NMR Spectra of Compound <b>2.1</b> .....	343
Annex 31: $^1\text{H}$ and $^{13}\text{C}$ NMR Spectra of Compound <b>2.2</b> .....	345
Annex 32: $^1\text{H}$ and $^{13}\text{C}$ NMR Spectra of Compound <b>2.3</b> .....	347
Annex 33: $^1\text{H}$ and $^{13}\text{C}$ NMR Spectra of Compound <b>2.4</b> .....	349

Annex 35: $^1\text{H}$ and $^{13}\text{C}$ NMR Spectra of Compound <b>2.21</b> .....	351
Annex 36: $^1\text{H}$ and $^{13}\text{C}$ NMR Spectra of Compound <b>2.22</b> .....	353
Annex 37: $^1\text{H}$ and $^{13}\text{C}$ NMR Spectra of Compound <b>2.30</b> .....	355
Annex 38: $^1\text{H}$ and $^{13}\text{C}$ NMR Spectra of Compound <b>2.38</b> .....	357
Annex 39: $^1\text{H}$ and $^{13}\text{C}$ NMR Spectra of Compound <b>3.14a</b> .....	359
Annex 40: $^1\text{H}$ and $^{13}\text{C}$ NMR Spectra of Compound <b>3.14b</b> .....	361
Annex 41: $^1\text{H}$ and $^{13}\text{C}$ NMR Spectra of Compound <b>3.14c</b> .....	363
Annex 42: $^1\text{H}$ and $^{13}\text{C}$ NMR Spectra of Compound <b>3.14d</b> .....	365
Annex 43: $^1\text{H}$ and $^{13}\text{C}$ NMR Spectra of Compound <b>3.14e</b> .....	367
Annex 44: $^1\text{H}$ and $^{13}\text{C}$ NMR Spectra of Compound <b>3.14f</b> .....	369
Annex 45: $^1\text{H}$ and $^{13}\text{C}$ NMR Spectra of Compound <b>3.14g</b> .....	371
Annex 46: $^1\text{H}$ and $^{13}\text{C}$ NMR Spectra of Compound <b>3.14h</b> .....	373
Annex 47: $^1\text{H}$ and $^{13}\text{C}$ NMR Spectra of Compound <b>3.15</b> .....	375
Annex 48: $^1\text{H}$ and $^{13}\text{C}$ NMR Spectra of Compound <b>3.19</b> .....	377
Annex 49: $^1\text{H}$ and $^{13}\text{C}$ NMR Spectra of Compound <b>3.20</b> .....	379
Annex 50: $^1\text{H}$ and $^{13}\text{C}$ NMR Spectra of Compound <b>3.21</b> .....	381
Annex 51: $^1\text{H}$ and $^{13}\text{C}$ NMR Spectra of Compound <b>4.3</b> .....	383
Annex 52: $^1\text{H}$ and $^{13}\text{C}$ NMR Spectra of Compound <b>4.6</b> .....	385
Annex 53: $^1\text{H}$ and $^{13}\text{C}$ NMR Spectra of Compound <b>4.7</b> .....	387
Annex 54: $^1\text{H}$ and $^{13}\text{C}$ NMR Spectra of Compound <b>4.8</b> .....	389
Annex 55: $^1\text{H}$ and $^{13}\text{C}$ NMR Spectra of Compound <b>4.9</b> .....	391
Annex 56: $^1\text{H}$ and $^{13}\text{C}$ NMR Spectra of Compound <b>4.10</b> .....	393
Annex 57: $^1\text{H}$ and $^{13}\text{C}$ NMR Spectra of Compound <b>4.11</b> .....	395
Annex 58: X-Ray Data for Compound <b>1.148</b> .....	397
Annex 59: X-Ray Data for Compound <b>3.20</b> .....	408

Annex 60: X-Ray Data for Compound <b>4.7</b> .....	417
Annex 61: X-Ray Data for Compound <b>4.8</b> .....	438
Annex 62: X-Ray Data for Compound <b>4.9</b> .....	445
Annex 63: X-Ray Data for Compound <b>4.11</b> .....	452

## List of Tables

<b>Table 1.</b> Binding affinities (nM) to SIP receptors. ....	8
<b>Table 2.</b> Mean IC <sub>50</sub> (in μM +/- SEM) of analogs in cell viability assays in a range of human cancer cell lines and BCR-Abl-expressing murine bone marrow (BM).....	57
<b>Table 3.</b> IC <sub>50</sub> values in other cancer cell lines.....	63
<b>Table 4.</b> Intermolecular reactions under “Barbier conditions” .....	212
<b>Table 5.</b> Screening of temperature and catalysts loading.....	237
<b>Table 6.</b> Screening of solvents. ....	238
<b>Table 7.</b> Screening of additives.....	239
<b>Table 8.</b> Screening of bases.....	241
<b>Table 9.</b> Chiral bases with and without LiBr. ....	244
<b>Table 10.</b> Equilibration reactions between <b>3.19</b> and <b>3.20</b> . ....	247
<b>Table 11.</b> Reactions with other triketones catalyzed by TBD with and without LiBr. ....	252
<b>Table 12.</b> Intermolecular Reactions in the presence of TBD with and without additives.....	253
<b>Table 13.</b> Reactions with benzyl triketone <b>4.6</b> . ....	254
<b>Table 14.</b> Equilibrium reactions between ketol <b>4.8</b> and <b>4.9</b> . ....	257
<b>Table 15.</b> Intramolecular aldol reaction of 1-phenylheptane-2,6-dione ( <b>4.10</b> ). ....	259

## List of Figures

<b>Figure 1.</b> Structure of rapamycin ( <b>1.1</b> ), cyclosporin A ( <b>1.2</b> ), FK506 ( <b>1.3</b> ) and ISP-I (myriocin, thermozytocidin, <b>1.4</b> ).....	2
<b>Figure 2.</b> Optimization of ISP-I ( <b>1.4</b> ) to FTY720 ( <b>1.8</b> ) .....	4
<b>Figure 3.</b> ( <i>S</i> )-FTY720 phosphate inhibits S1P/S1P <sub>1</sub> -dependent lymphocyte egress from lymphoid tissues by long-term internalization and degradation of S1P <sub>1</sub> .....	9
<b>Figure 4.</b> Examples of constrained analogues reported by Macdonald. ....	16
<b>Figure 5.</b> Constrained 2,3,5-trisubstituted pyrrolidine analogues.....	17
<b>Figure 6.</b> List of synthesized constrained <i>O</i> -arylmethylpyrrolidine analogues. ....	34
<b>Figure 7.</b> X ray structure of ester <b>1.148</b> . ....	43
<b>Figure 8.</b> List of synthesized constrained <i>C</i> -aryl substituted pyrrolidine analogues. ....	51
<b>Figure 9.</b> Cytotoxic action of different alkyl chain substituted L-prolinol analogues on murine hematopoietic FL5.12 cells.....	53
<b>Figure 10.</b> Cytotoxic action of diastereomeric 2-hydroxymethyl-4- <i>O</i> -arylmethylpyrrolidine analogues on Sup-B15 leukemia cells. ....	54
<b>Figure 11.</b> Cytotoxic action of diastereomeric 2-hydroxymethyl-3- <i>O</i> -arylmethylpyrrolidine analogues on Sup-B15 leukemia cells. ....	55
<b>Figure 12.</b> Cytotoxic action of 2-methoxymethyl- and 2-methyl-4- <i>O</i> -arylmethylpyrrolidine analogues, and 3- <i>O</i> -arylmethylpyrrolidine analogues on Sup-B15 leukemia cells.....	56
<b>Figure 13.</b> Diastereomeric 2-hydroxymethyl- and 2-methyl-4- <i>O</i> -arylmethylpyrrolidine (10 $\mu$ M) trigger nutrient transporter loss in Sup-B15 leukemia cells. ....	58
<b>Figure 14.</b> IC <sub>50</sub> values of 2,5-bis(hydroxymethyl)-3-arylpyrrolidine analogues in prostate cancer cell lines.....	59
<b>Figure 15.</b> IC <sub>50</sub> values of 2-hydroxymethyl-3-arylpyrrolidine analogues in prostate cancer cell lines.....	60
<b>Figure 16.</b> IC <sub>50</sub> values of 2-hydroxymethyl-3-aryl-lactam analogues in prostate cancer cell lines.....	60
<b>Figure 17.</b> IC <sub>50</sub> values of 2-methoxymethyl- and 2-methyl-3-arylpyrrolidine analogues in prostate cancer cell lines.....	61

<b>Figure 18.</b> IC <sub>50</sub> values of 2-hydroxymethyl-4-arylpyrrolidine analogues in prostate cancer cell lines. ....	62
<b>Figure 19.</b> IC <sub>50</sub> values of 3-arylpyrrolidine analogues in prostate cancer cell lines. ....	62
<b>Figure 20.</b> Nutrient transporter down-regulation in PC3 cells at 1X or 2X the IC <sub>50</sub> . ....	64
<b>Figure 21.</b> Cytotoxic action of phosphates <b>1.75</b> and <b>1.77</b> on Sup-B15 leukemia cells.....	65
<b>Figure 22.</b> Nutrient transporter down-regulation of phosphates <b>1.75</b> and <b>1.77</b> in Sup-B15 leukemia cells.....	65
<b>Figure 23.</b> General mechanism of a photoaffinity labeling (PAL) process. ....	138
<b>Figure 24.</b> Photolabeling groups: benzophenones, aryl azides and diazirines. ....	139
<b>Figure 25.</b> Possible photochemical processes of benzophenone.....	139
<b>Figure 26.</b> Possible photochemistry process of aryl azide. ....	140
<b>Figure 27.</b> Possible photochemistry process of diazirine.....	141
<b>Figure 28.</b> A general bioorthogonal chemical reaction.....	142
<b>Figure 29.</b> General mechanisms of the Staudinger reaction and the Bertozzi-Staudinger ligation. ....	143
<b>Figure 30.</b> General mechanisms of azide-alkyne Huisgen cycloaddition and CuAAC reaction. ....	145
<b>Figure 31.</b> General reaction of SPAAC and modified octyne analogues.....	147
<b>Figure 32.</b> Design of photoaffinity labeling (PAL) probes of <b>1.57</b> and <b>1.65</b> , and their ketone precursors <b>2.1</b> , <b>2.2</b> , <b>2.3</b> and <b>2.4</b> . ....	148
<b>Figure 33.</b> Cytotoxic action of different ketone side chain substituted analogues <b>2.1</b> , <b>2.2</b> , <b>2.3</b> and <b>2.4</b> on murine hematopoietic FL5.12 cells.....	157
<b>Figure 34.</b> Nutrient transporter down-regulation of ketone side-chain substituted analogues <b>2.1</b> , <b>2.2</b> , <b>2.3</b> , and <b>2.4</b> on FL5.12 cells.....	158
<b>Figure 35.</b> Diazirine analogues <b>2.21</b> and <b>2.22</b> .....	158
<b>Figure 36.</b> Cytotoxic action of diazirines <b>2.21</b> and <b>2.22</b> on FL5.12 cells. ....	161
<b>Figure 37.</b> Nutrient transporter down-regulation of diazirines <b>2.21</b> and <b>2.22</b> on FL5.12 cells. ....	162
<b>Figure 38.</b> Cytotoxic action of azide and alkyne analogues on FL5.12 cells. ....	163
<b>Figure 39.</b> Nutrient transporter down-regulation of azide and alkyne analogues on FL5.12 cells. ....	164

<b>Figure 40.</b> General structure of the desired photoaffinity probe and its retrosynthetic analysis.	165
<b>Figure 41.</b> Cytotoxic action of photoaffinity probes <b>2.31</b> and <b>2.39</b> on FL5.12 cells.	168
<b>Figure 42.</b> Nutrient transporter down-regulation of photoaffinity probes <b>2.31</b> and <b>2.39</b> on FL5.12 cells.	168
<b>Figure 43.</b> General projected PAL experiments for <b>2.31</b> and <b>2.39</b> .	169
<b>Figure 44.</b> The first reported Barbier reaction and the general concept of Barbier type reaction.	196
<b>Figure 45.</b> Barbier type reactions in aqueous media.	197
<b>Figure 46.</b> Intramolecular Barbier type reactions.	198
<b>Figure 47.</b> Proposed mechanisms for Barbier reactions.	199
<b>Figure 48.</b> General concept of the Grignard reaction.	200
<b>Figure 49.</b> Proposed mechanism for the formation of Grignard reagents.	200
<b>Figure 50.</b> Schlenk equilibrium and the dimer complex of alkyl magnesium chlorides.	201
<b>Figure 51.</b> Proposed mechanisms for Grignard reactions.	202
<b>Figure 52.</b> Proposed mechanisms for reduction reactions occurred in Grignard reactions.	204
<b>Figure 53.</b> Proposed mechanisms for pinacol coupling reactions in Grignard reactions.	205
<b>Figure 54.</b> Proposed mechanisms for enolization reactions occurred in Grignard reactions.	206
<b>Figure 55.</b> Example of self-aldol condensation in Grignard reactions and the possible mechanism.	207
<b>Figure 56.</b> Example of Grignard reaction with and without additive ( $\text{CeCl}_3$ ).	208
<b>Figure 57.</b> Retrosynthetic analysis for synthesizing key intermediate <b>3.9</b> .	209
<b>Figure 58.</b> Unusual Barbier reaction between 5-hexen-2-one ( <b>3.13</b> ) and <i>n</i> -butyl iodide.	210
<b>Figure 59.</b> $\beta$ -ketol formation from intramolecular cyclization of <b>3.18</b> .	214
<b>Figure 60.</b> Intramolecular reaction of <b>3.18</b> under “Barbier conditions”.	215
<b>Figure 61.</b> X ray structure of <b>3.20</b> .	215
<b>Figure 62.</b> Reaction of <b>3.13</b> using commercial Grignard reagents, and <i>t</i> -BuOMgBr.	216
<b>Figure 63.</b> Plausible mechanism for the intermolecular self-aldol reaction of ketones.	217
<b>Figure 64.</b> Plausible mechanism for the intramolecular aldol reaction.	217
<b>Figure 65.</b> Reaction of triketone <b>3.18</b> with <i>t</i> -BuOMgBr.	218
<b>Figure 66.</b> Aldol reaction under basic and acidic conditions.	230



<b>Figure 67.</b> Examples of $\beta$ -hydroxyl carbonyl units in natural products and drugs.....	231
<b>Figure 68.</b> Examples of Evans' oxazolidinone auxiliaries in the aldol reaction.....	232
<b>Figure 69.</b> Examples of chiral catalysts used in Mukaiyama aldol reaction.....	233
<b>Figure 70.</b> Examples of proline and its derivatives as catalysts in aldol reaction.....	233
<b>Figure 71.</b> Synthesis of <b>3.20</b> by Dauben and Bunce.....	234
<b>Figure 72.</b> Synthesis of <b>3.19</b> and <b>3.20</b> by Shibasaki and coworkers.....	235
<b>Figure 73.</b> Synthesis of <b>3.20</b> by Davies and coworkers.....	235
<b>Figure 74.</b> Synthesis of <b>3.20</b> by Mahrwald and coworkers.....	235
<b>Figure 75.</b> Kinetic profiles of DBU, with and without LiBr-catalyzed aldol reaction of <b>3.18</b> and the formation of <b>3.20</b> .....	242
<b>Figure 76.</b> Kinetic profiles of Eschenmoser amidine, with and without LiBr-catalyzed aldol reaction of <b>3.18</b> and the formation of <b>3.20</b> .....	242
<b>Figure 77.</b> Kinetic profiles of TBD, with and without LiBr catalyzed aldol reaction of <b>3.18</b> and the formation of <b>3.20</b> .....	242
<b>Figure 78.</b> Catalytic synthesis of $\beta$ -ketol <b>3.20</b> from triketone <b>3.18</b> .....	243
<b>Figure 79.</b> Proposed catalytic cycle in the LiBr pre-coordination model.....	245
<b>Figure 80.</b> $^{13}\text{C}$ NMR spectra study of <b>3.18</b> .....	246
<b>Figure 81.</b> Free energy profile of the DBU & LiBr-catalyzed reaction in THF at 233 K. ....	248
<b>Figure 82.</b> Proposed bifunctional H-bonded mechanism.....	249
<b>Figure 83.</b> Baati's proton shuffling general base mechanism.....	250
<b>Figure 84.</b> Free energy profile of the TBD-catalyzed reaction in THF at 233 K.....	251
<b>Figure 85.</b> Hypothesis for enantioselective synthesis of $\beta$ -ketol <b>4.7</b> from benzyl triketone <b>4.6</b> . .....	253
<b>Figure 86.</b> X-ray structure of ketols <b>4.7</b> , <b>4.8</b> and <b>4.9</b> .....	255
<b>Figure 87.</b> Proposed Li-coordinated and bifunctional H-bonding transition states model in the reaction of benzyl triketone <b>4.6</b> at - 40 °C.....	256
<b>Figure 88.</b> Proposed transition state model and effect of the temperature in the reaction of benzyl triketone <b>4.6</b> with DBU.....	257
<b>Figure 89.</b> X-ray structure of ketol <b>4.11</b> .....	259
<b>Figure 90.</b> Proposed transition state model in the cyclization of diketone <b>4.10</b> .....	260

**Figure 91.** Proposed bifunctional chiral amidine catalyst and the transition state model from DFT calculations. .... 261

## List of Schemes

<b>Scheme 1.</b> FTY720 ( <b>1.8</b> ) and sphingolipid metabolism.....	7
<b>Scheme 2.</b> Synthesis of constrained 2,3,5-trisubstituted pyrrolidine analogue <b>1.15</b> .....	18
<b>Scheme 3.</b> Design of two series of constrained pyrrolidine analogues of FTY720 ( <b>1.8</b> ).....	20
<b>Scheme 4.</b> Retrosynthesis of constrained <i>O</i> -arylmethyl-substituted pyrrolidine analogues ....	21
<b>Scheme 5.</b> Synthesis of (2 <i>R</i> ,3 <i>S</i> )-2-hydroxymethyl-3- <i>O</i> -arylmethylpyrrolidine <b>1.32</b> .....	22
<b>Scheme 6.</b> Synthesis of (2 <i>S</i> ,3 <i>R</i> )-2-hydroxymethyl-3- <i>O</i> -arylmethylpyrrolidine <b>1.39</b> .....	23
<b>Scheme 7.</b> Synthesis of (2 <i>R</i> ,3 <i>R</i> )-2-hydroxymethyl-3- <i>O</i> -arylmethylpyrrolidine <b>1.44</b> .....	24
<b>Scheme 8.</b> Synthesis of (2 <i>S</i> ,3 <i>S</i> )-2-hydroxymethyl-3- <i>O</i> -arylmethylpyrrolidine <b>1.49</b> .....	24
<b>Scheme 9.</b> Synthesis of (2 <i>S</i> ,4 <i>R</i> )-2-hydroxymethyl-4- <i>O</i> -arylmethylpyrrolidine <b>1.57</b> .....	26
<b>Scheme 10.</b> Synthesis of (2 <i>R</i> ,4 <i>S</i> )-2-hydroxymethyl-4- <i>O</i> -arylmethylpyrrolidine <b>1.65</b> .....	27
<b>Scheme 11.</b> Synthesis of (2 <i>R</i> ,4 <i>S</i> )-2-methoxymethyl-4- <i>O</i> -arylmethylpyrrolidine <b>1.67</b> .....	28
<b>Scheme 12.</b> Synthesis of (2 <i>R</i> ,4 <i>S</i> )-2-methyl-4- <i>O</i> -arylmethylpyrrolidine <b>1.70</b> .....	29
<b>Scheme 13.</b> Synthesis of (2 <i>S</i> ,4 <i>R</i> )-2-methyl-4- <i>O</i> -arylmethylpyrrolidine <b>1.73</b> .....	29
<b>Scheme 14.</b> Synthesis of (2 <i>S</i> ,4 <i>R</i> )- and (2 <i>R</i> ,4 <i>S</i> )-2-(methyl-dihydrophosphate)-4- <i>O</i> - arylmethylpyrrolidines <b>1.75</b> and <b>1.77</b> .....	30
<b>Scheme 15.</b> Synthesis of (2 <i>R</i> ,4 <i>R</i> )-2-hydroxymethyl-4- <i>O</i> -arylmethylpyrrolidine <b>1.83</b> .....	31
<b>Scheme 16.</b> Synthesis of (2 <i>S</i> ,4 <i>S</i> )-2-hydroxymethyl-4- <i>O</i> -arylmethylpyrrolidine <b>1.89</b> .....	31
<b>Scheme 17.</b> Synthesis of ( <i>R</i> )-3- <i>O</i> -arylmethylpyrrolidine <b>1.94</b> .....	32
<b>Scheme 18.</b> Synthesis of ( <i>S</i> )-3- <i>O</i> -arylmethylpyrrolidine <b>1.99</b> .....	33
<b>Scheme 19.</b> Retrosynthetic analysis of (2 <i>S</i> ,3 <i>S</i> ,5 <i>S</i> )-2,5-bis(hydroxymethyl)-3-aryl- pyrrolidine <b>1.100</b> .....	35
<b>Scheme 20.</b> Synthesis of (2 <i>S</i> ,3 <i>S</i> ,5 <i>S</i> )-2,5-bis(hydroxymethyl)-3-arylpyrrolidine <b>1.100</b> .....	36
<b>Scheme 21.</b> Synthesis of (2 <i>R</i> ,3 <i>R</i> ,5 <i>R</i> )-2,5-bis(hydroxymethyl)-3-arylpyrrolidine <b>1.101</b> .....	37

<b>Scheme 22.</b> Synthesis of 2-hydroxymethyl-3-arylpyrrolidines <b>1.114</b> , <b>1.117</b> , <b>1.120</b> and <b>1.123</b> . .....	38
<b>Scheme 23.</b> Synthesis of 2-hydroxymethyl-3-aryl-substituted lactams <b>1.124</b> , <b>1.125</b> , <b>1.126</b> and <b>1.127</b> .....	39
<b>Scheme 24.</b> Synthesis of 2-methoxymethyl-3-arylpyrrolidines <b>1.129</b> and <b>1.131</b> . ....	40
<b>Scheme 25.</b> Synthesis of 2-methyl-3-arylpyrrolidines <b>1.134</b> and <b>1.137</b> . ....	40
<b>Scheme 26.</b> Synthesis of 2-methyldihydrophosphate-3-arylpyrrolidines <b>1.139</b> and <b>1.141</b> .....	41
<b>Scheme 27.</b> Retrosynthetic analysis of 2-hydroxymethyl-4-arylpyrrolidines.....	42
<b>Scheme 28.</b> Synthesis of (2 <i>R</i> ,4 <i>S</i> )-2-hydroxymethyl-4-arylpyrrolidine <b>1.150</b> .....	43
<b>Scheme 29.</b> Synthesis of (2 <i>S</i> ,4 <i>R</i> )-2-hydroxymethyl-4-arylpyrrolidine <b>1.157</b> .....	44
<b>Scheme 30.</b> Studies of the reaction organolithium reagent addition on <b>1.145</b> . ....	45
<b>Scheme 31.</b> Proposed mechanism of epimerization of <b>1.158</b> followed by dehydrogenation...	46
<b>Scheme 32.</b> Synthesis of (2 <i>R</i> ,4 <i>R</i> )-2-hydroxymethyl-4-arylpyrrolidine <b>1.161</b> . ....	47
<b>Scheme 33.</b> Synthesis of (2 <i>S</i> ,4 <i>S</i> )-2-hydroxymethyl-4-arylpyrrolidine <b>1.164</b> . ....	47
<b>Scheme 34.</b> Retrosynthetic analysis for the synthesis of 3-arylpyrrolidine analogues. ....	48
<b>Scheme 35.</b> Synthesis of ( <i>S</i> )-3-arylpyrrolidine <b>1.170</b> . ....	49
<b>Scheme 36.</b> Synthesis of ( <i>R</i> )-3-arylpyrrolidine <b>1.175</b> .....	50
<b>Scheme 37.</b> Retrosynthetic analysis of ketone <b>2.1</b> (route I). ....	149
<b>Scheme 38.</b> Synthesis of ketone <b>2.1</b> (route I). ....	150
<b>Scheme 39.</b> Retrosynthetic analysis of ketone <b>2.1</b> (route II). ....	151
<b>Scheme 40.</b> Synthesis of ketone <b>2.1</b> (route II). ....	152
<b>Scheme 41.</b> Retrosynthetic analysis of ketone <b>2.2</b> . ....	152
<b>Scheme 42.</b> Synthesis of ketone <b>2.2</b> . ....	153
<b>Scheme 43.</b> Retrosynthetic analysis of ketone <b>2.3</b> . ....	154
<b>Scheme 44.</b> Synthesis of ketone <b>2.3</b> . ....	155

<b>Scheme 45.</b> Retrosynthetic analysis of ketone <b>2.4</b> .....	155
<b>Scheme 46.</b> Synthesis of ketone <b>2.4</b> .....	156
<b>Scheme 47.</b> Synthesis of diazirine <b>2.22</b> .....	159
<b>Scheme 48.</b> Synthesis of diazirine <b>2.21</b> .....	160
<b>Scheme 49.</b> Synthesis of photoaffinity probe <b>2.31</b> .....	166
<b>Scheme 50.</b> Synthesis of photoaffinity probe <b>2.39</b> .....	167
<b>Scheme 51.</b> Synthesis of key intermediate <b>3.9</b> by Barbier-Grignard type reaction. ....	209
<b>Scheme 52.</b> Synthesis of key intermediate <b>3.9</b> by intramolecular aldol reaction.....	210

## Abbreviations

Å	angstrom
$[\alpha]_D^{\text{Temp.}}$	Specific sodium D line rotation ( $\lambda = 589 \text{ nm}$ )
Ac	acetyl
AIBN	2, 2'-azo <i>bisisobutyronitrile</i>
ALL	acute lymphoblastic leukemia
ALO	aryl-less octyne
BARAC	biarylazacyclooctynone
BBB	blood–brain barrier
BCN	bicycle[6.1.0]nonyne
Bcl-2	B-cell lymphoma 2
BCR-ABL	breakpoint cluster region-Abelson murine leukemia viral oncogene
BM	bone marrow
Bn	benzyl
Boc	<i>tert</i> -butyloxycarbonyl
Calcd	calculated
c-hex	cyclohexyl
CLL	chronic lymphocytic leukemia
CNS	central nervous system
CML	chronic myelogenous leukemia
CuAAC	copper-catalyzed azide-alkyne cycloaddition
d	doublet
dba	dibenzylideneacetone
DBU	1,8-diazabicycloundec-7-ene
DCM	dichloromethane
dd	doublet of doublets
$\Delta G$	change in Gibbs free energy
DFT	density functional theory
DIBAC	dibenzoazacyclooctyne
DIBAL-H	diisobutylaluminium hydride

DIBO	dibenzocyclooctyne
DIEPA	<i>N,N</i> -diisopropylethylamine
DIFO	difluorinated cyclooctyne
DMAP	4-dimethylaminopyridine
DME	dimethoxyethane
DMF	dimethylformamide
DMS	dimethyl sulfide
DMTs	disease modifying therapies
DMSO	dimethyl sulfoxide
EAE	experimental autoimmune encephalomyelitis
ED <sub>50</sub>	effective dose causing 50 % inhibition
EDC	1-ethyl-3-(3-dimethylaminopropyl)carbodiimide
e.e.	enantiomeric excess
eq (equiv.)	equivalent
ERKs	extracellular-signal-regulated kinases
ESI	electrospray ionization
Et	ethyl
FAB	fast atom bombardment
FTIR	fourier transform infrared spectroscopy
g	gram
Gen.	generation
GPCRs	G-protein-coupled receptors
h	hour
HOBT	hydroxybenzotriazole
HPLC	high performance liquid chromatography
HRMS	high-resolution mass spectroscopy
Hz	hertz
IR	infrared spectroscopy
<i>J</i>	coupling constant
JNKs	c-Jun N-terminal kinases
IC <sub>50</sub>	half maximal inhibitory concentration

im	imidazolyl
<i>i</i> -Pr	<i>iso</i> -propyl
LC	liquid chromatography
LiHMDS	lithium <i>bis</i> (trimethylsilyl)amide
L-selectride	lithium tri- <i>sec</i> -butylborohydride
m	multiplet
<i>m</i> -CPBA	<i>meta</i> -chloroperoxybenzoic acid
Me	methyl
MHz	megahertz
min	minute
mL	milliliter
MLR	mouse allogeneic mixed lymphocyte reaction
MMF	mycophenolate mofetil
mmol	millimole
MOFO	monofluorinated cyclooctyne
Ms	methanesulfonyl
MS	multiple sclerosis or mass spectrometry or molecular sieve
MTBD	7-methyl-1,5,7-triazabicyclo[4.4.0]dec-5-ene
<i>n</i> -Bu	<i>neo</i> -butyl
NBS	<i>N</i> -bromosuccinimide
NMR	nuclear magnetic resonance
OCT	cyclooctyne
OTf	trifluoromethanesulfonate (triflate)
PAL	photoaffinity labeling
PAP	photoaffinity labeling probe
PBL	peripheral blood lymphocytes
ph	phenyl
Ph <sup>+</sup>	philadelphia chromosome-positive
Ph <sup>-</sup>	philadelphia chromosome-negative
pKa	acid dissociation constant
ppm	parts per million



PP-MS	primary progressive multiple sclerosis
PP2A	protein phosphatase 2A
PPTS	pyridinium <i>p</i> -toluenesulfonate
PR-MS	progressive relapsing multiple sclerosis
PTEN	phosphatase and tensin homolog
PTSA	<i>p</i> -toluenesulfonic acid
Py	pyridine
q	quartet
ROS	reactive oxygen species
RR-MS	relapsing-remitting multiple sclerosis
r.t.	room temperature
s	singlet
SAR	structure-activity relationship
SDS	solvent distillation system
SEM	standard error of the mean
SET	single electron transfer
SFC	supercritical fluid chromatography
SPAAC	strain-promoted alkyne-azide cycloaddition
SPhK	sphingosine kinases
SP-MS	secondary progressive multiple sclerosis
SPT	serine palmitoyl-transferase
S1P	sphingosine-1-phosphate
t	triplet
TBAF	tetra- <i>n</i> -butylammonium fluoride
TBAI	tetra- <i>n</i> -butylammonium iodide
TBD	triazabicyclodecene (1,5,7-triazabicyclo[4.4.0]dec-5-ene)
TBDPS	<i>tert</i> -butyldiphenylsilyl
TBS	<i>tert</i> -butyldimethylsilyl
<i>t</i> -Bu	<i>tert</i> -butyl
TEA	triethylamine
TEMPO	(2,2,6,6-tetramethylpiperidin-1-yl)oxyl

TFA	trifluoroacetic acid
THF	tetrahydrofuran
TLC	thin layer chromatography
TMS	trimethylsilyl
Tr	trityl (triphenylmethyl)
TS	transition state
$\mu\text{m}$	micromolar molar
UV	ultraviolet

*To my parents*

## Acknowledgments

Foremost, I would like to express my deepest gratitude to my supervisor Professor Stephen Hanessian, for his excellent guidance, patience, encouragement, and continuous support throughout all my M.Sc. and Ph.D. studies. He is not only an advisor with immense knowledge and a great passion for chemistry, but also a mentor who always keeps inspiring and motivating me in my life. It is an honor for me to study and work with him.

Besides my supervisor, I would like to thank the other members of my thesis committee: Prof. William D. Lubell, and Prof. Alexis Vallée-Bélisle, for their thoughtful and useful comments, assistance and encouragement in my research. I would also like to thank Prof. Jean-Philip G. Lumb, who was willing to serve as my external reader despite his busy schedule.

I would like to express my great appreciation to the past and present members in Hanessian group. Thanks to Dr. Rebecca Fransson, M.Sc. Jérémie Tessier, Dr. Michael Perryman, for great collaboration in the project of synthesis of FTY720 based analogues. Thanks to Dr. Gilles Berger for the DFT computation studies in the project of catalytic synthesis of  $\beta$ -ketols. Thanks to Drs. Eli Stoffman, Thomas Jennequin, Oscar Mario Saavedra, Miguel Angel Vilchis-Reyes, Étienne Chenard, Stéphane Dorich, Eduardo Sanchez Larios, Amit Kumar Chattopadhyay and Shashidhar Jakkepally for their kind discussion in my chemistry. Thanks to Benoit Deschenes Simard and Robert Giacometti, for their great help in the X-ray analysis. Thanks to Jean-Philippe Cusson for his useful information for the format of thesis. Thanks to Juan Salinas Hernandez, LoRena Rico and Phoebe Yap for their collaboration in managing the group's database. Thanks to Drs. Eli Stoffman and Michael Perryman for proof reading my thesis. Also, thanks to Dr. Sylvain Petit for preparing the Résumé. I am so thankful to Mrs. Michele Ursula Ammouche for her numerous favours and invaluable assistance.

I would like to extend my sincerest appreciation to our collaborators: Prof. Aimee L. Edinger and her group members at the University of California, Irvine; Prof. Andrea Huwiler and her group members at the University of Bern. They have made great effort in the biological testing of analogues of FTY720, provided important advice, and helped us to find the best lead compound. Especially, thanks to Dr. Alison McCrackn and Dr. Saurabh Ghosh Roy in the Edinger group, who have always been patient and friendly to answer all my questions related to the biological results.

I would like to acknowledge the chemistry department of Université de Montréal, especially for the great support from the Nuclear Magnetic Resonance Laboratory (Dr. Minh Tan Phan-Viet, Dr. Cédric Malveau, Silvie Bilodeau and Antoine Hamel), the Mass Spectrometry Laboratory (Alexandra Furtos, Karine Venne, Marie-Christine Tang, Karine Gilbert, and Louiza Mahrouche), and the X-ray Diffraction Laboratory (Michel Simard, Francine Bélanger-Gariépy). I want to thank Ms. Céline Millette, Prof. André Beauchamp and Prof. Christian Reber for their kind help. Many thanks to the library staffs who were always very helpful. I also need to thank Drs. Jinqiang Zhang and Yesica Garcia Ramos in the Lubell group for their help in HPLC analysis and Carl Trudel in the Lebel group for the help in GC analysis.

I would also like to thank Faculté des Études Supérieures et Postdoctorales in Université de Montréal, for their kind financial support during my Ph.D studies and thesis writing.

Thank you to all my friends for making my life in Montréal a lot of fun. I am lucky to have you, and I will remember the good times we had.

Last but not least, I am very grateful to my parents for their unconditional love, understanding and support through my entire life. I thank my aunt for her encouragement, and my girlfriend Lifeng Gu, who was always supportive, being patient and capable of cheering me up.

# Chapter 1: Design and Synthesis of Constrained Azacyclic Pyrrolidine Analogues of FTY720 as Anticancer Agents

## 1-1 Introduction

### 1-1-1 Discovery of FTY720

Organ transplantation is one of the most challenging medical procedures. One of the major problems being transplant rejection due to immune response from the patient. During the 1970s and 1980s, the discovery and development of immunosuppressive drugs, such as rapamycin<sup>1,2</sup> (isolated from a soil sample collected from Rapa Nui) (Figure 1, **1.1**), cyclosporin A<sup>3-5</sup> (isolated from fungus *Trichoderma polysporum*) **1.2**, and FK506<sup>6,7</sup> (isolated from bacterium *Streptomyces tsukubaensis*) **1.3**, have enhanced greatly the survival rate of organ transplant recipients, and inspired efforts of many scientists to find new immunosuppressant drugs from fungi and other microorganisms, as well as to synthesize derivatives.

In 1994, Tetsuro Fujita and coworkers reported a potent immunosuppressive agent, (2*S*,3*R*,4*R*)-(E)-2-amino-3,4-dihydroxy-2-hydroxymethyl-14-oxoeicos-6-enoic acid, termed as ISP-I, which was isolated from the fermentation broth of the fungus *Isaria sinclairii* (ATCC 24400) (Figure 1, **1.4**).<sup>8</sup> The structure of ISP-I (**1.4**) was found to be identical to the known antifungal agents myriocin<sup>9</sup> (isolated from *Myriococcum albomyces*) and thermozymocidin<sup>10</sup> (isolated from *Mycelia sterilia*). Also, Fujita et al. found for the first time that ISP-I (**1.4**) had strong immunosuppressive activity, being 5-10 fold more potent than cyclosporin A (**1.2**), suppressing the proliferation of lymphocytes in mouse allogeneic mixed lymphocyte reaction (MLR) assays *in vitro*,<sup>8</sup> and prolonging rat skin graft survival time *in vivo* at 0.1 mg / kg compared to 1.0 mg / kg of cyclosporin A (**1.2**).<sup>11</sup> However, ISP-I (**1.4**) was not suitable for clinical application due to its toxicity and poor solubility.

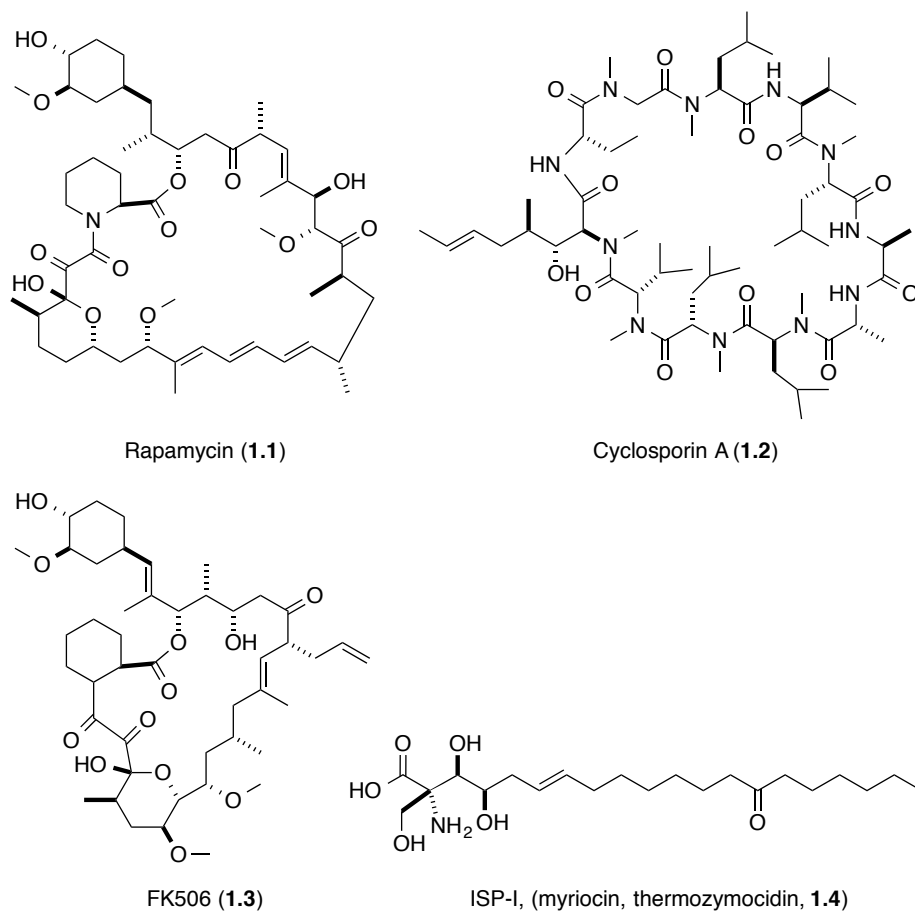


**Figure 1.** Structure of rapamycin (**1.1**), cyclosporin A (**1.2**), FK506 (**1.3**) and ISP-I (myriocin, thermozyiocidin, **1.4**).

Optimization of ISP-I (**1.4**) was carefully performed and guided by structure-activity relationship (SAR) studies to simplify the structure and improve the physicochemical and biological properties. The first important analogue, ISP-I-28 (Figure 2, **1.5**),<sup>11</sup> from the reduction of ISP-I (**1.4**), exhibited reduced toxicity (100 mg / kg compared to 1 mg / kg (ISP-I (**1.4**)) using *in vivo* rat skin graft assay),<sup>12</sup> and increased solubility compared to ISP-I (**1.4**).<sup>11,12</sup> ISP-I-28 prolonged rat skin graft survival time compared to cyclosporin A (**1.2**).<sup>11,12</sup> In the MLR assay, the activity of ISP-I-28 was however dramatically diminished (IC<sub>50</sub> : ISP-I-28 (**1.5**) 1630 nM compared to ISP-I (**1.4**) 3 ~ 8 nM).<sup>12,13</sup>

Further modification of ISP-I-28 (**1.5**) led to a more simplified achiral compound ISP-I-36 (Figure 2, **1.6**) by removing the three secondary alcohols.<sup>14</sup> This analogue showed good immunosuppressive activity in the MLR assay ( $IC_{50}$ : 12 nM)<sup>11</sup> and was more effective in prolonging rat skin graft survival time compared to ISP-I-28 (**1.5**).<sup>11</sup> Modification of the 18-carbon aliphatic side-chain to a shorter 14-carbon alkyl chain generated analogue ISP-I-55 (Figure 2, **1.7**),<sup>11,14</sup> which further improved the activities *in vitro* and *in vivo* compared to ISP-I-36 (**1.6**).<sup>11,14</sup> At this stage, it was clear that the 2-amino-propane-1,3-diol hydrophilic head was crucial to maintain the activity, however, the lipophilic tail chain could be further optimized.

Further optimization led to FTY720 (Figure 2, **1.8**),<sup>15,16</sup> which was obtained by introducing a phenyl moiety into the side-chain with the intention to restrict the conformation of the hydrophobic alkyl appendage. This modification facilitated to analytical detection compared to non-aromatic analogues in biological testing and future clinical studies. FTY720 (**1.8**) was active *in vitro* ( $IC_{50}$ : 6.1 nM in (MLR) assay),<sup>15</sup> and prolonged significantly survival time in the rat skin allograft assay *in vivo*.<sup>15,17</sup> It was also more favorable in terms of toxicology (less toxic) and physical properties (better solubility) compared to ISP-1 (**1.4**).<sup>15,17</sup> It should be noted that the activity was dependent on the position of the phenyl ring. Analogues bearing a phenyl group at other positions of the side-chain were less active than FTY720 (**1.8**).<sup>15,17</sup>



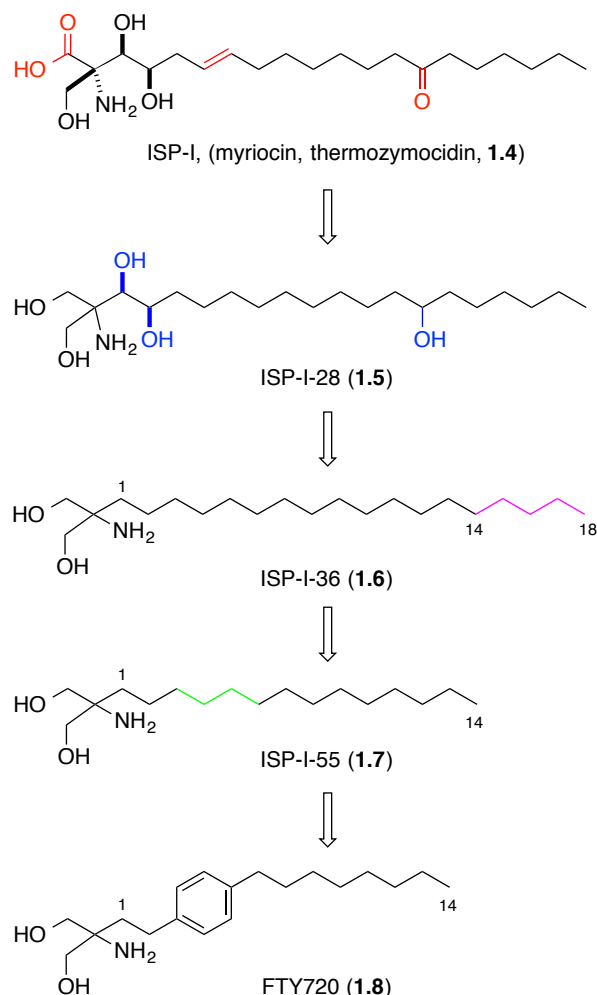


**Figure 2.** Optimization of ISP-I (**1.4**) to FTY720 (**1.8**)

## 1-1-2 FTY720 in immunosuppression

### 1-1-2-1 Mechanism of FTY720 in immunosuppression

During the discovery of FTY720 (**1.8**), the immunosuppressive ability of analogues was always evaluated by the MLR assay *in vitro* and the rat skin allograft assay *in vivo*, which were later found to be a crucial and fortunate choices that enabled the development of FTY720 as a drug. The serine palmitoyl-transferase (SPT) inhibition assay is used commonly for measuring the activity of immunosuppressants *in vitro* based on inhibition of serine palmitoyltransferase, which is an enzyme participating in the first step of sphingosine and sphingolipid biosynthesis. The lead compound ISP-I (**1.4**) had activity in the MLR assay<sup>8</sup> and

was also reported to inhibit SPT in 1995.<sup>18</sup> However, the analogues FTY720 (**1.8**) and ISI-55 (**1.7**) were found to only be active in the MLR assay, and not in the SPT assay.<sup>12,17</sup> This indicates that the mechanism of immunosuppression has changed at some stage of the structural modification, and there is another mechanism responsible for the activity of FTY720 (**1.8**). Thus, it is fortunate that all the analogues were screened by MLR assay; otherwise, FTY720 (**1.8**) may not have been discovered.

Since the discovery of FTY720 (**1.8**), efforts have been made to elucidate its mechanism of action. In 1996, Chiba, Fujita and coworkers noticed initially that FTY720 (**1.8**) induced a remarkable decrease of the number of peripheral blood lymphocytes (PBL), especially T cells, at doses that prolong allograft survival.<sup>19,20</sup> At first, they hypothesized that the decrease of PBL was caused by the apoptosis of lymphocytes induced by FTY720 (**1.8**).<sup>21</sup> After realizing the blood concentration of FTY720 (**1.8**) was too low to induce the cell death of PBL, they focused on the lymphocyte recirculation.<sup>22</sup> Lymphocytes are mobile and continuously travel in the body from the blood to the secondary lymphoid organs (spleen, lymph node), and return to the blood to complete circulation and maintain the immune system. Thus, the number of PBL could decrease without apoptosis of lymphocytes if FTY720 (**1.8**) modulated lymphocyte homing. This hypothesis was proven by an experiment in which single oral administration of FTY720 (**1.8**), at 0.1 to 1 mg/ kg, to rats caused the number of PBL to decrease significantly, while the number of lymphocytes in the lymph nodes was markedly increased.<sup>22</sup> Further experiments<sup>23-26</sup> illustrated a more acceptable mechanism for the immunosuppressive ability of FTY720 (**1.8**) involving induction of the sequestration of mature lymphocytes into the secondary lymphoid organs, resulting in a decrease in the number of lymphocytes circulating in the blood, and reduced autoimmune response to the grafted organs and inflamed tissues. The function of lymphocytes (including the activation and proliferation of T cells) was not impaired in this process, making FTY720 (**1.8**) potentially more advantageous and promising as an immunosuppressant compared to other immunosuppressive drugs that act *via* inhibition of mTOR (*e.g.*, rapamycin (**1.1**)<sup>2</sup>) and calcineurin (*e.g.*, cyclosporin A (**1.2**)<sup>27,28</sup>, FK506 (**1.3**)<sup>27,29</sup>), blocking the activation of T cells.

Although FTY720 (**1.8**) could induce redistribution of lymphocytes, the mechanism of action of FTY720 (**1.8**) was still not clear. Lymphocyte trafficking regulates lymphocyte recirculation *via* the lymphocyte-homing receptor. However, the lymphocyte-homing receptor was not required for FTY720 (**1.8**) to redistribute the recirculation of lymphocytes,<sup>30</sup> and its real target of was unclear. Researchers observed and surmised that FTY720 (**1.8**) targets possibly G-protein-coupled receptors (GPCRs).<sup>26, 31</sup> Based on this hypothesis, and the structural similarity of FTY720 (**1.8**) with sphingosine (Scheme 1), two groups<sup>32,33</sup> discovered independently that FTY720 (**1.8**) targeted sphingosine 1-phosphate receptors.

Sphingosine (2-amino-4-octadecene-1,3-diol) is the backbone of sphingolipids. Sphingolipids and their metabolites [*e.g.*, ceramide, sphingosine and sphingosine-1-phosphate (S1P) (Scheme 1)] are important signaling lipid molecules participating in a variety of cellular processes. In the sphingolipid metabolism (Scheme 1), sphingosine is generated from the *N*-deacylation of ceramide by ceramidase. Whereas ceramide can be formed thorough either degradation of sphingomyelin or *de novo* biosynthesis starting from palmitoyl-CoA and L-serine, sphingosine can be phosphorylated *in vivo via* sphingosine kinases (SphK1, 2) to give sphingosine-1-phosphate (S1P),<sup>34,35</sup> which functions as an activator for five different cell surface GPCRs, termed as S1P<sub>1-5</sub>. These receptors are ubiquitously expressed and regulate diverse biological processes.<sup>35,36</sup> S1P<sub>1-3</sub> are widely expressed in heart, lung, brain, spleen, liver, thymus, kidney, adipose and other tissues.<sup>37,38</sup> Specifically, S1P<sub>1</sub> is essential for lymphocyte trafficking. It regulates lymphocyte egress from both the thymus and peripheral lymphoid organs;<sup>39,40</sup> S1P<sub>3</sub> is also expressed in the heart and help regulate heart rate.<sup>39</sup> Expressing of S1P<sub>4-5</sub> is relatively restricted to the immune and nervous systems.<sup>38,41</sup>

As per the mechanism discovered in 2002,<sup>32,33</sup> FTY720 (**1.8**) is structurally close to sphingosine, and can be phosphorylated by sphingosine kinases (primarily by SphK2)<sup>42</sup> *in vivo* to form (*S*)-FTY720 phosphate<sup>43</sup> (Scheme 1). This phosphate is the biologically active molecule, rather than FTY720 (**1.8**), and acts as an agonist towards four of five S1P receptors (S1P<sub>1, 3, 4, 5</sub>) with high affinity (Table 1).<sup>32,33</sup>

**Scheme 1.** FTY720 (**1.8**) and sphingolipid metabolism.

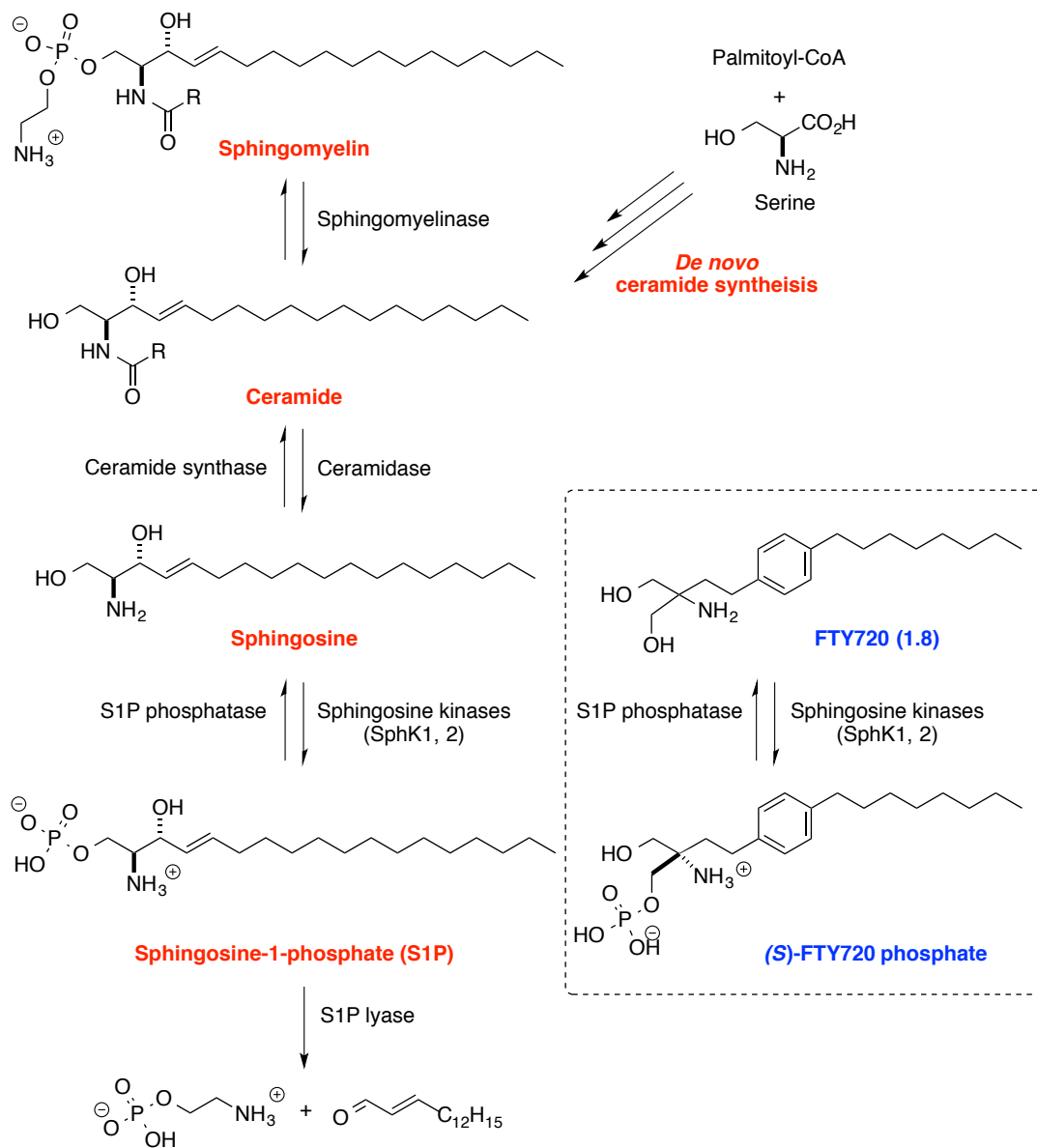


**Table 1.** Binding affinities (nM) to S1P receptors.<sup>32</sup>

	S1P <sub>1</sub>	S1P <sub>2</sub>	S1P <sub>3</sub>	S1P <sub>4</sub>	S1P <sub>5</sub>
S1P	0.47 ± 0.34	0.31 ± 0.02	0.17 ± 0.05	95 ± 25	0.61 ± 0.39
(S)-FTY720-P	0.21 ± 0.17	> 10000	5.0 ± 2.7	5.9 ± 2.3	0.59 ± 0.27
FTY720	300 ± 51	> 10000	> 10000	> 5000	2623 ± 317

IC<sub>50</sub> measurements determined by competition of S1P binding to membranes prepared from stably transfected CHO cells expressing the indicated S1P receptor.<sup>30</sup>

Further studies<sup>44-48</sup> suggest that (S)-FTY720 phosphate serves as both an agonist, and operates as a functional antagonist. Internalization, followed by degradation of S1P<sub>1</sub> on lymphocytes, results in the inhibition of S1P-S1P<sub>1</sub> signaling-dependent lymphocyte's egress from the thymus and secondary lymphoid organs (Figure 3). S1P, on the other hand, internalizes with S1P<sub>1</sub>, followed by recycling of the receptor without degradation.<sup>49</sup> This mechanism explains the previously reported observation that FTY720 (**1.8**) induced a decrease in the number of lymphocytes in the blood, while increasing their numbers in the lymph nodes.<sup>22</sup> Expression of S1P<sub>1</sub> on the surface of lymphocytes is dependent on the concentration of S1P, which is stringently regulated *in vivo*. S1P is abundant in blood and lymph. In the secondary lymphoid tissues, S1P is found in low concentrations due to regulation by S1P-degradating enzyme (S1P lyase). Therefore, the concentration gradient of S1P causes S1P<sub>1</sub> expression in lymphocytes to be down-regulated in blood but up-regulated in secondary lymphoid tissues. Lymphocyte egress from the secondary lymphoid organs is suggested to be mediated by S1P gradients, which are regulated by S1P lyase.<sup>50-52</sup> Therefore, targeting this enzyme may lead to new immunosuppressive agents.<sup>51,52</sup>

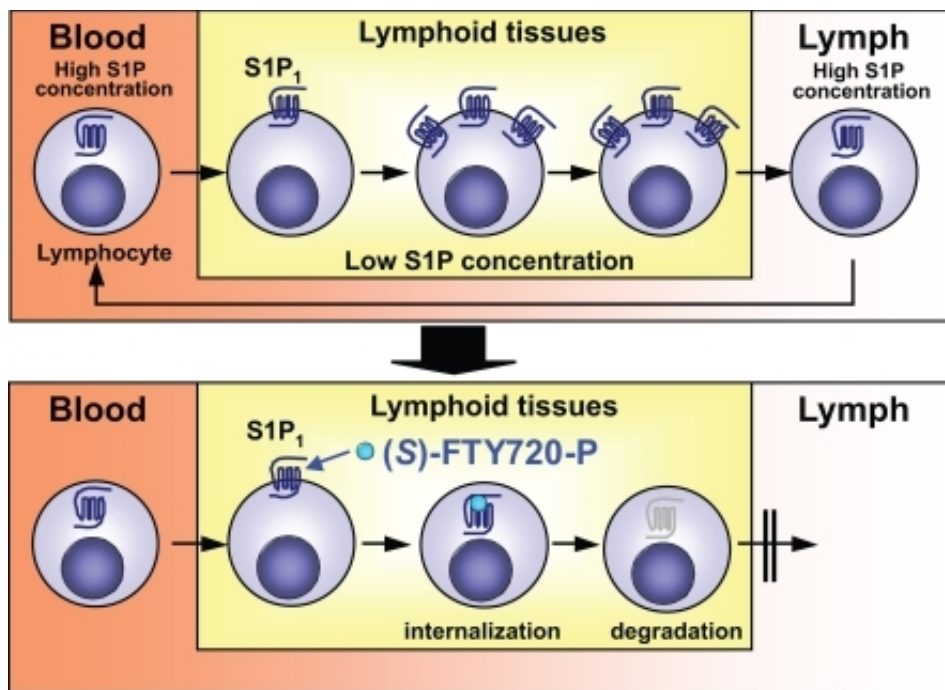


Diagram from Kunitomo Adachi et al.<sup>16a</sup>

**Figure 3.** (S)-FTY720 phosphate inhibits S1P/S1P<sub>1</sub>-dependent lymphocyte egress from lymphoid tissues by long-term internalization and degradation of S1P<sub>1</sub>.

Based on all the accumulated evidence, the generally recognized immunosuppressive mechanism is that FTY720 (**1.8**) is first phosphorylated by SphK2 *in vivo* to yield (S)-FTY720 phosphate. Then this phosphate mimics S1P, and activates the S1P<sub>1</sub> receptor on lymphocytes, which is followed by long-term internalization and degradation of the S1P<sub>1</sub> receptors, which resulting in a temporary state without S1P<sub>1</sub> at the surface of lymphocyte. These lymphocytes cells are then unable to sense the S1P gradient between lymphoid tissues and blood or lymph, which ultimately prevents lymphocytes from egressing out of the secondary lymphoid organs (Figure 3).

### 1-1-2-2 FTY720 in the treatment of multiple sclerosis (MS)

Since its discovery, FTY720 (**1.8**) has shown good immunosuppressive ability and potential to be used in organ transplantation. Early preclinical studies demonstrated that FTY720 (**1.8**), (daily dose from 0.1 ~ 10 mg / kg) prolonged remarkably skin and cardiac

allograft survival, as well as and host survival in rats.<sup>19,20,53,54</sup> A synergistic effect was obtained in combination therapy of FTY720 (**1.8**) with subtherapeutic doses of cyclosporin A (**1.2**) or FK506 (**1.3**) on canine renal allograft, as well as rat skin and cardiac allografts.<sup>21,23,24,54-57</sup> In experimental autoimmune encephalomyelitis (EAE), an animal model of human MS, FTY720 (**1.8**) was also highly advantageous (in the doses of 0.1 ~ 0.3 mg/Kg per day) for suppressing the development of EAE.<sup>31,58</sup> Being promising in animal models of organ transplantation, FTY720 (**1.8**) was advanced to clinical studies. In the phase I clinical trials for renal transplantation, FTY720 (**1.8**) showed a good safety profile (no serious side effects except for transient asymptomatic bradycardia when given at high doses to patient).<sup>59,60</sup> However, in phase II and III trials in *de novo* renal transplantation, combination therapy using FTY720 (**1.8**) and Neoral™ (cyclosporine A (**1.2**) microemulsion, Novartis) failed to show a clear advantage compared to the existing standard therapy (mycophenolate mofetil (MMF) and Neoral) for preventing acute allograft rejection in terms of efficacy, or adverse effects (bradycardia and other unexpected side effects including impairment of renal function and macula oedema).<sup>61-64</sup> After discontinuation of FTY720 (**1.8**) in trials in renal transplantation, the potential of FTY720 (**1.8**) was explored in the treatment of MS.

Multiple sclerosis (MS) is a chronic autoimmune disease of the central nervous system (CNS, including brain and spinal cord). First reported in 1868,<sup>65</sup> there were about 2.5 million MS patients all over the world in 2008.<sup>66</sup> MS is unpredictable, and its causes are still not clear. Most people are first affected by MS when they are 20 ~ 40 years old (women twice as often as men).<sup>67</sup> Studies show that MS is an inflammatory disease caused by myelin being attacked by the immune system. Myelin covers and protects nerves of the brain and spinal cord. Frequent demyelination and remyelination lead to scarring of axons, which leads to electrical signals being unable to conduct effectively.<sup>67,68</sup> Generally, there are four types of MS depending on the pattern of disease: relapsing-remitting MS (RR-MS), secondary progressive MS (SP-MS), primary progressive MS (PP-MS) and progressive relapsing MS (PR-MS).<sup>69</sup> It is noteworthy that 85% of patients have RR-MS.<sup>70</sup>

Although MS usually progresses slowly, to date there is no cure. Current therapies are focused on suppressing and slowing down the development of MS by reducing relapses and managing symptoms at the same time. Disease modifying therapies (DMTs) are the most common therapies used in the treatment of MS. Before 2010, the classic immunomodulator drugs for DMTs were interferon- $\beta$  (IFN- $\beta$ ) products (Avonex<sup>®</sup>, Betaseron<sup>®</sup>, Extavia<sup>®</sup> and Rebif<sup>®</sup>), glatiramer acetate (Copaxone<sup>®</sup>) and natalizumab (Tysabri<sup>®</sup>). These medications need to be administered by injection or intravenous (iv) infusion. They are limited due to their modest efficacy and side-effects. The discovery and development of more effective therapies for MS remains an important topic in drug discovery. In 2010, FTY720 (Gilenya<sup>™</sup>) (**1.8**) was approved by the Food and Drug Administration (FDA) as the first oral drug for treating MS. Then in 2014, two new oral drugs, Teriflunomide (Aubagio<sup>®</sup>) and dimethyl fumarate (Tecfidera<sup>™</sup>) were approved, as well as Alemtuzumab (Lemtrada<sup>™</sup>), which is given by iv infusion.

FTY720 (**1.8**) has significantly improved the efficacy in reducing relapse rate compared to a common therapy, IFN- $\beta$ -1a (Avonex<sup>®</sup>), in phase III clinic trials.<sup>71</sup> Mechanistic studies have demonstrated that, as an immunomodulator, FTY720 (Gilenya<sup>™</sup>) (**1.8**) works through sequestering lymphocytes in lymph tissues; therefore, there are less immune cells to infiltrate and attack the CNS causing autoimmune responses, and the resulting relapses are reduced.<sup>72</sup> The immune system of the patient is not affected by the administration of FTY720 (**1.8**), and can still respond to other infections, because FTY720 (**1.8**) does not impair the function of lymphocytes,<sup>73</sup> Besides effects on the immune system through phosphorylation, FTY720 (**1.8**) can also cross the blood–brain barrier (BBB),<sup>74</sup> and directly act on the CNS, which may contribute to its efficacy in the treatment of MS.<sup>73,75</sup>

Although FTY720 (Gilenya<sup>™</sup>) (**1.8**) has been approved for the treatment of MS, it can induce bradycardia,<sup>71,76</sup> a potentially fatal side-effect. Thus, it is advised that the first administration should be conducted and monitored in a hospital. Bradycardia, the decreasing of heart rate, is probably caused by FTY720-phosphate activating S1P<sub>3</sub> receptors which regulate heart rate.<sup>39</sup> However, recent studies have suggested that bradycardia is mediated by S1P<sub>1</sub>,<sup>77</sup> and may not be avoided, because S1P<sub>1</sub> is targeted by FTY720 (**1.8**). Safety and



tolerability studies in clinical trials have deemed FTY720 (**1.8**) safe and promising as therapy for MS.<sup>71,76</sup>

### 1-1-3 FTY720 in cancer therapy

FTY720 (**1.8**) is not only an immunomodulator, but also an efficient antitumor agent.<sup>78</sup> FTY720 (**1.8**) has been evaluated in multiple cancer cell lines *in vitro* and *in vivo*. For example, it acts against human glioma cell line T98G with an ED<sub>50</sub> of 1~10 µg/mL,<sup>79</sup> and markedly suppressed the proliferation of two glioblastoma cancel cell lines (U251MG and U87MG) at concentrations above 7 µM.<sup>80</sup> In breast cancer studies, it killed 80% of mouse breast cancer JygMC(A) cells *in vitro* at 10 µM after 12 h and significantly inhibited tumor growth *in vivo* at 5 mg/kg per day or higher doses without any notable adverse effects.<sup>81</sup> In test with three human breast cancer cell lines (MCF-7, MDA-MB-231 and Sk-Br-3), it also showed good antitumor activity with IC<sub>50</sub> 5~7 µM.<sup>82</sup> For human colon cancer cell lines (HCT-116 and SW620), it also maintained activity with IC<sub>50</sub> 5~7 µM.<sup>82</sup> FTY720 (**1.8**) has been evaluated against prostatic cancer shortly after it was discovered. In 1999, researchers found it induced rapid death of a human prostatic carcinoma cell line DU145 *in vitro* at concentrations of 20 µM or more.<sup>83</sup> The following *in vitro* studies with another human prostate cancer cell line (PC3), as well as DU145, indicated FTY720 (**1.8**) exhibited very strong anticancer ability (IC<sub>50</sub>: 1.48, 1.50 µM respectively),<sup>84</sup> and suppressed the growth of human prostate cancer LNCaP-AI cells.<sup>85</sup> In *in vivo* studies with nude mice xenografted with human prostate cancer cells CWR22R, the growth of tumor was significantly inhibited by treatment with FTY720 (**1.8**) at 10 mg/kg/day for 20 days, without notable side effects.<sup>86</sup> FTY720 (**1.8**) exhibits the potential to treat various forms of leukemia, such as acute lymphoblastic leukemia (ALL),<sup>87,88</sup> chronic lymphocytic leukemia (CLL)<sup>87</sup> and chronic myelogenous leukemia (CML).<sup>89</sup> It inhibits the proliferation of B-cell lines *in vitro*, including two ALL cell lines (697, RS4;11) and CLL B cells from CLL patients, MEC-1 CLL cells, and Burkitt lymphoma cell lines (Raji, Ramos).<sup>87</sup> In *in vivo* tests of FTY720 (**1.8**) using xenografted mice, a model of disseminated B-cell lymphoma/leukemia, it was found that the survival time of the mice was markedly prolonged.<sup>87</sup> Further studies in ALL indicated FTY720 (**1.8**) induced apoptosis in both Philadelphia positive (Ph<sup>+</sup>) and native (Ph<sup>-</sup>) cell lines.<sup>88</sup> For other blood cancers, FTY720 (**1.8**) also showed potential in the treatment of multiple myeloma,<sup>90</sup> lymphoblastic lymphoma<sup>87</sup> and

mantle cell lymphoma.<sup>91</sup> In addition to the cancers mentioned above, many studies have demonstrated that FTY720 (**1.8**) also has antitumor activity in lung cancer,<sup>92-95</sup> liver cancer,<sup>96,97</sup> ovarian cancer,<sup>98,99</sup> bladder cancer,<sup>100</sup> renal cancer<sup>101</sup> and other cancers.<sup>78</sup>

Since FTY720 (**1.8**) acts against a variety of cancers, the anticancer mechanisms involved are varied and complicated. It has been noted that FTY720-phosphate, which is essential for the immunosuppressive effect, did not inhibit the proliferation of breast cancer cells (MCF-7, MDA-MB-231, Sk-Br-3) or colon cancer cell lines (HCT-116, SW620).<sup>82</sup> In contrast, FTY720-phosphate induced a slight growth of MCF-7 cells at low concentration,<sup>82</sup> thus indicating that phosphorylation of FTY720 (**1.8**) is not responsible for the anticancer activity. Further studies, in 2010, found that both FTY720 (**1.8**) and one of its analogues, (*S*)-FTY720 vinylphosphonate induced apoptosis of MCF-7 and LNCaP-AI cancer cells due to inhibition followed by degradation of SphK1.<sup>102,103</sup> As discussed previously (Scheme 1), there are two types of sphingosine kinases (SphKs). FTY720 (**1.8**) is phosphorylated most by SphK2 to yield immunosuppressant FTY720-phosphate, while SphK1 is already highly recognized in association with various cancers, and it participates in the multiplication, migration and impairment of apoptosis in cancer cells.<sup>78,104</sup> Thus, FTY720 (**1.8**), as a SphK1 inhibitor, disturbs S1P/S1P receptor mediated signaling to induce the apoptosis of cancer cells.<sup>78</sup> Higher concentrations of FTY720 (**1.8**), and the related S1P receptor expression in tissues, may cause the former to act as an antitumor agent rather than as an immunomodulator.<sup>78</sup> In addition to SphK1, many other targets have been proposed, such as B-cell lymphoma 2 (Bcl-2), reactive oxygen species (ROS), protein phosphatase 2A (PP2A), extracellular-signal-regulated kinases (ERKs), c-Jun *N*-terminal kinases (JNKs), PI3K/AKT/mTOR signaling pathway, phosphatase and tensin homolog (PTEN), Cyclin D1 and 14-3-3 proteins.<sup>78</sup> By activating these molecular targets, FTY720 (**1.8**) induces apoptosis and cancer cell death.<sup>78</sup>

Besides apoptosis of cancer cells through a caspase-dependent pathway or caspase-independent cell death, autophagy was also found to contribute to the anticancer activity of FTY720 (**1.8**).<sup>78</sup> Autophagy is a term for cell self-degradation through lysosomes to remove unnecessary cytoplasmic components.<sup>105</sup> It's a survival process for cells to balance the energy

levels when they are under nutrient stress.<sup>105</sup> However, autophagy could also lead to cell death under excessive activation.<sup>106</sup> Autophagy has been reported to be induced by FTY720 (**1.8**) in cancer cells, such as ALL cell lines,<sup>88</sup> ovarian cancer cells,<sup>98,99</sup> and multiple myeloma U266 cell lines.<sup>107</sup> Cancer cell survival may be dependant on the type of cell. For example, FTY720 (**1.8**)-induced autophagy promoted the apoptosis of the multiple myeloma U266 cell line.<sup>107</sup> In ALL,<sup>88</sup> and ovarian cancer cells,<sup>98,99</sup> inhibition of induced autophagy protected cells from death resulting enhanced anticancer activity.<sup>98,99</sup> In addition, Edinger<sup>108</sup> reported that FTY720 (**1.8**) induced cell starvation in the presence of abundant nutrients by down regulating nutrient transporter proteins, which resulted in autophagy for self-protection. Cancer cells starved to death but normal cells can adapt to the nutrient stress and survive.<sup>108</sup> Meanwhile, this bioenergetic stress led to apoptosis even if it's found to be not necessary, because the nutrient stress was severe enough to kill cancer cells when apoptosis was block. Thus, FTY720 (**1.8**) can effectively and selectively starve cancer cells to death.<sup>108</sup> FTY720 (**1.8**) induced autophagy, and induced blockage of autophagy to enhance the anticancer efficacy of milatuzumab in mantle cell lymphoma.<sup>109,110</sup> Therefore, the autophagy and apoptosis induced by FTY720 (**1.8**) involved in its antitumor mechanisms are complicated. Although many targets and mechanisms have been proposed, the anticancer effects of FTY720 (**1.8**) remain unclear.

Bradycardia is a known side-effect of FTY720 (**1.8**) when used to treat MS, so the recommended dose is only 0.5 mg per day. Although FTY720 has anticancer activity against various cancers, the required dose for *in vivo* studies on mice generally are 5~10 mg per day,<sup>81,86</sup> which are much higher than those needed for immunosuppressive treatment. Even if no notable side effects were observed in mice at such high does,<sup>81, 86</sup> the increased chance of triggering bradycardia, and other potential adverse effects, limited the use of FTY720 (**1.8**) in human cancer treatment. Therefore, finding the right FTY720 (**1.8**) analogues lacking dose-limiting toxicity, but maintaining good anticancer proprieties, has attracted the attention of many scientists and has already shown promise in the discovery of new anticancer drugs. For example, AAL-149,<sup>33,111</sup> an analogue of FTY720 (**1.8**) tested by Edinger,<sup>108</sup> killed human ALL Sup-B15 cells by down-regulating nutrient transporter proteins, but does not induce bradycardia due to its inability to be phosphorylated and activate S1P receptors.

## 1-1-4 Constrained analogues of FTY720 in S1P receptors studies

As a prodrug, FTY720 (**1.8**) can be phosphorylated to generate FTY720-phosphate, which binds non-selectively to four of the five S1P receptors.<sup>32,33</sup> In general, in order to bind to a receptor, a ligand needs to change its conformation to adapt itself to a certain shape (bioactive conformation), which can fit the binding pocket of the receptor to be recognized. FTY720 (**1.8**) bears a lipophilic long alkyl chain and a hydrophilic amino-diol, which are linked by a phenylene group in a 1,4-configuration. This structure affords a high level of flexibility, even for the phosphorylated product, FTY720-phosphate. Thus, to understand how the conformations of FTY720 (**1.8**) affect these receptors, and further develop new FTY720 (**1.8**) analogues that can selectively target S1P receptors, constrained analogues were of particular interest. For instance, MacDonald and coworkers reported a series of constrained analogues based on modification of the polar moiety of FTY720 (**1.8**) (Figure 4), including bond 1-constrained analogues **1.9a-d**,<sup>112</sup> bond 2-constrained analogue **1.10**,<sup>112</sup> bond 3-constrained analogue **1.11**,<sup>112</sup> bond 1,2-constrained analogues **1.12a**,<sup>112</sup> **1.12b**,<sup>113</sup> **1.12c** and **1.12d**,<sup>114</sup> bond 2,3-constrained analogue **1.13**<sup>112,115</sup> and variety of heterocyclic analogues (**1.14a**,<sup>116</sup> **1.14b**<sup>117,118</sup>). It became clear that the constrained chemical space had a great influence on the biological activity. For example, **1.9b** and **1.9c** can be phosphorylated by SphK *in vivo*, while **1.10**, **1.11** and **1.12a** cannot be phosphorylated.<sup>112</sup> The phosphate of **1.9b** is an agonist for S1P<sub>1,3</sub> receptors,<sup>112</sup> but **1.12b**-phosphate is a selective S1P<sub>1,3</sub> antagonist.<sup>113</sup> The phosphates of **1.12c** and **1.12d** are S1P<sub>1</sub> agonists, but **1.12c**-phosphate is an antagonist of S1P<sub>3</sub> receptors. The indane-based analog **1.13a** cannot be phosphorylated, but the tetralin-based analog **1.13b** is phosphorylated by SphK2 and is a potent agonist for S1P<sub>1</sub>.<sup>112,115</sup> Phenylimidazole-based analogue **1.14a** is a selective S1P<sub>4</sub> agonist,<sup>116</sup> while the oxazole and oxadiazole heterocyclic compounds (*e.g.*, **1.14b-f**) are good substrates for SphK, and their phosphates have better S1P<sub>1</sub> / S1P<sub>3</sub> selectivity compared to FTY720-phosphate.<sup>117,118</sup> By evaluating these analogues, potential S1P ligands were discovered, and the structural requirements of the S1P receptors were better understood.

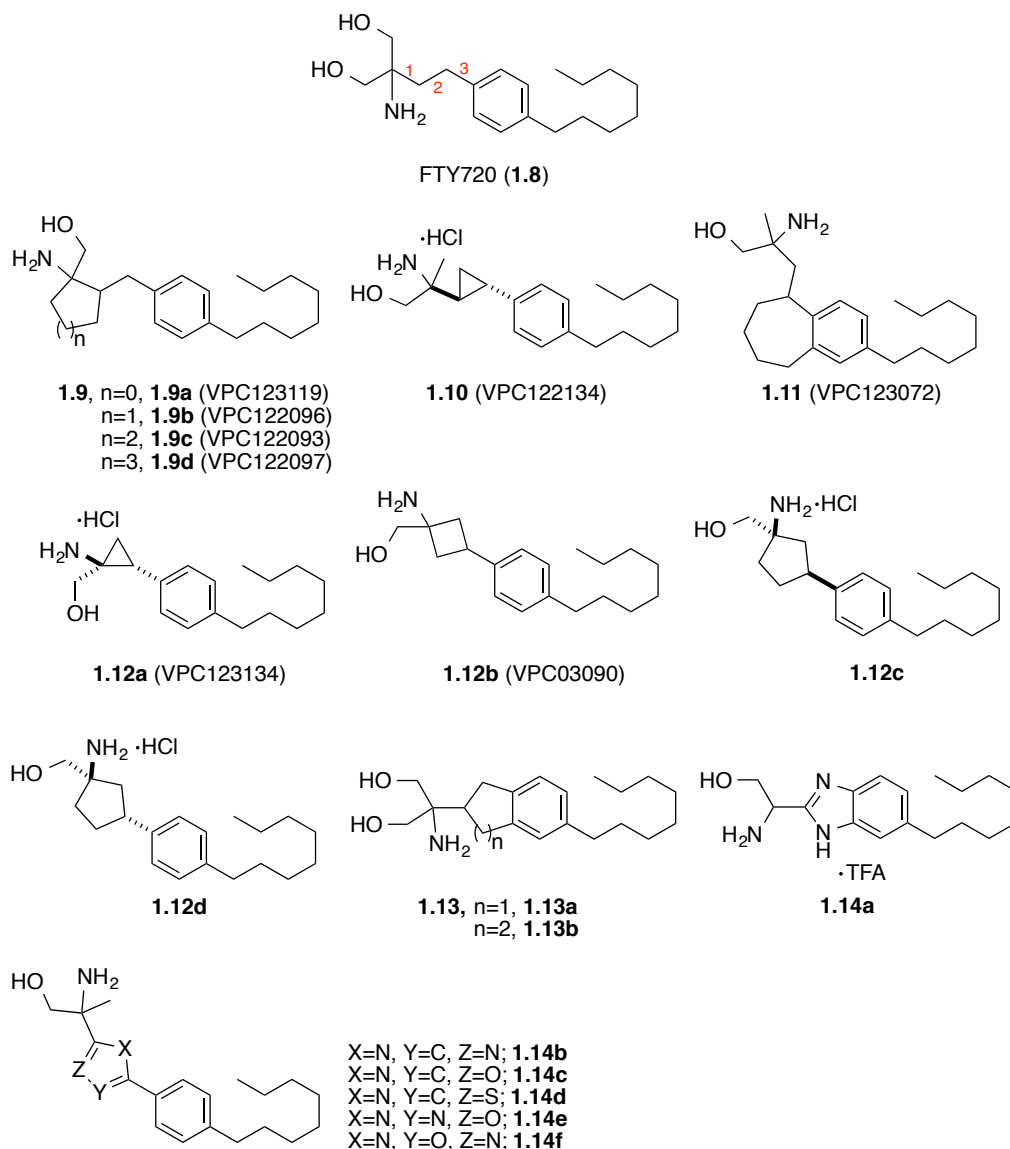


**Figure 4.** Examples of constrained analogues reported by Macdonald.<sup>112-113114115116117118</sup>

Our group has a long-standing interest in the design and synthesis of constrained analogues of FTY720 (**1.8**). In 2007, two enantiomeric 2,3,5-trisubstituted pyrrolidines (**1.15**, **1.16**), were made as constrained azacyclic analogues.<sup>119</sup> The corresponding phosphates (**1.17**, **1.18**, **1.19**, **1.20**) were also synthesized (Figure 5).<sup>119</sup> Starting from  $\alpha,\beta$ -unsaturated lactam **1.21**, cuprate 1,4-addition generated the aryl bromide **1.22** with good diastereomeric selectivity. The alkyl chain was then incorporated by a Suzuki coupling reaction followed by hydrogenation, to yield intermediate **1.23**. Reduction of the lactam with Super-hydride,

followed by trapping as the *O*-methyl aminal, and titanium-catalyzed allylation, afforded tetra substituted pyrrolidine **1.24** as the only diastereomer. With **1.24** in hand, the terminal olefin was isomerized to the 1,2-disubstituted alkene, which was then cleaved by ozonolysis and the aldehyde was reduced with sodium borohydride to obtain the alcohol **1.25**. Finally, deprotection with TBAF, followed by treatment with HCl, led to the constrained analogue **1.15**. The same protocol was used to prepare the enantiomeric analogue **1.16**.<sup>119</sup>

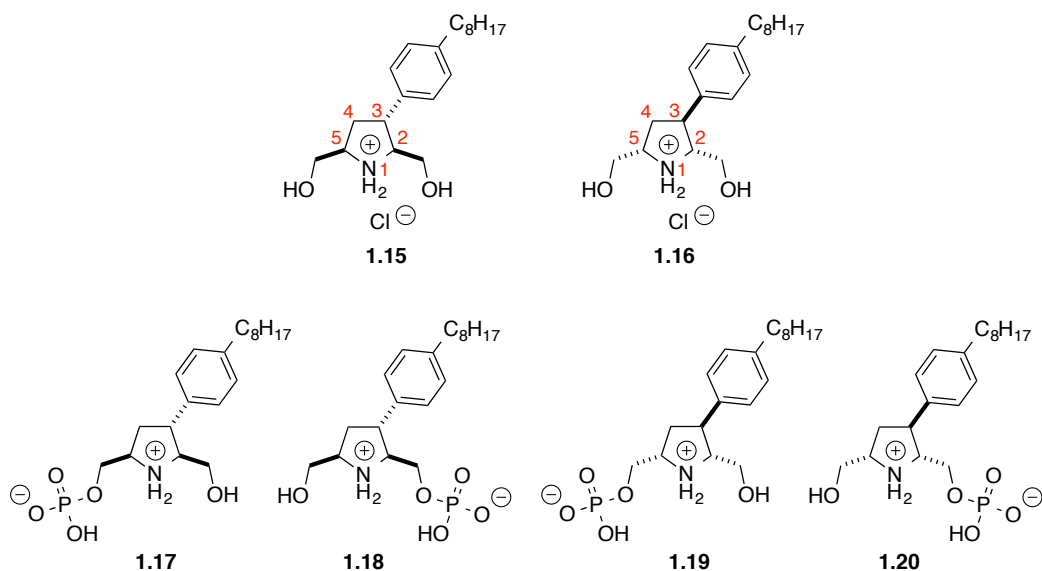
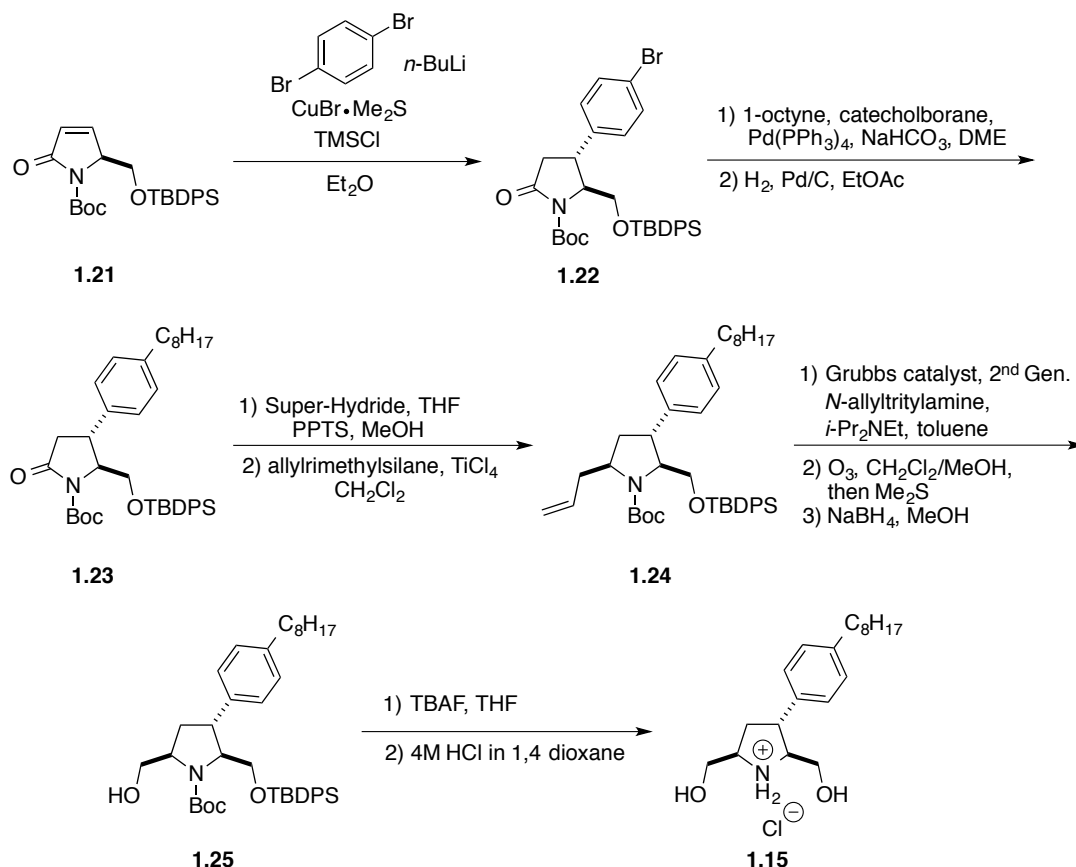


**Figure 5.** Constrained 2,3,5-trisubstituted pyrrolidine analogues.

**Scheme 2.** Synthesis of constrained 2,3,5-trisubstituted pyrrolidine analogue **1.15**.



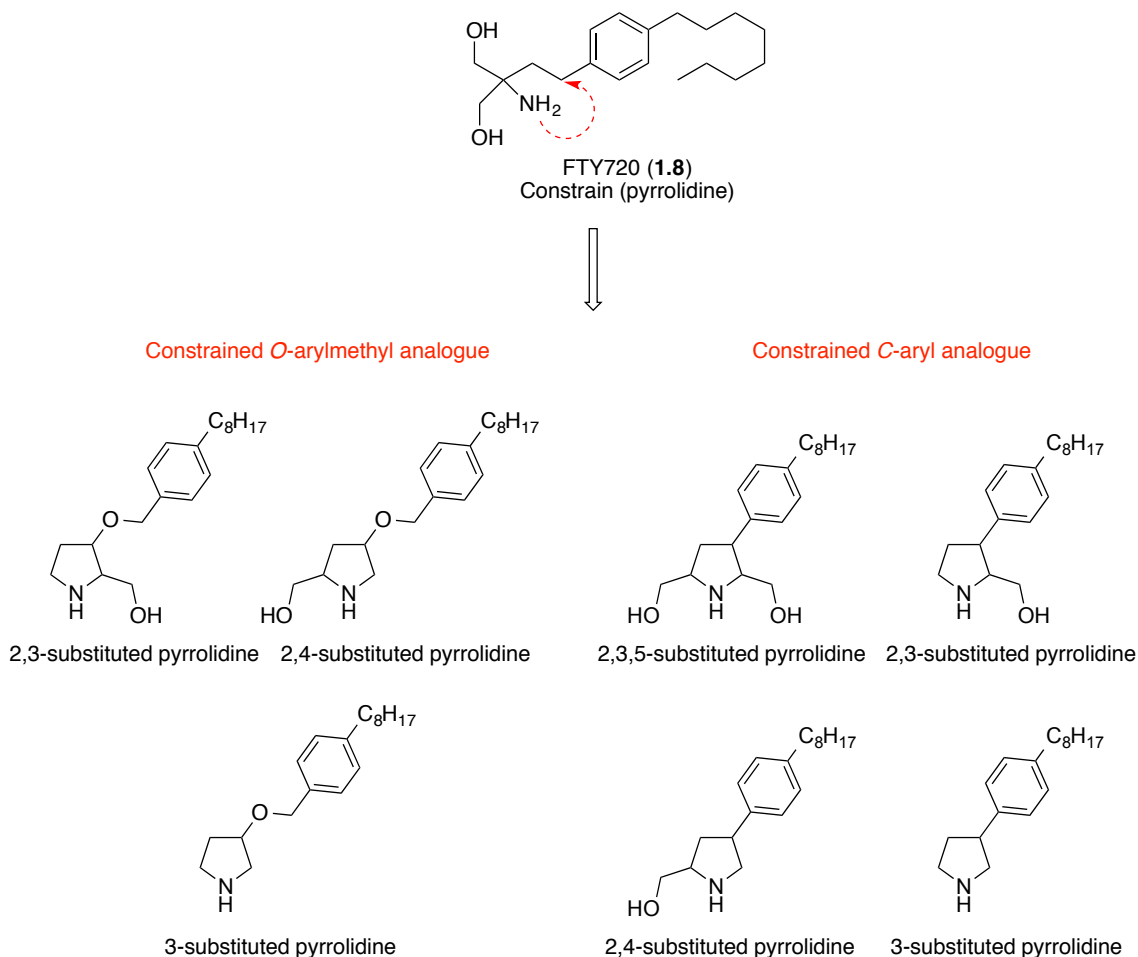
The biological activities of enantiomers **1.15** and **1.16** are quite different. Analogue **1.15** was rapidly phosphorylated by SphK2 *in vitro*, being 4 times faster than the phosphorylation of FTY720 (**1.8**), but **1.16** was not a substrate for SphK.<sup>119</sup> Further evaluation in calcium release assays demonstrated significant selective affinities for S1P<sub>4</sub> and S1P<sub>5</sub> receptors, over S1P<sub>1</sub> and S1P<sub>3</sub> receptors for all of the four chemically synthesized phosphates (**1.17**, **1.18**, **1.19**, **1.20**) compared to FTY720-phosphate and S1P. Among these phosphates, **1.17** and **1.18** were the most efficient agonists for S1P<sub>4</sub> and S1P<sub>5</sub>, and were generated enzymatically from **1.15**.<sup>119</sup> Thus, constraining the conformation of FTY720 (**1.8**), and changing the stereochemistry of the analogues has had significant influence on biological properties.

### 1-1-5 Design of new constrained pyrrolidine analogues of FTY720

Interesting biological results obtained using constrained FTY720 analogues,<sup>Error!</sup> **Bookmark not defined.** especially the observation of low affinity toward S1P<sub>1</sub> and S1P<sub>3</sub> for the phosphate analogues, indicate a path for lowering the chance of triggering bradycardia to enhance the potential for drug development. We decided to continue SAR studies of novel constrained analogues of FTY720 (**1.8**). To evaluate their effects on cancer cell lines, we have collaborated with the Edinger group in department of cell & developmental biology at the University of California-Irvine. Based on the idea of constraining FTY720 (**1.8**), we designed two new series of pyrrolidine analogues to test if both hydroxymethyl arms were necessary for activity (Scheme 3). One of the series was designed bearing *O*-substituted benzyl ethers to simplify the synthetic approach and increase conformational flexibility of the aryl appendage, and included substitution on the 2,3-, 2,4-, and 3-positions of the pyrrolidine ring,<sup>120</sup> The other C-aryl series pursued the design of our previous studies<sup>119</sup> to gain further understanding of the influence of stereochemistry and to optimize the molecular structure.



**Scheme 3.** Design of two series of constrained pyrrolidine analogues of FTY720 (**1.8**).



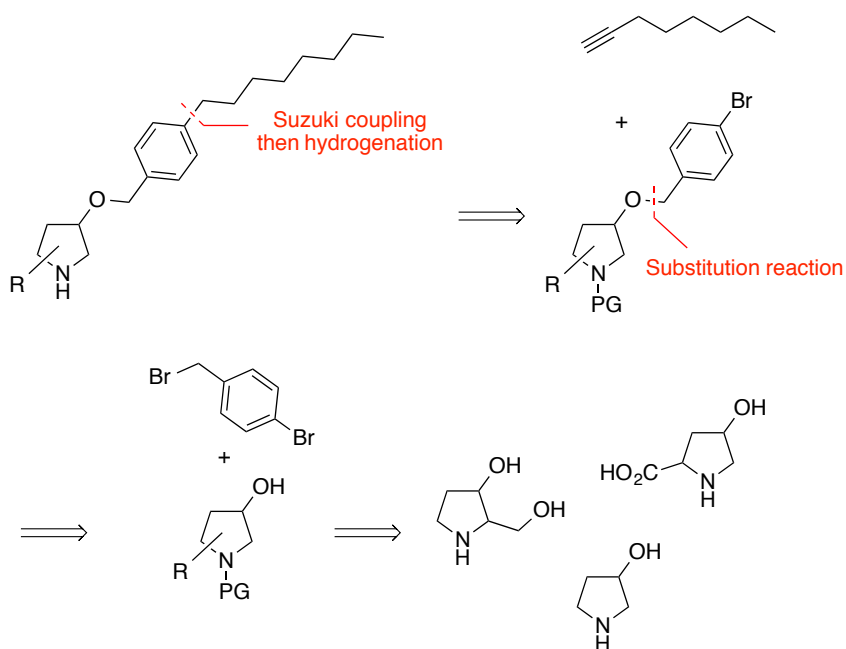
## 1-2 Results and Discussion

### 1-2-1 Synthesis of constrained *O*-arylmethyl-substituted pyrrolidine analogues

In our design of the *O*-arylmethyl substituted pyrrolidine series, one of the goals was to easily and rapidly access these analogues. In our retrosynthesis, outlined in Scheme 4, we envisioned that the C8 alkyl chain of the *O*-arylmethyl substituted pyrrolidine could be obtained through a Suzuki coupling with 1-octyne followed by hydrogenation; the same strategy used in the synthesis of **1.15** (Scheme 2). The aryl bromide reactant for the coupling

reaction could be obtained by a simple substitution reaction with 4-bromobenzyl bromide. The hydroxypyrrolidine scaffold can be easily accessed, either directly from enantiomerically pure natural products that already possess the same stereocenters (e.g. hydroxyproline, hydroxypyrrolidine), or by known procedures.<sup>120</sup>

**Scheme 4.** Retrosynthesis of constrained *O*-arylmethyl-substituted pyrrolidine analogues



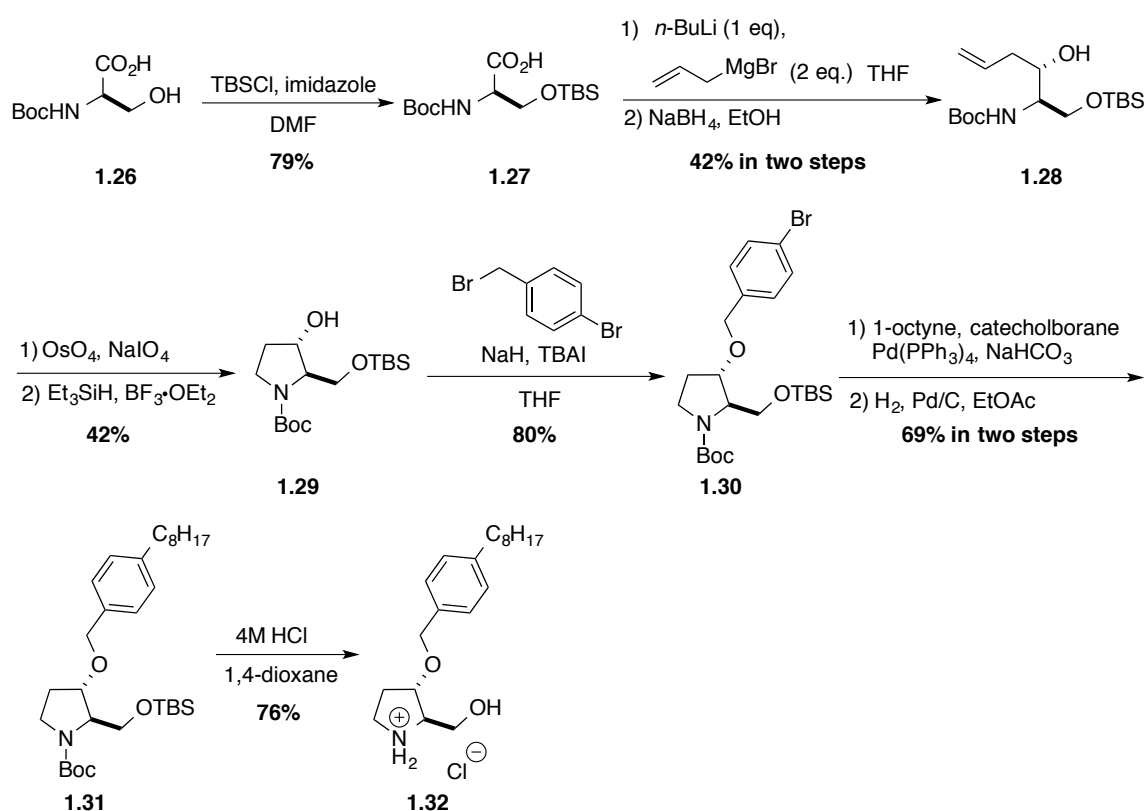
### 1-2-1-1 Synthesis of 2-hydroxymethyl-3-*O*-arylmethylpyrrolidine analogues

#### 1-2-1-1-1 Synthesis of *trans*-2-hydroxymethyl-3-*O*-arylmethylpyrrolidine analogues

As per our synthetic protocol (Scheme 4), pyrrolidine intermediate **1.29** was prepared by a known procedure starting from D-serine (**1.26**, Scheme 5).<sup>121</sup> Protection of the alcohol as a *tert*-butyldimethylsilyl ether afforded **1.27** in 79 % yield. The carboxylic acid group of **1.27** was then deprotonated by one equivalent of *n*-butyllithium and the lithium salt was reacted with two equivalents of allylmagnesium bromide to yield an allylketone intermediate, which was further reduced by sodium borohydride to give **1.28** as a single diastereomer in 42 % yield (two steps). Oxidative cleavage of the terminal olefin of **1.28**, followed by cyclization, led to an amina intermediate, which was then reduced using triethylsilane and boron trifluoride to afford the required (2*R*,3*S*)-2-(*tert*-butyldimethylsilyl)oxy)methyl-3-hydroxypyrrolidine

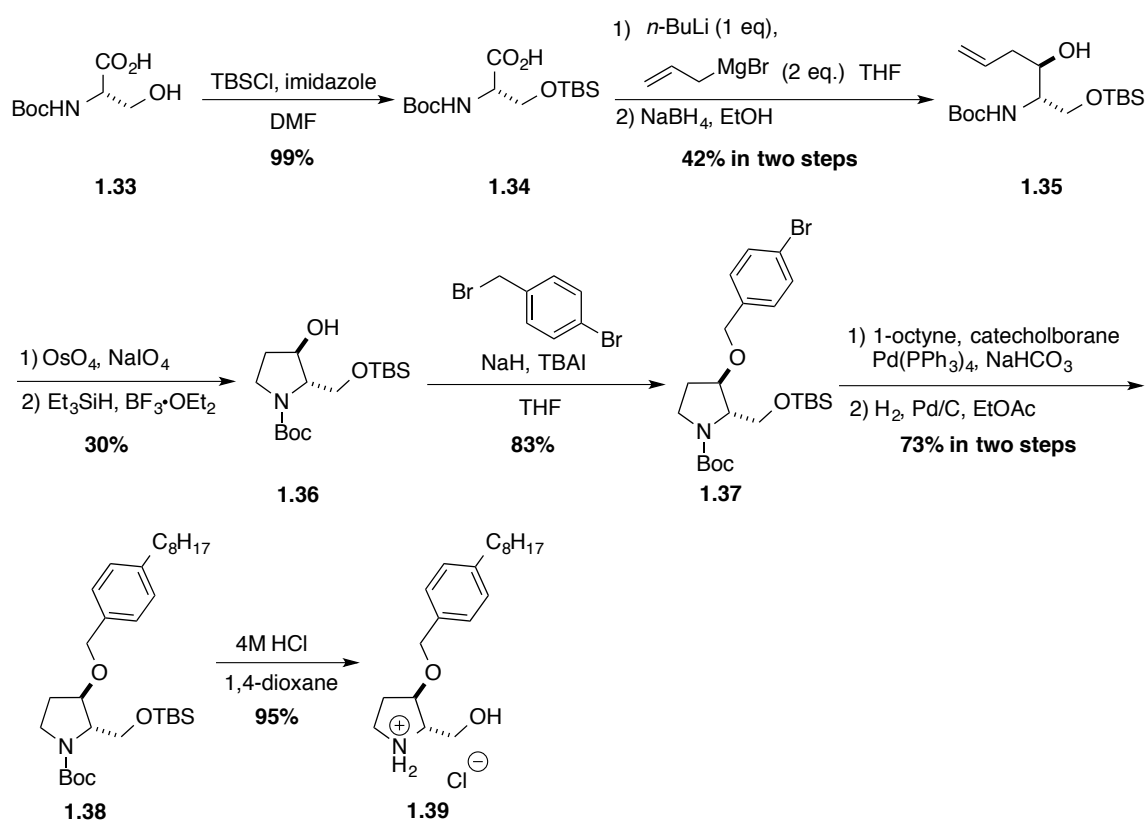
intermediate **1.29** (14 % yield from **1.26** in 5 steps). With **1.29** in hand, a substitution reaction on 4-bromobenzyl bromide furnished aryl bromide intermediate **1.30**. The alkyl chain was then introduced through a Suzuki coupling reaction followed by hydrogenation to afford **1.31** in 69% yield (two steps). Finally, global deprotection of **1.31** using hydrogen chloride in 1,4-dioxane gave the desired (2*R*,3*S*)-2-hydroxymethyl-3-*O*-arylmethylpyrrolidine analogue **1.32** as the hydrochloride salt in 9 steps from D-serine (**1.26**), and 6 % overall yield.

**Scheme 5.** Synthesis of (2*R*,3*S*)-2-hydroxymethyl-3-*O*-arylmethylpyrrolidine **1.32**.



After successfully synthesizing **1.32**, the enantiomer (**1.39**) was prepared from L-serine **1.33** via the same route in 7 % overall yield (Scheme 6).

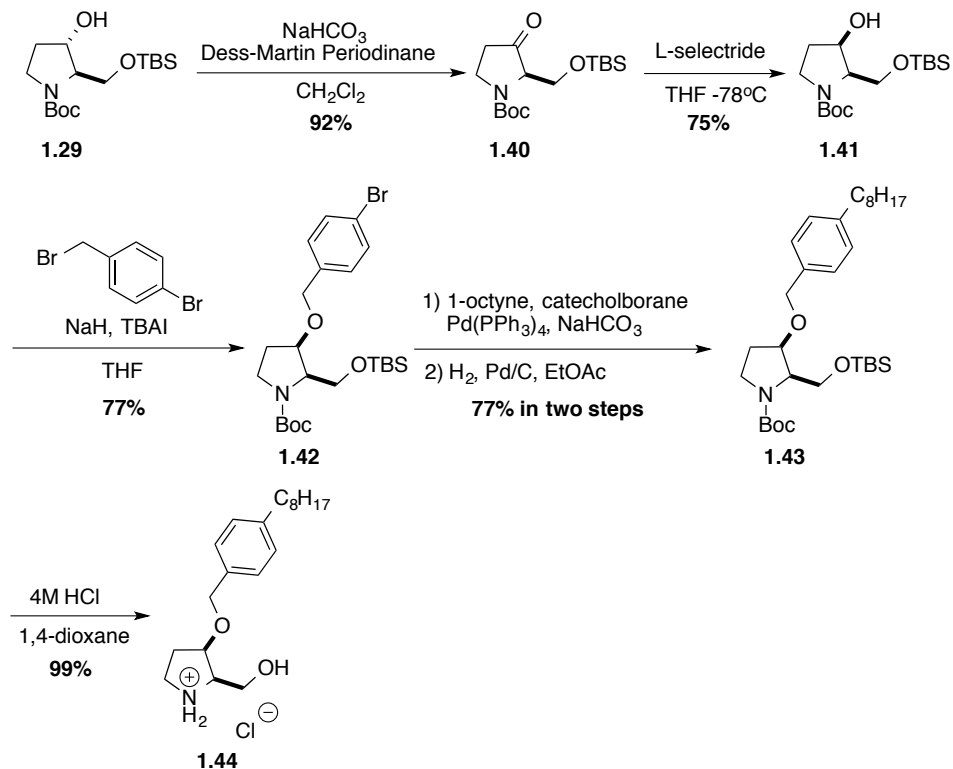
**Scheme 6.** Synthesis of (2*S*,3*R*)-2-hydroxymethyl-3-*O*-arylmethylpyrrolidine **1.39**.



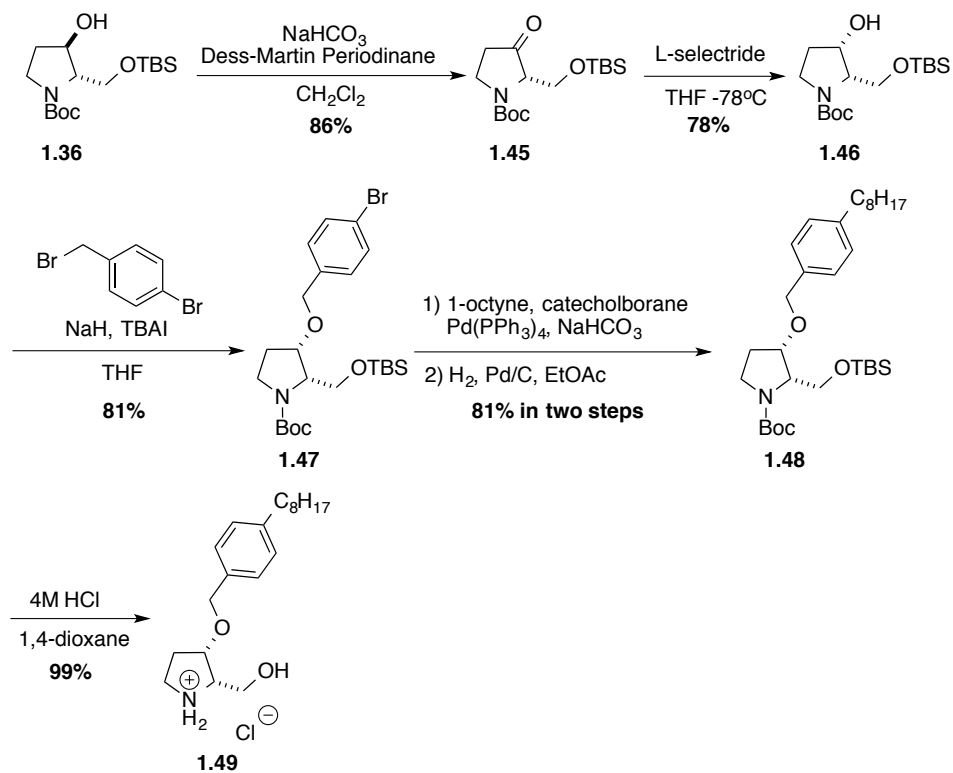
*1-2-1-1-2 Synthesis of cis-2-hydroxymethyl-3-*O*-arylmethylpyrrolidine analogues*

Starting with the key hydroxypyrrolidine intermediate **1.29**, the hydroxyl group was oxidized using Dess–Martin periodinane to yield ketone **1.40**, which was then reduced by L-selectride to provide the desired (2*R*,3*R*)-2-(*tert*-butyldimethylsilyl)oxy)methyl-3-hydroxypyrrolidine intermediate **1.41** as a single isomer. Hydride attack occurred from the bottom face of pyrrolidine due to the bulky OTBS group on the top face. With **1.41** in hand, we used the same protocol as in our synthesis of the *trans*-2,3-substituted analogues to afford *cis*-2,3-substituted pyrrolidine analogue **1.44** as the hydrochloride salt (6 steps from intermediate **1.29**, 41 % overall yield, Scheme 7). In this way, hydroxymethylpyrrolidine **1.49**, the enantiomer of **1.44**, was also prepared starting from the enantiomeric intermediate (2*S*, 3*R*)-**1.36** in 44 % overall yield (Scheme 8).

**Scheme 7.** Synthesis of (2*R*,3*R*)-2-hydroxymethyl-3-*O*-arylmethylpyrrolidine **1.44**.



**Scheme 8.** Synthesis of (2*S*,3*S*)-2-hydroxymethyl-3-*O*-arylmethylpyrrolidine **1.49**.

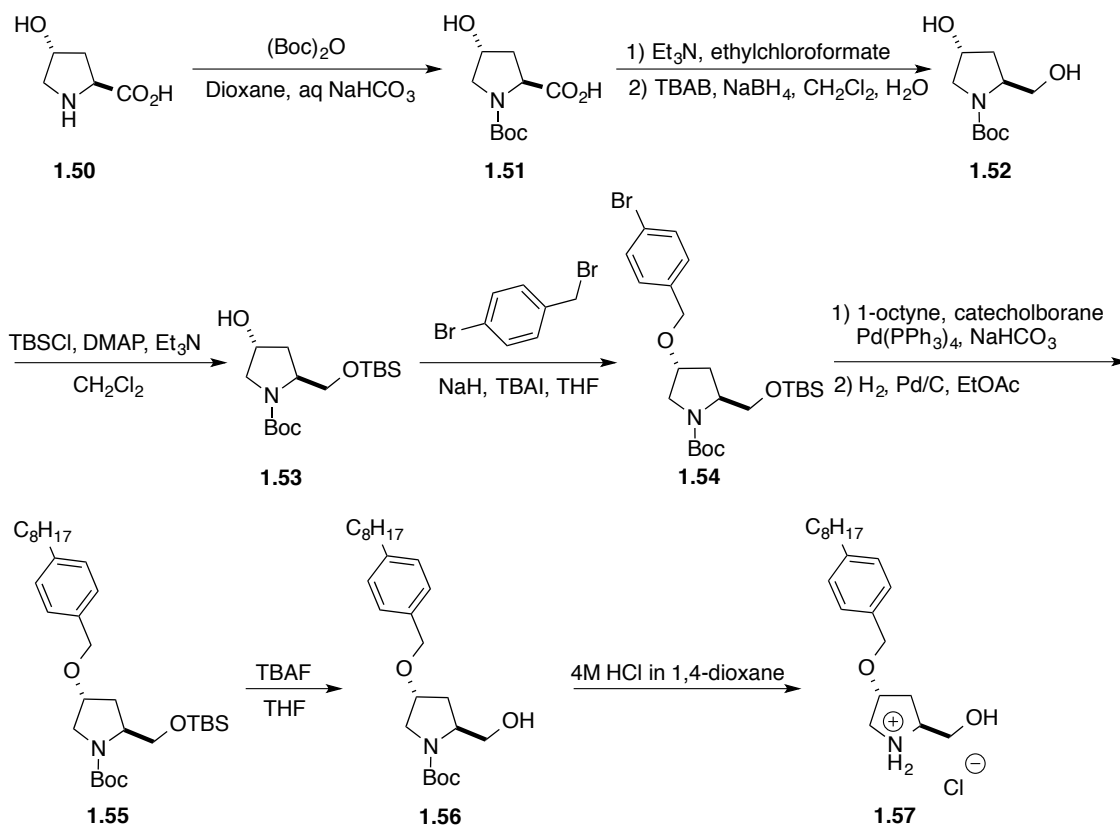


## 1-2-1-2 Synthesis of 2-hydroxymethyl-4-*O*-arylmethylpyrrolidine analogues

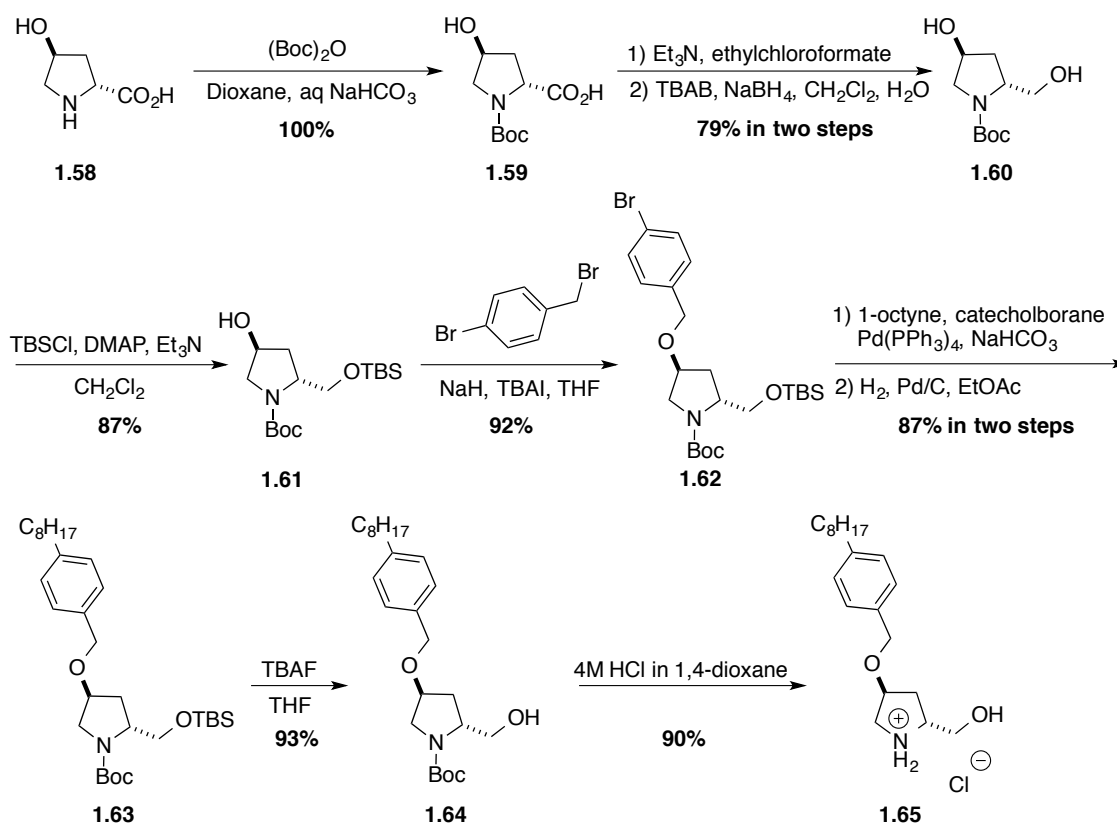
### 1-2-1-2-1 Synthesis of *trans*-2-hydroxymethyl-4-*O*-arylmethylpyrrolidine analogues

*trans*-2,4-Substituted pyrrolidine analogues were first synthesized by Dr. Rebecca Fransson in our group.<sup>120</sup> Starting from commercially available *trans*-4-hydroxy-L-proline **1.50**, protection of the free amine **1.50** as *tert*-butyl carbamate **1.51**, followed by the reduction of the carboxylic acid to the primary alcohol **1.52** using ethyl chloroformate to generate a mixed anhydride that was reduced by treatment with aqueous sodium borohydride and TBAB (as a phase transfer reagent).<sup>122</sup> The resulting primary alcohol was then protected as *tert*-butyldimethylsilyl ether **1.53**, to which was added the side-chain using the previously described substitution-coupling-hydrogenation route to give intermediate **1.55**. Removal of all the protecting groups from **1.55** using TBAF yielded alcohol **1.56**, and treatment with hydrogen chloride in 1,4-dioxane, led to (2*S*,4*R*)-2-hydroxymethyl-4-*O*-arylmethylpyrrolidine analogue **1.57** as the hydrochloride salt (Scheme 9). Similarly, the enantiomer **1.65** was prepared from *trans*-4-hydroxy-D-proline **1.58** (Scheme 10).

**Scheme 9.** Synthesis of (2*S*,4*R*)-2-hydroxymethyl-4-*O*-arylmethylpyrrolidine **1.57**.



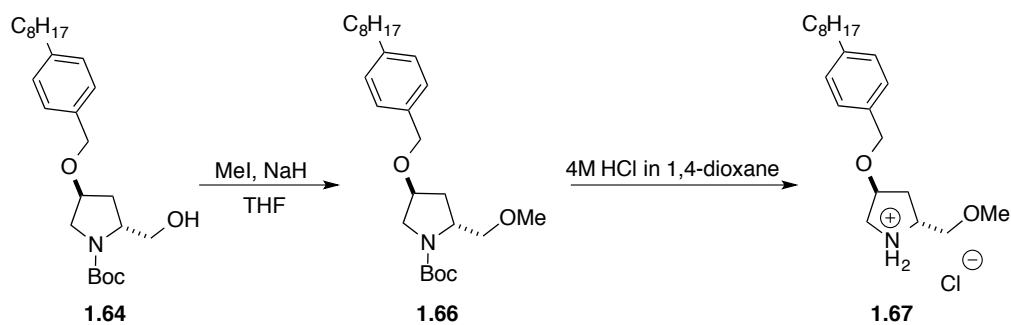
**Scheme 10.** Synthesis of (2*R*,4*S*)-2-hydroxymethyl-4-*O*-arylmethylpyrrolidine **1.65**.



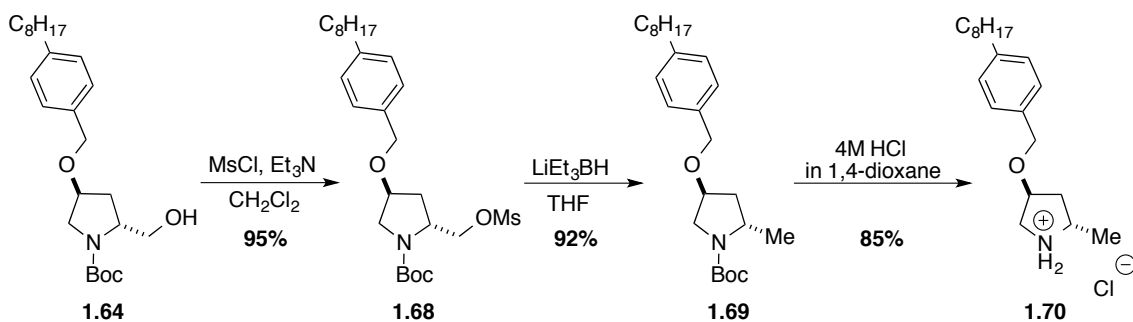
With the successful synthesis of *trans*-2-hydroxymethyl-4-*O*-arylmethylpyrrolidines **1.57** and **1.65**, we prepared several analogues modifying the hydroxymethyl arm. To prevent the analogues from being phosphorylated by cells, the hydroxyl group was removed. Protection of alcohol **1.63** as methyl ether **1.66**, followed by treatment with hydrogen chloride in 1,4-dioxane generated (2*R*,4*S*)-2-methoxymethyl-4-*O*-arylmethylpyrrolidine **1.67** (Scheme 11). Transformation of the alcohol **1.63** to the methanesulfonate **1.68** by reaction with MsCl and Et<sub>3</sub>N followed by deoxygenation using Super-hydride afforded methyl pyrrolidine **1.69** in 92 % yield.<sup>123,124</sup> Deprotection afforded (2*R*,4*S*)-2-methyl-4-*O*-aryl-methylpyrrolidine **1.70** (Scheme 12). With the same synthetic strategy, enantiomer **1.73** was prepared from intermediate **1.56** (Scheme 13).



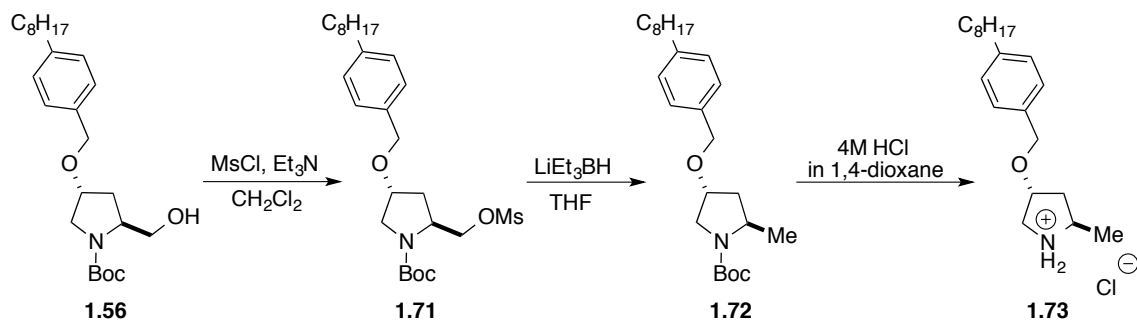
**Scheme 11.** Synthesis of (2*R*,4*S*)-2-methoxymethyl-4-*O*-arylmethylpyrrolidine **1.67**.



**Scheme 12.** Synthesis of (2*R*,4*S*)-2-methyl-4-*O*-arylmethylpyrrolidine **1.70**.



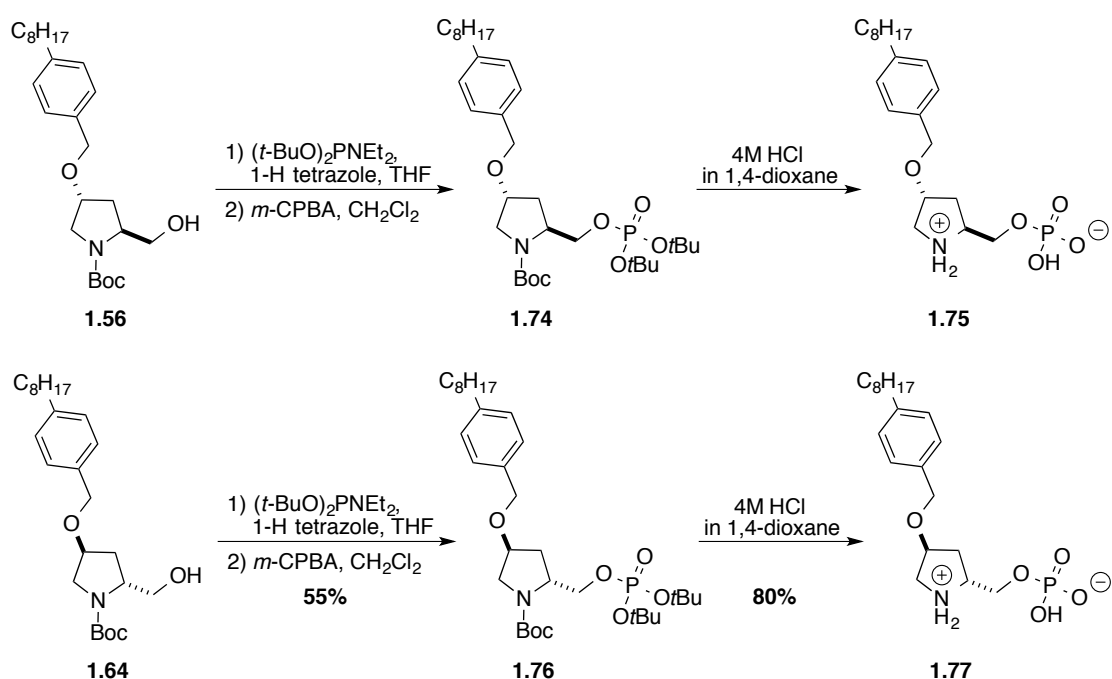
**Scheme 13.** Synthesis of (2*S*,4*R*)-2-methyl-4-*O*-arylmethylpyrrolidine **1.73**.



To evaluate the effects on S1P receptors of analogues **1.57** and **1.65**, their phosphates **1.75** and **1.77** were also prepared. Using the protocol that was described in Charron's work,<sup>119</sup> starting from the 2-hydroxymethyl-4-*O*-arylmethylpyrrolidine intermediate **1.56**. The primary

alcohol was converted to a di-*tert*-butyl phosphite ester using phosphoramidite chemistry, and then oxidized using *m*-CPBA to generate the desired di-*tert*-butyl phosphate ester **1.74**. Removal of the Boc protecting group using hydrogen chloride afforded phosphate **1.75** (the phosphorylated analogue of **1.57**) (Scheme 14). The enantiomeric phosphate analogue **1.77** was made in the same way from (2*R*, 4*S*)-**1.64** (Scheme 14).

**Scheme 14.** Synthesis of (2*S*,4*R*)- and (2*R*,4*S*)-2-(methyl-dihydrophosphate)-4-*O*-arylmethylpyrrolidines **1.75** and **1.77**.

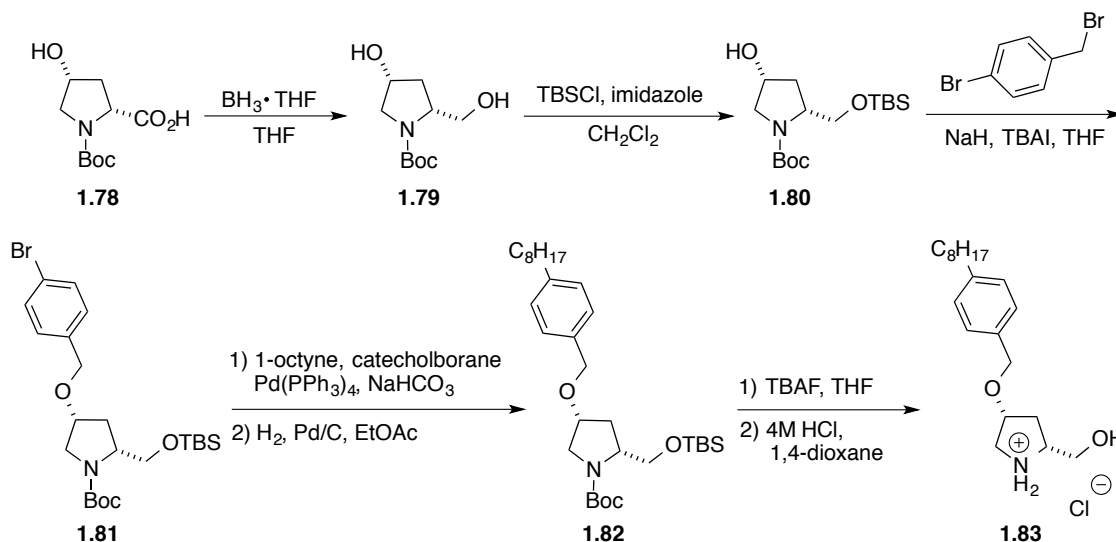


#### 1-2-1-2-2 Synthesis of *cis*-2-hydroxymethyl-4-*O*-arylmethylpyrrolidine analogues

The *cis*-2-hydroxymethyl-4-*O*-arylmethylpyrrolidine analogues were prepared by Dr. Rebecca Fransson.<sup>120</sup> Among these, analogue **1.83** was synthesized from the relatively cheap and commercially available *N*-Boc-*cis*-4-hydroxy-D-proline (**1.78**). Instead of the two steps sequence used in the synthesis of *trans*-analogues **1.56** and **1.65** (Scheme 9 and 10), the carboxylic acid of **1.78** was reduced with borane in THF to generate the primary alcohol **1.79**. With diol **1.79** in hand, the same synthetic protocol used for the synthesis of **1.56** and **1.65**

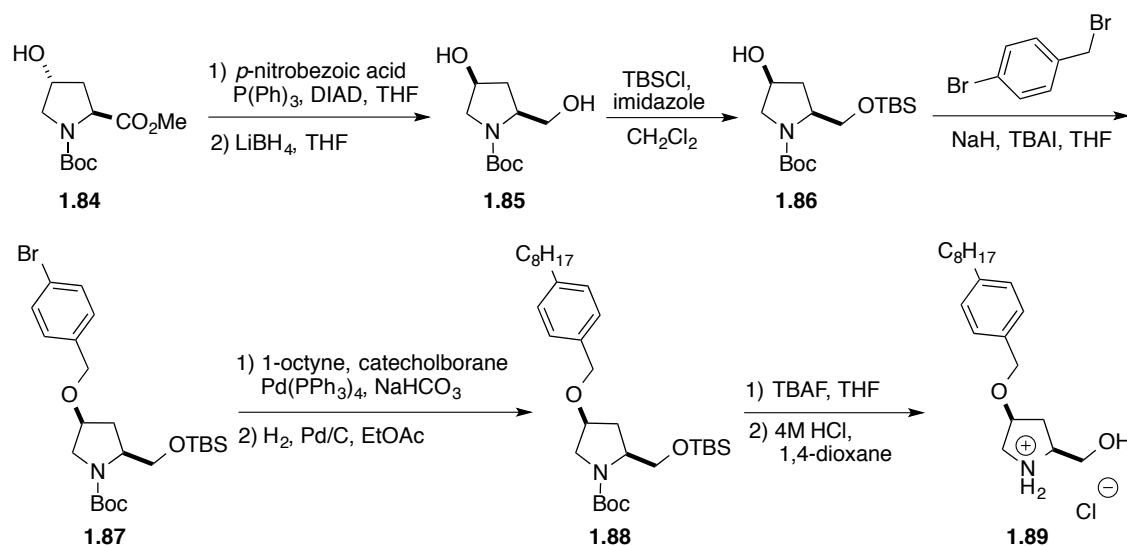
(Scheme 9 and 10) was employed to prepare (2*R*,4*R*)-2-hydroxymethyl-4-*O*-arylmethylpyrrolidine **1.83** as the hydrogen chloride salt (Scheme 15).

**Scheme 15.** Synthesis of (2*R*,4*R*)-2-hydroxymethyl-4-*O*-arylmethylpyrrolidine **1.83**.



To avoid using expensive *cis*-4-hydroxy-L-proline (120 \$ / mmol in Aldrich), a Mitsunobu reaction was performed on inexpensive *N*-Boc-*trans*-4-hydroxy-L-proline methyl ester (**1.84**) (7.5 \$ / mmol in Aldrich). The secondary alcohol was inverted to furnish the *cis*-4-hydroxyproline methyl ester intermediate, which was reduced using LiBH<sub>4</sub> to afford *cis*-4-hydroxy-L-prolinol **1.85**. (2*S*,4*S*)-2-hydroxymethyl-4-*O*-arylmethylpyrrolidine **1.89** was prepared using the same procedure as for **1.83** (Scheme 16).

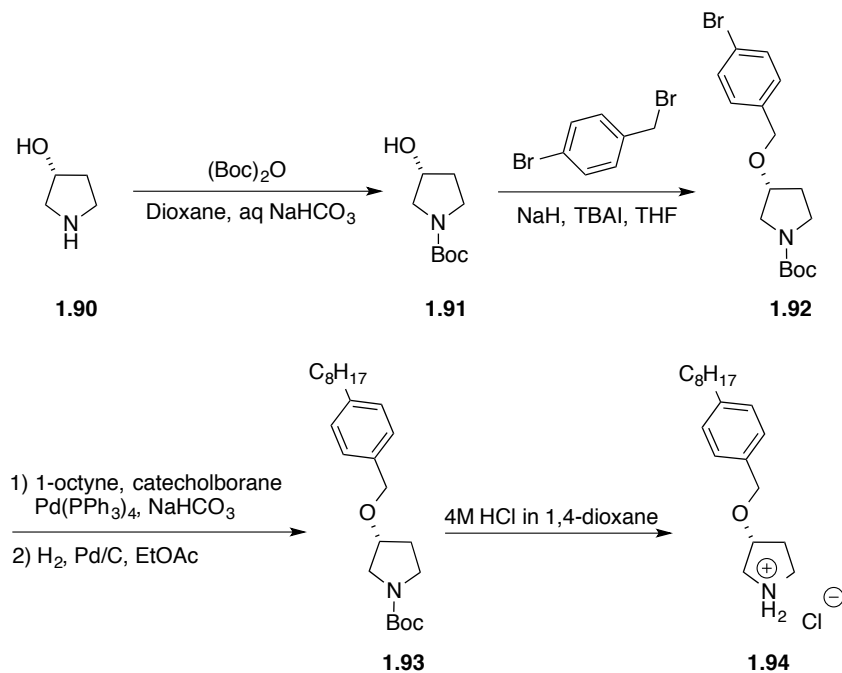
**Scheme 16.** Synthesis of (2*S*,4*S*)-2-hydroxymethyl-4-*O*-arylmethylpyrrolidine **1.89**.



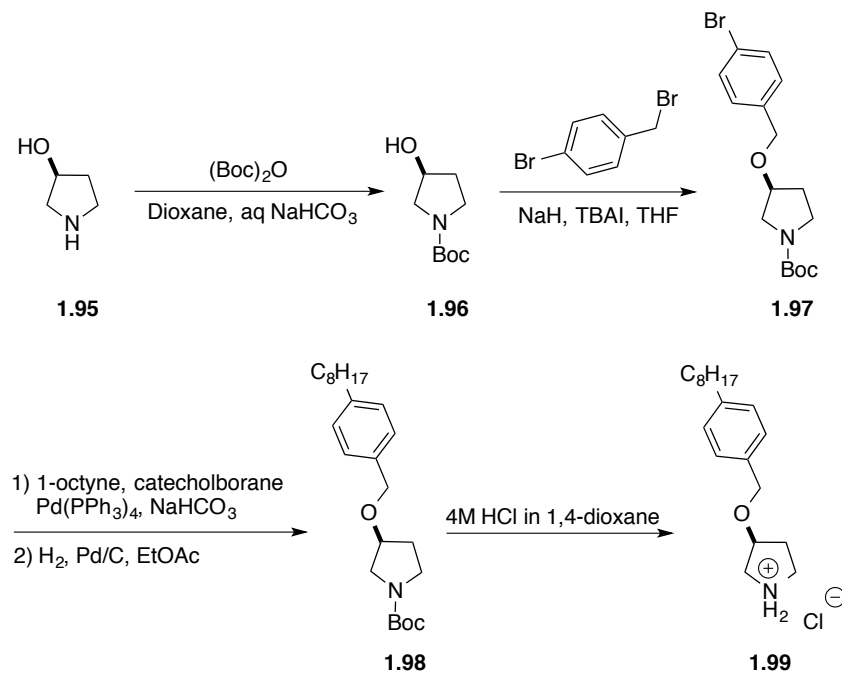
**1-2-1-3 Synthesis of 3-*O*-arylmethylpyrrolidine analogues**

Compared to the di-substituted pyrrolidine analogues, the 3-*O*-arylmethyl substituted analogues were easier to prepare. Starting from 3-hydroxy-pyrrolidine (**1.90**), Boc protection of the amine, followed by our previously described procedures to furnish the long alkyl chain yielded **1.93**, which was deprotected using hydrogen chloride afforded the (*R*)-3-*O*-arylmethylpyrrolidine **1.94** in five steps (Scheme 17). The same route was used for synthesis of the enantiomer **1.99** (Scheme 18). These two analogues were also prepared by Dr. Rebecca Fransson.<sup>120</sup>

**Scheme 17.** Synthesis of (*R*)-3-*O*-arylmethylpyrrolidine **1.94**.



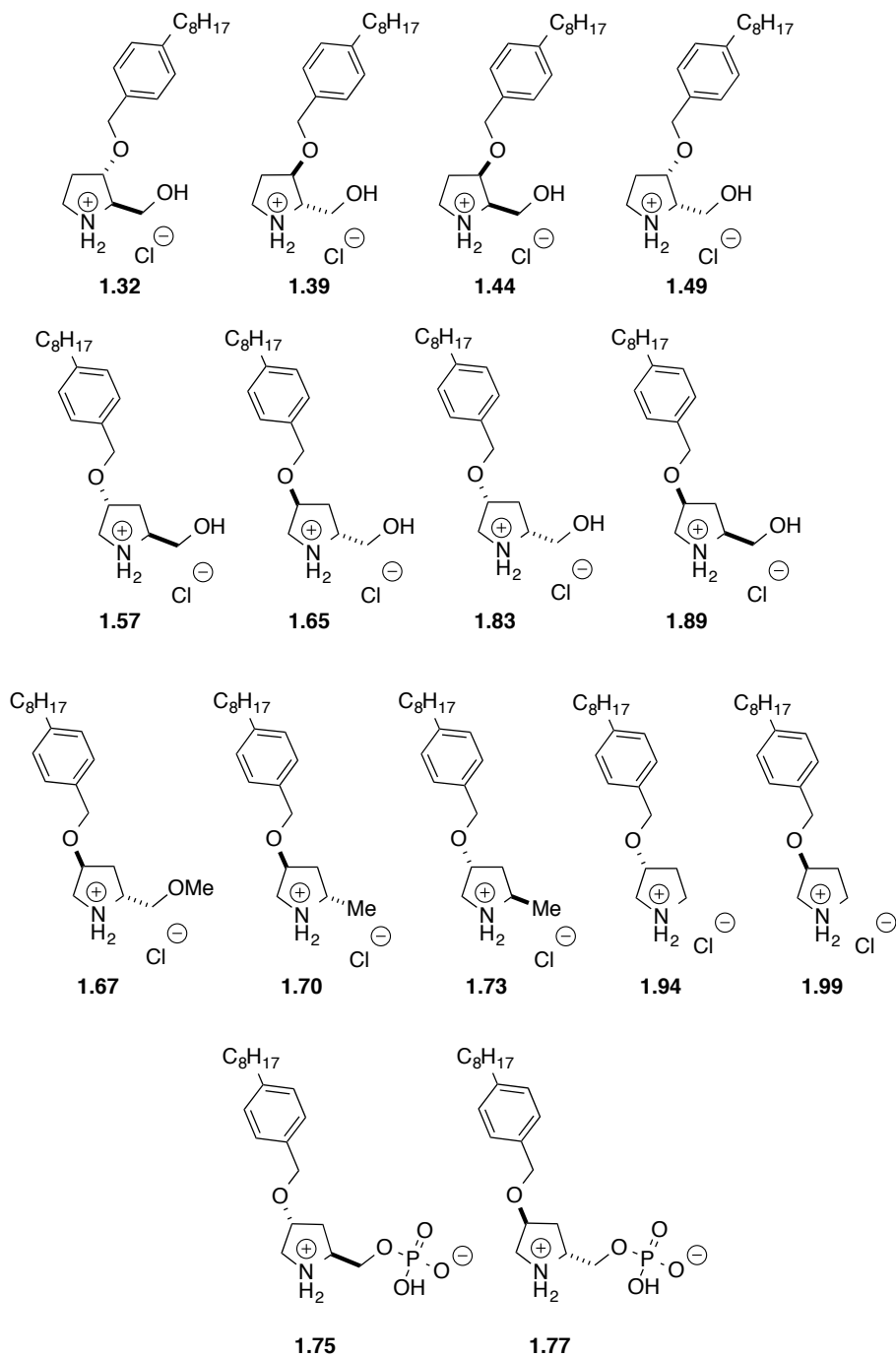
**Scheme 18.** Synthesis of (*S*)-3-*O*-arylmethylpyrrolidine **1.99**.



In sum, we prepared a series of constrained *O*-arylmethyl substituted pyrrolidine analogues (Figure 6), including all the diastereomers of 2-hydroxymethyl-3- and -4-

arylmethylpyrrolidine analogues, 3-*O*-arylmethylpyrrolidine analogues, and several 2-substituted-4-*O*-arylmethylpyrrolidine analogues with a modified 2-hydroxymethyl arm.

**Figure 6.** List of synthesized constrained *O*-arylmethylpyrrolidine analogues.

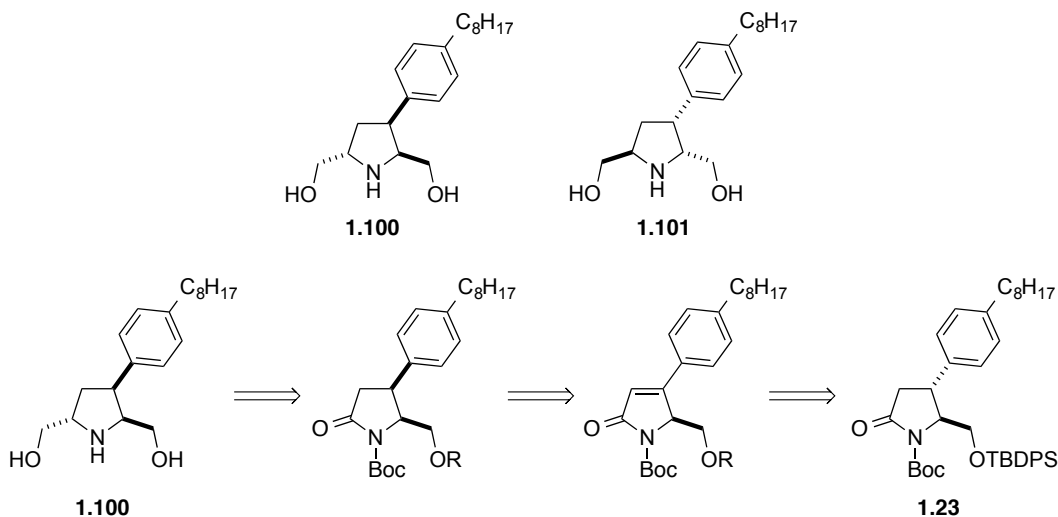


## 1-2-2 Synthesis of constrained C-aryl substituted pyrrolidine analogues

### 1-2-2-1 Synthesis of 2,5-bis(hydroxymethyl)-3-arylpyrrolidine analogues

Continuing Charron's research on 2,5-bis(hydroxymethyl)-3-arylpyrrolidine analogues **1.15** and **1.16** (Figure 5),<sup>119</sup> to understand the influence of stereochemistry on these tri-substituted analogues, two new diastereomers **1.100** and **1.101** were considered (Scheme 19). We envisioned that the second hydroxymethyl arm of **1.100** would be accessed from the (2*S*,3*S*)-2-hydroxymethyl-3-aryl substituted lactam intermediate using the same strategy as in the synthesis of **1.15**.<sup>119</sup> This lactam could be obtained from an  $\alpha,\beta$ -unsaturated lactam by hydrogenation, with hydrogen delivery from the opposite face of the bulky OTBDPS ether. The unsaturated lactam would be provided on selenoxide installation and elimination from the intermediate **1.23**, which was previous used in the synthesis of **1.15**.<sup>119</sup> Both enantiomers **1.101** and **1.100** could be obtained using the same protocol.

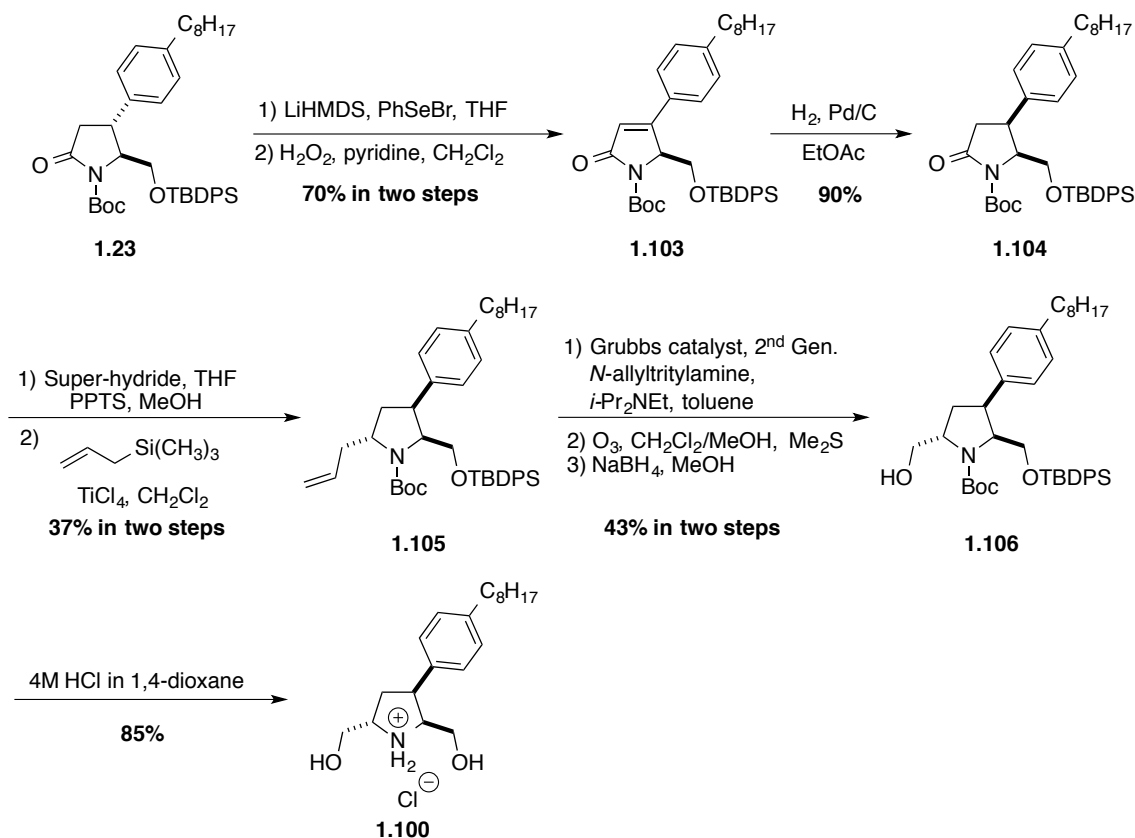
**Scheme 19.** Retrosynthetic analysis of (2*S*,3*S*,5*S*)-2,5-bis(hydroxymethyl)-3-arylpyrrolidine **1.100**.



Starting from **1.23**, which was prepared using Charron's procedure (Scheme 2),<sup>119</sup> the  $\alpha$ -position of the lactam was deprotonated with LiHMDS, and the anion was reacted with phenylselenenyl bromide to generate the selenide intermediate, which was oxidized with hydrogen peroxide to the selenoxide, and eliminated to afford  $\alpha,\beta$ -unsaturated lactam **1.103**.

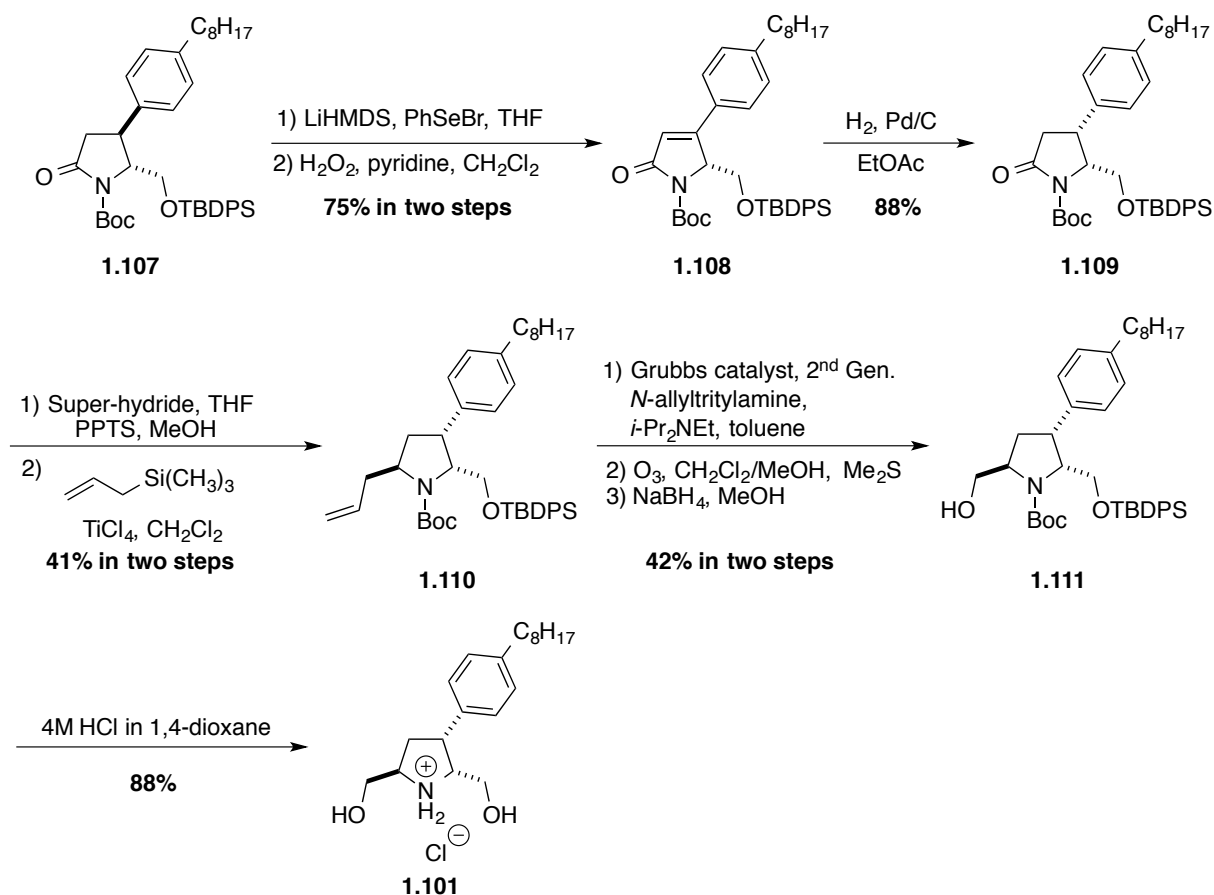
Hydrogenation with **1.103** provided the desired *cis*-2,3-substituted lactam **1.104** as a single isomer. With lactam **1.104** in hand, the protocol previously described for synthesizing **1.15** (Scheme 5), was used to provide (2*S*,3*S*,5*S*)-2,5-bis(hydroxymethyl)-3-arylpyrrolidine **1.100** as the hydrochloride salt in nine steps from **1.23**, and 9 % overall yield, Scheme 20). The enantiomer **1.101** was prepared in the same way from intermediate **1.107** (Scheme 21).

**Scheme 20.** Synthesis of (2*S*,3*S*,5*S*)-2,5-bis(hydroxymethyl)-3-arylpyrrolidine **1.100**.





**Scheme 21.** Synthesis of (2*R*,3*R*,5*R*)-2,5-bis(hydroxymethyl)-3-arylpyrrolidine **1.101**.



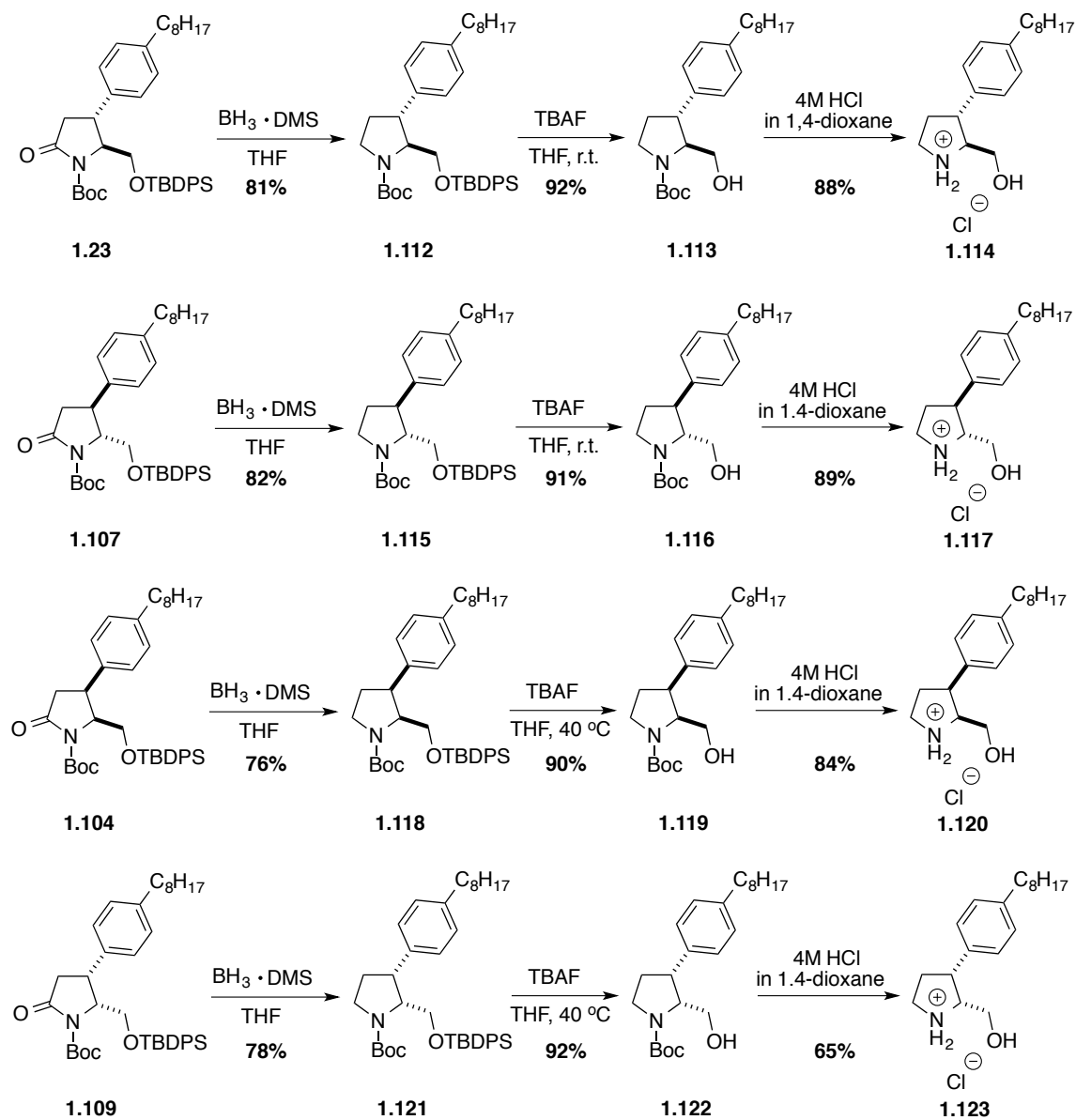
### 1-2-2-2 Synthesis of 2,3-substituted *C*-aryl analogues

#### 1-2-2-2-1 Synthesis of 2-hydroxymethyl-3-arylpyrrolidine analogues

2,3-Substituted *C*-aryl pyrrolidine analogues were designed to determine the importance of the second hydroxymethyl arm. These analogues were prepared from key lactam intermediates by reduction of the lactam. For example, treatment of lactam **1.23** with borane dimethyl sulfide complex gave pyrrolidine **1.112**. Removal of the TBDPS protecting group from **1.112** unveiled the primary alcohol **1.113**, and Boc group removal using hydrogen chloride afforded 2,3-substituted *C*-aryl pyrrolidine **1.114** in good yield (Scheme 22). Similarly, three other 2,3-substituted *C*-aryl pyrrolidine diastereomers **1.117**, **1.120** and **1.123** were prepared from the corresponding lactams (Scheme 22). The *cis*-configuration and

bulkiness of the OTBDPS group and the phenyl side chain in **1.118** and **1.121**, necessitated heating the reaction to 40 °C to cleave the silyl ether.

**Scheme 22.** Synthesis of 2-hydroxymethyl-3-arylpyrrolidines **1.114**, **1.117**, **1.120** and **1.123**.

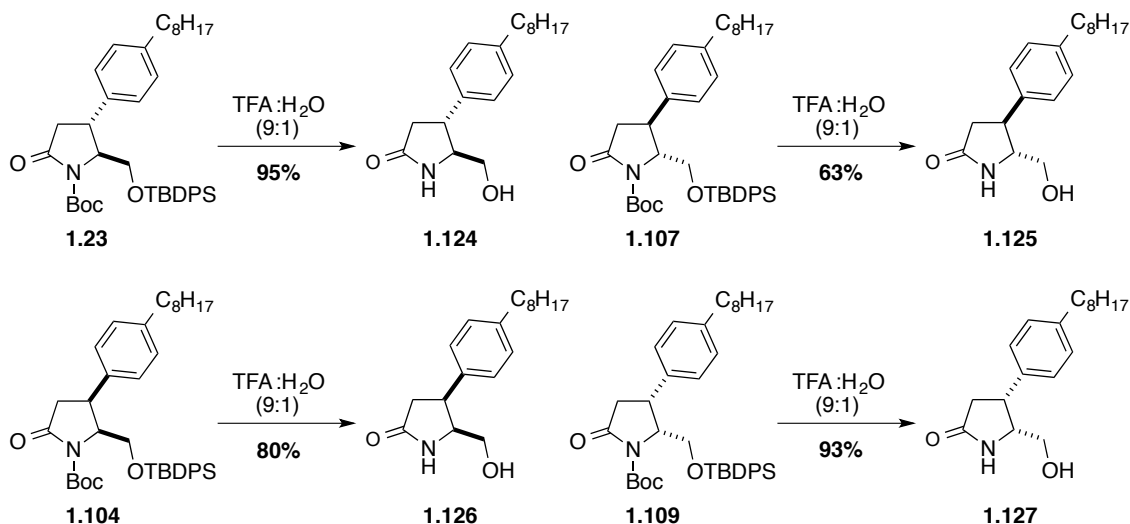


#### 1-2-2-2-2 Synthesis of 2-hydroxymethyl-3-aryl-substituted lactam analogues

To compare the effects of a lactam to those of a free amine (pyrrolidine), several lactams (*e.g.*, **1.124**, **1.125**, **1.126** and **1.127**) were prepared by removing all of the protecting

groups from key intermediates (e.g., **1.23**, **1.107**, **1.104** and **1.109**) using a 9:1 mixture of TFA and water (Scheme 23).

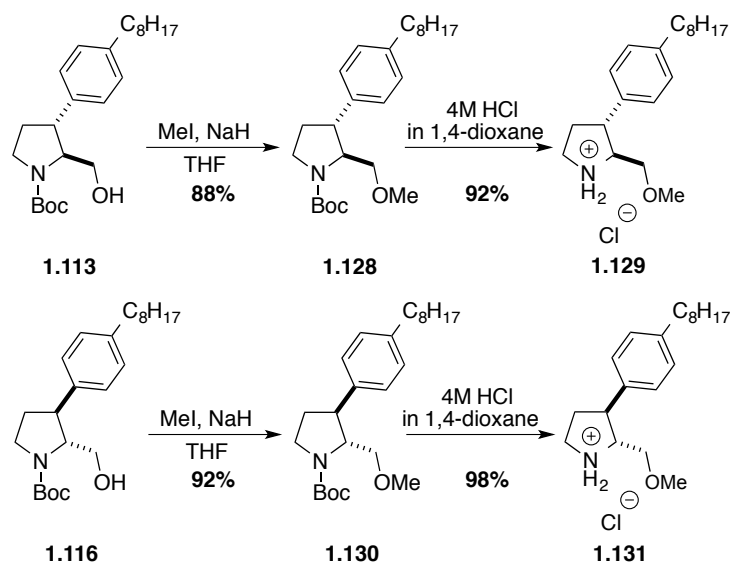
**Scheme 23.** Synthesis of 2-hydroxymethyl-3-aryl-substituted lactams **1.124**, **1.125**, **1.126** and **1.127**.



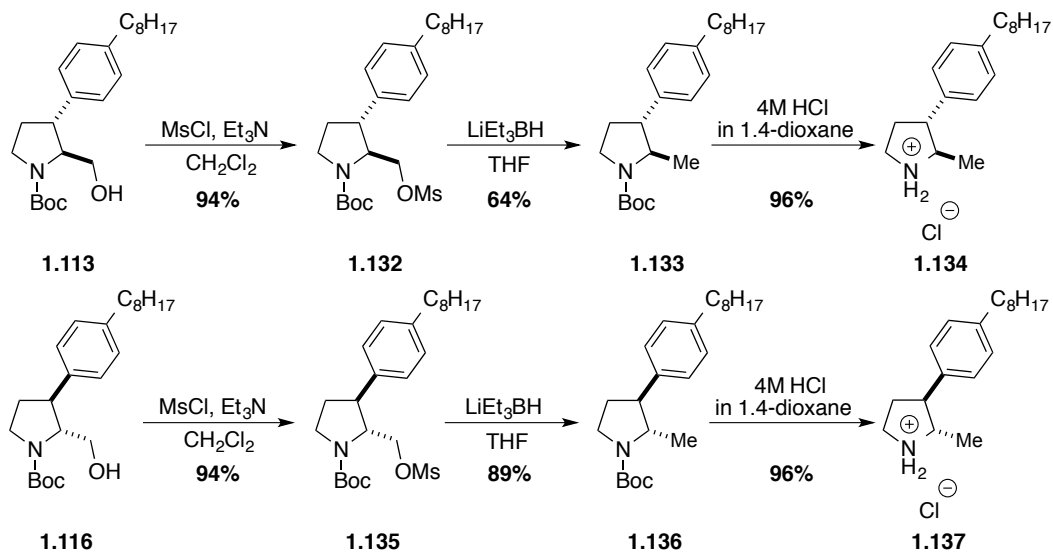
#### 1-2-2-2-3 Synthesis of 2-methoxymethyl- and 2-methyl-3-arylpyrrolidine analogues

As described for the constrained *O*-arylmethyl substituted pyrrolidine analogues (e.g., **1.67**, **1.70** and **1.73**, Scheme 11-13), to gauge the importance at the hydroxyl group for activity, alcohols **1.113** and **1.116** were converted to methyl ethers **1.129** and **1.131** (Scheme 24), and the hydroxyl group were removed to afford methyl analogues **1.134** and **1.137** in good yield (Scheme 25), employing similar same synthetic protocols as those described for preparing compounds **1.67**, **1.70** and **1.73** (Scheme 11-13).

**Scheme 24.** Synthesis of 2-methoxymethyl-3-arylpyrrolidines **1.129** and **1.131**.



**Scheme 25.** Synthesis of 2-methyl-3-arylpyrrolidines **1.134** and **1.137**.

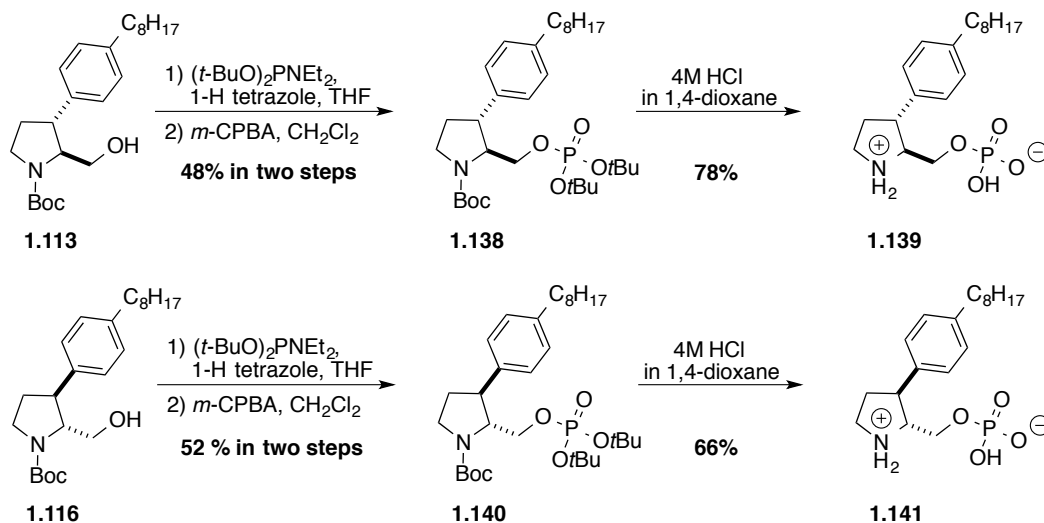


*1-2-2-2-4 Synthesis of phosphates of 2-hydroxymethyl-3-arylpyrrolidine analogues.*

In order to probe the effect of phosphorylation, the phosphates of **1.114** and **1.117** were prepared. Starting from alcohols **1.113** and **1.116**, using the same procedure as described for

the synthesis of phosphates **1.75** and **1.77**, the corresponding phosphates **1.139** and **1.141** were obtained in moderate yield (Scheme 26).

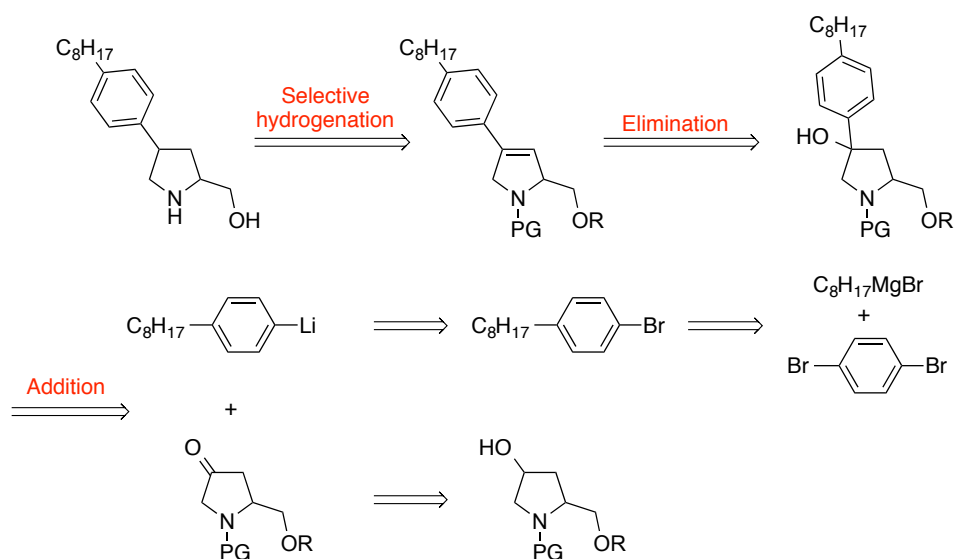
**Scheme 26.** Synthesis of 2-methyldihydrophosphate-3-arylpyrrolidines **1.139** and **1.141**.



### 1-2-2-3 Synthesis of 2-hydroxymethyl-4-arylpyrrolidine analogues

As shown in the retrosynthetic analysis, outlined in scheme 27, we envisioned that both *cis* and *trans*-2-hydroxymethyl-4-arylpyrrolidine analogues could be obtained by the selective hydrogenation of unsaturated pyrrolidine intermediates. *cis*-Diastereomers would be obtained by taking advantage of the bulky OR group to direct hydrogen addition from the opposite face. A free hydroxyl group may direct hydrogenation to the same face to generate the *trans*-diastereomers. The unsaturated pyrrolidine could result from by elimination of a tertiary alcohol intermediate, which could be obtained through addition of a phenyl lithium to a 4-oxopyrrolidine intermediate, derived from the corresponding 4-hydroxy-proline. The organolithium reagent could be prepared from 1-bromo-4-octylbenzene, which would be produced by a coupling reaction between 1,4-dibromobenzene and octyl magnesium bromide.

**Scheme 27.** Retrosynthetic analysis of 2-hydroxymethyl-4-arylpyrrolidines.



#### *1-2-2-3-1 Synthesis of cis-2-hydroxymethyl-4-arylpyrrolidine analogues*

We began with the synthesis of the common intermediate 1-bromo-4-octylbenzene **1.142**, which was prepared by a palladium-catalyzed coupling reaction between 1,4-dibromobenzene and octyl magnesium bromide (Scheme 28).<sup>125</sup> Protection of *cis*-4-hydroxyproline (**1.143**) as *tert*-butyl carbamate followed by oxidation using trichloroisocyanuric acid and TEMPO gave the 4-oxoproline **1.144** in 87 % yield over two steps. To introduce a bulky group, carbocyclic acid **1.144** was converted to *tert*-butyl ester **1.145**. Treatment of bromide **1.142** with *n*-BuLi generated the corresponding organolithium reagent, which was added to ketone **1.145** to give addition product **1.146**. Elimination of the tertiary alcohol from **1.146** using Burgess's reagent (methyl *N*-(triethylammoniumsulfonyl)carbamate)<sup>126</sup> led to unsaturated pyrrolidine intermediate **1.147** in 68 % yield. With olefin **1.147** in hand, hydrogenation catalyzed by palladium-on-activated-charcoal gave the *cis*-2,4-substituted pyrrolidine **1.148**, in 94 % yield. The structure of **1.148** was confirmed by X-ray analysis (Figure 7). Finally, reduction of ester **1.148** using LiAlH<sub>4</sub> generated primary alcohol **1.149**, which was treated with hydrogen chloride to give (2*R*,4*S*)-2-hydroxymethyl-4-aryl-substituted pyrrolidine **1.150** in good yield (Scheme 28).

**Scheme 28.** Synthesis of (2*R*,4*S*)-2-hydroxymethyl-4-arylpyrrolidine **1.150**.

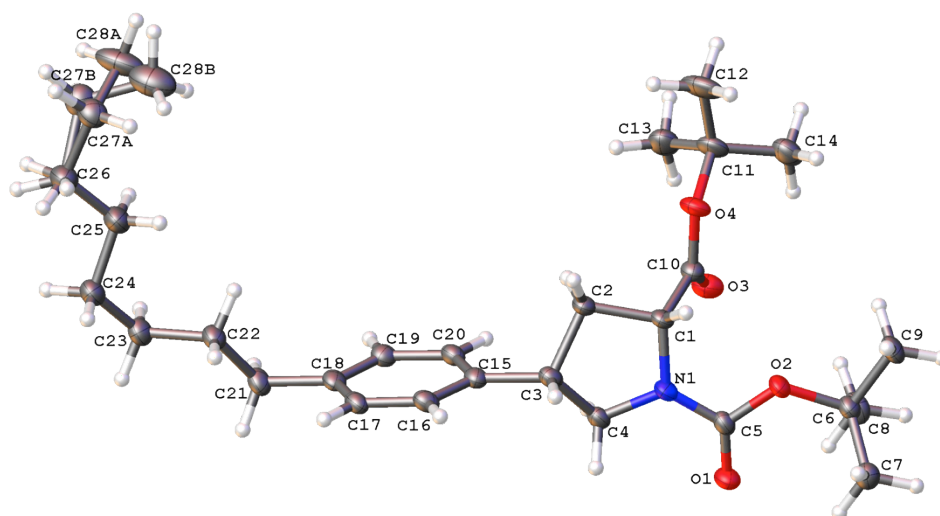
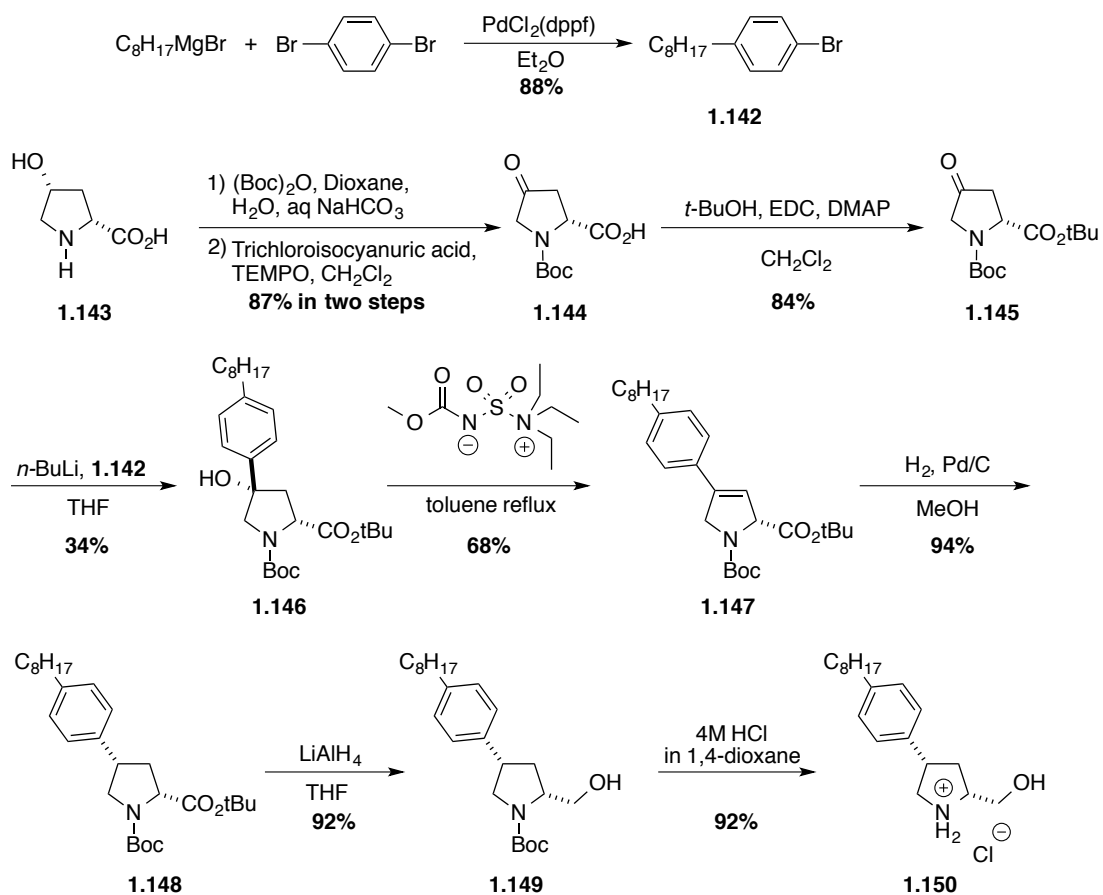
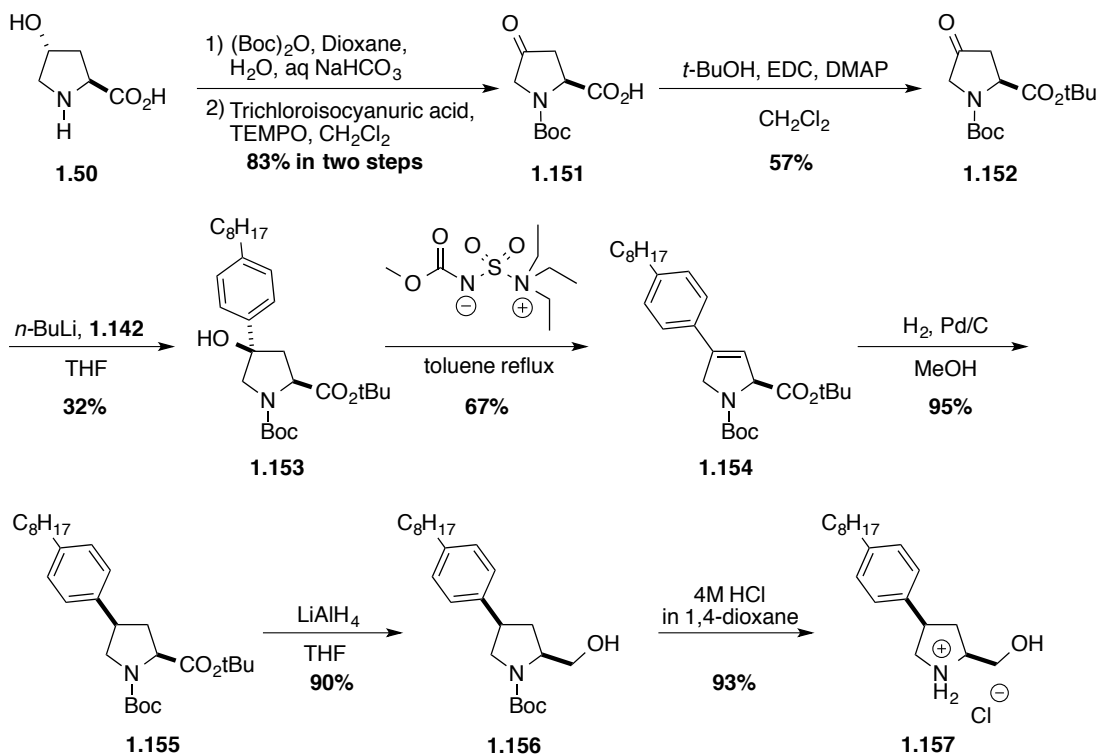


**Figure 7.** X ray structure of ester **1.148**.

Based on the same synthetic strategy, the enantiomer **1.157** was synthesized from *trans*-4-hydroxyl-L-proline (**1.50**) in eight steps and 8 % overall yield (Scheme 29).

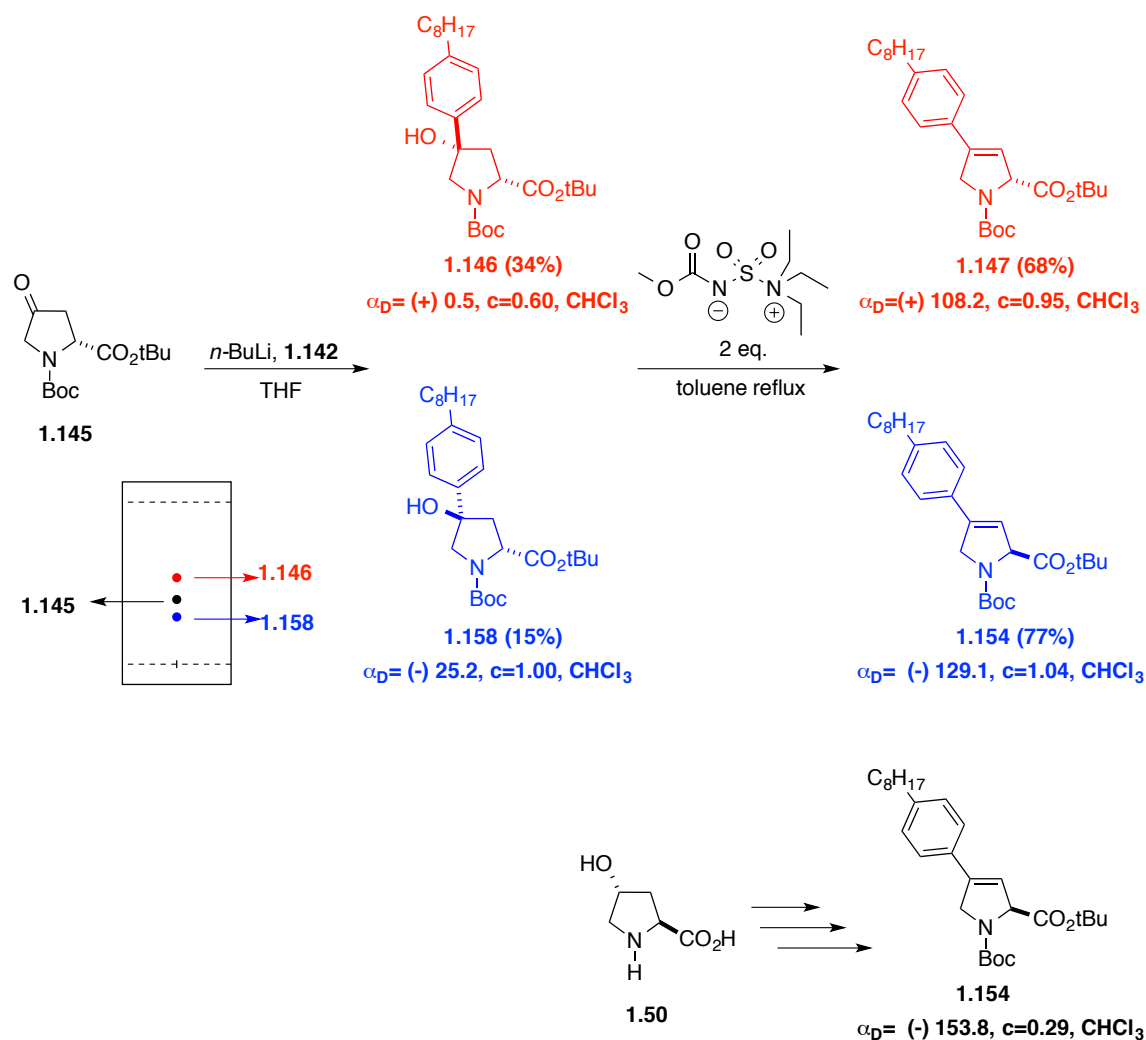
**Scheme 29.** Synthesis of (2*S*,4*R*)-2-hydroxymethyl-4-arylpyrrolidine **1.157**.



In the syntheses of **1.150** and the enantiomer **1.157**, one of the key reactions was the addition of an organolithium reagent to oxo-pyrrolidines **1.145** and **1.152**. The yield of this step was however usually around 30 %. Upon investigating this reaction further (Scheme 30), we found that the low yield was due to in part addition on the *tert*-butyl ester rather than the ketone, which increased ultimately the difficulty in the purification. Moreover, another diastereomer **1.158**, which had not previously been isolated, was obtained as a more polar product than **1.146** in up to 19% yield. Treatment of both alcohol isomers under the same conditions used to eliminate the tertiary alcohol gave products having the same r.f. and  $^1\text{H}$  NMR spectrum, but opposite optical rotation values, indicating that they were enantiomers.

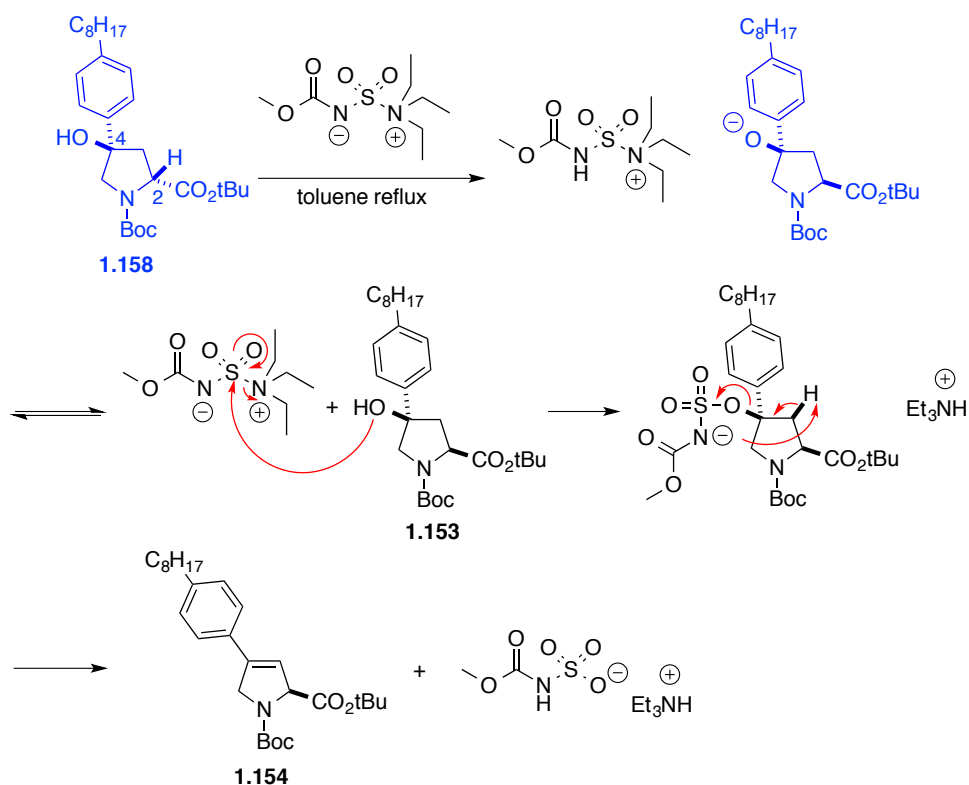


**Scheme 30.** Studies of the reaction organolithium reagent addition on **1.145**.



Based on these observations, we proposed that the stereocenter at the 2-position of **1.158** was epimerized due to the steric hindrance induced by the *cis*-2,4 configuration of **1.158** (Scheme 31). In the presence of the Burgess's reagent in toluene at reflux, **1.158** was epimerized at the 2-position, prior to elimination of the hydroxyl group, by the Burgess reagent to afford olefin **1.154**.

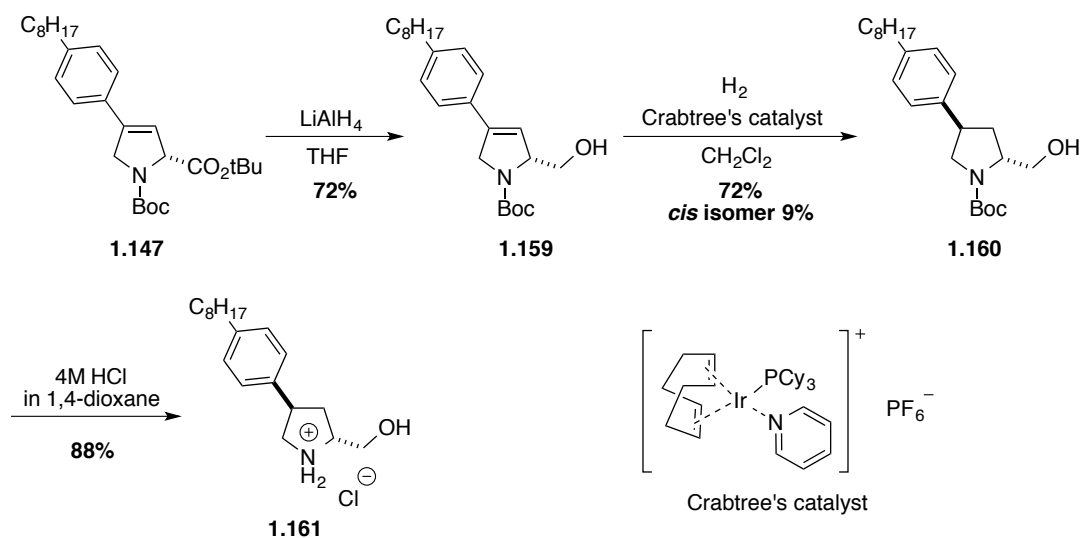
**Scheme 31.** Proposed mechanism of epimerization of **1.158** followed by dehydrogenation.



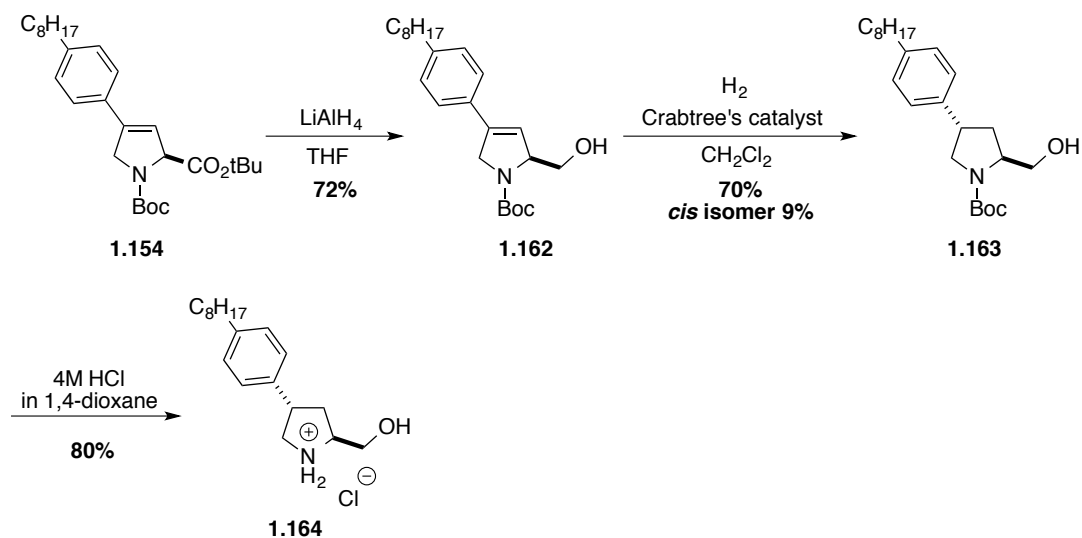
#### 1-2-2-3-2 Synthesis of *trans*-2-hydroxymethyl-4-arylpyrrolidine analogues

After successfully achieving the synthesis of *cis*-2-hydroxymethyl-4-arylpyrrolidines **1.150** and **1.157**, the *trans*-2-hydroxymethyl-4-arylpyrrolidine analogues were also prepared according to the initial plan (Scheme 27). The *tert*-butyl ester of unsaturated pyrrolidine **1.147** was reduced to primary alcohol **1.159**, which was treated with Carbtree's catalyst<sup>127,128</sup> and hydrogen, under hydrogen at 70 psi pressure, for 3 days. As expected, the hydrogenation was directed by the primary alcohol to the same face as the hydroxymethyl group of prolinol **1.159** to give *trans*-product **1.160** in 72 % yield. A minor amount of *cis*-isomer **1.149** (9 %) was also generated. Finally, the Boc group of **1.160** was removed using hydrogen chloride to afford (*2R,4R*)-2-hydroxylmethyl-4-arylpyrrolidine **1.161** (Scheme 32). The enantiomer **1.164** was prepared in the same way from **1.154** (Scheme 33).

**Scheme 32.** Synthesis of (2*R*,4*R*)-2-hydroxymethyl-4-arylpyrrolidine **1.161**.



**Scheme 33.** Synthesis of (2*S*,4*S*)-2-hydroxymethyl-4-arylpyrrolidine **1.164**.

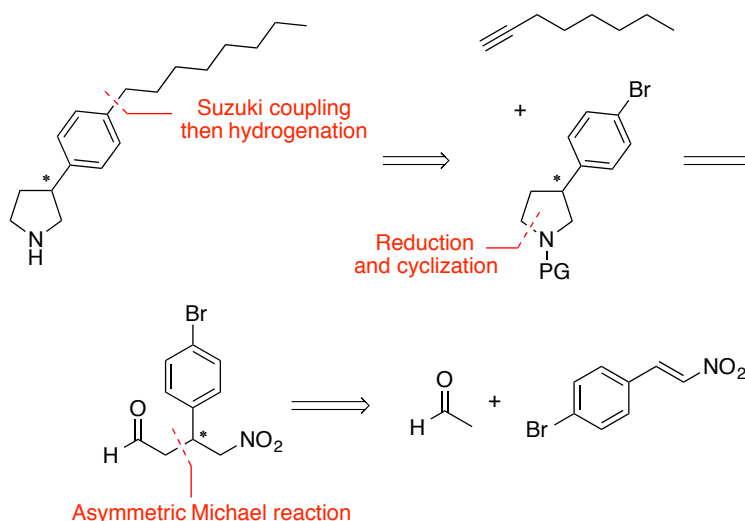


#### 1-2-2-4 Synthesis of 3-arylpyrrolidine analogues

We envisioned that the side-chain could be installed at a later point in the synthesis by our general coupling and hydrogenation strategy (Scheme 34). The 3-(*p*-bromophenyl)-pyrrolidine coupling precursor could be generated from a nitroaldehyde by reduction of the

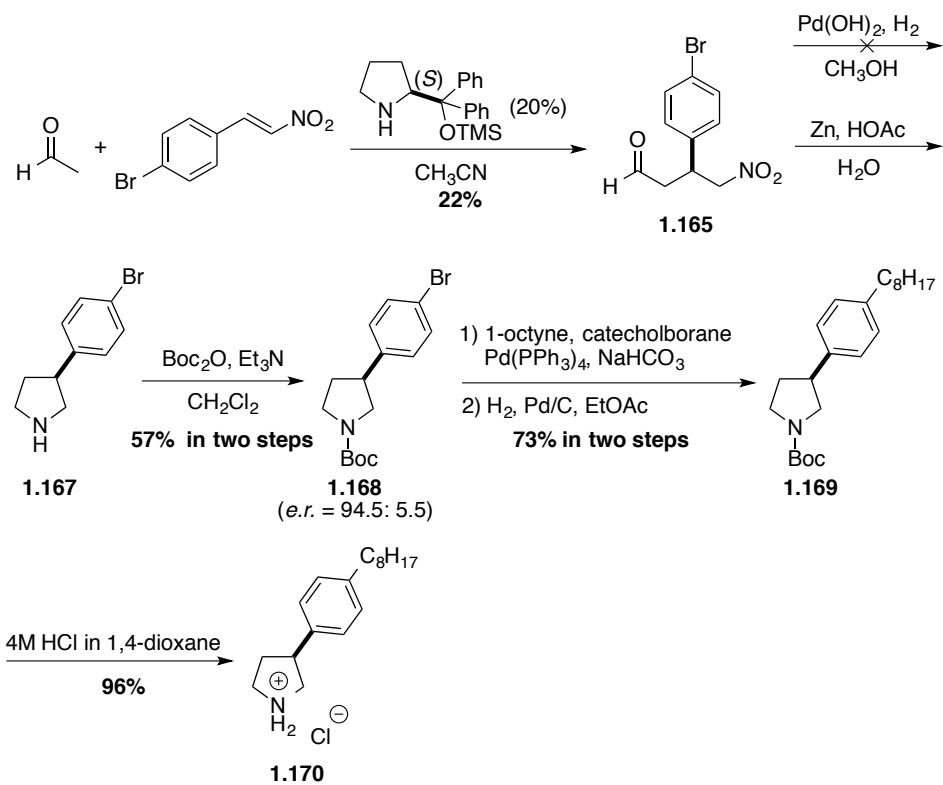
nitro group to the amine, followed by cyclization using reductive amination. The nitroaldehyde could be obtained by an asymmetric Michael reaction between acetaldehyde and *trans*-4-bromo- $\beta$ -nitrostyrene, based on the organo-catalytic method reported by List.<sup>129</sup>

**Scheme 34.** Retrosynthetic analysis for the synthesis of 3-arylpyrrolidine analogues.

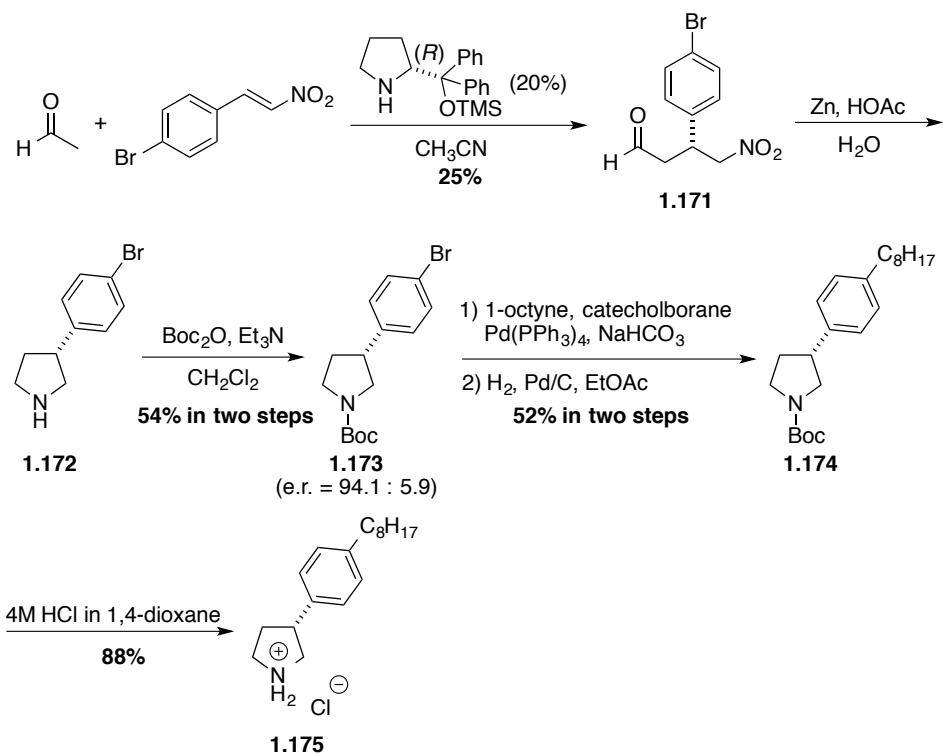


The reaction of acetaldehyde and *trans*-4-bromo- $\beta$ -nitrostyrene was performed in the presence of the Jørgensen–Hayashi-type of silyl ether catalyst, (*S*)-(-)- $\alpha,\alpha$ -diphenyl-2-pyrrolidinemethanol trimethylsilyl ether,<sup>130,131</sup> to afford the (*S*)-nitroaldehyde **1.165** in 22 % yield (Scheme 35). Treatment of nitroaldehyde **1.165** with Pd(OH)<sub>2</sub> under 5 bar pressure of hydrogen, as used previously in synthesis of 3-phenylpyrrolidine,<sup>129</sup> gave no reaction; however, switching to zinc and aqueous acetic acid<sup>132</sup> led to the required 3-substituted pyrrolidine **1.167**. Protection of **1.167** as the *tert*-butyl carbamate gave pyrrolidine **1.168**, which was ready for a Suzuki reaction. The purity of amine **1.168** was established by chiral SFC, which demonstrated a good enantiomeric ratio (e.r. = 94.5 : 5.5) had been obtained. The side-chain was installed using our general synthetic protocol to yield **1.169**, which was deprotected to give the (*S*)-3-arylpyrrolidine **1.170** as the hydrochloride salt (Scheme 35). The enantiomer **1.175** was obtained based on the same synthetic strategy employing (*R*)-(-)- $\alpha,\alpha$ -diphenyl-2-pyrrolidinemethanol trimethylsilyl ether as catalyst (Scheme 36).

**Scheme 35.** Synthesis of (*S*)-3-arylpyrrolidine **1.170**.

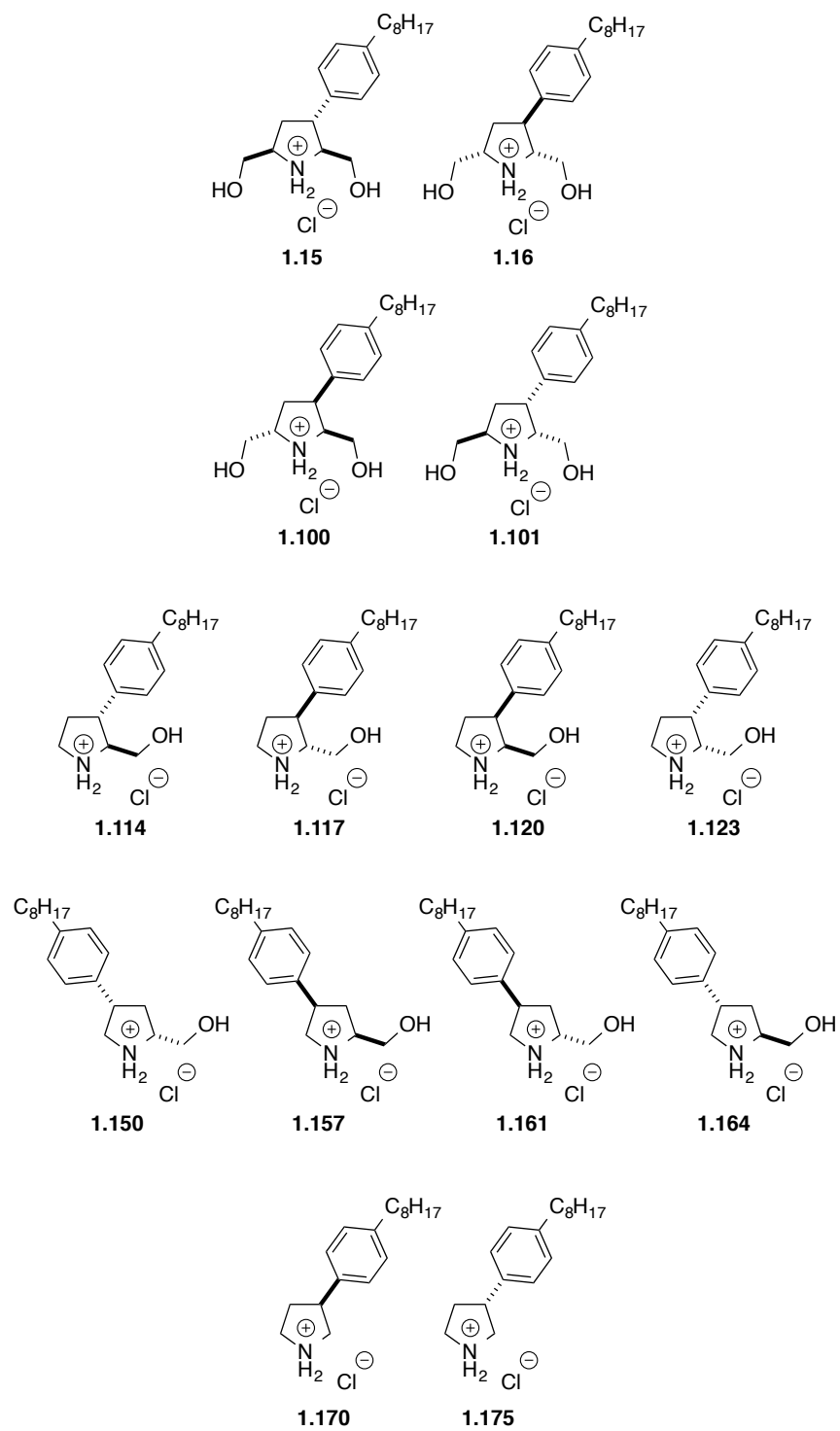


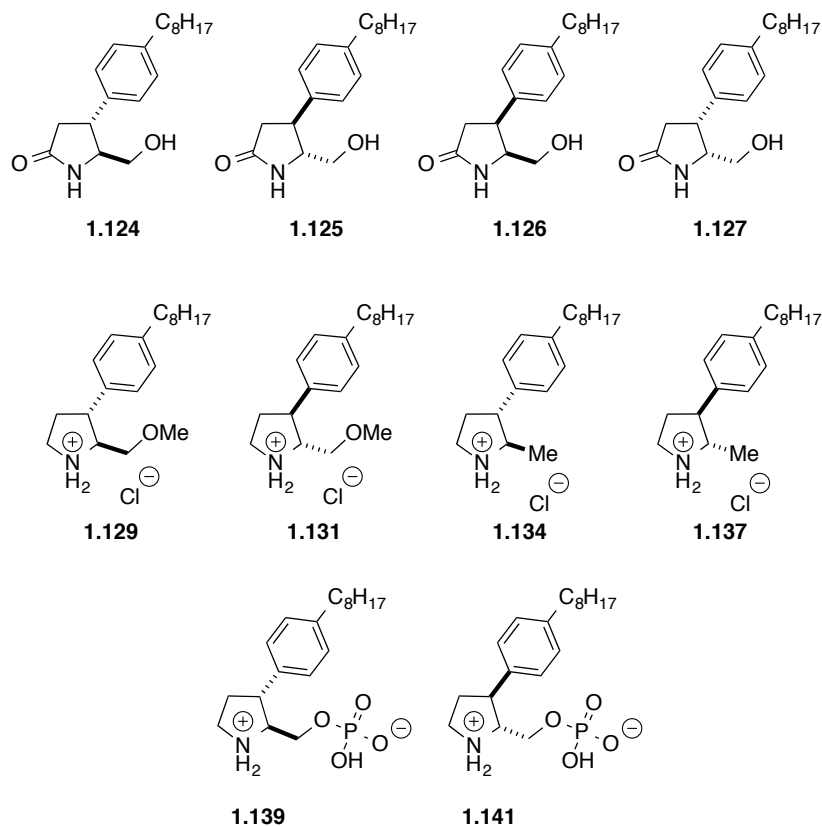
**Scheme 36.** Synthesis of (*R*)-3-arylpyrrolidine **1.175**.



In summary, we have prepared a series of constrained *C*-arylpyrrolidine analogues (Figure 8). These include all the diastereomers of the 2-hydroxymethyl-3- and 4-arylpyrrolidine, 3-arylpyrrolidine, 2-hydroxymethyl-3-aryl-lactam analogues, as well as several 2,3-substituted pyrrolidine analogues with modified 2-hydroxymethyl arm.

**Figure 8.** List of synthesized constrained C-aryl substituted pyrrolidine analogues.

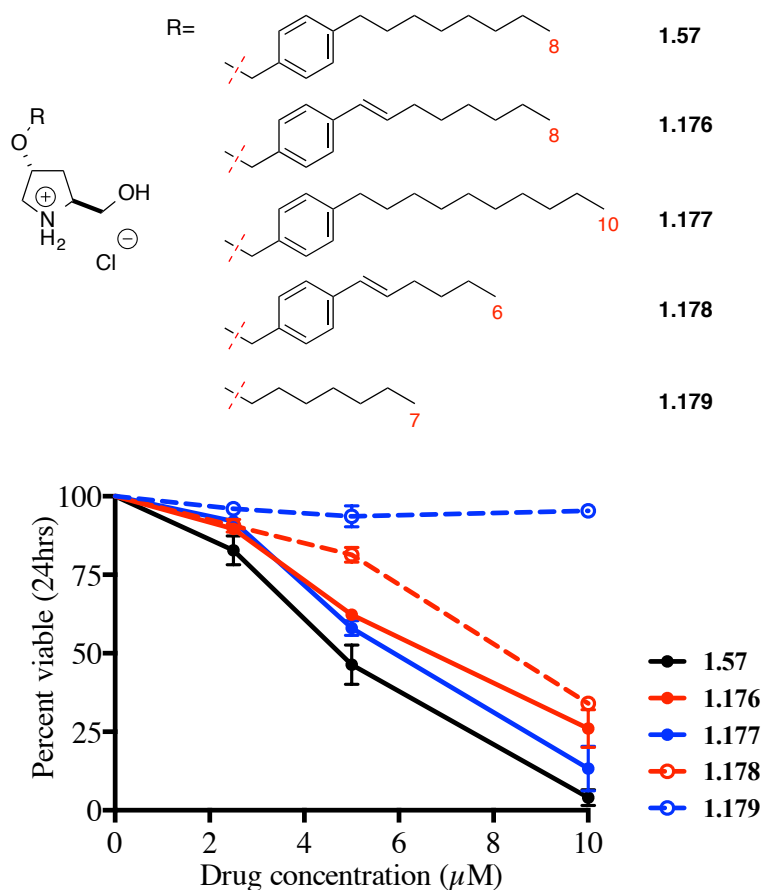




### 1-2-3 Biological evaluations of constrained *O*-arylmethyl substituted pyrrolidine analogues

We collaborated with Professor Edinger at the University of California-Irvine to evaluate the biological activities of our synthetic compounds (Figure 6) against various cancer cell lines. Firstly, the importance of the *O*-arylmethyl C-8 alkyl chain was studied. A series of analogues with modified aliphatic chain moieties were prepared by Dr. Rebecca Fransson (Figure 9).<sup>120</sup> These analogues were evaluated using cell viability assays with a murine hematopoietic FL5.12 cell line (Figure 9). Limiting the flexibility of the C-8 alkyl chain by introducing unsaturation (*e.g.*, **1.176**), and extending the chain length to a C-10 chain (*e.g.*, **1.177**), led to a slight decrease in activity compared to **1.57**. An obvious reduction in activity was observed in the shorter C-6 unsaturated chain (*e.g.*, **1.178**). Removal of the phenyl group (*e.g.*, **1.179**) resulted in a dramatic loss of activity. The *O*-benzyl group tethered to a C-8 alkyl chain was thus crucial for maintaining activity.

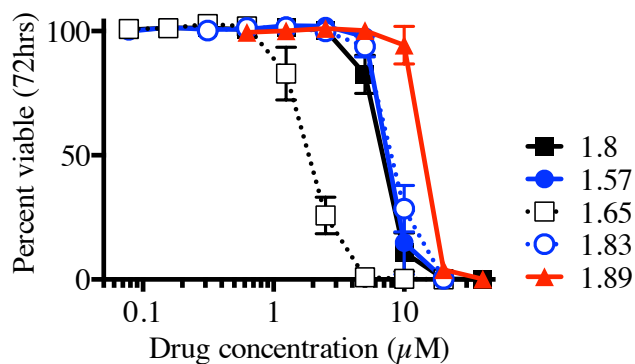
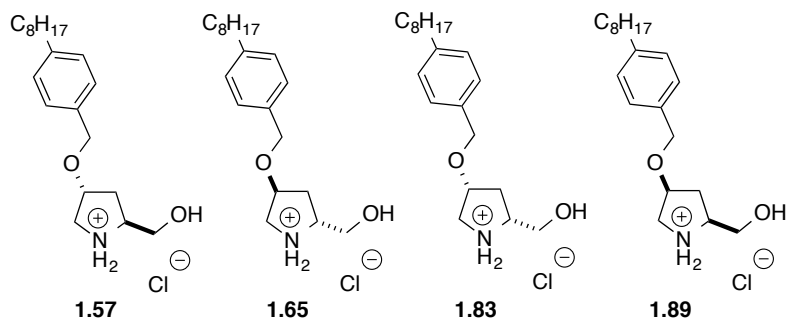




Cell viability was measured by vital dye exclusion and flow cytometry at 72h.

**Figure 9.** Cytotoxic action of different alkyl chain substituted L-prolinol analogues on murine hematopoietic FL5.12 cells.<sup>120</sup>

The constrained *O*-arylmethylpyrrolidine analogues were then tested in cell viability assays using Sup-B15, a Ph<sup>+</sup> ALL cell line. All the 2-hydroxymethyl-4-*O*-arylmethylpyrrolidine analogues induced leukemia cell death as efficiently as FTY720 (**1.8**) (Figure 10).<sup>120</sup> Among these, the *trans*-analogue **1.65** exhibited a 3-fold increase in efficacy compared to FTY720 (**1.8**), and a 4-fold increase compared to its enantiomer **1.57**. *cis*-Analogues were less active compared to the *trans*-isomers, especially **1.89**, which showed an 8-fold decrease in activity compared to **1.65**. These results indicated that constrained analogues could enhance the anticancer potency compared to FTY720 (**1.8**). The shape of the molecule, due to different stereochemistry of the benzyl ether appendage and the hydroxymethyl arm, has great influence on its anti-leukemia ability.

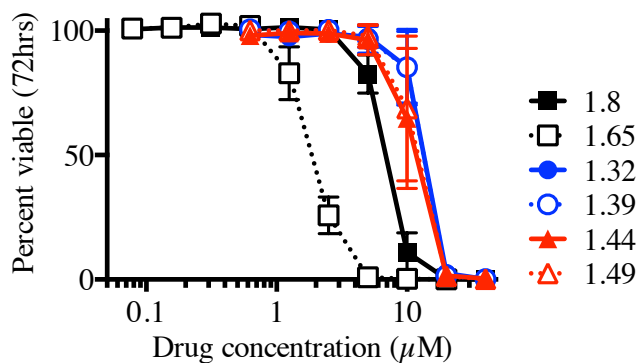
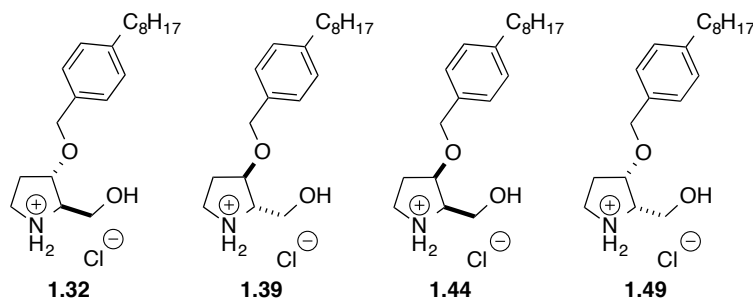


	<b>1.8</b>	<b>1.57</b>	<b>1.65</b>	<b>1.83</b>	<b>1.89</b>
Sup-B15	6.8 ± 0.7	7.7 ± 0.8	2.0 ± 0.2	8.3 ± 0.8	16.7 ± 2.4

Mean IC<sub>50</sub> (in μM +/- SEM). Cell viability was measured by vital dye exclusion and flow cytometry at 72h.

**Figure 10.** Cytotoxic action of diastereomeric 2-hydroxymethyl-4-*O*-arylmethylpyrrolidinium analogues on Sup-B15 leukemia cells.<sup>120</sup>

Next, the 2-hydroxymethyl-3-*O*-arylmethylpyrrolidinium analogues were evaluated (Figure 11). These analogues killed Sup-15 cells efficiently, but compared to **1.65**, they were 5 ~ 6 fold less active. Interestingly, their stereochemistry did not have much effect on their anti-leukemia activities as in the previously mentioned 2,4-substituted series. Thus, the high activity of **1.65** was caused by its unique structure, stereochemistry, and spatial orientation of the benzyl ether appendage and hydroxymethyl group.



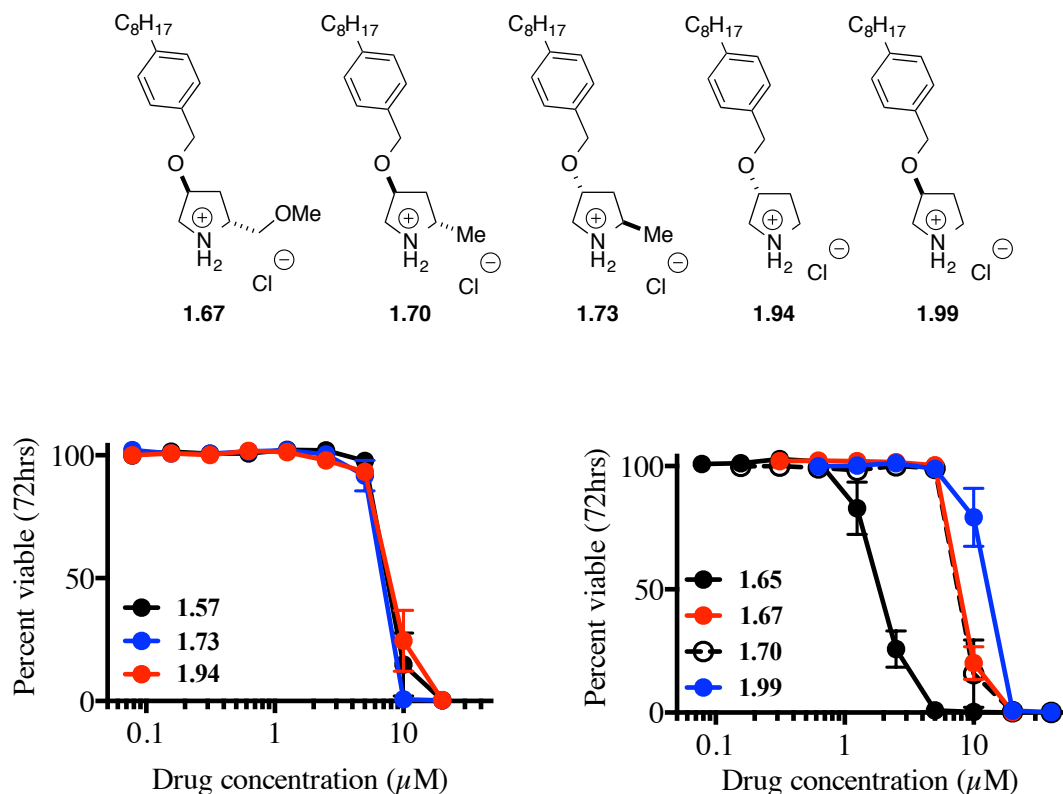
	<b>1.8</b>	<b>1.65</b>	<b>1.32</b>	<b>1.39</b>	<b>1.44</b>	<b>1.49</b>
Sup-B15	6.8 ± 0.7	2.0 ± 0.2	13.9 ± 2.2	12.9 ± 1.1	10.7 ± 2.0	11.0 ± 2.0

Mean IC<sub>50</sub> (in µM +/- SEM). Cell viability was measured by vital dye exclusion and flow cytometry at 72h.

**Figure 11.** Cytotoxic action of diastereomeric 2-hydroxymethyl-3-*O*-arylmethylpyrrolidine analogues on Sup-B15 leukemia cells.<sup>120</sup>

Although the 2-hydroxymethyl constrained analogues (**1.32**, **1.39**, **1.44**, **1.49**, **1.57**, **1.65**, **1.83** and **1.89**) showed good activities against Sup-B15 leukemia cells, their *in vivo* anticancer efficacies could be limited due to the chance of phosphorylation to activate S1P<sub>1</sub> and S1P<sub>3</sub> receptors, which could induce bradycardia. Taking the two most active analogues **1.57** and **1.65**, a series of analogues with modified hydroxymethyl arms was prepared (Figure 12). For **1.57**, there was almost no detrimental effect for either removal of the hydroxyl group (**1.73**) or the entire removal of the hydroxymethyl group (**1.94**). For the analogue **1.65**, protection and removal of the hydroxyl group (**1.67**, **1.70** and **1.99**) reduced activity. These results demonstrated that phosphorylation was not necessary to induce the death of Sup-B15 leukemia cells, In the case of **1.65**, a free hydroxyl group gave however the most active analogue. Recent results from the Edinger group have revealed that compound **1.77**, the

phosphate of **1.65**, appeared to further enhance the *in vitro* antileukemic activity without causing bradycardia (private communication, see discussion).



	<b>1.57</b>	<b>1.65</b>	<b>1.73</b>	<b>1.67</b>	<b>1.70</b>	<b>1.94</b>	<b>1.99</b>
Sup-B15	7.7 ± 0.8	2.0 ± 0.2	6.5 ± 0.3	8.1 ± 1.0	9.0 ± 1.0	8.1 ± 0.9	11.5 ± 0.7

Mean IC<sub>50</sub> (in μM ± SEM). Cell viability was measured by vital dye exclusion and flow cytometry at 72h.

**Figure 12.** Cytotoxic action of 2-methoxymethyl- and 2-methyl-4-*O*-arylmethylpyrrolidine analogues, and 3-*O*-arylmethylpyrrolidine analogues on Sup-B15 leukemia cells.<sup>120</sup>

Intrigued by the high activity of **1.65**, compared to its diastereomeric analogues, against Sup-B15 leukemia cells, it was evaluated against several other cancer cell lines (Table 2),<sup>120</sup> and **1.65** proved the most active analogue against another BCR-ABL positive ALL cell line, BV173. It also showed the best activity, with a 10-fold increase in activity compared to **1.57** against cell line BM-P190, a transformed murine bone marrow cell line bearing the BCR-ABL fusion protein p190. Against the other three non BCR-ABL fused protein expressed ALL cell lines (CCRF-CEM, Nalm-6 and Blin-1), **1.65** did not exhibit an obvious advantage

compared to the other analogues (**1.57**, **1.83** and **1.89**). In addition, **1.65** was active against the prostate cancer cell lines PC3 and DU145, but it was not as efficient as FTY720 (**1.8**). Thus, the effect of **1.65** seems to have a connection with the expression of BCR-ABL-fused protein, which was associated with CML and ALL. Several BCR-ABL tyrosine kinase inhibitors have been discovered to treat CML,<sup>133</sup> such as the well-known Imatinib (Gleevec),<sup>134</sup> which prolongs the survival of CML significantly. The constrained analogue **1.65** showed the potency necessary to be potentially used in clinical studies of BCR-ABL positive ALL.

**Table 2.** Mean IC<sub>50</sub> (in  $\mu\text{M}$  +/- SEM) of analogs in cell viability assays in a range of human cancer cell lines and BCR-Abl-expressing murine bone marrow (BM).<sup>120</sup>

	SupB15	BM-p190	BV173	CCRF-CEM	Nalm-6	Blin-1	PC3	DU145
	Ph+ ALL		Ph+ ALL	Ph- ALL	Ph- ALL	Ph- ALL	Prostate	Prostate
<b>1.8</b>	6.8 ± 0.7	3.3 ± 0.2	6.3 ± 0.4	6.8 ± 0.3	9.6 ± 1.9	5.5 ± 0.1	9.8 ± 0.9	6.5 ± 0.9
<b>1.57</b>	7.7 ± 0.8	5.7 ± 1.1	10.4 ± 0.7	11.0 ± 1.3	15.0 ± 2.1	7.5 ± 0.1	14.3 ± 1.2	10.8 ± 0.4
<b>1.65</b>	2.0 ± 0.2	0.5 ± 0.1	3.8 ± 0.4	8.2 ± 0.7	13.5 ± 2.4	6.9 ± 0.3	13.5 ± 2.6	15.1 ± 1.0
<b>1.83</b>	8.3 ± 0.8	4.0 ± 0.4	9.7 ± 1.0	8.1 ± 1.4				
<b>1.89</b>	16.7 ± 2.4	8.4 ± 1.5	13.8 ± 0.8	11.6 ± 1.1				

Viability was measured by vital dye exclusion and flow cytometry at 72 h.

Since the early studies of the anticancer effect of FTY720 (**1.8**), Edinger has found that FTY720 (**1.8**) could selectively starve cancer cells to death by down regulating nutrient transporter proteins.<sup>108</sup> Thus, these constrained analogues were also evaluated to see if they killed cancer cells through same mechanism as FTY720 (**1.8**) (Figure 13). In the assay of surface expression of 4F2hc, all of the constrained analogues **1.57**, **1.65**, **1.70**, and **1.73**, as well as FTY720 (**1.8**), induced rapid down-regulation of the amino acid transporter-associated

protein 4F2hc, which indicated that these novel constrained analogues were working through a common mechanism involving starving the cancer cells to death.

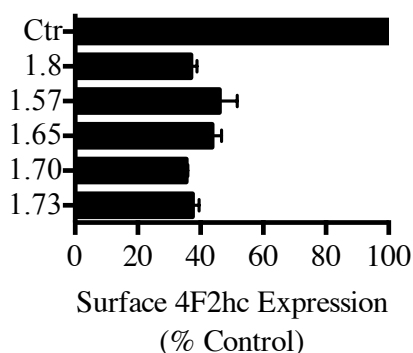
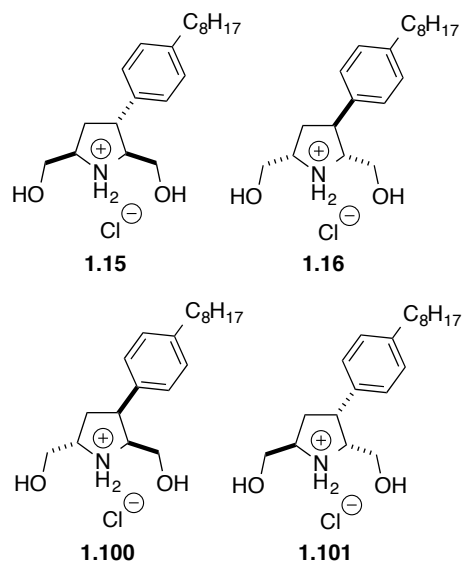


**Figure 13.** Diastereomeric 2-hydroxymethyl- and 2-methyl-4-*O*-arylmethylpyrrolidine (10  $\mu$ M) trigger nutrient transporter loss in Sup-B15 leukemia cells.

### 1-2-4 Biological evaluations of constrained *C*-aryl substituted pyrrolidine analogues

Although the constrained *O*-arylmethylpyrrolidine analogues showed greatly enhanced anti-leukemia activities compared to FTY720 (**1.8**) (Table 2), they were less efficient toward other types of cancer cell lines (PC3 and DU145). On the other hand, Charron's original *C*-aryl analogues<sup>119</sup> **1.15** and **1.16** were active against the prostate cancer cell lines (PC3 and DU145). To determine the relationship between stereochemistry and activity, as studied in the *O*-arylmethyl pyrrolidine analogues, two new synthetic 2,5-bis(hydroxymethyl)-3-arylpiperidine analogues (**1.100** and **1.101**) were synthesized and tested in a Cell Titer Glo assay (Figure 14). Compound **1.16**, which was shown previously to not be phosphorylated by SphK,<sup>119</sup> had same activities in both prostate cancer cell lines compared to **1.15**. The new analogues **1.100** and **1.101** showed similar *in vitro* activities against prostate cancer cell lines as **1.15** and **1.16**. Thus, the stereochemistry of 2,3,5-trisubstituted analogues had little effect on their activity against prostate cancer cell lines, but the stereochemistry was important for the compounds to be phosphorylated by SphK.<sup>119</sup>

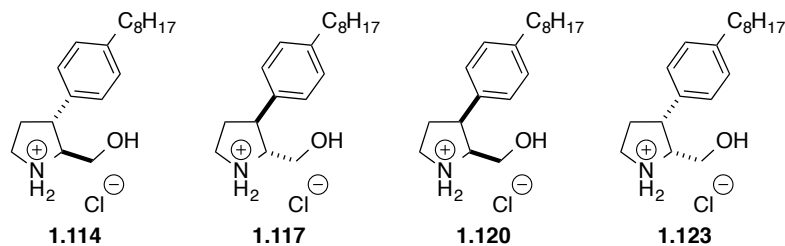


	FTY720 (1.8)	1.15	1.16	1.100	1.101
PC3	2.6 ± 0.2	7.0 ± 0.3	6.1 ± 1.0	3.4 ± 0.6	4.9 ± 0.6
DU145	3.2 ± 0.2	7.3 ± 0.8	5.7 ± 0.4	4.1 ± 0.6	5.3 ± 0.2

Values in  $\mu\text{M}$ , Mean  $\pm$  SEM is shown,  $n \geq 3$ .

**Figure 14.**  $\text{IC}_{50}$  values of 2,5-bis(hydroxymethyl)-3-arylpyrrolidinium analogues in prostate cancer cell lines.

Next, the 2-hydroxymethyl-3-arylpyrrolidinium analogues were evaluated for activity against prostate cancer cell lines (Figure 15). Compared to the 2,3,5-trisubstituted *C*-aryl analogues, these analogues are without a second hydroxymethyl arm. They retained the anti-prostate cancer activities as for 2,3,5-trisubstituted *C*-aryl analogues. Although **1.114** and **1.117** had better activities compared to the other two diastereomers, **1.120** and **1.123**, the configurations of the members in this series was not as important as in the *O*-arylmethyl substituted pyrrolidinium analogues in influencing the anti-cancer activities.

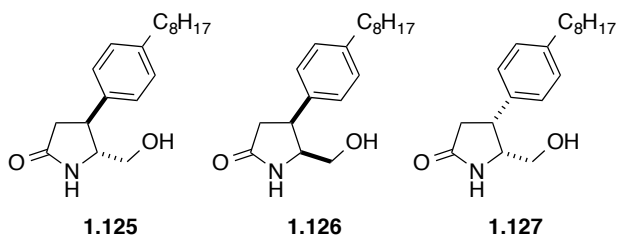


	<b>1.114</b>	<b>1.117</b>	<b>1.120</b>	<b>1.123</b>
PC3	4.0 ± 0.7	3.0 ± 0.4	6.5 ± 0.3	5.5 ± 0.7
DU145	3.8 ± 0.4	3.7 ± 0.4	5.4 ± 0.3	5.3 ± 0.7

Values in  $\mu\text{M}$ , Mean  $\pm$  SEM is shown,  $n \geq 3$ .

**Figure 15.**  $\text{IC}_{50}$  values of 2-hydroxymethyl-3-arylpyrrolidinium analogues in prostate cancer cell lines.

Meanwhile, the corresponding lactams of 2-hydroxymethyl-3-arylpyrrolidinium analogues were tested to see if the ammonium was important for the activity (Figure 16). The anti-prostate cancer activities were lost for all the lactams indicating that a charged nitrogen on the pyrrolidinium ring was crucial for anticancer activity likely through an electrostatic interaction with the target receptor.



	<b>1.125</b>	<b>1.126</b>	<b>1.127</b>
PC3	>20	>20	>20
DU145	>20	>20	>20

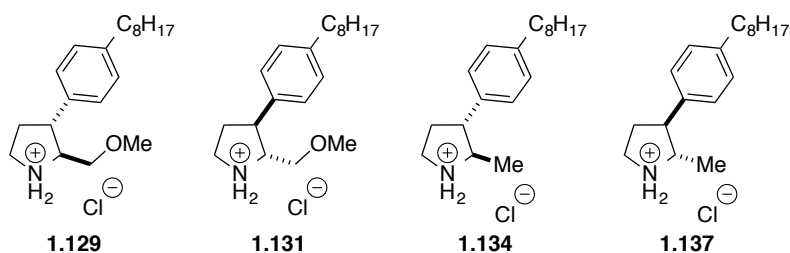
Values in  $\mu\text{M}$ , Mean  $\pm$  SEM is shown,  $n \geq 3$ .

**Figure 16.**  $\text{IC}_{50}$  values of 2-hydroxymethyl-3-aryl-lactam analogues in prostate cancer cell lines.

Considering that **1.114** and **1.117** showed as good anti-prostate cancer activities as FTY720 (**1.8**) (Figure 15), we wanted to know if they could be phosphorylated, and whether



their activities were associated with phosphorylation. Preliminary results suggested that **1.114** was phosphorylated to a similar degree as FTY720 (**1.8**) in PC3 and SW620 cells. Furthermore, analogues **1.114** and **1.117** activated only weakly S1P<sub>1</sub>, and were not substrates for the other S1P<sub>2,3,4,5</sub> receptors. Similar losses of activity at S1P receptors were observed in tests of the corresponding synthetic phosphates **1.139** and **1.141**. In order to eliminate any possibility of phosphorylation, a series of new **1.114** and **1.117** analogues (**1.129**, **1.131**, **1.134** and **1.137**) with modified hydroxymethyl groups were evaluated (Figure 17). Methyl ethers **1.129** and **1.131**, and methyl analogues **1.134** and **1.137** exhibited activities against prostate cancer cell lines which were as good as compounds **1.114** and **1.117**. This indicated further that the hydroxyl group and its phosphorylation were not crucial for the anti-cancer activity.

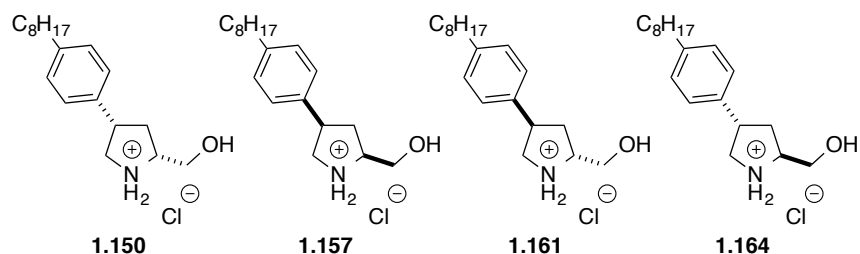


	<b>1.129</b>	<b>1.131</b>	<b>1.134</b>	<b>1.137</b>
PC3	6.3 ± 0.3	1.9 ± 0.3	4.4 ± 0.6	4.1 ± 0.4
DU145	5.9 ± 0.3	5.6 ± 0.1	5.1 ± 0.6	5.0 ± 0.1

Values in  $\mu\text{M}$ , Mean  $\pm$  SEM is shown,  $n \geq 3$ .

**Figure 17.** IC<sub>50</sub> values of 2-methoxymethyl- and 2-methyl-3-arylpyrrolidine analogues in prostate cancer cell lines.

Another series of 2,4-substituted pyrrolidine analogues were tested to investigate the importance of the relative positions of the phenyl side chain appendage and the hydroxymethyl arm (Figure 18). Against prostate cancer cell lines, **1.150**, **1.157** and **1.161** retained as good activities as the 2-hydroxymethyl-3-aryl substituted pyrrolidine analogues, and **1.164** was less active. This suggested that the relative position of the substituents on the pyrrolidine core could affect the anticancer activity in this series.

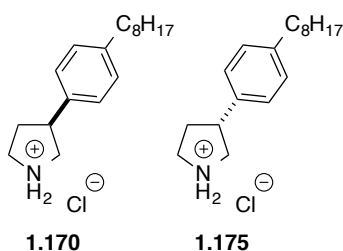


	<b>1.150</b>	<b>1.157</b>	<b>1.161</b>	<b>1.164</b>
PC3	6.6 ± 0.1	4.3 ± 0.3	6.4 ± 0.1	9.8 ± 1.3
DU145	5.8 ± 0.2	4.9 ± 0.1	6.8 ± 0.1	10.6 ± 1.0

Values in  $\mu\text{M}$ , Mean +/- SEM is shown,  $n \geq 3$ .

**Figure 18.**  $\text{IC}_{50}$  values of 2-hydroxymethyl-4-arylpyrrolidinium analogues in prostate cancer cell lines.

Simplification of the structure by removal of the hydroxymethyl group resulted in 3-arylpyrrolidinium analogues **1.170** and **1.175**, which exhibited moderate anti-prostate cancer activities (Figure 19). The hydroxyl group was thus not crucial for the anti-cancer activity. In general, analogues **1.114**, **1.117** and their modified analogue **1.131**, that cannot be phosphorylated by SphK, have potency that merits be further study in the treatment of prostate cancer.



	<b>1.170</b>	<b>1.175</b>
PC3	5.7 ± 0.1	5.5 ± 0.1
DU145	5.1 ± 0.1	5.0 ± 0.1

Values in  $\mu\text{M}$ , Mean +/- SEM is shown,  $n \geq 3$ .

**Figure 19.**  $\text{IC}_{50}$  values of 3-arylpyrrolidinium analogues in prostate cancer cell lines.

The *C*-aryl substituted pyrrolidinium analogues were also evaluated against several other cancer cell lines (Table 3). These analogues (**1.100**, **1.114**, **1.117** and **1.131**) exhibited as broad

anticancer activity as FTY720 (**1.8**) against colon cancer cell line (SW-620), lung cancer cell line (A-549), pancreas cancer cell lines (PANC-1), and breast cancer cell (MDA-MB-231). The *O*-arylmethyl substituted pyrrolidine analogues (*e.g.*, **1.57** and **1.65**) were less active in these cancer cell lines. Against for the leukemia cell line (SupB-15), the *C*-aryl substituted analogues had activities; however, **1.65** was still the most active analogue in the two series.

**Table 3.** IC<sub>50</sub> values in other cancer cell lines.

	<b>SW-620</b>	<b>A-549</b>	<b>PANC-1</b>	<b>MDA-MB-231</b>	<b>SupB-15</b>
	Colon	Lung	Pancreas	Breast	Leukemia
FTY720 ( <b>1.8</b> )	2.8 ± 0.1	6.0 ± 0.4	4.6 ± 0.5	4.0 ± 0.1	6.8 ± 0.7
<b>1.100</b>	2.6 ± 0.0	4.7 ± 0.6	3.5 ± 0.3	4.6 ± 0.5	ND
<b>1.114</b>	2.5 ± 0.1	8.9 ± 1.4	3.3 ± 0.5	2.1 ± 0.2	5.1 ± 0.9
<b>1.117</b>	2.1 ± 0.2	8.4 ± 1.2	5.0 ± 0.9	4.9 ± 0.6	5.9 ± 0.1
<b>1.131</b>	2.7 ± 0.2	7.8 ± 1.8	4.8 ± 0.6	4.0 ± 0.0	7.5 ± 0.4
<b>1.57</b>	7.0 ± 1.2	10.7 ± 0.2	8.0 ± 1.5	9.1 ± 0.3	7.7 ± 0.8
<b>1.65</b>	4.9 ± 0.9	9.5 ± 1.1	8.8 ± 0.6	6.4 ± 0.4	2.0 ± 0.2

Values in μM, Mean +/- SEM is shown, n≥3. SupB-15 viability was determined by flow cytometry, Cell Titer Glo assays were performed with the other cell lines. ND, not determined.

Analogues **1.110**, **1.114** and **1.117** were tested for the surface expression of 4F2hc at their IC<sub>50</sub>, and at twice this dose (Figure 20). As expected, these analogues, as well as FTY720 (**1.8**), triggered down-regulation of the amino acid transporter-associated protein 4F2hc at their IC<sub>50</sub>, and consistently at 2X IC<sub>50</sub>. This indicated that these *C*-aryl substituted pyrrolidine analogues killed cancer cells through the same “starve to death” mechanism.

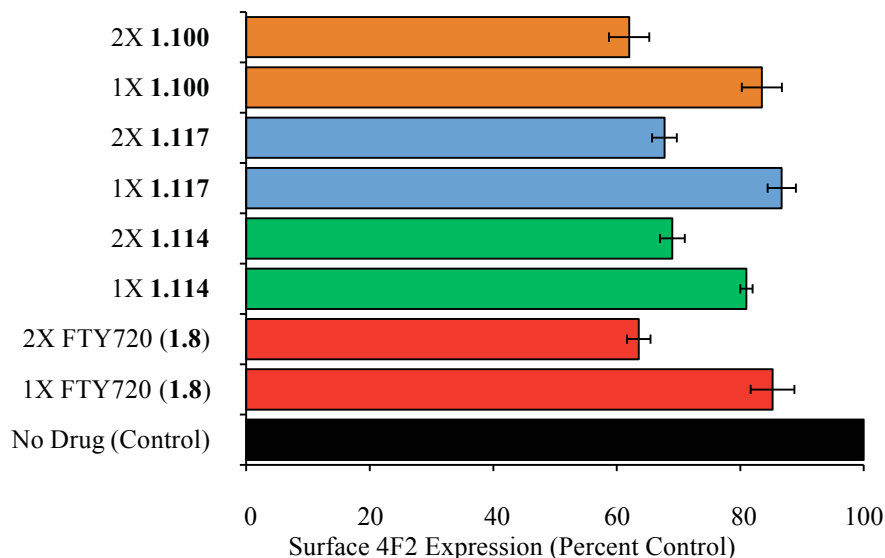


**Figure 20.** Nutrient transporter down-regulation in PC3 cells at 1X or 2X the IC<sub>50</sub>.

### 1-2-5 Discussion

Among the *O*-arylmethylpyrrolidine analogues, **1.57** and **1.65** were found to kill cancer cells by down-regulating nutrient transporters to starve cancer cells to death (Figure 13). Recent studies from the Huwiler group, in Bern, showed that **1.57** and **1.65** did not activate S1P<sub>1,2,4</sub> receptors, however, **1.57** could be partially phosphorylated by both SphK1 and SphK2, and **1.65** can be efficiently phosphorylated *in vivo* and *in vitro*, especially by SphK2. Further studies of the corresponding phosphates, **1.75** and **1.77**, indicated that these phosphates could activate S1P<sub>1,2,3,5</sub> receptors *in vitro*. The phosphates were active against the SupB-15 leukemia cell line (Figure 21). Furthermore, in the assay of surface expression of 4F2hc, no down-regulation of the amino acid transporter-associated protein 4F2hc was observed, up to 20 μM dose (Figure 22). Thus, phosphates **1.75** and **1.77** may act through another mechanism to kill the leukemia cells. The activity of **1.65** was actually enhanced by phosphorylation. Moreover, **1.75** and **1.77** could be dephosphorylated by cells, and their anti-leukemia activities may in fact be due to corresponding alcohols **1.57** and **1.65**, not the phosphates themselves. These results demonstrate that the anti-cancer mechanisms of **1.57** and **1.65** are complex, and merit study to identify their targets, especially for the most active analogue, **1.65**.

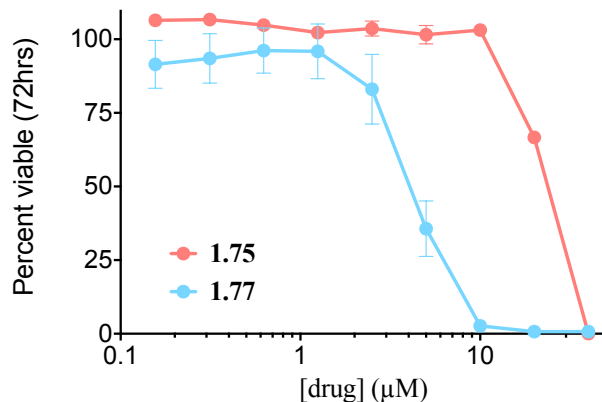


**Figure 21.** Cytotoxic action of phosphates **1.75** and **1.77** on Sup-B15 leukemia cells.

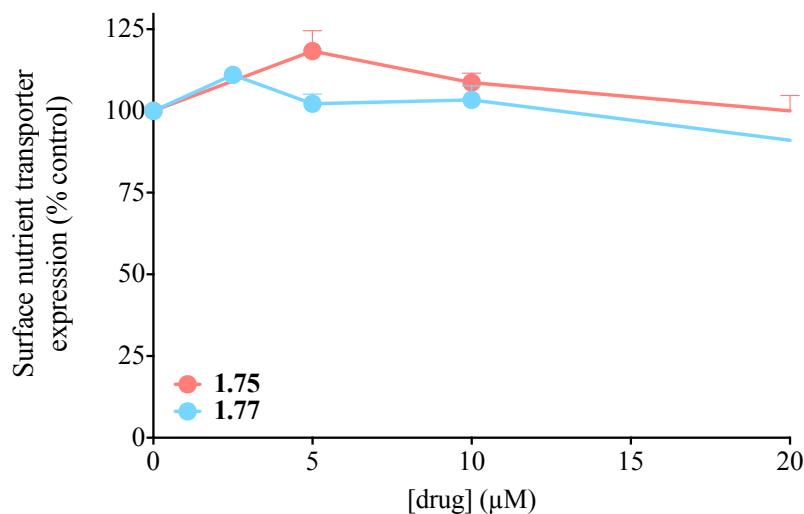


**Figure 22.** Nutrient transporter down-regulation of phosphates **1.75** and **1.77** in Sup-B15 leukemia cells.

### 1-3 Conclusion

In conclusion, we have synthesized two series of constrained FTY720 analogues, including all of the diastereomers of 2,3-, 2,4-, and 3-substituted pyrrolidine analogues, as well as a subset of these analogues with modified hydroxymethyl groups to limit the possibility of phosphorylation. Many of these analogues exhibited good anticancer activities in *in vitro* studies. The *O*-arylmethylpyrrolidine analogues were active against the BCR-ABL

positive ALL cancer cells, especially compound **1.65**, which showed the highest activity against the SupB-15 leukemia cell line among all the analogues, with a 3-fold increase in efficacy compared to FTY720 (**1.8**). The *C*-aryl pyrrolidine series were broadly active against human prostate, leukemia, colon, breast, and pancreatic cancer cell lines. Certain analogues (*e.g.*, **1.129**, **1.131**, **1.134** and **1.137**) were active without phosphorylation by SphK, exhibiting potency to be further studied in the treatment of cancer without inducing bradycardia.

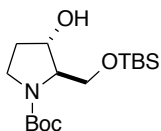
The mechanistic studies suggested that certain contained analogues killed cancer cells through the same bioenergetic mechanism as FTY720 proposed by Edinger.<sup>111</sup> By down-regulation of nutrient transporters, these analogues starved the cancer cells to death; however, their mechanism of action is still unclear. Photo-affinity labeling techniques have thus been used to find the target protein, and will be discussed in chapter 2.

The promising *in vitro* results of analogues **1.65**, **1.114**, and **1.129** have led to their examination *in vivo* in mice, and these experiments are now in progress.

## 1-4 Experimental

All non-aqueous reactions were run in flame-dried glassware under a positive pressure of argon. Anhydrous solvents were distilled under positive pressure of dry argon before use and dried by standard methods.<sup>135</sup> THF, ether, CH<sub>2</sub>Cl<sub>2</sub> and toluene were dried by passage through solvent delivery systems, commercial grade reagents were used without further purification. Reactions were monitored by *S*-2 analytical thin-layer chromatography (TLC) performed on pre-coated, glass-backed silica gel plates. Visualization of the developed chromatogram was performed by UV absorbance (wave length: 254 nm), and staining TLC plates with aqueous cerium ammonium molybdate, or aqueous potassium permanganate solution. Flash chromatography<sup>136</sup> was performed on 230-400 mesh silica gel with the indicated solvent systems. Nuclear magnetic resonance spectra (NMR) were recorded at 300, 400, 500 and 700 MHz spectrometers. Chemical shifts for <sup>1</sup>H NMR spectra are recorded in parts per million (ppm) from tetramethylsilane with the solvent resonance as the internal standard (CDCl<sub>3</sub> δ 7.27 ppm, CD<sub>3</sub>OD, δ 3.31 ppm, D<sub>2</sub>O, δ 4.80 ppm). Data are reported as

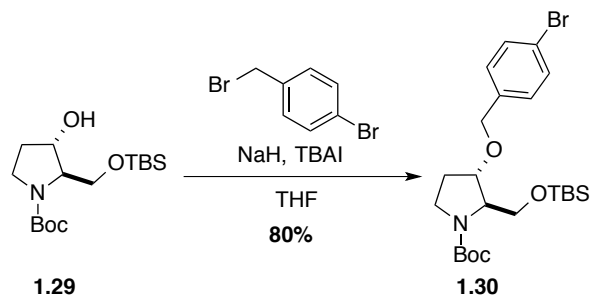
follows: chemical shift, multiplicity (s = singlet, d = doublet, t = triplet, q = quartet, quint = quintet, m = multiplet, and br = broad), coupling constants ( $J$ ) are reported in Hz, and integration. Chemical shifts for  $^{13}\text{C}$  NMR spectra are recorded in parts per million from tetramethylsilane using the central peak of the solvent resonance as the internal standard ( $\text{CDCl}_3$ ,  $\delta$  77.00 ppm,  $\text{CD}_3\text{OD}$ ,  $\delta$  49.00 ppm). All spectra were obtained with complete proton decoupling. Optical rotations were determined in a 1 dm cell at 589 nm at 20 °C. Data are reported as follows:  $[\alpha]_{\text{D}}$ , concentration ( $c$  in g/100 mL), and solvent. High-resolution mass spectra were performed using fast atom bombardment (FAB) or electrospray (ESI) techniques. Low-resolution mass spectra were obtained using electrospray ionization technique (ESI). Purity analysis was assessed by LC/MS. HPLC conditions: (A) The column used was an YMC ODS-AQ, 2.0 x 50 mm, particle size 3 $\mu$ ; the eluents were  $\text{H}_2\text{O}$  with 0.1 % formic acid and ACN 0.1 % formic acid; the gradient started at 20 % organic, then increased to 95 % in 6 minutes and stays at 95 % for another 1.5 min; the flow was set at 0.35 mL / min; UV det. 214 nm. (B) The column used was an SUNFIRE™ C18, 2.1 x 50 mm, particle size 3.5  $\mu$ ; the eluents were  $\text{H}_2\text{O}$  with 0.1 % formic acid and MeOH 0.1 % formic acid; the gradient started at 80 % organic, then increased to 95 % in 10 minutes and stays at 95 % for another 2.0 min; the flow was set at 0.40 mL / min; UV det. 214 nm; (C) The column used was an SUNFIRE™ C18, 2.1 x 50 mm, particle size 3.5  $\mu$ ; the gradient started at 50 % organic, then increased to 95 % in 10 minutes and stays at 95 % for another 2.0 min; the flow was set at 0.40 mL / min; UV det. 214 nm. (D) The column used was an Atlantis C18, 150 x 4.6 mm; the eluents were  $\text{H}_2\text{O}$  with 0.13 % formic acid and MeOH 0.13 % formic acid; the gradient started at 30 % organic, then increased to 95 % in 8 minutes and stays at 95 % for another 10 min; flow was set at 0.30 mL / min.



1.29

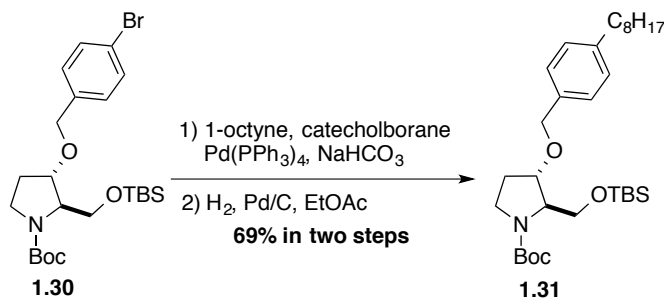
***tert*-Butyl (2*R*,3*S*)-2-(((*tert*-butyldimethylsilyl)oxy)methyl)-3-hydroxypyrrolidine-**

**1-carboxylate (1.29)** was synthesized from **1.26** according to the procedure report by Evano.<sup>121</sup> Spectroscopic data were in agreement with the proposed structures and matched those reported in the literature.<sup>121,137</sup>



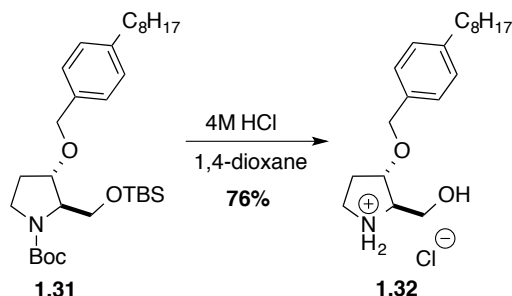
**tert-Butyl (2R,3S)-3-((4-bromobenzyl)oxy)-2-(((tert-butyldimethylsilyl)oxy)methyl)pyrrolidine-1-carboxylate (1.30).** Alcohol **1.29** (63 mg, 0.19 mmol) was dissolved in dry THF (1.3 mL). The solution was purged with argon, cooled to 0°C and treated with NaH (60 % in mineral oil, 23 mg, 0.57 mmol). The mixture was stirred for 30 min and treated sequentially with 4-bromobenzyl bromide (143 mg, 0.57 mmol) and TBAI (7 mg, 0.02 mmol). The reaction mixture was allowed to warm to room temperature and was stirred for 2 days. The reaction was quenched with water, diluted with EtOAc and washed with water and brine, dried over MgSO<sub>4</sub> and filtrated. The solvent was removed under reduced pressure and the residue was purified by flash chromatography (hexane: EtOAc, 12:1 to 8:1) to give **1.30** (76 mg, 80 %) as pale yellow oil. <sup>1</sup>H NMR (400 MHz, CDCl<sub>3</sub>): δ 7.47 (d, *J* = 8.0 Hz, 2H), 7.20 (d, *J* = 8.4 Hz, 2H), 4.48 (m, 2H), 4.07 (m, 1H), 3.94-3.74 (m, 2H), 3.61-3.35 (m, 3H), 1.99 (m, 2H), 1.46 (s, 9H), 0.87 (d, *J* = 4.0 Hz, 9H), 0.05 (s, 3H), 0.03 (d, *J* = 4.0 Hz, 3H); <sup>13</sup>C NMR (100 MHz, mixture of rotamers, CDCl<sub>3</sub>): δ 154.8, (154.7), 137.5, 131.6, (129.4), 129.3, 121.5, 81.3, (80.8), 79.7, (79.3), 69.8, 64.6, (64.2), 62.6, (62.2), (45.5), 45.1, 30.2, 28.8, 28.7, (28.6), 26.0, -5.6, -5.7; [α]<sub>D</sub> (-) 11.8° (*c* 1.60, CHCl<sub>3</sub>); HRMS (ESI) calcd for C<sub>23</sub>H<sub>38</sub>BrNNaO<sub>4</sub>Si [M+Na]<sup>+</sup> 522.1646, found 522.1659.



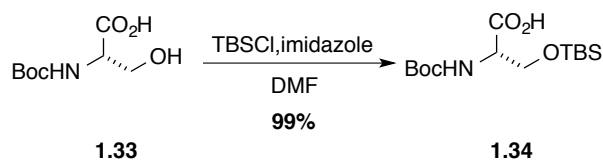


***tert*-Butyl (2*R*,3*S*)-2-(((*tert*-butyldimethylsilyloxy)methyl)-3-((4-octylbenzyl)oxy)**

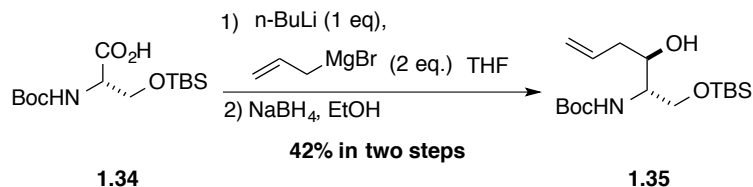
**pyrrolidine-1-carboxylate (1.31).** A solution of 1-octyne (31  $\mu$ L, 0.21 mmol) and catecholborane (1.0 M in THF, 0.21 mL, 0.21 mmol) was heated at reflux at 70  $^{\circ}$ C for 2 h under argon atmosphere, and cooled to room temperature. A solution of **1.30** (70 mg, 0.14 mmol) in DME (1.7 mL) was added to the reaction mixture followed by Pd(PPh<sub>3</sub>)<sub>4</sub> (5.0 mg, 0.004 mmol) and 1N aqueous NaHCO<sub>3</sub> (1.1 mL). The reaction mixture was heated at reflux with vigorous stirring for 4 h, cooled to room temperature and treated with a brine solution. The mixture was extracted three times with Et<sub>2</sub>O. The combined organic layers were dried over NaSO<sub>4</sub> and filtered. The filtrate was evaporated under reduced pressure and the residue was purified by flash chromatography (hexane: EtOAc, 10:1 to 8:1) to give pale yellow oil. The oil was dissolved in EtOAc (2.6 mL) treated with Pd/C (10 %, 15 mg, 0.014 mmol) and placed under an atmosphere of hydrogen by evacuation of the flask and refilling with H<sub>2</sub> gas. After completion of the hydrogenation as indicated by TLC (R<sub>f</sub>: 0.65, hexane: EtOAc, 4:1), the reaction mixture was filtered through a pipette containing a layer of Celite<sup>TM</sup> over a plus of cotton. The filtrate was evaporated under reduced pressure to give alkane **1.31** (53 mg, 69 % in two steps) as pale yellow oil. <sup>1</sup>H NMR (400 MHz, CDCl<sub>3</sub>):  $\delta$  7.24 (d,  $J$  = 8.0 Hz, 2H), 7.15 (d,  $J$  = 7.6 Hz, 2H), 4.50 (m, 2H), 4.10 (m, 1H), 3.81-3.74 (m, 2H), 3.64-3.35 (m, 3H), 2.59 (t,  $J$  = 7.6 Hz, 2H), 2.01 (m, 2H), 1.60 (m, 2H), 1.46 (d,  $J$  = 2.4 Hz, 9H), 1.28 (m, 10H), 0.87 (m, 12H), 0.05 (s, 3H), 0.03 (d,  $J$  = 4.4 Hz, 3H); <sup>13</sup>C NMR (100 MHz, mixture of rotamers, CDCl<sub>3</sub>):  $\delta$  (154.8), 154.7, 142.5, 135.6, 128.6, (127.9), 127.8, 81.1, (80.6), 79.5, (79.2), 70.6, 64.6, (64.3), 62.8, (62.3), (45.6), 45.2, 35.8, 32.0, (31.7), 30.2, 29.6, 29.5, 29.4, 28.8, 28.7, (28.7), 26.0, 22.8, 18.3, 14.2, -5.6, -5.7; [ $\alpha$ ]<sub>D</sub> (-) 13.0 $^{\circ}$  ( $c$  1.46, CHCl<sub>3</sub>); HRMS (ESI) calcd for C<sub>31</sub>H<sub>55</sub>NNaO<sub>4</sub>Si [M+Na]<sup>+</sup> 556.3793, found 556.3797.



**(2*R*,3*S*)-2-(Hydroxymethyl)-3-((4-octylbenzyl)oxy)pyrrolidin-1-ium chloride (1.32).** A 4M solution of HCl in 1,4-dioxane (1.4 mL, 5.6 mmol) was added to a flask with **1.31** (15 mg, 0.028 mmol) and the solution was stirred at room temperature until completion was showed by TLC (3h,  $R_f$ : 0.42,  $\text{CH}_2\text{Cl}_2$ : EtOH, 4:1). The volatiles were removed under reduced pressure. The residue was dissolved in 1,4-dioxane (2 mL) and the volatiles were evaporated to remove the residual HCl. The crude mixture was purified by flash chromatography ( $\text{CH}_2\text{Cl}_2$ : EtOH, 4:1 to 1:1) to give yellow oil. The oil was dissolved in water, filtered through a plastic syringe filter (pore size: 0.45  $\mu\text{m}$ ), and lyophilized to give hydrochloride **1.32** (7.6 mg, 76 %) as pale yellow solid.  $^1\text{H}$  NMR (400 MHz,  $\text{D}_2\text{O}$ ):  $\delta$  7.15 (d,  $J = 8.0$  Hz, 2H), 6.94 (d,  $J = 8.0$  Hz, 2H), 4.37, 4.34 (ABq,  $J = 11.8$  Hz, 2H), 3.97 (m, 1H), 3.73-3.58 (m, 3H), 3.38-3.24 (m, 2H), 2.37 (t,  $J = 7.6$  Hz, 2H), 2.07 (m, 1H), 1.94 (m, 1H), 1.38 (m, 2H), 1.23 (s. br, 10H), 0.88 (t,  $J = 6.4$  Hz, 3H);  $^{13}\text{C}$  NMR (100 MHz,  $\text{D}_2\text{O}$ ):  $\delta$  141.4, 134.6, 127.7, 78.2, 70.4, 64.7, 58.4, 43.7, 35.1, 31.5, 31.0, 29.6, 29.2, 29.1, 29.0, 22.2, 13.5;  $[\alpha]_D^{25}$  (+) 35.0° ( $c$  0.12, MeOH); HRMS (ESI) calcd for  $\text{C}_{20}\text{H}_{34}\text{NO}_2$   $[\text{M}+\text{H}]^+$  320.2584, found 320.2592. HPLC: condition (A),  $t_R = 5.99$  min; purity: > 99 %.

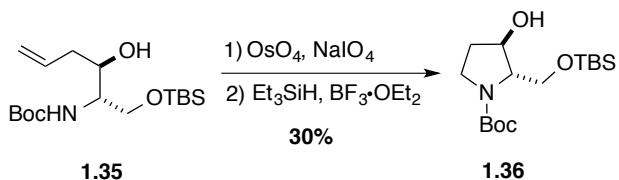


***N*-(*tert*-Butoxycarbonyl)-*O*-(*tert*-butyldimethylsilyl)-*L*-serine (1.34)** was obtained as pale yellow, sticky oil (7.7 g, 99 %) from *N*-(Boc)-*L*-serine **1.33** (4.0 g, 0.038 mol).<sup>121</sup> Spectroscopic data were in agreement with the proposed structure and matched those reported in the literature.<sup>138</sup>



***tert*-Butyl ((2*S*,3*R*)-1-((*tert*-butyldimethylsilyloxy)-3-hydroxyhex-5-en-2-yl)**

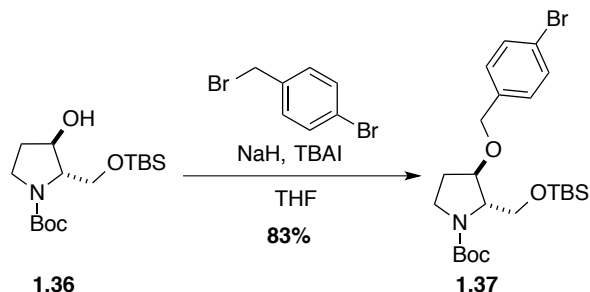
**carbamate (1.35)** was obtained as colorless oil (0.90 g, 42 % over two steps) from **1.34** (2.0 g, 6.3 mmol).<sup>121</sup> <sup>1</sup>H NMR (400 MHz, CDCl<sub>3</sub>): δ 5.87-5.79 (m, 1H), 5.24 (d, *J* = 8.0 Hz, 1H), 5.14-5.09 (m, 2H), 3.96 (dd, *J* = 2.8, 10.4 Hz, 1H), 3.78 (dd, *J* = 2.0, 10.4 Hz, 1H), 3.71 (quint, *J* = 7.2 Hz, 1H), 3.54 (br. m, 1H), 3.07 (d, *J* = 8.0 Hz, 1H), 2.33 (t, *J* = 6.4 Hz, 2H), 1.43 (s, 9H), 0.89 (s, 9H), 0.07 (s, 6H); <sup>13</sup>C NMR (100 MHz, CDCl<sub>3</sub>): δ 155.8, 134.7, 117.9, 79.5, 72.9, 63.3, 53.8, 39.4, 28.5, 25.9, 18.3, -5.7, -5.7; [α]<sub>D</sub> (+) 32.2° (*c* 1.32, CHCl<sub>3</sub>); HRMS (ESI) calcd for C<sub>17</sub>H<sub>35</sub>NNaO<sub>4</sub>Si [M+Na]<sup>+</sup> 368.2228, found 368.2238.



***tert*-Butyl (2*S*,3*R*)-2-(((*tert*-butyldimethylsilyloxy)methyl)-3-hydroxypyrrolidine-**

**1-carboxylate (1.36)** was obtained as white solid (230 mg, 30 %) from **1.35** (800 mg, 2.32 mmol).<sup>121</sup> Spectroscopic data were in agreement with the proposed structures and matched those reported in the literature.<sup>137</sup>

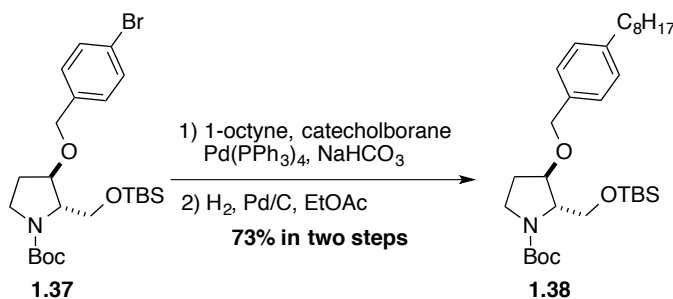
Compound **1.37** was obtained according to the procedure for synthesizing **1.30**.



***tert*-Butyl (2*S*,3*R*)-3-((4-bromobenzyl)oxy)-2-(((*tert*-butyldimethylsilyloxy)methyl)**

**pyrrolidine-1-carboxylate (1.37)** was obtained as pale yellow oil (75 mg, 83 %) from **1.36** (60 mg, 0.18 mmol).  $^1\text{H}$  NMR (400 MHz,  $\text{CDCl}_3$ ):  $\delta$  7.45 (d,  $J = 7.6$  Hz, 2H), 7.20 (d,  $J = 8.4$  Hz, 2H), 4.47 (m, 2H), 4.07 (m, 1H), 3.94-3.73 (m, 2H), 3.60-3.35 (m, 3H), 2.00 (m, 2H), 1.46 (s, 9H), 0.87 (d,  $J = 4.4$  Hz, 9H), 0.04 (s, 3H), 0.03 (d,  $J = 4.0$  Hz, 3H);  $^{13}\text{C}$  NMR (100 MHz,  $\text{CDCl}_3$ ):  $\delta$  (154.8), 154.7, (137.5), 137.4, 131.6, (129.3), 129.2, 121.5, 81.3, (80.8), 79.6, (79.3), 69.8, 64.5, (64.2), 62.7, (62.2), (45.5), 45.1, 30.2, 28.8, 28.7, (28.7), 25.9, -5.6, -5.7;  $[\alpha]_{\text{D}}^{25}$  (+) 10.6° ( $c$  1.08,  $\text{CHCl}_3$ ); HRMS (ESI) calcd for  $\text{C}_{23}\text{H}_{38}\text{BrNNaO}_4\text{Si}$   $[\text{M}+\text{Na}]^+$  522.1646, found 522.1645.

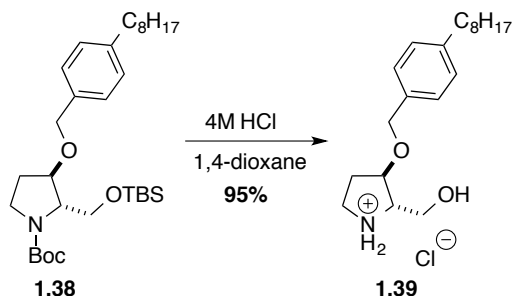
Compound **1.38** was obtained according to the procedure for synthesizing **1.31**.



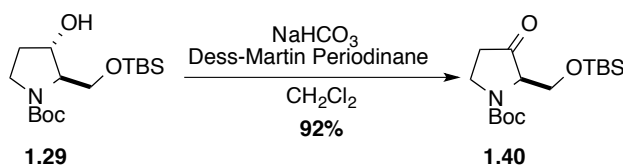
***tert*-Butyl (2*S*,3*R*)-2-(((*tert*-butyldimethylsilyl)oxy)methyl)-3-((4-octylbenzyl)oxy)**

**pyrrolidine-1-carboxylate (1.38)** was obtained as pale yellow oil (55 mg, 73 % over two steps) from **1.37** (70 mg, 0.14 mmol).  $^1\text{H}$  NMR (400 MHz,  $\text{CDCl}_3$ ):  $\delta$  7.24 (d,  $J = 8.0$  Hz, 2H), 7.15 (d,  $J = 7.6$  Hz, 2H), 4.50 (m, 2H), 4.10 (m, 1H), 3.97-3.74 (m, 2H), 3.64-3.35 (m, 3H), 2.59 (t,  $J = 7.6$  Hz, 2H), 2.02 (m, 2H), 1.60 (m, 2H), 1.47 (d,  $J = 2.8$  Hz, 9H), 1.29 (m, 10H), 0.88 (m, 12H), 0.05 (s, 3H), 0.03 (d,  $J = 4.4$  Hz, 3H);  $^{13}\text{C}$  NMR (100 MHz,  $\text{CDCl}_3$ ):  $\delta$  (154.8), 154.7, 142.5, 135.6, 128.6, (127.9), 127.8, 81.1, (80.6), 79.5, (79.2), 70.6, 64.6, (64.3), 62.8, (62.3), (45.6), 45.2, 35.8, 32.1, (31.7), 30.2, 29.6, 29.4, 29.4, 28.8, 28.7, (28.7), 26.0, 22.8, 18.3, 14.2, -5.6, -5.7;  $[\alpha]_{\text{D}}^{25}$  (+) 14.4° ( $c$  0.45,  $\text{CHCl}_3$ ); HRMS (ESI) calcd for  $\text{C}_{31}\text{H}_{55}\text{NNaO}_4\text{Si}$   $[\text{M}+\text{Na}]^+$  556.3793, found 556.3810.

Compound **1.39** was obtained according to the procedure for synthesizing **1.32**.

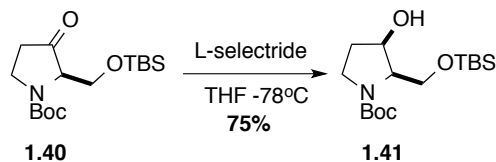


**(2*S*,3*R*)-2-(Hydroxymethyl)-3-((4-octylbenzyl)oxy)pyrrolidin-1-ium chloride (1.39)** was obtained as yellow solid (19.0 mg, 95 %) from **1.38** (30 mg, 0.056 mmol). <sup>1</sup>H NMR (400 MHz, D<sub>2</sub>O): δ 7.10 (d, *J* = 4.8 Hz, 2H), 6.94 (d, *J* = 6.8 Hz, 2H), 4.34-4.25 (m, 2H), 3.91 (s. br, 1H), 3.69-3.57 (m, 3H), 3.28-3.20 (m, 2H), 2.30 (br, 2H), 2.00 (m, 1H), 1.85 (m, 1H), 1.39 (br, 2H), 1.21 (br, 10H), 0.87 (t, *J* = 6.0 Hz, 3H); <sup>13</sup>C NMR (100 MHz, D<sub>2</sub>O): δ 141.0, 134.8, 127.5, 78.4, 70.3, 64.7, 58.6, 43.7, 35.2, 31.6, 31.1, 29.7, 29.4, 29.3, 29.2, 22.3, 13.5; [α]<sub>D</sub> (-) 30.0° (*c* 0.14, MeOH); HRMS (ESI) calcd for C<sub>20</sub>H<sub>34</sub>NO<sub>2</sub> [M+H]<sup>+</sup> 320.2584, found 320.2591. HPLC: condition (A), *t*<sub>R</sub> = 6.01 min; purity: > 99 %.



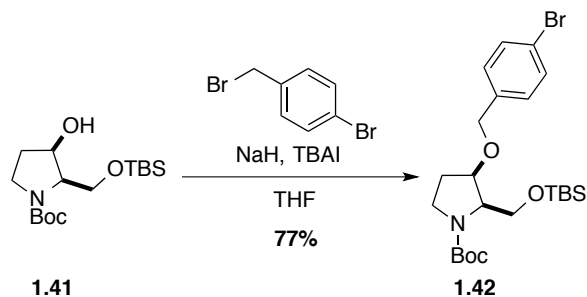
***tert*-Butyl (*R*)-2-(((*tert*-butyldimethylsilyl)oxy)methyl)-3-oxopyrrolidine-1-carboxylate (1.40)**. Solid NaHCO<sub>3</sub> (134 mg, 1.60 mmol) followed by Dess–Martin periodinane (134 mg, 0.32 mmol) were added to a solution of alcohol **1.29** (70 mg, 0.21 mmol) in CH<sub>2</sub>Cl<sub>2</sub> (1.0 mL) at room temperature. The resulting mixture was stirred for 1.5 h, when no more starting material was observed by TLC (*R*<sub>f</sub> = 0.50, hexane: EtOAc, 4:1). A saturated aqueous Na<sub>2</sub>S<sub>2</sub>O<sub>3</sub> solution was added to the mixture. The organic layer was separated. The aqueous layer was extracted with CH<sub>2</sub>Cl<sub>2</sub>. The combined organic layers were washed with brine, dried over MgSO<sub>4</sub>, filtered and concentrated under reduced pressure. The residue was purified by flash chromatography (hexane: EtOAc, 12:1 to 8:1) to give ketone **1.40** (64 mg, 92 %) as pale yellow oil. <sup>1</sup>H NMR (400 MHz, CDCl<sub>3</sub>): δ 4.17-3.77 (m, 4H), 3.63 (m, 1H), 2.50 (m, 2H), 1.47 (s, 9H), 0.83 (s, 9H), 0.02 (s, 3H) 0.01 (s, 3H); <sup>13</sup>C NMR (100 MHz, CDCl<sub>3</sub>): δ 213.6, (213.1), 154.3, 80.4, (80.2), 64.3, (64.0), 63.5, (62.5), (43.2), 42.6,

(37.1), 36.6, 28.6, 25.9, 18.2, -5.8, -6.0;  $[\alpha]_D$  (-) 144.9° (*c* 0.37, CHCl<sub>3</sub>); HRMS (ESI) calcd for C<sub>16</sub>H<sub>31</sub>NNaO<sub>4</sub>Si [M+Na]<sup>+</sup> 352.1915, found 352.1921.



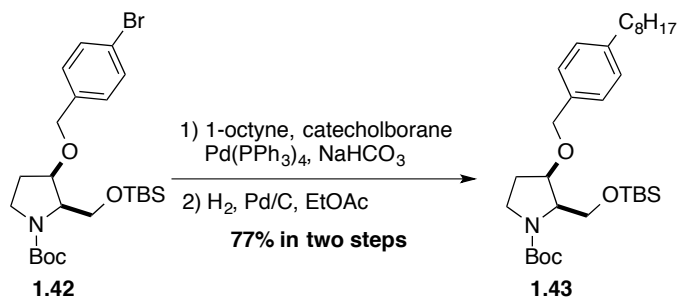
***tert*-Butyl (2*R*,3*R*)-2-(((*tert*-butyldimethylsilyloxy)methyl)-3-hydroxypyrrolidine-**

**1-carboxylate (1.41).** L-Selectride (1M in THF, 0.27 mL, 0.27 mmol) was added to a THF (1.8 mL) solution of **1.40** (60 mg, 0.18 mmol) at -78 °C. The resulting solution was stirred for 1 h at this temperature, when starting material was observed by TLC ( $R_f$  = 0.32, hexane: EtOAc, 4:1). A saturated aqueous NH<sub>4</sub>Cl was then added to the solution. The organic layer was separated. The aqueous layer was extracted with EtOAc. The combined organic layers were washed with brine, dried over MgSO<sub>4</sub>, filtered and concentrated under reduced pressure. The residue was purified by flash chromatography (hexane: EtOAc, 5:1) to give alcohol **1.41** (45 mg, 75 %) as colorless oil. <sup>1</sup>H NMR (400 MHz, CDCl<sub>3</sub>): δ 4.45 (m, 1H), 4.12-3.76 (m, 3H), 3.54-3.37 (m, 3H), 2.06 (m, 1H), 1.92 (m, 1H), 1.45 (s, 9H), 0.89 (s, 9H), 0.08 (s, 3H), 0.07 (s, 3H). <sup>13</sup>C NMR (100 MHz, CDCl<sub>3</sub>): δ = 154.7, (79.8), 79.5, (73.4), 73.0, (62.4), 61.8, 59.9, 44.6, (44.0), 33.8, (32.8), 28.6, 25.9, 18.1, -5.7;  $[\alpha]_D$  (-) 61.4° (*c* 0.28, CHCl<sub>3</sub>); HRMS (ESI) calcd for C<sub>16</sub>H<sub>33</sub>NNaO<sub>4</sub>Si [M+Na]<sup>+</sup> 354.2071, found 354.2073.



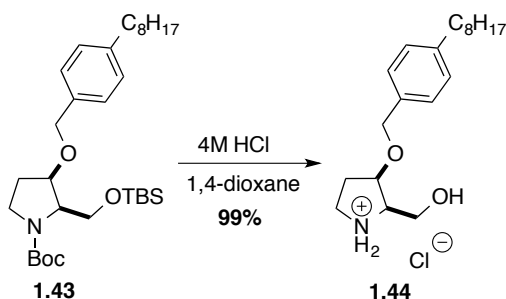
***tert*-Butyl (2*R*,3*R*)-3-((4-bromobenzyl)oxy)-2-(((*tert*-butyldimethylsilyloxy)methyl)-pyrrolidine-1-carboxylate (1.42)** was obtained as colorless oil (46 mg, 77 %) from **1.41** (40 mg, 0.12 mmol) according to the procedure previously described for synthesizing **1.30**. <sup>1</sup>H NMR (400 MHz, CDCl<sub>3</sub>): δ 7.46 (d, *J* = 8.4 Hz, 2H), 7.23 (d, *J* = 8.4 Hz, 2H), 4.54 (m, 2H),

4.10 (m, 1H), 3.92-3.85 (m, 3H), 3.41-3.28 (m, 2H), 2.15-2.08 (m, 1H), 2.04-1.97 (m, 1H), 1.47 (s, 9H), 0.89 (s, 9H), 0.05 (s, 3H), 0.03 (s, 3H);  $^{13}\text{C}$  NMR (100 MHz,  $\text{CDCl}_3$ ):  $\delta$  154.6, 137.7, 131.5, 129.0, 121.4, 79.6, (79.3), 78.5, (77.7), 71.2, 60.5, 59.8, (59.2), (44.2), 43.8, 36.7, 29.8, (29.1), (28.7), 26.0, 24.8, (23.5), 18.3, -5.7;  $[\alpha]_{\text{D}}^{25}$  (-) 11.9° (c 0.64,  $\text{CHCl}_3$ ); HRMS (ESI) calcd for  $\text{C}_{23}\text{H}_{38}\text{BrNNaO}_4\text{Si}$   $[\text{M}+\text{Na}]^+$  522.1646, found 522.1658.



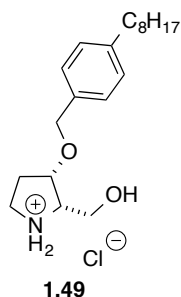
***tert*-Butyl (2*R*,3*R*)-2-(((*tert*-butyldimethylsilyloxy)methyl)-3-((4-octylbenzyl)oxy)**

**pyrrolidine-1-carboxylate (1.43)** was obtained as pale yellow oil (29 mg, 77 % over two steps) from **1.42** (35 mg, 0.06 mmol) according to the procedure previously described for synthesizing **1.31**.  $^1\text{H}$  NMR (400 MHz,  $\text{CDCl}_3$ ):  $\delta$  7.25 (d,  $J = 8.0$  Hz, 2H), 7.15 (d,  $J = 8.0$  Hz, 2H), 4.56 (m, 2H), 4.10 (m, 1H), 3.97-3.81 (m, 3H), 3.51-3.26 (m, 2H), 2.60 (t,  $J = 7.6$  Hz, 2H), 2.21-2.10 (m, 1H), 2.08-2.00 (m, 1H), 1.61 (m, 2H), 1.47 (s, 9H), 1.28 (m, 10H), 0.89 (m, 12H), 0.06 (s, 3H), 0.04 (s, 3H);  $^{13}\text{C}$  NMR (100 MHz,  $\text{CDCl}_3$ ):  $\delta$  154.7, 142.5, 135.8, 128.5, 127.6, 79.5, (79.2), 78.1, 71.9, 60.5, 59.7, (59.1), (44.2), 43.8, 35.8, 32.0, (31.7), 29.8, 29.6, 29.5, 29.4, 29.1, 28.7, 26.1, (25.9), 22.8, 18.3, 14.3, -5.6;  $[\alpha]_{\text{D}}^{25}$  (-) 9.8° (c 1.33,  $\text{CHCl}_3$ ); HRMS (ESI) calcd for  $\text{C}_{31}\text{H}_{55}\text{NNaO}_4\text{Si}$   $[\text{M}+\text{Na}]^+$  556.3793, found 556.3790.

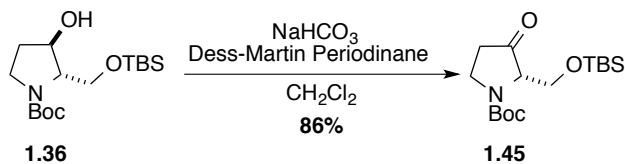


**(2*R*,3*R*)-2-(Hydroxymethyl)-3-((4-octylbenzyl)oxy)pyrrolidin-1-ium chloride (1.44)** was obtained as yellow solid (9.3 mg, 99 %) from **1.43** (14 mg, 0.026 mmol) according to the

procedure for synthesizing **1.32**.  $^1\text{H}$  NMR (400 MHz,  $\text{D}_2\text{O}$ ):  $\delta$  7.12 (d,  $J = 7.2$  Hz, 2H), 6.94 (d,  $J = 7.6$  Hz, 2H), 4.42 (d,  $J = 12.0$  Hz, 1H), 4.25 (d,  $J = 12.0$  Hz, 1H), 4.08 (m, 1H), 3.87-3.79 (m, 2H), 3.61 (m, 1H), 3.36-3.33 (m, 2H), 2.37 (t,  $J = 7.6$  Hz, 2H), 2.10 (m, 1H), 1.97 (m, 1H), 1.39 (m, 2H), 1.24 (s. br, 10H), 0.88 (t,  $J = 6.4$  Hz, 3H);  $^{13}\text{C}$  NMR (100 MHz,  $\text{D}_2\text{O}$ ):  $\delta$  141.3, 134.9, 127.7, 127.3, 76.6, 70.1, 64.0, 57.2, 42.7, 35.1, 31.5, 31.0, 29.2, 29.2, 29.0, 29.0, 22.3, 13.5;  $[\alpha]_{\text{D}}$  (-)  $29.0^\circ$  ( $c$  0.10, MeOH); HRMS (ESI) calcd for  $\text{C}_{20}\text{H}_{34}\text{NO}_2$   $[\text{M}+\text{H}]^+$  320.2584, found 320.2587. HPLC: condition (A),  $t_{\text{R}} = 5.97$  min; purity:  $> 99\%$ .

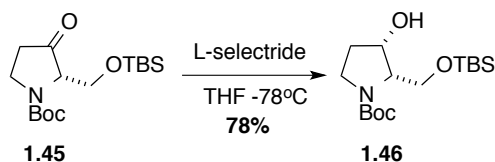


Ketone **1.49** was obtained according to the procedure for synthesizing **1.44**.



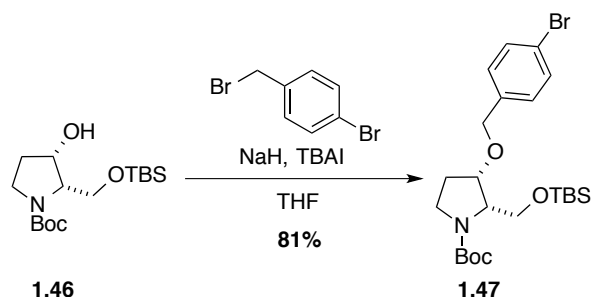
**tert-Butyl (S)-2-(((tert-butyl dimethylsilyl)oxy)methyl)-3-oxopyrrolidine-1-**

**carboxylate (1.45)** was obtained (60 mg, 86 %) as pale yellow oil from alcohol **1.36** (70 mg, 0.21 mmol).  $^1\text{H}$  NMR (400 MHz,  $\text{CDCl}_3$ ):  $\delta$  4.19-3.78 (m, 4H), 3.63 (m, 1H), 2.50 (m, 2H), 1.49 (s, 9H), 0.85 (s, 9H), 0.02 (s, 3H) 0.01 (s, 3H);  $^{13}\text{C}$  NMR (100 MHz,  $\text{CDCl}_3$ ):  $\delta$  213.6, (213.2), 154.3, 80.4, (80.2), 64.3, (64.1), 63.6, (62.6), (43.2), 42.6, (37.1), 36.6, 28.6, 25.9, 18.2, -5.8, -5.9;  $[\alpha]_{\text{D}}$  (+)  $150.0^\circ$  ( $c$  0.24,  $\text{CHCl}_3$ ); HRMS (ESI) calcd for  $\text{C}_{16}\text{H}_{31}\text{NNaO}_4\text{Si}$   $[\text{M}+\text{Na}]^+$  352.1915, found 352.1919.

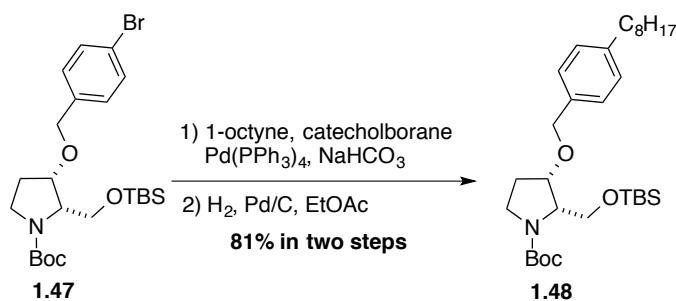




***tert*-Butyl (2*S*,3*S*)-2-(((*tert*-butyldimethylsilyl)oxy)methyl)-3-hydroxypyrrolidine-1-carboxylate (1.46)** was obtained (39 mg, 78 %) as colorless oil from **1.45** (50 mg, 0.15 mmol). <sup>1</sup>H NMR (400 MHz, CDCl<sub>3</sub>): δ 4.45 (m, 1H), 4.12-3.76 (m, 3H), 3.54-3.36 (m, 3H), 2.06 (m, 1H), 1.92 (m, 1H), 1.45 (s, 9H), 0.89 (s, 9H), 0.08 (s, 3H), 0.07 (s, 3H). <sup>13</sup>C NMR (100 MHz, CDCl<sub>3</sub>): δ 154.6, (154.5), (79.8), 79.4, (73.4), 73.0, (62.4), 61.8, 59.9, (59.8), 44.6, (44.0), 33.8, (32.8), 28.6, 25.9, 18.1, -5.8; [α]<sub>D</sub> (+) 66.7° (*c* 0.21, CHCl<sub>3</sub>); HRMS (ESI) calcd for C<sub>16</sub>H<sub>33</sub>NNaO<sub>4</sub>Si [M+Na]<sup>+</sup> 354.2071, found 354.2080.

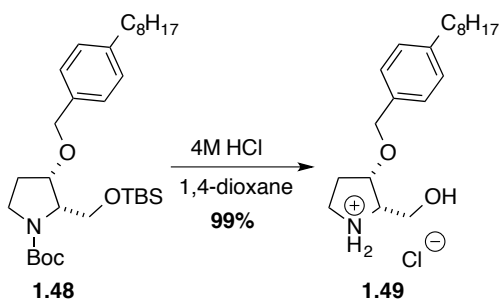


***tert*-Butyl (2*S*,3*S*)-3-((4-bromobenzyl)oxy)-2-(((*tert*-butyldimethylsilyl)oxy)methyl)pyrrolidine-1-carboxylate (1.47)** was obtained as colorless oil (43 mg, 81 %) from **1.46** (35 mg, 0.11 mmol). <sup>1</sup>H NMR (400 MHz, CDCl<sub>3</sub>): δ 7.46 (d, *J* = 8.4 Hz, 2H), 7.23 (d, *J* = 8.0 Hz, 2H), 4.54 (m, 2H), 4.10 (m, 1H), 3.92-3.85 (m, 3H), 3.41-3.28 (m, 2H), 2.15-2.08 (m, 1H), 2.05-2.00 (m, 1H), 1.47 (s, 9H), 0.89 (s, 9H), 0.05 (s, 3H), 0.03 (s, 3H); <sup>13</sup>C NMR (100 MHz, CDCl<sub>3</sub>): δ 154.7, 137.7, 131.5, 129.0, 121.4, 79.6, (79.3), 78.5, (77.8), 71.2, 60.5, 59.8, (59.2), (44.2), 43.8, 36.8, 29.8, (29.1), (28.7), 26.0, 24.8, (23.5), 18.3, -5.7; [α]<sub>D</sub> (+) 10.7° (*c* 0.30, CHCl<sub>3</sub>); HRMS (ESI) calcd for C<sub>23</sub>H<sub>38</sub>BrNNaO<sub>4</sub>Si [M+Na]<sup>+</sup> 522.1646, found 522.1656.

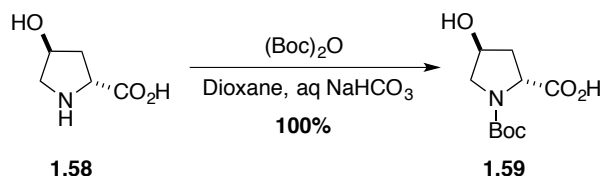


***tert*-Butyl (2*S*,3*S*)-2-(((*tert*-butyldimethylsilyl)oxy)methyl)-3-((4-octylbenzyl)oxy)**

**pyrrolidine-1-carboxylate (1.48)** was obtained as pale yellow oil (30 mg, 81 % over two steps) from **1.47** (35 mg, 0.06 mmol).  $^1\text{H}$  NMR (400 MHz,  $\text{CDCl}_3$ ):  $\delta$  7.26 (d,  $J = 8.0$  Hz, 2H), 7.15 (d,  $J = 8.0$  Hz, 2H), 4.56 (m, 2H), 4.10 (m, 1H), 3.92-3.81 (m, 3H), 3.41-3.24 (m, 2H), 2.60 (t,  $J = 7.6$  Hz, 2H), 2.19-2.09 (m, 1H), 2.04-2.01 (m, 1H), 1.60 (m, 2H), 1.46 (s, 9H), 1.29 (m, 10H), 0.89 (m, 12H), 0.06 (s, 3H), 0.04 (s, 3H);  $^{13}\text{C}$  NMR (100 MHz,  $\text{CDCl}_3$ ):  $\delta$  154.7, 142.5, 135.8, 128.5, 127.6, 79.5, (79.2), 78.1, 71.9, 60.5, 59.7, (59.1), (44.2), 43.8, 35.8, 32.0, (31.7), 29.8, 29.6, 29.5, 29.4, 29.1, 28.7, 26.1, (25.9), 22.8, 18.3, 14.3, -5.6;  $[\alpha]_{\text{D}}^{25}$  (+) 9.5° ( $c$  1.37,  $\text{CHCl}_3$ ); HRMS (ESI) calcd for  $\text{C}_{31}\text{H}_{55}\text{NNaO}_4\text{Si}$   $[\text{M}+\text{Na}]^+$  556.3793, found 556.3789.

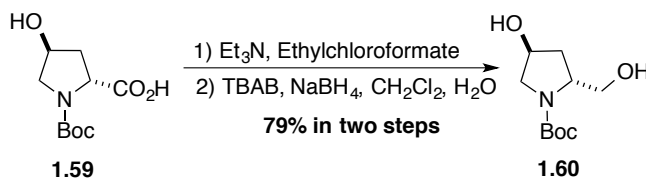


**(2*S*,3*S*)-2-(Hydroxymethyl)-3-((4-octylbenzyl)oxy)pyrrolidin-1-ium chloride (1.49)** was obtained as yellow solid (9.2 mg, 99 %) from **1.48** (14 mg, 0.026 mmol).  $^1\text{H}$  NMR (400 MHz,  $\text{D}_2\text{O}$ ):  $\delta$  7.12 (d,  $J = 7.2$  Hz, 2H), 6.94 (d,  $J = 7.6$  Hz, 2H), 4.44 (d,  $J = 12.0$  Hz, 1H), 4.27 (d,  $J = 12.0$  Hz, 1H), 4.08 (m, 1H), 3.87-3.79 (m, 2H), 3.61 (m, 1H), 3.36-3.33 (m, 2H), 2.37 (t,  $J = 7.6$  Hz, 2H), 2.10 (m, 1H), 1.97 (m, 1H), 1.39 (m, 2H), 1.24 (s. br, 10H), 0.88 (t,  $J = 6.4$  Hz, 3H);  $^{13}\text{C}$  NMR (100 MHz,  $\text{D}_2\text{O}$ ):  $\delta$  141.6, 135.3, 128.1, 127.7, 77.0, 70.6, 64.4, 57.6, 43.1, 35.5, 31.9, 31.4, 29.6, 29.5, 29.4, 29.4, 22.6, 13.9;  $[\alpha]_{\text{D}}^{25}$  (+) 29.1° ( $c$  0.11, MeOH); HRMS (ESI) calcd for  $\text{C}_{20}\text{H}_{34}\text{NO}_2$   $[\text{M}+\text{H}]^+$  320.2584, found 320.2586. HPLC: condition (A)  $t_{\text{R}} = 5.97$  min; purity: 95.1 %.

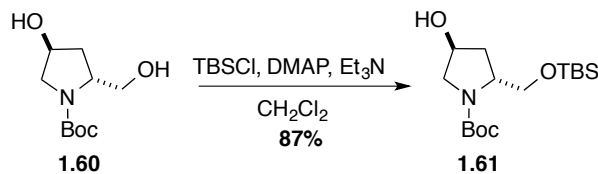


**(2*R*,4*S*)-1-(*tert*-Butoxycarbonyl)-4-hydroxyproline-2-carboxylic acid (1.59)**. Saturated aqueous  $\text{NaHCO}_3$  (160 mL) was added to a solution of *trans*-hydroxyproline **1.58** (4 g, 30.6

mmol) in dioxane and water (1:1, 80 mL). The solution was cooled to 0°C and (Boc)<sub>2</sub>O (7.7 mL, 33.7 mmol) was added drop wise. The reaction was stirred at room temperature over night. The pH was acidified to 3 by addition of 2M HCl and the reaction mixture was extracted with EtOAc. The organic layers were combined, dried over MgSO<sub>4</sub> and filtered. The volatiles were removed under reduced pressure to give alcohol **1.59** (7.1 g, 100 %) as colorless oil, which was used in the next step without purification. Spectroscopic data were in agreement with the proposed structures and matched those reported in the literature.<sup>139</sup>

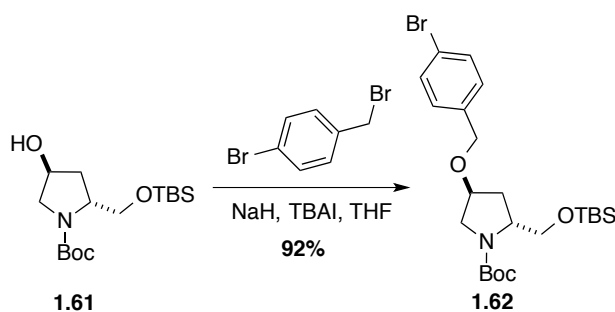


**tert-Butyl (2R,4S)-4-hydroxy-2-((tert-butylidimethylsilyloxy)methyl)pyrrolidine-1-carboxylate (1.60).** Acid **1.59** (3.5g, 15.2 mmol) dissolved in CH<sub>2</sub>Cl<sub>2</sub> (56 mL) on addition of Et<sub>3</sub>N (2.3 mL, 16.7 mmol). The solution was cooled to -30°C. Ethyl chloroformate (1.53 mL, 16.0 mmol) was added to the mixture, which was stirred for 40 min. To this mixture, TBAB (538 mg, 1.67 mmol) was added, followed slowly by a suspension of NaBH<sub>4</sub> (2.47 g, 65.4 mmol) in ice-cold water (4 mL). The reaction mixture was allowed to warm to -10°C, stirred for 1 h, warmed to 0°C, and stirred for an addition 1 h. The reaction mixture was acidified to pH 6 with 50 % acetic acid. The organic phase and the aqueous phase were separated. The aqueous phase was extracted with CH<sub>2</sub>Cl<sub>2</sub> three times. The organic phases were combined, dried over MgSO<sub>4</sub> and filtered. The solvent was removed under reduced pressure and the residue purified by flash chromatography (hexane: EtOAc, 3:7) to give **1.60** (2.61 g, 79 %) as colorless oil. Spectroscopic data were in agreement with the proposed structures and matched those reported in the literature.<sup>140</sup>

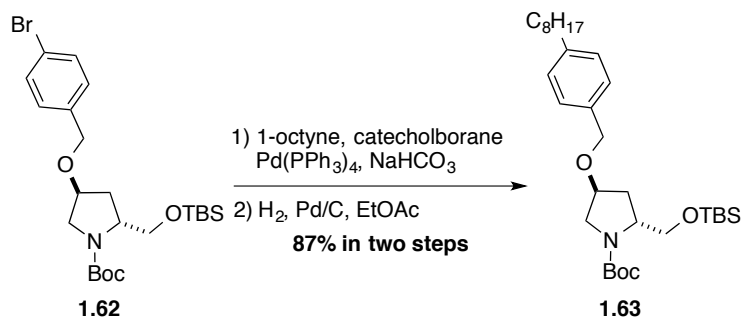


**tert-Butyl (2R,4S)-2-(((tert-butylidimethylsilyloxy)methyl)oxy)methyl-4-hydroxypyrrolidine-1-**

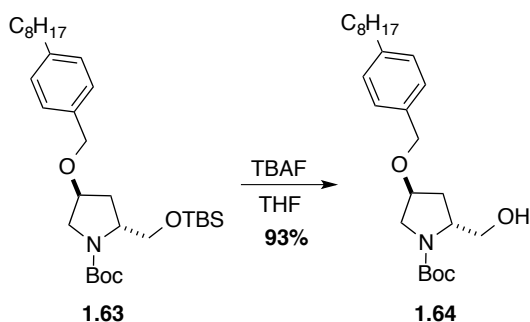
**carboxylate (1.61).** DMAP (136 mg, 1.1 mmol), Et<sub>3</sub>N (3.74 mL, 26.8 mmol) and TBDMSCl (3.7 g, 24.5 mmol) were added to a CH<sub>2</sub>Cl<sub>2</sub> solution of diol **1.60** (4.83 g, 22.3 mmol) at 0°C under argon atmosphere. The reaction was allowed to warm to room temperature and stirred for 2 days when completion was indicated by TLC (R<sub>f</sub> : 0.21, hexane: EtOAc, 3:1). The reaction was diluted with Et<sub>2</sub>O and the organic phase was washed with water two times, dried over MgSO<sub>4</sub>, filtered and concentrated under reduced pressure. The residue was purified by flash chromatography (hexane: EtOAc, 3:1) to give **1.61** (6.4 g, 87 %) as colorless oil. Spectroscopic data were in agreement with the proposed structures and matched those reported in the literature.<sup>140</sup>



***tert*-Butyl (2*R*,4*S*)-4-((4-bromobenzyl)oxy)-2-(((*tert*-butyldimethylsilyl)oxy)methyl)pyrrolidine-1-carboxylate (1.62)** was obtained as colorless oil (6.94 g, 92 %) from **1.61** (5.0 g, 15.1 mmol) according to the procedure for synthesizing **1.30**. <sup>1</sup>H NMR (300 MHz, CDCl<sub>3</sub>) δ 7.45 (d, *J* = 7.9 Hz, 2H), 7.19 (d, *J* = 8.2 Hz, 2H), 4.55-4.33 (m, 2H), 4.28-4.09 (m, 1H), 4.08-3.85 (m, 2H), 3.75-3.33 (m, 3H), 2.28 -2.11 (m, 1H), 2.10- 1.94 (m, 1H), 1.54-1.37 (m, 9H), 0.85 (s, 9H), 0.01 (brs, 6H); <sup>13</sup>C NMR (100 MHz, CDCl<sub>3</sub>) δ (154.7), 154.5, 137.4, 131.7, (129.4), 129.3, 121.6, (79.6), 79.4, 76.5, 70.5, 64.4, (63.6), 57.7, 52.5, (51.7), 35.2, 34.1, 28.7, 26.0, 18.3, -5.3; [α]<sub>D</sub> (+) 23.2° (*c* 2.17, CHCl<sub>3</sub>); HRMS (ESI) calcd for C<sub>23</sub>H<sub>38</sub>BrNNaO<sub>4</sub>Si: (M+Na)<sup>+</sup> 522.1646, found 522.1655.

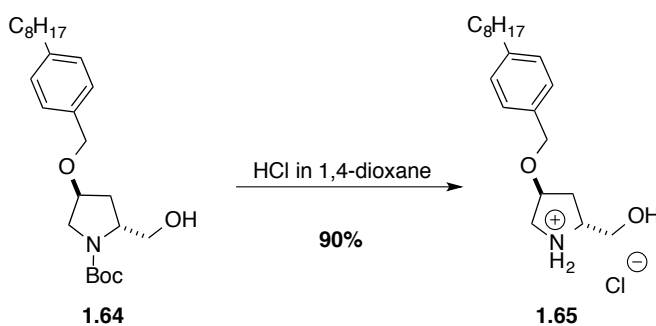


***tert*-Butyl (2*R*,4*S*)-2-(((*tert*-butyldimethylsilyl)oxy)methyl)-4-((4-octylbenzyl)oxy)pyrrolidine-1-carboxylate (**1.63**)** was obtained as pale yellow oil (3.25 g, 87 % over two steps) from **1.62** (3.5 g, 7.0 mmol) according to the procedure for synthesizing **1.31**. <sup>1</sup>H NMR (400 MHz, CDCl<sub>3</sub>) δ 7.23 (d, *J* = 8.0 Hz, 2H), 7.14 (d, *J* = 7.8 Hz, 2H), 4.54-4.39 (m, 2H), 4.28-4.16 (m, 1H), 4.05-3.86 (m, 2H), 3.72-3.49 (m, 2H), 3.48-3.37 (m, 1H), 2.63-2.55 (m, 2H), 2.23-2.14 (m, 1H), 2.12-1.97 (m, 1H), 1.63-1.54 (m, 2H), 1.46, 1.45 (s, 9H), 1.36-1.22 (m, 10H), 0.93-0.83 (m, 12H), 0.06- -0.02 (m, 6H); <sup>13</sup>C NMR (100 MHz, CDCl<sub>3</sub>) δ 154.7, 142.6, 135.5, (129.0), 128.6, (128.4), 128.0, 79.5, (79.3), 76.1, (71.2), 71.1, 64.5, (63.6), (57.8), 57.7, 52.5, (51.8), 35.8, 35.3, 34.1, 32.0, 31.7, 29.6, 29.5, 29.4, 28.7, 26.0, 22.8, 18.3, 14.2, -5.3; [α]<sub>D</sub> (+) 21.2° (*c* 0.17, CHCl<sub>3</sub>); HRMS (ESI) calcd for C<sub>31</sub>H<sub>55</sub>NNaO<sub>4</sub>Si: (M+Na)<sup>+</sup> 556.3793, found 556.3808.

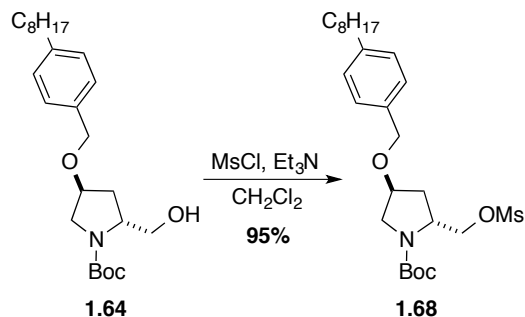


***tert*-Butyl (2*R*,4*S*)-2-(hydroxymethyl)-4-((4-octylbenzyl)oxy)pyrrolidine-1-carboxylate (**1.64**)** A solution of TBAF (1.0 M in THF, 9.8 mL, 9.8 mmol) was added to a solution of silyl ether **1.63** (3.0 g, 5.6 mmol) in dry THF (130 mL). The reaction was stirred at room temperature for 3 h, when completion was indicated by TLC (*R<sub>f</sub>* : 0.45, hexane: EtOAc, 1:1). The mixture was quenched with saturated aqueous NaHCO<sub>3</sub> and extracted three times with CH<sub>2</sub>Cl<sub>2</sub>. The organic layers were combined, dried over NaSO<sub>4</sub> and filtered. The volatiles

were removed under reduced pressure and the residue was purified by flash chromatography (hexane: EtOAc, 6:4) to give alcohol **1.64** (2.2 g, 93 %) as pale yellow oil.  $^1\text{H}$  NMR (400 MHz,  $\text{CDCl}_3$ )  $\delta$  7.22 (d,  $J = 8.1$  Hz, 2H), 7.15 (d,  $J = 8.1$  Hz, 2H), 4.95-2.90 (m, 1H), 4.54-4.40 (m, 2H), 4.19-4.08 (m, 1H), 4.09-4.00 (m, 1H), 3.78-3.59 (m, 2H), 3.55 (dd,  $J = 11.4, 7.2$  Hz, 1H), 3.46-3.33 (m, 1H), 2.62-2.54 (m, 2H), 2.23-2.13 (m, 1H), 1.66-1.53 (m, 2H), 1.47 (s, 9H), 1.35-1.22 (m, 10H), 0.91-0.85 (m, 3H);  $^{13}\text{C}$  NMR (100 MHz,  $\text{CDCl}_3$ )  $\delta$  157.2, 142.8, 135.2, 128.7, 127.8, 80.6, 76.0, 70.9, 67.4, 59.3, 53.1, 35.8, 34.7, 32.0, 31.7, 29.6, 29.5, 29.4, 28.6, 22.8, 14.2;  $[\alpha]_D +20.3^\circ$  ( $c$  1.3,  $\text{CHCl}_3$ ); HRMS (ESI) calcd for  $\text{C}_{25}\text{H}_{41}\text{NNaO}_4$ :  $(\text{M}+\text{Na})^+$  442.2928, found 442.2939.

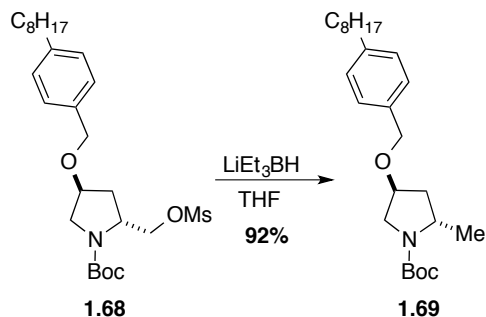


**(2R,4S)-2-(Hydroxymethyl)-4-((4-octylbenzyl)oxy)pyrrolidin-1-ium chloride (1.65)** was obtained as white solid (759 mg, 90 %) from **1.64** (1.0 g, 2.4 mmol) according to the procedure for synthesizing **1.32**.  $^1\text{H}$  NMR (400 MHz, MeOD)  $\delta$  7.27 (d,  $J = 8.0$  Hz, 2H), 7.17 (d,  $J = 8.1$  Hz, 2H), 4.53 (s, 2H), 4.39-4.33 (m, 1H), 3.95-3.83 (m, 2H), 3.63 (dd,  $J = 11.8, 6.4$  Hz, 1H), 3.46-3.32 (m, 2H), 2.64-2.56 (m, 2H), 2.30 (dd,  $J = 13.9, 6.6$  Hz, 1H), 1.91 (ddd,  $J = 14.7, 10.5, 4.5$  Hz, 1H), 1.66-1.54 (m, 2H), 1.37-1.20 (m, 10H), 0.89 (t,  $J = 6.9$  Hz, 3H);  $^{13}\text{C}$  NMR (75 MHz, MeOD)  $\delta$  143.9, 136.2, 129.5, 129.1, 78.4, 71.9, 61.5, 61.4, 51.8, 36.6, 33.6, 33.0, 32.7, 30.6, 30.4, 30.3, 23.7, 14.4;  $[\alpha]_D (-) 4.62^\circ$  ( $c$  0.26, MeOH); HRMS (ESI) calcd for  $\text{C}_{20}\text{H}_{34}\text{NO}_2$ :  $(\text{M}+\text{H})^+$  320.2584, found 320.2594. HPLC: condition (A),  $t_R = 5.99$  min; purity: > 99 %.



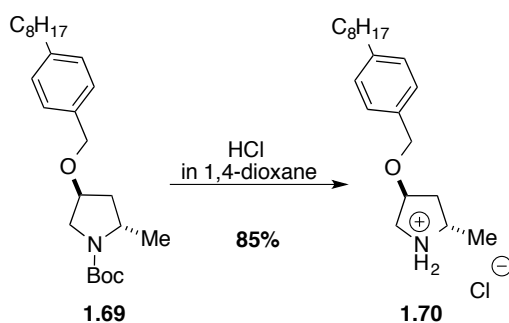
***tert*-Butyl (2*R*,4*S*)-2-(((methanesulfonyl)oxy)methyl)-4-((4-octylbenzyl)oxy)**

**pyrrolidine-1-carboxylate (1.68).** Alcohol **1.64** (100 mg, 0.238 mmol) was dissolved in CH<sub>2</sub>Cl<sub>2</sub> (0.8 mL), and Et<sub>3</sub>N (66 μL, 0.476 mmol) was added. The solution was cooled 0 °C. To this mixture, MsCl (28 μL, 0.357 mmol) was added. The resulting solution was stirred over night. The reaction mixture was poured into water and extracted with EtOAc. The combined organic phases were dried over MgSO<sub>4</sub>, filtered and concentrated under reduced pressure. The residue was purified by flash chromatography (hexane: EtOAc, 3:1) to give methanesulfonate **1.68** (112 mg, 95 %) as pale yellow oil. <sup>1</sup>H NMR (400 MHz, CDCl<sub>3</sub>) δ 7.22 (d, *J* = 8.0 Hz, 2H), 7.15 (d, *J* = 8.0 Hz, 2H), 4.59-4.25 (m, 4H), 4.15 (m, 2H), 3.83-3.56 (m, 1H), 3.44-3.39 (m, 1H), 2.98 (s, 3H), 2.61-2.57 (t, *J* = 7.6 Hz, 2H), 2.21 (m, 1H), 2.13-2.08 (m, 1H), 1.61-1.55 (m, 2H), 1.46 (s, 9H), 1.30-1.27 (m, 10H), 0.83 (t, *J* = 6.4 Hz 3H); <sup>13</sup>C NMR (100 MHz, CDCl<sub>3</sub>, mixture of rotamers) δ 154.8, (154.4), 142.7, 135.0, (129.7), 128.6, 127.8, (127.2), (80.5), 80.1, 76.1, (75.6), 71.0, 70.0, 55.0, 52.5, (51.7), (37.4), 36.9, 35.7, (35.3), 34.0, 31.9, 31.6, 29.5, 29.4, 29.3, 28.5, 22.7, 14.2; [α]<sub>D</sub> (+) 28.0° (*c* 0.54, CHCl<sub>3</sub>); HRMS (ESI) calcd. for C<sub>26</sub>H<sub>43</sub>NNaO<sub>6</sub>S: (M+Na)<sup>+</sup> 520.2703, found 520.2696.



***tert*-Butyl (2*S*,4*S*)-2-methyl-4-((4-octylbenzyl)oxy)pyrrolidine-1-carboxylate (1.69).** A solution of LiBHET<sub>3</sub> (1 M in THF, 0.644 mL, 0.644 mmol) was added slowly to an ice-cold

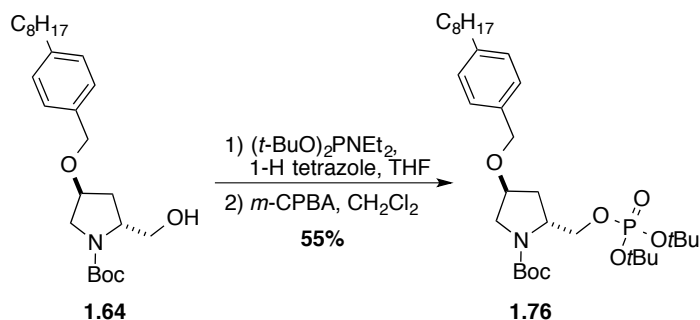
solution of methanesulfonate **1.68** (80 mg, 0.161 mmol) in THF (0.16 mL). The solution was allowed to warm to r.t. and stirred for 2 h, when completion was indicated by TLC ( $R_f$ : 0.55, hexane: EtOAc, 8:1). The reaction was quenched with water and poured into EtOAc. The aqueous and organic phases were separated. The aqueous phase was extracted with EtOAc. The combined organic phases were washed with brine, dried over  $MgSO_4$ , filtered and concentrated under reduced pressure. The residue was purified by flash chromatography (hexane: EtOAc, 16:1) to give pyrrolidine **1.69** (60 mg, 92 %) as pale yellow oil.  $^1H$  NMR (400 MHz,  $CDCl_3$ ) 7.23 (d,  $J = 7.6$  Hz, 2H), 7.15 (d,  $J = 8.0$  Hz, 2H), 4.48-4.46 (m, 2H), 4.10-3.97 (m, 2H), 3.68-3.43 (m, 2H), 2.59 (t,  $J = 8.0$  Hz, 2H), 2.17 (m, 1H), 1.75-1.69 (m, 1H), 1.61-1.57 (m, 2H), 1.48 (s, 9H), 1.31-1.21 (m, 13H), 0.89 (t,  $J = 6.0$  Hz, 3H);  $^{13}C$  NMR (100 MHz,  $CDCl_3$ , mixture of rotamers) 154.9, 142.6, 135.3, 128.6, 127.8, 79.2, (76.4), 75.9, 71.0, 51.9, (51.2), 40.3, (39.3), 35.8, 32.0, 31.6, 29.6, 29.4, 29.4, 28.6, 22.8, 21.5, 20.9, 14.2;  $[\alpha]_D^{25}$  (+) 11.1° ( $c$  0.18,  $CHCl_3$ ); HRMS calcd for  $C_{25}H_{41}NNaO_3$ :  $(M+Na)^+$  426.2979, found 426.2963.



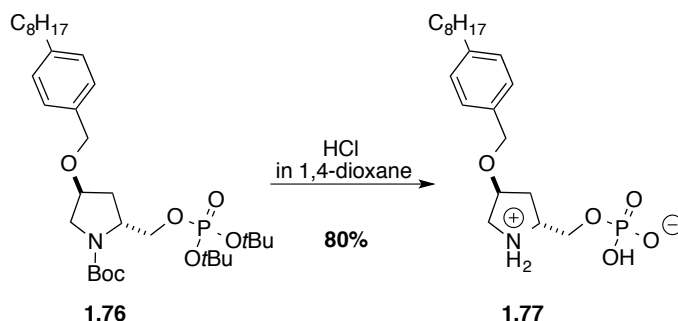
**(2S,4S)-2-Methyl-4-((4-octylbenzyl)oxy)pyrrolidin-1-ium chloride (1.70)** was obtained as white solid (20.1 mg, 85 %) from **1.69** (28 mg, 0.069 mmol) according to the procedure for synthesizing **1.32**.  $^1H$  NMR (400 MHz,  $D_2O$ ) 7.17 (d,  $J = 8.0$  Hz, 2H), 6.94 (d,  $J = 8.0$  Hz, 2H), 4.38 (d,  $J = 12.0$  Hz, 1H), 4.29 (d,  $J = 12.0$  Hz, 1H), 4.15 (m, 1H), 3.73-3.64 (m, 1H), 3.44 (dd,  $J = 13.2, 5.2$  Hz, 1H), 3.30 (d,  $J = 13.2$  Hz, 1H), 2.38 (t,  $J = 8.0$  Hz, 2H), 2.05 (dd,  $J = 14.0, 6.0$  Hz, 1H), 1.58-1.66 (m, 1H), 1.45 (m, 2H), 1.30 (d,  $J = 6.8$  Hz, 3H), 1.25-1.30 (m, 10H), 0.90 (t,  $J = 5.2$  Hz, 3H);  $^{13}C$  NMR (100 MHz,  $D_2O$ ) 141.6, 135.2, 128.0, 77.0, 70.3, 54.7, 50.0, 38.0, 35.5, 32.0, 31.5, 29.7, 29.6, 29.5, 22.7, 16.3, 13.9;  $[\alpha]_D^{25}$  (+) 3.5° ( $c$  0.34,



MeOH); HRMS calcd for C<sub>20</sub>H<sub>34</sub>NO : (M+H)<sup>+</sup> 304.2635, found 304.2644. HPLC: condition (A), *t*<sub>R</sub> = 6.20 min; purity: > 99 %.

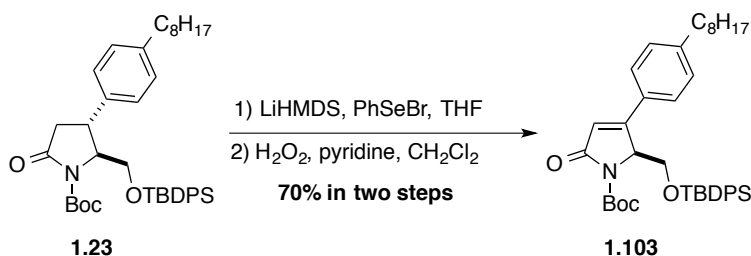


***tert*-Butyl (2*R*,4*S*)-2-(((di-*tert*-butoxyphosphoryl)oxy)methyl)-4-((4-octylbenzyl)oxy)pyrrolidine-1-carboxylate (1.76).** Di-*tert*-butyl *N,N*-diethylphosphoramidite (97  $\mu$ L, 87 mg, 0.35 mmol) and 1H-tetrazole (50 mg, 0.71 mmol) were sequentially added to a solution of alcohol **1.64** (50 mg, 0.12 mmol) in anhydrous THF (1.6 mL) under argon atmosphere at r.t. The mixture was stirred over night and then cooled to -78 °C. A solution of *m*-CPBA (77%, 83 mg, 0.35 mmol) in CH<sub>2</sub>Cl<sub>2</sub> (1.6 ml) was added to the mixture and the reaction was warmed back to r.t. After 0.5 h, the reaction was quenched with saturated aqueous NaHCO<sub>3</sub> and extracted three times with EtOAc. The organic layers were washed with brine, dried over MgSO<sub>4</sub> and filtered. The filtrate was evaporated under reduced pressure and the residue was purified by flash chromatography (hexane: EtOAc, 4:1 to 2:1) to give phosphate **1.76** (40 mg, 55 %) as colorless oil. <sup>1</sup>H NMR (400 MHz, CDCl<sub>3</sub>)  $\delta$  7.19 (d, *J* = 7.6 Hz, 2H), 7.11 (d, *J* = 7.6 Hz, 2H), 4.48-4.38 (m, 2H), 4.18-3.92 (m, 4H), 3.74 – 3.36 (m, 2H), 2.55 (t, *J* = 7.6 Hz, 2H), 2.13 (m, 2H), 1.56 (m, 2H), 1.49 (s, 9H), 1.44 (m, 18H), 1.26 (m, 10H), 0.85 (m, 3H). <sup>13</sup>C NMR (100 MHz, CDCl<sub>3</sub>, mixture of rotamers)  $\delta$  154.3, 142.4, 135.0, 128.3, (127.6), 127.6, 82.7, (82.6), 82.1, (82.0), 79.7, (79.3), 75.7, 70.9, (70.8), 67.8, (67.2), 55.6, 52.1, 51.4, 35.5, 35.1, 33.7, 31.7, 31.4, 30.2, 30.2, 29.8, 29.7, 29.3, 29.2, 29.1, 28.3, 22.5, 14.0; <sup>31</sup>P NMR (162 MHz, CDCl<sub>3</sub>, mixture of rotamers) -9.62, -10.01; [ $\alpha$ ]<sub>D</sub> (+) 17.0° (*c* 1.95, CHCl<sub>3</sub>); HRMS (ESI) calcd for C<sub>33</sub>H<sub>58</sub>NNaO<sub>7</sub>P (M+Na)<sup>+</sup> 634.3843, found 634.3848.



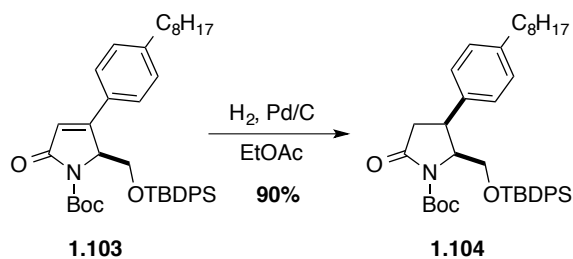
**((2*R*,4*S*)-4-((4-Octylbenzyl)oxy)pyrrolidin-1-ium-2-yl)methyl hydrogen phosphate (1.77).**

A solution of HCl (4M) in 1,4-dioxane (1.6 mL, 6.4 mmol) was added to a flask containing carbamate **1.76** (30 mg, 0.05 mmol) and the solution was stirred overnight at room temperature. The volatiles were removed under reduced pressure. 1,4-Dioxane (2 mL) was added to the residue and the contents were evaporated to remove residual HCl. The crude mixture was purified by flash chromatography (*i*-PrOH : NH<sub>4</sub>OH : H<sub>2</sub>O, 8 : 2 : 1) to give a colorless oil. The oil was dissolved in CHCl<sub>3</sub>, filtered through a plastic syringe filter (pore size: 0.45 μm), and lyophilized to give phosphate **1.77** (16.0 mg, 88 %) as white solid. <sup>1</sup>H NMR (500 MHz, MeOD) δ 7.26 (d, *J* = 8.0 Hz, 2H), 7.16 (d, *J* = 8.0 Hz, 2H), 4.53 (s, 2H), 4.37 (t, *J* = 4.0 Hz, 1H), 4.21 (ddd, *J* = 12.5, 8.5, 2.5 Hz, 1H), 4.05-3.99 (m, 1H), 3.92 (ddd, *J* = 12.5, 11.0, 5.5 Hz, 1H), 3.44 (m, 1H), 3.31 (m, overlapped with MeOD, 1H), 2.60 (t, *J* = 7.5 Hz, 2H), 2.32 (m, 1H), 2.05 (m, 1H), 1.60 (m, 2H), 1.31-1.13 (m, 10H), 0.89 (t, *J* = 7.0 Hz, 3H). <sup>13</sup>C NMR (100 MHz, D<sub>2</sub>O) δ 144.0, 136.4, 129.7, 129.3, 78.7, 71.9, 64.1, 60.6, 51.6, 36.7, 33.3, 33.2, 32.9, 30.7, 30.5, 30.4, 23.9, 14.6; [α]<sub>D</sub> (-) 20.0° (*c* 0.05, MeOH); <sup>31</sup>P NMR (202 MHz, MeOD) 2.36; HRMS (ESI) calcd for C<sub>20</sub>H<sub>34</sub>NNaO<sub>5</sub>P (M+Na)<sup>+</sup> 422.2069, found 422.2064.



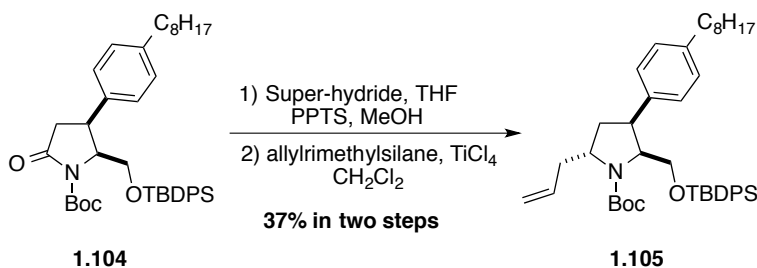
***tert*-Butyl (*S*)-2-(((*tert*-butyldiphenylsilyl)oxy)methyl)-3-(4-octylphenyl)-5-oxo-**

**2,5-dihydro-1*H*-pyrrole-1-carboxylate (1.103).** A solution of lactam **1.23** (257 mg, 0.40 mmol) in anhydrous THF (4.0 mL) under argon atmosphere was cooled to -78 °C. A solution of LiHMDS (1M) in THF (0.44 mL, 0.44 mmol) was added dropwise to the solution. The mixture was stirred at -78 °C for 1 h. In another flask under argon atmosphere, a solution of PhSeBr (104 mg, 0.44 mmol) in anhydrous THF (1 mL) was cooled to -78 °C, and transferred dropwise by canula to the reaction mixture, which was stirred at -78 °C for 2 h. The reaction was quenched with saturated aqueous NH<sub>4</sub>Cl, diluted with CH<sub>2</sub>Cl<sub>2</sub> and the two phases were separated. The aqueous phase was extracted twice with CH<sub>2</sub>Cl<sub>2</sub>. The combined organic phases were dried over MgSO<sub>4</sub> and filtered. The volatiles were removed under reduced pressure to a residue that was dissolved in CH<sub>2</sub>Cl<sub>2</sub> (2 mL), cooled to -78 °C and treated with a solution of hydrogen peroxide (30 % (w/w) in H<sub>2</sub>O, 204 μL), followed by pyridine (160 μL, 2.2 mmol). The reaction mixture was allowed to warm to room temperature and stirred for 1 h, when completion was indicated by TLC (R<sub>f</sub> : 0.41, hexane: EtOAc, 4:1). The mixture was quenched with saturated aqueous NH<sub>4</sub>Cl, and extracted three times with CH<sub>2</sub>Cl<sub>2</sub>. The organic layers were combined, dried over NaSO<sub>4</sub> and filtered. The filtrate was evaporated under reduced pressure and the residue was purified by flash chromatography (hexane: EtOAc, 6:1) to give olefin **1.103** (180 mg, 70 % over two steps) as yellow oil. <sup>1</sup>H NMR (400 MHz, CDCl<sub>3</sub>) δ 7.51-7.27 (m, 10H), 7.16-7.08 (m, 4H), 6.42 (s, 1H), 5.12 (s, 1H), 4.28 (dd, *J* = 2.4, 10.4 Hz, 1H), 3.84 (dd, *J* = 1.2, 10.4 Hz, 1H), 2.71 (t, 7.6 Hz, 2H), 1.69 (m, 2H), 1.52 (s, 9H), 1.41-1.27 (m, 10H), 0.90 (m, 12H); <sup>13</sup>C NMR (100 MHz, CDCl<sub>3</sub>) δ 169.4, 159.2, 149.5, 146.2, 135.3, 135.2, 132.6, 132.6, 129.7, 129.4, 129.1, 128.5, 127.7, 127.4, 127.2, 120.6, 82.6, 63.2, 60.9, 35.9, 31.8, 31.3, 29.4, 29.3, 29.2, 28.1, 26.4, 22.6, 19.1, 14.1; [α]<sub>D</sub> (-) 183.8° (*c* 0.40, CHCl<sub>3</sub>); HRMS (ESI) calcd for C<sub>40</sub>H<sub>53</sub>NNaO<sub>4</sub>Si (M+Na)<sup>+</sup> 662.3636, found 662.3616.



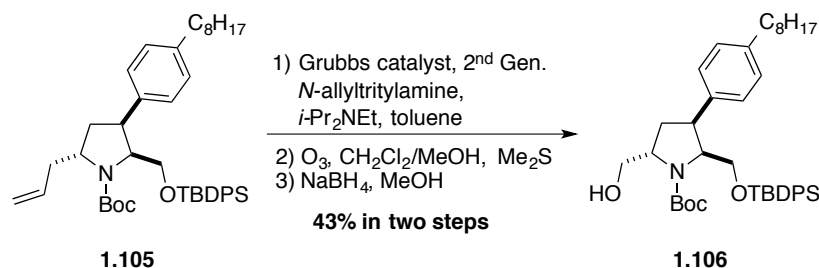
***tert*-Butyl (2*S*,3*S*)-2-(((*tert*-butyldiphenylsilyl)oxy)methyl)-3-(4-octylphenyl)-5-**

**oxopyrrolidine-1-carboxylate (1.104).** To a solution of olefin **1.103** (300 mg, 0.47 mmol) in EtOAc (9.5 mL), Pd/C (10 %, 50 mg, 0.047 mmol) was added. The flask was evacuated under vacuum and filled with H<sub>2</sub>. After stirring overnight, TLC showed complete reaction (R<sub>f</sub> : 0.41, hexane: EtOAc, 4:1). The reaction mixture was filtered over Celite<sup>TM</sup>. The filtrate was evaporated under reduced pressure. The residue was purified by flash chromatography (hexane: EtOAc, 6:1) to give lactam **1.104** (270 mg, 90 %) as pale yellow oil. <sup>1</sup>H NMR (500 MHz, CDCl<sub>3</sub>) δ 7.54 (m, 2H), 7.52-7.25 (m, 4H), 7.23-7.19 (m, 8H), 4.36 (d, *J* = 7.2 Hz, 1H), 3.87-3.79 (m, 2H), 3.59-3.51 (m, 2H), 2.75-2.67 (m, 3H), 1.68 (m, 2H), 1.43 (s, 9H), 1.43-1.30 (m, 10H), 1.00 (s, 9H), 0.91 (t, *J* = 6.8 Hz, 3H); <sup>13</sup>C NMR (125 MHz, CDCl<sub>3</sub>) δ 174.0, 149.6, 141.9, 135.6, 135.4, 133.9, 132.6, 132.1, 129.7, 129.4, 128.6, 127.7, 127.7, 127.4, 82.6, 62.5, 61.3, 40.3, 37.0, 35.6, 31.8, 31.5, 29.4, 29.3, 29.2, 27.9, 26.7, 22.6, 18.8, 14.0; [α]<sub>D</sub> (-) 41.6° (*c* 1.60, CHCl<sub>3</sub>); HRMS (ESI) calcd for C<sub>40</sub>H<sub>55</sub>NNaO<sub>4</sub>Si (M+Na)<sup>+</sup> 664.3793, found 664.3799.



***tert*-Butyl (2*S*,3*S*,5*R*)-5-allyl-2-(((*tert*-butyldiphenylsilyl)oxy)methyl)-3-(4-octylphenyl)pyrrolidine-1-carboxylate (1.105).** Lactam **1.104** (105 mg, 0.16 mmol) was dissolved in anhydrous THF (6.0 mL) in a dry flask under argon atmosphere, cooled to -78 °C, treated dropwise with lithium triethylborohydride (1.0 M in THF, 180 μL, 0.18 mmol), and stirred for 1 hat -78 °C. In another dry flask, pyridinium *p*-toluenesulfonate (48.0 mg, 0.19 mmol) was dissolved in anhydrous MeOH (4.0 mL) under argon, cooled to -78°C, then transferred dropwise by canula to the reaction mixture. The pH was verified to be slightly acidic (pH~6); otherwise, more pyridinium *p*-toluenesulfonate was added. The mixture was allowed to warm to room temperature and stirred overnight. The reaction was quenched with saturated aqueous NaHCO<sub>3</sub>, and extracted three times with CH<sub>2</sub>Cl<sub>2</sub>. The organic layers were combined, dried over NaSO<sub>4</sub> and filtered. The filtrate was evaporated under reduced pressure to give *O*-methyl

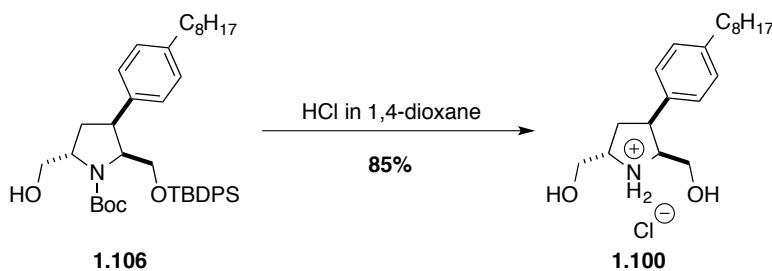
aminal product as yellow oil, that was dissolved in anhydrous CH<sub>2</sub>Cl<sub>2</sub> (0.74 mL) under argon atmosphere and cooled to -78 °C. Allyltrimethylsilane (128 μL, 0.80 mmol) and titanium tetrachloride (1.0 M in CH<sub>2</sub>Cl<sub>2</sub>, 180 μL, 0.180 mmol) were added sequentially to the -78 °C solution. The resulting orange mixture was stirred for 1 h at -78 °C, quenched with water and extracted three times with CH<sub>2</sub>Cl<sub>2</sub>. The organic layers were combined, dried over NaSO<sub>4</sub> and filtered. The filtrate was evaporated under reduced pressure and the residue purified by flash chromatography (hexane: EtOAc, 6:1) to give the olefin **1.105** (40 mg, 37 % over two steps) as pale yellow oil. <sup>1</sup>H NMR (400 MHz, CDCl<sub>3</sub>, mixture of rotamers) δ 7.51-7.48 (m, 2H), 7.39-7.10 (m, 12H), 5.87 (m, 1H), 5.10 (m, 2H), 4.20-4.04 (m, 2.5H), 3.78 (dd, *J* = 2.8, 10.8 Hz, 0.5H), 3.67 (m, 1H), 3.39 (d, *J* = 10.4 Hz, 0.5H), 3.29 (d, *J* = 10.8 Hz, 0.5H), 2.94 (m, 1.5H), 2.74 (dd, *J* = 6.4, 12.8 Hz, 0.5H), 2.65 (m, 2H), 2.29 (m, 1H), 2.01 (td, *J* = 6.4, 11.6 Hz, 1H), 1.65 (m, 2H), 1.55 (s, 5H), 1.32 (m, 10H), 1.26 (s, 4H), 1.00 (s, 5H), 0.98 (s, 4H), 0.91 (t, *J* = 7.2 Hz, 3H); <sup>13</sup>C NMR (100 MHz, CDCl<sub>3</sub>, mixture of rotamers) δ (153.8), 153.5, (141.1), 141.1, (136.1), 135.8, (135.7), 135.7, (135.6), 135.5, 133.4, (133.1), (132.9), 132.8, (129.5), 129.4, (129.2), 129.2, 128.3, 127.7, (127.4), 127.3, 117.1, (117.0), 79.2, (79.1), (62.4), 62.2, 61.9, 60.2, 57.1, (56.9), (43.5), 43.0, 39.5, 37.8, 35.6, 32.4, 31.9, (31.7), 31.6, (31.4), 29.5, 29.4, 29.3, 28.6, (28.4), 26.8, (26.8), 22.7, 19.0, (18.8), 14.1; [α]<sub>D</sub> (-) 30.2° (*c* 0.42, CHCl<sub>3</sub>); HRMS (ESI) calcd for C<sub>43</sub>H<sub>61</sub>NNaO<sub>3</sub>Si (M+Na)<sup>+</sup> 690.4313, found 690.4297.



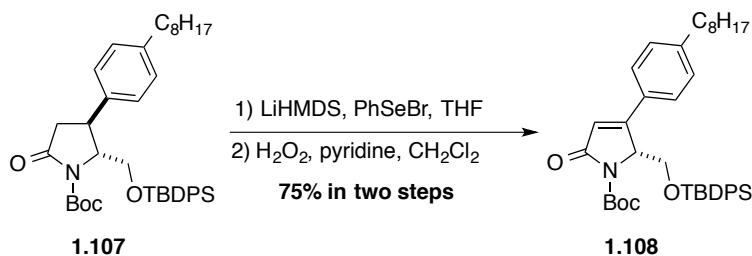
***tert*-Butyl (2*S*,3*S*,5*S*)-2-(((*tert*-butyldiphenylsilyl)oxy)methyl)-5-(hydroxymethyl)-3-(4-octylphenyl)pyrrolidine-1-carboxylate (1.106).** Olefin **1.105** (55 mg, 0.082 mmol) was dissolved in anhydrous toluene (1.8 mL) in a dry flask equipped with a condenser, under argon atmosphere.

*N*-Allyltrimethylamine (49 mg, 0.16 mmol) and Grubb's catalyst 2<sup>nd</sup> generation (14 mg, 0.016 mmol) were sequentially added to the reaction mixture, which was heated to reflux for 3 days, cooled to room temperature and quenched with brine. The mixture was extracted

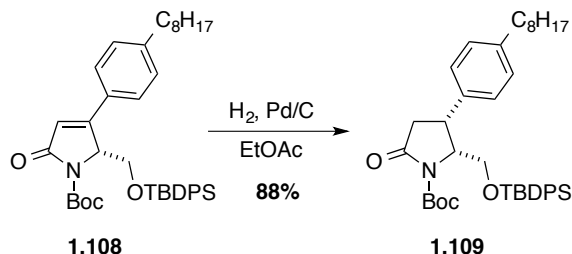
three times with CH<sub>2</sub>Cl<sub>2</sub>. The organic layers were combined, dried over NaSO<sub>4</sub> and filtered. The filtrate was evaporated under reduced pressure and the residue was purified by flash chromatography (hexane: EtOAc, 40:1 to 20:1) to give the disubstituted alkene isomer (40 mg, 73 %) as yellow oil. The oil (40 mg, 0.06 mmol) was dissolved in a solution of MeOH and CH<sub>2</sub>Cl<sub>2</sub> (1:1, 6 mL), cooled to -78 °C, and treated with ozone bubbles until a deep blue color persisted. Argon was bubbled through the solution to remove residual ozone until no blue color was observed. Dimethyl sulfide (0.4 mL) was added carefully. The reaction was allowed to slowly warm to room temperature with stirring overnight. The volatiles were removed under reduced pressure. The residue was dissolved in MeOH (1.96 mL), cooled to 0 °C, treated with sodium borohydride (6.8 mg, 0.180 mmol) and stirred at 0 °C for 4 h, when completion was indicated by TLC (R<sub>f</sub>: 0.15, hexane: EtOAc, 8:1). The reaction was quenched with saturated aqueous NH<sub>4</sub>Cl, extracted three times with CH<sub>2</sub>Cl<sub>2</sub>. The organic layers were combined, dried over NaSO<sub>4</sub> and filtered. The filtrate was evaporated under reduced pressure and the residue was purified by flash chromatography (hexane: EtOAc, 8:1 to 4:1) to give alcohol **1.106** (23.2 mg, 59 % over two steps) as yellow oil (23.2 mg, 43% over three steps). <sup>1</sup>H NMR (400 MHz, CDCl<sub>3</sub>, mixture of rotamers) δ 7.52-7.47 (m, 2H), 7.41-7.06 (m, 12H), 4.80 (br, 1H), 4.41 (m, 1H), 4.20-3.74 (m, 3H), 3.65 (m, 1H), 3.40-3.29 (m, 1H), 3.16-2.98 (m, 1H), 2.68-2.59 (m, 2H), 1.93-1.89 (m, 1H), 1.67-1.60 (m, 3H), 1.35-1.26 (m, 19H), 1.10 (s, 2H), 1.00 (s, 7H), 0.90 (t, *J*=6.8 Hz, 3H); <sup>13</sup>C NMR (100 MHz, CDCl<sub>3</sub>, mixture of rotamers) δ 156.4, 141.3, (141.1), 135.7, (135.6), (135.5), 135.4, 133.0, 132.7, 129.6, (129.5), 129.4, (129.3), 128.4, (128.3), 128.1, 127.7, (127.4), 127.4, 80.6, (79.9), 69.3, (65.3), 63.4, (62.5), 61.5, 60.4, (59.9), (59.1), 44.5, (43.6), 35.6, (32.1), 31.9, 31.6, (31.5), 29.7, 29.5, 29.4, 29.3, 28.6, 28.3, 26.8, 22.7, (19.0), 18.8, 14.1; [α]<sub>D</sub> (-) 31.8° (*c* 0.78, CHCl<sub>3</sub>); HRMS (ESI) calcd for C<sub>41</sub>H<sub>59</sub>NNaO<sub>4</sub>Si (M+Na)<sup>+</sup> 680.4106, found 680.4103.



**(2*S*,3*S*,5*S*)-2,5-Bis(hydroxymethyl)-3-(4-octylphenyl)pyrrolidin-1-ium chloride (1.100)** was obtained as a yellow solid (10.6 mg, 85 %) from silyl ether **1.106** (23 mg, 0.035 mmol) according to the procedure for synthesizing alcohol **1.32**. <sup>1</sup>H NMR (400 MHz, D<sub>2</sub>O) δ 7.09 (d, *J* = 8.0 Hz, 2H), 6.93 (d, *J* = 7.6 Hz, 2H), 4.01-3.91 (m, 2H), 3.75-3.60 (m, 3H), 3.28-3.19 (m, 2H), 2.38-2.28 (m, 3H), 1.94-1.90 (m, 1H), 1.47 (br, 2H), 1.27 (br. s, 10H), 0.90 (t, *J* = 6.8 Hz, 3H); <sup>13</sup>C NMR (100 MHz, D<sub>2</sub>O) δ 140.9, 134.1, 128.2, 128.1, 63.3, 61.5, 58.8, 58.3, 43.8, 35.4, 32.0, 31.3, 30.2, 29.8, 29.6, 29.6, 22.7, 13.9; [α]<sub>D</sub> (+) 37.7° (*c* 0.22, MeOH); HRMS (ESI) calcd for C<sub>20</sub>H<sub>34</sub>NO<sub>2</sub> (M+H)<sup>+</sup> 320.2584, found 320.2586. HPLC: condition (B), *t*<sub>R</sub> = 6.05 min; purity: 95.6 %.

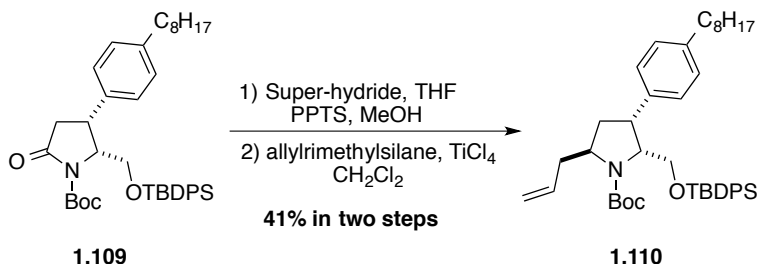


***tert*-Butyl (*R*)-2-(((*tert*-butyldiphenylsilyl)oxy)methyl)-3-(4-octylphenyl)-5-oxo-2,5-dihydro-1*H*-pyrrole-1-carboxylate (1.108)** was obtained as yellow oil (192 mg, 75 % over two steps) from lactam **1.107** (257 mg, 0.40 mmol) according to the procedure for synthesizing lactam **1.103**. <sup>1</sup>H NMR (400 MHz, CDCl<sub>3</sub>) δ 7.51-7.27 (m, 10H), 7.16-7.08 (m, 4H), 6.42 (s, 1H), 5.12 (s, 1H), 4.28 (dd, *J* = 2.4, 10.4 Hz, 1H), 3.84 (dd, *J* = 1.6, 10.4 Hz, 1H), 2.71 (t, 7.6 Hz, 2H), 1.68 (m, 2H), 1.53 (s, 9H), 1.37-1.27 (m, 10H), 0.89 (m, 12H); <sup>13</sup>C NMR (100 MHz, CDCl<sub>3</sub>) δ 169.4, 159.2, 149.5, 146.2, 135.4, 135.2, 132.6, 132.6, 129.7, 129.4, 129.2, 128.5, 127.7, 127.4, 127.2, 120.7, 82.6, 63.2, 61.0, 35.9, 31.9, 31.3, 29.5, 29.3, 29.2, 28.1, 26.4, 22.7, 19.1, 14.1; [α]<sub>D</sub> (+) 163.0° (*c* 2.20, CHCl<sub>3</sub>); HRMS (ESI) calcd for C<sub>40</sub>H<sub>53</sub>NNaO<sub>4</sub>Si (M+Na)<sup>+</sup> 662.36361, found 662.36401.



***tert*-Butyl (2*R*,3*R*)-2-(((*tert*-butyldiphenylsilyl)oxy)methyl)-3-(4-octylphenyl)-5-**

**oxopyrrolidine-1-carboxylate (1.109)** was obtained as pale yellow oil (150 mg, 88 %) from olefin **1.108** (170 mg, 0.27 mmol) according to the procedure for synthesizing **1.104**.  $^1\text{H}$  NMR (500 MHz,  $\text{CDCl}_3$ )  $\delta$  7.53 (m, 2H), 7.41-7.32 (m, 4H), 7.25-7.20 (m, 8H), 4.36 (d,  $J = 6.4$  Hz, 1H), 3.85-3.80 (m, 2H), 3.58-3.51 (m, 2H), 2.74-2.67 (m, 3H), 1.68 (m, 2H), 1.44 (s, 9H), 1.38-1.31 (m, 10H), 1.01 (s, 9H), 0.91 (t,  $J = 5.2$  Hz, 3H);  $^{13}\text{C}$  NMR (125 MHz,  $\text{CDCl}_3$ )  $\delta$  174.0, 149.6, 141.9, 135.6, 135.4, 133.9, 132.6, 132.1, 129.7, 129.4, 128.6, 127.7, 127.7, 127.4, 82.6, 62.5, 61.3, 40.3, 37.0, 35.6, 31.8, 31.5, 29.4, 29.3, 29.2, 27.9, 26.7, 22.6, 18.8, 14.0;  $[\alpha]_{\text{D}}^{20}$  (+) 30.2° ( $c$  1.50,  $\text{CHCl}_3$ ); HRMS (ESI) calcd for  $\text{C}_{40}\text{H}_{55}\text{NNaO}_4\text{Si}$  ( $\text{M}+\text{Na}$ )<sup>+</sup> 664.3793, found 664.379.

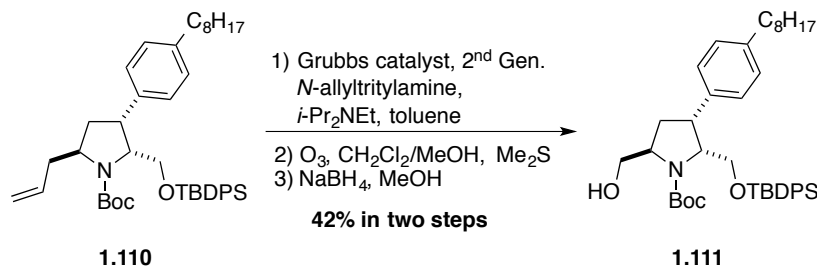


***tert*-Butyl (2*R*,3*R*,5*S*)-5-allyl-2-(((*tert*-butyldiphenylsilyl)oxy)methyl)-3-**

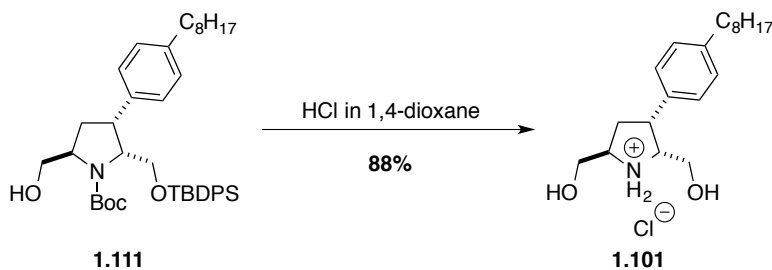
**(4-octylphenyl)pyrrolidine-1-carboxylate (1.110)** was obtained as pale yellow oil (20 mg, 41 %) from **1.109** (47 mg, 0.073 mmol) according to the procedure for synthesizing **1.105**.  $^1\text{H}$  NMR (400 MHz,  $\text{CDCl}_3$ , mixture of rotamers)  $\delta$  7.51-7.49 (m, 2H), 7.39-7.10 (m, 12H), 5.88 (m, 1H), 5.10 (m, 2H), 4.19-4.04 (m, 2.5H), 3.80 (dd,  $J = 2.8, 10.8$  Hz, 0.5H), 3.70 (m, 1H), 3.39 (d,  $J = 10.4$  Hz, 0.5H), 3.29 (d,  $J = 10.8$  Hz, 0.5H), 2.94 (m, 1.5H), 2.74 (dd,  $J = 5.6, 12.8$  Hz, 0.5H), 2.64 (m, 2H), 2.28 (m, 1H), 2.02 (td,  $J = 6.4, 11.6$  Hz, 1H), 1.65 (m, 2H), 1.56 (s, 5H), 1.31 (m, 10H), 1.26 (s, 4H), 1.01 (s, 5H), 0.98 (s, 4H), 0.91 (t,  $J = 7.2$  Hz, 3H);  $^{13}\text{C}$  NMR (100 MHz,  $\text{CDCl}_3$ , mixture of rotamers)  $\delta$  153.8, (153.4), (141.1), 141.0, (136.0), 135.8,



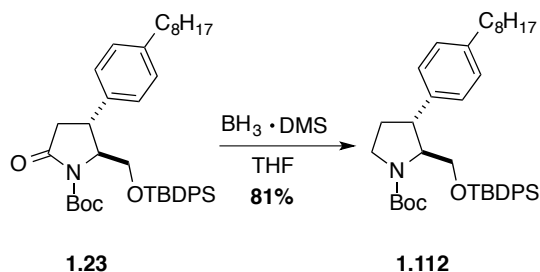
(135.8), 135.7, (135.7), 135.6, (135.6), 135.5, 133.4, (133.1), (132.8), 132.8, (129.4), 129.4, (129.2), 129.2, 128.3, (128.2), 127.7, (127.4), 127.3, 117.1, (117.0), 79.2, (79.1), (62.4), 62.2, 61.9, 60.1, 57.1, (56.9), (43.4), 43.0, 39.4, 37.7, (35.6), 35.6, (32.3), 31.9, (31.6), 31.6, 31.4, (29.5), 29.4, 29.2, 28.6, (28.3), 26.8, (26.7), 22.7, 19.0, (18.8), 14.1;  $[\alpha]_D$  (+) 43.8° (*c* 0.16, CHCl<sub>3</sub>); HRMS (ESI) calcd for C<sub>43</sub>H<sub>61</sub>NNaO<sub>3</sub>Si (M+Na)<sup>+</sup> 690.4313, found 690.4309.



***tert*-Butyl (2*R*,3*R*,5*R*)-2-(((*tert*-butyldiphenylsilyl)oxy)methyl)-5-(hydroxymethyl)-3-(4-octylphenyl)pyrrolidine-1-carboxylate (1.111)** was obtained as pale yellow oil (23.8 mg, 42 % over three steps) from olefin **1.110** (57 mg, 0.085 mmol) according to the procedure for synthesizing **1.106**. <sup>1</sup>H NMR (400 MHz, CDCl<sub>3</sub>, mixture of rotamers) δ 7.52-7.47 (m, 2H), 7.41-7.07 (m, 12H), 4.80 (br, 1H), 4.41 (m, 1H), 4.19-3.74 (m, 3H), 3.65 (m, 1H), 3.40-3.29 (m, 1H), 3.16-3.00 (m, 1H), 2.67-2.59 (m, 2H), 1.93-1.89 (m, 1H), 1.67-1.62 (m, 3H), 1.35-1.26 (m, 19H), 1.10 (s, 2H), 1.00 (s, 7H), 0.90 (t, *J*=6.8 Hz, 3H); <sup>13</sup>C NMR (100 MHz, CDCl<sub>3</sub>, mixture of rotamers) δ 156.4, 141.3, (141.1), 135.7, (135.6), (135.5), 135.5, 133.0, 132.7, 129.6, (129.5), 129.4, (129.3), 128.4, (128.3), 128.1, 127.7, (127.4), 127.4, 80.6, (79.9), 69.4, (65.4), 63.4, (62.5), 61.5, 60.4, (59.9), (59.1), 44.5, (43.6), 35.6, (32.1), 31.9, 31.6, (29.7), 29.6, 29.5, 29.4, (29.3), 29.3, 28.6, 28.3, 26.8, 22.7, (19.0), 18.8, 14.1;  $[\alpha]_D$  (+) 36.6° (*c* 0.32, CHCl<sub>3</sub>); HRMS (ESI) calcd for C<sub>41</sub>H<sub>59</sub>NNaO<sub>4</sub>Si (M+Na)<sup>+</sup> 680.4106, found 680.4105.



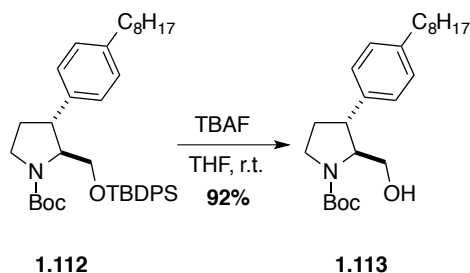
**(2*R*,3*R*,5*R*)-2,5-Bis(hydroxymethyl)-3-(4-octylphenyl)pyrrolidin-1-ium chloride (1.101)** was obtained as pale yellow solid (10.0 mg, 88 %) from silyl ether **1.111** (21 mg, 0.032 mmol) as yellow solid according to the procedure for synthesizing **1.32**.  $^1\text{H}$  NMR (400 MHz,  $\text{D}_2\text{O}$ )  $\delta$  7.08 (d,  $J = 7.6$  Hz, 2H), 6.92 (d,  $J = 8.0$  Hz, 2H), 3.99-3.89 (m, 2H), 3.74-3.58 (m, 3H), 3.27-3.18 (m, 2H), 2.35-2.29 (m, 3H), 1.92-1.88 (m, 1H), 1.45 (br, 2H), 1.26 (br. s, 10H), 0.89 (t,  $J = 6.8$  Hz, 3H);  $^{13}\text{C}$  NMR (100 MHz,  $\text{D}_2\text{O}$ )  $\delta$  140.5, 133.8, 127.8, 127.7, 62.9, 61.1, 58.4, 58.0, 43.4, 35.0, 31.6, 31.0, 29.8, 29.4, 29.2, 29.2, 22.3, 13.5;  $[\alpha]_{\text{D}}^{25}$  (-)  $38.7^\circ$  ( $c$  0.30, MeOH); HRMS (ESI) calcd. for  $\text{C}_{20}\text{H}_{34}\text{NO}_2$  ( $\text{M}+\text{H}$ ) $^+$  320.2584, found 320.2587. HPLC: condition (B),  $t_{\text{R}} = 5.46$  min; purity: 93.3 %.



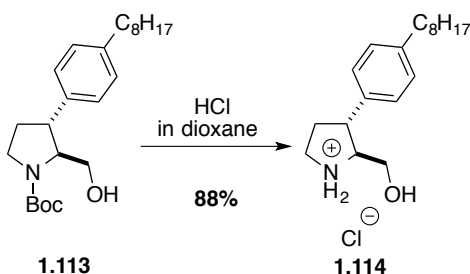
***tert*-Butyl (2*S*,3*R*)-2-(((*tert*-butyldiphenylsilyl)oxy)methyl)-3-(4-octylphenyl)**

**pyrrolidine-1-carboxylate (1.112)** A solution of lactam **1.23** (120 mg, 0.187 mmol) in anhydrous THF (2.4 mL) was cooled to  $0^\circ\text{C}$ . Borane dimethyl sulfide complex (2M in THF, 0.37 mL, 0.748 mmol) was added to the reaction mixture, which was allowed to warm to room temperature and stirred overnight, when completion was indicated by TLC ( $R_{\text{f}}$ : 0.53, hexane: EtOAc, 8:1). The volatiles were removed under reduced pressure. After the residue was co-evaporated twice with MeOH (2 mL), it was dissolved in  $\text{CH}_2\text{Cl}_2$ , and washed three times with saturated aqueous  $\text{NaHCO}_3$ . The organic layer was washed with brine, dried over  $\text{MgSO}_4$  and filtered. The filtrate was evaporated under reduced pressure and the residue was purified by flash chromatography (hexane: EtOAc, 8:1) to give carbamate **1.112** (94.6 mg, 81 %) as pale yellow oil.  $^1\text{H}$  NMR (400 MHz,  $\text{CDCl}_3$ , mixture of rotamers)  $\delta$  7.68-7.67 (m, 4H), 7.66-7.37 (m, 6H), 7.12-7.11 (m, 4H), 4.17 (dd,  $J = 3.6, 10.0$  Hz, 0.4H), 3.92-3.57 (m, 4.6H), 3.44 (m, 1H), 2.59 (t,  $J = 7.2$  Hz, 2H), 2.30-2.24 (m, 1H), 1.98-1.90 (m, 1H), 1.61 (br. s, 2H), 1.52 (s, 3H), 1.35-1.29 (m, 16H), 1.08 (s, 9H), 0.90 (t,  $J = 6.8$  Hz, 3H);  $^{13}\text{C}$  NMR (100 MHz,  $\text{CDCl}_3$ ,

mixture of rotamers)  $\delta$  154.3, 141.2, (140.9), 140.2, 135.6, 133.8, 133.5, (133.4), 129.6, (129.5), 128.6, (127.7), 127.7, (127.3), 127.1, 79.3, (79.0), 65.5, (65.3), 63.5, 62.0, 47.2, (46.4), 46.2, 45.3, 35.5, 32.9, 31.9, 31.5, 29.5, 29.4, 29.2, 28.6, 28.4, 26.9, 22.7, (19.4), 19.3, 14.1;  $[\alpha]_D$  (-) 8.0° (*c* 1.17, CHCl<sub>3</sub>); HRMS (ESI) calcd for C<sub>40</sub>H<sub>57</sub>NNaO<sub>3</sub>Si (M+Na)<sup>+</sup> 650.4000, found 650.3998.



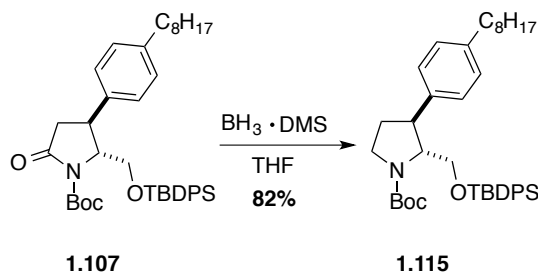
***tert*-Butyl (2*S*,3*R*)-2-(hydroxymethyl)-3-(4-octylphenyl)pyrrolidine-1-carboxylate (1.113)** was obtained as colorless oil (155 mg, 92 %) from silyl ether **1.112** (271 mg, 0.432 mmol) according to the procedure for synthesizing alcohol **1.64**. <sup>1</sup>H NMR (400 MHz, CDCl<sub>3</sub>)  $\delta$  7.14 (s, 4H), 5.10 (br, 1H), 3.93 (m, 1H), 3.90-3.70 (m, 2H), 3.65-3.56 (m, 1H), 3.35 (td, *J*=6.4, 10.5 Hz, 1H), 2.86 (m, 1H), 2.58 (t, *J*=8.0 Hz, 2H), 2.14 (m, 1H), 1.96 (m, 1H), 1.60 (m, 2H), 1.51 (s, 9H), 1.31-1.23 (m, 10H), 0.89 (t, *J*=7.2 Hz, 3H); <sup>13</sup>C NMR (100 MHz, CDCl<sub>3</sub>)  $\delta$  156.9, 141.9, 137.7, 128.7, 127.4, 80.5, 67.1, 66.2, 47.6, 47.1, 35.5, 33.0, 31.9, 31.5, 29.5, 29.3, 29.2, 28.5, 22.7, 14.1;  $[\alpha]_D$  (-) 7.6° (*c* 1.44, CHCl<sub>3</sub>); HRMS (ESI) calcd for C<sub>24</sub>H<sub>39</sub>NNaO<sub>3</sub> (M+Na)<sup>+</sup> 412.2822, found 412.2838.



**(2*S*,3*R*)-2-(Hydroxymethyl)-3-(4-octylphenyl)pyrrolidin-1-ium chloride (1.114)** was obtained as a pale yellow solid (11.0 mg, 88 %) from carbamate **1.113** (15 mg, 0.039 mmol) according to the procedure for synthesizing **1.32**. <sup>1</sup>H NMR (400 MHz, D<sub>2</sub>O)  $\delta$  7.15 (d, *J* = 8.0

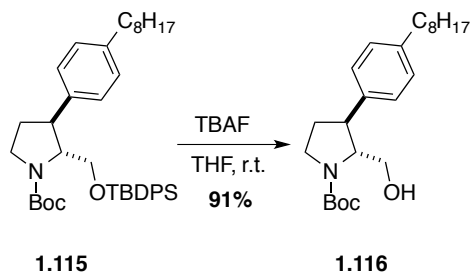
Hz, 2H), 6.91 (d,  $J = 7.6$  Hz, 2H), 3.59 (m, 2H), 3.50 (m, 2H), 3.35-3.27 (m, 1H), 3.18-3.11 (m, 1H), 2.33 (t,  $J = 7.6$  Hz, 2H), 2.15 (m, 1H), 2.06-1.95 (m, 1H), 1.42 (m, 2H), 1.23 (s, 10H), 0.86 (t,  $J = 6.8$  Hz, 3H);  $^{13}\text{C}$  NMR (100 MHz,  $\text{D}_2\text{O}$ )  $\delta$  141.2, 136.0, 128.5, 127.6, 66.4, 58.2, 44.7, 44.5, 35.4, 32.4, 31.9, 31.3, 29.7, 29.5, 29.5, 22.6, 13.9;  $[\alpha]_{\text{D}}^{20}$  (+)  $20.0^\circ$  ( $c$  0.06, MeOH); HRMS (ESI) calcd for  $\text{C}_{19}\text{H}_{32}\text{NO}$  ( $\text{M}+\text{H}$ ) $^+$  290.2478, found 290.2477. HPLC: condition (B),  $t_{\text{R}} = 6.00$  min; purity: 98.5 %.

Compounds **1.117**, **1.120** and **1.123** were prepared according to the procedure for synthesizing **1.114**.

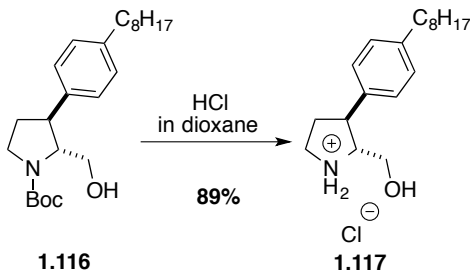


***tert*-Butyl (2*R*,3*S*)-2-(((*tert*-butyldiphenylsilyl)oxy)methyl)-3-(4-octylphenyl)**

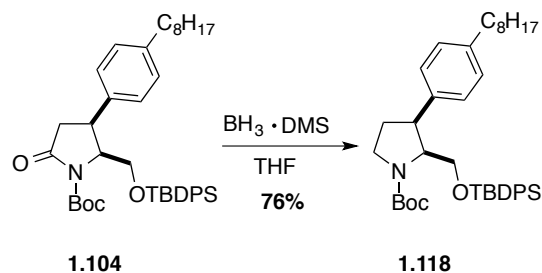
**pyrrolidine-1-carboxylate (1.115)** was obtained as pale yellow oil (120 mg, 82 %) from **1.107** (150 mg, 0.234 mmol).  $^1\text{H}$  NMR (400 MHz,  $\text{CDCl}_3$ , mixture of rotamers)  $\delta$  7.70-7.69 (m, 4H), 7.68-7.39 (m, 6H), 7.15-7.11 (m, 4H), 4.18 (dd,  $J = 3.6, 10.0$  Hz, 0.4H), 3.92-3.57 (m, 4.6H), 3.44 (m, 1H), 2.60 (t,  $J = 7.2$  Hz, 2H), 2.33-2.25 (m, 1H), 1.99-1.90 (m, 1H), 1.61 (m, 2H), 1.53 (s, 3H), 1.36-1.30 (m, 16H), 1.09 (s, 9H), 0.91 (t,  $J = 6.8$  Hz, 3H);  $^{13}\text{C}$  NMR (100 MHz,  $\text{CDCl}_3$ , mixture of rotamers)  $\delta$  154.3, (154.2), 141.2, (140.9), 140.2, 135.6, (133.8), 133.6, 133.5, (133.4), 129.6, (129.5), 128.6, (127.7), 127.7, (127.2), 127.1, 79.3, (79.0), 65.5, (65.3), 63.5, 62.0, 47.2, (46.4), 46.2, 45.4, 35.5, 32.9, 31.9, 31.5, 29.5, 29.4, 29.2, 28.6, 28.4, 26.9, 22.7, (19.4), 19.3, 14.1;  $[\alpha]_{\text{D}}^{20}$  (+)  $7.2^\circ$  ( $c$  0.60,  $\text{CHCl}_3$ ); HRMS (ESI) calcd for  $\text{C}_{40}\text{H}_{57}\text{NNaO}_3\text{Si}$  ( $\text{M}+\text{Na}$ ) $^+$  650.4000, found 650.3980.



***tert*-Butyl (2*R*,3*S*)-2-(hydroxymethyl)-3-(4-octylphenyl)pyrrolidine-1-carboxylate (1.116)** was obtained as pale yellow oil (58 mg, 91%) from silyl ether **1.115** (100 mg, 0.159 mmol).  $^1\text{H}$  NMR (400 MHz,  $\text{CDCl}_3$ )  $\delta$  7.14 (s, 4H), 5.10 (br, 1H), 3.92 (m, 1H), 3.90-3.60 (m, 2H), 3.65-3.56 (m, 1H), 3.35 (td,  $J=6.4, 10.5$  Hz, 1H), 2.86 (m, 1H), 2.58 (t,  $J=8.0$  Hz, 2H), 2.13 (m, 1H), 1.95 (m, 1H), 1.60 (m, 2H), 1.51 (s, 9H), 1.31-1.23 (m, 10H), 0.89 (t,  $J=7.2$  Hz, 3H);  $^{13}\text{C}$  NMR (100 MHz,  $\text{CDCl}_3$ )  $\delta$  156.9, 141.8, 137.7, 128.7, 127.4, 80.4, 67.1, 66.1, 47.5, 47.1, 35.5, 32.9, 31.9, 31.5, 29.4, 29.3, 29.2, 28.4, 22.6, 14.1;  $[\alpha]_{\text{D}}^{25}$  (+) 8.1° ( $c$  1.65,  $\text{CHCl}_3$ ); HRMS (ESI) calcd for  $\text{C}_{24}\text{H}_{39}\text{NNaO}_3$  ( $\text{M}+\text{Na}$ ) $^+$  412.2822, found 412.2807.

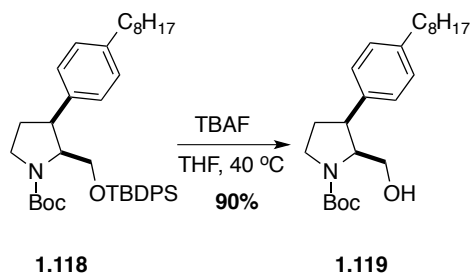


**(2*R*,3*S*)-2-(Hydroxymethyl)-3-(4-octylphenyl)pyrrolidin-1-ium chloride (1.117)** was obtained as yellow solid (10 mg, 89 %) from carbamate **1.116** (15 mg, 0.039 mmol).  $^1\text{H}$  NMR (400 MHz,  $\text{D}_2\text{O}$ )  $\delta$  7.16 (d,  $J = 8.0$  Hz, 2H), 6.91 (d,  $J = 8.0$  Hz, 2H), 3.60 (m, 2H), 3.51 (m, 2H), 3.36-3.29 (m, 1H), 3.20-3.13 (m, 1H), 2.33 (t,  $J = 7.6$  Hz, 2H), 2.18-2.12 (m, 1H), 2.06-1.95 (m, 1H), 1.44 (m, 2H), 1.27 (s, 10H), 0.90 (t,  $J = 6.8$  Hz, 3H);  $^{13}\text{C}$  NMR (100 MHz,  $\text{D}_2\text{O}$ )  $\delta$  141.2, 136.0, 128.5, 127.6, 66.4, 58.2, 44.7, 44.5, 35.4, 32.4, 31.9, 31.3, 29.7, 29.5, 29.5, 22.7, 13.9;  $[\alpha]_{\text{D}}^{25}$  (-) 19.1° ( $c$  0.11, MeOH); HRMS (ESI) calcd for  $\text{C}_{19}\text{H}_{32}\text{NO}$  ( $\text{M}+\text{H}$ ) $^+$  290.2478, found 290.2473. HPLC: condition (B),  $t_{\text{R}} = 5.56$  min; purity: 96.9%.



***tert*-Butyl (2*S*,3*S*)-2-(((*tert*-butyldiphenylsilyl)oxy)methyl)-3-(4-octylphenyl)**

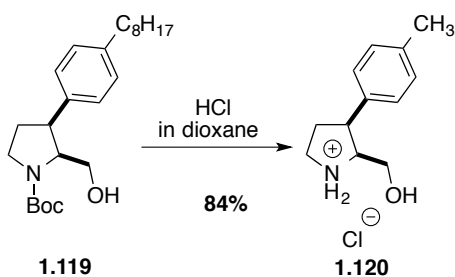
**pyrrolidine-1-carboxylate (1.118)** was obtained as pale yellow oil (22 mg, 76 %) from lactam **1.104** (30 mg, 0.047 mmol).  $^1\text{H}$  NMR (400 MHz,  $\text{CDCl}_3$ , mixture of rotamers)  $\delta$  7.54-7.52 (m, 2H), 7.39-7.13 (m, 12H), 4.11 (d,  $J = 7.2$  Hz, 0.4H), 3.98 (d,  $J = 6.8$  Hz, 0.6H), 3.90 (dd,  $J = 2.8, 11.2$  Hz, 0.4H), 3.78-3.70 (m, 1.6H), 3.62-3.49 (m, 2H), 3.36 (dd,  $J = 10.8, 17.2$  Hz, 1H), 2.86 (m, 1H), 2.65 (m, 2H), 2.17 (m, 1H), 1.65 (m, 2H), 1.54 (s, 4H), 1.41-1.27 (m, 15H), 0.99 (s, 4.4H), 0.98 (s, 4.6H), 0.90 (t,  $J = 6.8$  Hz, 3H);  $^{13}\text{C}$  NMR (100 MHz,  $\text{CDCl}_3$ , mixture of rotamers)  $\delta$  (154.4), 154.3, 141.2, 136.0, 135.6, 135.5, 135.4, (133.4), 133.1, 132.9, 129.5, (129.3), 128.3, (127.7), 127.5, 127.4, 79.2, (79.0), 62.4, 61.8, (61.6), 61.5, 46.4, (46.3), 45.9, 35.7, 31.9, 31.7, 29.5, 29.4, 29.3, (28.6), 28.4, 27.6, 26.7, 22.7, (19.0), 18.8, 14.1;  $[\alpha]_{\text{D}}^{25}$  (-) 38.2° ( $c$  1.90,  $\text{CHCl}_3$ ); HRMS (ESI) calcd for  $\text{C}_{40}\text{H}_{57}\text{NNaO}_3\text{Si}$  ( $\text{M}+\text{Na}$ ) $^+$  650.4000, found 650.3995.



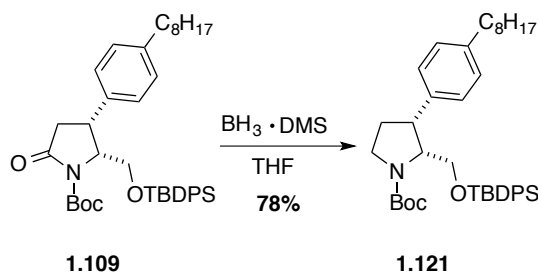
***tert*-Butyl (2*S*,3*S*)-2-(hydroxymethyl)-3-(4-octylphenyl)pyrrolidine-1-carboxylate (1.119)**

A solution of silyl ether **1.118** (22 mg, 0.035 mmol) in anhydrous THF (1.14 mL) was cooled to 0 °C. Tetrabutylammonium fluoride solution (1M in THF, 61  $\mu\text{L}$ , 0.061 mmol) was added. The reaction was allowed to warm to room temperature and stirred overnight, when completion was indicated by TLC ( $R_f$ : 0.33, hexane: EtOAc, 4:1). The reaction was heated to 40 °C for 48 h, quenched with saturated aqueous  $\text{NaHCO}_3$  extracted three times with  $\text{CH}_2\text{Cl}_2$ . The organic layers were washed with brine, dried over  $\text{MgSO}_4$  and filtered. The volatiles were

removed under reduced pressure. The residue was purified by flash chromatography (hexane: EtOAc, 6:1 to 4:1) to give **1.119** (12.2 mg, 90 %) as colorless oil.  $^1\text{H}$  NMR (400 MHz,  $\text{CDCl}_3$ , mixture of rotamers)  $\delta$  7.13 (s, 4H), 4.26 (m, 0.7H), 4.07 (m, 0.3H), 3.63 (m, 1H), 3.47 (m, 2.3H), 3.33 (m, 1.7H), 2.58 (t,  $J=7.6$  Hz, 2H), 2.44-2.28 (m, 1H), 2.15-2.09 (m, 1H), 1.59 (m, 2H), 1.50 (s, 9H), 1.30-1.26 (m, 10H), 0.88 (t,  $J=6.8$  Hz, 3H);  $^{13}\text{C}$  NMR (100 MHz,  $\text{CDCl}_3$ , mixture of rotamers)  $\delta$  157.1, 141.8, 134.9, (134.8), 128.6, (127.7), 127.7, 80.3, 64.7, 62.4, (46.2), 45.7, 35.5, 31.9, 31.5, 29.7, 29.5, 29.3, 29.2, 28.5, 28.0, 22.7, 14.1;  $[\alpha]_{\text{D}}^{25}$  (+)  $9.8^\circ$  ( $c$  1.22,  $\text{CHCl}_3$ ); HRMS (ESI) calcd for  $\text{C}_{24}\text{H}_{39}\text{NNaO}_3$  ( $\text{M}+\text{Na}$ ) $^+$  412.2822, found 412.2829.

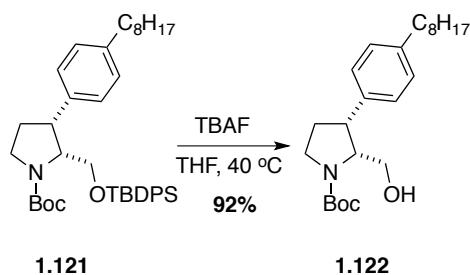


**(2S,3S)-2-(Hydroxymethyl)-3-(4-octylphenyl)pyrrolidin-1-ium chloride (1.120)** was obtained as yellow solid (7.0 mg, 84 %) from carbamate **1.119** (10 mg, 0.026 mmol).  $^1\text{H}$  NMR (400 MHz,  $\text{D}_2\text{O}$ )  $\delta$  7.10 (d,  $J = 7.6$  Hz, 2H), 6.91 (d,  $J = 7.6$  Hz, 2H), 3.99 (m, 1H), 3.59 (m, 2H), 3.35 (m, 1H), 3.27-3.16 (m, 2H), 2.38 (t,  $J = 7.2$  Hz, 2H), 2.22 (m, 1H), 2.09 (m, 1H), 1.46 (m, 2H), 1.29 (s, 10H), 0.91 (t,  $J = 6.8$  Hz, 3H);  $^{13}\text{C}$  NMR (100 MHz,  $\text{D}_2\text{O}$ )  $\delta$  141.1, 133.6, 128.2, 62.6, 58.3, 44.3, 44.0, 35.4, 32.0, 31.3, 29.8, 29.6, 29.5, 27.9, 22.7, 13.9;  $[\alpha]_{\text{D}}^{25}$  (+)  $42.9^\circ$  ( $c$  0.10, MeOH); HRMS (ESI) calcd for  $\text{C}_{19}\text{H}_{32}\text{NO}$  ( $\text{M}+\text{H}$ ) $^+$  290.2478, found 290.2478. HPLC: condition (B),  $t_{\text{R}} = 5.57$  min; purity: 98.0 %.



***tert*-Butyl (2*R*,3*R*)-2-(((*tert*-butyldiphenylsilyl)oxy)methyl)-3-(4-octylphenyl)**

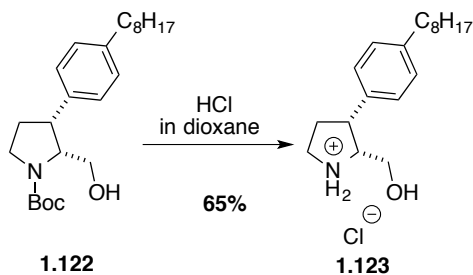
**pyrrolidine-1-carboxylate (1.121)** was obtained as pale yellow oil (22 mg, 76 %) from lactam **1.109** (30 mg, 0.047 mmol). <sup>1</sup>H NMR (400 MHz, CDCl<sub>3</sub>, mixture of rotamers) δ 7.54-7.52 (m, 2H), 7.40-7.13 (m, 12H), 4.11 (d, *J* = 7.2 Hz, 0.4H), 3.98 (d, *J* = 6.8 Hz, 0.6H), 3.90 (dd, *J* = 2.8, 10.8 Hz, 0.4H), 3.78-3.69 (m, 1.6H), 3.61-3.49 (m, 2H), 3.36 (dd, *J* = 10.8, 16.8 Hz, 1H), 2.86 (m, 1H), 2.65 (m, 2H), 2.17 (m, 1H), 1.65 (m, 2H), 1.55 (s, 4H), 1.42-1.23 (m, 15H), 0.99 (s, 3.5H), 0.98 (s, 4.5H), 0.90 (t, *J* = 6.8 Hz, 3H); <sup>13</sup>C NMR (100 MHz, CDCl<sub>3</sub>, mixture of rotamers) δ (154.4), 154.3, 141.2, 136.0, 135.6, 135.5, 135.4, (133.4), 133.1, 132.8, 129.5, (129.3), 128.3, 127.7, (127.5), 127.4, 79.2, (79.0), 62.4, 61.8, (61.6), 61.5, 46.4, (46.3), 45.9, 35.7, 31.9, 31.7, 29.5, 29.4, 29.3, (28.6), 28.4, 27.5, 26.7, 22.7, (19.0), 18.8, 14.1; [α]<sub>D</sub> (+) 34.0° (*c* 2.10, CHCl<sub>3</sub>); HRMS (ESI) calcd for C<sub>40</sub>H<sub>57</sub>NNaO<sub>3</sub>Si(M+Na)<sup>+</sup> 650.4000, found 650.4012.



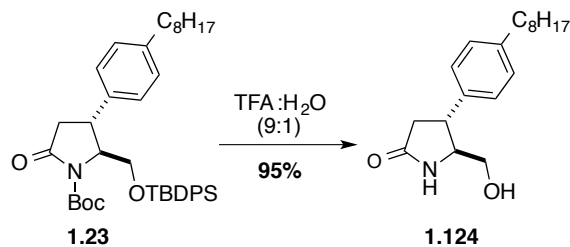
***tert*-Butyl (2*R*,3*R*)-2-(hydroxymethyl)-3-(4-octylphenyl)pyrrolidine-1-carboxylate (1.122)**

was obtained as colorless oil (12.5 mg, 92 %) from silyl ether **1.121** (22 mg, 0.035 mmol). <sup>1</sup>H NMR (400 MHz, CDCl<sub>3</sub>, mixture of rotamers) δ 7.13 (s, 4H), 4.28 (m, 0.7H), 4.06 (m, 0.3H), 3.63 (m, 1H), 3.47 (m, 2.3H), 3.33 (m, 1.7H), 2.58 (t, *J* = 7.6 Hz, 2H), 2.43-2.28 (m, 1H), 2.15-2.09 (m, 1H), 1.61-1.50 (m, 2H), 1.50 (s, 9H), 1.29-1.22 (m, 10H), 0.87 (t, *J* = 6.8 Hz, 3H); <sup>13</sup>C NMR (100 MHz, CDCl<sub>3</sub>) δ 157.1, 141.8, 134.9, 128.6, 127.8, 80.3, 64.7, 62.4, (46.2), 45.7, 35.5, 31.9, 31.4, 29.7, 29.4, 29.3, 29.2, 28.5, 28.0, 22.6, 14.1; [α]<sub>D</sub> (-) 9.3° (*c* 1.25, CHCl<sub>3</sub>); HRMS (ESI) calcd for C<sub>24</sub>H<sub>39</sub>NNaO<sub>3</sub>(M+Na)<sup>+</sup> 412.2822, found 412.2816.





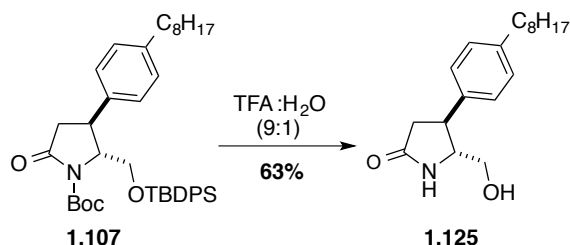
**(2*R*,3*R*)-2-(Hydroxymethyl)-3-(4-octylphenyl)pyrrolidin-1-ium chloride (1.123)** was obtained as yellow solid (5.4 mg, 65 %) from **1.22** (10 mg, 0.026 mmol). <sup>1</sup>H NMR (400 MHz, D<sub>2</sub>O) δ 7.10 (d, *J* = 7.2 Hz, 2H), 6.91 (d, *J* = 7.6 Hz, 2H), 3.98 (m, 1H), 3.59 (m, 2H), 3.38-3.31 (m, 1H), 3.27-3.17 (m, 2H), 2.38 (t, *J* = 7.2 Hz, 2H), 2.25-2.17 (m, 1H), 2.11 (m, 1H), 1.47 (m, 2H), 1.27 (s, 10H), 0.90 (t, *J* = 6.8 Hz, 3H); <sup>13</sup>C NMR (100 MHz, D<sub>2</sub>O) δ 140.8, 133.3, 127.8, 127.8, 62.2, 58.0, 43.9, 43.6, 34.9, 31.5, 30.9, 29.3, 29.1, 29.0, 27.6, 22.2, 13.5; [α]<sub>D</sub> (-) 43.2° (*c* 0.10, MeOH); HRMS (ESI) calcd for C<sub>19</sub>H<sub>32</sub>NO (M+H)<sup>+</sup> 290.2478, found 290.2471. HPLC: condition (B), *t*<sub>R</sub> = 6.13 min; purity: 94.2%.



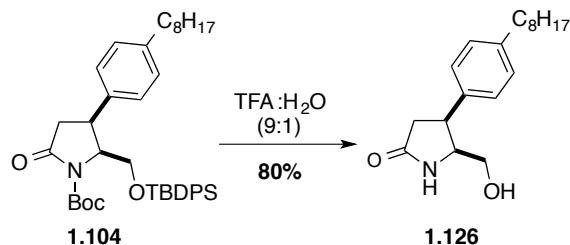
**(4*R*,5*S*)-5-(Hydroxymethyl)-4-(4-octylphenyl)pyrrolidin-2-one (1.124)**. A (9:1) solution of trifluoroacetic acid (0.48 mL, 6.2 mmol) and H<sub>2</sub>O (0.05 mL) was added to a flask containing carbamate **1.23** (40 mg, 0.062 mmol) at 0 °C. After 15 min, the solution was warmed to room temperature and stirred overnight, when completion was indicated by TLC (*R*<sub>f</sub> : 0.17, CH<sub>2</sub>Cl<sub>2</sub>: MeOH: NH<sub>4</sub>OH, 100: 8: 1). The volatiles were removed under reduced pressure. The residue was dissolved in CH<sub>2</sub>Cl<sub>2</sub>, washed three times with saturated aqueous NaHCO<sub>3</sub>. The organic layer was washed with brine, dried over MgSO<sub>4</sub> and filtered. The volatiles were removed under reduced pressure and the residue was purified by flash chromatography (CH<sub>2</sub>Cl<sub>2</sub>: MeOH: NH<sub>4</sub>OH, 100: 8: 1) to give lactam **1.124** (18.0 mg, 95 %) as white solid. <sup>1</sup>H NMR (400 MHz, CDCl<sub>3</sub>) δ 7.38 (s, 1H), 7.16 (s, 4H), 3.93-3.72 (m, 3H), 3.63-3.48 (m, 1H), 3.30 (m, 1H), 2.81 (dd, *J* = 17.6, 9.6 Hz, 1H), 2.66-2.51 (m, 3H), 1.60 (p, *J* = 7.2 Hz, 2H), 1.41-

1.18 (m, 10H), 0.94-0.81 (m, 3H);  $^{13}\text{C}$  NMR (100 MHz,  $\text{CDCl}_3$ )  $\delta$  177.9, 142.1, 138.7, 128.9, 127.1, 64.3, 64.2, 42.0, 39.3, 35.5, 31.9, 31.5, 29.5, 29.3, 29.2, 22.6, 14.1;  $[\alpha]_{\text{D}}$  (+) 25.8° (*c* 0.12,  $\text{CHCl}_3$ ); HRMS (ESI) calcd for  $\text{C}_{19}\text{H}_{29}\text{NNaO}_2$  ( $\text{M}+\text{Na}$ ) $^+$  326.2091, found. 326.2100.

Compounds **1.125**, **1.126** and **1.127** were prepared according to the procedure for synthesizing **1.124**.

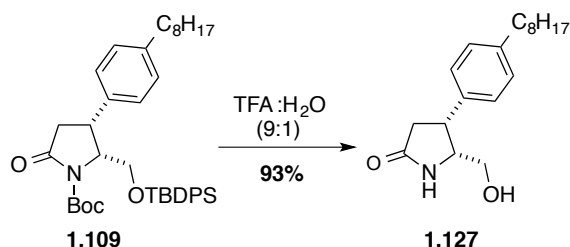


**(4*S*,5*R*)-5-(Hydroxymethyl)-4-(4-octylphenyl)pyrrolidin-2-one (1.125)** was obtained as white solid (12.0 mg, 63 %) from silyl ether **1.107** (40 mg, 0.062 mmol).  $^1\text{H}$  NMR (400 MHz,  $\text{CDCl}_3$ )  $\delta$  7.17 (s, 4H), 6.61 (s, 1H), 3.85-3.75 (m, 2H), 3.57 (m, 1H), 3.28 (td,  $J = 9.0, 6.7$  Hz, 1H), 2.80 (dd,  $J = 17.3, 9.4$  Hz, 1H), 2.69-2.45 (m, 4H), 1.59 (dd,  $J = 14.9, 7.2$  Hz, 2H), 1.37-1.22 (m, 10H), 0.89 (t,  $J = 6.9$  Hz, 3H);  $^{13}\text{C}$  NMR (100 MHz,  $\text{D}_2\text{O}$ )  $\delta$  177.2, 142.1, 138.6, 128.9, 127.1, 64.6, 63.7, 42.2, 39.1, 35.5, 31.9, 31.5, 29.4, 29.3, 29.2, 22.6, 14.1;  $[\alpha]_{\text{D}}$  (-) 23.0° (*c* 0.60,  $\text{CHCl}_3$ ); HRMS (ESI) calcd for  $\text{C}_{19}\text{H}_{29}\text{NNaO}_2$  ( $\text{M}+\text{Na}$ ) $^+$  326.2091, found 326.2090. HPLC: condition (C),  $t_{\text{R}} = 6.16$  min; purity: > 99 %.

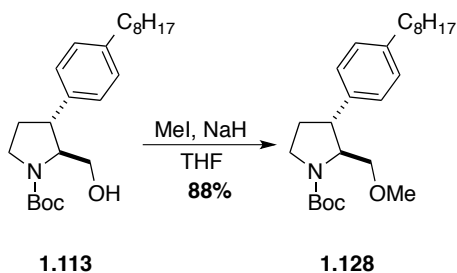


**(4*S*,5*S*)-5-(Hydroxymethyl)-4-(4-octylphenyl)pyrrolidin-2-one (1.126)** was obtained as white solid (5.7 mg, 80 %) from silyl ether **1.104** (15 mg, 0.023 mmol).  $^1\text{H}$  NMR (700 MHz,  $\text{CDCl}_3$ )  $\delta$  7.16 (s, 4H), 6.22 (m, 1H), 3.99-3.96 (td,  $J = 7.6, 3.9$  Hz, 1H), 3.85-3.82 (dd,  $J = 16.9, 8.6$  Hz, 1H), 3.36-3.34 (dd,  $J = 11.3, 3.7$  Hz, 1H), 3.24-3.22 (m, 1H), 2.79-2.64 (ddd,  $J =$

77.3, 16.8, 8.8 Hz, 2H), 2.60-2.58 (t,  $J = 7.7$  Hz, 2H), 1.61 (m, 2H), 1.32-1.26 (m, 10H), 0.90 (t,  $J = 7.7$  Hz, 3H);  $^{13}\text{C}$  NMR (100 MHz,  $\text{CDCl}_3$ )  $\delta$  177.6, 142.3, 134.9, 128.8, 127.6, 63.5, 59.1, 41.9, 35.6, 35.5, 31.9, 31.4, 29.4, 29.3, 29.2, 22.6, 14.1;  $[\alpha]_{\text{D}}^{25}$  (+) 130.2° ( $c$  0.56,  $\text{CHCl}_3$ ); HRMS (ESI) calcd for  $\text{C}_{19}\text{H}_{29}\text{NNaO}_2$  ( $\text{M}+\text{Na}$ ) $^{+}$  326.2091, found 326.2095. HPLC: condition (C),  $t_{\text{R}} = 6.57$  min; purity: > 99 %.



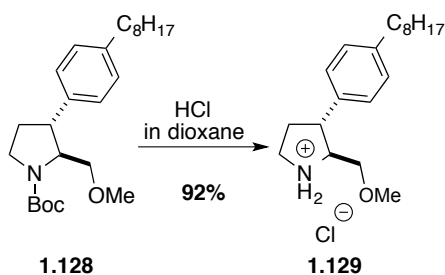
**(4*R*,5*R*)-5-(Hydroxymethyl)-4-(4-octylphenyl)pyrrolidin-2-one (1.127)** was obtained as white solid (6.6 mg, 93 %) from silyl ether **1.109** (15 mg, 0.023 mmol).  $^1\text{H}$  NMR (700 MHz,  $\text{CDCl}_3$ )  $\delta$  7.16 (s, 4H), 6.06 (m, 1H), 3.99-3.96 (td,  $J = 7.8, 3.9$  Hz, 1H), 3.86-3.82 (dd,  $J = 16.8, 8.7$  Hz, 1H), 3.37-3.35 (dd,  $J = 11.1, 3.8$  Hz, 1H), 3.24-3.22 (m, 1H), 2.79-2.65 (ddd,  $J = 71.7, 16.8, 8.8$  Hz, 2H), 2.60-2.58 (t,  $J = 7.7$  Hz, 2H), 1.59 (m, 2H), 1.31-1.26 (m, 10H), 0.89 (t,  $J = 7.0$  Hz, 3H);  $^{13}\text{C}$  NMR (100 MHz,  $\text{CDCl}_3$ )  $\delta$  177.9, 142.3, 134.9, 128.8, 127.6, 63.5, 59.3, 41.9, 35.6, 35.6, 31.9, 31.5, 29.5, 29.4, 29.3, 22.7, 14.1;  $[\alpha]_{\text{D}}^{25}$  (-) 131.3° ( $c$  0.45,  $\text{CHCl}_3$ ); HRMS (ESI) calcd for  $\text{C}_{19}\text{H}_{29}\text{NNaO}_2$  ( $\text{M}+\text{Na}$ ) $^{+}$  326.2091, found 326.2095. HPLC: condition (C),  $t_{\text{R}} = 5.62$  min; purity: > 99 %.



***tert*-Butyl (2*S*,3*R*)-2-(methoxymethyl)-3-(4-octylphenyl)pyrrolidine-1-carboxylate (1.128)**

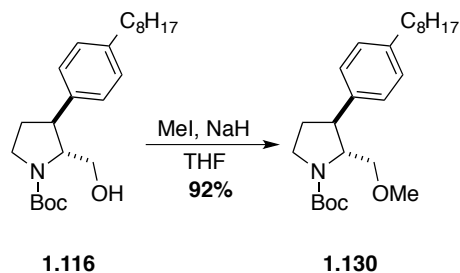
A solution of alcohol **1.113** (35 mg, 0.090 mmol) in anhydrous THF (0.75 mL) was cooled to

0 °C. Sodium hydride (60 % dispersion in mineral oil, 7.2 mg, 0.180 mmol) was added to the solution followed by methyl iodide (26 mg, 12  $\mu$ L, 0.180 mmol). The reaction was allowed to warm to room temperature and stirred overnight. The mixture was poured into water and extracted three times with EtOAc. The organic layers were combined, washed with brine, dried over MgSO<sub>4</sub> and filtered. The filtrate was evaporated under reduced pressure and the residue was purified by flash chromatography (hexane: EtOAc, 4:1) to give ether **1.128** (32 mg, 88 %) as colorless oil. <sup>1</sup>H NMR (400 MHz, CDCl<sub>3</sub>)  $\delta$  7.11 (s, 4H), 3.95-3.86 (br, 1H), 3.68 (br, 2H), 3.47 (m, 2H), 3.36 (m, 4H), 2.57 (t,  $J=7.6$  Hz, 2H), 2.24 (m, 1H), 1.89 (m, 1H), 1.59 (m, 2H), 1.49 (s, 9H), 1.29 (m, 10H), 0.88 (m, 3H); <sup>13</sup>C NMR (100 MHz, CDCl<sub>3</sub>)  $\delta$  154.4, 141.2, 140.6, 128.6, 127.1, 79.4, 72.6, 71.4, 63.5, 59.1, 46.5, 46.0, 35.5, 31.9, 31.5, 29.5, 29.4, 29.2, 28.5, 22.7, 14.1;  $[\alpha]_D$  (+) 13.3° ( $c$  0.68, CHCl<sub>3</sub>); HRMS (ESI) calcd for C<sub>25</sub>H<sub>41</sub>NNaO<sub>3</sub> (M+Na)<sup>+</sup> 426.2979, found 426.2981.

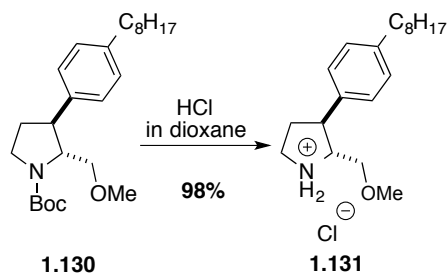


**(2S,3R)-2-(Methoxymethyl)-3-(4-octylphenyl)pyrrolidin-1-ium chloride (1.129)** was obtained as yellow oil (13.1 mg, 92 %) from ether **1.128** (19 mg, 0.047 mmol) according the procedure for synthesizing **1.32**. <sup>1</sup>H NMR (400 MHz, D<sub>2</sub>O)  $\delta$  7.17 (d,  $J=8.0$  Hz, 2H), 6.92 (d,  $J=7.6$  Hz, 2H), 3.64 (m, 2H), 3.56 (m, 1H), 3.42-3.30 (m, 2H), 3.18-3.12 (m, 4H), 2.36 (t,  $J=7.6$  Hz, 2H), 2.21 (m, 1H), 2.06 (m, 1H), 1.46 (m, 2H), 1.28 (s, 10H), 0.90 (m, 3H); <sup>13</sup>C NMR (100 MHz, D<sub>2</sub>O)  $\delta$  140.8, 135.7, 128.2, 127.3, 68.5, 64.0, 58.2, 44.7, 44.4, 35.0, 32.3, 31.6, 31.0, 29.3, 29.2, 29.0, 22.3, 13.5;  $[\alpha]_D$  (+) 33.5° ( $c$  0.49, MeOH); HRMS (ESI) calcd for C<sub>20</sub>H<sub>34</sub>NO (M+H)<sup>+</sup> 304.2635, found 304.2643. HPLC: condition (B),  $t_R = 7.20$  min; purity: 96.6 %.

Compound **1.131** was prepared according to the procedure for synthesizing **1.129**.

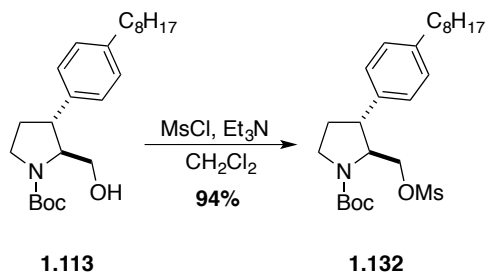


***tert*-Butyl (2*R*,3*S*)-2-(methoxymethyl)-3-(4-octylphenyl)pyrrolidine-1-carboxylate (1.130)** was obtained as colorless oil (33 mg, 92 %) from **1.116** (35 mg, 0.090 mmol).  $^1\text{H}$  NMR (400 MHz,  $\text{CDCl}_3$ )  $\delta$  7.12 (s, 4H), 3.97 (br, 1H), 3.67 (br, 2H), 3.45 (m, 2H), 3.37 (m, 4H), 2.58 (t,  $J=7.6$  Hz, 2H), 2.24 (m, 1H), 1.90 (m, 1H), 1.59 (m, 2H), 1.50 (s, 9H), 1.29 (m, 10H), 0.89 (m, 3H);  $^{13}\text{C}$  NMR (100 MHz,  $\text{CDCl}_3$ )  $\delta$  154.4, 141.2, 140.6, 128.6, 127.0, 79.4, 72.6, 71.4, 63.5, 59.1, 46.4, 46.0, 35.5, 31.9, 31.5, 29.4, 29.3, 29.2, 28.5, 22.6, 14.1;  $[\alpha]_{\text{D}} (-) 16.9^\circ$  ( $c$  1.1,  $\text{CHCl}_3$ ); HRMS (ESI) calcd for  $\text{C}_{25}\text{H}_{41}\text{NNaO}_3$  ( $\text{M}+\text{Na}$ ) $^+$  426.2979, found 426.2988.

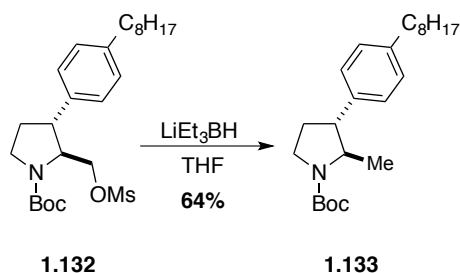


**(2*R*,3*S*)-2-(Methoxymethyl)-3-(4-octylphenyl)pyrrolidin-1-ium chloride (1.131)** was obtained as yellow oil (9.9 mg, 98 %) from carbamate **1.130** (12 mg, 0.030 mmol).  $^1\text{H}$  NMR (400 MHz,  $\text{D}_2\text{O}$ )  $\delta$  7.17 (d,  $J = 8.0$  Hz, 2H), 6.93 (d,  $J = 8.0$  Hz, 2H), 3.66 (m, 2H), 3.57 (m, 1H), 3.43-3.31 (m, 2H), 3.17 (m, 4H), 2.37 (m, 2H), 2.22 (m, 1H), 2.06 (m, 1H), 1.47 (m, 2H), 1.28 (s, 10H), 0.91 (m, 3H);  $^{13}\text{C}$  NMR (100 MHz,  $\text{D}_2\text{O}$ )  $\delta$  141.2, 136.1, 128.6, 127.7, 68.9, 64.4, 58.5, 45.0, 44.7, 35.4, 32.6, 31.9, 31.4, 29.6, 29.5, 29.4, 22.6, 13.9;  $[\alpha]_{\text{D}} (-) 32.8^\circ$  ( $c$  0.29, MeOH); HRMS (ESI) calcd for  $\text{C}_{20}\text{H}_{34}\text{NO}$  ( $\text{M}+\text{H}$ ) $^+$  304.2635, found 304.2640. HPLC: condition (B),  $t_{\text{R}} = 6.48$  min; purity: 96.8 %.

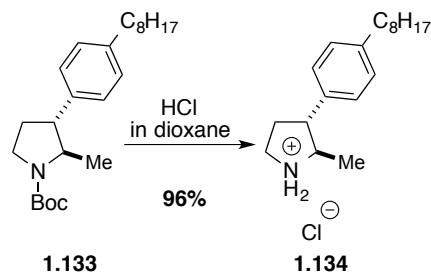
Compounds **1.134** and **1.137** were prepared according to the procedure for synthesizing **1.70**.



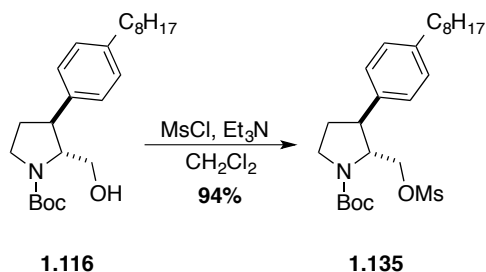
***tert*-Butyl (2*S*,3*R*)-2-(((methanesulfonyl)oxy)methyl)-3-(4-octylphenyl)pyrrolidine-1-carboxylate (1.132)** was obtained as colorless oil (68 mg, 94 %) from alcohol **1.113** (60 mg, 0.154 mmol). <sup>1</sup>H NMR (400 MHz, CDCl<sub>3</sub>, mixture of rotamers) δ 7.15 (s, 4H), 4.71 (br, 0.6H), 4.44 (br, 0.4H), 4.28-4.21 (m, 1H), 3.95 (br, 1H), 3.81-3.69 (br, 1H), 3.44-3.34 (m, 2H), 2.98 (s, 3H), 2.58 (t, *J*=7.6 Hz, 2H), 2.24-2.19 (m, 1H), 2.00-1.95 (m, 1H), 1.58 (m, 2H), 1.50 (s, 9H), 1.31-1.27 (m, 10H), 0.88 (t, *J*=6.8 Hz, 3H); <sup>13</sup>C NMR (100 MHz, CDCl<sub>3</sub>, mixture of rotamers) δ 154.4, (153.9), 141.9, 138.1, 128.9, 127.2, (80.6), 80.0, 67.9, 62.9, 46.9, (46.5), 45.7, (37.5), 36.9, 35.5, 32.6, 31.9, 31.5, 29.4, 29.3, 29.2, 28.4, 22.6, 14.1; [α]<sub>D</sub> (+) 3.0° (*c* 2.9, CHCl<sub>3</sub>); HRMS (ESI) calcd for C<sub>25</sub>H<sub>41</sub>NNaO<sub>5</sub>S (M+Na)<sup>+</sup> 490.2598, found 490.2594.



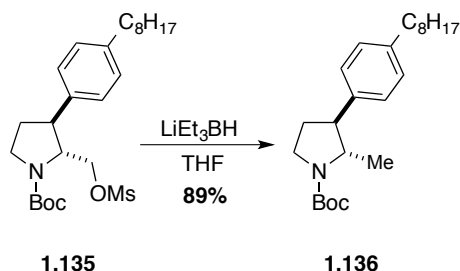
***tert*-Butyl (2*R*,3*R*)-2-methyl-3-(4-octylphenyl)pyrrolidine-1-carboxylate (1.133)** was obtained as colorless oil (33.4 mg, 64 %) from methanesulfonate **1.132** (65 mg, 0.139 mmol). <sup>1</sup>H NMR (400 MHz, CDCl<sub>3</sub>) δ 7.13 (s, 4H), 3.75 (br, 2H), 3.40-3.34 (m, 1H), 2.92-2.87(m, 1H), 2.58 (t, *J*=7.6 Hz, 2H), 2.21-2.13 (m, 1H), 1.96-1.89 (m, 1H), 1.60 (m, 2H), 1.49 (s, 9H), 1.28 (m, 13H), 0.89 (t, *J*=6.8 Hz, 3H); <sup>13</sup>C NMR (100 MHz, CDCl<sub>3</sub>) δ 154.6, 141.4, 139.5, 128.6, 127.2, 79.1, 59.9, 52.9, 45.9, 35.5, 32.1, 31.9, 31.5, 29.5, 29.4, 29.2, 28.6, 22.7, 20.2, 14.1; [α]<sub>D</sub> (+) 8.8° (*c* 0.68, CHCl<sub>3</sub>); HRMS (ESI) calcd for C<sub>25</sub>H<sub>39</sub>NNaO<sub>2</sub> (M+Na)<sup>+</sup> 396.2873, found 396.2868.



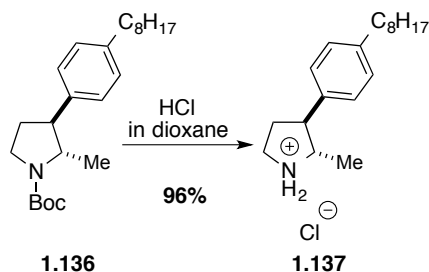
**(2*R*,3*R*)-2-Methyl-3-(4-octylphenyl)pyrrolidin-1-ium chloride (1.134)** was obtained as yellow solid (26 mg, 96 %) from carbamate **1.133** (33 mg, 0.088 mmol).  $^1\text{H}$  NMR (400 MHz,  $\text{D}_2\text{O}$ )  $\delta$  7.10 (d,  $J = 8.0$  Hz, 2H), 6.90 (d,  $J = 7.6$  Hz, 2H), 3.47 (m, 2H), 3.35 (m, 1H), 2.91 (m, 1H), 2.34 (m, 2H), 2.15 (m, 1H), 1.99 (m, 1H), 1.45 (m, 2H), 1.29 (s, 10H), 1.10 (d,  $J = 6.4$  Hz, 3H), 0.91 (m, 3H);  $^{13}\text{C}$  NMR (100 MHz,  $\text{D}_2\text{O}$ )  $\delta$  141.0, 136.0, 128.4, 127.6, 61.2, 50.3, 43.7, 35.5, 32.1, 32.0, 31.4, 29.8, 29.6, 29.6, 22.7, 14.5, 13.9;  $[\alpha]_{\text{D}}^{25}$  (+) 23.3° ( $c$  0.58, MeOH); HRMS (ESI) calcd for  $\text{C}_{19}\text{H}_{32}\text{N}$  ( $\text{M}+\text{H}$ ) $^+$  274.2529, found 274.2540. HPLC: condition (B),  $t_{\text{R}} = 6.93$  min; purity: 95.6 %.



***tert*-Butyl (2*R*,3*S*)-2-(((methylsulfonyl)oxy)methyl)-3-(4-octylphenyl)pyrrolidine-1-carboxylate (1.135)** was obtained as colorless oil (34.0 mg, 94 %) from **1.116** (30 mg, 0.077 mmol).  $^1\text{H}$  NMR (400 MHz,  $\text{CDCl}_3$ , mixture of rotamers)  $\delta$  7.15 (s, 4H), 4.72 (br, 0.6H), 4.45 (br, 0.4H), 4.27-4.21 (m, 1H), 3.96 (br, 1H), 3.81-3.68 (br, 1H), 3.44-3.34 (m, 2H), 2.98 (s, 3H), 2.58 (t,  $J = 7.6$  Hz, 2H), 2.25-2.21 (m, 1H), 2.00 (m, 1H), 1.62-1.56 (m, 2H), 1.50 (s, 9H), 1.28 (m, 10H), 0.89 (t,  $J = 6.8$  Hz, 3H);  $^{13}\text{C}$  NMR (100 MHz,  $\text{CDCl}_3$ , mixture of rotamers)  $\delta$  154.4, (153.9), 141.9, 138.6, 138.1, 128.8, 127.2, (80.5), 79.9, 68.0, 67.9, 62.8, 46.8, (46.4), 45.6, (37.5), 36.8, 35.5, 32.5, 31.8, 31.4, 29.4, 29.3, 29.2, 28.4, 22.6, 14.1;  $[\alpha]_{\text{D}}^{25}$  (-) 2.5° ( $c$  1.4,  $\text{CHCl}_3$ ); HRMS (ESI) calcd for  $\text{C}_{25}\text{H}_{41}\text{NNaO}_5\text{S}$  ( $\text{M}+\text{Na}$ ) $^+$  490.2598, found 490.2608.



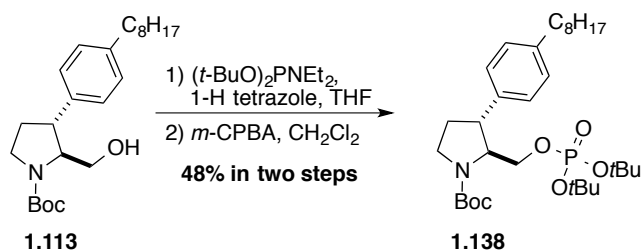
***tert*-Butyl (2*S*,3*S*)-2-methyl-3-(4-octylphenyl)pyrrolidine-1-carboxylate (1.136)** was obtained as colorless oil (20.7 mg, 89 %) from methanesulfonate **1.135** (29 mg, 0.062 mmol).  $^1\text{H}$  NMR (400 MHz,  $\text{CDCl}_3$ )  $\delta$  7.13 (s, 4H), 3.75 (br, 2H), 3.41-3.34 (m, 1H), 2.92-2.87(m, 1H), 2.58 (t,  $J=7.6$  Hz, 2H), 2.21-2.14 (dtd,  $J=10.8, 6.6, 4.2$  Hz, 1H), 1.96-1.87 (m, 1H), 1.61 (m, 2H), 1.49 (s, 9H), 1.28 (m, 13H), 0.89 (t,  $J=6.8$  Hz, 3H);  $^{13}\text{C}$  NMR (100 MHz,  $\text{CDCl}_3$ )  $\delta$  154.6, 141.4, 139.5, 128.6, 127.2, 79.1, 59.9, 52.9, 45.9, 35.5, 32.1, 31.9, 31.5, 29.5, 29.4, 29.2, 28.6, 22.7, 20.2, 14.1;  $[\alpha]_{\text{D}}^{25}$  (-)  $6.7^\circ$  ( $c$  0.09,  $\text{CHCl}_3$ ); HRMS (ESI) calcd for  $\text{C}_{25}\text{H}_{39}\text{NNaO}_2$  ( $\text{M}+\text{Na}$ ) $^+$  396.2873, found 396.2877.



**(2*S*,3*S*)-2-Methyl-3-(4-octylphenyl)pyrrolidin-1-ium chloride (1.137)** was obtained as yellow solid (8.0 mg, 96 %) from carbamate **1.136** (10 mg, 0.027 mmol).  $^1\text{H}$  NMR (400 MHz,  $\text{D}_2\text{O}$ )  $\delta$  7.10 (d,  $J=7.6$  Hz, 2H), 6.90 (d,  $J=7.6$  Hz, 2H), 3.46 (m, 2H), 3.35 (m, 1H), 2.91 (m, 1H), 2.35 (m, 2H), 2.15 (m, 1H), 1.99 (m, 1H), 1.46 (m, 2H), 1.29 (s, 10H), 1.11 (d,  $J=6.4$  Hz, 3H), 0.86 (m, 3H);  $^{13}\text{C}$  NMR (100 MHz,  $\text{D}_2\text{O}$ )  $\delta$  141.1, 136.0, 128.4, 127.6, 61.2, 50.3, 43.7, 35.4, 32.1, 31.9, 31.3, 29.7, 29.6, 29.5, 22.7, 14.5, 13.9;  $[\alpha]_{\text{D}}^{25}$  (-)  $26.2^\circ$  ( $c$  0.13, MeOH); HRMS (ESI) calcd for  $\text{C}_{19}\text{H}_{32}\text{N}$  ( $\text{M}+\text{H}$ ) $^+$  274.2529, found 274.2540. HPLC: condition (B),  $t_{\text{R}} = 5.98$  min; purity: 96.2 %.

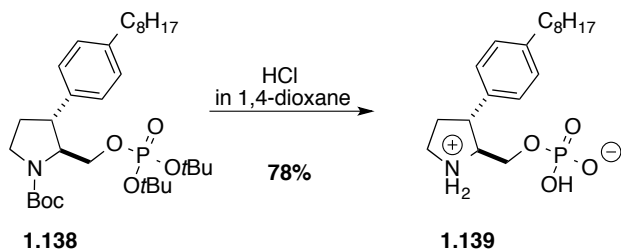


Compounds **1.139** and **1.141** were prepared according to the procedure for synthesizing **1.77**.



***tert*-Butyl (2*S*,3*R*)-2-(((di-*tert*-butoxyphosphoryl)oxy)methyl)-3-(4-octylphenyl)**

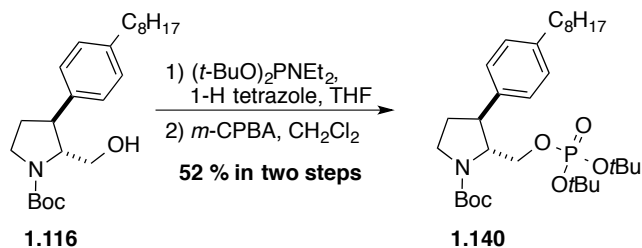
**pyrrolidine-1-carboxylate (1.138)** was obtained as colorless oil (10.0 mg, 48 % over two steps) from carbamate **1.113** (14 mg, 0.036 mmol). <sup>1</sup>H NMR (400 MHz, CDCl<sub>3</sub>) δ 7.13 (s, 4H), 4.36 (m, 0.5H), 4.12 (m, 0.5H), 4.01-3.87 (m, 2H), 3.75-3.64 (m, 1H), 3.50 (m, 1H), 3.38 (m, 1H), 2.58 (m, 2H), 2.24 (m, 1H), 1.94 (m, 1H), 1.60 (m, 2H), 1.49-1.48 (m, 27H), 1.28 (m, 10H), 0.88 (m, 3H); <sup>13</sup>C NMR (100 MHz, CDCl<sub>3</sub>, mixture of rotamers) δ 154.1, 141.4, 139.9, 139.5, 128.7, 127.2, 127.1, 82.2, 79.9, 79.3, 65.5, 64.8, 63.8, 63.7, 46.7, 46.2, 46.1, 45.0, 35.5, 31.9, 31.5, 29.9, 29.8, 29.4, 29.3, 29.2, 28.5, 22.6, 14.1; <sup>31</sup>P NMR (162 MHz, CDCl<sub>3</sub>, mixture of rotamers) -9.34, -9.79; [α]<sub>D</sub> (+) 4.0° (*c* 0.80, CHCl<sub>3</sub>); HRMS (ESI) calcd for C<sub>32</sub>H<sub>56</sub>NNaO<sub>6</sub>P (M+Na)<sup>+</sup> 604.3738, found 604.3732.



**((2*S*,3*R*)-3-(4-Octylphenyl)pyrrolidin-1-ium-2-yl)methyl hydrogen phosphate (1.139)**

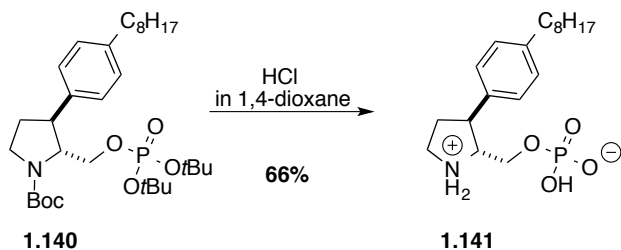
was obtained as white solid (2.5 mg, 78 %) from **1.138** (5 mg, 0.009 mmol). <sup>1</sup>H NMR (400 MHz, MeOD) δ 7.17 (d, *J* = 8.0 Hz, 2H), 7.09 (d, *J* = 8.0 Hz, 2H), 4.05 (ddd, *J* = 10.4, 7.6, 2.8 Hz, 1H), 3.79 (ddd, *J* = 12.8, 10.4, 5.6 Hz, 1H), 3.62 (ddd, *J* = 8.0, 5.2, 2.4 Hz, 1H), 3.46 (ddd, *J* = 11.2, 8.4, 2.4 Hz, 1H), 3.30 (qd, *J* = 11.2, 7.2 Hz, 2H), 2.50 (t, *J* = 7.6 Hz, 2H), 2.34 (dtd, *J* = 13.6, 6.8, 2.8 Hz, 1H), 2.15 (m, 1H), 1.50 (m, 2H), 1.27-1.12 (m, 10H), 0.80 (t, *J* = 6.8 Hz, 3H). <sup>13</sup>C NMR (100 MHz, MeOD, mixture of rotamers) δ 143.9, 136.8, 130.4, 128.8, 67.4, 67.4, 62.8, 62.7, 46.2, 46.1, 36.7, 34.2, 33.2, 32.9, 30.8, 30.6, 30.5, 23.9, 14.6; [α]<sub>D</sub> (+) 52.0°

(*c* 0.05, MeOH);  $^{31}\text{P}$  NMR (162MHz, MeOD) 3.65; HRMS (ESI) calcd for  $\text{C}_{19}\text{H}_{33}\text{NO}_4\text{P}$  ( $\text{M}+\text{H}$ ) $^+$  370.2142, found 370.2134. HPLC: condition (D),  $t_{\text{R}} = 7.14$  min; purity: 94.7 %.



***tert*-Butyl (2*R*,3*S*)-2-(((di-*tert*-butoxyphosphoryl)oxy)methyl)-3-(4-octylphenyl)**

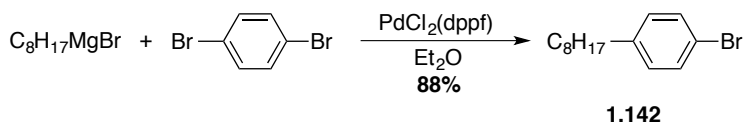
**pyrrolidine-1-carboxylate (1.140)** was obtained as colorless oil (11.0 mg, 52 % over two steps) from **1.116** (14 mg, 0.036 mmol).  $^1\text{H}$  NMR (400 MHz,  $\text{CDCl}_3$ )  $\delta$  7.13 (s, 4H), 4.37 (m, 0.5H), 4.12 (m, 0.5H), 4.01-3.87 (m, 2H), 3.75-3.62 (m, 1H), 3.50 (m, 1H), 3.38 (m, 1H), 2.58 (t,  $J = 8.0$  Hz, 2H), 2.24 (m, 1H), 1.94 (m, 1H), 1.60 (m, 2H), 1.49-1.48 (m, 27H), 1.31-1.26 (m, 10H), 0.89 (t,  $J = 6.8$  Hz, 3H);  $^{13}\text{C}$  NMR (100 MHz,  $\text{CDCl}_3$ , mixture of rotamers)  $\delta$  154.2, 141.4, 139.9, 128.7, 127.2, 127.1, 82.2, 79.9, 79.4, 65.5, 64.8, 63.8, 63.7, 46.7, 46.2, 46.1, 45.0, 35.5, 31.9, 31.5, 29.9, 29.8, 29.5, 29.4, 29.3, 28.5, 22.7, 14.1;  $^{31}\text{P}$  NMR (162 MHz,  $\text{CDCl}_3$ , mixture of rotamers) -8.72, -9.18;  $[\alpha]_{\text{D}}^{25}$  (-) 4.2 $^\circ$  (*c* 0.50,  $\text{CHCl}_3$ ); HRMS (ESI) calcd for  $\text{C}_{32}\text{H}_{56}\text{NNaO}_6\text{P}$  ( $\text{M}+\text{Na}$ ) $^+$  604.3738, found 604.3733.



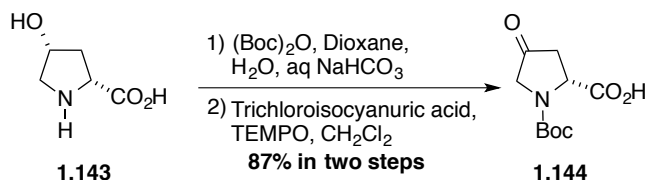
**((2*R*,3*S*)-3-(4-Octylphenyl)pyrrolidin-1-ium-2-yl)methyl hydrogen phosphate (1.139)**

was obtained as white solid (2.1 mg, 66 %) from **1.140** (5 mg, 0.009 mmol).  $^1\text{H}$  NMR (400 MHz, MeOD)  $\delta$  7.17 (d,  $J = 8.0$  Hz, 2H), 7.09 (d,  $J = 8.0$  Hz, 2H), 4.05 (ddd,  $J = 10.4, 8.0, 2.8$  Hz, 1H), 3.78 (ddd,  $J = 12.8, 10.4, 5.6$  Hz, 1H), 3.61 (ddd,  $J = 8.0, 5.2, 2.4$  Hz, 1H), 3.45 (ddd,  $J = 11.2, 8.4, 2.4$  Hz, 1H), 3.30 (m, 2H), 2.50 (t,  $J = 7.6$  Hz, 2H), 2.33 (dtd,  $J = 13.6, 6.8, 2.4$  Hz, 1H), 2.12 (m, 1H), 1.50 (m, 2H), 1.27-1.12 (m, 10H), 0.80 (m, 3H).  $^{13}\text{C}$  NMR (100 MHz, MeOD, mixture of rotamers)  $\delta$  143.8, 136.8, 130.3, 128.8, 67.4, 67.3, 62.7, 62.6, 46.2, 46.0,

36.6, 34.2, 33.2, 32.9, 30.7, 30.6, 30.5, 23.9, 14.6;  $[\alpha]_D$  (-) 55.0° (*c* 0.10, MeOH);  $^{31}\text{P}$  NMR (162MHz, MeOD) 2.98; HRMS (ESI) calcd for  $\text{C}_{19}\text{H}_{33}\text{NO}_4\text{P}$  ( $\text{M}+\text{H}$ ) $^+$  370.2142, found 370.2148.

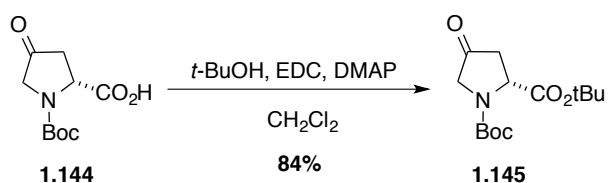


**1-Bromo-4-octylbenzene (1.142)** was synthesized according to a procedure to generate 1-bromo-4-dodecylbenzene reported by Dorn et al.<sup>125</sup> A solution of octylmagnesium bromide (2.0 M) in diethyl ether, (21.2 mL, 42.4 mmol) was added dropwise to a diethyl ether solution (25.0 mL) of 1,4-dibromobenzene (10 g, 42.4 mmol) and  $\text{PdCl}_2(\text{dppf})$  at 0 °C under argon. After stirring for 48 h at room temperature, the mixture was heated at reflux for 2.5 h, exposed to air, poured into water and extracted three times with diethyl ether. The combined organic layers were washed with brine, dried over  $\text{MgSO}_4$  and filtered. The filtrate was evaporated under reduced pressure and the residue was purified by preparative thin-layer chromatography (20 x 20 cm, 1000  $\mu\text{m}$ , 8 plates in hexane) to give bromide **1.142** (9.9 g, 88 %) as colorless oil. The product contained a minor impurity and was used as such in the subsequent reaction.  $^1\text{H}$  NMR (400 MHz,  $\text{CDCl}_3$ )  $\delta$  7.55 (d,  $J = 8.4$  Hz, 2H), 7.20 (d,  $J = 8.4$  Hz, 2H), 2.72 (t,  $J = 7.6$  Hz, 2H), 1.75 (m, 2H), 1.46 (m, 10H), 1.08 (m, 3H);  $^{13}\text{C}$  NMR (100 MHz,  $\text{CDCl}_3$ )  $\delta$  141.7, 131.2, 130.1, 119.2, 35.3, 31.9, 31.3, 29.4, 29.3, 29.2, 22.7, 14.1.

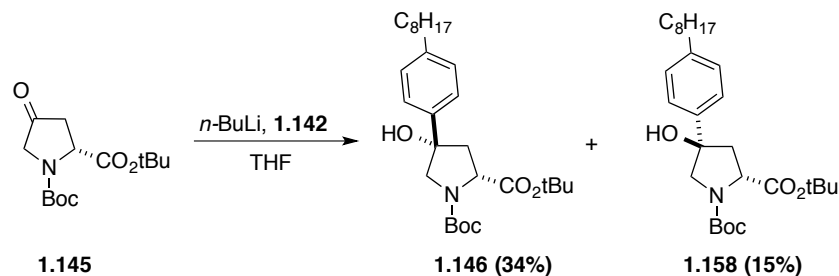


**(R)-1-(tert-Butoxycarbonyl)-4-oxopyrrolidine-2-carboxylic acid (1.144)**. Saturated aqueous  $\text{NaHCO}_3$  (120 mL) was added to a solution of *cis*-4-hydroxy-D-proline (**1.143**, 3.0 g, 23.0 mmol) in dioxane and water (1:1, 60 mL). The solution was cooled to 0°C and  $(\text{Boc})_2\text{O}$  (5.52 g, 5.8 mL, 25.3 mmol) was added drop wise. The reaction was stirred at room temperature over night. The pH was adjusted to 3 by addition of 2M HCl and the reaction mixture was extracted with EtOAc. The organic layers were combined, dried over  $\text{MgSO}_4$  and filtered. The

filtrate was evaporated under reduced pressure to give a white solid (5.0 g, 94 %). The solid (3.0 g, 13.0 mmol) was dissolved in CH<sub>2</sub>Cl<sub>2</sub> (64 mL), treated with trichloroisocyanuric acid (3.0 g, 13.0 mmol) in one portion, cooled to 0 °C and treated with TEMPO (102 mg, 0.65 mmol). The mixture was stirred at 0 °C for 0.5 h, warmed to room temperature, and stirred for 0.5 h. when completion was indicated by TLC (R<sub>f</sub> : 0.30, hexane: EtOAc: AcOH, 10: 10: 1). Water (10 mL) was added to the mixture. After stirring for 10 min, the mixture was concentrated *in vacuo*, diluted with ethyl acetate (40 mL), and filtered through Celite™. The filtrate was acidified with 1N HCl solution (80 mL), washed four times with water (20 mL), washed with brine (20 mL), dried over MgSO<sub>4</sub> and filtered. The filtrate was evaporated under reduced pressure to give ketone **1.144** (2.75 g, 93 %) as white solid (2.75 g, 87 over two steps), which was used in the next step without purification. Spectroscopic data were in agreement with the proposed structures and matched those reported in the literature.<sup>141</sup>



**Di-*tert*-butyl (*R*)-4-oxopyrrolidine-1,2-dicarboxylate (1.145).** A solution of ketone **1.144** (2.3 g, 10.0 mmol) in anhydrous CH<sub>2</sub>Cl<sub>2</sub> (46 mL) was cooled to 0 °C. *tert*-Butyl alcohol (2.9 mL, 30.0 mmol) and DMAP (122 mg, 1.0 mmol) were added to the solution. After stirring for 5 min, 1-ethyl-3-(3-dimethylaminopropyl)carbodiimide hydrochloride (2.0 g, 10.5 mmol) was added to the solution. The reaction was allowed to warm to room temperature and stirred overnight. The mixture was quenched with saturated aqueous NaHCO<sub>3</sub> and extracted three times with CH<sub>2</sub>Cl<sub>2</sub>. The organic layers were washed with brine, dried over MgSO<sub>4</sub> and filtered. The filtrate was evaporated under reduced pressure and the residue was purified by flash chromatography (hexane: EtOAc, 8:1) to give ester **1.145** (2.41 g, 84 %) as pale yellow oil. <sup>1</sup>H NMR (400 MHz, CDCl<sub>3</sub>, mixture of rotamers) δ 4.62-4.53 (dd, *J* = 29.2, 10.0 Hz, 1H), 3.82 (m, 2H), 2.93-2.81 (m, 1H), 2.49-2.44 (dd, *J* = 18.8, 2.0 Hz, 1H), 1.43 (2s, 18H); <sup>13</sup>C NMR (100 MHz, CDCl<sub>3</sub>, mixture of rotamers) δ (208.8), 208.0, 170.8, (154.2), 153.6, 82.2, 80.9, 56.9, (56.5), (52.8), 52.4, 41.3, (40.8), 28.1, 27.8; [α]<sub>D</sub> (-) 8.9° (*c* 1.28, CHCl<sub>3</sub>); HRMS (ESI) calcd for C<sub>14</sub>H<sub>23</sub>NNaO<sub>5</sub> (M+Na)<sup>+</sup> 308.1468, found 308.1473.



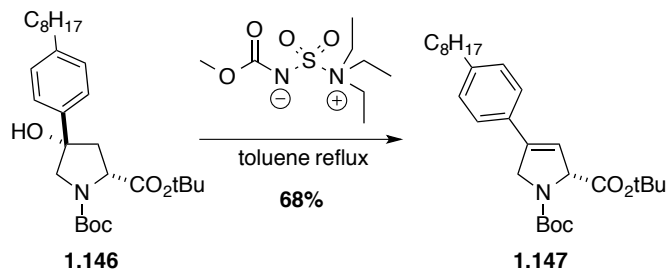
**Di-*tert*-butyl (2*R*,4*S*)-4-hydroxy-4-(4-octylphenyl)pyrrolidine-1,2-dicarboxylate (1.146).**

*n*-BuLi (2.5 M in hexane, 450  $\mu$ L, 1.12 mmol) was added dropwise to a solution of 1-bromo-4-octylbenzene (**1.142**, 288 mg, 1.07 mmol) in THF (2.0 mL) at  $-78$   $^{\circ}$ C. After stirring for 0.5 h, a solution of ketone **1.145** (123 mg, 0.43 mmol) in THF (0.3 mL) was added to the mixture, and the solution was stirred for an additional 2 h at  $-78$   $^{\circ}$ C. The reaction was warmed to  $-40$   $^{\circ}$ C and stirred overnight at this temperature. The reaction mixture was quenched at  $-40$   $^{\circ}$ C with saturated aqueous  $\text{NH}_4\text{Cl}$  and allowed to warm to room temperature. The organic layer was separated. The aqueous layer was extracted three times with  $\text{CH}_2\text{Cl}_2$ . The combined organic layers were washed with brine, dried over  $\text{MgSO}_4$  and filtered. The filtrate was evaporated under reduced pressure. The residue was purified by flash chromatography (hexane: EtOAc, 12:1 to 8:1) to give less polar alcohol **1.146** (70 mg, 34 %) as pale yellow oil, and more polar product **1.158** (32 mg, 15 %) as pale yellow oil.

**1.146:**  $^1\text{H}$  NMR (400 MHz,  $\text{CDCl}_3$ )  $\delta$  7.41 (m, 2H), 7.19 (m, 2H), 4.54 (s, 0.4H), 4.42-4.33 (dd,  $J=24.8, 9.6$  Hz, 1H), 4.17 (s, 0.6H), 3.97-3.86 (m, 1H), 3.77-3.65 (dd,  $J=37.6, 11.6$  Hz, 1H), 2.71-2.63 (m, 1H), 2.60 (t,  $J=7.6$  Hz, 2H), 2.27 (m, 1H), 1.62 (m, 2H), 1.53 (s, 9H), 1.48-1.47 (m, 9H), 1.29 (m, 10H), 0.88 (t,  $J=6.8$  Hz, 3H);  $^{13}\text{C}$  NMR (100 MHz,  $\text{CDCl}_3$ , mixture of rotamers)  $\delta$  (174.2), 173.9, (154.3), 153.8, 142.4, 138.7, (138.6), 128.4, 125.2, (125.1), (82.8), 82.6, 80.4, (80.2), (80.0), 79.1, (61.4), 60.6, 59.5, (59.4), 44.4, (43.3), 35.5, 31.9, (31.4), 29.4, 29.3, 29.2, 28.4, 28.0, 27.9, 22.6, 14.1;  $[\alpha]_D$  (+)  $3.5^{\circ}$  ( $c$  0.57,  $\text{CHCl}_3$ ); HRMS (ESI) calcd for  $\text{C}_{28}\text{H}_{45}\text{NNaO}_5$  ( $\text{M}+\text{Na}$ ) $^+$  498.3190, found 498.3182.

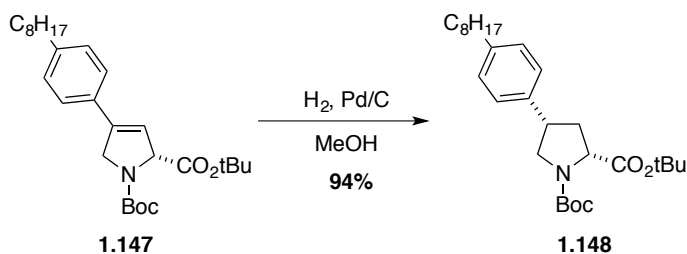
**1.158:**  $^1\text{H}$  NMR (400 MHz,  $\text{CDCl}_3$ )  $\delta$  7.36 (d,  $J=8.0$  Hz, 2H), 7.19 (d,  $J=8.0$  Hz, 2H), 4.51-4.40 (m, 1H), 4.05-3.87 (m, 1H), 3.86-3.72 (m, 1H), 2.70-2.50 (m, 2H), 2.35-2.18 (m, 1H), 2.05 (s, 1H), 1.65-1.55 (m, 3H), 1.53 (s, 18H), 1.48 (m, 10H), 0.88 (m, 3H);  $^{13}\text{C}$  NMR (100 MHz,  $\text{CDCl}_3$ )  $\delta$  171.9, 154.3, 143.0, 138.8, 128.7, 125.2, 81.1, 80.2, 79.2, 59.4, 59.0, 44.6,

35.5, 31.9, 31.4, 29.4, 29.3, 29.2, 28.4, 28.0, 22.6, 14.1;  $[\alpha]_D$  (-) 25.2° (*c* 1.00, CHCl<sub>3</sub>); HRMS (ESI) calcd for C<sub>28</sub>H<sub>45</sub>NNaO<sub>5</sub> (M+Na)<sup>+</sup> 498.3190, found 498.3193.



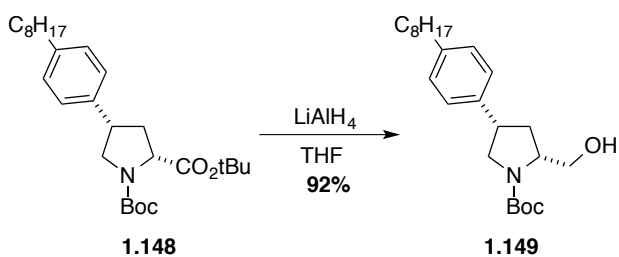
**Di-tert-butyl (R)-4-(4-octylphenyl)-2,5-dihydro-1H-pyrrole-1,2-dicarboxylate (1.147).**

Burgess' reagent (68 mg, 0.286 mmol) was added to a solution of alcohol **1.146** (68 mg, 0.143 mmol) in toluene (1.1 mL). The mixture was heated at reflux under argon for 4 h, cooled to room temperature and diluted with EtOAc. The mixture was washed with water, and brine, dried over MgSO<sub>4</sub> and filtered. The filtrate was evaporated under reduced pressure and the residue was purified by flash chromatography (hexane: EtOAc, 12:1 to 8:1) to give **1.147** (44 mg, 67%) as pale yellow oil. <sup>1</sup>H NMR (400 MHz, CDCl<sub>3</sub>) δ 7.32 (d, *J* = 8.0 Hz, 2H), 7.18 (d, *J* = 8.4 Hz, 2H), 6.05 (m, 0.3H), 6.00 (0.7H), 5.04 (m, 0.3H), 4.97 (m, 0.7H), 4.67-4.47 (m, 2H), 2.61 (t, *J* = 7.6 Hz, 2H), 1.61 (m, 2H), 1.53-1.47 (m, 18H), 1.29 (m, 10H), 0.88 (*J* = 6.8 Hz, 3H); <sup>13</sup>C NMR (100 MHz, CDCl<sub>3</sub>, mixture of rotamers) δ 169.6, (169.5), (153.8), 153.5, 143.8, (143.7), (140.5), 140.4, (130.1), 130.0, 128.7, (128.6), 125.6, (125.5), (117.5), 117.3, 81.5, (81.5), 80.0, (79.9), 68.0, (67.9), (53.6), 53.5, 35.7, 31.8, (31.3), 29.4, 29.3, 29.2, 28.5, 28.4, 28.0, (28.0), 22.6, 14.1;  $[\alpha]_D$  (+) 108.2° (*c* 0.95, CHCl<sub>3</sub>); HRMS (ESI) calcd for C<sub>28</sub>H<sub>43</sub>NNaO<sub>4</sub> (M+Na)<sup>+</sup> 480.30843, found 480.30792.



**Di-tert-butyl (2R,4S)-4-(4-octylphenyl)pyrrolidine-1,2-dicarboxylate (1.148)** was obtained as white solid (30 mg, 94 %) from olefin **1.147** (32 mg, 0.070 mmol) according to a modified

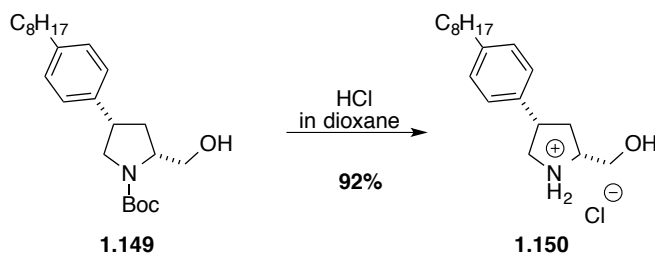
procedure for synthesizing **1.104**. To a solution of olefin **1.147** in MeOH (1.6 mL), Pd/C (10 %, 7.5 mg, 0.007 mmol) was added. The flask was evacuated and filled with H<sub>2</sub> atmosphere. The reaction was stirred overnight. The mixture was filtered through Celite™. The filtrate was evaporated under reduced pressure and the residue purified by flash chromatography (hexane: EtOAc, 12:1 to 8:1) to give **1.148**. m.p. (82.7 - 83.5°C); <sup>1</sup>H NMR (400 MHz, CDCl<sub>3</sub>) δ 7.14 (s, 4H), 4.22 (m, 1H), 4.07 (m, 0.65H), 3.91 (m, 0.35H), 3.43-3.36 (m, 1H), 3.36-3.24 (m, 1H), 2.69 (m, 1H), 2.57 (t, *J* = 7.6 Hz, 2H), 2.02-1.93 (m, 1H), 1.58 (m, 2H), 1.47-1.46 (2s, 18H), 1.28 (m, 10H), 0.88 (m, 3H); <sup>13</sup>C NMR (100 MHz, CDCl<sub>3</sub>, mixture of rotamers) δ 172.0, (171.9), (154.0), 153.7, 141.7, (137.0), 136.9, 128.6, (127.0), 127.0, 80.9, 79.9, (79.6), (60.0), 60.0, (53.2), 52.4, (43.3), 42.4, 38.5, (37.5), 35.5, 31.8, (31.5), 29.4, 29.3, 29.2, 28.4, 28.3, 28.0, (27.9), 22.6, 14.1; [α]<sub>D</sub> (+) 25.4° (*c* 0.39, CHCl<sub>3</sub>); HRMS (ESI) calcd for C<sub>28</sub>H<sub>45</sub>NNaO<sub>4</sub> (M+Na)<sup>+</sup> 482.3241, found 482.3243.



***tert*-Butyl (2*R*,4*S*)-2-(hydroxymethyl)-4-(4-octylphenyl)pyrrolidine-1-carboxylate (**1.149**).**

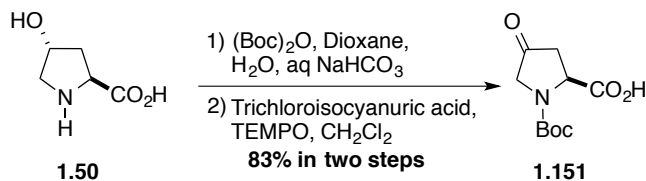
A mixture of lithium aluminium hydride (2.1 mg, 0.054 mmol) in anhydrous THF (1.5 mL) was cooled to 0 °C, treated slowly with ester **1.148** (25 mg, 0.054 mmol) in THF (1.5 mL), and stirred at 0 °C for 1 h. The reaction was quenched with water, diluted with CH<sub>2</sub>Cl<sub>2</sub>. The organic layer was separated, washed with water and brine, dried over MgSO<sub>4</sub> and filtered. The filtrate was evaporated under reduced pressure. The residue was purified by flash chromatography (hexane: EtOAc, 4:1) to give alcohol **1.149** (19.5 mg, 92 %) as pale yellow oil. <sup>1</sup>H NMR (400 MHz, CDCl<sub>3</sub>) δ 7.14 (s, 4H), 5.28 (m, 1H), 4.11-4.06 (m, 1H), 3.97 (m, 1H), 3.79-3.65 (m, 2H), 3.24 (m, 2H), 2.58 (t, *J* = 7.6 Hz, 2H), 2.42-2.36 (m, 1H), 1.59 (m, 2H), 1.49 (s, 9H), 1.28 (m, 10H), 0.89 (t, *J* = 6.8 Hz, 3H); <sup>13</sup>C NMR (100 MHz, CDCl<sub>3</sub>) δ 156.9, 141.8, 137.2, 128.6, 126.9, 80.6, 67.7, 61.5, 54.1, 42.2, 36.5, 35.5, 31.9, 31.5, 29.5,

29.3, 29.2, 28.4, 22.7, 14.1;  $[\alpha]_D$  (-) 4.6° (*c* 0.28, CHCl<sub>3</sub>); HRMS (ESI) calcd for C<sub>24</sub>H<sub>39</sub>NNaO<sub>3</sub> (M+Na)<sup>+</sup> 412.2822, found 412.2836.



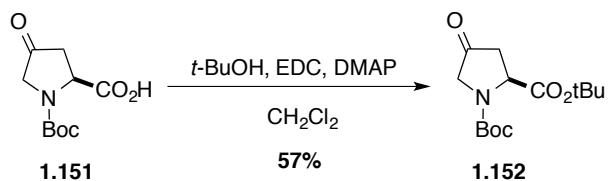
**(2R,4S)-2-(Hydroxymethyl)-4-(4-octylphenyl)pyrrolidin-1-ium chloride (1.150)** was obtained as pale yellow solid (8.5 mg, 92 %) from **1.149** ( 11 mg, 0.028 mmol) according the procedure for synthesizing **1.32**. <sup>1</sup>H NMR (400 MHz, D<sub>2</sub>O) δ 7.13 (d, *J* = 8.0 Hz, 2H), 6.91 (d, *J* = 8.0 Hz, 2H), 3.81 (m, 2H), 3.68-3.57 (m, 2H), 3.46 (m, 1H), 3.09 (m, 1H), 2.32 (m, 2H), 2.15 (m, 1H), 1.70 (m, 1H), 1.42 (m, 2H), 1.27 (s, 10H), 0.91 (m, 3H); <sup>13</sup>C NMR (100 MHz, D<sub>2</sub>O) δ 141.0, 136.3, 128.4, 127.2, 61.3, 59.9, 50.5, 42.5, 35.4, 34.2, 32.0, 31.3, 29.7, 29.6, 29.5, 22.7, 13.9;  $[\alpha]_D$  (-) 23.5° (*c* 0.17, MeOH); HRMS (ESI) calcd. For C<sub>19</sub>H<sub>32</sub>NO (M+H)<sup>+</sup> 290.2478, found 290.2469. HPLC: condition (B), *t<sub>R</sub>* = 5.97 min; purity: > 99 %.

Compound **1.157** was prepared according to the procedure for synthesizing **1.150**.

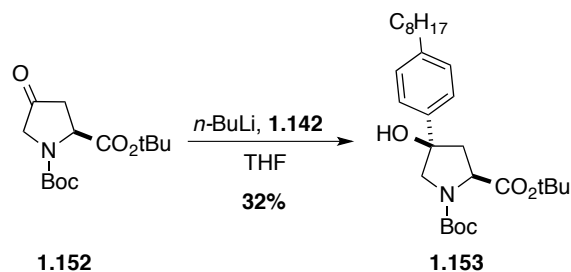


**(S)-1-(tert-butoxycarbonyl)-4-Oxopyrrolidine-2-carboxylic acid (1.151)** was obtained as white solid (1.35 g, 83 % over two steps) from **1.50**. Spectroscopic data were in agreement with the proposed structures and matched those reported in the literature.<sup>142,143</sup>

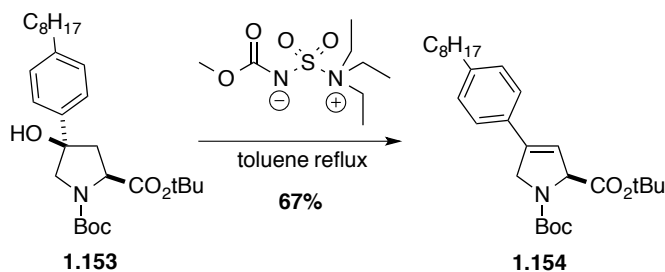




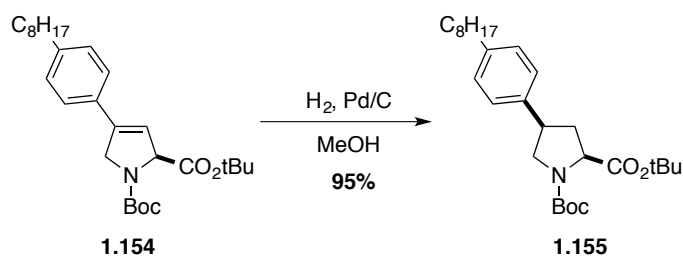
**Di-*tert*-butyl (*S*)-4-oxopyrrolidine-1,2-dicarboxylate (1.152)** was obtained as pale yellow oil (0.96 g, 57 %) from **1.151** (1.35 g, 5.9 mmol). Spectroscopic data were in agreement with the proposed structures and matched those reported in the literature.<sup>142</sup>



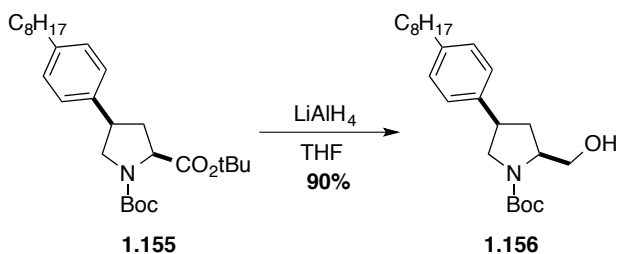
**Di-*tert*-butyl (2*S*,4*R*)-4-hydroxy-4-(4-octylphenyl)pyrrolidine-1,2-dicarboxylate (1.153)** was obtained as pale yellow oil (21 mg, 32 %) from **1.152** (40 mg, 0.14 mmol). <sup>1</sup>H NMR (400 MHz, CDCl<sub>3</sub>) δ 7.42 (m, 2H), 7.20 (m, 2H), 4.54 (s, 0.4H), 4.42-4.33 (dd, *J*=24.8, 10.0 Hz, 1H), 4.16 (s, 0.6H), 3.97-3.83 (m, 1H), 3.77-3.65 (dd, *J*=37.2, 11.6 Hz, 1H), 2.71-2.63 (m, 1H), 2.60 (t, *J*=7.6 Hz, 2H), 2.26 (m, 1H), 1.62 (m, 2H), 1.53 (s, 9H), 1.48-1.47 (m, 9H), 1.28 (m, 10H), 0.88 (t, *J*=6.8 Hz, 3H); <sup>13</sup>C NMR (100 MHz, CDCl<sub>3</sub>, mixture of rotamers) δ (174.2), 174.0, (154.3), 153.8, 142.4, (142.4), 138.7, (138.6), 128.4, 125.2, (125.1), (82.8), 82.6, 80.4, (80.3), (80.0), 79.1, (61.4), 60.6, 59.4, (59.4), 44.3, (43.2), 35.5, 31.9, (31.4), 29.4, 29.3, 29.2, 28.4, 28.0, 27.9, 22.6, 14.1; [α]<sub>D</sub> (-) 5.3° (*c* 0.19, CHCl<sub>3</sub>); HRMS (ESI) calcd for C<sub>28</sub>H<sub>45</sub>NNaO<sub>5</sub> (M+Na)<sup>+</sup> 498.31900, found 498.3188.



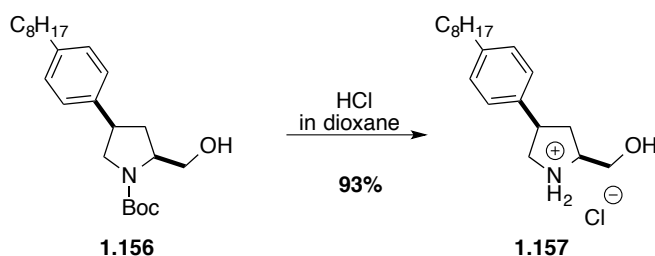
**Di-*tert*-butyl (*S*)-4-(4-octylphenyl)-2,5-dihydro-1*H*-pyrrole-1,2-dicarboxylate (1.154)** was obtained as pale yellow oil (10 mg, 67 %) from **1.153** (15 mg, 0.032 mmol). <sup>1</sup>H NMR (400 MHz, CDCl<sub>3</sub>) δ 7.32 (d, *J* = 8.0 Hz, 2H), 7.17 (d, *J* = 8.0 Hz, 2H), 6.05 (m, 0.3H), 6.00 (0.7H), 5.04 (m, 0.3H), 4.97 (m, 0.7H), 4.70-4.48 (m, 2H), 2.61 (m, 2H), 1.61 (m, 2H), 1.57-1.47 (m, 18H), 1.30 (m, 10H), 0.88 (m, 3H); <sup>13</sup>C NMR (100 MHz, CDCl<sub>3</sub>, mixture of rotamers) δ 169.6, (169.5), (153.8), 153.5, 143.8, (143.7), (140.5), 140.4, (130.1), 130.0, 128.7, (128.6), 125.6, (125.5), (117.5), 117.2, 81.5, (81.4), 80.0, (79.9), 67.9, (67.9), (53.6), 53.5, 35.7, 31.8, (31.3), 29.4, 29.2, 29.2, 28.5, 28.3, 28.0, (28.0), 22.6, 14.1; [α]<sub>D</sub> (-) 129.1° (*c* 1.04, CHCl<sub>3</sub>); HRMS (ESI) calcd for C<sub>28</sub>H<sub>43</sub>NNaO<sub>4</sub> (M+Na)<sup>+</sup> 480.3084, found 480.3091.



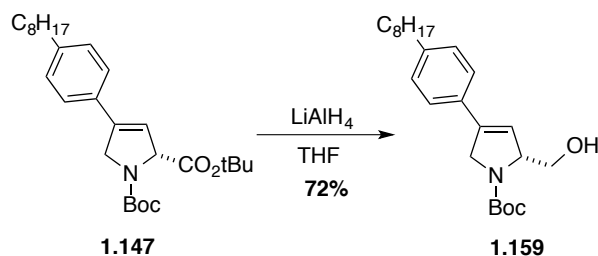
**Di-*tert*-butyl (2*S*,4*R*)-4-(4-octylphenyl)pyrrolidine-1,2-dicarboxylate (1.155)** was obtained as white solid (19 mg, 95 %) from **1.154** (20 mg, 0.044 mmol). m.p. ( 82.5-83.5°C); <sup>1</sup>H NMR (400 MHz, CDCl<sub>3</sub>) δ 7.14 (s, 4H), 4.21 (m, 1H), 4.06 (m, 0.65H), 3.91 (m, 0.35H), 3.43-3.34 (m, 1H), 3.34-3.24 (m, 1H), 2.69 (m, 1H), 2.57 (t, *J* = 7.6 Hz, 2H), 2.02-1.93 (m, 1H), 1.58 (m, 2H), 1.47-1.46 (2s, 18H), 1.28 (m, 10H), 0.88 (m, 3H); <sup>13</sup>C NMR (100 MHz, CDCl<sub>3</sub>, mixture of rotamers) δ 172.0, (172.0), (154.0), 153.8, 141.8, (137.1), 137.0, 128.6, (127.0), 127.0, 81.0, 80.0, (79.7), (60.0), 60.0, (53.30, 52.5, (43.3), 42.4, 38.5, (37.5), 35.5, 31.9, (31.5), 29.5, 29.3, 29.2, 28.4, 28.4, 28.0, (28.0), 22.7, 14.1; [α]<sub>D</sub> (-) 24.2° (*c* 1.08, CHCl<sub>3</sub>); HRMS (ESI) calcd for C<sub>28</sub>H<sub>45</sub>NNaO<sub>4</sub> (M+Na)<sup>+</sup> 482.3241, found 482.3243.



***tert*-Butyl (2*S*,4*R*)-2-(hydroxymethyl)-4-(4-octylphenyl)pyrrolidine-1-carboxylate (1.156)** was obtained as pale yellow oil (11.4 mg, 90 %) from **1.155** (15 mg, 0.033 mmol). <sup>1</sup>H NMR (400 MHz, CDCl<sub>3</sub>) δ 7.14 (s, 4H), 5.28 (m, 1H), 4.11-4.04 (m, 1H), 3.97 (m, 1H), 3.79-3.65 (m, 2H), 3.24 (m, 2H), 2.58 (t, *J* = 7.6 Hz, 2H), 2.42-2.38 (m, 1H), 1.58 (m, 2H), 1.49 (s, 9H), 1.28 (m, 10H), 0.89 (t, *J* = 6.8 Hz, 3H); <sup>13</sup>C NMR (100 MHz, CDCl<sub>3</sub>) δ 156.9, 141.8, 137.1, 128.6, 126.9, 80.6, 67.7, 61.5, 54.1, 42.2, 36.5, 35.5, 31.9, 31.5, 29.4, 29.3, 29.2, 28.4, 22.6, 14.1; [α]<sub>D</sub> (+)4.31° (*c* 0.58, CHCl<sub>3</sub>); HRMS (ESI) calcd for C<sub>24</sub>H<sub>39</sub>NNaO<sub>3</sub> (M+Na)<sup>+</sup> 412.2822, found 412.2827.

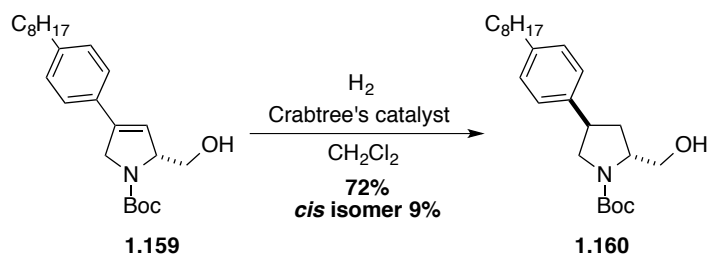


**(2*S*,4*R*)-2-(hydroxymethyl)-4-(4-octylphenyl)Pyrrolidin-1-ium chloride (1.157)** was obtained as pale yellow solid (7.0 mg, 93 %) from **1.156** (9 mg, 0.023 mmol). <sup>1</sup>H NMR (400 MHz, D<sub>2</sub>O) δ 7.13 (d, *J* = 7.2 Hz, 2H), 6.91 (d, *J* = 7.2 Hz, 2H), 3.81-3.76 (m, 2H), 3.70-3.57 (m, 2H), 3.46 (m, 1H), 3.13-3.08 (m, 1H), 2.32 (m, 2H), 2.15 (m, 1H), 1.69 (m, 1H), 1.44 (m, 2H), 1.27 (s, 10H), 0.90 (m, 3H); <sup>13</sup>C NMR (100 MHz, D<sub>2</sub>O) δ 140.7, 135.8, 128.0, 126.8, 60.9, 59.5, 50.1, 42.1, 34.9, 33.8, 31.5, 30.9, 29.3, 29.1, 29.1, 22.3, 13.5; [α]<sub>D</sub> (+) 20.0° (*c* 0.21, MeOH); HRMS (ESI) calcd for C<sub>19</sub>H<sub>32</sub>NO (M+H)<sup>+</sup> 290.2478, found 290.2477. HPLC: condition (B), *t<sub>R</sub>* = 5.93 min; purity: > 99%.

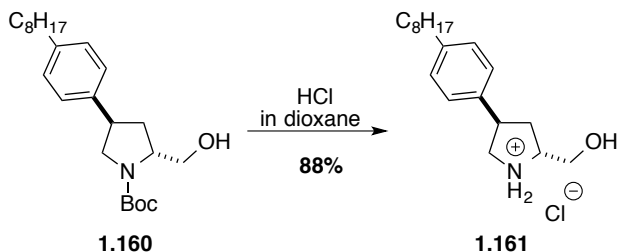


***tert*-Butyl (*R*)-2-(hydroxymethyl)-4-(4-octylphenyl)-2,5-dihydro-1*H*-pyrrole-**

**1-carboxylate (1.159)** was obtained as colorless oil (20.0 mg, 72 %) from **1.147** (33 mg, 0.072 mmol) according to the procedure for synthesizing **1.149**. <sup>1</sup>H NMR (400 MHz, CDCl<sub>3</sub>) δ 7.29 (d, *J* = 8.0 Hz, 2H), 7.17 (d, *J* = 8.0 Hz, 2H), 6.02 (s, 0.2H), 5.93 (s, 0.8H), 4.91 (m, 1H), 4.74-4.65 (m, 1H), 4.56-4.43 (m, 2H), 3.85 (m, 1H), 3.78-3.63 (m, 1H), 2.61 (t, *J* = 7.6 Hz, 2H), 1.61 (m, 2H), 1.54 (s, 9H), 1.28 (m, 10H), 0.89 (t, *J* = 6.8 Hz, 3H); <sup>13</sup>C NMR (100 MHz, CDCl<sub>3</sub>) δ 156.6, 143.6, 138.3, 130.1, 125.4, 119.0, 80.8, 68.6, 67.5, 54.3, 35.7, 31.8, 31.3, 29.4, 29.2, 29.2, 28.5, 22.6, 14.1; [α]<sub>D</sub> (+) 34.0° (*c* 2.0, CHCl<sub>3</sub>); HRMS (ESI) calcd for C<sub>24</sub>H<sub>37</sub>NNaO<sub>3</sub> (M+Na)<sup>+</sup> 410.2666, found 410.2662.

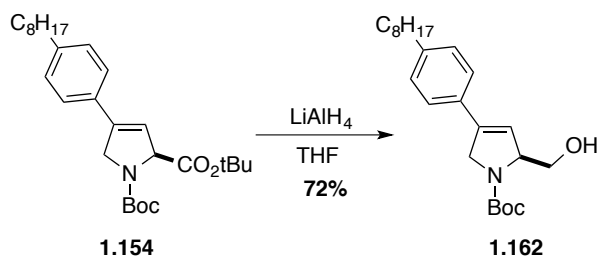


***tert*-Butyl (2*R*,4*R*)-2-(hydroxymethyl)-4-(4-octylphenyl)pyrrolidine-1-carboxylate (1.160).** Crabtree's catalyst (5.0 mg, 0.006 mmol) was added to a solution of olefin **1.159** (16 mg, 0.041 mmol) in anhydrous CH<sub>2</sub>Cl<sub>2</sub> (0.8 mL). The resulting light orange mixture was subjected to a hydrogen pressure of 70 psi for 72 h. The volatiles were removed under reduced pressure and the residue was purified by flash chromatography (hexane: EtOAc, 10:1 to 8:1) to give the *trans*-pyrrolidine **1.160** (11.6 mg, 72 %) as pale yellow oil. <sup>1</sup>H NMR (400 MHz, CDCl<sub>3</sub>) δ 7.14 (s, 4H), 4.31-3.18 (m, 1H), 3.81-3.67 (m, 3H), 3.41 (m, 2H), 2.59 (t, *J* = 7.6 Hz, 2H), 2.21-2.13 (m, 1H), 2.01-1.95 (m, 1H), 1.59 (m, 2H), 1.49 (s, 9H), 1.28 (m, 10H), 0.89 (m, 3H); <sup>13</sup>C NMR (100 MHz, CDCl<sub>3</sub>) δ 157.1, 141.7, 138.2, 128.6, 126.8, 80.5, 68.0, 59.8, 54.0, 42.0, 35.9, 35.5, 31.9, 31.5, 29.5, 29.3, 29.2, 28.5, 22.7, 14.1; [α]<sub>D</sub> (+) 37.2° (*c* 1.16, CHCl<sub>3</sub>); HRMS (ESI) calcd for C<sub>24</sub>H<sub>39</sub>NNaO<sub>3</sub> (M+Na)<sup>+</sup> 412.2822, found 412.2811.



**(2*R*,4*R*)-2-(Hydroxymethyl)-4-(4-octylphenyl)pyrrolidin-1-ium chloride (1.161)** was obtained as pale yellow solid (8.5 mg, 88 %) from **1.160** (11.6 mg, 0.030 mmol) according to the procedure for synthesizing **1.32**. <sup>1</sup>H NMR (400 MHz, CDCl<sub>3</sub>) δ 7.15 (dd, *J* = 8.4, 14.0 Hz, 4H), 4.14 (m, 1H), 4.08-4.01 (m, 1H), 3.99-3.91 (m, 1H), 3.87-3.83 (m, 1H), 3.67 (m, 1H), 3.32 (m, 1H), 2.56 (t, *J* = 7.6 Hz, 2H), 2.31-2.23 (m, 1H), 2.23- 2.14 (m, 1H), 1.58 (m, 2H), 1.36-1.22 (m, 10H), 0.88 (m, 3H); <sup>13</sup>C NMR (100 MHz, CDCl<sub>3</sub>) δ 142.3, 135.8, 129.0, 127.0, 61.6, 61.4, 51.5, 42.6, 35.5, 34.4, 31.9, 31.4, 29.4, 29.3, 29.2, 22.6, 14.1; [α]<sub>D</sub> (-) 8.7° (*c* 0.85, CHCl<sub>3</sub>); HRMS (ESI) calcd for C<sub>19</sub>H<sub>32</sub>NO (M+H)<sup>+</sup> 290.2478, found 290.2477. HPLC: condition (B), *t*<sub>R</sub> = 6.30 min; purity: > 99 %.

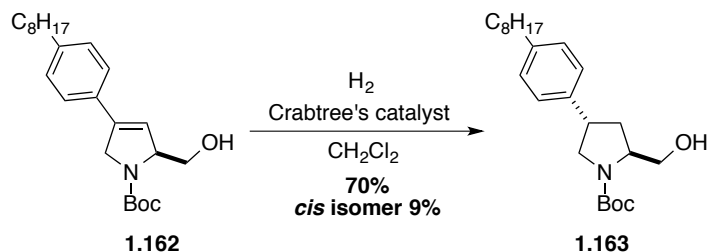
Compound **1.164** was prepared according to the procedure for synthesizing **1.161**.



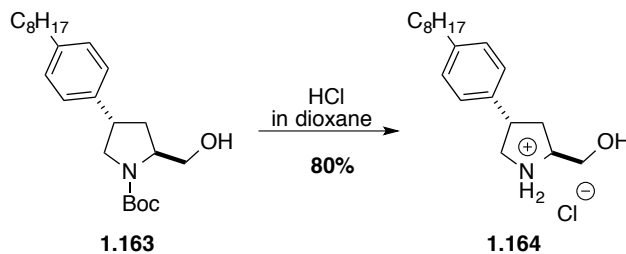
**tert-Butyl (S)-2-(hydroxymethyl)-4-(4-octylphenyl)-2,5-dihydro-1*H*-pyrrole-**

**1-carboxylate (1.162)** was obtained as colorless oil (20.0 mg, 72 %) from **1.154** (38 mg, 0.083 mmol). <sup>1</sup>H NMR (400 MHz, CDCl<sub>3</sub>) δ 7.29 (d, *J* = 8.4 Hz, 2H), 7.17 (d, *J* = 8.0 Hz, 2H), 6.01 (s, 0.2H), 5.93 (m, 0.8H), 4.91 (m, 1H), 4.70 (m, 1H), 4.49-4.43 (m, 2H), 3.86 (m, 1H), 3.78-3.63 (m, 1H), 2.61 (t, *J* = 7.6 Hz, 2H), 1.60 (m, 2H), 1.54 (s, 9H), 1.28 (m, 10H), 0.89 (t, *J* = 6.8 Hz, 3H); <sup>13</sup>C NMR (100 MHz, CDCl<sub>3</sub>) δ 156.6, 143.6, 138.3, 130.1, 125.5, 119.1, 80.8,

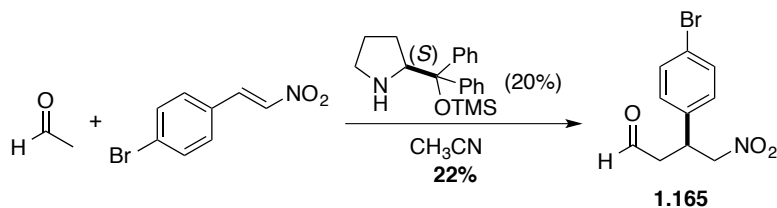
68.6, 67.6, 54.3, 35.7, 31.8, 31.4, 29.4, 29.3, 29.2, 28.5, 22.7, 14.1;  $[\alpha]_D$  (-) 28.6° (*c* 0.14, CHCl<sub>3</sub>); HRMS (ESI) calcd for C<sub>24</sub>H<sub>37</sub>NNaO<sub>3</sub> (M+Na)<sup>+</sup> 410.2666, found 410.2657.



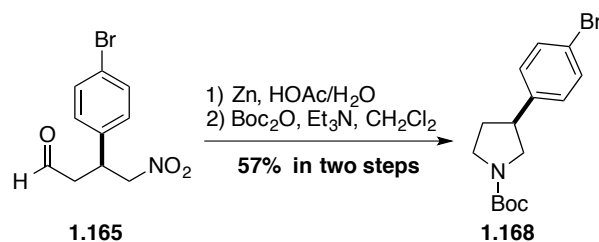
***tert*-Butyl (2*S*,4*S*)-2-(hydroxymethyl)-4-(4-octylphenyl)pyrrolidine-1-carboxylate (1.163)** was obtained as pale yellow oil (8.4 mg, 70 %) from **1.162** (12 mg, 0.031 mmol). <sup>1</sup>H NMR (400 MHz, CDCl<sub>3</sub>) δ 7.14 (s, 4H), 4.30-3.20 (m, 1H), 3.81-3.69 (m, 3H), 3.43 (m, 2H), 2.58 (t, *J* = 7.6 Hz, 2H), 2.21-2.13 (m, 1H), 1.98 (m, 1H), 1.59 (m, 2H), 1.48 (s, 9H), 1.28 (m, 10H), 0.89 (m, 3H); <sup>13</sup>C NMR (100 MHz, CDCl<sub>3</sub>) δ 157.1, 141.7, 138.2, 128.6, 126.8, 80.5, 67.9, 59.8, 54.0, 42.0, 35.8, 35.5, 31.9, 31.5, 29.5, 29.3, 29.2, 28.4, 22.6, 14.1;  $[\alpha]_D$  (-) 20.0° (*c* 0.40, CHCl<sub>3</sub>); HRMS (ESI) calcd for C<sub>24</sub>H<sub>39</sub>NNaO<sub>3</sub> (M+Na)<sup>+</sup> 412.2822, found 412.2824.



**(2*S*,4*S*)-2-(Hydroxymethyl)-4-(4-octylphenyl)pyrrolidin-1-ium chloride (1.164)** was obtained as pale yellow solid (3.2 mg, 80 %) from **1.163** (4.8 mg, 0.012 mmol). <sup>1</sup>H NMR (700 MHz, CDCl<sub>3</sub>) δ 7.15 (m, 4H), 4.13 (m, 1H), 4.03-3.97 (m, 1H), 3.93-3.88 (m, 1H), 3.86-3.81 (m, 1H), 3.67 (m, 1H), 3.32 (m, 1H), 2.56 (t, *J* = 7.7 Hz, 2H), 2.28-2.25 (m, 1H), 2.20-2.16 (m, 1H), 1.58 (m, 2H), 1.35-1.22 (m, 10H), 0.88 (t, *J* = 7.0 Hz, 3H); <sup>13</sup>C NMR (175 MHz, CDCl<sub>3</sub>) δ 142.4, 135.7, 129.0, 127.0, 61.6, 61.4, 51.5, 42.6, 35.5, 34.4, 31.9, 31.4, 29.4, 29.4, 29.3, 29.2, 22.6, 14.1;  $[\alpha]_D$  (+) 9.4° (*c* 0.18, CHCl<sub>3</sub>); HRMS (ESI) calcd for C<sub>19</sub>H<sub>32</sub>NO (M+H)<sup>+</sup> 290.2478, found 290.2482. HPLC: condition (B), *t<sub>R</sub>* = 5.85 min; purity: > 99 %.

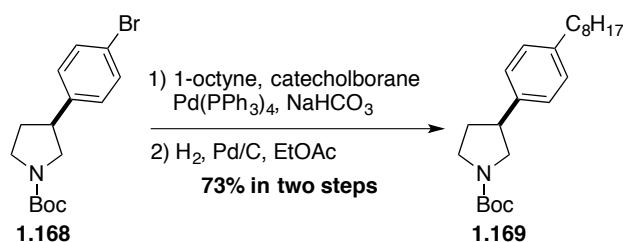


**(S)-3-(4-Bromophenyl)-4-nitrobutanal (1.165)** was prepared according to the procedure reported by List,<sup>129</sup> starting from acetaldehyde (5M in CH<sub>3</sub>CN, 3mL, 15 mmol) and *trans*-4-bromo- $\beta$ -nitrostyrene (684 mg), After 71 h, aldehyde **1.165** was obtained as pale yellow oil (180 mg, 22%). <sup>1</sup>H NMR (400 MHz, CDCl<sub>3</sub>)  $\delta$  9.69 (s, 1H), 7.47 (d, *J* = 8.4 Hz, 2H), 7.12 (d, *J* = 8.4 Hz, 2H), 4.70-4.56 (m, 2H), 4.05 (p, *J* = 7.2 Hz, 1H), 2.94 (m, 2H); <sup>13</sup>C NMR (100 MHz, CDCl<sub>3</sub>)  $\delta$  198.4, 137.2, 132.3, 129.1, 122.0, 79.0, 46.2, 37.3; [ $\alpha$ ]<sub>D</sub> (-) 6.8° (*c* 0.47 CHCl<sub>3</sub>); HRMS (ESI) calcd for C<sub>10</sub>H<sub>10</sub>BrNO<sub>3</sub> (M-H)<sup>+</sup> 269.9771, found 269.9771. The spectroscopic data were in agreement with the proposed structures and matched those reported in the literature.<sup>144,145</sup>

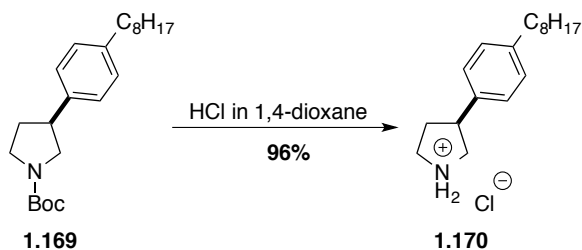


**tert-Butyl (S)-3-(4-bromophenyl)pyrrolidine-1-carboxylate (1.168)** was synthesized according to the reported procedure.<sup>132</sup> Zinc powder was added in three portions over 10 min to a solution of aldehyde **1.165** in HOAc/H<sub>2</sub>O (1:1, 2 mL) at 0 °C. The mixture was stirred at room temperature for 3-4 h and filtered, and the filter cake was washed with water. The pH OF THE combined filtrate and washings was adjusted to pH = 12 with 4N aqueous KOH. The aqueous layer was extracted with CH<sub>2</sub>Cl<sub>2</sub> (5 mL) three times. The organic phases were combined, dried over MgSO<sub>4</sub> and filtered. The filtrate was evaporated under reduced pressure. The residue was directly used without purification. The residue (80 mg, 0.36 mmol) was dissolved in CH<sub>2</sub>Cl<sub>2</sub> (0.44 mL) and treated with Et<sub>3</sub>N (57  $\mu$ L, 41 mg, 0.40 mmol), cooled to 0°C and treated dropwise with (Boc)<sub>2</sub>O (82  $\mu$ L, 79 mg, 0.36 mmol). The reaction mixture was stirred at room temperature for 2 days and then quenched with saturated aqueous NH<sub>4</sub>Cl. The aqueous layer

was extracted with  $\text{CH}_2\text{Cl}_2$ . The organic layers were combined, dried over  $\text{MgSO}_4$  and filtered. The filtrate was evaporated under reduced pressure. The residue was purified by flash chromatography (hexane: EtOAc, 1:8 with) to give carbamate **1.168** (68 mg, 57 % in two steps) as colorless oil.  $^1\text{H}$  NMR (400 MHz,  $\text{CDCl}_3$ )  $\delta$  7.43 (d,  $J = 8.4$  Hz, 2H), 7.10 (d,  $J = 8.4$  Hz, 2H), 3.90-3.70 (m, 1H), 3.70-3.50 (m, 1H), 3.44-3.20 (m, 3H), 2.25 (m, 1H), 1.93 (m, 1H), 1.47 (s, 9H);  $^{13}\text{C}$  NMR (100 MHz,  $\text{CDCl}_3$ , mixture of rotamers)  $\delta$  154.4, 140.5, 131.6, 128.7, 120.4, 79.3, 52.3, (51.6), (45.8), 45.5, 43.7, (42.7), (33.2), 32.3, 28.5;  $[\alpha]_{\text{D}} (-) 17.4^\circ$  ( $c$  1.55,  $\text{CHCl}_3$ ); HRMS (ESI) calcd for  $\text{C}_{15}\text{H}_{20}[^{79}\text{Br}]\text{NNaO}_2$  ( $\text{M}+\text{Na}$ ) $^+$  348.0570, found. 348.0563. SFC conditions: LUX AMYLOSE 2, 150 x 4.6 mm, particle size 3  $\mu\text{m}$ , 10 % MeOH, 150 bar  $\text{CO}_2$ , Column temperature: 35  $^\circ\text{C}$ , flow rate: 3 mL/min, detection: UV 210 nm, major  $t_{\text{R}}$  2.92 min, minor  $t_{\text{R}}$  2.36 min, e.r. = 94.5 : 5.5.



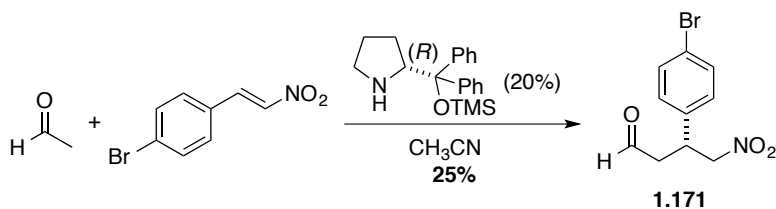
**tert-Butyl (S)-3-(4-octylphenyl)pyrrolidine-1-carboxylate (1.169)** was obtained as colorless oil (24 mg, 73% over two steps) from **1.168** (30 mg, 0.092 mmol) according to the procedure for synthesizing **1.31**.  $^1\text{H}$  NMR (400 MHz,  $\text{CDCl}_3$ )  $\delta$  7.15 (m, 4H), 3.90-3.70 (m, 1H), 3.68-3.51 (m, 1H), 3.45-3.20 (m, 3H), 2.59 (m, 2H), 2.24 (m, 1H), 1.98 (m, 1H), 1.61 (m, 2H), 1.48 (m, 9H), 1.40-1.20 (m, 10H), 0.89 (m, 3H);  $^{13}\text{C}$  NMR (100 MHz,  $\text{CDCl}_3$ )  $\delta$  154.5, 141.5, 141.4, 138.6, 128.6, 126.9, 79.1, 52.7, 51.8, 46.0, 45.6, 44.0, 43.0, 35.5, 33.4, 32.5, 31.9, 31.5, 29.5, 29.3, 29.2, 28.5, 22.6, 14.1;  $[\alpha]_{\text{D}} (-) 11.6^\circ$  ( $c$  0.80,  $\text{CHCl}_3$ ); HRMS (ESI) calcd for  $\text{C}_{23}\text{H}_{37}\text{NNaO}_2$  ( $\text{M}+\text{Na}$ ) $^+$  382.2717, found. 382.2704.



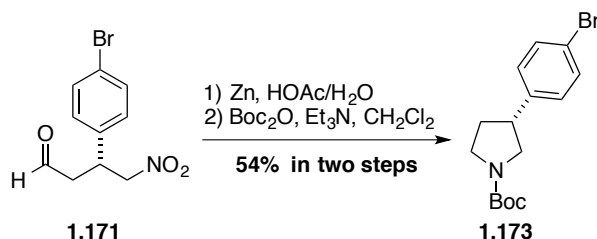


**(S)-3-(4-Octylphenyl)pyrrolidin-1-ium chloride (1.170)** was obtained as pale yellow solid (12.6 mg, 96 %) from carbamate **1.169** (16 mg, 0.045 mmol) according the procedure for synthesizing **1.32**.  $^1\text{H}$  NMR (400 MHz,  $\text{D}_2\text{O}$ )  $\delta$  7.09 (d,  $J = 8.0$  Hz, 2H), 6.85 (d,  $J = 8.0$  Hz, 2H), 3.58-3.49 (m, 1H), 3.48-3.39 (m, 1H), 3.38-3.20 (m, 2H), 2.99 (t,  $J = 11.2$  Hz, 1H), 2.29 (m, 2H), 2.06 (m, 1H), 1.78 (m, 1H), 1.42 (m, 2H), 1.27 (m, 10H), 0.91 (m, 3H);  $^{13}\text{C}$  NMR (100 MHz,  $\text{D}_2\text{O}$ )  $\delta$  140.8, 136.6, 128.3, 127.3, 50.5, 45.4, 42.6, 35.4, 32.0, 31.9, 31.4, 29.9, 29.7, 29.6, 22.7, 13.9;  $[\alpha]_{\text{D}} (-) 8.0^\circ$  ( $c$  0.40,  $\text{CHCl}_3$ ); HRMS (ESI) calcd for  $\text{C}_{18}\text{H}_{30}\text{N}$  ( $\text{M}+\text{H}$ ) $^+$  260.2373, found. 260.2384.

Compound **1.175** was prepared according to the procedure for synthesizing **1.170**.

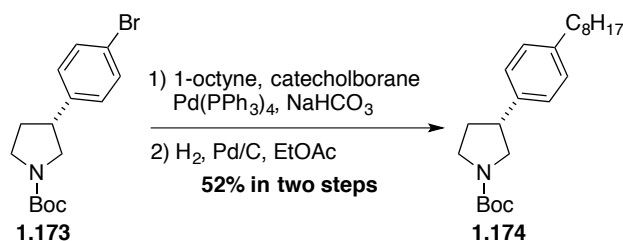


**(R)-3-(4-Bromophenyl)-4-nitrobutanal (1.171)**. Starting from acetaldehyde (5M in  $\text{CH}_3\text{CN}$ , 3mL, 15 mmol) and *trans*-4-bromo- $\beta$ -nitrostyrene (684 mg), After 71 h, **1.171** was obtained as pale yellow oil (200 mg, 25%).  $^1\text{H}$  NMR (400 MHz,  $\text{CDCl}_3$ )  $\delta$  9.66 (s, 1H), 7.46 (d,  $J = 8.4$  Hz, 2H), 7.11 (d,  $J = 8.4$  Hz, 2H), 4.70-4.52 (m, 2H), 4.03 (p,  $J = 7.2$  Hz, 1H), 2.92 (m, 2H);  $^{13}\text{C}$  NMR (100 MHz,  $\text{CDCl}_3$ )  $\delta$  198.4, 137.2, 132.2, 129.1, 121.9, 78.9, 46.1, 37.2;  $[\alpha]_{\text{D}} (+) 6.4^\circ$  ( $c$  0.45,  $\text{CHCl}_3$ ); HRMS (ESI) calcd for  $\text{C}_{10}\text{H}_{10}\text{BrNO}_3$  ( $\text{M}-\text{H}$ ) $^+$  269.9771, found 269.9771.

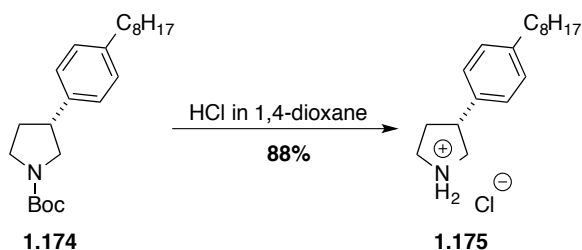


**tert-Butyl (R)-3-(4-bromophenyl)pyrrolidine-1-carboxylate (1.173)** was obtained as colorless oil (65 mg, 54 % over two steps) from **1.171** (100 mg, 0.37 mmol).  $^1\text{H}$  NMR (400 MHz,  $\text{CDCl}_3$ )  $\delta$  7.43 (d,  $J = 8.0$  Hz, 2H), 7.10 (d,  $J = 8.0$  Hz, 2H), 3.88-3.71 (m, 1H), 3.68-

3.48 (m, 1H), 3.46-3.18 (m, 3H), 2.24 (m, 1H), 1.94 (m, 1H), 1.47 (s, 9H);  $^{13}\text{C}$  NMR (100 MHz,  $\text{CDCl}_3$ , mixture of rotamers)  $\delta$  154.4, 140.4, 131.6, 128.7, 120.4, 79.3, 52.3, (51.6), (45.7), 45.5, 43.6, (42.7), (33.2), 32.3, 28.5;  $[\alpha]_{\text{D}}^{25}$  (+) 17.3° (*c* 1.65,  $\text{CHCl}_3$ ); HRMS (ESI) calcd for  $\text{C}_{15}\text{H}_{20}[^{79}\text{Br}]\text{NNaO}_2$  ( $\text{M}+\text{Na}$ ) $^{+}$  348.0570, found. 348.0563. SFC conditions: LUX AMYLOSE 2, 150 x 4.6 mm, particle size 3  $\mu\text{m}$ , 10 % MeOH, 150 bar  $\text{CO}_2$ , Column temperature: 35 °C, flow rate: 3 mL/min, detection: UV 210 nm, major  $t_{\text{R}}$  2.31 min, minor  $t_{\text{R}}$  3.06 min, e.r. = 94.1: 5.9.



***tert*-Butyl (*R*)-3-(4-octylphenyl)pyrrolidine-1-carboxylate (1.174)** was obtained as colorless oil (17 mg, 52 % over two steps) from **1.173** (30 mg, 0.092 mmol).  $^1\text{H}$  NMR (400 MHz,  $\text{CDCl}_3$ )  $\delta$  7.15 (m, 4H), 3.88-3.72 (m, 1H), 3.68-3.51 (m, 1H), 3.45-3.22 (m, 3H), 2.59 (m, 2H), 2.24 (m, 1H), 1.98 (m, 1H), 1.61 (m, 2H), 1.48 (m, 9H), 1.39-1.20 (m, 10H), 0.89 (m, 3H);  $^{13}\text{C}$  NMR (100 MHz,  $\text{CDCl}_3$ )  $\delta$  154.5, 141.5, 141.4, 138.6, 128.6, 126.9, 79.1, 52.7, 51.8, 46.0, 45.7, 44.0, 43.0, 35.5, 33.4, 32.5, 31.9, 31.5, 29.5, 29.4, 29.2, 28.5, 22.7, 14.1;  $[\alpha]_{\text{D}}^{25}$  (+) 10.8° (*c* 0.50,  $\text{CHCl}_3$ ); HRMS (ESI) calcd for  $\text{C}_{23}\text{H}_{37}\text{NNaO}_2$  ( $\text{M}+\text{Na}$ ) $^{+}$  382.2717, found. 382.2730.



**(*R*)-3-(4-Octylphenyl)pyrrolidin-1-ium chloride (1.175)** was obtained as pale yellow solid (7.2 mg, 88 %) from **1.174** (10 mg, 0.028 mmol).  $^1\text{H}$  NMR (400 MHz,  $\text{D}_2\text{O}$ )  $\delta$  7.09 (d, *J* = 8.0 Hz, 2H), 6.85 (d, *J* = 8.0 Hz, 2H), 3.57-3.49 (m, 1H), 3.48-3.38 (m, 1H), 3.38-3.20 (m, 2H), 2.98 (t, *J* = 11.2 Hz, 1H), 2.29 (m, 2H), 2.06 (m, 1H), 1.78 (m, 1H), 1.42 (m, 2H), 1.27 (m,

10H), 0.91 (m, 3H);  $^{13}\text{C}$  NMR (100 MHz,  $\text{D}_2\text{O}$ )  $\delta$  140.8, 136.6, 128.3, 127.3, 50.5, 45.4, 42.6, 35.4, 32.0, 31.9, 31.3, 29.8, 29.6, 29.6, 22.7, 13.9;  $[\alpha]_{\text{D}}^{20}$  (+) 5.9° (*c* 0.22,  $\text{CHCl}_3$ ); HRMS (ESI) calcd for  $\text{C}_{18}\text{H}_{30}\text{N}(\text{M}+\text{H})^+$  260.2373, found. 260.2363.

## 1-5 References

1. Vézina, C.; Kudelski, A.; Sehgal, S. N. *J. Antibiot.* **1975**, *28*, 721.
2. Sehgal, S. N. *Transplant. Proc.* **2003**, *35*, 7S.
3. Dreyfuss, M.; Härrri, E.; Hofmann, H.; Kobel, H.; Pache, W.; Tschertter, H. *Eur. J. Appl. Microbiol.* **1976**, *3*, 125.
4. Borel, J. F.; Feurer, C.; Gubler, H. U.; Stähelin, H. *Agents Action*, **1976**, *6*, 468.
5. Borel, J. F. *Wien. Klin. Wochenschr.* **2002**, *114*, 433.
6. Kino, T.; Hatanaka, H.; Hashimoto, M.; Nishiyama, M.; Goto, T.; Okuhara, M.; Kohsaka, M.; Aoki, H.; Imanaka, H. *J. Antibiot.* **1987**, *40*, 1249.
7. Tanaka, H.; Kuroda, A.; Marusawa, H.; Hatanaka, H.; Kino, T.; Goto, T.; Hashimoto, M.; Taga, T. *J. Am. Chem. Soc.* **1987**, *109*, 5031.
8. Fujita, T.; Inoue, K.; Yamamoto, S.; Ikumoto, T.; Sasaki, S.; Toyama, R.; Chiba, K.; Hoshino, Y.; Okumoto, T. *J. Antibiot.* **1994**, *47*, 208.
9. Kluepfel, D.; Bagli, J.; Baker, H.; Charest, M. P.; Kudelski, A.; Sehgal, S. N.; Vezina, C. *J. Antibiot.* **1972**, *25*, 109.
10. Aragozzini, F.; Manachini, P. L.; Craveri, R.; Rindone, B.; Scolastico, C. *Tetrahedron*, **1972**, *28*, 5493.
11. Fujita, T.; Yoneta, M.; Hirose, R.; Sasaki, S.; Inoue, K.; Kiuchi, M.; Hirase, S.; Adachi, K.; Arita, M.; Chiba, K. *Bioorg. Med. Chem. Lett.* **1995**, *5*, 847.
12. Fujita, T.; Hirose, R.; Yoneta, M.; Sasaki, S.; Inoue, K.; Kiuchi, M.; Hirase, S.; Chiba, K.; Sakamoto, H.; Arita, M. *J. Med. Chem.* **1996**, *39*, 4451.
13. Fujita, T.; Hirose, R.; Hamamichi, N.; Kitao, Y.; Sasaki, S.; Yoneta, M.; Chiba, K. *Bioorg. Med. Chem. Lett.* **1995**, *5*, 1857.
14. Fujita, T.; Hamamichi, N.; Kiuchi, M.; Matsuzaki, T.; Kitao, Y.; Inoue, K.; Hirose, R.;

- Yoneta, M.; Sasaki, S.; Chiba, K. *J. Antibiot.* **1996**, *49*, 846.
15. Adachi, K.; Kohara, T.; Nakao, N.; Arita, M.; Chiba, K.; Mishina, T.; Sasaki, S.; Fujita, T. *Bioorg. Med. Chem. Lett.* **1995**, *5*, 853.
  16. For reviews on the discovery and development of FTY720, see: (a) Adachi, K.; Chiba, K. *Perspect. Medicin. Chem.* **2007**, *1*, 11; (b) Brinkmann, V.; Billich, A.; Baumruker, T.; Heining, P.; Schmouder, R.; Francis, G.; Aradhye, S.; Burtin, P. *Nat. Rev. Drug Discov.* **2010**, *9*, 883; (c) Strader, C. R.; Pearce, C. J.; Oberlies, N. H. *J. Nat. Prod.* **2011**, *74*, 900; (d) Chun, J.; Brinkmann, V. *Discov Med.* **2011**, *12*, 213; Chiba, K.; Adachi, K. *Future Med. Chem.* **2012**, *4*, 771.
  17. Kiuchi, M.; Adachi, K.; Kohara, T.; Minoguchi, M.; Hanano, T.; Aoki, Y.; Mishina, T.; Arita, M.; Nakao, N.; Ohtsuki, M.; Hoshino, Y.; Teshima, K.; Chiba, K.; Sasaki, S.; Fujita, T. *J. Med. Chem.* **2000**, *43*, 2946.
  18. Miyake, Y.; Kozutsumi, Y.; Nakamura, S.; Fujita, T.; Kawasaki, T. *Biochem. Biophys. Res. Commun.* **1995**, *211*, 396.
  19. Chiba, K.; Hoshino, Y.; Suzuki, C.; Masubuchi, Y.; Yanagawa, Y.; Ohtsuki, M.; Sasaki, S.; Fujita, T. *Transplant. Proc.* **1996**, *28*, 1056.
  20. Hoshino, Y.; Suzuki, C.; Ohtsuki, M.; Masubuchi, Y.; Amano, Y.; Chiba, K. *Transplant. Proc.* **1996**, *28*, 1060.
  21. Suzuki S.; Li, X. K.; Enosawa, S.; Shinomiya, T. *Immunology.* **1996**, *89*, 518.
  22. Chiba, K.; Yanagawa, Y.; Masubuchi, Y.; Kataoka, H.; Kawaguchi, T.; Ohtsuki, M.; Hoshino, Y. *J. Immunol.* **1998**, *160*, 5037.
  23. Yanagawa, Y.; Sugahara, K.; Kataoka, H.; Kawaguchi, T.; Masubuchi, Y.; Chiba, K. *J. Immunol.* **1998**, *160*, 5493.
  24. Yanagawa, Y.; Masubuchi, Y.; Chiba, K. *Immunology*, **1998**, *95*, 591.
  25. Chiba, K.; Yanagawa, Y.; Kataoka, H.; Kawaguchi, T.; Ohtsuki, M.; Hoshino, Y. *Transplant. Proc.* **1999**, *31*, 1230.
  26. Brinkmann, V.; Pinschewer, D.; Chiba, K.; Feng, L. *Trends Pharmacol. Sci.* **2000**, *21*, 49.
  27. Ho, S.; Clipstone, N.; Timmermann, L.; Northrop, J.; Graef, I.; Fiorentino, D.; Nourse, J.; Crabtree, G. R. *Clin Immunol Immunopathol.* **1996**, *80*, S40.

28. Matsuda, S.; Koyasu, S. *Immunopharmacology*. **2000**, *47*, 119.
29. Thomson, A. W.; Bonham, C. A.; Zeevi, A. *Ther Drug Monit*. **1995**, *17*, 584.
30. Henning, G.; Ohl, L.; Junt, T.; Reiterer, P.; Brinkmann, V.; Nakano, H.; Hohenberger, W.; Lipp, M.; Förster, R. *J. Exp. Med.* **2001**, *194*, 1875.
31. Brinkmann, V.; Wilt, C.; Kristofic, C.; Nikolova, Z.; Hof, R. P.; Chen, S.; Albert, R.; Cottens, S. *Transplant. Proc.* **2001**, *33*, 3078.
32. Mandala, S.; Hajdu, R.; Bergstrom, J.; Quackenbush, E.; Xie, J.; Milligan, J.; Thornton, R.; Shei, G. J.; Card, D.; Keohane, C.; Rosenbach, M.; Hale, J.; Lynch, C. L.; Rupprecht, K.; Parsons, W.; Rosen, H. *Science*, **2002**, *296*, 346.
33. Brinkmann, V.; Davis, M. D.; Heise, C. E.; Albert, R.; Cottens, S.; Hof, R.; Bruns, C.; Prieschl, E.; Baumruker, T.; Hiestand, P.; Foster, C. A.; Zollinger, M.; Lynch, K. R. *J. Biol. Chem.* **2002**, *277*, 21453.
34. Kharel, Y.; Lee, S.; Snyder, A. H.; Sheasley-O'Neill, S. L.; Morris, M. A.; Setiady, Y.; Zhu, R.; Zigler, M. A.; Burcin, T. L.; Ley, K.; Tung, K. S. K.; Engelhard, V. H.; Macdonald, T. L.; Pearson-White, S.; Lynch, K. R. *J. Biol. Chem.* **2005**, *280*, 36865.
35. Brinkmann, V. *Pharmacol. Ther.* **2007**, *115*, 84.
36. Chun, J.; Hartung, H. P.; *Clin. Neuropharmacol.* **2010**, *33*, 91.
37. Zhang, G. F.; Contos, J. J. A.; Weiner, J. A.; Fukushima, N.; Chun, J. *Gene*, **1999**, *227*, 89.
38. Ishii, I.; Friedman, B.; Ye, X.; Kawamura, S.; McGiffert, C.; Contos, J. J.; Kingsbury, M. A.; Zhang, G.; Brown, J. H.; Chun, J. *J. Biol. Chem.* **2001**, *276*, 33697.
39. Sanna, M. G.; Liao, J.; Jo, E.; Alfonso, C.; Ahn, M. Y.; Peterson, M. S.; Webb, B.; Lefebvre, S.; Chun, J.; Gray, N.; Rosen, H. *J. Biol. Chem.* **2004**, *279*, 13839.
40. Lo, C. G., Xu, Y., Proia, R. and Cyster, J. G. *J. Exp. Med.* **2005**, *20*, 291.
41. Anliker, B.; Chun, J. *J. Biol. Chem.* **2004**, *279*, 20555.
42. Zemann, B.; Kinzel, B.; Müller, M.; Reuschel, R.; Mechtcheriakova, D.; Urtz, N.; Bornancin, F.; Baumruker, T.; Billich, A. *Blood*, **2006**, *107*, 1454.
43. Albert, R.; Hinterding, K.; Brinkmann, V.; Guerini, D.; Müller-Hartweg, C.; Knecht, H.; Simeon, C.; Streiff, M.; Wagner, T.; Welzenbach, K.; Zécri, F.; Zollinger, M.; Cooke, N.; Francotte, E. *J. Med. Chem.* **2005**, *48*, 5373.

44. Matloubian, M.; Lo, C. G.; Cinamon, G.; Lesneski, M. J.; Xu, Y.; Brinkmann, V.; Allende, M. L.; Proia, R. L.; Cyster, J. G. *Nature*, **2004**, *427*, 355.
45. Sanna, M. G.; Wang, S-K.; Gonzalez-Cabrera, P. J.; Don, A.; Marsolais, D.; Matheu, M. P.; Wei, S. H.; Parker, I.; Jo, E.; Cheng, W.-C.; Cahalan, M.D.; Wong, C.-H.; Rosen, H. *Nature Chem. Biol.* **2006**, *2*, 434.
46. Gräler, M. H.; Goetzl, E. J. *FASEB J.* **2004**, *3*, 551.
47. Oo, M. L.; Thangada S, Wu, M. T.; Liu, C. H.; Macdonald, T. L.; Lynch, K. R.; Lin, C. Y.; Hla, T. *J. Biol. Chem.* **2007**, *282*, 9082.
48. Pappu, R.; Schwab, S. R.; Cornelissen, I.; Pereira, J. P.; Regard, J. B.; Xu, Y.; Camerer, E.; Zheng, Y. W.; Huang, Y.; Cyster, J. G.; Coughlin, S. R. *Science*, **2007**, *316*, 295.
49. Jo, E., M., Sanna, M. G., Gonzalez-Cabrera, P. J., Thangada, S., Tigyi, G., Osborne, D. A., Hla, T., Parrill, A. L.; Rosen, H. *Chem. Biol.* **2005**, *12*, 705.
50. Bandhuvula, P.; Tam, Y. Y.; Oskouian, B.; Saba, J. D. *J. Biol. Chem.* **2005**, *280*, 33697.
51. Schwab, S. R.; Pereira, J. P.; Matloubian, M.; Xu, Y.; Huang, Y.; Cyster, J. G. *Science*, **2005**, *309*, 1735.
52. Schwab, S. R.; Cyster, J. G. *Nat. Immunol.* **2007**, *8*, 1295.
53. Masubuchi, Y.; Kawaguchi, T.; Ohtsuki, M.; Suzuki, C.; Amano, Y.; Hoshino, Y.; Chiba, K. *Transplant. Proc.* **1996**, *28*, 1064.
54. Brinkmann, V.; Lynch, K. R. *Curr. Opin. Immunol.* **2002**, *14*, 569.
55. Suzuki, S.; Enosawa, S.; Kakefuda, T.; Shinomiya, T.; Amari, M.; Naoe, S.; Hoshino, Y.; Chiba, K. *Transplantation*, **1996**, *61*, 200.
56. Kawaguchi, T.; Hoshino, Y.; Rahman, F.; Amano, Y.; Higashi, H.; Kataoka, H.; Ohtsuki, M.; Teshima, K.; Chiba, K.; Kakefuda, T.; Suzuki, S. *Transplant. Proc.* **1996**, *28*, 1062.
57. Hoshino, Y.; Yanagawa, Y.; Ohtsuki, M.; Nakayama, S.; Hashimoto, T.; Chiba, K. *Transplant. Proc.* **1999**, *31*, 1224.
58. Foster, C. A.; Howard, L. M.; Schweitzer, A.; Persohn, E.; Hiestand, P. C.; Balatoni, B.; Reuschel, R.; Beerli, C.; Schwartz, M.; Billich, A. *J. Pharmacol. Exp. Ther.* **2007**, *323*, 469.
59. Budde, K.; Schmouder, R. L.; Brunkhorst, R.; Nashan, B.; Lücker, P. W.; Mayer, T.;

- Choudhury, S.; Skerjanec, A.; Kraus, G.; Neumayer, H. H. *J. Am. Soc. Nephrol.* **2002**, *13*, 1073.
60. Kahan, B. D.; Karlix, J. L.; Ferguson, R. M.; Leichtman, A. B.; Mulgaonkar, S.; Gonwa, T. A.; Skerjanec, A.; Schmouder, R. L.; Chodoff, L. *Transplantation*, **2003**, *76*, 1079.
61. Tedesco-Silva, H.; Mourad, G.; Kahan, B. D.; Boira, J. G.; Weimar, W.; Mulgaonkar, S.; Nashan, B.; Madsen, S.; Charpentier, B.; Pellet, P.; Vanrenterghem, Y. *Transplantation*, **2005**, *79*, 1553.
62. Tedesco-Silva, H.; Pescovitz, M. D.; Cibrik, D.; Rees, M. A.; Mulgaonkar, S.; Kahan, B. D.; Gugliuzza, K. K.; Rajagopalan, P. R.; Esmeraldo, Rde. M.; Lord, H.; Salvadori, M.; Slade, J. M.; FTY720 Study Group. *Transplantation*, **2006**, *82*, 1689.
63. Mulgaonkar, S.; Tedesco, H.; Oppenheimer, F.; Walker, R.; Kunzendorf, U.; Russ, G.; Knoflach, A.; Patel, Y.; Ferguson, R.; FTYA121 study group. *Am. J. Transplant.* **2006**, *6*, 1848.
64. Salvadori, M.; Budde, K.; Charpentier, B.; Klempnauer, J.; Nashan, B.; Pallardo, L. M.; Eris, J.; Schena, F. P.; Eisenberger, U.; Rostaing, L.; Hmissi, A.; Aradhye, S.; FTY720 0124 Study Group. *Am. J. Transplant.* **2006**, *6*, 2912.
65. Charcot, J. M. *Gazette des hopitaux*, **1868**, *41*, 554.
66. *Atlas Multiple Sclerosis Resources in the World 2008*; WHO Press, Geneva, **2008**; p 15-16.
67. Compston, A.; Coles, A. *Lancet*, **2002**, *359*, 1221.
68. Nakahara, J.; Maeda, M.; Aiso, S.; Suzuki, N. *Clin. Rev. Allergy Immunol.* **2012**, *42*, 26.
69. Lublin, F. D.; Reingold, S. C. *Neurology*, **1996**, *46*, 907.
70. Hafler, D. A. *J. Clin. Invest.* **2004**, *113*, 788.
71. Cohen, J. A.; Barkhof, F.; Comi, G.; Hartung, H. P.; Khatri, B. O.; Montalban, X.; Pelletier, J.; Capra, R.; Gallo, P.; Izquierdo, G.; Tiel-Wilck, K.; de Vera, A.; Jin, J.; Stites, T.; Wu, S.; Aradhye, S.; Kappos, L.; TRANSFORMS Study Group. *N. Engl. J. Med.* **2010**, *362*, 402.
72. Chun, J.; Hartung, H. P. *Clin. Neuropharmacol.* **2010**, *33*, 91.
73. Brinkmann, V.; Chen, S.; Feng, L.; Pinschewer, D.; Nikolova, Z.; Hof, R. *Transplant. Proc.* **2001**, *33*, 530.

74. Foster, C. A.; Howard, L. M.; Schweitzer, A.; Persohn, E.; Hiestand, P. C.; Balatoni, B.; Reuschel, R.; Beerli, C.; Schwartz, M.; Billich, A. *J. Pharmacol. Exp. Ther.* **2007**, *323*, 469.
75. Groves, A.; Kihara, Y.; Chun, J. *J. Neurol. Sci.* **2013**, *328*, 9.
76. Kappos, L.; Radue, E. W.; O'Connor, P.; Polman, C.; Hohlfeld, R.; Calabresi, P.; Selmaj, K.; Agoropoulou, C.; Leyk, M.; Zhang-Auberson, L.; Burtin, P. *N. Engl. J. Med.* **2010**, *362*, 387.
77. Fryer, R. M.; Muthukumarana, A.; Harrison, P. C.; Nodop Mazurek, S.; Chen, R. R.; Harrington, K. E.; Dinallo, R. M.; Horan, J. C.; Patnaude, L.; Modis, L. K.; Reinhart, G. A. *PLOS One*, **2012**, *7*, e52985.
78. For review of FTY720 in cancer therapy, see: (a) Zhang, L.; Wang, H. D.; Ji, X. J.; Cong, Z. X.; Zhu, J. H.; Zhou, Y. *Oncol. Rep.* **2013**, *30*, 2571. (b) *The Role of Sphingolipids in Cancer Development and Therapy*, 1st Edition, Norris, J. S. **2013**, Academic Press, p161-175.
79. Sonoda, Y.; Yamamoto, D.; Sakurai, S.; Hasegawa, M.; Aizu-Yokota, E.; Momoi, T.; Kasahara, T. *Biochem. Biophys. Res. Commun.* **2001**, *281*, 282.
80. Zhang, L.; Wang, H.; Zhu, J.; Ding, K.; Xu, J. *Tumour Biol.* **2014**, *35*, 10707.
81. Azuma, H.; Takahara, S.; Ichimaru, N.; Wang, J. D.; Itoh, Y.; Otsuki, Y.; Morimoto, J.; Fukui, R.; Hoshiga, M.; Ishihara, T.; Nonomura, N.; Suzuki, S.; Okuyama, A.; Katsuoka, Y. *Cancer Res.* **2002**, *62*, 1410.
82. Nagaoka, Y.; Otsuki, K.; Fujita, T.; Uesato, S. *Biol. Pharm. Bull.* **2008**, *31*, 1177.
83. Wang, J. D.; Takahara, S.; Nonomura, N.; Ichimaru, N.; Toki, K.; Azuma, H.; Matsumiya, K.; Okuyama, A.; Suzuki, S. *Prostate.* **1999**, *40*, 50.
84. Zhou, C.; Ling, M. T.; Kin-Wah Lee, T.; Man, K.; Wang, X.; Wong, Y. C. *Cancer Lett.* **2006**, *233*, 36.
85. Tonelli, F.; Lim, K. G.; Loveridge, C.; Long, J.; Pitson, S. M.; Tigyi, G.; Bittman, R.; Pyne, S.; Pyne, N. *J. Cell. Signalling*, **2010**, *22*, 1536.
86. Chua C. W.; Lee D. T.; Ling M. T.; Zhou C.; Man K.; Ho J.; Chan F. L.; Wang X.; Wong Y. C. *Int. J. Cancer*, **2005**, *117*, 1039.



87. Liu, Q.; Zhao, X.; Frissora, F.; Ma, Y.; Santhanam, R.; Jarjoura, D.; Lehman, A.; Perrotti, D.; Chen, C. S.; Dalton, J. T.; Muthusamy, N.; Byrd, J. C. *Blood*. **2008**, *111*, 275.
88. Wallington-Beddoe, C. T.; Hewson, J.; Bradstock, K. F.; Bendall, L. J. *Autophagy*. **2011**, *7*, 707.
89. Neviani, P.; Santhanam, R.; Oaks, J. J.; Eiring, A. M.; Notari, M.; Blaser, B. W.; Liu, S.; Trotta, R.; Muthusamy, N.; Gambacorti-Passerini, C.; Druker, B. J.; Cortes, J.; Marcucci, G.; Chen, C. S.; Verrills, N. M.; Roy, D. C.; Caligiuri, M. A.; Bloomfield, C. D.; Byrd, J. C.; Perrotti, D. *J Clin Invest*. **2007**, *117*, 2408.
90. Yasui, H.; Hideshima, T.; Raje, N.; Roccaro, A. M.; Shiraishi, N.; Kumar, S.; Hamasaki, M.; Ishitsuka, K.; Tai, Y. T.; Podar, K.; Catley, L.; Mitsiades, C. S.; Richardson, P. G.; Albert, R.; Brinkmann, V.; Chauhan, D.; Anderson, K. C. *Cancer Res*. **2005**, *65*, 7478.
91. Liu, Q.; Alinari, L.; Chen, C. S.; Yan, F.; Dalton, J. T.; Lapalombella, R.; Zhang, X.; Mani, R.; Lin, T.; Byrd, J. C.; Baiocchi, R. A.; Muthusamy, N. *Clin. Cancer Res*. **2010**, *16*, 3182.
92. Schmid, G.; Guba, M.; Pappan, A.; Ischenko, I.; Brückel, M.; Bruns, C. J.; Jauch, K. W.; Graeb, C. *Transplant. Proc*. **2005**, *37*, 110.
93. Lucas da Silva, L. B.; Ribeiro, D. A.; Cury, P. M.; Cordeiro, J. A.; Bueno, V. *J. Exp. Ther. Oncol*. **2008**, *7*, 9.
94. Salinas, N. R.; Lopes, C. T.; Palma, P. V.; Oshima, C. T.; Bueno, V. *Pathol. Oncol. Res*. **2009**, *15*, 549.
95. Saddoughi, S. A.; Gencer, S.; Peterson, Y. K.; Ward, K. E.; Mukhopadhyay, A.; Oaks, J.; Bielawski, J.; Szulc, Z. M.; Thomas, R. J.; Selvam, S. P.; Senkal, C. E.; Garrett-Mayer, E.; De Palma, R. M.; Fedarovich, D.; Liu, A.; Habib, A. A.; Stahelin, R. V.; Perrotti, D.; Ogretmen, B. *EMBO Mol. Med*. **2013**, *5*, 105.
96. Ng, K. T.; Man, K.; Ho, J. W.; Sun, C. K.; Lee, T. K.; Zhao, Y.; Lo, C. M.; Poon, R. T.; Fan, S. T. *Int. J. Oncol*. **2007**, *30*, 375.
97. Li, C. X.; Shao, Y.; Ng, K. T.; Liu, X. B.; Ling, C. C.; Ma, Y. Y.; Geng, W.; Fan, S. T.; Lo, C. M.; Man, K. *PLoS One*. **2012**, *7*, e32380.
98. Zhang, N.; Qi, Y.; Wadham, C.; Wang, L.; Warren, A.; Di, W.; Xia, P. *Autophagy*. **2010**, *6*, 1157.

99. Zhang, N.; Dai, L.; Qi, Y.; Di, W.; Xia, P. *Int. J. Oncol.* **2013**, *42*, 2053.
100. Azuma, H.; Takahara, S.; Horie, S.; Muto, S.; Otsuki, Y.; Katsuoka, Y. *J. Urol.* **2003**, *169*, 2372.
101. Ubai, T.; Azuma, H.; Kotake, Y.; Inamoto, T.; Takahara, K.; Ito, Y.; Kiyama, S.; Sakamoto, T.; Horie, S.; Muto, S.; Takahara, S.; Otsuki, Y.; Katsuoka, Y. *Anticancer Res.* **2007**, *27*, 75.
102. Tonelli, F.; Lim, K. G.; Loveridge, C.; Long, J.; Pitson, S. M.; Tigyi, G.; Bittman, R.; Pyne, S.; Pyne, N. J. *Cell Signal.* **2010**, *22*, 1536.
103. Lim, K. G.; Tonelli, F.; Li, Z.; Lu, X.; Bittman, R.; Pyne, S.; Pyne, N. J. *J. Biol. Chem.* **2011**, *286*, 18633.
104. Vadas, M.; Xia, P.; McCaughan, G.; Gamble, J. *Biochim. Biophys. Acta.* **2008**, *1781*, 442.
105. Glick, D.; Barth, S.; Macleod, K. F. *J. Pathol.* **2010**, *221*, 3.
106. Maiuri, M. C.; Zalckvar, E.; Kimchi, A.; Kroemer, G. *Nat. Rev. Mol. Cell Biol.* **2007**, *8*, 741.
107. Liao, A.; Hu, R.; Zhao, Q.; Li, J.; Li, Y.; Yao, K.; Zhang, R.; Wang, H.; Yang, W.; Liu, Z. *Eur. J. Pharm. Sci.* **2012**, *45*, 600.
108. Romero Rosales, K.; Singh, G.; Wu, K.; Chen, J.; Janes, M. R.; Lilly, M. B.; Peralta, E. R.; Siskind, L. J.; Bennett, M. J.; Fruman, D. A.; Edinger, A. L. *Biochem. J.* **2011**, *439*, 299.
109. Alinari, L.; Mahoney, E.; Patton, J.; Zhang, X.; Huynh, L.; Earl, C. T.; Mani, R.; Mao, Y.; Yu, B.; Quinion, C.; Towns, W. H.; Chen, C. S.; Goldenberg, D. M.; Blum, K. A.; Byrd, J. C.; Muthusamy, N.; Praetorius-Ibba, M.; Baiocchi, R. A. *Blood.* **2011**, *118*, 6893.
110. Alinari, L.; Baiocchi, R. A.; Praetorius-Ibba, M. *Autophagy.* **2012**, *8*, 416.
111. LaMontagne, K.; Littlewood-Evans, A.; Schnell, C.; O'Reilly, T.; Wyder, L.; Sanchez, T.; Probst, B.; Butler, J.; Wood, A.; Liau, G.; Billy, E.; Theuer, A.; Hla, T.; Wood, J. *Cancer Res.* **2006**, *66*, 221.
112. *Synthesis of Conformation-Restricted Analogs of FTY720 as Sphingosine 1-Phosphate Receptor Pro-drugs.* Huang, T. University of Virginia, ProQuest, UMI Dissertations Publishing, **2012**. 3516185.

113. Kennedy, P. C.; Zhu, R.; Huang, T.; Tomsig, J. L.; Mathews, T. P.; David, M.; Peyruchaud, O.; Macdonald, T. L.; Lynch, K. R. *J. Pharmacol. Exp. Ther.* **2011**, 338, 879.
114. Zhu, R.; Snyder, A. H.; Kharel, Y.; Schaffter, L.; Sun, Q.; Kennedy, P. C.; Lynch, K. R.; Macdonald, T. L. *J. Med. Chem.* **2007**, 50, 6428.
115. Ma, B.; Guckian, K. M.; Lin, E. Y.; Lee, W. C.; Scott, D.; Kumaravel, G.; Macdonald, T. L.; Lynch, K. R.; Black, C.; Chollate, S.; Hahm, K.; Hetu, G.; Jin, P.; Luo, Y.; Rohde, E.; Rossomando, A.; Scannevin, R.; Wang, J.; Yang, C. *Bioorg. Med. Chem. Lett.* **2010**, 20, 2264.
116. Clemens, J. J.; Davis, M. D.; Lynch, K. R.; Macdonald, T. L. *Bioorg. Med. Chem. Lett.* **2004**, 14, 4903.
117. Clemens, J. J.; Davis, M. D.; Lynch, K. R.; Macdonald, T. L. *Bioorg. Med. Chem. Lett.* **2005**, 15, 3568.
118. Foss, F.W. Jr.; Mathews, T. P.; Kharel, Y.; Kennedy, P. C.; Snyder, A. H.; Davis, M. D.; Lynch, K. R.; Macdonald, T. L. *Bioorg. Med. Chem.* **2009**, 17, 6123.
119. Hanessian, S.; Charron, G.; Billich, A.; Guerini, D. *Bioorg. Med. Chem. Lett.* **2007**, 17, 491.
120. Fransson, R.; McCracken, A. N.; Chen, B.; McMonigle, R. J.; Edinger, A. L.; Hanessian, S. *ACS. Med. Chem. Lett.* **2013**, 4, 969.
121. Toumi, M.; Couty, F.; Evano, G. *Angew. Chem. Int. Ed.* **2007**, 46, 572.
122. Zlatopolskiy, B. D.; Kroll, H. P.; Melotto, E.; Meijere, A. *Eur. J. Org. Chem.* **2004**, 4492.
123. Rosen, T.; Chu, D. T. W.; Lico, I. M.; Fernandes, P. B.; Marsh, K.; Shen, L.; Cepa, V. G.; Pernet, A. G. *J. Med. Chem.* **1988**, 31, 1598.
124. Mitsumori, S.; Zhan, H.; Cheong, P. H. Y.; Houk, K. N.; Tanaka, F.; Barbas, III, C. F. *J. Am. Chem. Soc.* **2006**, 128, 1040.
125. Dorn, H.; Rodezno, J. M.; Brunnhöfer, B.; Rivard, E.; Massey, J. A.; Manners, I. *Macromolecules*, **2003**, 36, 291.
126. Atkins Jr, G. M., Burgess, E. M. *J. Am. Chem. Soc.* **1968**, 90, 4744.
127. Crabtree, R. H. *Acc. Chem. Res.* **1979**, 12, 331.

128. Brown, J. M. *Angew. Chem. Int. Ed.* **1987**, *26*, 190.
129. García-García, P.; Ladépêche, A.; Halder, R.; List, B. *Angew. Chem.* **2008**, *120*, 4797.
130. Marigo, M.; Wabnitz, T. C.; Fielenbach, D.; Jørgensen, K. A. *Angew. Chem. Int. Ed.* **2005**, *44*, 794.
131. Hayashi, Y.; Gotoh, H.; Hayashi, T.; Shoji, M. *Angew. Chem. Int. Ed.* **2005**, *44*, 4212.
132. Zhu, S. L.; Yu, S. Y.; Wang, Y.; Ma, D. W. *Angew. Chem. Int. Ed.* **2010**, *49*, 4656.
133. An, X.; Tiwari, A. K.; Sun, Y.; Ding, P. R.; Ashby Jr, C. R.; Chen, Z. S. *Leuk. Res.* **2010**, *34*, 1255.
134. Savage, D. G.; Antman, K. H. *N. Engl. J. Med.* **2002**, *346*, 683.
135. *Purification of Laboratory Chemicals*, (7 edition), Armarego, W. L. F.; Chai, C. L. L. Butterworth-Heinemann; **2012**.
136. Still, W. C.; Kahn, M.; Mitra A. *J. Org. Chem.* **1978**, *43*, 2923.
137. Kumar, T. P.; Chandrasekhar, S. *Synthesis*, **2012**, *44*, 2889.
138. Mina, J. G.; Mosely, J. A.; Ali, H. A.; Denny, P. W.; Steel, P. G. *Org. Biomol. Chem.* **2011**, *9*, 1823.
139. Koskinen, A. M. P.; Helaja, J.; Kumpulainen, E. T. T.; Koivisto, J.; Mansikkamäki, H.; Rissanen, K. *J. Org. Chem.* **2005**, *70*, 6447.
140. Watanabe, A.; Yamasaki, T.; Tanda, K.; Miyagoe, T.; Sakamoto, M.; Kiyota, N.; Otsuka, M. *J. Heterocyclic Chem.* **2011**, *48*, 1132.
141. Chabaud, P.; Pépe, G.; Courcambeck, J.; Camplo, M. *Tetrahedron*, **2005**, *61*, 3725.
142. Barraclough, P.; Hudhomme, P.; Spray, C. A.; Young, D. W. *Tetrahedron*, **1995**, *51*, 4195.
143. Van Huis, C. A.; Casimiro-Garcia, A.; Bigge, C. F.; Cody, W. L.; Dudley, D. A.; Filipinski, K. J.; Heemstra, R. J.; Kohrt, J. T.; Leadley, R. J. Jr.; Narasimhan, L. S.; McClanahan, T.; Mochalkin, I.; Pamment, M.; Peterson, J. T.; Sahasrabudhe, V.; Schaum, R. P.; Edmunds, J. J. *Bioorg. Med. Chem.* **2009**, *17*, 2501-2511.
144. Gotoh, H.; Ishikawa, H.; Hayashi, Y. *Org. Lett.* **2007**, *9*, 5307.
145. Wang, Y. C.; Li, P. Y.; Liang, X. M.; Zhang, T. Y.; Ye, J. X. *Chem. Commun.* **2008**, 1232.

## Chapter 2: Design and Synthesis of Photoaffinity Labeling Probe of Amino Alcohol 1.57 and 1.65

### 2-1 Introduction

#### 2-1-1 General mechanism of photoaffinity labeling (PAL)

Protein–ligand interactions are ubiquitous and essential in living organisms. Study of the interactions between bioactive ligands and their corresponding receptor proteins is not only required in the fundamental life sciences, but is also helpful for understanding the pathology of diseases, to aid drug discovery and medical science.<sup>1-3</sup> The major challenges to elucidate the structures of the complex biological molecules involved in such processes has led to the development of several techniques,<sup>4</sup> such as X-ray crystallography<sup>4-6</sup> and NMR spectroscopy.<sup>4,7,8</sup> Analysis of structures of crystalline protein-ligand complexes by X-ray crystallography can directly provide details of their interactions in three dimensions, but this static structural information is usually insufficient for determining or predicting solution-state interactions. NMR spectroscopy is a powerful technique for probing protein-ligand interactions in solution, because it can provide dynamic structural information of the complex by analysis of the resonance signals of the ligand or the protein, but it may be limited by macromolecular size.<sup>9</sup> Both of these methods require usually protein samples of high purity, which may be a challenge due to difficulties in the purification of proteins. In 1962, Westheimer and coworkers<sup>10</sup> described the successful labeling of chymotrypsin by acylation with *p*-nitrophenyl diazoacetate followed by photolysis. Based on their success, the concept of photoaffinity labeling (PAL) was introduced and proposed as a new method for mapping the active site of an enzyme.<sup>10</sup> With this revolutionary idea, new photoaffinity probes and methods for detection of the labeled receptor soon were developed, which led PAL to become one of most important techniques in structural biology today.<sup>11</sup>

In PAL experiments, a bifunctional ligand probe, possessing a photoreactive group and a reporter group, bind to the macromolecule of interest, usually a protein (Figure 23). Upon

irradiation with UV light, a highly reactive intermediate (typically a carbene, nitrene or a diradical) is generated from the photolabile moiety and inserts into the bonds of the large molecule forming a covalent link. Thus, the previously reversible binding is turned to permanent binding. The ligand-receptor complex may then be purified by tagging ligand to allow identification of the macromolecule, and particularly its binding region. In PAL processes, purification of the target macromolecule is initially not needed, and only required after tagging of the ligand-receptor complex. Therefore, PAL is advantageous for studies of complex systems (*e.g.* ribosomes and transcription factors) and unknown macromolecules.

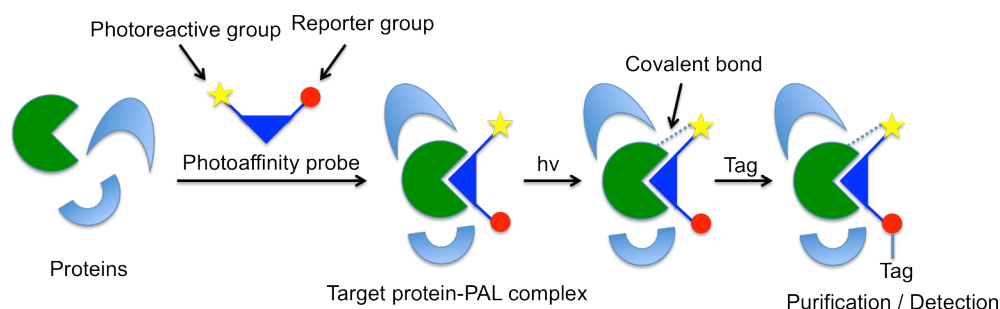


**Figure 23.** General mechanism of a photoaffinity labeling (PAL) process.

### 2-1-2 Photoaffinity probe (PAP)

The design of a suitable photoaffinity probe is a crucial factor for success in PAL studies. The PAP is usually prepared by modification of a ligand for the receptor. This modification should not decrease the biological activity (including affinity). The photoreactive group on the probe should be highly reactive, and activated at mild conditions to avoid any damage to the biosystem. The active intermediate after irradiation should readily react not only with X-H nucleophiles, but ideally with the C-H bonds of the target protein. The reporter group should be easily detected. The crosslinking reaction should give high yield. There is no such thing as an ideal PAP; however, many efforts have been made, to create diverse photoreactive groups and reporter groups. Design of the most suitable PAP is typically done on a case by case basis.<sup>11</sup>

### 2-1-2-1 Photoreactive groups

Since the diazoacetyl group was used by Westheimer and coworkers in the labeling of chymotrypsin,<sup>10</sup> many other photoreactive groups have been developed.<sup>11</sup> Among these, benzophenones, aryl azides, and diazirines are among the most widely used in PAL experiments (Figure 24).

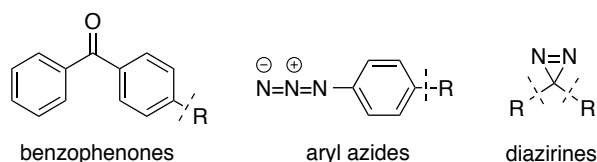


**Figure 24.** Photolabeling groups: benzophenones, aryl azides and diazirines.

Benzophenone<sup>11,12</sup> can be photoactivated at wavelengths of 350~360 nm to generate a highly reactive triplet state benzhydryl diradical (Figure 25).<sup>11d</sup> This diradical can exist up to 120  $\mu$ s before it converts back to the ground state. It abstracts hydrogen from the nearby X-H bonds on a protein, and undergoes fast recombination to form a benzhydryl alcohol. Water does not deactivate the photochemical reactivity of benzophenone, because the diradical can react with water and generate a hydrate, that dehydrates to give back benzophenone. This enhances PAL efficiency when using benzophenone. Benzophenones also have advantages in terms of chemical stability and commercial availability; however, they have drawbacks, such as the bulkiness of benzophenone may affect the biological activity of the ligand and the interaction between the ligand and receptor. Benzophenones often require prolonged irradiation times, which may cause damage to biosystems.

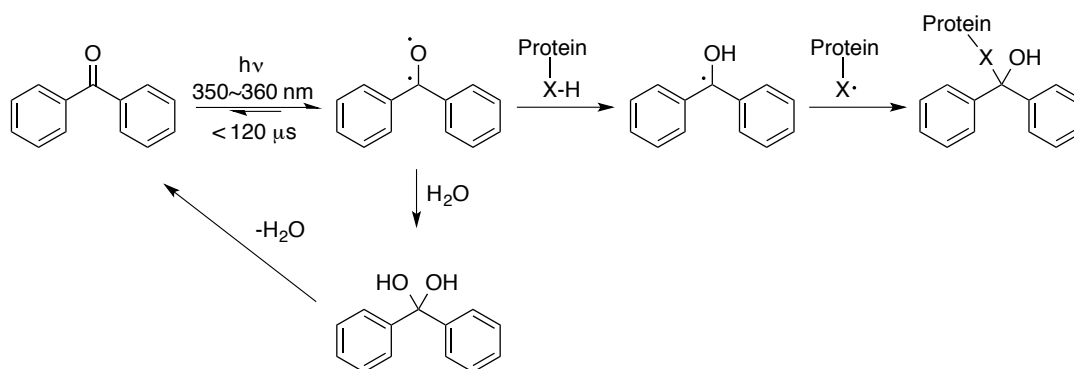


**Figure 25.** Possible photochemical processes of benzophenone.<sup>11d</sup>

Aryl azides<sup>11,13</sup> can be irradiated (major wavelengths < 300 nm) to generate the reactive singlet state nitrenes, which can directly insert into the X-H bonds of the protein receptor (Figure 26). The short-lived nitrene can be transformed to a lower energy triplet state nitrene through intersystem crossing, abstract a hydrogen from an X-H bond, and form a covalent N-X bond with the protein receptor, the same complex as generated by the singlet nitrene. The singlet nitrene can also be converted to a benzazirine, which rearrange to a dehydroazepine. Both benzazirine and dehydroazepine can react with a variety of nucleophiles.<sup>14</sup> In addition to these possible photolysis reactions, there are many other side reactions, including the reduction of aryl azides to the corresponding amines, oxidation of triplet nitrenes to nitro intermediates, and dimerization of triplet nitrenes to azobenzene. Due to the many reaction pathways, the crosslinking efficiencies of aryl azides in PAL are usually low (< 30% yield).<sup>15</sup> Irradiating at wavelengths less than 300 nm may also damage the biosystems, which further limits the use of aryl azides in PAL studies. Compared to benzophenones, aryl azides are however relatively small in size, and relatively easy to synthesize from the corresponding aromatic amines.<sup>16</sup> Modification of the substituents on the aryl ring may increase crosslinking efficiencies.<sup>11a</sup> These advantages combined make aryl azides one of the most popular photoreactive groups.

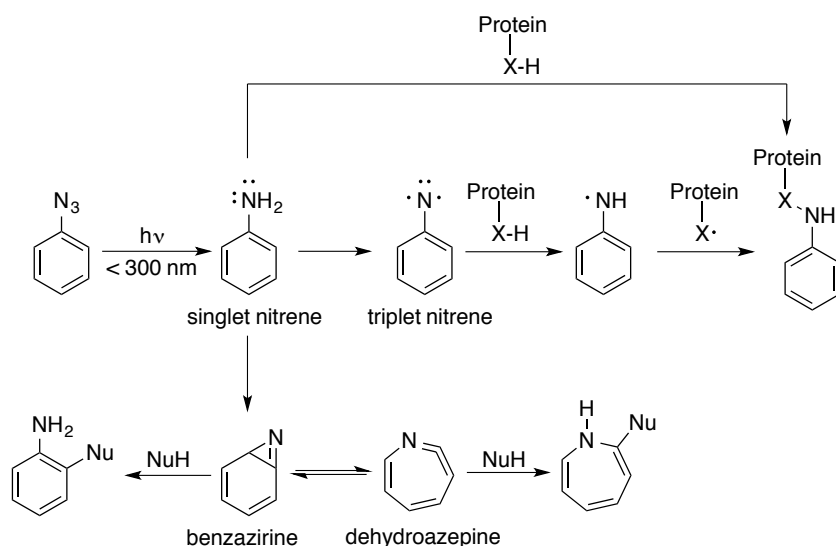


**Figure 26.** Possible photochemistry process of aryl azide.<sup>11d</sup>



Diazirines<sup>11,15,17</sup> can be efficiently excited at wavelengths 350-380 nm, and generate a singlet carbene and a diazo isomer (> 30 %) (Figure 27). The short-lived singlet carbene can directly insert into an X-H bond of the protein, and can also go through intersystem crossing to give a lower energy triplet carbene, which could abstract a hydrogen from an X-H bond, and recombine to form the ligand-protein complex, the same product generated from the singlet carbene. The diazo isomer may also transform into a singlet carbene, but this process is slow, and it could lead to the unspecific labeling, or hydrolysis.<sup>11d</sup> A solution to this problem is to use the 3-trifluoromethyl-3-phenyldiazirine (Figure 27),<sup>18</sup> because this diazo derivative is stabilized due to the strong electron-withdrawing effect of the trifluoromethyl group and resists side reactions. Compared to other photoreactive groups, diazirines are more difficult to synthesize often requiring more steps.<sup>17c,19</sup> Diazirines are relatively small in size, and require long wavelengths to activate, which decreases the risk of damaging the target biomolecules. They are chemically stable under various conditions (strong acids, bases, etc.). Due to these advantages, diazirines have become the most useful photo-reactive groups in PAL studies.

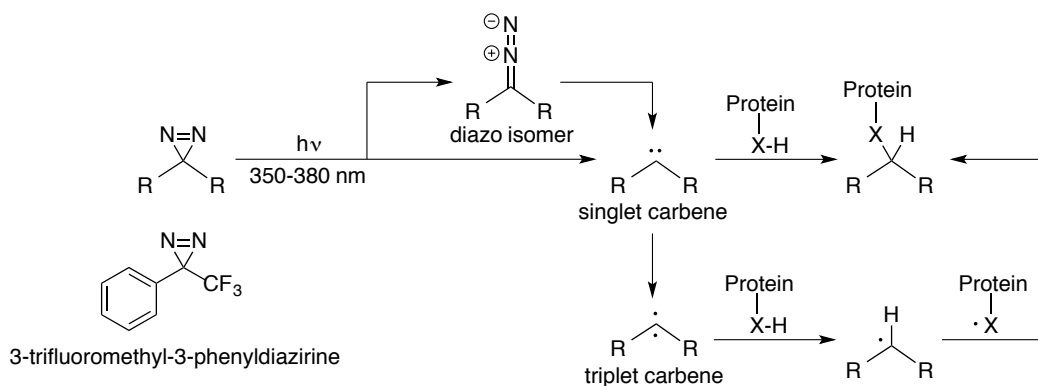


**Figure 27.** Possible photochemistry process of diazirine.<sup>11d</sup>

### 2-1-2-2 Reporter groups

Reporter groups facilitate the detection of the photolabeled complex, and help isolation and identification. A number of reporter groups have been developed based on different methods,<sup>11e,g, 20</sup> such as radiolabels (radioactive isotopes <sup>125</sup>I, <sup>3</sup>H),<sup>20</sup> fluorophores (e.g. fluorescein, pyrene),<sup>21</sup> and affinity tags (e.g. biotin, epitope tags).<sup>11d</sup> Although widely used, radiolabels suffer several significant drawbacks, because they are quickly degraded, harmful,

and require special handling techniques. The incorporation of fluorophores and affinity tags may augment size, and cell permeability, and thus alter the biological activities of the probe. In the absence of cell permeability, photoaffinity probes are unable to capture receptor targets in live cells.

In 2003, Bertozzi and coworkers coined the term “bioorthogonal chemistry”,<sup>22,23</sup> which is used to enable the study the biomolecules in living cells. In concept, a chemical reaction could occur inside of living systems, but it should neither interact with the biosystem, nor interfere with any native biochemical processes.<sup>24</sup> This type of reaction was achieved by incorporating certain functional groups as reporter groups on biomolecules, which could be selectively ligated in a second step (Figure 28). Bioorthogonal chemistry provides a strategy in PAL studies, using chemical reporters that perform tandem photoaffinity labeling–bioorthogonal conjugation to detect the photoaffinity probe-receptor complex,<sup>11e</sup> and to allow the capture of targets in live cells.

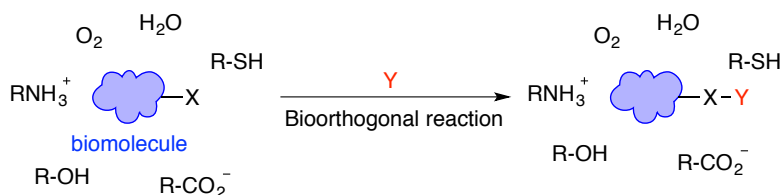
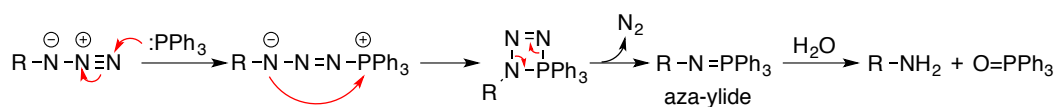


**Figure 28.** A general bioorthogonal chemical reaction.

Bioorthogonal chemistry requires unique reporter and ligation groups. A number of bioorthogonal reactions have been developed,<sup>25</sup> including: condensation reactions of ketones/aldehydes with amines/hydrazide,<sup>26</sup> the Bertozzi-Staudinger ligation of azides and triarylphosphines,<sup>27</sup> 1,3-dipolar cycloaddition between azides and alkynes<sup>28-30</sup> Diels–Alder cycloadditions between tetrazines and strained alkenes/alkynes,<sup>31,32</sup> cross-metathesis,<sup>33,34</sup> and Suzuki-Miyaura coupling reactions.<sup>35,36</sup> Among these reactions, the Bertozzi-Staudinger ligation and 1,3-dipolar azide-alkyne cycloaddition have been the most well studied reactions in bioorthogonal chemistry.

The Bertozzi-Staudinger ligation was the first successful bioorthogonal reaction in this field.<sup>37</sup> In the classic Staudinger reaction, an azide reacts with a phosphine (e.g. triphenylphosphine) or a phosphite to generate an unstable aza-ylide intermediate,<sup>38,39</sup> which then can be hydrolyzed to give the amine (Figure 29). In 2000, Bertozzi and coworkers modified this reaction, by introducing an electrophilic trap, a methyl ester group, *ortho* to the phosphorus atom on one of the phenyl rings in triphenylphosphine, the generated aza-ylide was directed to form an amide bond through intramolecular cyclization, instead of hydrolysis. The five-member ring intermediate is then hydrolyzed to afford a stable ligation product (Figure 29).<sup>37</sup>

**Staudinger reaction:**



**Bertozzi-Staudinger ligation:**

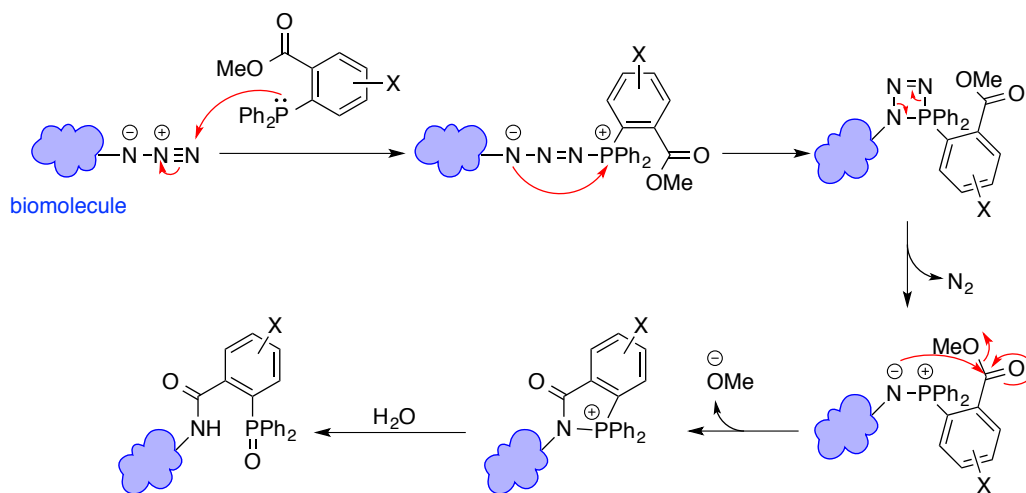
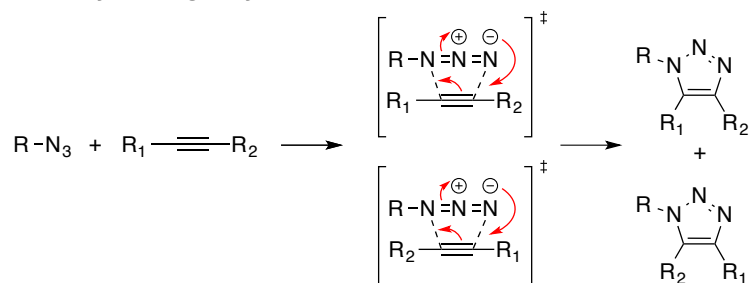


**Figure 29.** General mechanisms of the Staudinger reaction and the Bertozzi-Staudinger ligation.

Bertozzi-Staudinger ligations have been practically used in living cells<sup>40</sup> and animals;<sup>41</sup> however, they suffer drawbacks: aryl azides can be reduced by thiols,<sup>23a</sup> phosphine reagents can be slowly oxidized by air or enzymes,<sup>23a,c</sup> the kinetics of the reactions are slow (second order rate constant:  $0.0020 \text{ M}^{-1}\cdot\text{s}^{-1}$ ) resulting in a higher concentration of phosphine reagents, which also lead to the problems of phosphine oxidation and high background signals in cell fluorescence image applications.<sup>42</sup> Although limited by these problems, the Bertozzi-Staudinger ligation is a common choice in bioorthogonal chemistry due to high selectivity and wide compatibility.<sup>25</sup>

1,3-Dipolar azide-alkyne cycloadditions are also commonly considered for bioorthogonal chemistry. This [3+2] cycloaddition reaction was first described by Arthur Michael in 1893,<sup>43</sup> followed by extensive studies by Rolf Huisgen,<sup>44</sup> This reaction is presently known as “Azide-alkyne Huisgen cycloaddition” (Figure 30). For bioorthogonal chemistry, azides are absent in biological systems, both azides and alkynes are small in size, and their incorporation should have minimal effect of biological activity, nor perturb biosystems. Although there could be many benefits, the classic Huisgen cycloaddition cannot be used as a bioorthogonal reaction due to the harsh reaction conditions (high temperature and pressure) and the slow kinetics. In 2002, both K. Barry Sharpless<sup>45</sup> and Morten Meldal<sup>46</sup> reported efficient Copper (I) catalyzed 1,3-dipolar cycloaddition reactions between azides and terminal alkynes, which overcame these obstacles for use in bioorthogonal chemistry (Figure 30). The mechanism of the copper (I) catalyzed 1,3-dipolar azide-alkyne cycloaddition, termed as “CuAAC”,<sup>47,48</sup> and known as “click chemistry”,<sup>49</sup> is different from the standard [3+2] Huisgen cycloaddition. The generally recognized mechanism involves dinuclear copper interactions.<sup>50-</sup><sup>52</sup> One molecular copper (I) catalyst first interacts with the terminal alkyne substrate to form a pi-complex. The terminal hydrogen is then deprotonated by a base to generate a second molecular copper (I) species, which binds to the copper acetylide intermediate, and activates the azide substrate to generate a copper-azide-acetylide complex. Upon cyclization and protonation, the complex transforms to a 1,4-disubstituted triazole as a specific isomer, and the copper (I) catalyst was regenerated (Figure 30).

**Azide-alkyne Huisgen cycloaddition:**



**CuAAC reaction:**

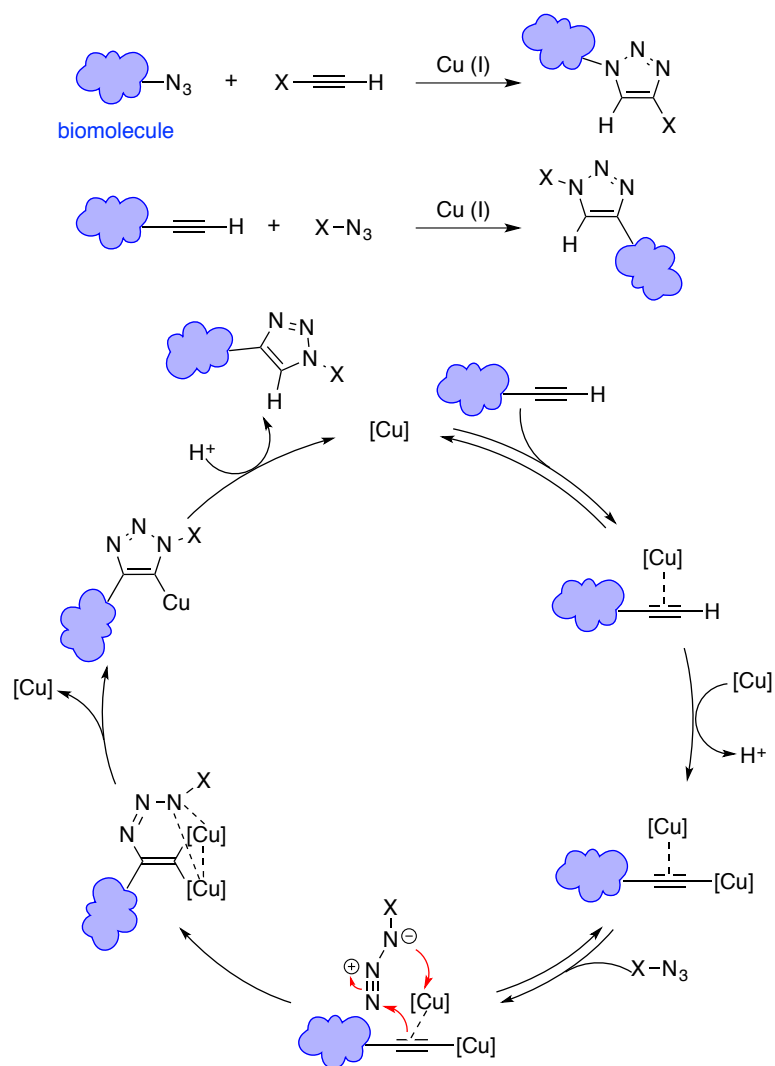


**Figure 30.** General mechanisms of azide-alkyne Huisgen cycloaddition and CuAAC reaction.

The CuAAC reaction has a faster reaction rate compared to Bertozzi-Staudinger ligation, is relatively simple and readily occurs in aqueous solution. Widely used as a popular bioorthogonal reaction in chemical biology studies,<sup>47,53</sup> the CuAAC reaction has wide compatibility with biosystems; however, Cu (I) catalysts are toxic to living cells.<sup>54</sup> To decrease cytotoxicity, a number of ligands have been developed,<sup>55-60</sup> which enable labeling biomolecules in living cells through the CuAAC reaction.

To further optimize the CuAAC reaction and avoid the use of Cu (I) completely, Bertozzi developed “Cu-free click chemistry” by employing ring strain (cyclooctyne)<sup>61-63</sup> to facilitate alkyne-azide cycloaddition in the absence of Cu (I) (Figure 31).<sup>64</sup> Termed “strain-promoted alkyne-azide cycloaddition” (SPAAC), the first generation of this method employed OCT-botin for labeling glycoproteins without cytotoxicity.<sup>64</sup> The reaction suffers from drawbacks: the kinetics of the reaction are typically slower than the Bertozzi-Staudinger ligation, and significantly slower compared to CuAAC reactions; OCT is poorly water soluble. To improve the SPAAC reaction, modified cyclooctynes have been prepared, such as ALO (aryl-less octyne),<sup>65</sup> which has better solubility in water compared to OCT, but similarly poor kinetics. MOFO (monofluorinated cyclooctyne)<sup>65</sup> and DIFO (difluorinated cyclooctyne)<sup>66</sup> have enhanced reaction rates due to the electron-withdrawing property of fluoride, DIBO (dibenzocyclooctyne)<sup>67</sup> increases reactivity by fusing two aryl rings to increase strain. BARAC (biarylazacyclooctynone)<sup>68</sup> and DIBAC (dibenzoazacyclooctyne)<sup>69, 70</sup> have accelerated the reaction rates due in part to an amide bond on the ring. BCN (bicyclo[6.1.0]nonyne)<sup>71</sup> has improved the kinetics due to the added strain of the cyclopropane, and gives a single regioisomer due to symmetry (Figure 31). These modified cyclooctynes effectively promoted SPAAC in biological systems, especially *in vivo* imaging studies.<sup>66,72,73</sup> “Click chemistry”, including CuAAC and SPAAC, has become the most common and promising reaction in bioorthogonal chemistry, and a popular strategy in PAL studies.

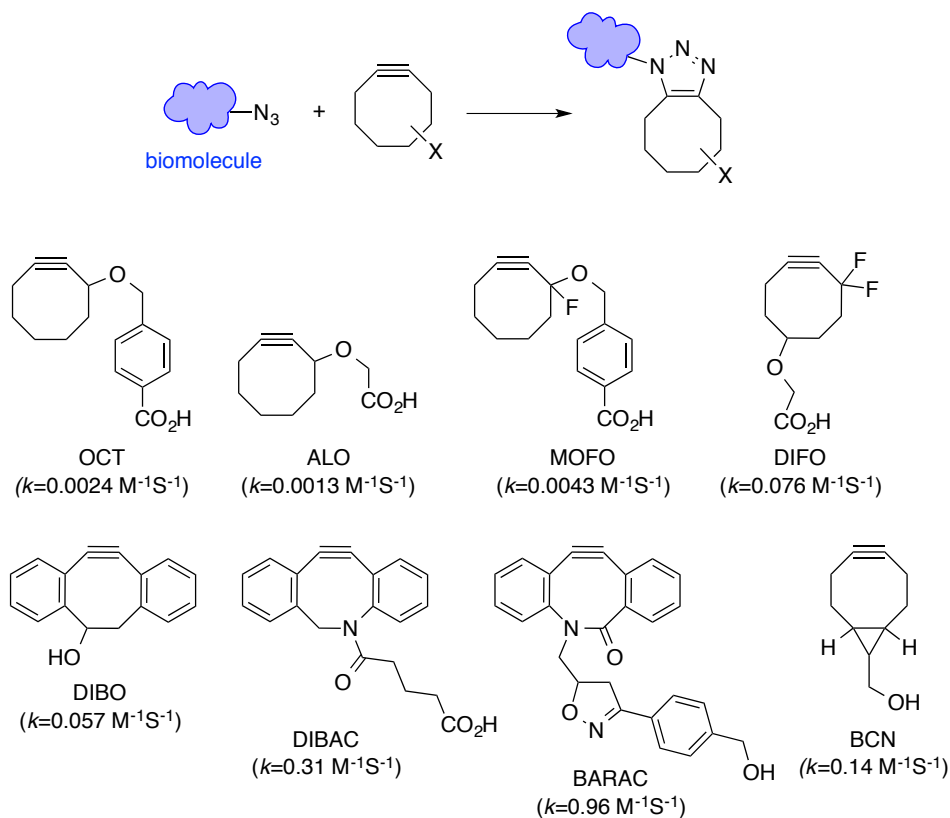


**Figure 31.** General reaction of SPAAC and modified octyne analogues.

### 2-1-3 Design of photoaffinity labeling probes from **1.57** and **1.65**

In our studies of constrained azacyclic pyrrolidine analogues of FTY720, amino alcohol **1.65** exhibited better activity against Sup-B15 leukemia cell line compared to FTY720 (**1.8**) and analogues (Tables 2 and 3). Furthermore, **1.65** could trigger down-regulation of the nutrient transporter to kill cancer cells (Figure 13). To further understand its anti-cancer mechanism, and the affect of stereochemistry compared to its enantiomer **1.57**, we decided to use PAL to identify the target receptor, and ultimately facilitate design of more effective analogues.

To make photoaffinity labeling probes from **1.57** and **1.65**, we chose to incorporate a diazirine as the photoreactive group on the C-8 aliphatic long chain (Figure 32). Diazirines are usually prepared from the corresponding ketones.<sup>17c</sup> To determine the best position to install

the diazirine, four analogues (**2.1**, **2.2**, **2.3**, and **2.4**) of **1.65** bearing ketone moieties at the 1-, 3-, 4-, 7-positions on the chain were respectively prepared (Figure 32).

For reporter groups, we planed to use “click chemistry”, and install an azide or terminal alkyne on the hydroxymethyl arm (Figure 32). In general, these small photo reactive groups and reporter groups were expected to not have much negative influence on bioactivity. The most suitable reporter group would depend on the bioactivity after modification and the difficulty of synthesis.

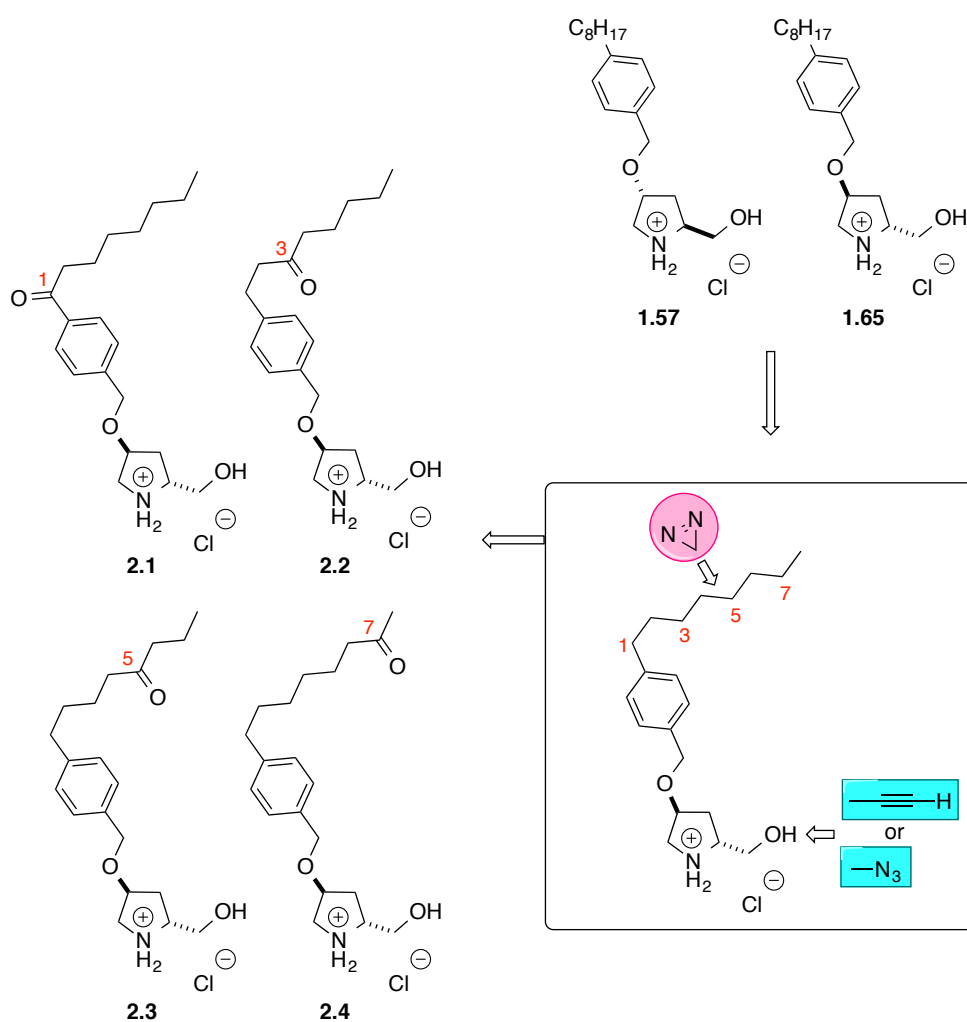


**Figure 32.** Design of photoaffinity labeling (PAL) probes of **1.57** and **1.65**, and their ketone precursors **2.1**, **2.2**, **2.3** and **2.4**.



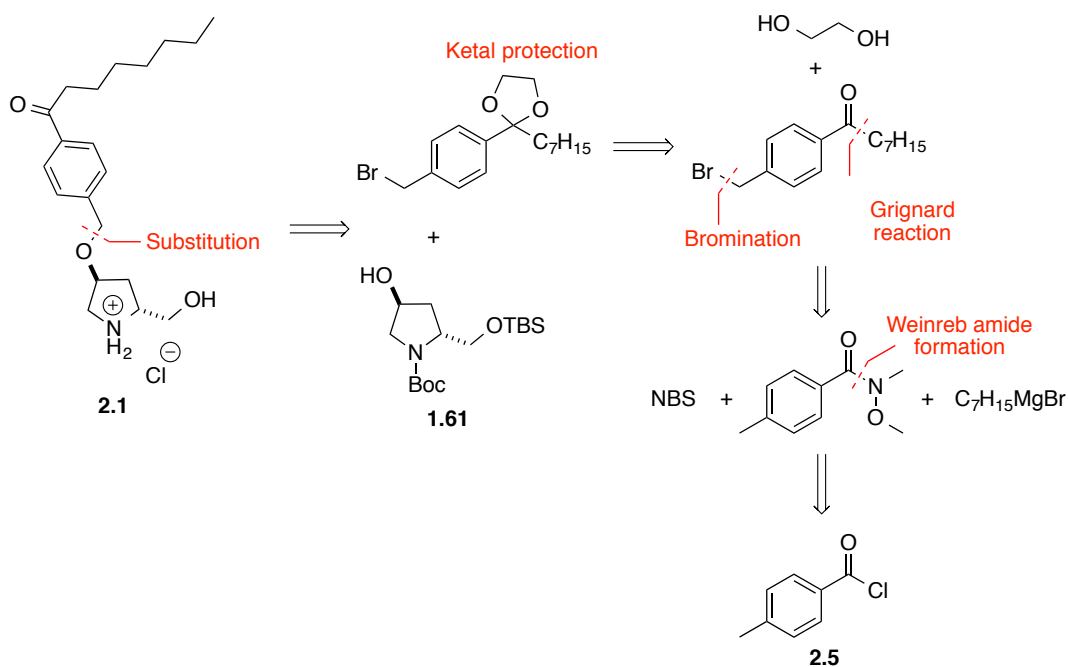
## 2-2 Results and Discussion

### 2-2-1 Screening of the position of diazirine

#### 2-2-1-1 Synthesis of ketone 2.1

In our initial retrosynthetic analysis (Scheme 37), we envisioned that compound **2.1** could be easily assembled from the available (2*R*)-hydroxymethyl-(4*S*)-hydroxyl-pyrrolidine intermediate **1.61** (Scheme 10) and a ketal protected benzyl bromide through a substitution reaction. This ketal intermediate could be prepared from the corresponding ketone, which could be generated through a Grignard reaction between *n*-heptylmagnesium bromide and phenyl Weinreb amide. The required bromide can be accessed through benzylic bromination using NBS. The Weinreb amide intermediate could be easily prepared from the corresponding 4-methylbenzoyl chloride (**2.5**).

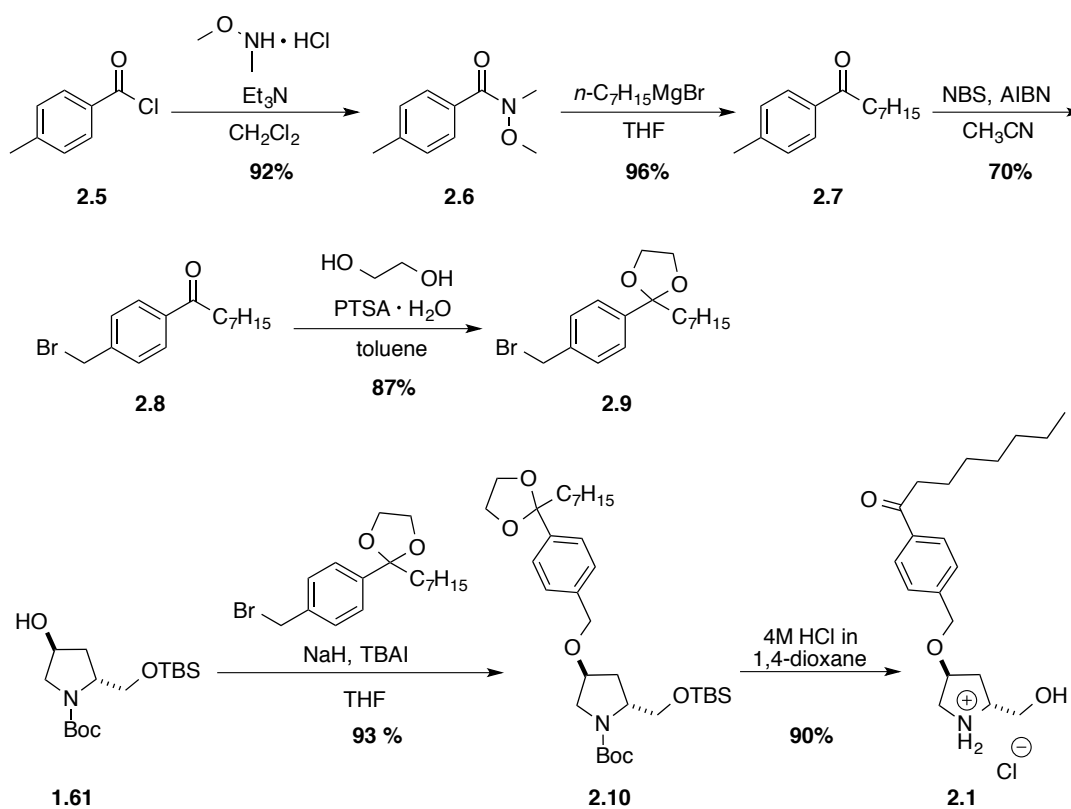
**Scheme 37.** Retrosynthetic analysis of ketone **2.1** (route I).



Silyl ether **1.61** was available from a previous synthesis (Scheme 10), and to be alkylated with benzyl bromide **2.9**, in a substitution reaction (Scheme 38). The synthesis of bromide **2.9** began by the reaction of *N,O*-dimethylhydroxylamine hydrochloride,

triethylamine and 4-methylbenzoyl chloride (**2.5**) to provide Weinreb amide **2.6** in 92 % yield. The Grignard reagent, *n*-heptylmagnesium bromide was prepared *in situ* from 1-bromoheptane and magnesium turnings, and reacted with **2.6** to provide the desired ketone **2.7** in 96 % yield. Treatment of **2.7** with NBS and AIBN then afforded the required bromide **2.8**. Protection of ketone **2.8** as the ketal **2.9** left us ready for the substitution reaction using protected prolinol **1.61**. Thus, the reaction of **1.61** and **2.9** in the presence of NaH and TBAI generated successfully ether **2.10** in 93 % yield. Global deprotection of **2.10** was accomplished using HCl in 1,4-dioxane to remove the ketal, TBS, and Boc groups in one step. The desired ketone **2.1** was obtained in 90 % yield (Scheme 38).

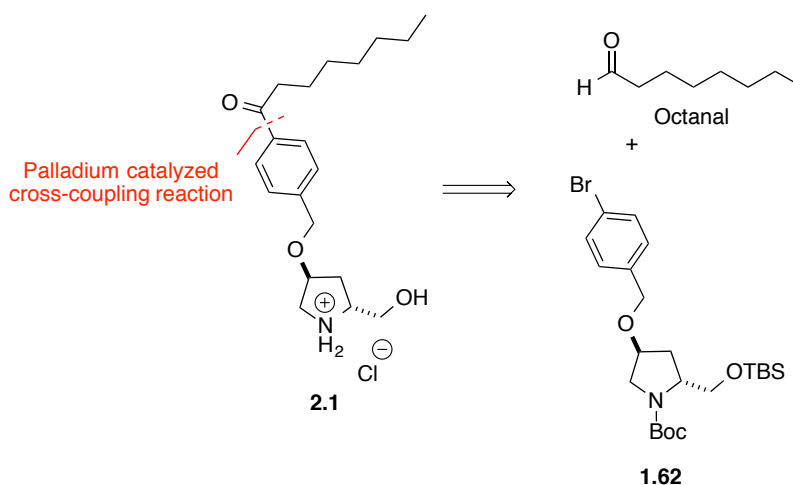
**Scheme 38.** Synthesis of ketone **2.1** (route I).



Although ketone **2.1** was successfully synthesized, the route was relatively long and inefficient. A simpler route was devised for the synthesis of **2.1**. The Suzuki coupling reaction was commonly used to install the C8 side-chain in our strategy to synthesize constrained

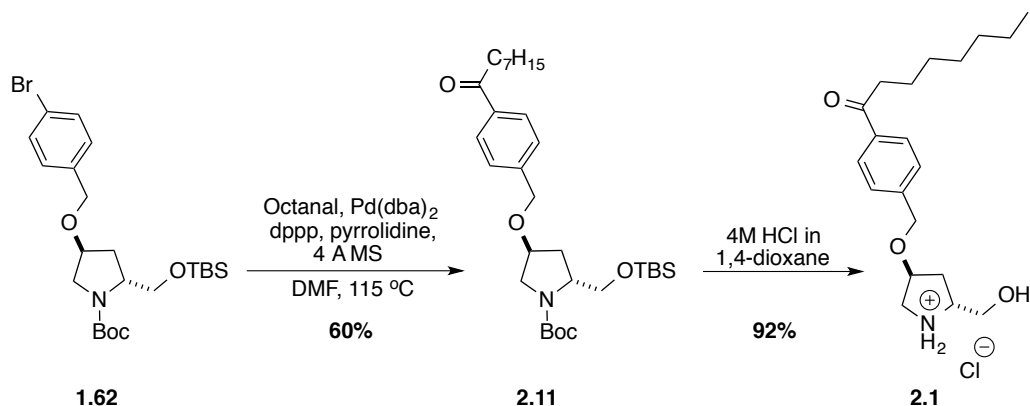
FTY720 analogues (Chapter 1). We thought that the aryl ketone side chain in **2.1** could be accessed through a palladium-catalyzed cross-coupling reaction<sup>74</sup> between octanal and aryl bromide intermediate **1.62**, which was available from our previous synthesis (see Schemes 10 and 39).

**Scheme 39.** Retrosynthetic analysis of ketone **2.1** (route II).



Thus, treatment of the bromide **1.62** with octanal in DMF, using Pd(dba)<sub>2</sub> and dppp as catalysts in the presence of pyrrolidine and 4Å molecular sieves gave aryl ketone **2.11** in 60 % yield (Scheme 40).<sup>74</sup> Removal of the TBS and Boc protecting groups in **2.11** using HCl in 1,4-dioxane provided ketone **2.1** in 92 % yield. This route significantly simplified the synthesis of **2.1** (two steps from available intermediate **1.62**, total 55 % yield).

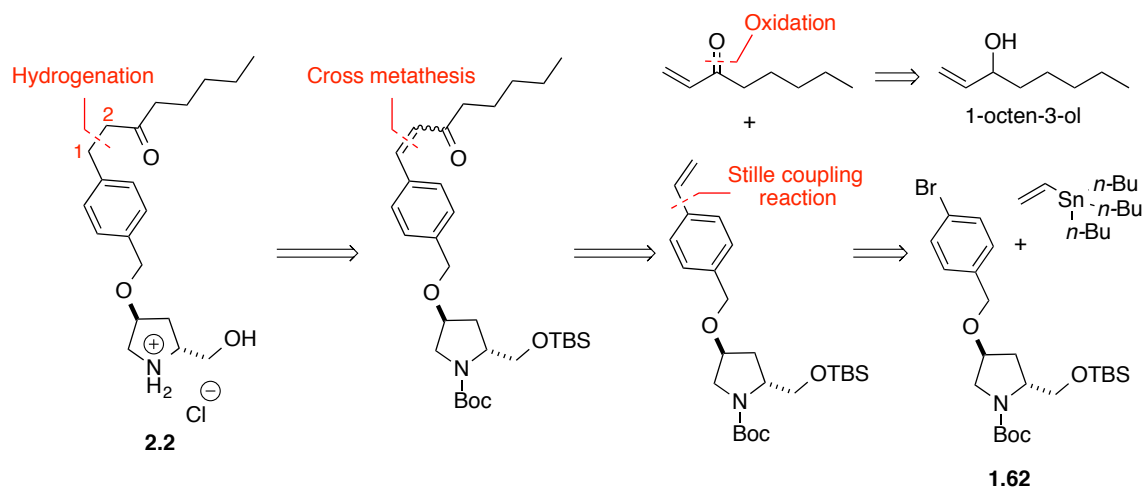
**Scheme 40.** Synthesis of ketone **2.1** (route II).



**2-2-1-2 Synthesis of ketone 2.2**

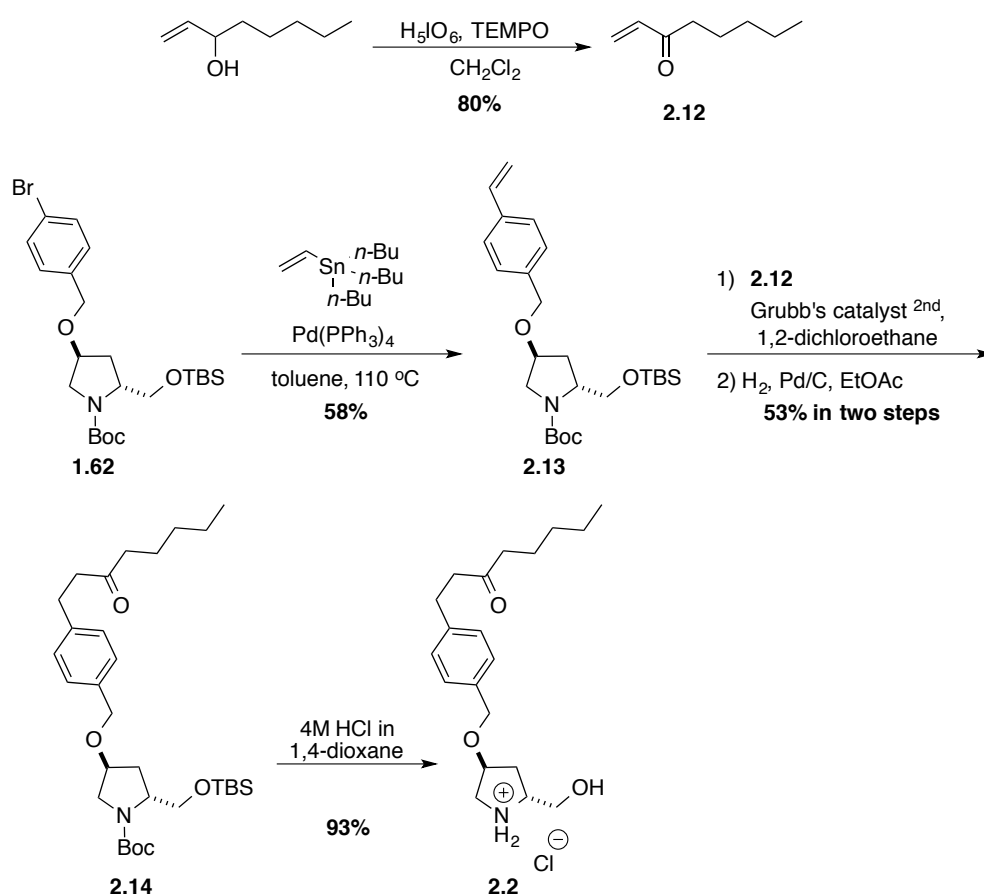
To make ketone **2.2**, we envisioned that a hydrogenation of the olefin from the cross metathesis between 1-octen-3-one and a vinyl benzyl hydroxyprolinol (Scheme 41). 1-Octen-3-one can be easily prepared from 1-octen-3-ol by oxidation.<sup>75</sup> Vinyl benzyl hydroxyprolinol could be generated from the available intermediate **1.62** and vinyltributylstannane, through a Stille coupling reaction (Scheme 41).

**Scheme 41.** Retrosynthetic analysis of ketone **2.2**.



Based on a known procedure,<sup>75</sup> 1-octen-3-ol was treated with periodic acid and TEMPO, and 1-octen-3-one (**2.12**) was obtained in 80 % yield (Scheme 41). Bromide **1.62** was transformed to the desired styrene **2.13** by reaction with vinyltributylstannane, which was catalyzed by Pd(PPh<sub>3</sub>)<sub>4</sub> (Stille coupling). Olefin **2.13** was mixed with enone **2.12** in 1,2-dichloroethane in the presence of Grubb's II catalyst to afford the cross metathesis product, which was reduced by hydrogenation to give the ketone **2.14** (53 %, in two steps). Finally, deprotection of **2.14** using HCl afforded the required ketone **2.2** in 93 % yield (Scheme 42).

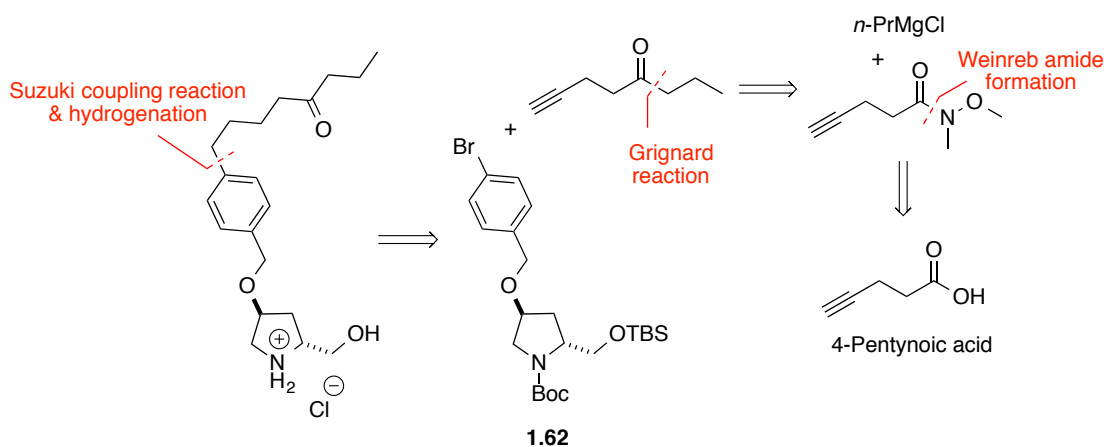
**Scheme 42.** Synthesis of ketone **2.2**.



### 2-2-1-3 Synthesis of ketone 2.3

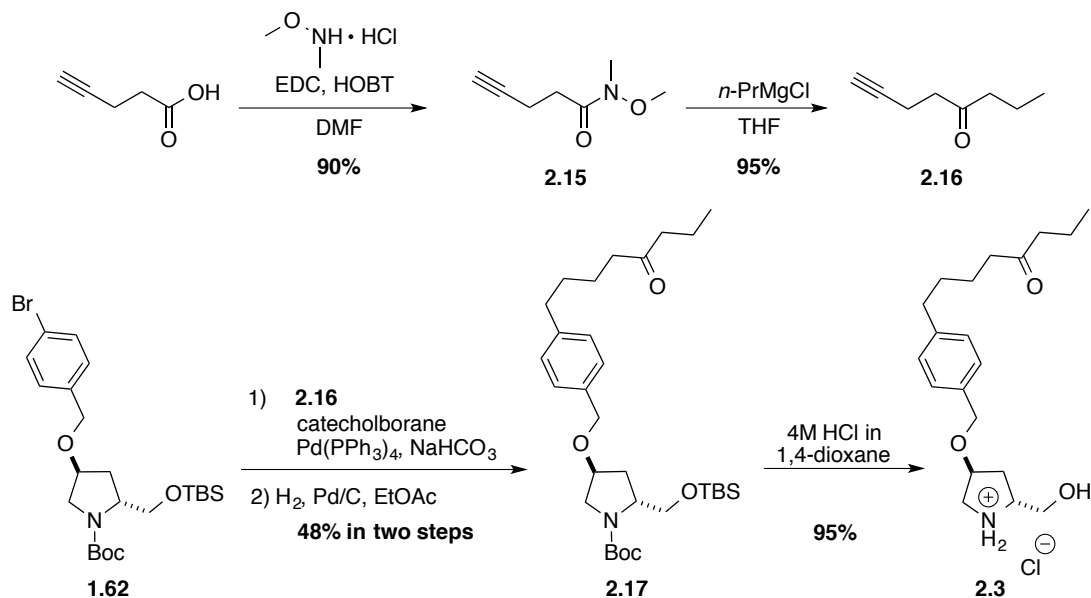
We envisioned that ketone **2.3** could be obtained through our common strategy for installing the side chain through a Suzuki coupling reaction with aryl bromide **1.62** followed by hydrogenation (Scheme 43). The alkyne could be generated by a Grignard reaction between the corresponding Weinreb amide and propylmagnesium chloride. This Weinreb amide could be prepared from commercially available 4-pentynoic acid (Scheme 43).

**Scheme 43.** Retrosynthetic analysis of ketone **2.3**.



4-Pentynoic acid reacted in the presence of EDC and HOBT with *N,O*-dimethylhydroxylamine hydrochloride to give the corresponding Weinreb amide **2.15** in 90 % yield (Scheme 44). Treatment of amide **2.15** with propylmagnesium chloride afforded ketone **2.16** in 95 % yield. Using our Suzuki coupling and hydrogenation strategy, **1.62** was reacted with alkyne **2.16** and transformed to ketone **2.17** (48 % yield, in two steps). Finally, HCl was used to remove the TBS and Boc protecting groups from **2.17**, and provide ketone **2.3** in 95 % yield.

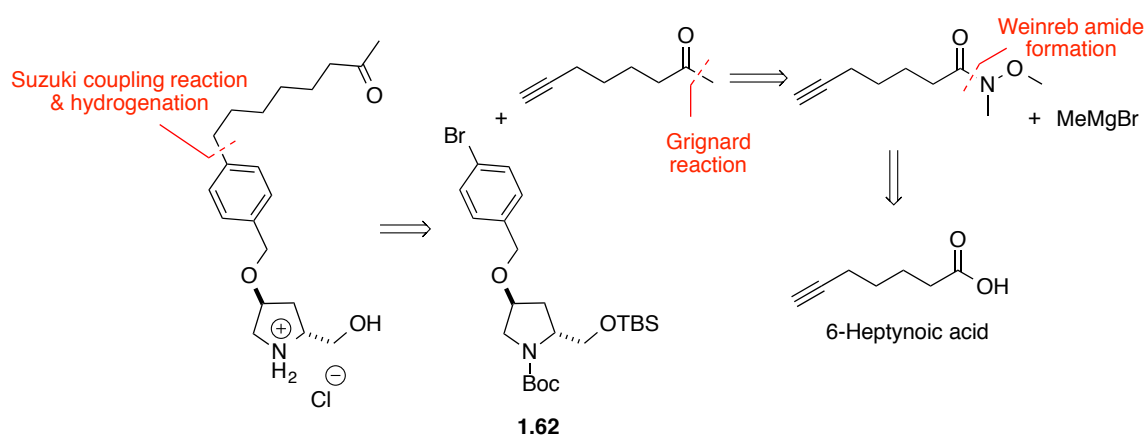
### Scheme 44. Synthesis of ketone 2.3.



### 2-2-1-4 Synthesis of ketone 2.4

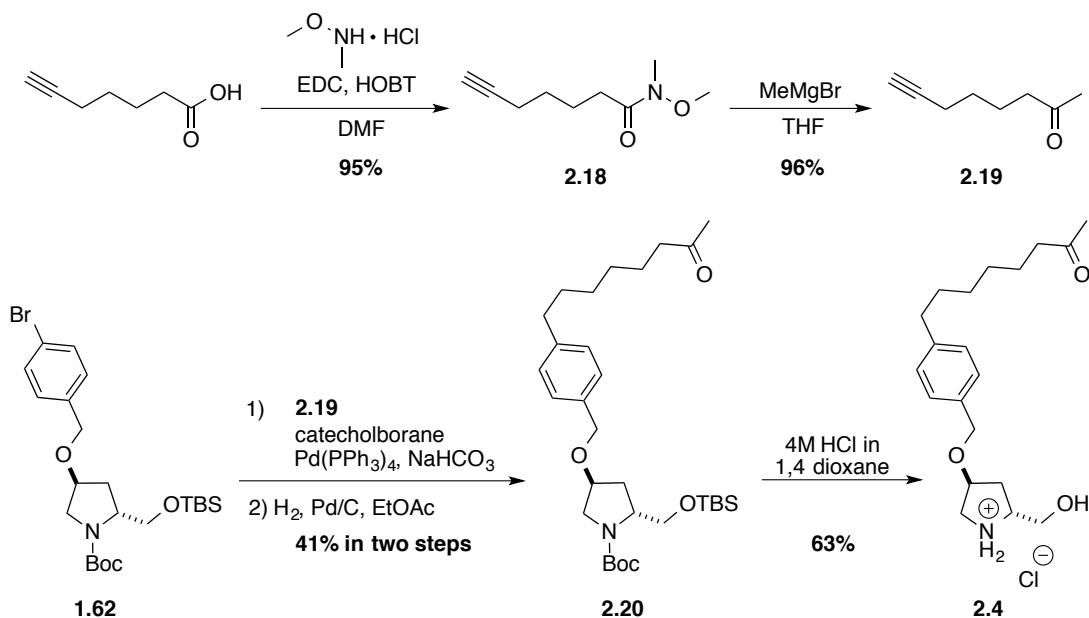
Ketone 2.4 was prepared using a similar strategy as for the synthesis of 2.3 (Scheme 44) from commercially available 6-heptynoic acid (Scheme 45).

### Scheme 45. Retrosynthetic analysis of ketone 2.4.



6-Heptynoic acid was transformed to Weinreb amide **2.18** in 95 % yield (Scheme 46), which was treated with methylmagnesium bromide to afford ketone **2.19** in 96 % yield. From **2.19**, a two-step sequence of Suzuki coupling and hydrogenation, gave ketone **2.20** in 41 % yield. Finally, all the protecting groups were removed from **2.20** using HCl to generate ketone **2.4** in 63 % yield.

**Scheme 46.** Synthesis of ketone **2.4**.



### 2-2-1-5 Biological evaluation of ketones **2.1**, **2.2**, **2.3** and **2.4**

With all four ketone analogues in hand, they were tested in a cell viability assay to compare their cytotoxic activities on murine hematopoietic FL5.12 cells (Figure 33). Preliminary results suggested that all the analogues were less cytotoxic to FL5.12 cells than FTY720 (**1.8**). Ketone **2.1** was the most active of all four analogues, and **2.2** was less active than **2.1**, but more active than **2.3** and **2.4**. The activities of **2.3** and **2.4** were dramatically lower than the activities of **2.1** and **2.2**. These results indicated that the closer the side chain ketone carbonyl was to the phenyl ring, the more active the analogue. We hypothesized that the long aliphatic chain may have interactions with a hydrophobic pocket in the target, such that, modification closer to the phenyl ring minimized the negative effect on activity.



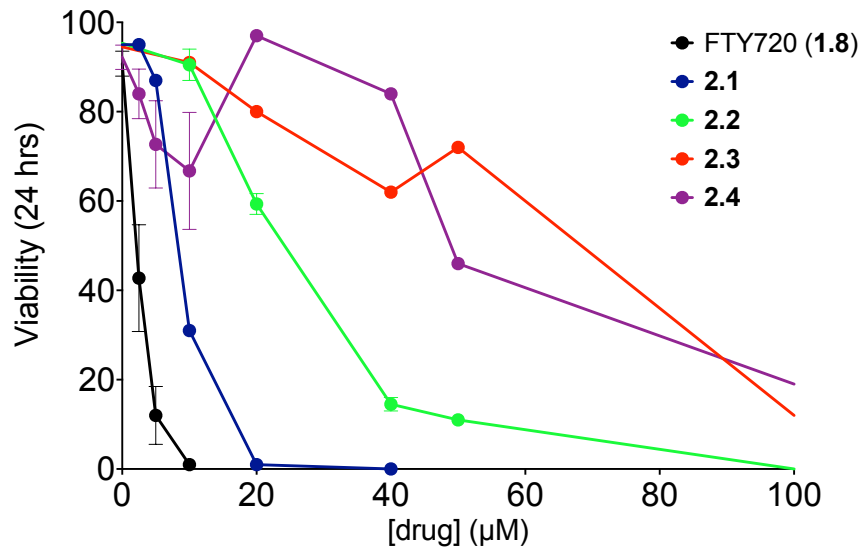
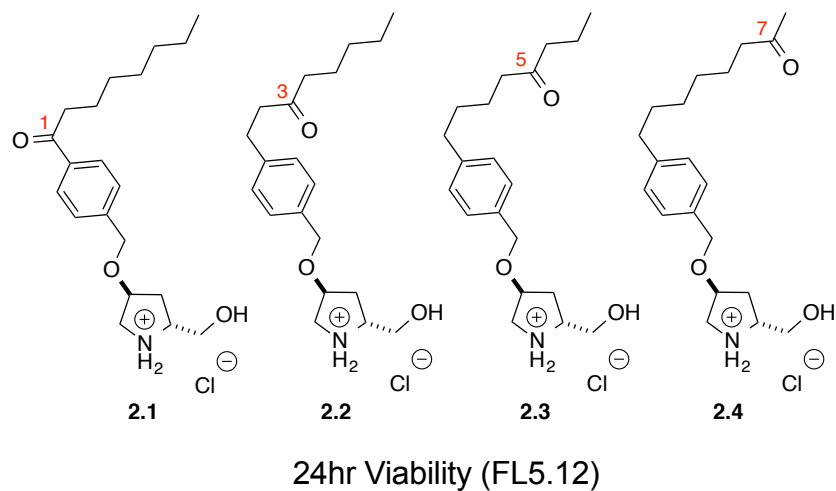


**Figure 33.** Cytotoxic action of different ketone side chain substituted analogues **2.1**, **2.2**, **2.3** and **2.4** on murine hematopoietic FL5.12 cells.

The same position-activity trend was also observed in the surface 4F2hc expression assay on FL5.12 cells. Although all four analogues induced nutrient transporter down-regulation, analogue **2.1** was still the most active one, and exhibited almost the same activity as FTY720 (**1.8**). Therefore, the C-1 position on the side chain was considered to be the best position to install the diazirine photo-reactive group.

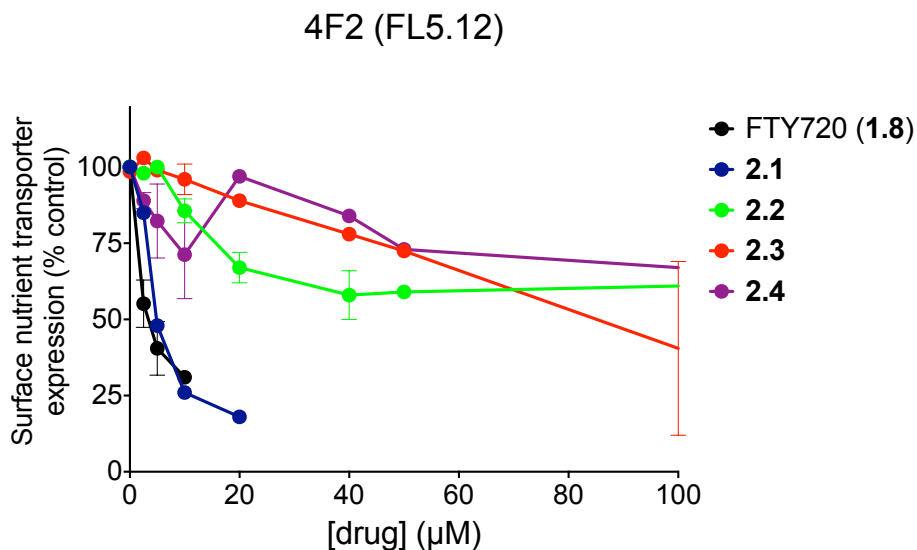


**Figure 34.** Nutrient transporter down-regulation of ketone side-chain substituted analogues **2.1**, **2.2**, **2.3**, and **2.4** on FL5.12 cells.

#### 2-2-1-6 Synthesis of diazirines **2.21** and **2.22**.

using ketone **2.1**, because it was the most active analogue, we proposed the synthesis of diazirine **2.21** (Figure 35). In addition, diazirine **2.22** was prepared from ketone **2.2**, and tested as well (Figure 35).

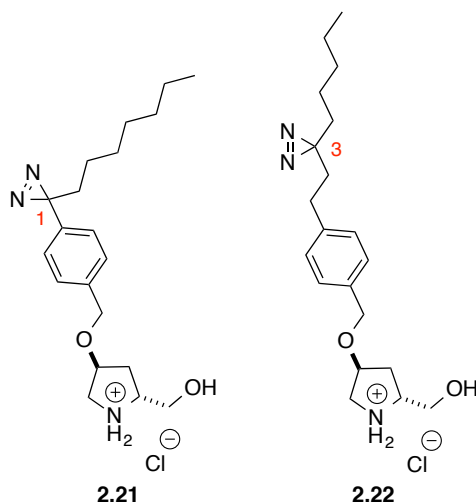
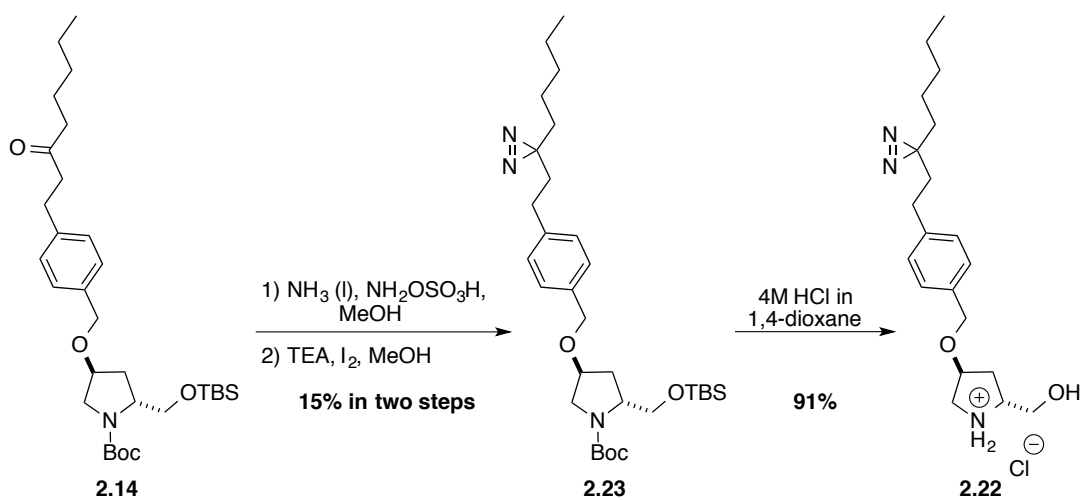


**Figure 35.** Diazirine analogues **2.21** and **2.22**.

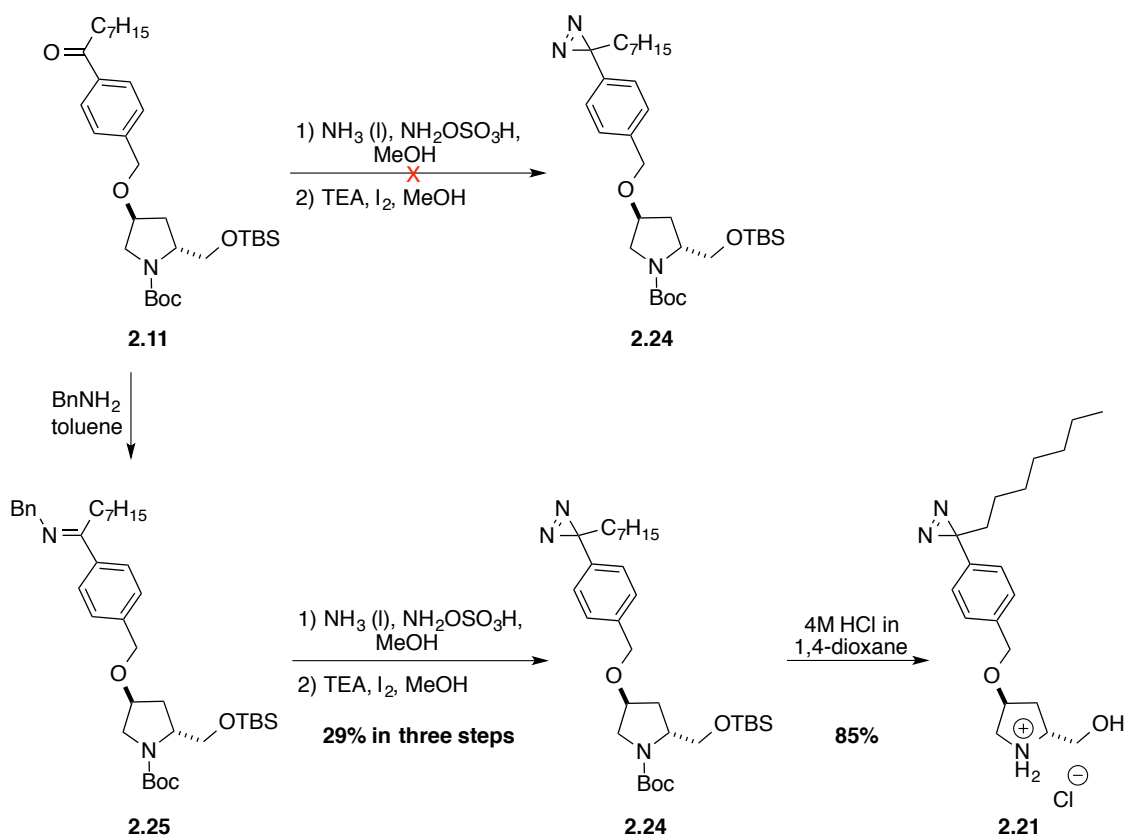
Diazirines were synthesized from the corresponding ketones by diaziridine formation, and oxidation.<sup>17c</sup> Ketone **2.14** was treated with liquid ammonia and hydroxylamine-*O*-sulfonic acid to generate the corresponding unstable diaziridine intermediate, which was immediately oxidized with triethylamine and iodine to give diazirine **2.23** in 15 % yield over two steps (Scheme 46). The low yield was due to inefficient diaziridine formation in the first step. With diazirine **2.23** in hand, the protecting groups were removed using HCl in 1,4-dioxane to afford the desired diazirine analogue **2.22** in 91 % yield (Scheme 47).

**Scheme 47.** Synthesis of diazirine **2.22**.



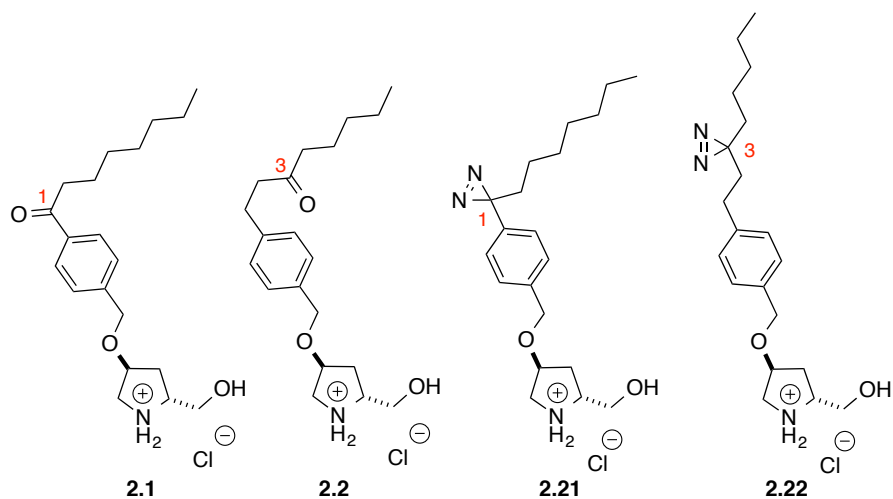
The same synthetic protocol was used to prepare the other diazirine **2.21** (Scheme 48); however, treatment of ketone **2.11** with liquid ammonia and hydroxylamine-*O*-sulfonic acid, followed by oxidation using triethylamine and iodine, did not give the expected diazirine **2.24**. Considering the electrophilicity of the carbonyl was decreased at the benzylic position, ketone **2.11** was transformed into a more electrophilic benzylimine **2.25**, by reaction with benzylamine in toluene. Imine **2.25** was submitted to the same reaction conditions as used previously, and provided the diazirine **2.24** in 29 % yield over three steps. Finally, deprotection of **2.24** afforded the required diazirine **2.21** in 85 % yield (Scheme 48).

### Scheme 48. Synthesis of diazirine **2.21**.



### 2-2-1-7 Biological evaluation of diazirines **2.21** and **2.22**.

Diazirines **2.21** and **2.22** were used in the same cell viability assay as for their corresponding ketones to examine their cytotoxic activities on FL5.12 cells (Figure 36). Preliminary results suggested both **2.21** and **2.22** were active against FL5.12 cells as their corresponding ketones **2.1** and **2.2** at almost the same concentration, and diazirine **2.21** was more active than **2.22**, with the same position-activity trend as in the ketones (Figure 33). These results suggested that our strategy to use the precursor ketones to predict the activity trend was reasonable, and the most suitable position to install a diazirine group on the side chain was the C-1 position (the closest carbon to phenyl ring).



24hr Viability (FL5.12)

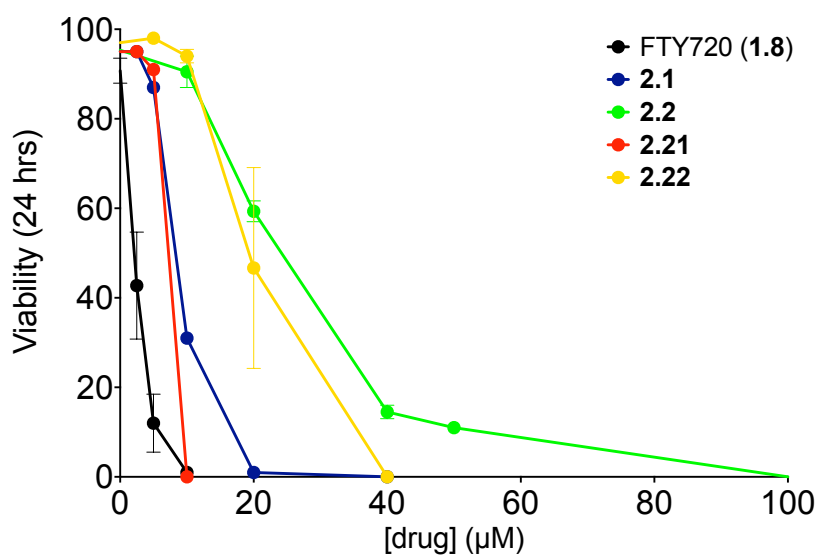


**Figure 36.** Cytotoxic action of diazirines **2.21** and **2.22** on FL5.12 cells.

Diazirines **2.21** and **2.22** were also tested using a surface 4F2hc expression assay, on FL5.12 cells (Figure 37). The same activity trend was observed in this test and **2.11** was more active than **2.22** in inducing nutrient transporter down-regulation.

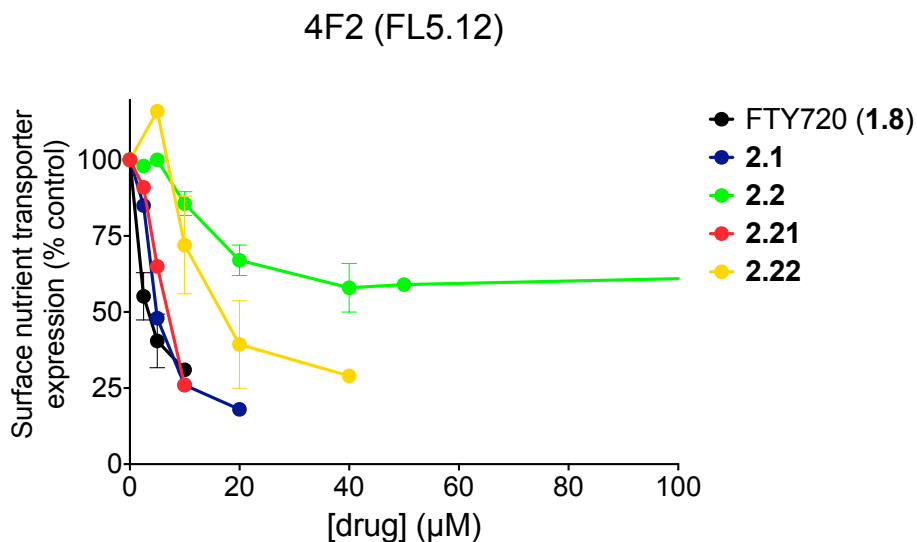
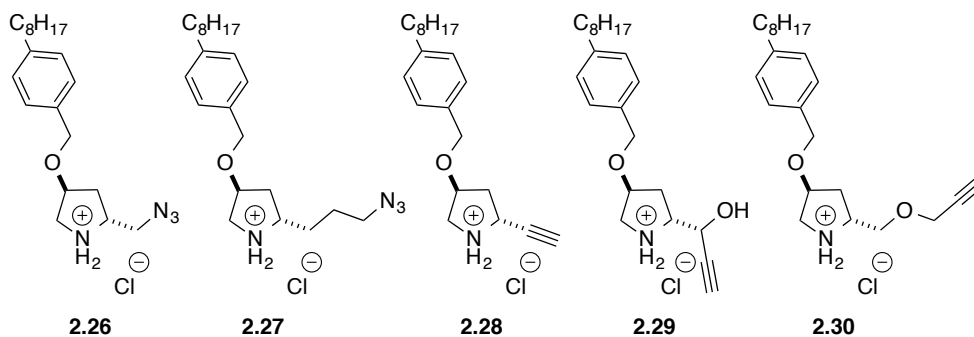


**Figure 37.** Nutrient transporter down-regulation of diazirines **2.21** and **2.22** on FL5.12 cells.

### 2-2-2 Screening of the reporter group

“Click chemistry” was explored for use in the reporter groups (Figure 32). To find the most suitable reporter alkyne, and the right position to install it, five analogues of **1.65** were prepared by Jérémie Tessier in our group (Figure 38). These included analogues **2.26** and **2.27**, bearing an azide group with different chain lengths, and analogues **2.28**, **2.29** and **2.30**, equipped with a terminal alkyne in different chain lengths. They were tested in the cell viability assay to compare their cytotoxic activities on FL5.12 cells (Figure 38). Preliminary results suggested azide analogue **2.27** was the most active among all five compounds (Figure 38). Alkyne analogue **2.30** was slightly less active than **2.27**. The other three analogues were much less active than **2.27** and **2.30**. Although there was not much difference in the activity between **2.27** and **2.30**, the synthesis of **2.27** was significantly longer than **2.30**. Based on this information, we decided to employ the terminal alkyne **2.30**.



24hr Viability (FL5.12)

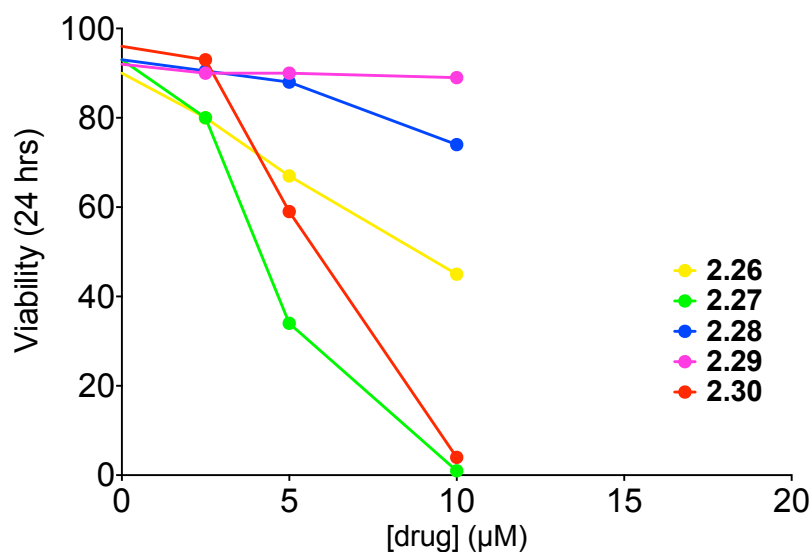


**Figure 38.** Cytotoxic action of azide and alkyne analogues on FL5.12 cells.

In the surface 4F2hc expression assay on FL5.12 cells (Figure 39), analogues **2.27** and **2.30** were also the most active compounds, and **2.30** was slightly more active than **2.27** in inducing nutrient transporter down-regulation. All of these results suggested that the terminal alkyne group in **2.30** should be used in the photoaffinity probe.

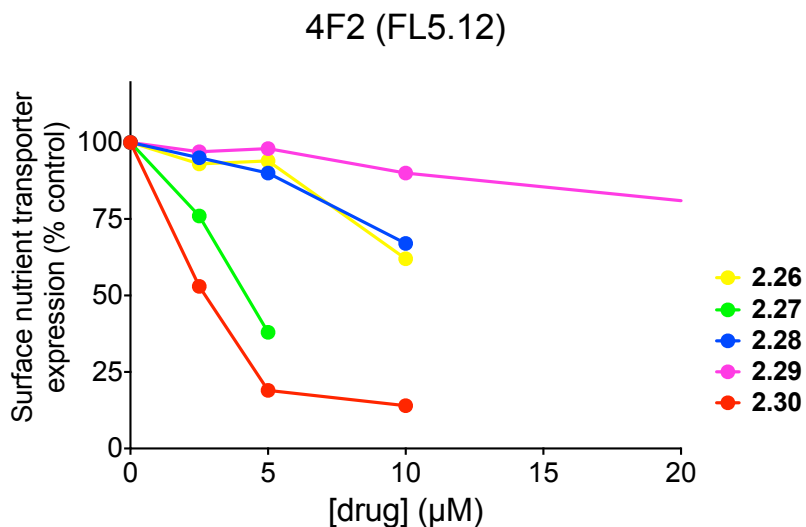


**Figure 39.** Nutrient transporter down-regulation of azide and alkyne analogues on FL5.12 cells.

### 2-2-3 Synthesis of the photoaffinity probes 2.31 and 2.39

Based on the screening results, the diazirine and terminal alkyne functional groups were selected to be installed in probe **2.31** (Figure 40). From **2.24**, a substitution reaction between prolinol **2.32** and propargyl bromide was envisioned to give ether **2.31** after carbamate removal (Scheme 48).



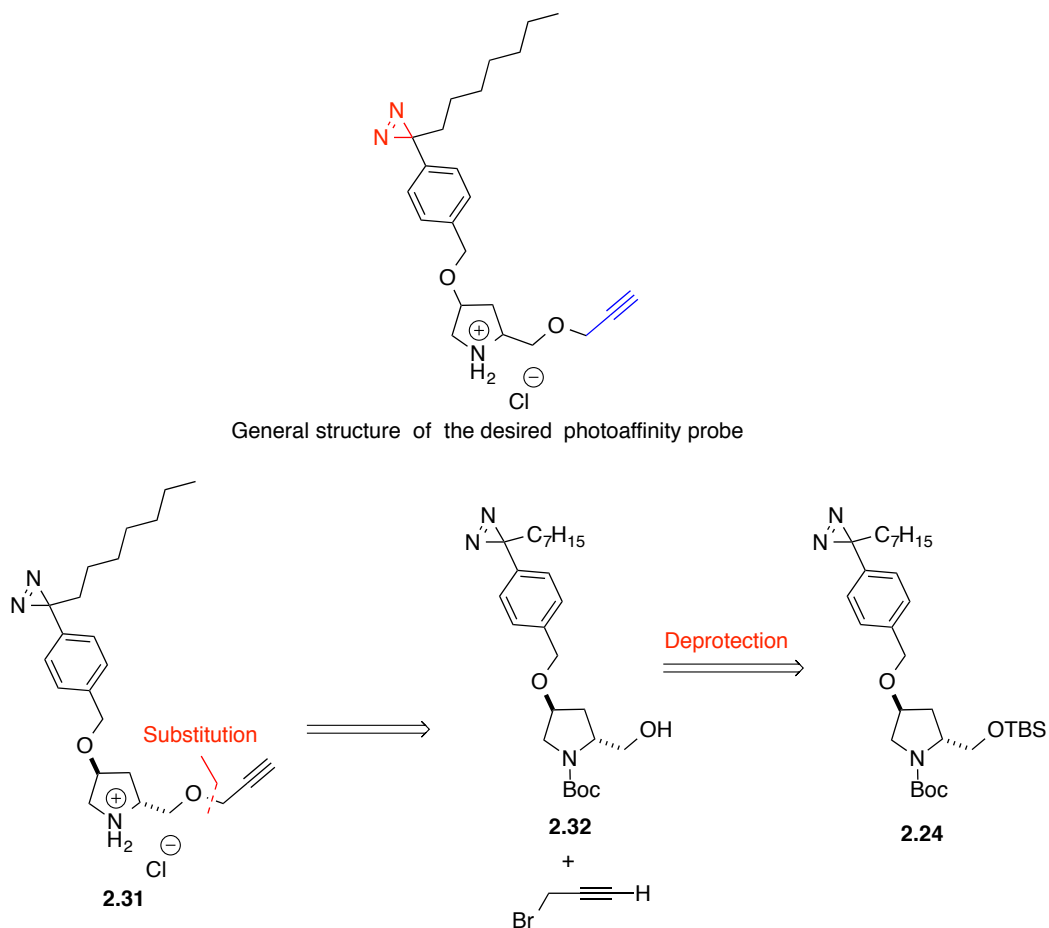
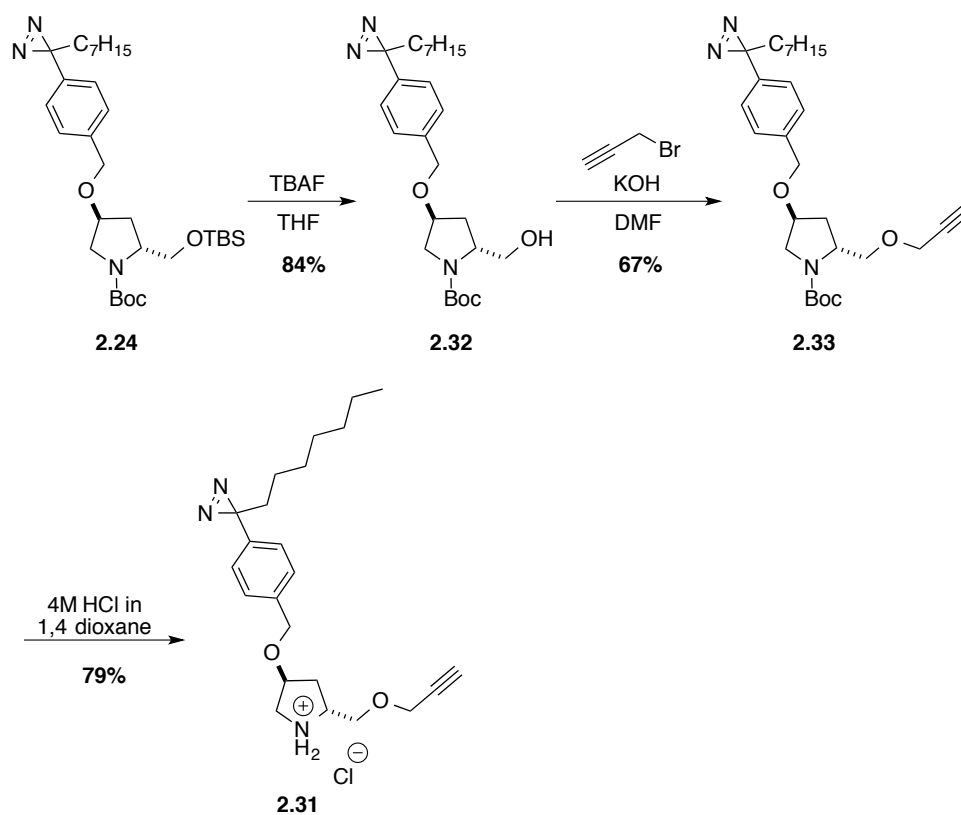


**Figure 40.** General structure of the desired photoaffinity probe and its retrosynthetic analysis.

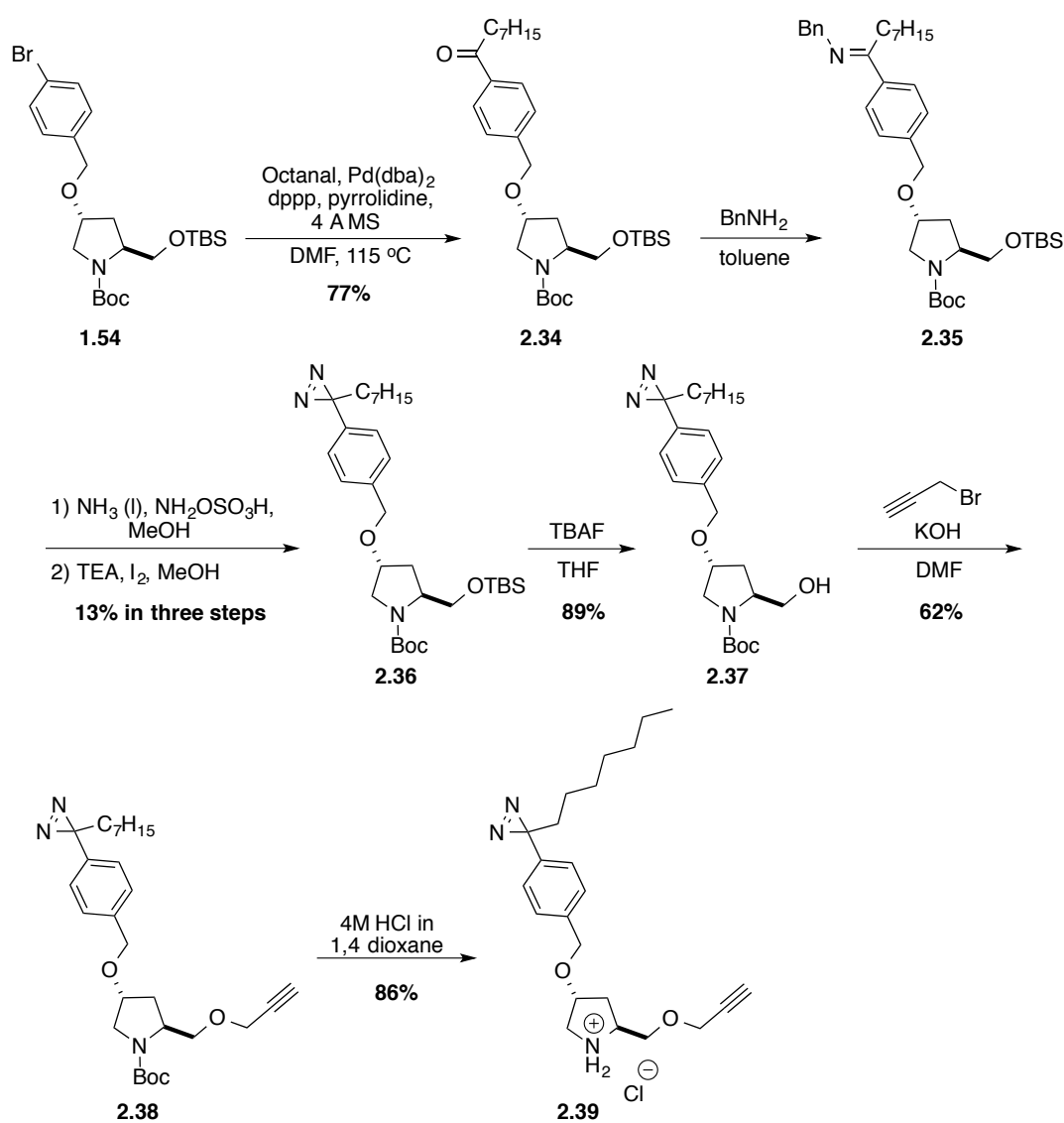
Silyl ether **2.24** was treated with TBAF to remove the TBS protecting group (Scheme 49), and prolinol **2.32** was obtained in 84 % yield. Alcohol **2.32** was reacted with propargyl bromide in the presence of potassium hydroxide to generate alkyne **2.33** in 67 % yield. Finally, removal of the Boc protecting group using HCl in 1,4-dioxane afforded probe **2.31** in 79 % yield (Scheme 49).

**Scheme 49.** Synthesis of photoaffinity probe **2.31**.



Using the same synthetic strategy, the enantiomer of compound **2.31** (the photoaffinity probe **2.39** for analogue **1.57**) was successfully prepared from bromide **1.54** (Scheme 50).

**Scheme 50.** Synthesis of photoaffinity probe **2.39**.



**2-2-4 Biological evaluations of photoaffinity probes 2.31 and 2.39**

With photoaffinity probes **2.31** and **2.39** in hand, a cell viability assay was used to test their cytotoxic activities on FL5.12 cells (Figure 41). Preliminary results suggested that both **2.31** and **2.39** exhibited similar activity in killing the FL5.12 cells as FTY720 (**1.8**), indicating that the positions of the diazirine and alkyne groups were compatible with the expected activity.

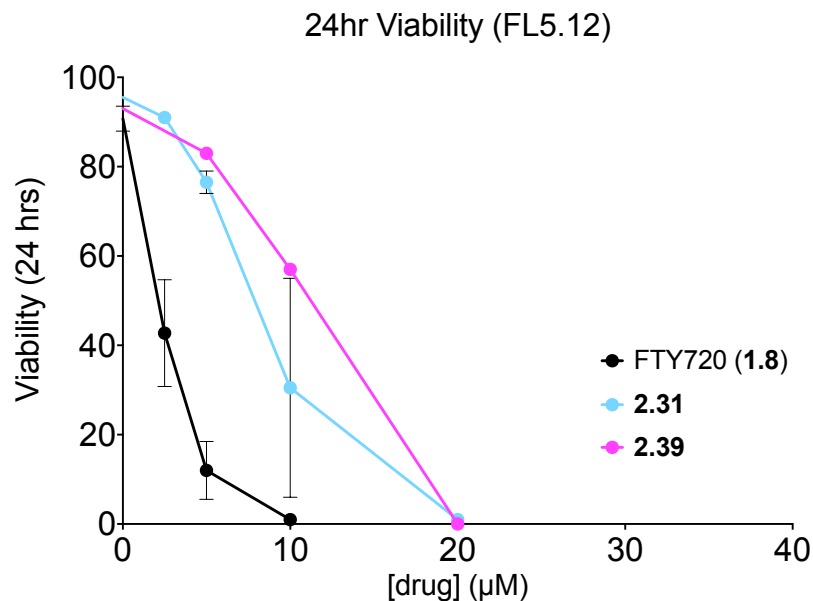


**Figure 41.** Cytotoxic action of photoaffinity probes **2.31** and **2.39** on FL5.12 cells.

Diazirines **2.31** and **2.39** were also tested in the surface 4F2hc expression assay on FL5.12 cells (Figure 42). Both probes induced nutrient transporter down-regulation, further indicating that our design was successful, and did not compromise activity.

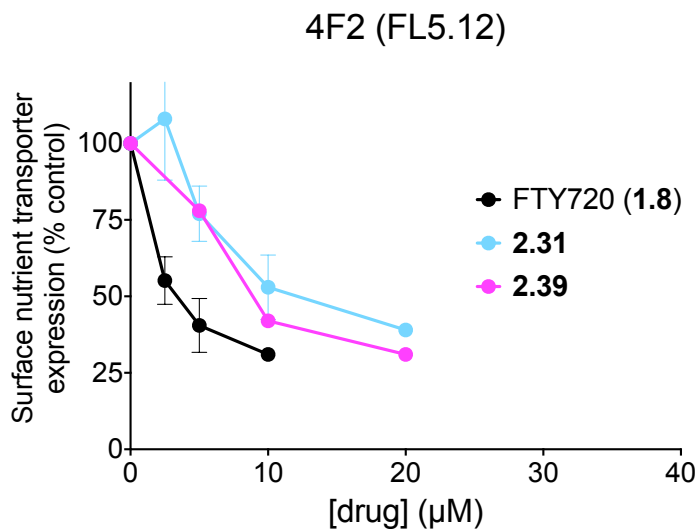


**Figure 42.** Nutrient transporter down-regulation of photoaffinity probes **2.31** and **2.39** on FL5.12 cells.

With these promising results, photoaffinity probes **2.31** and **2.39** were subjected to PAL experiments (Figure 43). In general, the probes should bind to the target receptor. Upon irradiation, a covalent bond will be formed between the probe and receptor. The terminal alkyne on the receptor-probe complex could be “clicked” onto an azide linked to a biotin based tag (Figure 43). After generation of the corresponding triazole, the complex would be purified using a streptavidin column, which would bind to biotin with high affinity. With the avidin-biotin complex in hand, the receptor could be digested into small pieces by trypsin, and by analyzed with LC/MS/MS to identify the target receptor and active site (Figure 43). These experiments are currently in progress.

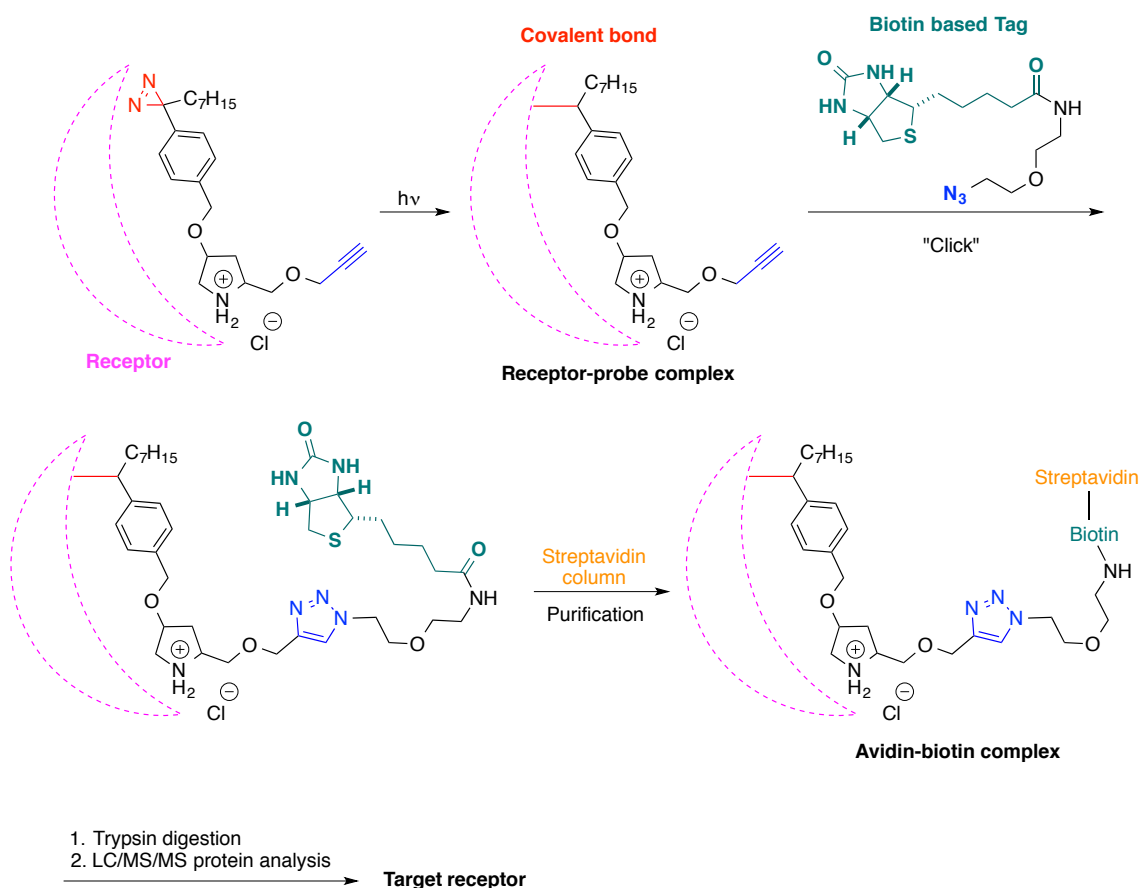


**Figure 43.** General projected PAL experiments for **2.31** and **2.39**.

## 2-3 Conclusion

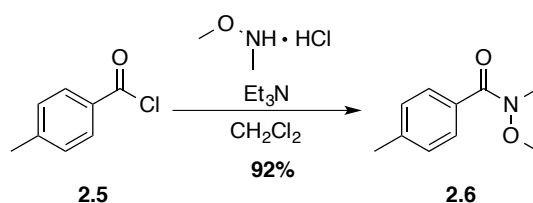
To further understand the anticancer mechanism of amino alcohols **1.57** and **1.65**, we designed and synthesized successfully photoaffinity probes **2.39** and **2.31** in an effort to fish out their target receptors by using PAL techniques.

Systematic studies on the photoreactive group and receptor group were crucial in designing these probes. The position of the diazirine on the side chain was screened using both ketone precursors and the corresponding diazirines. Screening was also used to compare azide and alkyne groups to determine the best position for their installation.

Preliminary results indicated probes **2.39** and **2.31** maintained activity, PAL experiments using these compounds are in progress now.

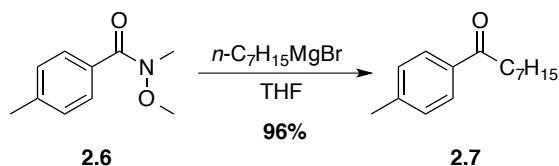
## 2-4 Experimental

General methods are same as described in the experimental section of Chapter 1.

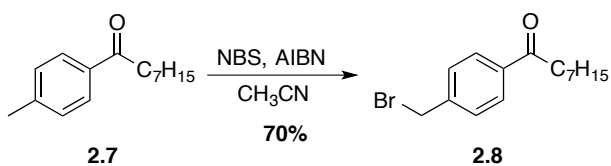


*N*-Methoxy-*N*,4-dimethylbenzamide (**2.6**) was prepared according a reported procedure.<sup>76</sup> Triethylamine (1.67 mL, 1.21 g, 12.0 mmol) was added dropwise to a solution of *N*,*O*-dimethylhydroxylamine hydrochloride (878 mg, 9.0 mmol) in  $\text{CH}_2\text{Cl}_2$  (14 mL) at 0 °C. After stirring for 10 min, the mixture was treated with a solution of 4-methylbenzoyl chloride (**2.5**, 0.53 mL, 927 mg, 6 mmol) in  $\text{CH}_2\text{Cl}_2$  (5 mL), allowed to warm to room temperature, stirred overnight and quenched by the addition of water. The aqueous layer was extracted three times with  $\text{CH}_2\text{Cl}_2$  (10 mL). The organic phases were combined, washed with brine, dried over  $\text{MgSO}_4$  and filtered. The volatiles were removed under reduced pressure. The residue was purified by flash chromatography (hexane: EtOAc, 4:1 to 2:1) to give hydroxamate **2.6** (990 mg, 92 %) as colorless oil.  $^1\text{H}$  NMR (500 MHz,  $\text{CDCl}_3$ )  $\delta$  7.51-7.49 (m, 2H), 7.11-7.09 (m,

2H), 3.48-3.43 (m, 3H), 3.27-3.22 (m, 3H), 2.28-2.27 (m, 3H);  $^{13}\text{C}$  NMR (125 MHz,  $\text{CDCl}_3$ )  $\delta$  169.5, 140.4, 130.8, 128.2, 127.9, 60.5, 33.4, 21.0; HRMS (ESI) calcd for  $\text{C}_{10}\text{H}_{13}\text{NNaO}_2$  ( $\text{M}+\text{Na}$ ) $^+$  202.0839, found 202.0833.

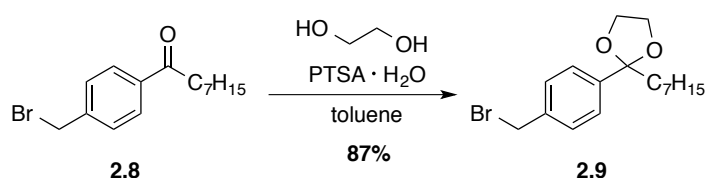


**1-(*p*-Tolyl)octan-1-one (2.7).** Magnesium turnings (41 mg, 1.7 mmol) were added to a dry flask equipped with condenser, followed by a solution of 1-bromoheptane (304 mg, 1.7 mmol) in anhydrous THF (1.7 mL). 1,2-Dibromoethane was then added to the flask to initiate the reaction. The mixture was stirred and started to reflux. After stirring for 1 h, the flask was cooled to  $-40\text{ }^\circ\text{C}$ , a solution of hydroxamate **2.6** (60 mg, 0.34 mmol) in THF (1.0 mL) was added dropwise to the mixture. The reaction was slowly warmed to  $0\text{ }^\circ\text{C}$ , stirred for 2 h, then quenched with saturated aqueous  $\text{NH}_4\text{Cl}$  and extracted three times with  $\text{Et}_2\text{O}$ . The organic layers were washed with brine, dried over  $\text{MgSO}_4$  and filtered. The filtrate was evaporated under reduced pressure and the residue was purified by flash chromatography (hexane: EtOAc, 16:1) to give **2.7** (70 mg, 96 %) as colorless oil.  $^1\text{H}$  NMR (500 MHz,  $\text{CDCl}_3$ )  $\delta$  7.86 (d,  $J = 8.0$  Hz, 2H), 7.25 (d,  $J = 8.5$  Hz, 2H), 2.93 (t,  $J = 7.5$  Hz, 2H), 2.41 (s, 3H), 1.76-1.68 (m, 2H), 1.42-1.24 (m, 8H), 0.89 (m, 3H);  $^{13}\text{C}$  NMR (125 MHz,  $\text{CDCl}_3$ )  $\delta$  200.2, 143.5, 134.6, 129.2, 128.1, 38.5, 31.7, 29.3, 29.1, 24.5, 22.6, 21.5, 14.0; HRMS (ESI) calcd for  $\text{C}_{15}\text{H}_{22}\text{NaO}$  ( $\text{M}+\text{Na}$ ) $^+$  241.1563, found 241.1560.



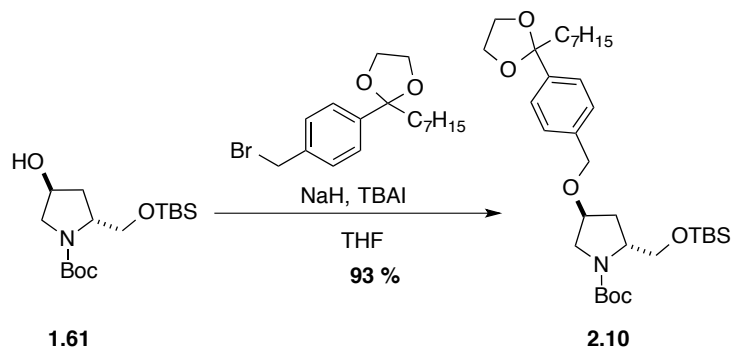
**1-(4-(Bromomethyl)phenyl)octan-1-one (2.8).** *N*-bromosuccinimide (323 mg, 1.82 mmol) and AIBN (27 mg, .017 mmol) were added to a solution of ketone **2.7** (360 mg, 1.65 mmol) in anhydrous  $\text{CH}_3\text{CN}$  (1.8 mL) under argon. The solution was heated to  $90\text{ }^\circ\text{C}$ , stirred for 14 h, and evaporated under reduced pressure. The residue was dissolved in toluene, filtered. The

filtrate was evaporated under reduced pressure and the residue was purified by flash chromatography (hexane: EtOAc, 40:1 to 15:1) to give bromide **2.8** (343 mg, 70 %) as white solid. In some cases, bromide **2.8** was purified by preparative thin-layer chromatography (hexane: toluene 7:1). m.p. (60.7-61.5 °C); <sup>1</sup>H NMR (400 MHz, CDCl<sub>3</sub>) δ 7.89 (d, *J* = 8.4 Hz, 2H), 7.43 (d, *J* = 8.4 Hz, 2H), 4.46 (s, 2H), 2.91 (m, 2H), 1.70 (quint., *J* = 7.3 Hz, 2H), 1.40-1.21 (m, 8H), 0.86 (m, 3H); <sup>13</sup>C NMR (100 MHz, CDCl<sub>3</sub>) δ 199.4, 142.3, 136.6, 129.0, 128.3, 38.5, 32.0, 31.5, 29.1, 29.0, 24.1, 22.4, 13.9; HRMS (ESI) calcd for C<sub>15</sub>H<sub>22</sub>[<sup>79</sup>Br]O (M+H)<sup>+</sup> 297.0849, found 297.0843.

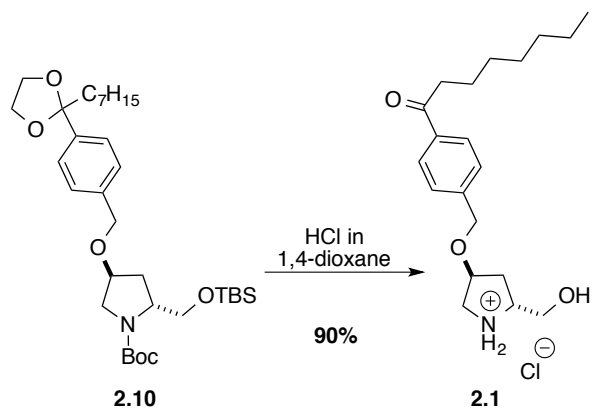


**2-(4-(Bromomethyl)phenyl)-2-heptyl-1,3-dioxolane (2.9).** A solution of ketone **2.8** (70 mg, 0.24 mmol) in toluene and ethylene glycol (40 μL, 45 mg, 0.72 mmol) were added to a flask equipped with a Dean-Stark apparatus and condenser. *p*-Toluenesulfonic acid monohydrate (4 mg, 0.02 mmol) was added to the reaction mixture, which was heated to reflux and stirred for 48 h, quenched with saturated aqueous NaHCO<sub>3</sub> and concentrated under reduced pressure. The reduced volume was extracted with EtOAc (5 mL) three times. The combined organic phases were washed with brine, dried over MgSO<sub>4</sub> and filtered. The volatiles were removed under reduced pressure and the residue was purified by preparative thin-layer chromatography (hexane: EtOAc, 16:1) to give acetal **2.9** (68 mg, 87 %) as pale yellow oil. <sup>1</sup>H NMR (400 MHz, CDCl<sub>3</sub>) δ 7.43 (d, *J* = 8.4 Hz, 2H), 7.35 (d, *J* = 8.4 Hz, 2H), 4.48 (s, 2H), 4.03-3.95 (m, 2H), 3.78-3.70 (m, 2H), 1.91-1.84 (m, 2H), 1.39-1.18 (m, 10H), 0.86 (m, 3H); <sup>13</sup>C NMR (100 MHz, CDCl<sub>3</sub>) δ 143.1, 137.0, 128.6, 126.1, 110.1, 64.3, 40.4, 33.0, 31.6, 29.5, 29.0, 23.4, 22.5, 13.9; HRMS (ESI) calcd for C<sub>17</sub>H<sub>26</sub>[<sup>79</sup>Br]O<sub>2</sub> (M+H)<sup>+</sup> 341.1111, found 341.1122.

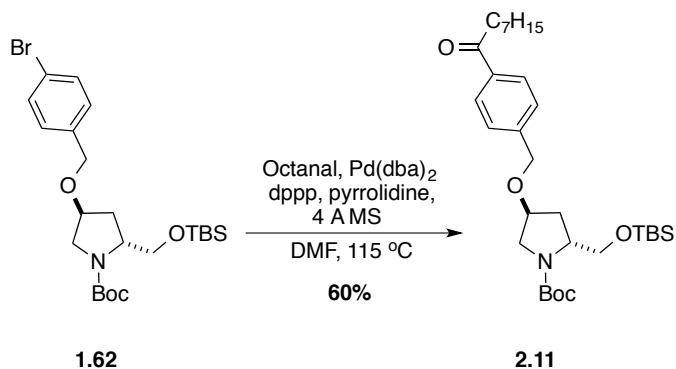




***tert*-Butyl (2*R*,4*S*)-2-(((*tert*-butyldimethylsilyloxy)methyl)-4-((4-(2-heptyl-1,3-dioxolan-2-yl)benzyl)oxy)pyrrolidine-1-carboxylate (2.10).** Sodium hydride (60 % in mineral oil, 8.3 mg, 0.20 mmol) was added to a solution of alcohol **1.61** (60 mg, 0.18 mmol) in anhydrous THF (1.2 mL) at 0 °C. The mixture was warmed to room temperature, stirred for 30 min, and cooled to 0 °C. A solution of bromide **2.9** (68 mg, 0.20 mmol) in THF (0.5 mL) and TBAI (7 mg, 0.018 mmol) were sequentially added to the mixture, which was warmed to room temperature, stirred for 4 h, quenched with saturated aqueous NH<sub>4</sub>Cl, and extracted three times with EtOAc (10 mL). The combined organic phases were washed with brine, dried over MgSO<sub>4</sub> and filtered. The filtrate was evaporated under reduced pressure. The residue was purified by flash chromatography (hexane: EtOAc, 10:1 to 6:1) to give ether **2.10** (100 mg, 93 %) as colorless oil. <sup>1</sup>H NMR (400 MHz, CDCl<sub>3</sub>) δ 7.39 (d, *J* = 6.8 Hz, 2H), 7.27 (d, *J* = 8.0 Hz, 2H), 4.54-4.40 (m, 2H), 4.28-4.14 (m, 1H), 4.04-3.97 (m, 3H), 3.75-3.68 (m, 2H), 3.68-3.36 (m, 4H), 2.21-2.16 (m, 1H), 2.09-2.00 (m, 1H), 1.86-1.82 (m, 2H), 1.45-1.43 (m, 9H), 1.29-1.20 (m, 10H), 0.84-0.81 (m, 12H), -0.01 (m, 6H); <sup>13</sup>C NMR (100 MHz, CDCl<sub>3</sub>, mixture of rotamers) δ (154.3), 154.2, 142.1, 137.5, (127.2), 127.2, 125.7, 110.3, (79.2), 78.9, 76.8, 76.2, 70.7, (70.6), 64.3, (64.2), 63.3, 57.5, (57.4), 52.2, (51.5), 40.5, 35.0, 33.8, 31.6, 29.5, 29.1, 28.4, 25.7, 23.4, 22.5, 18.0, 13.9, (-5.5), -5.6; [α]<sub>D</sub> (+) 22.8° (*c* 1.22, CHCl<sub>3</sub>); HRMS (ESI) calcd for C<sub>33</sub>H<sub>57</sub>NNaO<sub>6</sub>Si (M+Na)<sup>+</sup> 614.3847, found 614.3847.

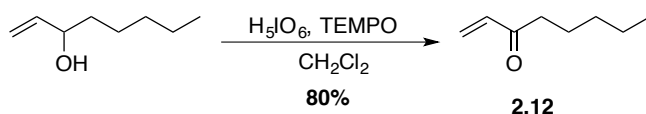


**(2*R*,4*S*)-2-(hydroxymethyl)-4-((4-octanoylbenzyl)oxy)Pyrrolidin-1-ium chloride (2.1)** was obtained as white solid (11 mg, 90 %) from carbamate **2.10** (20 mg, 0.033 mmol) according to the procedure for synthesizing **1.32**.  $^1\text{H NMR}$  (400 MHz,  $\text{D}_2\text{O}$ )  $\delta$  7.90 (d,  $J = 7.6$  Hz, 2H), 7.46 (d,  $J = 7.2$  Hz, 2H), 4.62 (s, 2H), 4.41 (s, 1H), 3.94-3.87 (m, 2H), 3.71-3.65 (m, 1H), 3.52-3.41 (m, 2H), 2.96 (m, 2H), 2.29-2.25 (m, 1H), 1.90 (m, 1H), 1.61 (m, 2H), 1.41-1.17 (m, 8H), 0.83 (m, 3H);  $^{13}\text{C NMR}$  (100 MHz,  $\text{CDCl}_3$ )  $\delta$  200.3, 142.2, 136.6, 128.3, 127.5, 70.4, 60.6, 60.3, 50.1, 38.7, 32.8, 31.7, 29.7, 29.3, 29.1, 24.3, 22.6, 14.1;  $[\alpha]_D^{25}$  (-)  $8.0^\circ$  ( $c$  0.20,  $\text{CHCl}_3$ ); HRMS (ESI) calcd for  $\text{C}_{20}\text{H}_{31}\text{NO}_3$  ( $\text{M}+\text{H}$ ) $^+$  334.2377, found 334.2377.

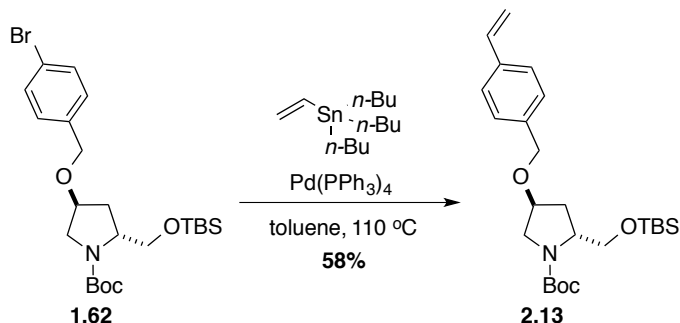


***tert*-Butyl (2*R*,4*S*)-2-(((*tert*-butyldimethylsilyl)oxy)methyl)-4-((4-octanoylbenzyl)oxy)pyrrolidine-1-carboxylate (2.11)** was prepared according to a reported procedure for similar reactions.<sup>74</sup> Starting from bromide **1.62** (250 mg, 0.50 mmol), ketone **2.11** was obtained as pale yellow oil (164 mg, 60 %).  $^1\text{H NMR}$  (500 MHz,  $\text{CDCl}_3$ )  $\delta$  7.93 (d,  $J = 5.5$  Hz, 2H), 7.41 (d,  $J = 7.5$  Hz, 2H), 4.62-4.48 (m, 2H), 4.28-4.15 (m, 1H), 4.05-3.98 (m, 0.5H), 3.97-3.89 (m, 1H), 3.73-3.52 (m, 2H), 3.50-3.38 (m, 1.5H), 2.95 (t,  $J = 7.5$  Hz, 2H), 2.24-2.16 (m, 1H), 2.14-2.00 (m, 1H), 1.73 (p,  $J = 7.5$  Hz, 2H), 1.50-1.42 (m, 9H), 1.41-1.23 (m, 8H),

0.89 (t,  $J = 6.0$  Hz, 3H), 0.88-0.81 (m, 9H), 0.01 (m, 6H);  $^{13}\text{C}$  NMR (125 MHz,  $\text{CDCl}_3$ , mixture of rotamers)  $\delta$  200.2, (154.5), 154.3, 143.5, 136.4, 128.2, (127.4), 127.3, (79.5), 79.2, 76.6, 70.4, (64.3), 63.4, 57.6, (57.5), 52.3, (51.6), 38.6, (35.1), 33.9, 31.7, 29.3, 29.1, 28.5, 25.8, 24.4, 22.6, 18.1, 14.1, -5.5;  $[\alpha]_{\text{D}}^{20}$  (+)  $21.1^\circ$  ( $c$  0.47,  $\text{CHCl}_3$ ); HRMS (ESI) calcd for  $\text{C}_{31}\text{H}_{53}\text{NNaO}_5\text{Si}$  ( $\text{M}+\text{Na}$ ) $^+$  570.3585, found 570.3572.



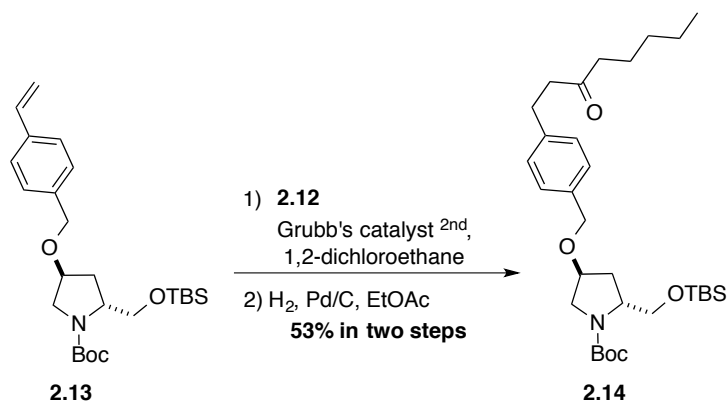
**Oct-1-en-3-one (2.12)** was synthesized according to a known procedure.<sup>75</sup> Starting from oct-1-en-3-ol (464  $\mu\text{L}$ , 385 mg, 3 mmol), **2.12** was obtained as yellow oil (300mg, 80%).  $^1\text{H}$  NMR (400 MHz,  $\text{CDCl}_3$ )  $\delta$  6.37-6.17 (m, 2H), 5.81-5.78 (m, 1H), 2.56 (t,  $J = 7.5$  Hz, 2H), 1.61 (quint,  $J = 7.4$  Hz, 2H), 1.37-1.22 (m, 4H), 0.88 (t,  $J = 6.8$  Hz, 3H);  $^{13}\text{C}$  NMR (100 MHz,  $\text{CDCl}_3$ )  $\delta$  201.0, 136.5, 127.7, 39.6, 31.4, 23.6, 22.4, 13.8; HRMS (ESI) calcd for  $\text{C}_8\text{H}_{14}\text{O}$  ( $\text{M}+\text{H}$ ) $^+$  127.1117, found 127.1112.



***tert*-Butyl (2*R*,4*S*)-2-(((*tert*-butyldimethylsilyl)oxy)methyl)-4-((4-vinylbenzyl)**

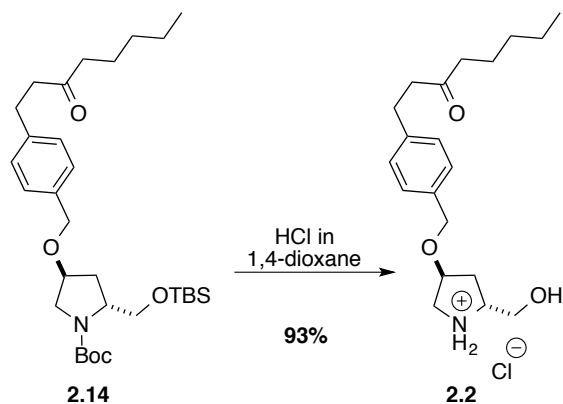
**oxy)pyrrolidine-1-carboxylate (2.13).**  $\text{Pd}(\text{Ph}_3)_4$  (6.9 mg, 0.006 mmol) was added to a solution of **1.62** (100 mg, 0.20 mmol) in toluene (2.6 mL). After stirring at room temperature for 15 min, a solution of vinyltributylstannane (129  $\mu\text{L}$ , 140 mg, 0.44 mmol) in toluene (1.7 mL) was added dropwise to the reaction mixture, which was heated to 110  $^\circ\text{C}$  and stirred for 48 h. The flask was then cooled to room temperature, the volatiles were removed under reduced pressure and the residue was purified by flash chromatography (hexane: EtOAc, 10:1 to 8:1) to give olefin **2.13** (52 mg, 58 %) as colorless oil.  $^1\text{H}$  NMR (400 MHz,  $\text{CDCl}_3$ )  $\delta$  7.38 (d,  $J = 7.6$  Hz, 2H), 7.28 (d,  $J = 8.0$  Hz, 2H), 6.70 (dd,  $J = 17.6, 6.8$  Hz, 1H), 5.74 (d,  $J = 17.6$

Hz, 1H), 5.23 (d,  $J = 10.8$  Hz, 1H), 4.54-4.41 (m, 2H), 4.27-4.13 (m, 1H), 4.05-3.97 (m, 0.5 H), 3.96-3.86 (m, 1H), 3.72-3.49 (m, 2H), 3.47-3.36 (m, 1.5H), 2.21-2.15 (m, 1H), 2.10-2.00 (m, 1H), 1.47-1.45 (m, 9H), 0.86 (s, 9H), 0.01 (m, 6H);  $^{13}\text{C}$  NMR (100 MHz,  $\text{CDCl}_3$ , mixture of rotamers)  $\delta$  (154.5), 154.4, 137.8, (137.7), 137.0, 136.5, (127.9), 127.8, 126.2, 113.7, (79.4), 79.1, 76.8, (76.1), 70.8, (70.8), (64.3), 63.4, 57.6, (57.5), 52.3, (51.6), 35.1, 33.9, 28.5, 25.8, 18.1, (-5.4), -5.5;  $[\alpha]_{\text{D}}^{20}$  (+) 26.2° ( $c$  1.56,  $\text{CHCl}_3$ ); HRMS (ESI) calcd for  $\text{C}_{25}\text{H}_{42}\text{NO}_4\text{Si}$  ( $\text{M}+\text{H}$ )<sup>+</sup> 448.2878, found 448.2872.

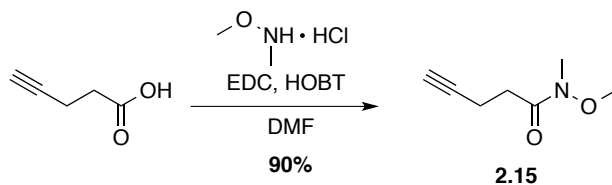


***tert*-Butyl (2*R*,4*S*)-2-(((*tert*-butyldimethylsilyl)oxy)methyl)-4-((4-(3-oxooctyl)benzyl)oxy)pyrrolidine-1-carboxylate (2.14).** Olefin **2.12** (35 mg, 0.078 mmol) and **2.13** (44 mg, 0.351 mmol) were dissolved in 1,2-dichloroethane (0.6 mL) in a pressure tube. Grubb's 2<sup>nd</sup> generation catalyst (2 mg, 0.002 mmol) was then added to the solution. The tube was sealed with a PTFE cap, and heated to 40 °C. After stirring for 24 h, the volatiles were removed under reduced pressure and the residue was purified by flash chromatography (hexane: EtOAc, 8:1 to 7:1) to give the unsaturated ketone (23.4 mg, 54 %) as colorless oil. Hydrogenation of the unsaturated ketone was performed according to the procedure for synthesizing **1.31**. Ketone **2.14** was obtained as a colorless oil (23.0 mg, 98 %).  $^1\text{H}$  NMR (400 MHz,  $\text{CDCl}_3$ )  $\delta$  7.24 (d,  $J = 8.0$  Hz, 2H), 7.15 (d,  $J = 7.2$  Hz, 2H), 4.52-4.38 (m, 2H), 4.27-4.13 (m, 1H), 4.05-3.97 (m, 0.5H), 3.96-3.87 (m, 1H), 3.72-3.51 (m, 2H), 3.48-3.36 (m, 1.5H), 2.86 (t,  $J = 7.6$  Hz, 2H), 2.71 (t,  $J = 7.6$  Hz, 2H), 2.38 (t,  $J = 7.5$  Hz, 2H), 2.21-2.16 (m, 1H), 2.11-1.99 (m, 1H), 1.56 (quint,  $J = 7.6$  Hz, 2H), 1.47-1.45 (m, 9H), 1.35-1.18 (m, 4H), 0.90-0.86 (m, 12H), 0.00 (m, 6H);  $^{13}\text{C}$  NMR (100 MHz,  $\text{CDCl}_3$ , mixture of rotamers)  $\delta$  210.3, (154.5), 154.4, 140.7, 135.9, 128.4, (128.0), 127.9, (79.4), 79.1, (76.8), 76.1, 70.8, (64.3),

63.4, 57.6, (57.5), 52.4, (51.6), (44.2), 43.0, 35.1, 33.9, 31.4, 29.4, 28.5, 25.8, 23.5, 22.4, 18.1, 13.9, (-5.4), -5.5;  $[\alpha]_D$  (+) 22.3° (*c* 0.80, CHCl<sub>3</sub>); HRMS (ESI) calcd for C<sub>31</sub>H<sub>53</sub>NNaO<sub>5</sub>Si (M+Na)<sup>+</sup> 570.3585, found 570.3559.

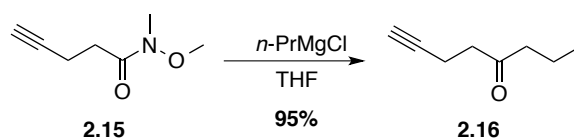


**(2*R*,4*S*)-2-(Hydroxymethyl)-4-((4-(3-oxooctyl)benzyl)oxy)pyrrolidin-1-ium chloride (2.2)** was obtained as white solid (10.0 mg, 93 %) from **2.14** (16 mg, 0.029 mmol) according to the procedure for synthesizing **1.32**. <sup>1</sup>H NMR (400 MHz, D<sub>2</sub>O) δ 7.33 (d, *J* = 8.4 Hz, 2H), 7.26 (d, *J* = 8.4 Hz, 2H), 4.56 (s, 2H), 4.46 (m, 1H), 4.01-3.88 (m, 2H), 3.70 (dd, *J* = 12.4, 6.8 Hz, 1H), 3.54-3.41 (m, 2H), 2.89 (s, 4H), 2.47 (t, *J* = 7.2 Hz, 2H), 2.31 (dd, *J* = 14.1, 6.6 Hz, 1H), 1.93 (ddd, *J* = 14.8, 10.8, 4.8 Hz, 1H), 1.47 (quint, *J* = 7.2 Hz, 2H), 1.33-1.09 (m, 4H), 0.82 (t, *J* = 7.2 Hz, 3H); <sup>13</sup>C NMR (100 MHz, D<sub>2</sub>O) δ 218.4, 141.0, 134.7, 128.7, 76.9, 70.6, 59.9, 59.8, 50.2, 43.3, 42.6, 32.3, 30.5, 29.1, 23.0, 21.7, 13.1;  $[\alpha]_D$  (-) 8.6° (*c* 0.14, CHCl<sub>3</sub>); HRMS (ESI) calcd for C<sub>20</sub>H<sub>31</sub>NO<sub>3</sub> (M+H)<sup>+</sup> 334.2377, found 334.2378.

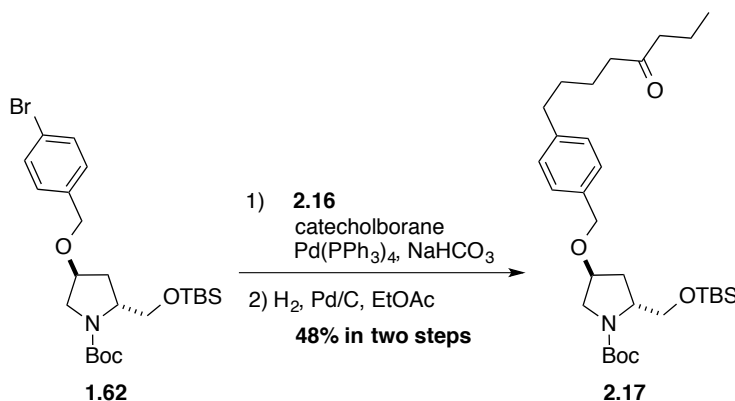


***N*-Methoxy-*N*-methylpent-4-ynamide (2.15).** Pent-4-ynoic acid (95 % grade, 1.64 g, 15.85 mmol) was added to a dried flask with CH<sub>2</sub>Cl<sub>2</sub> (174 mL), followed by EDC·HCl (4.56 g, 23.78 mmol) and HOBT (3.21g, 23.78 mmol). The mixture was cooled to 0°C, and *N,O*-dimethylhydroxylamine hydrochloride (1.7 g, 17.44 mmol) was added. The reaction was stirred at room temperature overnight. The volatiles were removed under reduced pressure and

the residue was dissolved in EtOAc, and washed three times with brine. The volatiles were removed under reduced pressure and the residue was purified by flash chromatography (hexane: EtOAc, 2:1 to 1:1) to give **2.15** (2.02 g, 90 %) as colorless oil.  $^1\text{H}$  NMR (400 MHz,  $\text{CDCl}_3$ )  $\delta$  3.69 (s, 3H), 3.18 (s, 3H), 2.68 (t,  $J = 7.4$  Hz, 2H), 2.53-2.48 (m, 2H), 1.96 (t,  $J = 2.6$  Hz, 1H);  $^{13}\text{C}$  NMR (100 MHz,  $\text{CDCl}_3$ )  $\delta$  172.3, 83.4, 68.6, 61.2, 32.1, 31.0, 13.8; HRMS (ESI) calcd for  $\text{C}_7\text{H}_{12}\text{NO}_2$  ( $\text{M}+\text{H}$ ) $^+$  142.0863, found 148.0867.

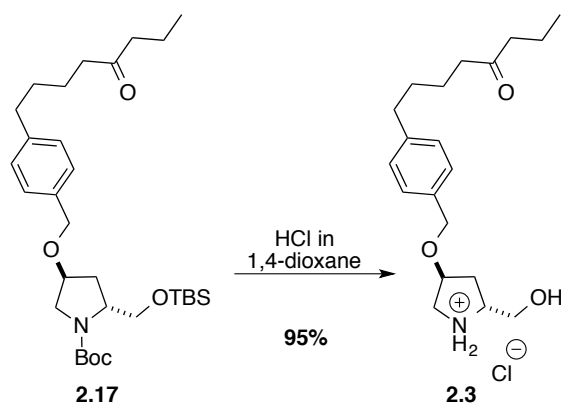


**Oct-7-yn-4-one (2.16).** A solution of hydroxamate **2.15** (700 mg, 4.96 mmol) in THF (17 mL) was cooled to  $0^\circ\text{C}$ , treated dropwise with  $n\text{-PrMgCl}$  (2M in  $\text{Et}_2\text{O}$  solution, 5.2 mL, 10.4 mmol) in 15 min, and the reaction mixture was allowed to warm to room temperature, stirred for 1 h and quenched with saturated aqueous  $\text{NH}_4\text{Cl}$  (2 mL). The aqueous layer was extracted three times with  $\text{Et}_2\text{O}$  (10 mL). The organic layers was combined, dried over  $\text{MgSO}_4$ , filtered and concentrated under reduced pressure to give ketone **2.16** (585 mg, 95 %) as yellow oil, which was used in next step without purification.  $^1\text{H}$  NMR (500 MHz,  $\text{CDCl}_3$ )  $\delta$  2.52 (t,  $J = 7.3$  Hz, 2H), 2.32 -2.24 (m, 4H), 1.82 (t,  $J = 3.0$  Hz, 1H), 1.47 (sext,  $J = 7.3$  Hz, 2H), 0.77 (t,  $J = 7.5$  Hz, 3H);  $^{13}\text{C}$  NMR (125 MHz,  $\text{CDCl}_3$ )  $\delta$  208.2, 82.8, 68.3, 44.2, 40.8, 16.8, 13.3, 12.5; HRMS (ESI) calcd for  $\text{C}_8\text{H}_{13}\text{O}$  ( $\text{M}+\text{H}$ ) $^+$  125.0961, found 125.0960.



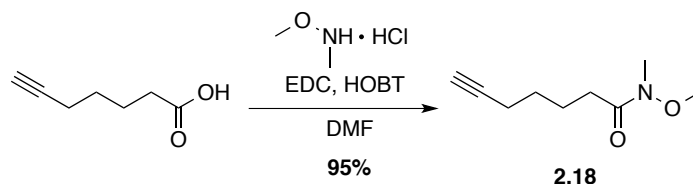
***tert*-Butyl (2*R*,4*S*)-2-(((*tert*-butyldimethylsilyl)oxy)methyl)-4-((4-(5-oxooctyl)benzyl)**

oxy)pyrrolidine-1-carboxylate (**2.17**) was obtained as pale yellow oil (130 mg, 48 % over two steps) from **1.62** (250 mg, 0.5 mmol) and **2.16** (249 mmol, 2 mmol) according to the procedure for synthesizing **1.31**.  $^1\text{H}$  NMR (400 MHz,  $\text{CDCl}_3$ )  $\delta$  7.23 (d,  $J = 8.0$  Hz, 2H), 7.14 (d,  $J = 7.6$  Hz, 2H), 4.53-4.39 (m, 2H), 4.28-4.15 (m, 1H), 4.05-3.96 (m, 0.5H), 3.96-3.86 (m, 1H), 3.72-3.51 (m, 2H), 3.48-3.36 (m, 1.5H), 2.61 (t,  $J = 6.8$  Hz, 2H), 2.43-2.35 (m, 4H), 2.20-2.16 (m, 1H), 2.11-1.99 (m, 1H), 1.62-1.45 (m, 6H), 1.50-1.44 (m, 9H), 0.91 (t,  $J = 7.6$  Hz, 3H), 0.86 (s, 9H), 0.01 (m, 6H);  $^{13}\text{C}$  NMR (100 MHz,  $\text{CDCl}_3$ , mixture of rotamers)  $\delta$  211.1, (154.5), 154.4, 141.7, 135.6, 128.4, (127.9), 127.8, (79.4), 79.1, 76.0, 71.0, (64.3), 63.5, 57.6, (57.5), 52.4, (51.6), 44.7, (42.6), 35.5, (35.1), 34.0, 31.1, (30.0), 29.7, 28.5, 25.9, 23.5, 18.2, 17.3, 13.8, -5.5;  $[\alpha]_{\text{D}}$  (+) 20.4° ( $c$  0.70,  $\text{CHCl}_3$ ); HRMS (ESI) calcd for  $\text{C}_{31}\text{H}_{53}\text{NNaO}_5\text{Si}$  ( $\text{M}+\text{Na}$ ) $^+$  570.3585, found 570.3571.

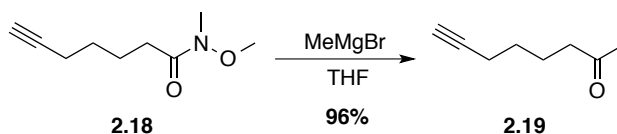


(2*R*,4*S*)-2-(Hydroxymethyl)-4-((4-(5-oxooctyl)benzyl)oxy)pyrrolidin-1-ium chloride (**2.3**) was obtained as white solid (18.0 mg, 95 %) from **2.17** (28 mg, 0.051 mmol), according to the procedure for synthesizing **1.32**.  $^1\text{H}$  NMR (500 MHz,  $\text{D}_2\text{O}$ )  $\delta$  7.34 (d,  $J = 8.0$  Hz, 2H), 7.28 (d,  $J = 8.0$  Hz, 2H), 4.56 (s, 2H), 4.47 (m, 1H), 4.04-3.88 (m, 2H), 3.72 (dd,  $J = 12.5, 6.5$  Hz, 1H), 3.55-3.43 (m, 2H), 2.63 (t,  $J = 7.2$  Hz, 2H), 2.53 (t,  $J = 6.9$  Hz, 2H), 2.47 (t,  $J = 7.3$  Hz, 2H), 2.32 (dd,  $J = 13.5, 6.5$  Hz, 1H), 1.95 (ddd,  $J = 14.6, 10.6, 4.7$  Hz, 1H), 1.63-1.48 (m, 6H), 0.84 (t,  $J = 7.5$  Hz, 3H);  $^{13}\text{C}$  NMR (125 MHz,  $\text{D}_2\text{O}$ )  $\delta$  217.4, 143.0, 134.3, 128.8, 128.6, 76.9, 70.6, 59.9, 59.8, 50.2, 44.3, 42.1, 34.4, 32.3, 30.1, 22.9, 17.1, 12.9;  $[\alpha]_{\text{D}}$  (-) 9.2° ( $c$  0.13,  $\text{CHCl}_3$ ); HRMS (ESI) calcd for  $\text{C}_{20}\text{H}_{31}\text{NO}_3$  ( $\text{M}+\text{H}$ ) $^+$  334.2377, found 334.2379.

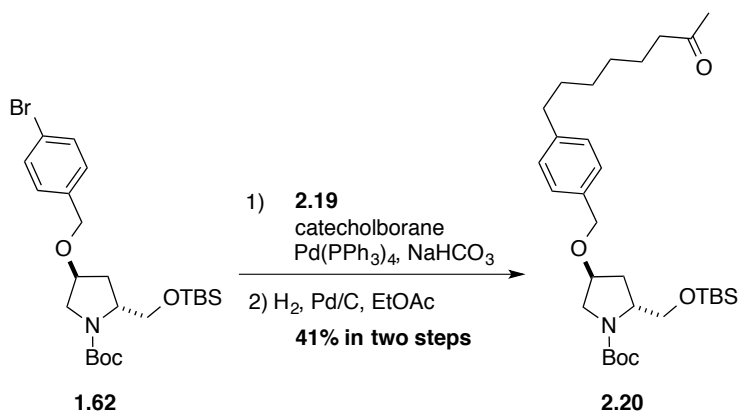
Compound **2.4** was prepared according to the procedure for synthesizing **2.3**.



***N*-Methoxy-*N*-methylhept-6-ynamide (2.18)** was obtained as colorless oil (766 mg, 95 %) from hept-6-ynoic acid (0.67 mL, 4.76 mmol). <sup>1</sup>H NMR (400 MHz, CDCl<sub>3</sub>) δ 3.67 (s, 3H), 3.16 (s, 3H), 2.43 (t, *J* = 7.5 Hz, 2H), 2.21 (td, *J* = 7.1, 2.7 Hz, 2H), 1.93 (t, *J* = 2.6 Hz, 1H), 1.79-1.69 (m, 2H) 1.64-1.54 (m, 2H); <sup>13</sup>C NMR (100 MHz, CDCl<sub>3</sub>) δ 174.2, 84.1, 68.4, 61.2, 32.1, 31.2, 28.1, 23.6, 18.2; HRMS (ESI) calcd for C<sub>9</sub>H<sub>15</sub>NO<sub>2</sub> (M+H)<sup>+</sup> 170.1176, found 170.1176.



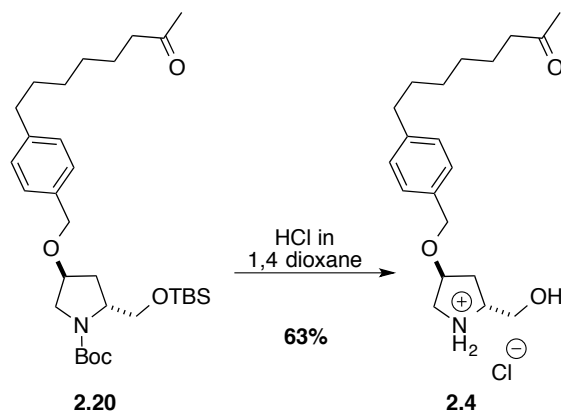
**Oct-7-yn-2-one (2.19)** was obtained as colorless oil (510 mg, 96 %) from **2.18** (726 mg, 4.29 mmol). <sup>1</sup>H NMR (400 MHz, CDCl<sub>3</sub>) δ 2.43 (t, *J* = 7.2 Hz, 2H), 2.18 (td, *J* = 7.2, 2.8 Hz, 2H), 2.12 (s, 3H), 1.93 (t, *J* = 2.6 Hz, 1H), 1.72-1.62 (m, 2H) 1.55-1.45 (m, 2H); <sup>13</sup>C NMR (100 MHz, CDCl<sub>3</sub>) δ 208.5, 83.9, 68.5, 43.0, 29.8, 27.8, 22.7, 18.1; HRMS (ESI) calcd for C<sub>8</sub>H<sub>12</sub>O (M+H)<sup>+</sup> 125.0961, found 125.0966.



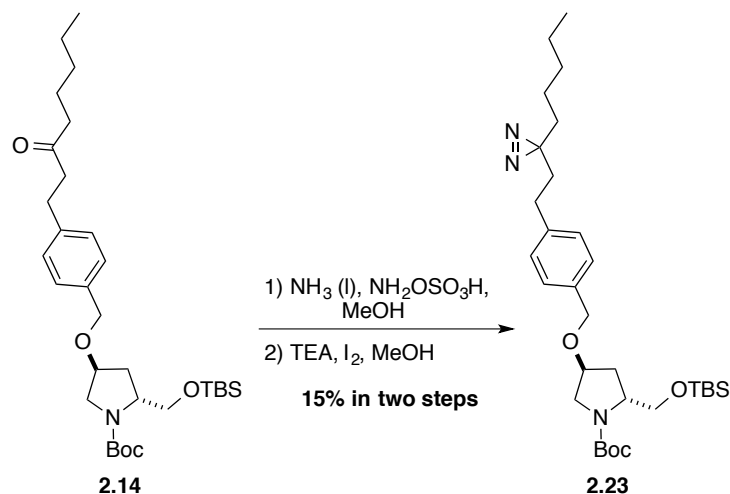
***tert*-Butyl (2*R*,4*S*)-2-(((*tert*-butyldimethylsilyl)oxy)methyl)-4-((4-(7-oxooctyl)benzyl)**



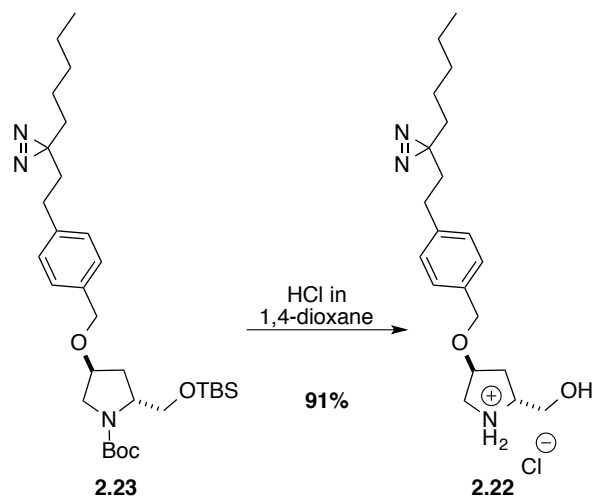
**oxy)pyrrolidine-1-carboxylate (2.20)** was obtained as pale yellow oil (112 mg, 41% over two steps) from **1.62** (250 mg, 0.5 mmol) and **2.19** (249 mg, 2 mmol).  $^1\text{H}$  NMR (400 MHz,  $\text{CDCl}_3$ )  $\delta$  7.23 (d,  $J = 8.0$  Hz, 2H), 7.14 (d,  $J = 7.6$  Hz, 2H), 4.54-4.39 (m, 2H), 4.28-4.15 (m, 1H), 4.05-3.96 (m, 0.5H), 3.96-3.87 (m, 1H), 3.72-3.50 (m, 2H), 3.48-3.37 (m, 1.5H), 2.59 (t,  $J = 7.7$  Hz, 2H), 2.42 (t,  $J = 7.4$  Hz, 2H), 2.24-2.15 (m, 1H), 2.13 (s, 3H), 2.11-2.01 (m, 1H), 1.65-1.52 (m, 2H), 1.50-1.43 (m, 9H), 1.38-1.25 (m, 6H), 0.86 (s, 9H), 0.01 (m, 6H);  $^{13}\text{C}$  NMR (100 MHz,  $\text{CDCl}_3$ , mixture of rotamers)  $\delta$  209.2, (154.5), 154.4, 142.2, 135.4, 128.4, (127.8), 127.7, (79.4), 79.1, 76.0, 71.0, (64.3), 63.5, (57.6), 57.5, 52.4, (51.6), 43.7, 35.6, 35.1, 34.0, 31.3, 29.8, 29.0, 28.5, 25.9, 23.8, 18.2, -5.5;  $[\alpha]_D$  (+)  $19.5^\circ$  ( $c$  0.98,  $\text{CHCl}_3$ ); HRMS (ESI) calcd for  $\text{C}_{31}\text{H}_{53}\text{NNaO}_5\text{Si}$  ( $\text{M}+\text{Na}$ ) $^+$  570.3585, found 570.3578.



**(2R,4S)-2-(Hydroxymethyl)-4-((4-(7-oxooctyl)benzyl)oxy)pyrrolidin-1-ium chloride (2.4)** was obtained as white solid (8.5 mg, 63%) from **2.20** (20 mg, 0.037 mmol).  $^1\text{H}$  NMR (400 MHz,  $\text{D}_2\text{O}$ )  $\delta$  7.35 (d,  $J = 8.0$  Hz, 2H), 7.29 (d,  $J = 8.0$  Hz, 2H), 4.58 (s, 2H), 4.49 (t,  $J = 4.0$  Hz, 1H), 4.04-3.90 (m, 2H), 3.76-3.68 (m, 1H), 3.56-3.43 (m, 2H), 2.64 (t,  $J = 7.5$  Hz, 2H), 2.52 (t,  $J = 7.3$  Hz, 2H), 2.34 (dd,  $J = 14.4, 6.8$  Hz, 1H), 2.19 (s, 3H), 1.95 (ddd,  $J = 14.9, 11.0, 4.8$  Hz, 1H), 1.61 (t,  $J = 6.8$  Hz, 2H), 1.53 (t,  $J = 6.8$  Hz, 2H), 1.30 (m, 4H);  $^{13}\text{C}$  NMR (100 MHz,  $\text{D}_2\text{O}$ )  $\delta$  217.4, 143.2, 133.8, 128.5, 128.2, 76.5, 70.2, 59.5, 59.4, 49.8, 42.8, 34.2, 31.9, 30.0, 28.8, 27.6, 27.5, 22.9;  $[\alpha]_D$  (-)  $6.5^\circ$  ( $c$  0.40, MeOH); HRMS (ESI) calcd for  $\text{C}_{20}\text{H}_{31}\text{NO}_3$  ( $\text{M}+\text{H}$ ) $^+$  334.2377, found 334.2389.

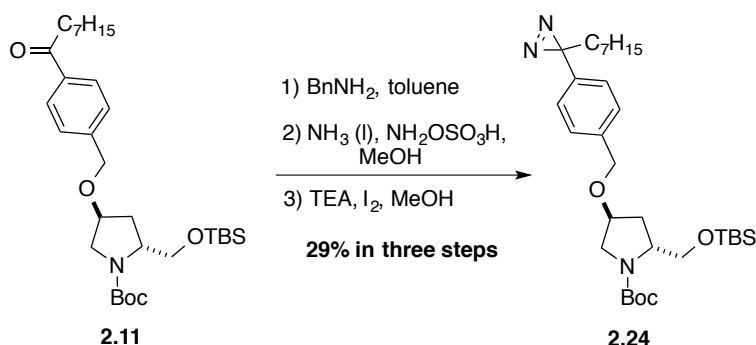


***tert*-Butyl (2*R*,4*S*)-2-(((*tert*-butyldimethylsilyl)oxy)methyl)-4-((4-(2-(3-pentyl-3*H*-diazirin-3-yl)ethyl)benzyl)oxy)pyrrolidine-1-carboxylate (2.23).** A solution of ketone **2.14** (33 mg, 0.060 mmol) in MeOH (1.0 mL) was cooled to 0 °C. Ammonia was bubbled into the solution for 5 h. To the solution, NH<sub>2</sub>OSO<sub>3</sub>H (7.8 mg, 0.069 mmol) in MeOH (0.5 mL) were slowly added over 30 min. The mixture was allowed to warm to room temperature, stirred overnight, and filtered. The filter cake was washed with MeOH. The filtrate and washings were evaporated under reduced pressure to give a white residue. Methanol (0.5 mL) was added to the residue. The resulting mixture was cooled to 0 °C, treated with Et<sub>3</sub>N (8.4 μL, 6.1 mg, 0.060 mmol), followed by I<sub>2</sub> until a brown color was formed. The reaction was warmed to room temperature, stirred for 1 h, and evaporated under reduced pressure. The residue was dissolved in EtOAc, washed with brine, dried over MgSO<sub>4</sub> and filtered. The filtrate was evaporated under reduced pressure. The residue was purified by flash chromatography (hexane: EtOAc, 8:1) to give diazirine **2.23** (5.0 mg, 15 % over two steps) as pale yellow oil. <sup>1</sup>H NMR (400 MHz, CDCl<sub>3</sub>) δ 7.24 (d, *J* = 8.0 Hz, 2H), 7.12 (d, *J* = 7.2 Hz, 2H), 4.53-4.38 (m, 2H), 4.26-4.13 (m, 1H), 4.05-3.96 (m, 0.5H), 3.95-3.87 (m, 1H), 3.72-3.51 (m, 2H), 3.48-3.36 (m, 1.5H), 2.39 (t, *J* = 8.4 Hz, 2H), 2.21-2.15 (m, 1H), 2.12-1.98 (m, 1H), 1.69-1.65 (m, 2H), 1.47-1.45 (m, 9H), 1.38-1.34 (m, 2H), 1.29-1.17 (m, 4H), 1.12-1.05 (m, 2H), 0.91-0.86 (m, 12H), 0.02 (m, 6H); <sup>13</sup>C NMR (100 MHz, CDCl<sub>3</sub>, mixture of rotamers) δ (154.1), 154.0, 140.7, 135.6, 127.9, (127.6), 127.5, (79.0), 78.8, 75.7, 70.5, (63.9), 63.1, 57.3, (57.2), 52.0, (51.2), 34.7, 33.6, 32.5, 31.0, 29.3, 28.4, 28.2, 25.5, 23.1, 22.0, 17.8, 13.5, -5.8; [α]<sub>D</sub> (+) 22.0° (*c* 0.50, CHCl<sub>3</sub>); HRMS (ESI) calcd for C<sub>31</sub>H<sub>53</sub>N<sub>3</sub>NaO<sub>4</sub>Si (M+Na)<sup>+</sup> 582.3698, found 582.3698.



**(2*R*,4*S*)-2-(Hydroxymethyl)-4-((4-(2-(3-pentyl-3*H*-diazirin-3-yl)ethyl)benzyl)oxy)**

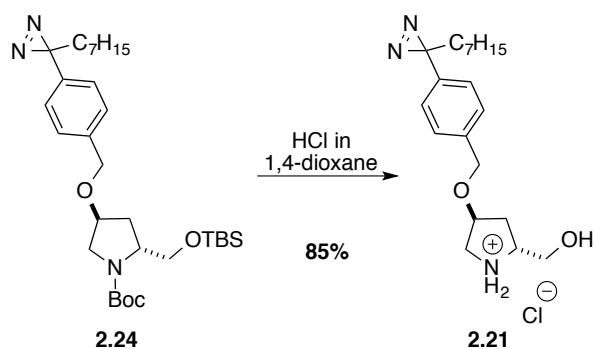
**pyrrolidin-1-ium chloride (2.22)** was obtained as yellow solid (3.1 mg, 91 %) from **2.23** (5 mg, 0.009 mmol) according to the procedure for synthesizing **1.32**. <sup>1</sup>H NMR (700 MHz, CDCl<sub>3</sub>) δ 7.24 (d, *J* = 7.7 Hz, 2H), 7.12 (d, *J* = 8.4 Hz, 2H), 4.50 (d, *J* = 11.9 Hz, 1H), 4.42 (d, *J* = 11.2 Hz, 1H), 4.25 (s, 1H), 4.06-3.97 (m, 2H), 3.77 (dd, *J* = 12.6, 6.3 Hz, 1H), 3.50 (d, *J* = 12.6 Hz, 1H), 3.42 (m, 1H), 2.38 (t, *J* = 8.4 Hz, 2H), 2.13 (dd, *J* = 14.0, 6.3 Hz, 1H), 1.98 (m, 1H), 1.67 (t, *J* = 8.4 Hz, 2H), 1.36 (t, *J* = 7.7 Hz, 2H), 1.25 (m, 2H + OH), 1.21 (m, 2H), 1.80 (m, 2H), 0.87 (t, *J* = 7.0 Hz, 3H); <sup>13</sup>C NMR (175 MHz, CDCl<sub>3</sub>) δ 140.8, 134.9, 128.5, 128.1, 76.7, 70.8, 60.7, 60.3, 50.2, 35.0, 32.8, 31.4, 29.7, 28.7, 23.5, 22.4, 13.9; [α]<sub>D</sub> (-) 9.4° (c 0.16, CHCl<sub>3</sub>); HRMS (ESI) calcd for C<sub>20</sub>H<sub>32</sub>N<sub>3</sub>O<sub>2</sub> (M+H)<sup>+</sup> 346.2489, found 346.2496.



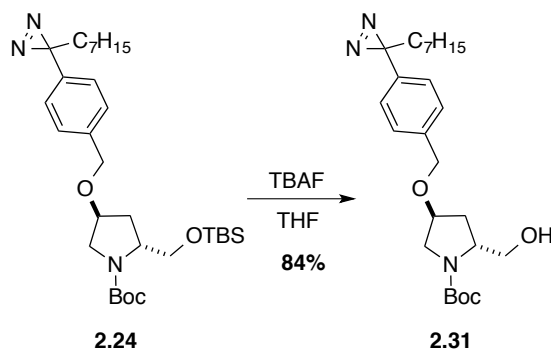
***tert*-Butyl (2*R*,4*S*)-2-(((*tert*-butyldimethylsilyl)oxy)methyl)-4-((4-(3-heptyl-3*H*-**

**diazirin-3-yl)benzyl)oxy)pyrrolidine-1-carboxylate (2.24).** A solution of ketone **2.11** (40 mg, 0.073 mmol) and benzyl amine (25 μL, 25 mg, 0.221 mmol) in toluene (1.0 mL) in a dry

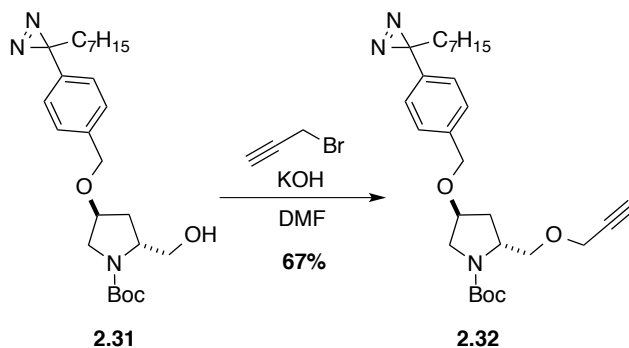
flask equipped with a Dean-Stark apparatus and condenser, was heated to reflux and stirred for 48 h. The volatiles were then removed under reduced pressure. To the yellow residue liquid ammonia (1 mL) was added at - 60 °C. The reaction mixture was stirred for 30 min, NH<sub>2</sub>OSO<sub>3</sub>H (12.8 mg, 0.115 mmol) in MeOH (1.0 mL) was added slowly to the reaction mixture over 15 min. The mixture was stirred at - 60 °C for 3 h, warmed to room temperature, stirred overnight, and filtered. The filtrate was evaporated under reduced pressure to give a white residue. Water (2 mL) was added to the residue, and the resulting mixture was extracted three times with Et<sub>2</sub>O (10 mL). The combined organic phases were dried over MgSO<sub>4</sub> and filtered. The filtrate was evaporated under reduced pressure to give a white residue. MeOH (1.1 mL) was added to the residue. The resulting mixture was cooled to 0 °C, and treated with Et<sub>3</sub>N (11.0 μL, 8.0 mg, 0.079 mmol), followed by I<sub>2</sub> until a brown color was formed. The reaction mixture was warmed to room temperature, stirred for 1 h, an evaporated under reduced pressure to a residue that was dissolved in EtOAc, washed with brine, dried over MgSO<sub>4</sub> and filtered. The filtrate was evaporated under reduced pressure and the residue was purified by flash chromatography (hexane: EtOAc, 8:1) to give diazirine **2.24** (12.0 mg, 29 % over three steps) as pale yellow oil. <sup>1</sup>H NMR (400 MHz, CDCl<sub>3</sub>) δ 7.31-7.26 (m, overlapped with CDCl<sub>3</sub>, 2H), 6.92 (d, *J* = 7.6 Hz, 2H), 4.54-4.42 (m, 2H), 4.25-4.13 (m, 1H), 4.04-3.96 (m, 0.5H), 3.95-3.86 (m, 1H), 3.72-3.50 (m, 2H), 3.46-3.37 (m, 1.5H), 2.21-2.15 (m, 1H), 2.11-1.98 (m, 1H), 1.94 (m, 2H), 1.49-1.43 (m, 9H), 1.34-1.18 (m, 10H), 0.93-0.81 (m, 12H), 0.00 (m, 6H); <sup>13</sup>C NMR (100 MHz, CDCl<sub>3</sub>, mixture of rotamers) δ (154.5), 154.4, 138.7, 137.4, (127.6), 127.5, 125.7, (79.4), 79.2, 76.2, 70.6, (64.3), 63.4, 57.6, 52.3, (51.6), 35.1, 33.9, 31.7, 30.2, 29.2, 29.0, 28.5, 25.8, 24.1, 22.6, 18.1, 14.0, -5.5; [α]<sub>D</sub> (+) 20.2° (*c* 0.60, CHCl<sub>3</sub>); HRMS (ESI) calcd for C<sub>31</sub>H<sub>53</sub>N<sub>3</sub>NaO<sub>4</sub>Si (M+Na)<sup>+</sup> 582.3698, found 582.3679.



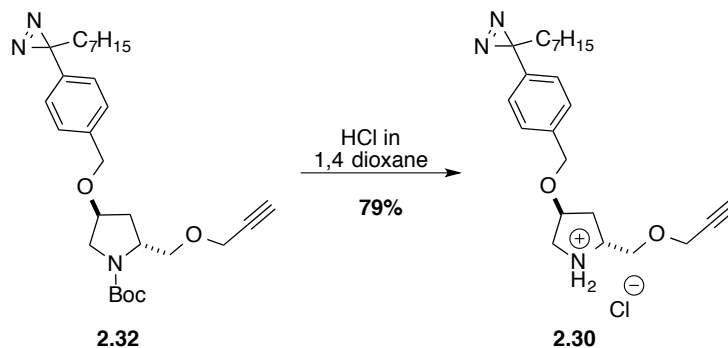
**(2*R*,4*S*)-4-((4-(3-Heptyl-3*H*-diazirin-3-yl)benzyl)oxy)-2-(hydroxymethyl)pyrrolidin-1-ium chloride (2.21)** was obtained as yellow solid (7.0 mg, 85 %) from **2.24** (12 mg, 0.021 mmol) according to the procedure for synthesizing **1.32**. <sup>1</sup>H NMR (400 MHz, CDCl<sub>3</sub>) δ 7.30 (d, *J* = 8.4 Hz, 2H), 6.92 (d, *J* = 8.4 Hz, 2H), 4.53 (d, *J* = 12.0 Hz, 1H), 4.42 (d, *J* = 11.6 Hz, 1H), 4.24 (m, 1H), 4.08-3.97 (m, 2H), 3.77 (dd, *J* = 12.7, 6.0 Hz, 1H), 3.53 (d, *J* = 12.4 Hz, 1H), 3.41 (dd, *J* = 12.6, 4.3 Hz, 1H), 2.14 (dd, *J* = 13.8, 6.4 Hz, 1H), 2.02-1.89 (m, 3H), 1.35-1.18 (m, 10H), 0.88 (t, *J* = 6.8 Hz, 3H); <sup>13</sup>C NMR (100 MHz, CDCl<sub>3</sub>) δ 139.1, 136.3, 127.7, 125.8, 70.5, 60.6, 60.2, 50.2, 32.8, 31.7, 30.1, 29.2, 29.0, 24.0, 22.6, 13.9; [α]<sub>D</sub> (-) 8.0° (*c* 0.10, CHCl<sub>3</sub>); HRMS (ESI) calcd for C<sub>20</sub>H<sub>32</sub>N<sub>3</sub>O<sub>2</sub> (M+H)<sup>+</sup> 346.2489, found 346.2481.



***tert*-Butyl (2*R*,4*S*)-4-((4-(3-heptyl-3*H*-diazirin-3-yl)benzyl)oxy)-2-(hydroxymethyl)pyrrolidine-1-carboxylate (2.31)** was obtained as pale yellow oil (14.4 mg, 84 %) from **2.24** (20 mg, 0.036 mmol) according to the procedure for synthesizing **1.64**. <sup>1</sup>H NMR (400 MHz, CDCl<sub>3</sub>) δ 7.27 (d, *J* = 8.0 Hz, 2H), 6.93 (d, *J* = 8.0 Hz, 2H), 4.85 (s, 1H), 4.53-4.40 (m, 2H), 4.18-3.98 (m, 2H), 3.74-3.48 (m, 3H), 3.42-3.32 (m, 1H), 2.21-2.14 (m, 1H), 1.96-1.89 (m, 2H), 1.68-1.55 (m, 1H), 1.47 (s, 9H), 1.27 (m, 10H), 0.88 (t, *J* = 6.4 Hz, 3H); <sup>13</sup>C NMR (100 MHz, CDCl<sub>3</sub>) δ 157.0, 138.8, 137.1, 127.4, 125.8, 80.5, 76.2, 70.3, 67.2, 59.1, 52.9, 34.5, 31.7, 30.1, 29.2, 29.2, 29.0, 28.4, 24.1, 22.6, 14.0; [α]<sub>D</sub> (+) 20.5° (*c* 1.44, CHCl<sub>3</sub>); HRMS (ESI) calcd for C<sub>25</sub>H<sub>39</sub>N<sub>3</sub>NaO<sub>4</sub> (M+Na)<sup>+</sup> 468.2833, found 468.2828.

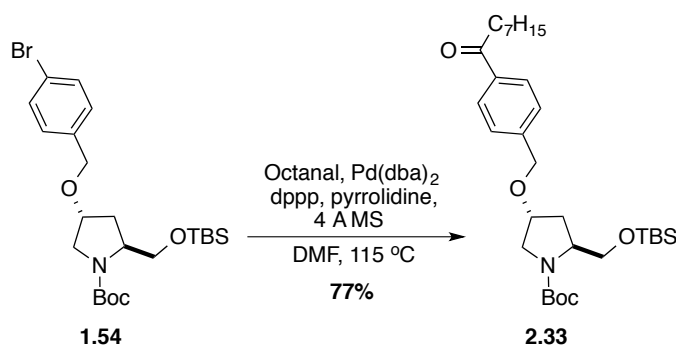


**tert-Butyl (2R,4S)-4-((4-(3-heptyl-3H-diazirin-3-yl)benzyl)oxy)-2-((prop-2-yn-1-yloxy)methyl)pyrrolidine-1-carboxylate (2.32)** was synthesized using a reported procedure for similar reactions.<sup>77</sup> Potassium hydroxide (9 mg, 0.16 mmol) was added to a solution of alcohol **2.31** (14.4 mg, 0.032 mmol) in anhydrous DMF (0.4 mL), followed by propargyl bromide (80 % in toluene, 7.1  $\mu$ L, 9.5 mg, 0.064 mmol) over 5 min. After stirring at room temperature for 18 h, the solution was poured into water (10 mL), and extracted three times with  $\text{CH}_2\text{Cl}_2$  (10 mL). The organic layers were concentrated under reduce pressure and the residue was dissolved in  $\text{Et}_2\text{O}$  (15 mL), washed three times by water (20 mL) and brine (10 mL). The ether solution was dried over  $\text{MgSO}_4$  and filtered. The filtrate was evaporated under reduced pressure and the residue was purified by flash chromatography (hexane: EtOAc, 8:1) to give ether **2.32** (10.4 mg, 67 %) as pale yellow oil.  $^1\text{H}$  NMR (400 MHz,  $\text{CDCl}_3$ )  $\delta$  7.29 (m, overlapped with  $\text{CDCl}_3$ , 2H), 6.92 (d,  $J = 8.4$  Hz, 2H), 4.54-4.44 (m, 2H), 4.20-4.08 (m, 4H), 3.74-3.37 (m, 4H), 2.41 (t,  $J = 2.4$  Hz, 1H), 2.14 (t,  $J = 6.0$  Hz, 2H), 1.94 (m, 2H), 1.47 (s, 9H), 1.36-1.18 (m, 10H), 0.88 (m, 3H);  $^{13}\text{C}$  NMR (100 MHz,  $\text{CDCl}_3$ )  $\delta$  154.6, 138.7, 137.3, 127.5, 125.7, 79.8, 76.2, 74.3, 71.2, 70.7, 70.5, 58.5, 55.6, 52.2, 51.4, 35.6, 34.3, 31.7, 30.2, 29.2, 29.0, 28.5, 24.1, 22.6, 14.0;  $[\alpha]_{\text{D}}^{20}$  (+) 19.0° ( $c$  1.04,  $\text{CHCl}_3$ ); HRMS (ESI) calcd for  $\text{C}_{28}\text{H}_{41}\text{N}_3\text{NaO}_4$  ( $\text{M}+\text{Na}$ )<sup>+</sup> 506.2989, found 506.2982.



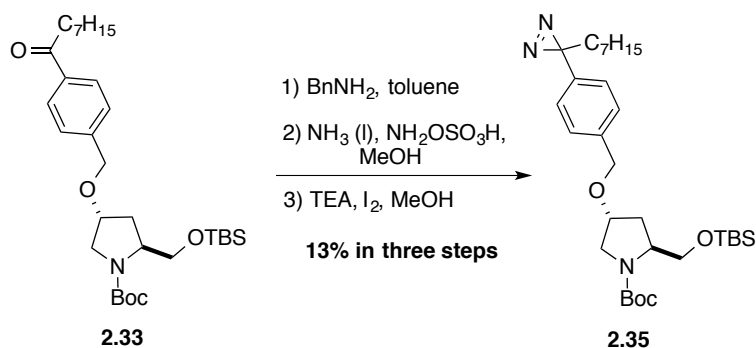
**(2*R*,4*S*)-4-((4-(3-Heptyl-3*H*-diazirin-3-yl)benzyl)oxy)-2-((prop-2-yn-1-yloxy)methyl)pyrrolidin-1-ium chloride (2.30)** was obtained as pale yellow oil (3.4 mg, 79 %) from **2.32** (5 mg, 0.010 mmol) according to the procedure for synthesizing **1.32**.  $^1\text{H}$  NMR (400 MHz,  $\text{CDCl}_3$ )  $\delta$  7.29 (d,  $J = 8.4$  Hz, 2H), 6.92 (d,  $J = 8.4$  Hz, 2H), 4.47 (ABq,  $\Delta\delta_{\text{AB}} = 0.02$ ,  $J_{\text{AB}} = 12.0$  Hz, 2H), 4.22 (d,  $J = 2.4$  Hz, 2H), 4.17-4.12 (m, 1H), 3.75-3.67 (m, 1H), 3.64 (dd,  $J = 9.2, 4.4$  Hz, 1H), 3.55 (dd,  $J = 9.2, 6.4$  Hz, 1H), 3.17 (d,  $J = 4.0$  Hz, 2H), 2.44 (t,  $J = 2.4$  Hz, 1H), 2.10-2.04 (m, 1H), 1.94 (m, 2H), 1.73 (ddd,  $J = 14.1, 8.8, 5.8$  Hz, 1H), 1.35-1.18 (m, 10H), 0.88 (m, 3H);  $^{13}\text{C}$  NMR (100 MHz,  $\text{CDCl}_3$ )  $\delta$  138.7, 137.2, 127.5, 125.8, 79.5, 79.0, 74.7, 71.6, 70.4, 58.5, 56.8, 51.8, 34.7, 31.7, 30.2, 29.2, 29.0, 24.1, 22.6, 14.1;  $[\alpha]_{\text{D}}^{25}$  (-) 13.3° ( $c$  0.27,  $\text{CHCl}_3$ ); HRMS (ESI) calcd for  $\text{C}_{23}\text{H}_{34}\text{N}_3\text{O}_2$  ( $\text{M}+\text{H}$ ) $^+$  384.2646, found 384.2645.

Compound **2.38** was prepared according the procedure for synthesizing **2.30**.



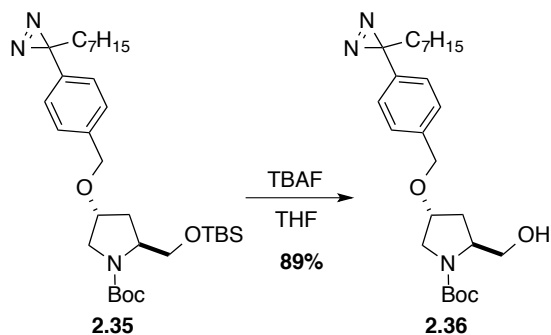
***tert*-Butyl (2*S*,4*R*)-2-(((*tert*-butyldimethylsilyl)oxy)methyl)-4-((4-octanoylbenzyl)oxy)pyrrolidine-1-carboxylate (2.33)** was obtained as pale yellow oil (84 mg, 77%) from **1.54** (100 mg, 0.20 mmol) according to the procedure for synthesizing **2.11**.  $^1\text{H}$  NMR (400 MHz,  $\text{CDCl}_3$ )  $\delta$  7.92 (d,  $J = 7.2$  Hz, 2H), 7.40 (d,  $J = 8.0$  Hz, 2H), 4.61-4.45 (m, 2H), 4.28-

4.15 (m, 1H), 4.05-3.97 (m, 0.5H), 3.97-3.88 (m, 1H), 3.73-3.49 (m, 2H), 3.49-3.38 (m, 1.5H), 2.95 (t,  $J = 7.6$  Hz, 2H), 2.24-2.15 (m, 1H), 2.14-1.98 (m, 1H), 1.76-1.7 (m, 2H), 1.50-1.40 (m, 9H), 1.39-1.19 (m, 8H), 0.91-0.78 (m, 12H), 0.00 (s, 6H);  $^{13}\text{C}$  NMR (100 MHz,  $\text{CDCl}_3$ , mixture of rotamers)  $\delta$  200.1, (154.4), 154.3, 143.4, 136.3, 128.2, (127.3), 127.2, (79.4), 79.2, 76.6, 70.4, (64.2), 63.4, 57.6, (57.5), 52.3, (51.6), 38.6, (35.0), 33.9, 31.6, 29.3, 29.1, 28.5, 25.8, 24.4, 22.5, 18.1, 14.0, -5.5;  $[\alpha]_{\text{D}}^{20}$  (-) 20.8° ( $c$  0.48,  $\text{CHCl}_3$ ); HRMS (ESI) calcd for  $\text{C}_{31}\text{H}_{53}\text{NNaO}_5\text{Si}$  ( $\text{M}+\text{Na}$ ) $^+$  570.3585, found 570.3575.

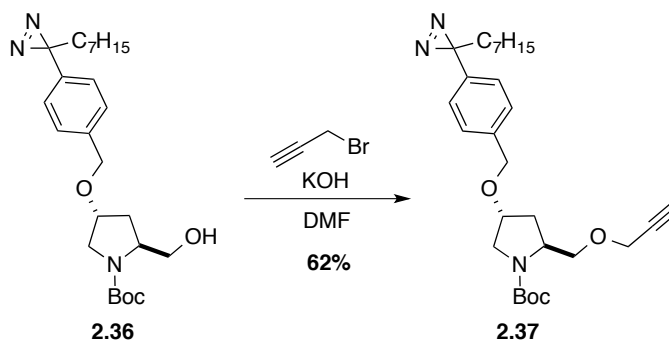


***tert*-Butyl (2*S*,4*R*)-2-(((*tert*-butyldimethylsilyloxy)methyl)-4-((4-(3-heptyl-3*H*-diazirin-3-yl)benzyl)oxy)pyrrolidine-1-carboxylate (2.35)** was obtained as pale yellow oil (10 mg, 13 % in three steps) from **2.33** (78 mg, 0.143 mmol) according to the procedure for synthesizing **2.24**.  $^1\text{H}$  NMR (400 MHz,  $\text{CDCl}_3$ )  $\delta$  7.28 (m, overlapped with  $\text{CDCl}_3$ , 2H), 6.92 (d,  $J = 7.6$  Hz, 2H), 4.54-4.41 (m, 2H), 4.26-4.12 (m, 1H), 4.05-3.97 (m, 0.5H), 3.96-3.88 (m, 1H), 3.72-3.50 (m, 2H), 3.48-3.36 (m, 1.5H), 2.21-2.15 (m, 1H), 2.12-1.98 (m, 1H), 1.94 (t,  $J = 8.0$  Hz, 2H), 1.52-1.43 (m, 9H), 1.34-1.18 (m, 10H), 0.93-0.81 (m, 12H), 0.01 (m, 6H);  $^{13}\text{C}$  NMR (100 MHz,  $\text{CDCl}_3$ , mixture of rotamers)  $\delta$  (154.5), 154.4, 138.7, 137.4, (127.6), 127.5, 125.7, (79.4), 79.2, 76.2, 70.6, (64.3), 63.5, 57.6, 52.3, (51.6), 35.1, 33.9, 31.7, 30.2, 29.2, 29.0, 28.5, 25.9, 24.1, 22.6, 18.1, 14.0, -5.5;  $[\alpha]_{\text{D}}^{20}$  (-) 20.6° ( $c$  1.01,  $\text{CHCl}_3$ ); HRMS (ESI) calcd for  $\text{C}_{31}\text{H}_{53}\text{N}_3\text{NaO}_4\text{Si}$  ( $\text{M}+\text{Na}$ ) $^+$  582.3698, found 582.3695.



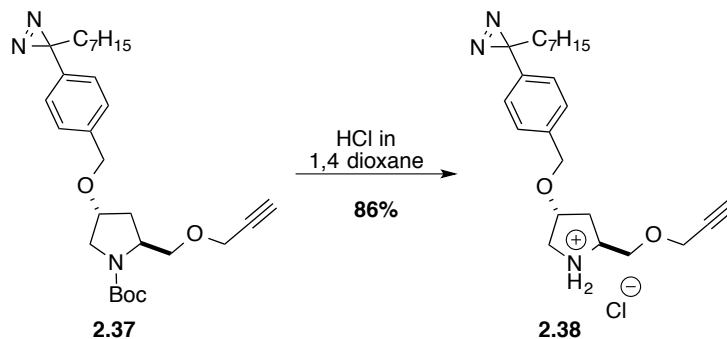


**tert-Butyl (2S,4R)-4-((4-(3-heptyl-3H-diazirin-3-yl)benzyl)oxy)-2-(hydroxymethyl)pyrrolidine-1-carboxylate (2.36)** was obtained as pale yellow oil (12.6 mg, 89 %) from **2.35** (18 mg, 0.032 mmol).  $^1\text{H}$  NMR (400 MHz,  $\text{CDCl}_3$ )  $\delta$  7.27 (d,  $J = 8.4$  Hz, 2H), 6.93 (d,  $J = 8.0$  Hz, 2H), 4.85 (s, 1H), 4.54-4.43 (m, 2H), 4.17-3.98 (m, 2H), 3.76-3.44 (m, 3H), 3.44-3.35 (m, 1H), 2.23-2.14 (m, 1H), 1.99-1.92 (m, 2H), 1.68-1.58 (m, 1H), 1.47 (s, 9H), 1.27 (m, 10H), 0.88 (m, 3H);  $^{13}\text{C}$  NMR (100 MHz,  $\text{CDCl}_3$ )  $\delta$  157.0, 138.8, 137.2, 127.4, 125.8, 80.5, 76.2, 70.3, 67.2, 59.1, 52.9, 34.5, 31.7, 30.2, 29.2, 29.2, 29.0, 28.4, 24.1, 22.6, 14.0;  $[\alpha]_{\text{D}}^{20}$  (-) 21.0° (c 1.26,  $\text{CHCl}_3$ ); HRMS (ESI) calcd for  $\text{C}_{25}\text{H}_{39}\text{N}_3\text{NaO}_4$  ( $\text{M}+\text{Na}$ ) $^+$  468.2833, found 468.2837.



**tert-Butyl (2S,4R)-4-((4-(3-heptyl-3H-diazirin-3-yl)benzyl)oxy)-2-((prop-2-yn-1-yloxy)methyl)pyrrolidine-1-carboxylate (2.37)** was obtained as pale yellow oil (8.0 mg, 62 %) from **2.36** (12 mg, 0.027 mmol).  $^1\text{H}$  NMR (400 MHz,  $\text{CDCl}_3$ )  $\delta$  7.29 (m, overlapped with  $\text{CDCl}_3$ , 2H), 6.92 (d,  $J = 8.4$  Hz, 2H), 4.54-4.44 (m, 2H), 4.21-4.08 (m, 4H), 3.74-3.37 (m, 4H), 2.41 (s, 1H), 2.14 (t,  $J = 5.6$  Hz, 2H), 1.94 (m, 2H), 1.47 (s, 9H), 1.36-1.18 (m, 10H), 0.88 (m, 3H);  $^{13}\text{C}$  NMR (100 MHz,  $\text{CDCl}_3$ )  $\delta$  154.6, 138.7, 137.3, 127.5, 125.7, 79.8, 76.3, 74.3, 71.2, 70.67, 70.5, 58.5, 55.6, 52.2, 51.4, 35.5, 34.3, 31.7, 30.2, 29.2, 29.0, 28.5, 24.1,

22.6, 14.1;  $[\alpha]_D$  (-) 19.7° (*c* 0.70, CHCl<sub>3</sub>); HRMS (ESI) calcd for C<sub>28</sub>H<sub>41</sub>N<sub>3</sub>NaO<sub>4</sub> (M+Na)<sup>+</sup> 506.2989, found 506.2969.



**(2*S*,4*R*)-4-((4-(3-Heptyl-3*H*-diazirin-3-yl)benzyl)oxy)-2-((prop-2-yn-1-yloxy)methyl)pyrrolidin-1-ium chloride (2.38)** was obtained as pale yellow oil (5.1 mg, 86 %) from **2.37** (7 mg, 0.014 mmol). <sup>1</sup>H NMR (700 MHz, CDCl<sub>3</sub>) δ 7.29 (d, *J* = 8.4 Hz, 2H), 6.92 (d, *J* = 7.7 Hz, 2H), 4.47 (ABq, Δδ<sub>AB</sub> = 0.02, J<sub>AB</sub> = 11.9 Hz, 2H), 4.21 (dd, *J* = 2.4, 1.2 Hz, 2H), 4.16-4.12 (m, 1H), 3.73-3.67 (m, 1H), 3.63 (dd, *J* = 9.5, 4.2 Hz, 1H), 3.55 (dd, *J* = 9.5, 6.4 Hz, 1H), 3.21-3.14 (m, 2H), 2.44 (t, *J* = 2.4 Hz, 1H), 2.09-2.03 (m, 1H), 1.94 (m, 2H), 1.73 (ddd, *J* = 14.0, 8.9, 5.7 Hz, 1H), 1.33-1.18 (m, 10H), 0.88 (t, *J* = 7.0 Hz, 3H); <sup>13</sup>C NMR (175 MHz, CDCl<sub>3</sub>) δ 138.7, 137.2, 127.5, 125.8, 79.5, 79.0, 74.7, 71.5, 70.4, 58.5, 56.8, 51.7, 34.6, 31.7, 30.2, 29.2, 29.0, 24.1, 22.6, 14.0;  $[\alpha]_D$  (+) 10.0° (*c* 0.20, CHCl<sub>3</sub>); HRMS (ESI) calcd for C<sub>23</sub>H<sub>34</sub>N<sub>3</sub>O<sub>2</sub> (M+H)<sup>+</sup> 384.2646, found 384.2653.

## 2-5 References

1. Henry, C. M. *Chem. Eng. News: Sci. Technol.* **2001**, 79, 69.
2. van Dongen M.; Weigelt, J.; Uppenberg, J.; Schultz, J.; Wikström, M. *Drug Discov. Today*, **2002**, 7, 471.
3. Leach, A. R.; Harren J. *Structure-based Drug Discovery*. Berlin: Springer, **2007**.
4. Nienhaus, G. U. *Protein-Ligand Interactions: Methods and Applications*. Humana Press: Totowa, **2005**.
5. Palmer, R. A.; Niwa, H. *Biochem. Soc. Trans.* **2003**, 31, 973.
6. Schlichting, I. *Methods Mol. Biol.* **2005**, 305, 155.

7. Mayer, M.; Meyer, B. *Angew. Chem. Int. Ed.* **1999**, *38*, 1784.
8. Meyer, B.; Peters, T. *Angew. Chem. Int. Ed.* **2003**, *42*, 864.
9. Chowdhry, V.; Westheimer, F. H. *Annu. Rev. Biochem.* **1979**, *48*, 293.
10. Singh, A.; Thornton, E. R.; Westheimer, F. H. *J. Biol. Chem.* **1962**, *237*, 3006.
11. For review of photoaffinity labeling, see: (a) Kotzybahibert, F.; Kapfer, I.; Goeldner, M.; *Angew. Chem. Int. Ed.* **1995**, *34*, 1296. (b) Dormán, G.; Prestwich, G. D. *Trends Biotechnol.* **2000**, *18*, 64. (c) Vodovozova, E. L. *Biochemistry (Mosc)*. **2007**, *72*, 1. (d) Geurink, P. P.; Prely, L. M.; van der Marel, G. A.; Bischoff, R.; Overkleeft, H. S. *Top. Curr. Chem.* **2012**, *324*, 85-113. (e) Lapinsky, D. J. *Bioorg. Med. Chem.* **2012**, *20*, 6237. (f) Sumranjit, J.; Chung, S. J. *Molecules*, **2013**, *18*, 10425. (g) Smith, E.; Collins, I. *Future Med. Chem.* **2015**, *7*, 159.
12. For review and use of benzophenones, see: (a) Galardy, R. E.; Craig, L. C.; Printz, M. P. *Nature New Biol.*, **1973**, *242*, 127. (b) Dormán, G.; Prestwich, G. D. *Biochemistry*, **1994**, *33*, 5661. Prestwich, G. D.; Dormán, G.; Elliott, J. T.; Marecak, D. M.; Chaudhary, A. *Photochem Photobiol.* **1997**, *65*, 222.
13. For review and use of aryl azides, see: (a) Fleet, G. W. J.; Porter, R. R.; Knowles, J. R. *Nature*, **1969**, *224*, 511. (b) Pinney, K. G.; Carlson, K. E.; Katzenellenbogen, B. S.; Katzenellenbogen, J. A. *Biochemistry*. **1991**, *30*, 2421. (c) David, A.; Steer, D.; Bregant, S.; Devel, L.; Makaritis, A.; Beau, F.; Yiotakis, A.; Dive, V. *Angew. Chem. Int. Ed.* **2007**, *46*, 3275.
14. Borden, W. T.; Gritsan, N. P.; Hadad, C. M.; Karney, W. L.; Kemnitz, C. R.; Platz, M. S. *Acc. Chem. Res.* **2000**, *33*, 765.
15. Hashimoto, M.; Hatanaka, Y. *Eur. J. Org. Chem.* **2008**, 2513.
16. For synthesis of aryl azides, see: (a) Liu, Q.; Tor, Y. *Org. Lett.* **2003**, *5*, 2571. (b) Goddard-Borger, E. D.; Stick, R. V. *Org. Lett.* **2007**, *9*, 3797. (c) Katritzky, A. R.; Khatib, E. M.; Bol'shakov, O.; Khelashvili, L.; Steel, P. J. *J. Org. Chem.* **2010**, *75*, 6532.
17. For review and use of diazirines, see: (a) Blencowe, A.; Hayes, W. *Soft Matter*, **2005**, *1*, 178. (b) Das, J.; *Chemical Reviews*, **2011**, *111*, 4405. (c) Dubinsky, L.; Krom, B. P.; Meijler, M. M. *Bioorg. Med. Chem.* **2012**, *20*, 554.
18. Brunner, J.; Senn, H.; Richards, F. M. *J. Biol. Chem.* **1980**, *255*, 3313.

19. For synthesis of diazirines, see: (a) Delfino, J. M.; Schreiber, S. L.; Richards, F. M. *J. Am. Chem. Soc.* **1993**, *115*, 3458. (b) Vila-Perello, M.; Pratt, M. R.; Tulin, F.; Muir, T. W. *J. Am. Chem. Soc.* **2007**, *129*, 8068. (c) Li, Z. Q.; Hao, P. L.; Li, L.; Tan, C. Y. J.; Cheng, X. M.; Chen, G. Y. J.; Sze, S. K.; Shen, H. M.; Yao, S. Q. *Angew. Chem. Int. Ed.*, **2013**, *52*, 8551.
20. Sadaghiani, A. M.; Verhelst, S. H.; Bogyo, M. *Curr. Opin. Chem. Biol.* **2007**, *11*, 20.
21. Chang, I. N.; Lin, J. N.; Andrade, J. D.; Herron, J. N. *Anal. Chem.* **1995**, *67*, 959.
22. Hang, H. C.; Yu, C.; Kato, D. L.; Bertozzi, C. R. *Proc. Natl. Acad. Sci.* **2003**, *100*, 14846.
23. For review of bioorthogonal chemistry, see: (a) Sletten, E. M.; Bertozzi, C. R. *Angew. Chem. Int. Ed.* **2009**, *48*, 6974. (b) Lim, R. K.; Lin, Q. *Chem. Commun.* **2010**, *46*, 1589. (c) Sletten, E. M.; Bertozzi, C. R. *Acc. Chem. Res.* **2011**, *44*, 666. (d) Grammel, M.; Hang, H. C. *Nat. Chem. Biol.* **2013**, *9*, 475. (e) Ramil, C. P.; Lin, Q. *Chem. Commun.* **2013**, *49*, 11007. (f) Yang, M. Y.; Li, J.; Chen, P. R. *Chem. Soc. Rev.* **2014**, *43*, 6511. (g) Lang, K.; Chin, J. W. *ACS Chem. Biol.* **2014**, *9*, 16. (h) Gong, Y. K.; Pan, L. F. *Tetrahedron Lett.* **2015**, *56*, 2123. (i) Zheng, M.; Zheng, L.; Zhang, P.; Li, J.; Zhang, Y. *Molecules*, **2015**, *20*, 3190.
24. Prescher, J. A.; Bertozzi, C. R. *Nat. Chem. Biol.* **2005**, *1*, 13.
25. Patterson, D. M.; Nazarova, L. A.; Prescher, J. A. *ACS Chem Biol.* **2014**, *9*, 592.
26. Yarema, K. J.; Mahal, L. K.; Bruehl, R. E.; Rodriguez, E. C.; Bertozzi, C. R. *J. Biol. Chem.* **1998**, *273*, 31168.
27. Saxon, E.; Bertozzi, C. R. *Science*, **2000**, *287*, 2007.
28. Kolb, H. C.; Finn, M. G.; Sharpless, K. B. *Angew. Chem., Int. Ed.* **2001**, *40*, 2004.
29. Baskin, J. M.; Prescher, J. A.; Laughlin, S. T.; Agard, N. J.; Chang, P. V.; Miller, I. A.; Lo, A.; Codelli, J. A.; Bertozzi, C. R. *Proc. Natl. Acad. Sci.* **2007**, *104*, 16793.
30. Hein, J. E.; Fokin, V. V. *Chem. Soc. Rev.* **2010**, *39*, 1302.
31. Blackman, M. L.; Royzen, M.; Fox, J. M. *J. Am. Chem. Soc.* **2008**, *130*, 13518.
32. Liu, D. S.; Tangpeerachaikul, A.; Selvaraj, R.; Taylor, M. T.; Fox, J. M.; Ting, A. Y. *J. Am. Chem. Soc.* **2012**, *130*, 13518.
33. Lin, Y. A.; Chalker, J. M.; Floyd, N.; Bernardes, G. J.; Davis, B. G. *J. Am. Chem. Soc.* **2008**, *130*, 9642.

34. Lin, Y. A.; Boutureira, O.; Lercher, L.; Bhushan, B.; Paton, R. S.; Davis, B. G. *J. Am. Chem. Soc.* **2013**, *135*, 12156.
35. Chalker, J. M.; Wood, C. S.; Davis, B. G. *J. Am. Chem. Soc.* **2009**, *131*, 16346.
36. Spicer, C. D.; Triemer, T.; Davis, B. G. *J. Am. Chem. Soc.* **2012**, *134*, 800.
37. Saxon, E.; Bertozzi, C. R. *Science*. **2000**, *287*, 2007.
38. Staudinger, H.; Meyer, J. *Helv. Chim. Acta.* **1919**, *2*, 635.
39. Gololobov, Y. G. *Tetrahedron*, **1981**, *37*, 437.
40. Griffin, B. A.; Adams, S. R.; Tsien, R. Y. *Science*, **1998**, *281*, 269.
41. Prescher, J. A.; Dube, D. H.; Bertozzi, C. R. *Nature*, **2004**, *430*, 873.
42. Chang, P. V.; Prescher, J. A.; Hangauer, M. J.; Bertozzi, C. R. *J. Am. Chem. Soc.* **2007**, *129*, 8400.
43. Michael, A. *J. Prakt. Chem.* **1893**, *48*, 94.
44. Huisgen, R. *Angew. Chem. Int. Ed.* **1963**, *2*, 565.
45. Rostovtsev, V. V.; Green, L. G.; Fokin, V. V.; Sharpless, K. B. *Angew. Chem. Int. Ed.* **2002**, *41*, 2596.
46. Tornøe, C. W.; Christensen, C.; Meldal, M. *J. Org. Chem.* **2002**, *67*, 3057.
47. Wu, P.; Fokin, V. V. *Aldrichimica. Acta.* **2007**, *40*, 7.
48. Amblard, F.; Cho, J. H.; Schinazi, R. F. *Chem. Rev.* **2009**, *109*, 4207.
49. Kolb, H. C.; Finn, M. G.; Sharpless, K. B. *Angew. Chem. Int. Ed.* **2001**, *40*, 2004.
50. Himo, F.; Lovell, T.; Hilgraf, R.; Rostovtsev, V. V.; Noodleman, L.; Sharpless, K. B.; Fokin, V. V. *J. Am. Chem. Soc.* **2005**, *127*, 210.
51. Rodionov, V. O.; Fokin, V. V.; Finn, M. G. *Angew. Chem. Int. Ed.* **2005**, *44*, 2210.
52. Worrell, B. T.; Malik, J. A.; Fokin, V. V. *Science*. **2013**, *340*, 457.
53. McKay, C. S.; Finn, M. G. *Chem. Biol.* **2014**, *21*, 1075.
54. Hong, V.; Steinmetz, N. F.; Manchester, M.; Finn, M. G. *Bioconjugate Chem.* **2010**, *21*, 1912.
55. Rodionov, V. O.; Presolski, S. I.; Díaz Díaz, D.; Fokin, V. V.; Finn, M. G. *J. Am. Chem. Soc.* **2007**, *129*, 12705.
56. Presolski, S. I.; Hong, V.; Cho, S. H.; Finn, M. G. *J. Am. Chem. Soc.* **2010**, *132*, 14570.
57. Soriano del Amo, D.; Wang, W.; Jiang, H.; Besanceney, C.; Yan, A. C.; Levy, M.; Liu, Y.;

- Marlow, F. L.; Wu, P. *J. Am. Chem. Soc.* **2010**, *132*, 16893.
58. Kennedy, D. C.; McKay, C. S.; Legault, M. C. B.; Danielson, D. C.; Blake, J. A.; Pegoraro, A. F.; Stolow, A.; Mester, Z.; Pezacki, J. P. *J. Am. Chem. Soc.* **2011**, *133*, 17993.
59. Besanceney-Webler, C.; Jiang, H.; Zheng, T.; Feng, L.; Soriano del Amo, D.; Wang, W.; Klivansky, L. M.; Marlow, F. L.; Liu, Y.; Wu, P. *Angew. Chem., Int. Ed.* **2011**, *50*, 8051.
60. Uttamapinant, C.; Tangpeerachaikul, A.; Grecian, S.; Clarke, S.; Singh, U.; Slade, P.; Gee, K. R.; Ting, A. Y. *Angew. Chem., Int. Ed.* **2012**, *51*, 5852.
61. Alder, K.; Stein, G.; Finzenhagen, H. *Justus Liebigs Ann. Chem.* **1931**, *485*, 211.
62. Alder, K.; Stein, G. *Justus Liebigs Ann. Chem.* **1933**, *501*, 1.
63. Wittig, G.; and Krebs, A. *Chem. Ber.* **1961**, *94*, 3260.
64. Agard, N. J.; Prescher, J. A.; Bertozzi, C. R. *J. Am. Chem. Soc.* **2004**, *126*, 15046.
65. Agard, N. J.; Baskin, J. M.; Prescher, J. A.; Lo, A.; Bertozzi, C. R. *ACS Chem. Biol.* **2006**, *1*, 644.
66. Baskin, J. M.; Prescher, J. A.; Laughlin, S. T.; Agard, N. J.; Chang, P. V.; Miller, I. A.; Lo, A.; Codelli, J. A.; Bertozzi, C. R. *Proc. Natl. Acad. Sci.* **2007**, *104*, 16793.
67. Ning, X.; Guo, J.; Wolfert, M. A.; Boons, G.-J. *Angew. Chem., Int. Ed.* **2008**, *47*, 2253.
68. Jewett, J. C.; Sletten, E. M.; Bertozzi, C. R. *J. Am. Chem. Soc.* **2010**, *132*, 3688.
69. Debets, M. F.; van Berkel, S. S.; Schoffelen, S.; Rutjes, F. P. J. T.; van Hest, J. C. M.; van Delft, F. L. *Chem. Commun.* **2010**, *46*, 97.
70. Kuzmin, A.; Poloukhine, A.; Wolfert, M. A.; Popik, V. V. *Bioconjugate Chem.* **2010**, *21*, 2076.
71. Dommerholt, J.; Schmidt, S.; Temming, R.; Hendriks, L. J. A.; Rutjes, F. P. J. T.; van Hest, J. C. M.; Lefeber, D. J.; Friedl, P.; van Delft, F. L. *Angew. Chem., Int. Ed.* **2010**, *49*, 9422.
72. Laughlin, S. T.; Baskin, J. M.; Amacher, S. L.; Bertozzi, C. R. *Science*, **2008**, *320*, 664.
73. Laughlin, S. T.; Bertozzi, C. R. *ACS Chem. Biol.* **2009**, *4*, 1068.
74. Ruan, J. W.; Saidi, O.; Iggo, J. A.; Xiao, J. L. *J. Am. Chem. Soc.*, **2008**, *130*, 10510.
75. Kim, S. S.; Nehru, K. *Synlett.* **2002**, *4*, 616.
76. Kishore Kumar, G. D.; Chavarria, G. E.; Charlton-Sevcik, A. K.; Arispe, W. M.; Macdonough, M. T.; Strecker, T. E.; Chen, S. E.; Siim, B. G.; Chaplin, D. J.; Trawick, M. L.; Pinney, K. G. *Bioorg. Med. Chem. Lett.* **2010**, *20*, 1415.

77. Smith, G.; Glaser, M.; Perumal, M.; Nguyen Q. D.; Shan, B.; Årstad, E.; Aboagye, E. O. *J. Med. Chem.*, **2008**, *51*, 8057.

# Chapter 3: Studies of Unusual Barbier-Grignard Type Reactions

## 3-1 Introduction

### 3-1-1 Barbier reaction

In 1899, Philippe Barbier reported a reaction forming 2,6-dimethylhept-5-en-2-ol (**3.2**) from 6-methylhept-5-en-2-one (**3.1**) and methyl iodide, in the presence of metallic magnesium (Figure 44).<sup>1</sup> This reaction was named after him, as the Barbier reaction. Following this discovery, a series of similar reactions, using different metals, were developed, which are also referred to as Barbier reactions.<sup>2</sup> In general, the Barbier reaction is a one-pot reaction between a carbonyl substrate (aldehyde and ketone) and an alkyl halide in the presence of certain metals, or their salts. After aqueous workup, the reaction generates the corresponding alcohol as the addition product (Figure 44).

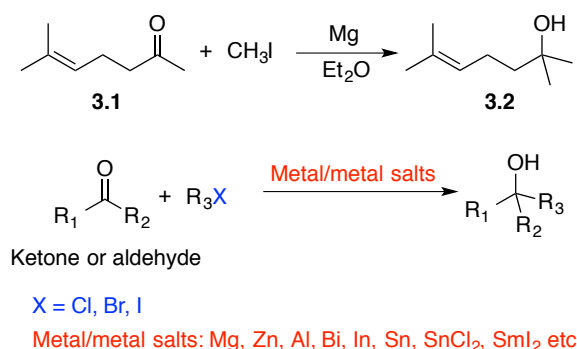


**Figure 44.** The first reported Barbier reaction and the general concept of Barbier type reaction.

The Barbier reaction is an important process for the formation of carbon-carbon bonds. The advantages of this type of reaction include a one-step procedure that may occur in water,<sup>2c</sup> as environmentally benign solvent. The Barbier reaction may thus be considered as “green chemistry”.<sup>3</sup> Applications include Barbier-type allylation,<sup>2c,4</sup> propargylation,<sup>2c,5</sup> alkylation using unactivated alkyl halides,<sup>6</sup> and arylation of aryl aldehydes<sup>7</sup> (Figure 45).



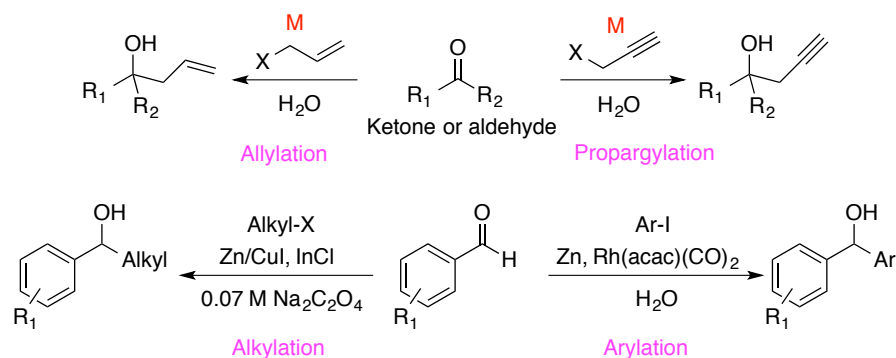


**Figure 45.** Barbier type reactions in aqueous media.

In addition to its wide use in intermolecular reactions, the Barbier reaction is a useful tool for intramolecular cyclizations (Figure 46).<sup>2c</sup> Examples include tin/aluminum mediated allylic cyclizations in aqueous THF,<sup>8</sup> zinc and indium promoted cyclizations to give homoallylic or homoallenic alcohols in five- or six-membered rings,<sup>9</sup> SmI<sub>2</sub> mediated cyclization to produce tetracyclic polyquinines,<sup>10</sup> and CrCl<sub>2</sub> with NiCl<sub>2</sub> catalyzed Nozaki-Hiyama-Kishi (NHK) reaction<sup>11</sup> in the synthesis of macrocyclic nature products,<sup>12</sup> e.g. bipinnatin J<sup>13</sup> (Figure 46).

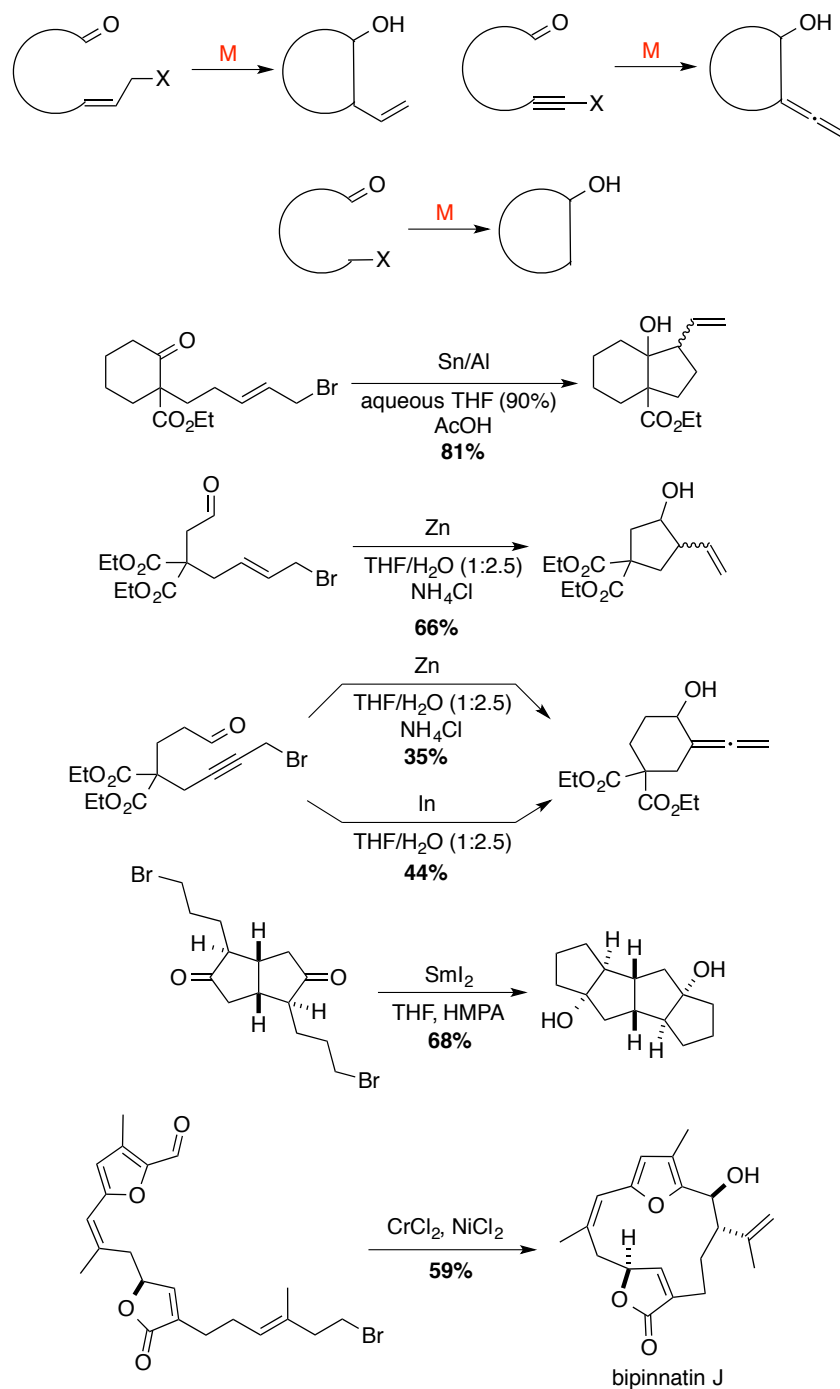
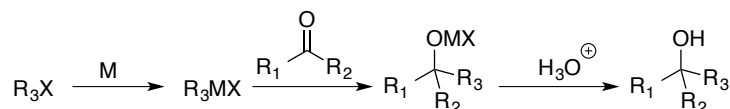


**Figure 46.** Intramolecular Barbier type reactions.

Although the Barbier reaction was discovered more than 100 years ago, its mechanism is still widely debated. In the organometallic-pathway, intermediate  $R_3MgX$  has been

suggested to be generated *in situ* and attacks the carbonyl group in the substrate to afford the corresponding metal salt, which is transformed to the alcohol product through an aqueous workup (Figure 47). Considering organometallic reagents often react violently with water, this mechanism is unlikely for aqueous Barbier reactions. Radical mechanisms,<sup>14,15</sup> featuring single-electron transfer (SET) between metal and halide substrate have been suggested to take place on the surface of the metal to generate a radical anion  $R_3\dot{X}^-$  that reacts with the carbonyl substrate to produce a radical adduct. Following another SET from the metal to the adduct an anion ensues. Aqueous workup affords the alcohol (Figure 47).<sup>16</sup> Alternatively, a ketyl intermediate could be generated through SET between the metal and ketone substrates. This reactive species could couple to the radical-anion  $R_3\dot{X}^-$  generated from the halide, to give an alkoxide intermediate, which would be transformed to the alcohol during aqueous work-up (Figure 47). These mechanisms may be applicable to all Barbier reactions with the actual pathway being dependent on the reaction conditions, metal, halide and ketone substrates.<sup>2c</sup>

**Organometallic pathway:**



**Radical pathway:**

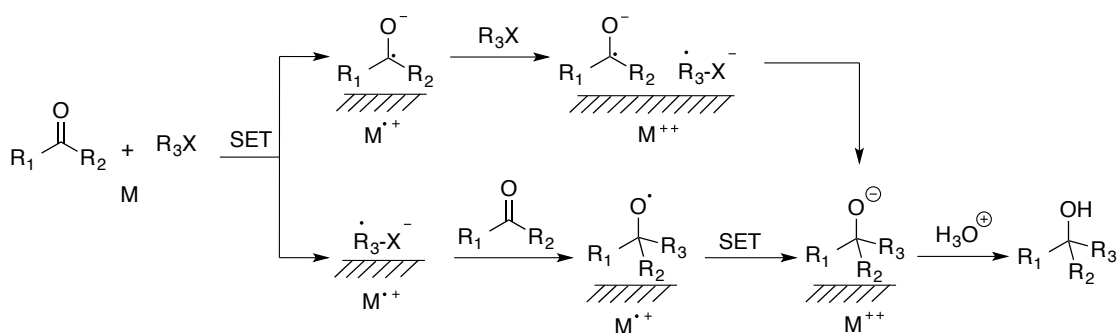


**Figure 47.** Proposed mechanisms for Barbier reactions.

### 3-1-2 Grignard reaction

Continuing Barbier's studies on organomagnesium chemistry, in 1900, François Auguste Victor Grignard, a student of Barbier, reasoned that  $RMgX$  was the active intermediate in the Barbier reaction.<sup>17</sup> He proposed a two-step reaction sequence whereby

formation of the RMgX complex occurs first, followed by the addition of this reactive species to the carbonyl substrates (Figure 48).<sup>17</sup> This novel proposal revolutionized organometallic methods for carbon-carbon bond formation. Grignard was awarded the Nobel Prize in 1912 for this contribution. Nowadays, the Grignard reaction has become one of the most useful reactions, not only in C-C bond formation, but also in the formation of carbon-boron, carbon-silicon, and other carbon-heteroatom bonds.

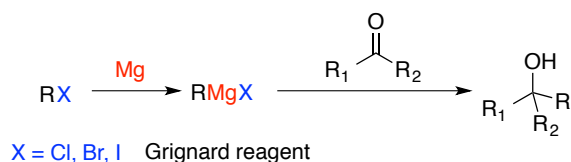


**Figure 48.** General concept of the Grignard reaction.

The active organomagnesium halides (RMgX) are called Grignard reagents<sup>18</sup> (Figure 48). They are usually prepared through the addition of alkyl or aryl halides to magnesium metal in ethereal solvent (typically diethyl ether or tetrahydrofuran). A SET mechanism is believed to be involved in the formation of Grignard reagents (Figure 49).<sup>18e,19</sup> On the surface of the magnesium metal, a radical anion ( $\text{R}\cdot\text{X}^-$ ) is generated through a SET from magnesium to the halide. This radical anion then decomposes, and a subsequent combination of radical  $\text{R}\cdot$ , magnesium radical cation ( $\text{Mg}^{\cdot+}$ ) and halide anion  $\text{X}^-$  leads to the organomagnesium halide complex (RMgX) (Figure 49). Metallic magnesium is usually covered by a layer of  $\text{Mg}(\text{OH})_2$ ,<sup>19b</sup> which results in sluggish formation of Grignard reagents. To accelerate the reaction, fresh magnesium metal may be pre-crushed, and iodine, methyl iodide, or 1,2-dibromoethane may be added as an initiation agent. Sonication and heating is often necessary for initiating the reaction in many cases.

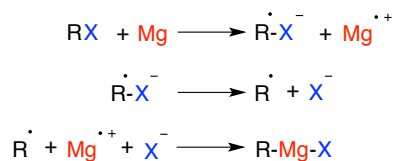


**Figure 49.** Proposed mechanism for the formation of Grignard reagents.

In an ether solution, Grignard reagents (RMgX) are stabilized by the formation of a tetrahedral magnesium (II) species, in which the ether coordinates to the magnesium in complex with the formula RMgX(S)<sub>2</sub> (S = ether solvent). Additionally, an equilibrium has been observed between two molecules of RMgX (Grignard complex) and one molecular of dialkyl magnesium Mg(R)<sub>2</sub> compound with the magnesium halide salt (Figure 50); this was named as Schlenk equilibrium.<sup>20</sup> The composition of the equilibrium is dependent on the solvent, temperature, concentration, organic moiety (R) and halide.<sup>21</sup> For simple organomagnesium halides, in mono-ether solvents, the equilibrium usually favors the RMgX complex.<sup>21,22</sup> In dioxane, MgX<sub>2</sub> may precipitate,<sup>23</sup> driving the equilibrium to the dialkyl magnesium. Grignard reagents have also been found to exist as dimers, and higher-order oligomers, in solution.<sup>24</sup> For example, alkyl-magnesium chlorides were observed to form dimers in diethyl ether<sup>25</sup> (Figure 50), with formation of aggregates at high concentration.

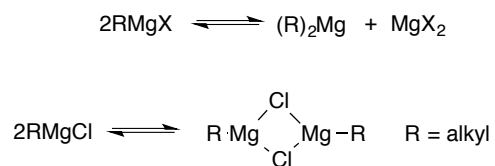
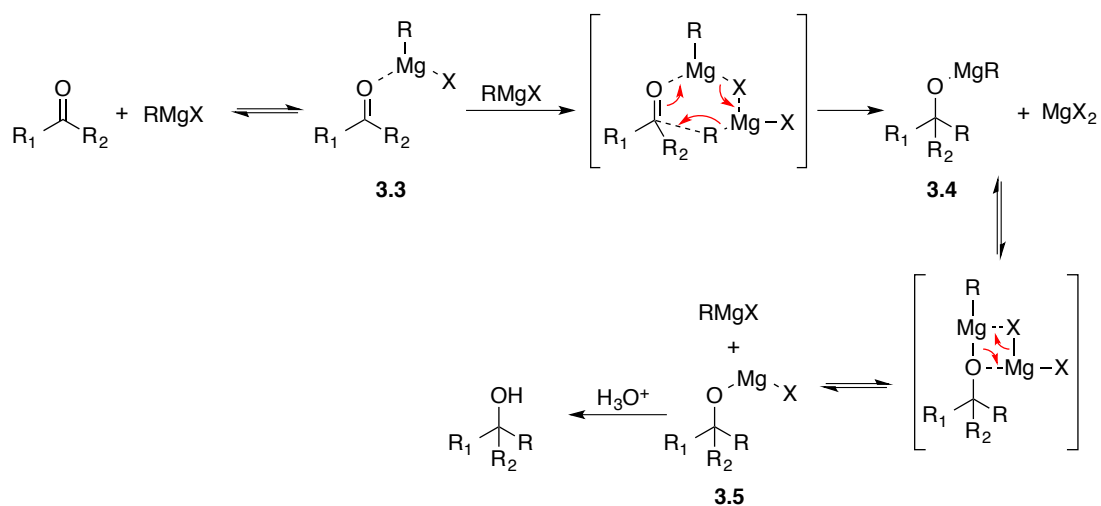


**Figure 50.** Schlenk equilibrium and the dimer complex of alkyl magnesium chlorides.

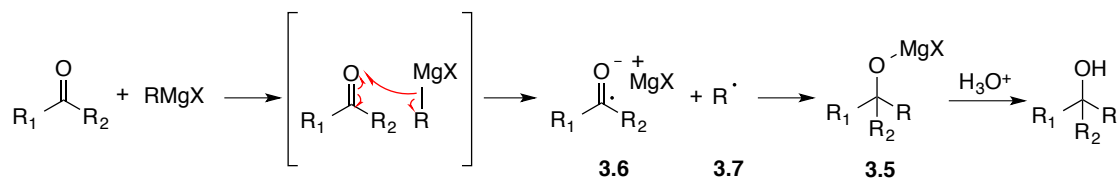
Grignard reagents can react with a variety of carbonyl substrates, such as ketones, aldehydes, esters, acyl halide, amides and carbon dioxide. The mechanism of the Grignard reaction is complex and, so far, there are two widely accepted mechanisms: the polar pathway and the SET pathway (Figure 51).<sup>24-27</sup> In the polar pathway, one molecule of a Grignard reagent RMgX could activate the ketone substrate and form a coordination complex **3.3** (Figure 51), that reacts with another molecule of RMgX, through a six-membered transition state to give the magnesium alkoxide **3.4** and MgX<sub>2</sub> salt. Intermediate **3.4** may transformed into salt **3.5** by interacting with MgX<sub>2</sub> to regenerate one molecule of the Grignard reagent (RMgX). Alkoxide **3.5** undergoes hydrolysis to give alcohol product (Figure 51). In the SET pathway, one electron is transferred from the Grignard reagent (RMgX) to the ketone substrate generating a ketyl radical anion, magnesium halide cation complex **3.6**, and the free radical **3.7** (Figure 51). Coupling of complex **3.6** and radical **3.7** affords the alkoxide intermediate **3.5**,

which is transformed to the corresponding alcohol by hydrolysis (Figure 51). These mechanisms are considered to be competitive and suggested to depend on the ketone substrate, organic moiety R, solvent and purity of the magnesium metal.<sup>27</sup> In relatively non-polar solvent, with high purity magnesium metal, the reaction between ketone substrate with a low tendency to be reduced and Grignard reagent with a low tendency to be oxidized would favor the polar pathway. In polar solvents with magnesium that contains transition metal impurities, the Grignard reaction between ketone with a high tendency to be reduced and Grignard reagent with a high tendency to be oxidized would favor the SET pathway.<sup>27</sup>

**Polar pathway:**



**SET pathway:**

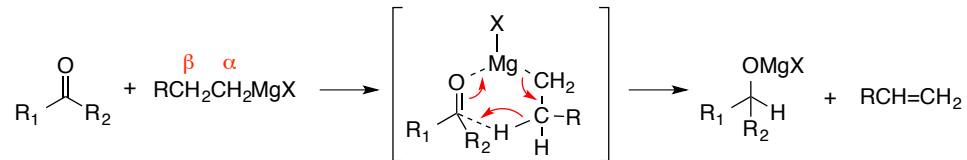
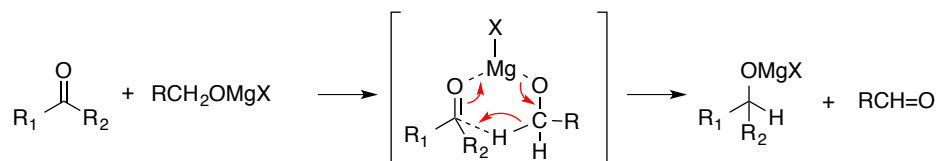
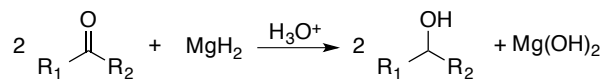
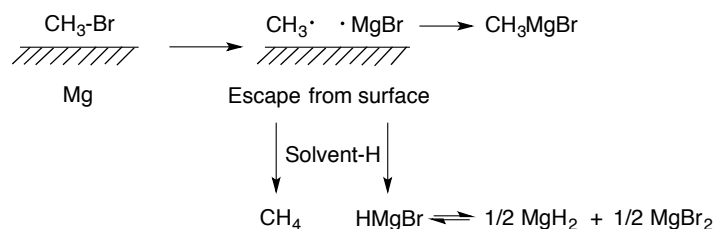


**Figure 51.** Proposed mechanisms for Grignard reactions.

The Grignard reaction is well known as an efficient method for obtaining addition products from RMgX and carbonyl substrates. However, in some cases, the product of the reaction may not be expected.<sup>28</sup> Such “unusual” or “abnormal” Grignard reactions include the

reduction of carbonyl substrates,<sup>28-32</sup> the pinacol coupling of carbonyl substrates<sup>28,33</sup> and the enolization and condensation of carbonyl substrates.<sup>28,30,34,35</sup>

During the discovery of the Grignard reaction, Grignard himself had noticed a reduction product, benzyl alcohol, from the reaction of benzaldehyde with isoamylmagnesium bromide.<sup>36</sup> Further studies on the reduction products in Grignard reactions gave rise to several possible mechanisms for this process (Figure 52).<sup>28</sup> Whitmore proposed that carbonyl substrates could be reduced by a  $\beta$ -hydride attack from a Grignard reagent through a six-membered transition state (Figure 52).<sup>37</sup> Some carbonyl substrates were considered to be reduced by magnesium alkoxide<sup>38,39</sup> in a manner analogue to the Meerwein-Ponndorf-Verley reduction,<sup>40</sup> through a six-membered transition state (Figure 52).<sup>28</sup> Ashby suggested that benzophenone could be reduced by magnesium hydride ( $\text{MgH}_2$ ) (Figure 52).<sup>25</sup> By using deuterated diethyl ether, they could conclude that the hydride involved in the reduction was from the solvent, and  $\text{MgH}_2$  was generated during the formation of the Grignard reagent ( $\text{CH}_3\text{MgBr}$ ).<sup>25</sup>

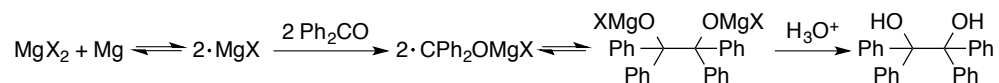
**$\beta$ -Hydride reduction:****Alkoxide reduction:****Magnesium hydride reduction:****Figure 52.** Proposed mechanisms for reduction reactions occurred in Grignard reactions.

The pinacol coupling species is a common side product of the Grignard reaction. In 1906, Schmidlin reported a Grignard reaction between benzophenone and triphenylmethylmagnesium chloride, which gave benzopinacol, instead of the expected addition product pentaphenylethanol.<sup>41</sup> Gomberg continued the study of the Grignard reaction with benzophenone and proposed a radical based mechanism (Figure 53).<sup>42</sup> Radical magnesium halide  $\cdot\text{MgX}$ , generated from  $\text{MgX}_2$  salt and magnesium metal, could react with benzophenone and afford the corresponding benzophenone radicals, which then could be coupled to give the pinacol product, benzpinacol (Figure 53). Blicke and Powers<sup>43</sup> also studied these types of coupling reactions and suggested an alternative radical mechanism: a SET between the Grignard reagent  $(\text{CH}_3)_3\text{CMgCl}$  and benzophenone would generate the



magnesium benzophenone ketyl radical anion and a *tert*-butyl radical. These radical anions could couple to give the pinacol product, benzopinacol (Figure 53).<sup>25,44-46</sup> Observation of pinacol coupling products was important evidence for the SET mechanism in Grignard reactions (Figure 51).

**Magnesium halide pathway:**



**Radical anion pathway:**

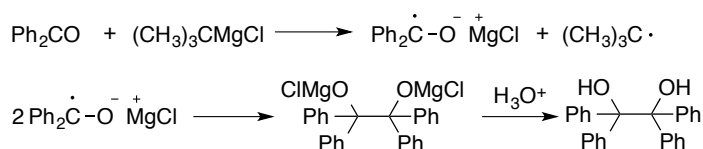


**Figure 53.** Proposed mechanisms for pinacol coupling reactions in Grignard reactions.

Grignard reagents can react as nucleophiles, and as bases. In the case of latter, the first example of enolization was described by Grignard.<sup>47,48</sup> Attempting a Grignard reaction between ethyl acetoacetate and methylmagnesium iodide, he observed that considerable amounts of methane were liberated and most of the keto-ester was recovered.<sup>47,48</sup> Further studies indicated that enolization was competitive with the normal addition reaction in Grignard reaction, and in certain cases, enolization was favored.<sup>28</sup> For example, Whitmore and co-workers<sup>30,34,35</sup> reported up to quantitative enolization during the reactions between sterically hindered methyl dineopentylmethyl ketone and isobutyl-, *tert*-butyl-, isopropylmagnesium halides.<sup>35</sup> They suggested that the presence of an acidic  $\alpha$ -hydrogen was important, otherwise, the addition reaction was favored.<sup>35</sup> Although the enolizations occurring in Grignard reactions were considered to occur through an acid-base mechanism, the actual mechanism for enolization was not clear due to the complicated composition of the Grignard reaction components.<sup>28</sup> Based on the proposals of Brecht-Savelsburg<sup>49</sup> and Arnold,<sup>50</sup> in the mechanism (Figure 54),<sup>28</sup> the ketone interacts with the Grignard reagent to form a complex that decomposes to give the corresponding enolate (Figure 54). Enolization may also occur through a concerted process, in a six-membered transition state as proposed by Lutz and Kibler (Figure 54).<sup>51</sup>

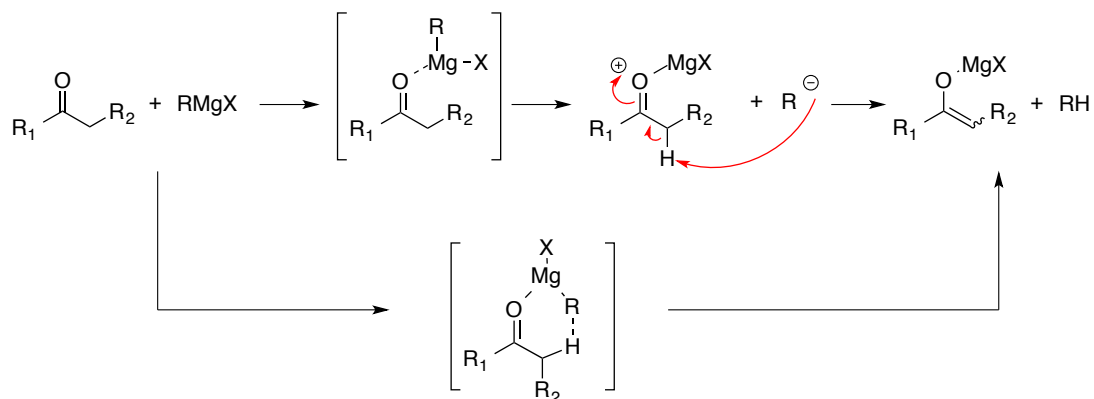


**Figure 54.** Proposed mechanisms for enolization reactions occurred in Grignard reactions.

Ketone substrates may be enolized under the Grignard conditions, moreover, aldol reaction of ketones to give  $\beta$ -ketols has been reported, initially by Grignard, who noticed product form the self-aldol condensation as a side-reaction.<sup>36</sup> For example, isoamylmagnesium bromide and acetone reacted to give tertiary alcohol, and small quantities of mesityl oxide and phorone, which arise from self-aldol reaction of acetone followed by elimination (Figure 55).<sup>36</sup> Other Grignard reactions has led to isolation of the self-aldol condensation products from ketone substrates.<sup>28</sup> For self-aldol reactions to occur, enolate  $R_1R_2C=CR_3OMgX$  should be first generated from ketone  $R_1R_2CHCR_3O$  by a base, and then react with another molecule of the ketone (Figure 55). Grignard realized these reactions were taking place through a base-catalyzed pathway, and suggested alkoxide  $ROMgX$  species to serve as base.<sup>52,53</sup> The actual base (*e.g.*,  $ROMgX$ , Grignard reagent) involved in the enolate formation is difficult to identify, due to the complicated composition of Grignard reaction mixtures.

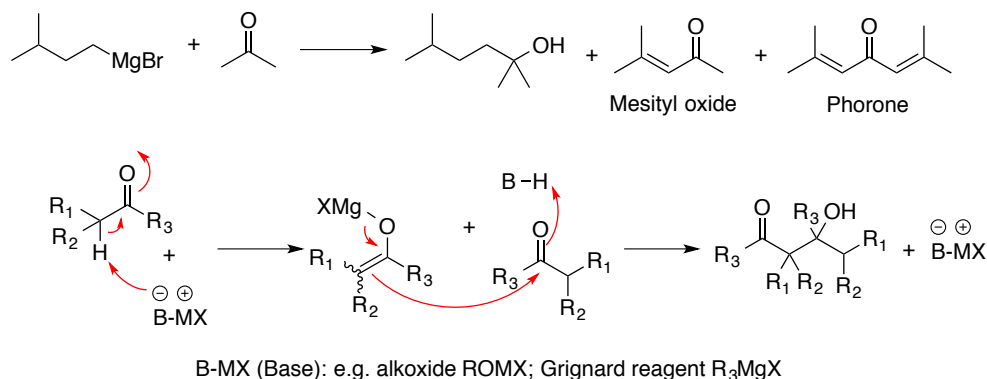


**Figure 55.** Example of self-aldol condensation in Grignard reactions and the possible mechanism.

To inhibit side reactions, additives (e.g.  $\text{MgBr}_2$ ,<sup>54-56</sup>  $\text{LiClO}_4$ ,<sup>57</sup>  $(n\text{-Bu})_4\text{NBr}$ ,<sup>57</sup>  $(i\text{-PrO})_3\text{TiCl}$ ,<sup>58</sup>  $(n\text{-BuO})_3\text{ZrCl}$ ,<sup>58</sup>  $\text{CeCl}_3$ <sup>59</sup>) have been used to enhance the addition reaction, by increasing the electrophilicity of the carbonyl group and decreasing the basicity of the organometallic reagent. For example, Imamoto<sup>59</sup> reported up to 80 % yield self-aldol reaction product from the reaction between cyclopentanone and  $i\text{-PrMgCl}$ , with addition product obtained in only 3 % yield. Employing  $\text{CeCl}_3$  as additive, the yield of the expected addition product was increased to 72 % and only trace amount of ketol was observed (Figure 56). The same additive effect was found in the reaction of cyclohexanone and  $i\text{-PrMgCl}$  (Figure 56).

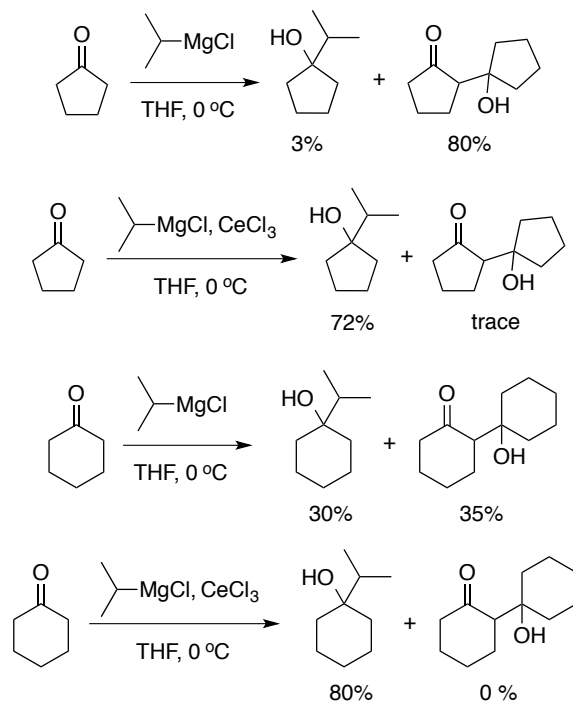


**Figure 56.** Example of Grignard reaction with and without additive (CeCl<sub>3</sub>).

### 3-1-3 An unsuccessful Barbier-Grignard type intramolecular cyclization

In a collaboration with Isis Pharmaceuticals to synthesize tricyclic nucleoside **3.8** (Figure 57) involving Drs. Waggener and Merner,<sup>60</sup> we envisioned using a Barbier-Grignard type intramolecular cyclization to construct tricycle **3.9** from iodide **3.10**. Primary alcohol **3.11** was converted to iodide **3.10** by the Appel reaction. Alcohol **3.11** was prepared from olefin **3.12** by hydroboration (Figure 57).

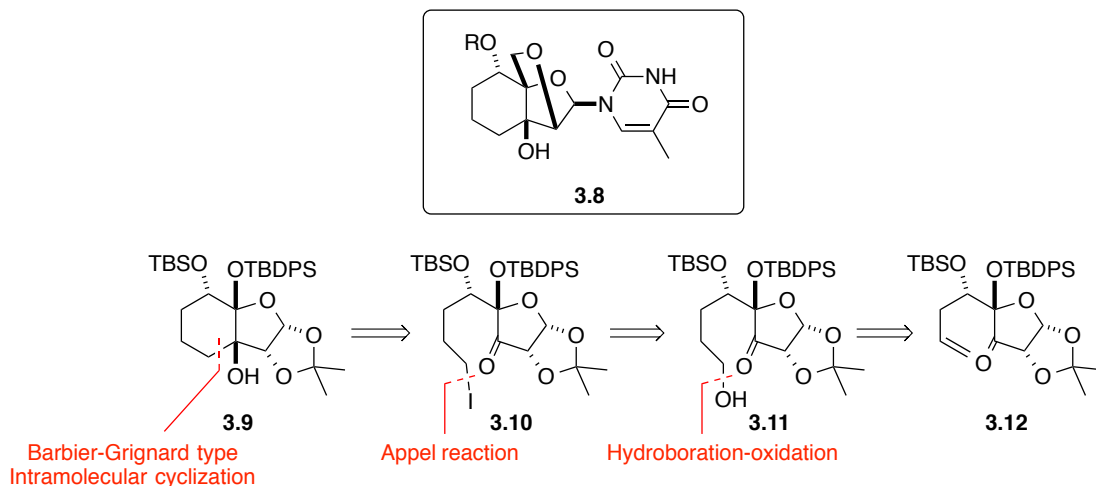
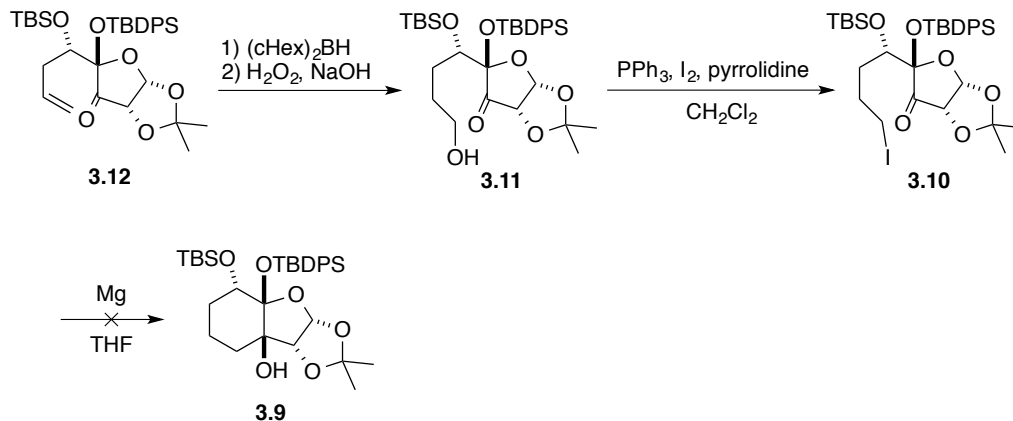


**Figure 57.** Retrosynthetic analysis for synthesizing key intermediate **3.9**.

Treatment of olefin **3.12** with dicyclohexylborane followed by hydrogen peroxide and sodium hydroxide gave primary alcohol **3.11** (Scheme 51). Alcohol **3.11** was converted to iodide **3.10** using triphenylphosphine and iodine. Treatment of iodide **3.10** with magnesium metal in THF, with heating or sonication to initialize the designed Barbier-Grignard type reaction provide no cyclization product and iodide starting material **3.10** was recovered (Scheme 51).

**Scheme 51.** Synthesis of key intermediate **3.9** by Barbier-Grignard type reaction.



The unsuccessful Barbier reaction inspired examination of a simpler reaction to involving 5-hexen-2-one (**3.13**), *n*-butyl iodide (5 equiv.) and magnesium (10 equiv.) in THF (Figure 58). Neither heating nor sonication triggered reaction. On the other hand, 1,2-dibromoethane caused the reaction to occur; however, ketol **3.14a** was isolated as the major product (44 % yield), instead of the expected addition product **3.15** (5 % yield) (Figure 58).

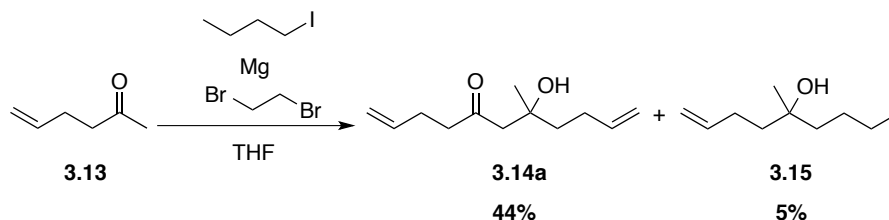
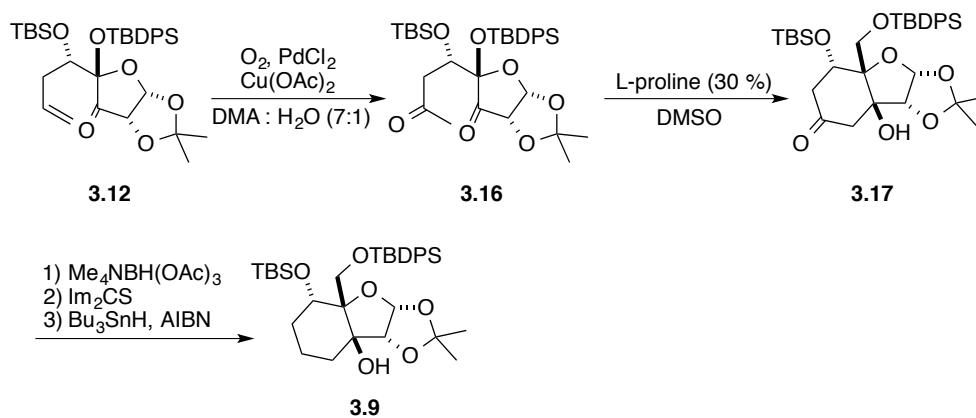


**Figure 58.** Unusual Barbier reaction between 5-hexen-2-one (**3.13**) and *n*-butyl iodide.

Faced with no success using the Barbier cyclization strategy, a new route based on proline catalyzed intramolecular aldol reaction was proposed and achieved successfully by Drs. Jernej Waggener and Bradley L. Merner (Scheme 52).<sup>60</sup> Alkene **3.12** was transformed methyl ketone **3.16** by a Wacker oxidation. Tricyclic **3.17** was successfully furnished through L-proline catalyzed intramolecular aldol reaction. The resulting ketone was reduced, and deoxygenated using the by Barton–McCombie reaction to give tricycle **3.9** (Scheme 52).

**Scheme 52.** Synthesis of key intermediate **3.9** by intramolecular aldol reaction.



Although the Barbier type reaction failed to give tricycle **3.9**, the interesting ketol product from the model reaction between 5-hexen-2-one (**3.13**) and *n*-butyl iodide attracted our attention (Figure 58). We decided to expand the scope of this reaction to afford  $\beta$ -ketols in one step.

## 3-2 Results

### 3-2-1 Intermolecular reactions

Intrigued by the formation of ketol **3.14a** from 5-hexen-2-one (**3.13**) (Figure 58), we screened other aliphatic methyl ketone substrates (Table 4, entries 1-10), as well as cyclic ketones (Table 4, entries 11-12) and aromatic methyl ketones (Table 4, entries 13-16). Similar self-aldol reactions were obtained with these ketones (Table 4). Reducing the amount of *n*-butyl iodide from 5 equiv. to 1 equiv., decreased slightly the average yield of  $\beta$ -ketols (Table 4). The yields of ketol product from cyclohexanone (Table 4, entries 11-12) were similar to that reported for the reaction between cyclohexanone and *i*-PrMgCl (Figure 56).<sup>59</sup> For aromatic ketones, 2-methoxyacetophenone gave lower yields (Table 4, entries 13-14), probably due to the steric bulk inhibiting formation of the ketol compared with the reaction of acetophenone (Table 4, entries 15-16).

**Table 4.** Intermolecular reactions under “Barbier conditions”

Entry	Substrate	<i>n</i> -BuI (equiv.)	$\beta$ -ketol product	Yield (%) <sup>a</sup>
1		1		38
2		5		44
3		1		35
4		5		38
5		1		34
6		5		40
7		1		38
8		5		45
9		1		48 <sup>b</sup>
10		5		76 <sup>b</sup>
11		1		32
12		5		44
13		1		22
14		5		24
15		1		39
16		5		42

The reactions were run with 1 mmol methyl ketone, 10 mmol magnesium turnings in 2 mL THF with heating (<1 min), then r.t. 2 h. <sup>a</sup> Average isolated yield. <sup>b</sup> Calculated from <sup>1</sup>H NMR spectra of crude sample.



### 3-2-2 Intramolecular reaction

With the promising results in intermolecular reactions (Table 4), we decided to investigate intramolecular reactions to form  $\beta$ -ketol. For intramolecular  $\beta$ -ketol formation, we selected to study the cyclization of triketone **3.18**, a reaction previously made famous by Zoltan G. Hajos and David R. Parrish at Hoffmann-La Roche and Schering AG over 40 years ago (Figure 59).<sup>61,62</sup> In their studies, triketone **3.18** was treated with aqueous piperidinium acetate, which gave racemic crystalline [3.2.1]-bicyclooctane: (**3.19**, m.p. 115 °C). Enolization was preferred in the cyclic rather than the aliphatic ketones, and enolate **3.18a**, which possessed a maximum  $\pi$ -orbital overlap reacted by a favorable alignment of the enolic double bond and the side-chain carbonyl group. On treatment with piperidine, followed by neutralizing acetic acid,  $\beta$ -ketol **3.19** could be isomerized to a more stable ketol **3.20** (m.p. 164 °C), in which the hydroxyl group adopted an axial orientation. Ketol **3.20** was considered the thermodynamic product compared to **3.19**. Enolate **3.18b** may thus undergo a retro-aldol reaction. In contrast, using piperidinium acetate in ether, the cyclization of **3.18** afforded the  $\beta$ -ketol **3.21**, which could be further dehydrated to give the enone **3.22**.<sup>61</sup> In an asymmetric version, treatment of triketone **3.18** with 3 mol % of L-proline in DMF gave  $\beta$ -ketol **3.23** in quantitative yield with an optical purity of > 93 % (Figure 59). The structure of ketol **3.23** was characterized by single-crystal X-ray analysis of its racemic mixture. Dehydration of **3.23** led to the corresponding  $\alpha,\beta$ -unsaturated diketone **3.24** (Hajos-Parrish diketone), which after recrystallization gave a product with an enantiomeric purity of > 97%.<sup>62</sup> This remarkable success in accessing enantiomerically enriched bicyclic ketol **3.21** through a proline-catalyzed intramolecular aldol reaction, is highly recognized as a pioneering example of organocatalysis.<sup>62,63</sup>

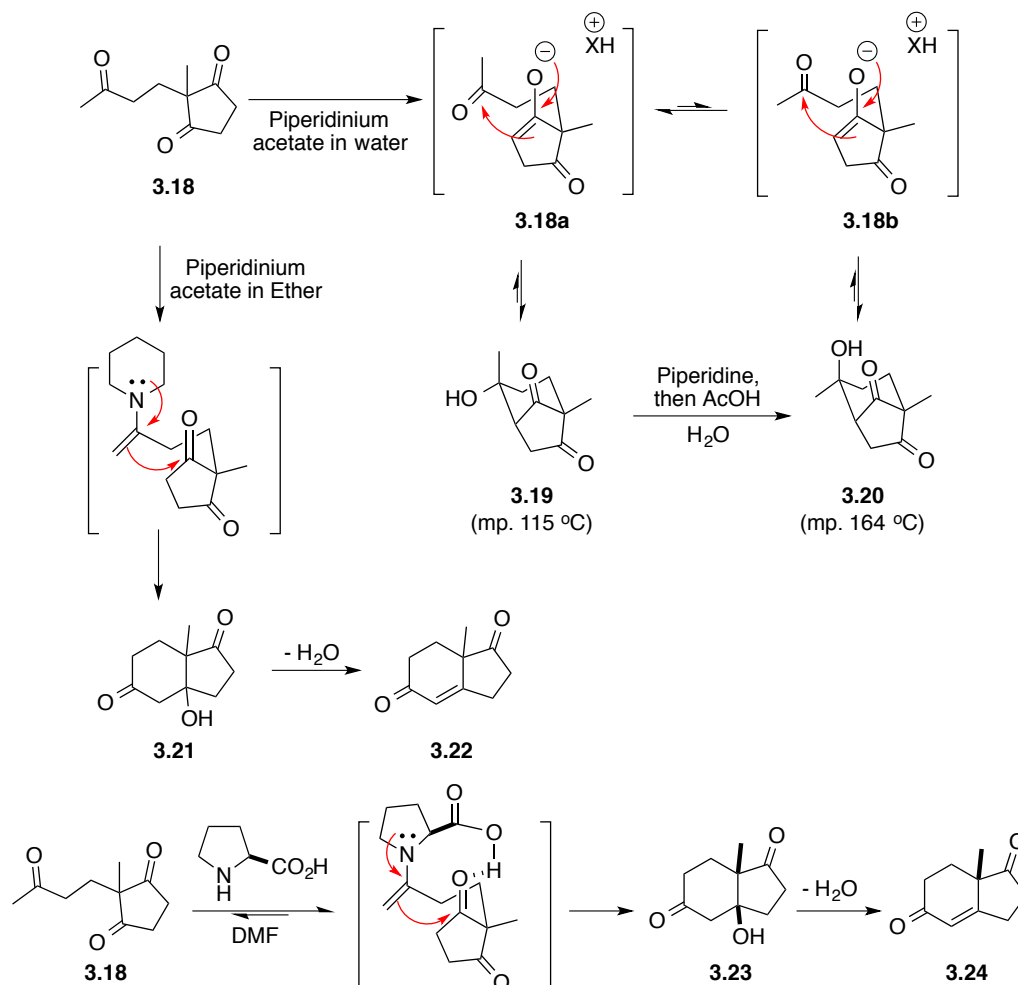


**Figure 59.**  $\beta$ -ketol formation from intramolecular cyclization of **3.18**.

In testing triketone **3.18** under our “Barbier conditions”, we hypothesized that  $\beta$ -ketols may form by intramolecular and intermolecular reactions. Indeed, the reaction between triketone **3.18** and *n*-butyl iodide generated a complicated mixture from which a major component was isolated as white solid in 35 % yield (Figure 60). X-ray analysis of the solid confirmed the structure of  $\beta$ -ketol **3.20** bearing an axial hydroxyl group arising from intramolecular reaction (Figure 61).

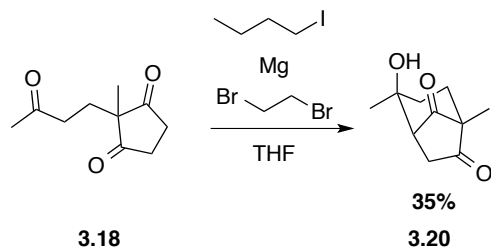


**Figure 60.** Intramolecular reaction of **3.18** under “Barbier conditions”

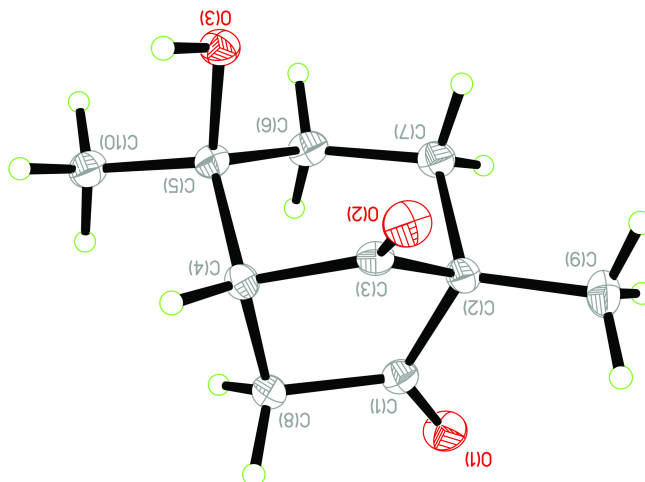
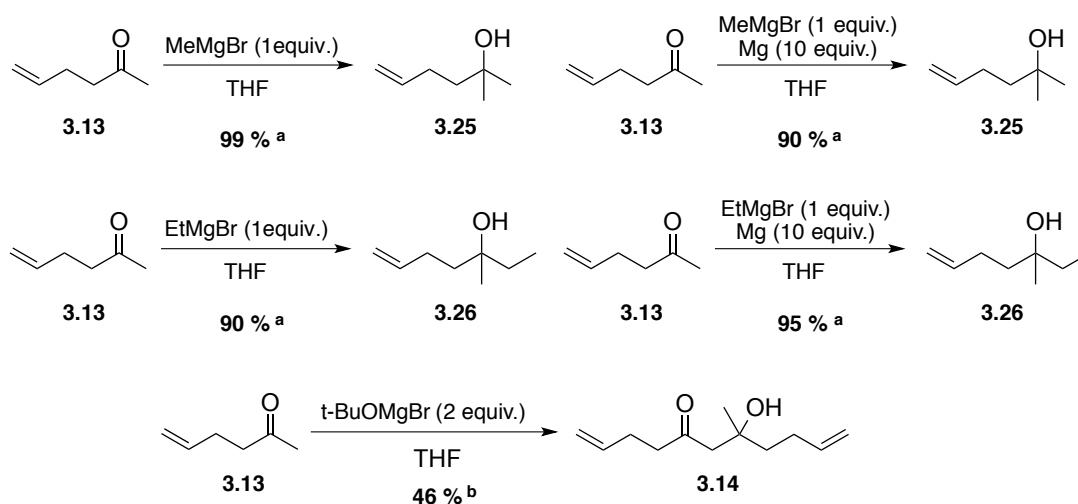


**Figure 61.** X ray structure of **3.20**.

### 3-3 Discussion

In self-aldol reactions of ketones, one molecule of ketone is enolized and the enolate reacts with another molecule of ketone to yield the ketol product. A base is usually required for enolate formation. Under our “Barbier reaction” conditions, the reaction mixture of ketone, *n*-BuI and magnesium metal, is treated with 1,2-dibromoethane in THF. The actual base (*e.g.*, ROMgI, Grignard reagent *n*-BuMgI) responsible for enolization is difficult to identify as discussed before in Grignard reactions (Figures 50, 54 and 55). Using commercially available Grignard reagents, MeMgBr and EtMgBr, in the presence or absence of magnesium metal, 5-hexen-2-one (**3.13**) reacted exclusively to give the addition products, with only trace amount ketol products (Figure 62). The Grignard reagent acted as nucleophile rather than a base. Although the Grignard reagent was not excluded as base, the magnesium alkoxide (ROMgI) generated in the reaction was considered as base (Figure 62). A tertiary magnesium alkoxide, *t*-BuOMgBr was prepared and reacted with ketone **3.13**. Ketol **3.14** was isolated in 46 % yield

(Figure 62). Similar aldol condensations were performed between a methyl ketone and an  $\alpha$ -bromoketone in the presence of *t*-BuOMgBr·Et<sub>2</sub>O in benzene, and a Et<sub>2</sub>NMgBr·Et<sub>2</sub>O in toluene to give the corresponding bromo  $\beta$ -ketols, as reported by Kulinkovich and Kel'in.<sup>64</sup>



<sup>a</sup> Calculated from <sup>1</sup>H NMR spectra of crude sample. <sup>b</sup> Isolated yield.

**Figure 62.** Reaction of **3.13** using commercial Grignard reagents, and *t*-BuOMgBr

Herein, for the sake of simplicity, R<sub>2</sub>MI represents any possible base (ROMgI, *n*-BuMgI etc.) involved in the self-aldol reaction mechanism (Figure 63). In the presence of base, the methyl ketone R<sub>1</sub>C=OCH<sub>3</sub> could be deprotonated to generate a magnesium enolate, which attacks another molecule of methyl ketone substrate to lead to the ketol product after hydrolysis (Figure 63). A magnesium chelated 6-membered transition state maybe involved in the aldol reaction.

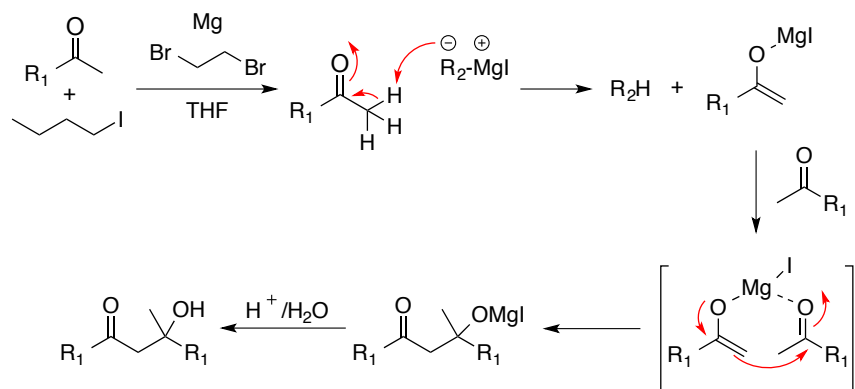


**Figure 63.** Plausible mechanism for the intermolecular self-aldol reaction of ketones.

For the intramolecular reaction of triketone **3.18**, a similar magnesium chelated transition state is proposed, because the hydroxyl group in the major product **3.20** is in the axial orientation, parallel to one of the carbonyl groups in the ring (Figure 64). The reaction of **3.18** with *t*-BuOMgBr lead to the formation of only **3.20** in 60 % yield (Figure 65), which also supports the existence of magnesium chelation.

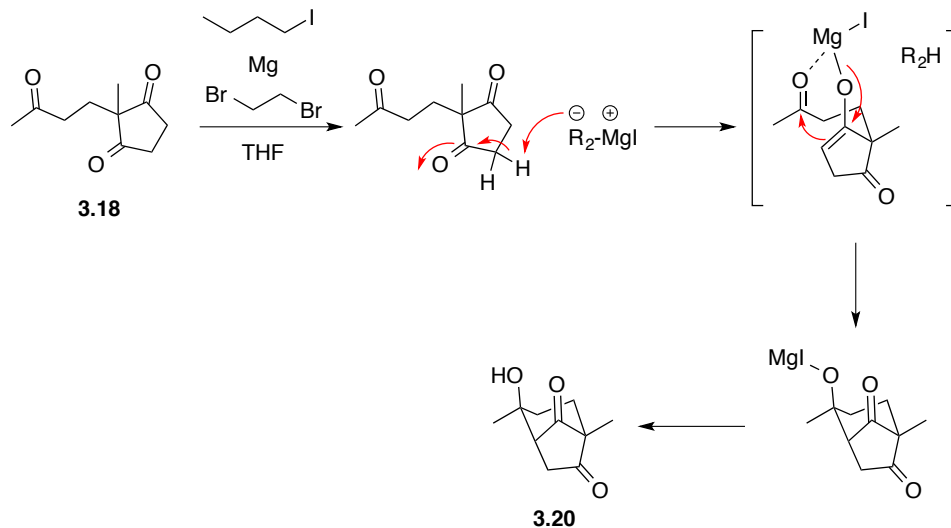


**Figure 64.** Plausible mechanism for the intramolecular aldol reaction.

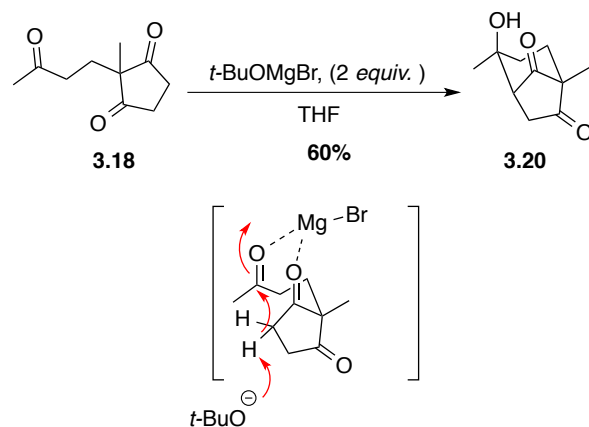


**Figure 65.** Reaction of triketone **3.18** with *t*-BuOMgBr

### 3-4 Conclusion

Intrigued by the discovery of an unusual result in a Barbier reaction, we conducted studies of intermolecular and intramolecular reactions to produce  $\beta$ -ketol products in moderate yield. We propose a mechanism involving a base promoted, magnesium chelated transition state (Figure 63 and 64). Furthermore, based on the selectivity of the intramolecular aldol cyclization in the generation of ketol **3.20** from triketone **3.18**, we hypothesized that a more efficient reaction for the formation of **3.20** could be developed by screening of bases and chelating additives. These will be discussed in Chapter four.

A direct method to access  $\beta$ -ketol is the aldol reaction. In the case of a methyl ketone, such as **3.13**, addition of a half equiv. of LDA should in principle, generate kinetic enolate to attack the ketone (**3.13**) and produce  $\beta$ -ketol **3.14**. Indeed, when such a reaction was tried, the  $\beta$ -ketol **3.14** was formed, but accompanied by unreacted ketone **3.13**. Organocatalytic aldol reactions catalyzed by proline leads to  $\beta$ -ketol; however, self-aldol reaction of ketones has not been explored to the best of my knowledge. Such aldol reactions are more common between methyl ketones and aldehydes.

In spite of the modest yields, the Barbier type synthesis of  $\beta$ -ketol as described in this thesis appears to be novel. In the original work, Barbier<sup>1</sup> had prepared the addition product **3.2** when using methyl iodide, and magnesium metal in ether (Figure 44). It is therefore curious

that using butyl iodide would lead to a  $\beta$ -ketol in substantial amount relative to direct addition. A critical experiments to be done is to determine the difference between methyl iodide and butyl iodide by using ethyl, propyl, isopropyl iodides to assess the effect of bulk on the tendency to promote self-aldol reaction versus direct addition. We have already established that a Grignard reactions with MeMgI and EtMgBr with ketone **3.13** led to tertiary alcohol addition products (Figure 62). The addition of BuMgCl also led to the tertiary alcohol contrary to the presently used Barbier conditions. Several by-products in the Barbier reaction of keonte **3.13** account for the modest yield of the  $\beta$ -ketol.

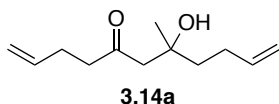
$\beta$ -Ketol was provided from the reaction of cyclopentanone and *i*-PrMgBr (Figure 56),<sup>59</sup> however, cyclohexanone gave a lower yield (Figure 56).<sup>59</sup> The same results appear to be taking place under Barbier condition with butyl iodide (Table 4, entries 11 and 12).

### 3-5 Experimental

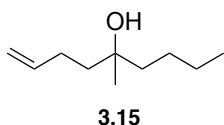
General methods are same as described in the experimental section of Chapter 1.

All the intermolecular reactions of methylketone under Barbier-Grignard type conditions were run with 1 mmol methyl ketone, 10 mmol magnesium turnings, in 2 mL THF and the typical procedure is shown below:

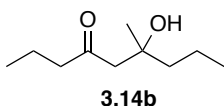
5-Hexene-2-one (**3.13**, 101 mg, 1.03 mmol, 120  $\mu$ L), magnesium turnings (247 mg, 10.3 mmol) and THF (2 mL) were added to a dried flask equipped with a condenser, following by *n*-butyl iodide (948 mg, 5.15 mmol, 586  $\mu$ L) and 2 drops of 1,2-dibromoethane at r.t. The reaction was initiated using a heat gun and after it was heated to reflux, the mixture was cooled to r.t., and stirred for 2 h when the clear solution turned cloudy. The reaction was quenched with saturated aqueous NH<sub>4</sub>Cl and extracted three times with CH<sub>2</sub>Cl<sub>2</sub> (3 $\times$ 10 mL). The combined organic phases were washed with brine, dried over MgSO<sub>4</sub> and filtered. The filtrate was evaporated under reduced pressure and the residue was purified by flash chromatography (hexane: EtOAc, 8:1 to 4:1) to give **3.14** (44 mg, 44 %) as pale yellow oil, and **3.15** (8.1 mg, 5 %) as pale yellow oil.



**7-Hydroxy-7-methylundeca-1,10-dien-5-one (3.14a).**  $^1\text{H}$ NMR (400 MHz,  $\text{CDCl}_3$ )  $\delta$  5.85-5.74 (m, 2H), 5.14-4.85 (m, 4H), 2.70-2.44 (m, 4H), 2.32 (q,  $J = 7.2$  Hz, 2H), 2.22-2.00 (m, 2H), 1.69-1.46 (m, 2H), 1.21 (s, 3H);  $^{13}\text{C}$  NMR (100 MHz,  $\text{CDCl}_3$ )  $\delta$  212.3, 138.6, 136.6, 115.5, 114.4, 71.5, 51.6, 43.5, 41.1, 28.2, 27.3, 26.7; FTIR ( $\text{cm}^{-1}$ ) (neat) 3478, 3077, 2976, 2924, 1699, 1641, 1374, 1132, 996, 910; HRMS (ESI) calcd for  $\text{C}_{12}\text{H}_{21}\text{O}_2$  ( $\text{M}+\text{H}$ ) $^+$  197.1536, found 197.1546.

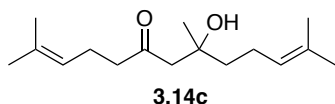


**5-Methylnon-1-en-5-ol (3.15)**  $^1\text{H}$  NMR (400 MHz,  $\text{CDCl}_3$ )  $\delta$  5.85 (ddt,  $J = 16.8, 10.4, 6.4$  Hz, 1H), 5.04 (dq,  $J = 17.2, 1.6$  Hz, 1 H), 4.97-4.93 (m, 1H), 2.15- 2.08 (m, 2H), 1.56-1.52 (m, 2H), 1.48-1.43 (m, 2H), 1.37-1.28 (m, 5H), 1.17 (s, 3H), 0.92 (t,  $J = 6.8$  Hz, 3H);  $^{13}\text{C}$  NMR (100 MHz,  $\text{CDCl}_3$ )  $\delta$  139.1, 114.3, 72.6, 41.7, 40.7, 28.3, 26.8, 26.1, 23.2, 14.1; FTIR ( $\text{cm}^{-1}$ ) (neat) 3383, 3078, 2958, 2931, 2861, 1640, 1465, 1375, 1298, 1260, 1232, 1143, 1088, 1030, 994, 948, 907.

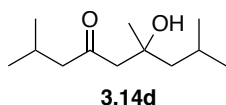


**6-Hydroxy-6-methylnonan-4-one (3.14b)** was obtained as pale yellow oil (31 mg, 35 %) using 1.03 mmol *n*-butyl iodide [34 mg, 38 % using 5.15 mmol *n*-butyl iodide].  $^1\text{H}$  NMR (400 MHz,  $\text{CDCl}_3$ )  $\delta$  3.88 (s, 1H), 2.56 (q,  $J = 17.0$  Hz, 2H), 2.39 (t,  $J = 7.3$  Hz, 2H), 1.64-1.55 (m, 2H), 1.48-1.43 (m, 2H), 1.38-1.30 (m, 2H), 1.18 (s, 3H), 0.91 (m, 6H);  $^{13}\text{C}$  NMR (100 MHz,  $\text{CDCl}_3$ )  $\delta$  213.5, 71.7, 51.3, 46.5, 44.5, 26.7, 17.2, 16.9, 14.5, 13.6; FTIR ( $\text{cm}^{-1}$ ) (neat) 3470, 2960, 2934, 2874, 1697, 1458, 1373, 1148, 1055, 1019, 939, 888.; HRMS (ESI) calcd for  $\text{C}_{10}\text{H}_{20}\text{NaO}_2$  ( $\text{M}+\text{Na}$ ) $^+$  195.1356, found 195.1356.

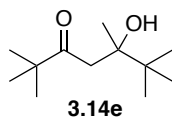




**8-Hydroxy-2,8,12-trimethyltrideca-2,11-dien-6-one (3.14c)** was obtained as yellow oil (44 mg, 34 %) using 1.03 mmol *n*-butyl iodide [52 mg, 40 % using 5.15 mmol *n*-butyl iodide].  $^1\text{H}$  NMR (400 MHz,  $\text{CDCl}_3$ )  $\delta$  5.09-5.02 (m, 2H), 3.85 (s, 1H), 2.57 (q,  $J = 17.0$  Hz, 2H), 2.44 (t,  $J = 7.3$  Hz, 2H), 2.24 (q,  $J = 7.2$  Hz, 2H), 2.10-1.95 (m, 2H), 1.67 (s, 6H), 1.60 (s, 6H), 1.53-1.47 (m, 2H), 1.20 (s, 3H);  $^{13}\text{C}$  NMR (100 MHz,  $\text{CDCl}_3$ )  $\delta$  213.3, 133.2, 131.9, 124.4, 122.5, 71.8, 51.7, 44.8, 42.1, 26.9, 25.9, 25.8, 22.8, 22.4, 17.8, 17.8; FTIR ( $\text{cm}^{-1}$ ) (neat) 3411, 2971, 2929, 1706, 1450, 1376, 1147, 1056, 982; HRMS (ESI) calcd for  $\text{C}_{16}\text{H}_{28}\text{NaO}_2$  ( $\text{M}+\text{Na}$ ) $^+$  275.1982, found 275.1982.

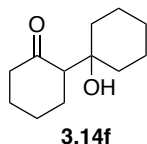


**6-Hydroxy-2,6,8-trimethylnonan-4-one (3.14d)** was obtained as pale yellow oil (39 mg, 38 %) using 1.03 mmol *n*-butyl iodide, [46 mg, 45 % using 5.15 mmol *n*-butyl iodide].  $^1\text{H}$  NMR (400 MHz,  $\text{CDCl}_3$ )  $\delta$  3.87 (s, 1H), 2.55 (q,  $J = 17.2$  Hz, 2H), 2.28 (d,  $J = 6.9$  Hz, 2H), 2.18-2.08 (m, 1H), 1.82-1.72 (m, 1H), 1.40 (qd,  $J = 14.2, 5.9$  Hz, 2H), 1.21 (s, 3H), 1.00-0.91 (m, 12H);  $^{13}\text{C}$  NMR (100 MHz,  $\text{CDCl}_3$ )  $\delta$  213.3, 72.2, 53.6, 52.6, 50.5, 27.2, 24.8, 24.5, 24.4, 24.1, 22.5, 22.4; FTIR ( $\text{cm}^{-1}$ ) (neat) 3489, 2955, 2871, 1697, 1466, 1367, 1152, 1055 947, 894; HRMS (ESI) calcd for  $\text{C}_{12}\text{H}_{24}\text{NaO}_2$  ( $\text{M}+\text{Na}$ ) $^+$  223.1669, found 223.1674.

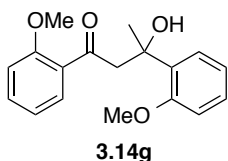


**5-Hydroxy-2,2,5,6,6-pentamethylheptan-3-one (3.14e)** was obtained as yellow oil (crude without purification) (49 mg, 48 %) using 1.03 mmol *n*-butyl iodide, [78 mg, 76 % using 5.15 mmol *n*-butyl iodide].  $^1\text{H}$  NMR (400 MHz,  $\text{CDCl}_3$ )  $\delta$  4.60 (s, 1H), 2.86 (d,  $J = 16.8$  Hz, 1H), 2.46 (d,  $J = 16.8$  Hz, 1H), 1.13 (s, 12H), 0.94 (s, 9H);  $^{13}\text{C}$  NMR (100 MHz,  $\text{CDCl}_3$ )  $\delta$  220.2, 75.5, 45.3, 40.2, 37.7, 26.0, 25.1, 21.9; FTIR ( $\text{cm}^{-1}$ ) (neat)

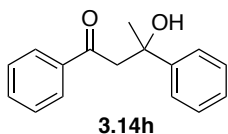
3484, 2958, 2873, 1691, 1478, 1465, 1395, 1369, 1324, 1215, 1155, 1101, 1067, 1008, 939, 873, 845, 810; HRMS (ESI) calcd for C<sub>12</sub>H<sub>24</sub>NaO<sub>2</sub> (M+Na)<sup>+</sup> 223.1669, found 223.1662.



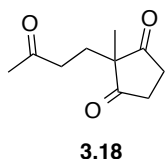
**1'-Hydroxy-[1,1'-bi(cyclohexan)]-2-one (3.14f)** was obtained as colorless oil (32 mg, 32 %) using 1.03 mmol *n*-butyl iodide, [44 mg, 44 % using 5.15 mmol *n*-butyl iodide]. <sup>1</sup>H NMR (400 MHz, CDCl<sub>3</sub>) δ <sup>1</sup>H NMR (400 MHz, CDCl<sub>3</sub>) 3.67 (s, 1H), 2.40-2.31 (m, 3H), 2.20-2.16 (m, 1H), 2.14-2.07 (m, 1H), 1.96-1.89 (m, 1H), 1.76-1.53 (m, 8H), 1.46-1.35 (m, 3H), 1.33-1.10 (m, 2H); <sup>13</sup>C NMR (100 MHz, CDCl<sub>3</sub>) δ 216.4, 72.0, 58.9, 43.9, 36.1, 33.2, 29.0, 28.3, 25.9, 25.5, 21.7, 21.4; FTIR (cm<sup>-1</sup>) (neat) 3513, 2928, 2858, 1693, 1448, 1395, 1348, 1308, 1258, 1217, 1179, 1040, 996, 966, 947, 894, 853, 836; HRMS (ESI) calcd for C<sub>12</sub>H<sub>20</sub>NaO<sub>2</sub> (M+Na)<sup>+</sup> 219.1356, found 219.1364.



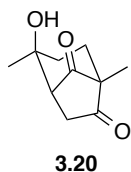
**3-Hydroxy-1,3-bis(2-methoxyphenyl)butan-1-one (3.14g)** was obtained as yellow oil (33 mg, 24 %) using 1.0 mmol *n*-butyl iodide, [36 mg, 24% using 5.0 mmol *n*-butyl iodide]. <sup>1</sup>H NMR (400 MHz, CDCl<sub>3</sub>) 7.70 (dd, *J* = 7.7, 1.7 Hz, 1H), 7.43-7.38 (m, 1H), 7.25 (d, *J* = 1.8 Hz, 1H), 7.21-7.15 (m, 1H), 6.98 (td, *J* = 7.6, 1.0 Hz, 1H), 6.93-6.86 (m, 2H), 6.72 (d, *J* = 8.2 Hz, 1H), 4.90 (s, 1H), 4.18 (d, *J* = 16.6 Hz, 1H), 3.89 (s, 3H), 3.63 (s, 3H), 3.39 (d, *J* = 16.6 Hz, 1H), 1.63 (s, 3H); <sup>13</sup>C NMR (100 MHz, CDCl<sub>3</sub>) δ 204.9, 158.3, 155.4, 134.8, 133.3, 129.7, 129.2, 128.0, 127.1, 120.7, 120.5, 111.3, 110.7, 73.5, 55.5, 54.8, 52.3, 28.1; FTIR (cm<sup>-1</sup>) (neat) 3468, 2931, 2837, 1671, 1596, 1485, 1462, 1435, 1357, 1282, 1240, 1179, 1162, 1124, 1023, 950, 805, 753; HRMS (ESI) calcd for C<sub>18</sub>H<sub>20</sub>NaO<sub>4</sub> (M+Na)<sup>+</sup> 323.1254, found 323.1258.



**3-Hydroxy-1,3-diphenylbutan-1-one (3.14h)** was obtained as pale yellow oil (47 mg, 39 %) using 1.0 mmol *n*-butyl iodide, [50 mg, 42% using 5.0 mmol *n*-butyl iodide]. <sup>1</sup>H NMR (400 MHz, CDCl<sub>3</sub>) δ 7.92 (dd, *J* = 8.1, 0.8 Hz, 2H), 7.70-7.56 (m, 1H), 7.56-7.37 (m, 4H), 7.37-7.16 (m, 3H), 4.89 (s, 1H), 3.80 (d, *J* = 17.4 Hz, 1H), 3.36 (d, *J* = 17.5 Hz, 1H), 1.64 (s, 3H); <sup>13</sup>C NMR (100 MHz, CDCl<sub>3</sub>) δ 201.3, 147.6, 136.9, 133.7, 128.7, 128.2, 128.0, 126.6, 124.3, 73.5, 48.8, 30.9; FTIR (cm<sup>-1</sup>) (neat) 3454, 3058, 3026, 2972, 2927, 1665, 1597, 1579, 1492, 1447, 1368, 1341, 1282, 1214, 1181, 1071, 1027, 1003, 936, 868, 817, 754, 724, 700, 689; HRMS (ESI) calcd for C<sub>16</sub>H<sub>16</sub>NaO<sub>2</sub> (M+Na)<sup>+</sup> 263.1043, found 263.1031.



**2-Methyl-2-(3-oxobutyl)cyclopentane-1,3-dione (3.18)** was prepared according to a known procedure.<sup>65</sup> The spectroscopic data were in agreement with the proposed structures and matched those reported in the literature<sup>65,66</sup> <sup>1</sup>H NMR (400 MHz, CDCl<sub>3</sub>) δ 2.79-2.50 (m, 4H), 2.29 (t, *J* = 7.3 Hz, 2H), 1.94 (s, 3H), 1.70 (t, *J* = 7.3 Hz, 2H), 0.93 (s, 3H); <sup>13</sup>C NMR (100 MHz, CDCl<sub>3</sub>) δ 215.5, 207.5, 54.7, 37.0, 34.4, 29.6, 27.4, 18.5.

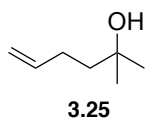


**(±)-4β-Hydroxy-1β,4α-dimethylbicyclo[3.2.1]octane-7,8-dione (3.20).** For intramolecular reactions under Barbier conditions, triketone **3.18** (50 mg, 0.28 mmol), magnesium turnings (67 mg, 2.8 mmol) and THF (0.5 mL) were added to a dried flask equipped with a condenser, following by *n*-butyl iodide (52mg, 0.28 mmol, 32 uL) and 2 drops of 1,2-dibromoethane at r.t. The reaction was initiated using a heat gun and after it was heated to reflux, the mixture was cooled to r.t., and stirred for 3 h when the clear solution turned orange/red. The reaction

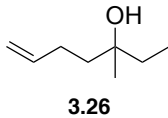
was quenched by saturated aqueous  $\text{NH}_4\text{Cl}$  and extracted three times with  $\text{CH}_2\text{Cl}_2$  ( $3 \times 5$  mL). The combined organic phases were washed with brine, dried over  $\text{MgSO}_4$  and filtered. The volatiles were removed under reduced pressure and the residue was purified by flash chromatography (hexane: EtOAc, 2:1 to 1:1) to give alcohol **3.20** (17.5 mg, 35 %) as white solid. m.p. 163-164 °C (lit.<sup>67</sup>, m.p. 160-161 °C). The spectroscopic data were in agreement with the proposed structures and matched those reported in the literature.<sup>68</sup>  $^1\text{H}$  NMR (400 MHz,  $\text{CDCl}_3$ )  $\delta$  2.79 (m, 1H), 2.68-2.53 (m, 2H), 2.14 (td,  $J = 12.6, 6.9$  Hz, 1H), 2.06 (s, 1H), 1.85 (ddd,  $J = 12.5, 5.3, 1.9$  Hz, 1H), 1.80-1.62 (m, 2H), 1.41 (s, 3H), 1.08 (s, 3H);  $^{13}\text{C}$  NMR (100 MHz,  $\text{CDCl}_3$ )  $\delta$  214.3, 211.3, 80.7, 58.3, 57.5, 42.8, 38.6, 32.3, 28.6, 11.9; FTIR ( $\text{cm}^{-1}$ ) (neat) 3465, 2972, 2932, 1763, 1717, 1448, 1402, 1382, 1371, 1357, 1332, 1285, 1247, 1217, 1185, 1165, 1127, 1106, 1072, 1055, 1018, 978, 957, 942, 919, 858, 809; HRMS (ESI) calcd for  $\text{C}_{10}\text{H}_{14}\text{NaO}_3$  ( $\text{M}+\text{Na}$ )<sup>+</sup> 205.0835, found 205.0833.

Typical procedure for reaction of ketone **3.13** with Grignard reagents:

5-Hexene-2-one (**3.13**, 53 mg, 0.54 mmol, 64  $\mu\text{L}$ ), with or without magnesium turnings (130 mg, 5.4 mmol), and THF (1 mL) were added to a dried flask equipped with a condenser, following by the addition of methyl magnesium bromide (3M in  $\text{Et}_2\text{O}$ , 0.54 mmol, 180  $\mu\text{L}$ ) at r.t. The reaction was stirred for 0.5 h before being quenched with saturated aqueous  $\text{NH}_4\text{Cl}$ . The resulting mixture was extracted three times with  $\text{CH}_2\text{Cl}_2$  ( $3 \times 5$  mL). The combined organic phases were washed with brine, dried over  $\text{MgSO}_4$  and then filtered. The solvent was removed under reduced pressure to give a crude residue, which was directly examined by  $^1\text{H}$  NMR spectroscopy to calculate the ratio of addition product and self-addition product.



**2-Methylhex-5-en-2-ol (3.25)** is a known compound, and the spectroscopic data were in agreement with the proposed structures and matched those reported in the literature.<sup>69</sup>  $^1\text{H}$  NMR (400 MHz,  $\text{CDCl}_3$ )  $\delta$  5.83 (ddt,  $J = 16.8, 10.2, 6.6$  Hz, 1H), 5.02 (dd,  $J = 17.1, 1.4$  Hz, 1H), 4.93 (d,  $J = 10.1$  Hz, 1H), 2.12 (dd,  $J = 16.2, 6.8$  Hz, 2H), 1.70 (s, 1H), 1.63 - 1.45 (m, 2H), 1.20 (s, 6H);  $^{13}\text{C}$  NMR (100 MHz,  $\text{CDCl}_3$ )  $\delta$  139.0, 114.2, 70.6, 42.7, 29.1, 28.7.



**3-Methylhept-6-en-3-ol (3.26).** The spectroscopic data were in agreement with the proposed structures and matched those reported in the literature (one of its enantiomer).<sup>70</sup> <sup>1</sup>H NMR (400 MHz, CDCl<sub>3</sub>) δ 5.85 (ddt, *J* = 16.8, 10.2, 6.6 Hz, 1H), 5.04 (dd, *J* = 17.1, 1.7 Hz, 1H), 4.95 (dd, *J* = 10.2, 1.8 Hz, 1H), 2.11 (m, 2H), 1.78-1.40 (m, 4H), 1.16 (s, 3H), 0.90 (t, *J* = 7.5 Hz, 3H); <sup>13</sup>C NMR (100 MHz, CDCl<sub>3</sub>) δ 139.1, 114.3, 72.8, 40.2, 34.3, 28.3, 26.2, 8.2.

Reaction of trione **3.18** with *t*-BuOMgBr:

*t*-BuOMgBr (0.5 M in THF) was prepared by treating methyl magnesium bromide (3M in Et<sub>2</sub>O, 9 mmol, 3 mL) with anhydrous *t*-butyl alcohol (0.667 g, 9 mmol, 0.84 mL) in THF (14.16 mL) at 0 °C, followed by stirring for 1h at r.t.

To trione **3.18** (50 mg, 0.27 mmol) dissolved in THF (2 mL) freshly prepared *t*-BuOMgBr (0.5 M in THF, 0.27 mmol, 0.54 mL) was added at r.t. After stirring for 12 h, one more equivalent of *t*-BuOMgBr (0.5 M in THF, 0.27 mmol, 0.54 mL) was added. The reaction was stirred for another 12 h, quenched by the addition of saturated aqueous NH<sub>4</sub>Cl and extracted with CH<sub>2</sub>Cl<sub>2</sub> (3×5 mL). The combined organic phases were washed with brine, dried over MgSO<sub>4</sub> and then filtered. The volatiles were removed under reduced pressure and the residue was purified by flash chromatography (hexane: EtOAc, 2:1 to 1:1) to give **3.20** (30 mg, 60 %) as a white solid.

### 3-6 References

1. Barbier, P. *C. R. Acad. Sci.* **1899**, 128, 110.
2. For review of Barbier reactions, see (a) Trost, B.; M. *Comprehensive Organic Synthesis*. Fleming I., Ed. Pergamon Press: Oxford, **1991**; Vol. 1, Part 1, 255-266. (b) Blomberg, C. *The Barbier Reaction and Related One-Step Processes, in Reactivity and Structure: Concepts in Organic Chemistry*, Vol. 31, Hafner, K.; Lehn, J. M.; Rees, C. W.; von Ragué Schleyer, P.; Trost, B. M.; Zahradník, R. Springer-Verlag, **1993**. (c) Li, C. J. *Tetrahedron*, **1996**, 52, 5643.

3. Li, C. J. *The Greening of a Fundamental Reaction: Metal-Mediated Reactions in Water*, Chapter 7, 74–86, in *Green Chemical Syntheses and Processes*, Editor(s): Paul, T.; Anastas, P. T.; Heine, L. G.; Williamson, T. C. **2000**, vol. 767.
4. For Barbier-type allylation: see (a) Nokami, J.; Otera, J.; Sudo, T.; Okawara, R. *Organometallics*, **1983**, 2, 191. (b) Li, C. J.; Chan, T. H. *Tetrahedron Lett.* **1991**, 32, 7017. (c) Paquette, L. A.; Mitzelm T. M. *Tetrahedron Lett.* **1995**, 36, 6863. (d) Isaak, M. B.; Chan, T. H. *Tetrahedron Lett.* **1995**, **36**, 8957. (e) Paquette, L. A.; Mitzel, T. M. *J. Am. Chem. Soc.* **1996**, *118*, 1931. (f) Zhou, J. Y.; Jia, Y.; Sun, G. F.; Wu, S. H. *Synth. Commun.* **1997**, 27, 1899. (g) Paquette, L. A.; Lobben, P. C. *J. Org. Chem.* **1998**, 63, 5604. (h) Loh, T. P.; Hu, Q. Y.; Chok, Y. K.; Tan, K. T. *Tetrahedron Lett.* **2001**, 42, 9277.
5. For Barbier-type propargylation, see: (a) Isaac, M. B.; Chan, T. H. *J. Chem. Soc. Chem. Commun.* **1995**, 1003. (b) Yi, X. H.; Meng, Y.; Li, C. J. *Chem. Commun.* **1998**, 449. (c) Jögi, A.; Mäeorg, U. *Molecules*, **2001**, 6, 964. (d) Mitzel, T. M.; Palomo, C.; Jendza, K. *J. Org. Chem.* **2001**, 67, 136. (e) Liu, L.; Zhang, Y.; Zhang, H.; Huang, K.; Gao, B. X.; Zou, M.; Zhou, X.; Wang, H.; Li, J. *Org. Biomol. Chem.* **2014**, 12, 5393.
6. Keh, C. C. K.; Wei, C.; Li, C. J. *J. Am. Chem. Soc.* **2003**, 125, 4062.
7. Zhou, F.; Li, C. J. *Nat. Commun.* **2014**, 5, 4254.
8. Nokami, J.; Wakabayashi, S.; Okawara, R. *Chem. Lett.* **1984**, 869.
9. Ivković, A.; Matović, R.; Saičić, R. N. *J. Serb. Chem. Soc.* **2002**, 67, 141.
10. Lannoye, G.; Sambasivarao, K.; Wehrli, S.; Cook, J. M.; Weiss, U. *J. Org. Chem.* **1988**, 53, 2327.
11. (a) Okude, Y.; Hirano, S.; Hiyama, T.; Nozaki, H. *J. Am. Chem. Soc.* **1977**, 99, 3179. (b) Fürstner, A. *Chem. Rev.* **1999**, 99, 991. (c) Kishi, Y. *Tetrahedron*, **2002**, 58, 6239.
12. (a) Still, W. C.; Mobilio, D. *J. Org. Chem.* **1983**, 48, 4785. (b) Aicher, T.; Buszek, K.; Fang, F.; Forsyth, C.; Jung, S.; Kishi, Y.; Matelich, M.; Scola, P.; Spero, D.; Yoon, S. *J. Am. Chem. Soc.* **1992**, 114, 3162. (c) MacMillan, D. W. C.; Overman, L. E. *J. Am. Chem. Soc.* **1995**, 117, 10391. (d) Chen, X. T.; Bhattacharya, S. K.; Zhou, B. S.; Gutteridge, C. E.; Pettus, T. R. R.; Danishefsky, S. J. *J. Am. Chem. Soc.* **1999**, 121, 6563. (e) Lotesta, S. D.; Liu, J.; Yates, E. V.; Krieger, I.; Sacchettini, J. C.; Freundlich, J. S.; Sorensen, E. J. *Chem. Sci.* **2011**, 2, 1258.

13. Roethle, P. A.; Trauner, D. *Org. Lett.* **2006**, *8*, 345.
14. Molle, G.; Bauer, P. *J. Am. Chem. Soc.* **1982**, *104*, 3481.
15. Li, C. J.; Zhang, W. C. *J. Am. Chem. Soc.* **1998**, *120*, 9102.
16. Li, C. J.; Chan, T. H. *Organic Reactions In Aqueous Media*; Wiley & Sons: New York, **1997**.
17. Grignard, V. *C. R. Acad. Sci.* **1900**, *130*, 1322.
18. For reviews of Grignard reagents, see (a) Negishi, E. *Organometallics in Organic Synthesis*, Vol.1, Wiley- VCH: New york, **1980**. (b) Lai, Y. H. *Synthesis*, **1981**, 585. (c) Wakefield, B. J. *Organomagnesium Methods in Organic Chemistry*, Academic Press: San Diego, CA, **1995**. (d) Silverman, G. S.; Rakita, P. E. *Handbook of Grignard Reagents*, Marcel Dekker: New York, **1996**. (e) Richey, H. G., Jr. *Grignard Reagents: New Development*; Wiley: Chichester, UK, **2000**. (f) Knochel, P.; Dohle, W.; Gommermann, N.; Kneisel, F. F.; Kopp, F.; Korn, T.; Sapountzis, I.; Vu, V. A. *Angew. Chem., Int. Ed.* **2003**, *42*, 4302. (g) Hoffmann, R. W. *Chem. Soc. Rev.* **2003**, *32*, 225. (h) Garst, J. F.; Soriaga, M. P. *Coord. Chem. Rev.* **2004**, *248*, 623. (i) Knochel, P. *Handbook of Functionalized Organometallics*, Wiley-VCH: Weinheim, Germany, **2005**. (j) Hatano, M.; Ishihara, K. *Synthesis*, **2008**, *11*, 1647. Luderer, M. R.; Bailey, W. F.; Luderer, M. R.; Fair, J. D.; Dancer, R. J.; Sommer, M. B. *Tetrahedron Asymmetry*, **2009**, *20*, 981.
19. (a) Rogers, H. R.; Hill, C. L.; Fujiwara, Y.; Rogers, R. J.; Mitchell, H. L.; Whitesides, G. M. *J. Am. Chem. Soc.* **1980**, *102*, 217. (b) Carey, F. A.; Sundberg, R. J. *Advanced Organic chemistry Part B: Reactions and Synthesis. 5th edition*. Springer, **2010**, PP 620-624.
20. Schlenk; W.; Schlenk, Jr. W. *Chem. Ber.* **1929**, *62*, 920.
21. Parris, G. E.; Ashby, E. C. *J. Am. Chem. Soc.* **1971**, *93*, 1206.
22. Allen, P. E. M.; Hagias, S.; Lincoln, S. F.; Mair, C.; Williams, E. H. *Ber. Bunsenges. Phys. Chem.* **1982**, *86*, 515.
23. Strohmeier, W.; Seifert, F. *Chem. Ber.* **1961**, *94*, 2356.
24. Ashby, E. C. *Q. Rev. Chem. Soc.* **1967**, *21*, 259.
25. Ashby, E. C. *Pure Appl. Chem.* **1980**, *52*, 545.
26. Ashby, E. C.; Duke, R. B.; Neuman, H. M. *J. Am. Chem. Soc.* **1967**, *89*, 1964.
27. Ashby, E. C.; Laemmle, J.; Neumann, H. M. *Acc. Chem. Res.* **1974**, *7*, 272.

28. Kharasch, M. S.; Reinmuth, O. *Grignard Reactions of Nonmetallic Substances*, Prentice-Hall, Inc., London, **1954**.
29. Blicke, F. F.; Powers, L. D. *J. Am. Chem. Soc.* **1929**, *51*, 3378.
30. Whitmore, F. C.; George, R. S. *J. Am. Chem. Soc.* **1942**, *64*, 1239.
31. Casnati, G.; Pochini, A.; Salerno, G.; Ungaro, R. *Tetrahedron Lett.* **1974**, *12*, 959.
32. Kang, S. H.; Jun, H. S. *Chem. Commun.* **1998**, 1929.
33. Blomberg, C.; Mosher, H. S. *J. Organometal. Chem.* **1968**, *13*, 519.
34. Whitmore, F. C.; Randall, D. I. *J. Am. Chem. Soc.* **1942**, *64*, 1242.
35. Whitmore, F. C.; Lester, C. T. *J. Am. Chem. Soc.* **1942**, *64*, 1247.
36. Grignard, V. *Ann. Chim.* **1901**, *7*, 433.
37. Mosher, H. S.; Combe, E. L.; *J. Am. Chem. Soc.* **1950**, *72*, 3994.
38. Marshall, J. *J. Chem. Soc., Trans.* **1914**, *105*, 527.
39. Marshall, J. *J. Chem. Soc., Trans.* **1915**, *107*, 509.
40. Meerwein, H.; Schmidt, R. *Liebigs Ann.* **1925**, *444*, 221.
41. Schmidlin, J. *Ber. Dtsch. Chem. Ges.* **1906**, *39*, 4198.
42. (a) Gomberg, M.; Bachmann, W. E. *J. Am. Chem. Soc.* **1927**, *49*, 236. (b) Bachmann, W. E.; Shankland, R. V. *J. Am. Chem. Soc.* **1929**, *51*, 306. (c) Gomberg, M.; Bailar Jr., J. C. *J. Am. Chem. Soc.* **1929**, *51*, 2229.
43. Blicke, F. F.; Powers, L. D. *J. Am. Chem. Soc.* **1929**, *51*, 3378.
44. Arbuzov, A. E.; Arbuzova, I. A. *J. Gen. Chem. USSR*, **1932**, *2*, 388.
45. Blomberg, C.; Salinger, R. M.; Mosher, H. S. *J. Org. Chem.* **1969**, *34*, 2385.
46. Holm, T.; Crossland, I. *Acta Chem. Scand.* **1971**, *25*, 59.
47. Grignard, V. *C. R. Acad. Sci.* **1902**, *134*, 849.
48. Grignard, V. *J. Chem. Soc., Abstr.* **1902**, *82*, A420.
49. Bredt-Savelsberg, M. *J. Prakt. Chem.* **1924**, *107*, 65.
50. Arnold, R. T.; Bank, H.; Liggett, R. W. *J. Am. Chem. Soc.* **1941**, *63*, 3444.
51. Lutz, R. E.; Kibler, C. J. *J. Am. Chem. Soc.* **1940**, *62*, 360.
52. Grignard, V.; Dubien, M. *C. R. Acad. Sci.* **1923**, *177*, 299.
53. Grignard, V.; Fluchaire, M. *Ann. Chim.* **1928**, *9*, 5.
54. Swain, C. G.; Boyles, H. B. *J. Am. Chem. Soc.* **1951**, *73*, 870.



55. McBee, E. T.; Pierce, O. R.; Higgins, J. F. *J. Am. Chem. Soc.* **1952**, *74*, 1736.
56. Chastrette, M.; Amouroux, R. *Bull. Soc. Chim. Fr.* **1970**, 4348.
57. Chastrett, M.; Amouroux, R. *J. Chem. Soc., Chem. Commun.* **1970**, 470.
58. Weidmann, B.; Seebach, D. *Angew. Chem., Int. Ed.* **1983**, *22*, 31.
59. Imamoto, T.; Takiyama, N.; Nakamura, K.; Hatajima, T.; Kamiya, Y. *J. Am. Chem. Soc.* **1989**, *111*, 4392.
60. Hanessian, S.; Waggener, J.; Merner, B. L.; Giacometti, R. D.; Østergaard, M. E.; Swayze, E. E.; Seth, P. P. *J. Org. Chem.* **2013**, *78*, 9064.
61. Hajos, Z. G.; Parrish, D. R. *J. Org. Chem.*, **1974**, *39*, 1612.
62. Hajos, Z. G.; Parrish, D. R. *J. Org. Chem.*, **1974**, *39*, 1615.
63. Berkessel, A.; Gröger, H. *Asymmetric Organocatalysis*, First Edition, Wiley-VCH, **2005**.
64. Kel'in, A. V.; Kulinkovich, O. G. *Synthesis* **1996**, 330.
65. Lacoste, E.; Vaique, E.; Berlande, M.; Pianet, I.; Vincent, J.-M.; Landais, Y. *Eur. J. Org. Chem.* **2007**, 167.
66. Bunce, R. A.; Dauben, W. G. *J. Org. Chem.* **1983**, *48*, 4642.
67. Dauben, W. G.; Bunce, R. A. *J. Org. Chem.* **1983**, *48*, 4642.
68. Davies, S. G.; Russell, A. J.; Sheppard, R. L.; Smith, A. D.; Thomson, J. E. *Org. Biomol. Chem.* **2007**, *5*, 3190.
69. Nicolai, S.; Waser, J. *Org. Lett.* **2011**, *13*, 6324.
70. Pulis, A. P.; Blair, D. J.; Torres, E.; Aggarwal, V. K. *J. Am. Chem. Soc.*, **2013**, *135*, 16054.

# Chapter 4: From Synthetic Study of 2-hydroxy-2,5-dimethylbicyclo[3.2.1]octane-6,8-dione (a constitutional isomer of the Hajos-Parrish ketone), to Catalytic Synthesis of Tertiary $\beta$ -Ketols

## 4-1 Introduction

### 4-1-1 $\beta$ -Ketols from Aldol reaction

The aldol reaction, between two aldehydes, was first introduced by Charles-Adolphe Wurtz in 1872<sup>1,2</sup> and has been widely recognized as one of most important methods for the construction carbon-carbon bonds.<sup>3</sup> Joining two carbonyl compounds (aldehydes, ketones or esters) to give a  $\beta$ -ketol product (Figure 66), in the process one of the carbonyl compounds bearing an  $\alpha$ -proton is enolized and the nucleophilic enolate (basic conditions), or a enol (acidic conditions), performs nucleophilic attack on another carbonyl compound (Figure 66).

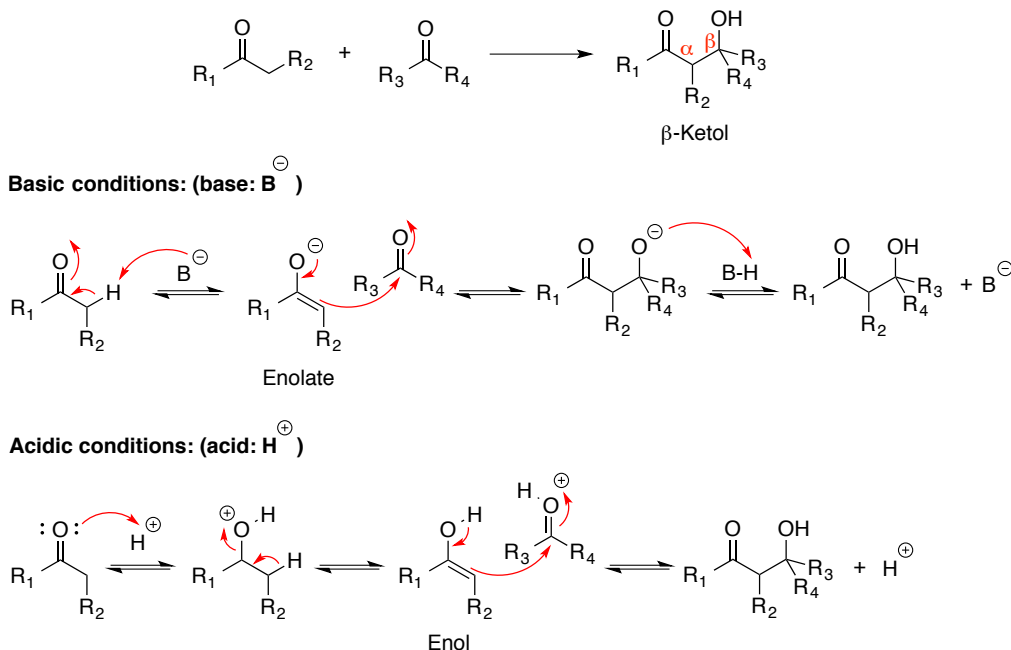


**Figure 66.** Aldol reaction under basic and acidic conditions.

The resulting  $\beta$ -hydroxyl carbonyl moiety is a common structural unit exhibited in many important natural products and drugs. Such as FK-506,<sup>4,6</sup> epothilones A and B,<sup>7-10</sup> and Taxol<sup>11,12</sup> (Figure 67).

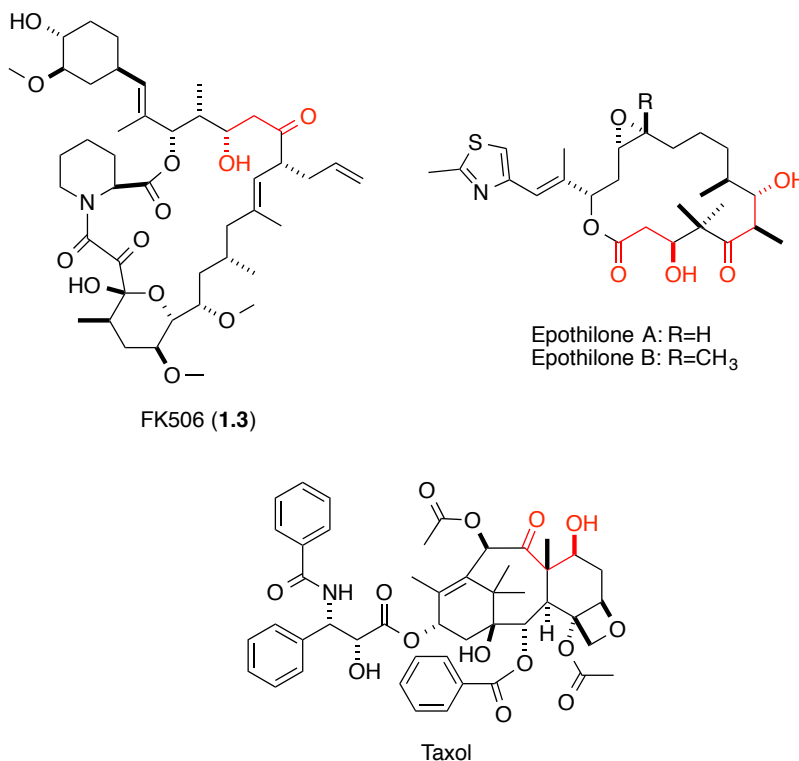


**Figure 67.** Examples of  $\beta$ -hydroxyl carbonyl units in natural products and drugs.

An aldol reaction may generate two new stereogenic centers (at the  $\alpha$  and  $\beta$ -positions). The challenge of stereoselectively obtaining a specific  $\beta$ -ketol has led to great efforts to develop asymmetric aldol reactions, using a variety of chiral auxiliaries, ligands and catalysts.<sup>3</sup> Evans,<sup>13</sup> and others,<sup>14,15</sup> discovered a series of chiral oxazolidinone auxiliaries, that provide high diastereoselectivity in the presence of a Lewis acid (*n*-Bu<sub>2</sub>BOTf,<sup>13,14</sup> (c-hex)<sub>2</sub>BCl,<sup>16</sup> Sn(OTf)<sub>2</sub>,<sup>17</sup> TiCl<sub>4</sub>,<sup>15,17</sup> MgCl<sub>2</sub>,<sup>18</sup> MgBr<sub>2</sub>·(OEt)<sub>2</sub><sup>19</sup> etc.) and base (DIPEA, TEA etc.) (Figure 68). Mukaiyama and coworkers discovered a type of aldol reaction, termed Mukaiyama aldol reaction, which uses silyl enol ethers as nucleophiles.<sup>20</sup> This reaction was widely used in synthesis of  $\beta$ -ketols, and chiral catalysts were developed by Mukaiyama,<sup>21</sup> Corey,<sup>22</sup> Carreira,<sup>23</sup> Evans,<sup>24</sup> Denmark,<sup>25</sup> and Yamamoto<sup>26</sup> to achieve asymmetric versions (Figure 69).

More recently, organocatalysis has been extensively explored in the aldol reaction.<sup>27</sup> As mentioned in Chapter 3, in 1974, Hajos and Parrish used proline to catalyze the intramolecular aldol reaction of triketone **3.18** (Figure 59).<sup>28</sup> Later List<sup>29</sup> and Barbas<sup>29,30</sup> developed L-proline catalyzed asymmetric aldol reactions between acetone and aldehydes (Figure 70). MacMillan<sup>31</sup> used L-proline successfully to achieve a cross-aldol reaction between aldehydes (Figure 70). Based on the success of proline, derivatives were developed to catalyze aldol reactions (Figure 70).<sup>30,32-36</sup> Although these versatile chiral auxiliaries, ligands, and catalysts have advanced the stereoselective synthesis of  $\beta$ -ketols from aldol reactions, catalytic asymmetric aldol reactions remain a topic of interest in organic synthesis.

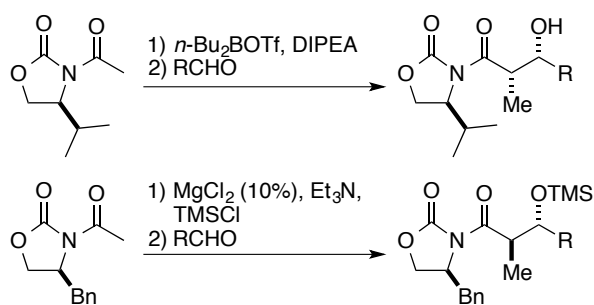


**Figure 68.** Examples of Evans' oxazolidinone auxiliaries in the aldol reaction.

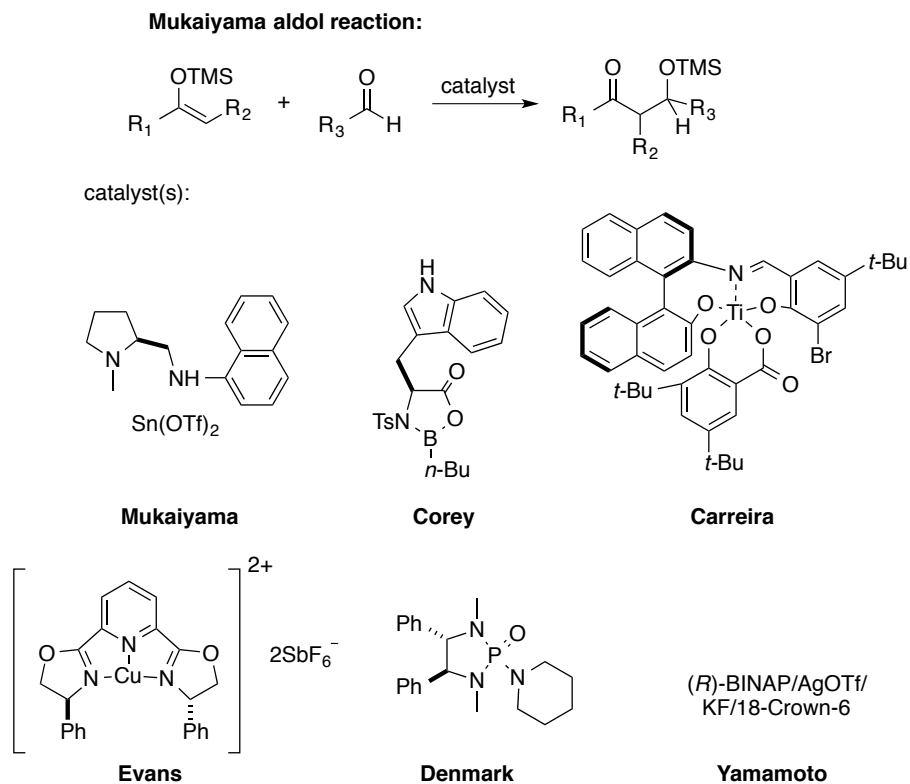


**Figure 69.** Examples of chiral catalysts used in Mukaiyama aldol reaction.

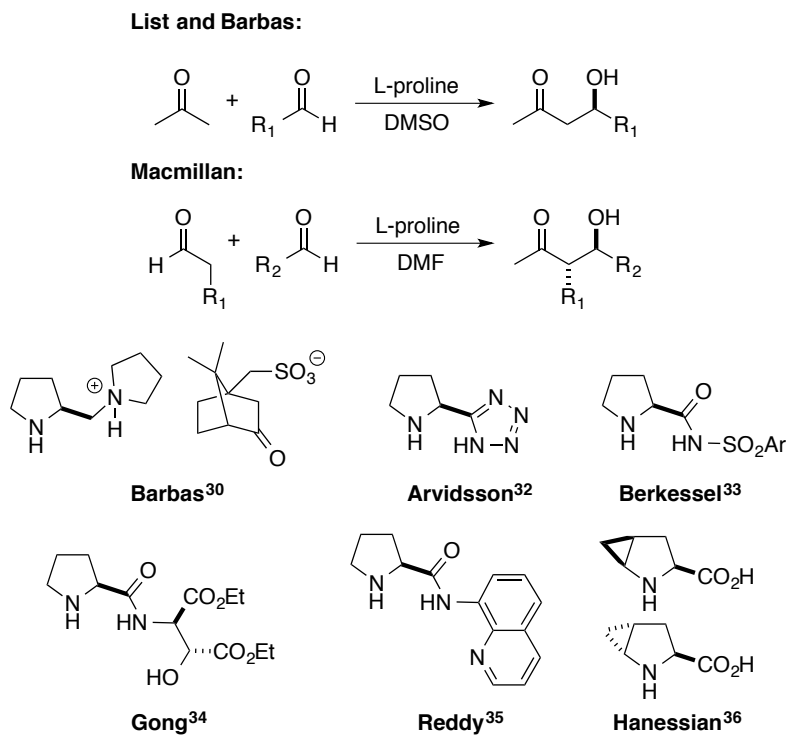


**Figure 70.** Examples of proline and its derivatives as catalysts in aldol reaction.

### 4-1-2 Synthetic background of $\beta$ -ketol **3.20** from triketone **3.18**

Since Hajos and Parrish disclosed the  $\beta$ -ketol products from triketone **3.18** via intramolecular aldol reaction (Figure 59, Chapter 3, section 3-2-1),<sup>28, 37</sup> catalytic enantioselective synthesis of  $\beta$ -ketol **3.21** has been studied to determine the mechanism and enhance the methodologies.<sup>38</sup> Formation of other ketol products (**3.19** and **3.20**) has been scarcely explored.

For the synthesis of ketol **3.20**, few examples have been reported. Dauben and Bunce<sup>39</sup> studied the reaction between 2-methyl-1,3-cyclopentanedione and methyl vinyl ketone at high pressure. Under 15 kbar in the presence of acetonitrile and  $\text{Et}_3\text{N}$ , ketol **3.20** was generated in 52 % yield (Figure 71). Shibasaki and coworkers<sup>40</sup> discovered a series of rare earth metal alkoxides that catalyze aldol reactions. In the intramolecular aldol cyclization of **3.18** with 10 mol%  $\text{Zr}(\text{O}-t\text{-Bu})_4$ , ketol **3.20** was generated in 30 % yield. Using  $\text{La}_3(\text{O}-t\text{-Bu})_9$  as the catalyst, both  $\beta$ -ketol **3.19** and **3.20** were obtained in 30 % and 40 % yield respectively. Yttrium alkoxide reacted selectively to generate **3.20** in almost quantitative yield. No cyclized product was observed using  $\text{Al}(\text{O}-t\text{-Bu})_3$ . To achieve enantioselectivity in the synthesis of **3.20**, a chiral ytterbium alkoxide was prepared and tested. After 6 days at  $-52\text{ }^\circ\text{C}$ , ketol **3.20** was obtained in 60 % yield with 52 % *e.e.* (Figure 72).<sup>40</sup> To the best of our knowledge, this is the only example of enantioselective synthesis of ketol **3.20**. Although Davies and coworkers<sup>41</sup> reported using (1'*R*, 2'*S*)-5-(2'-aminocyclopentan-1'-yl) tetrazole as a chiral catalyst in an attempt to achieve asymmetric synthesis of **3.20** from **3.18** (Figure 73), they obtained **3.20** in 67 % yield without enantioselectivity. Mahrwald and coworkers<sup>42</sup> employed a tetranuclear BINOL-titanium complex as catalyst, obtained racemic **3.20** in 44 % yield (Figure 74).

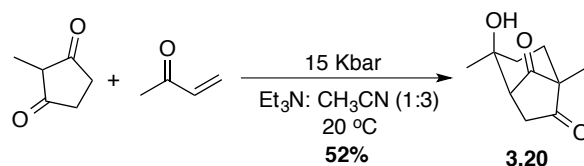


**Figure 71.** Synthesis of **3.20** by Dauben and Bunce.

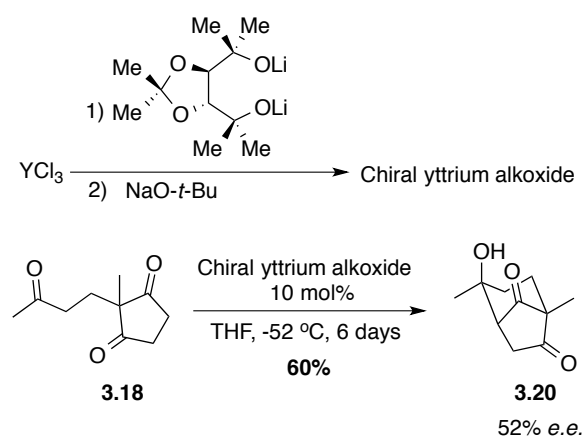
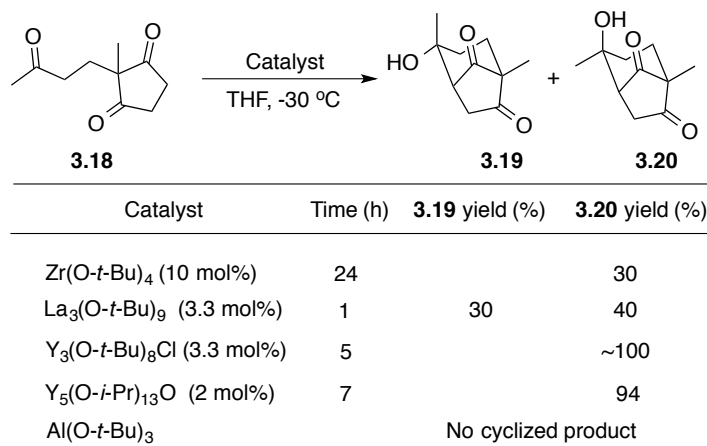


**Figure 72.** Synthesis of **3.19** and **3.20** by Shibasaki and coworkers.

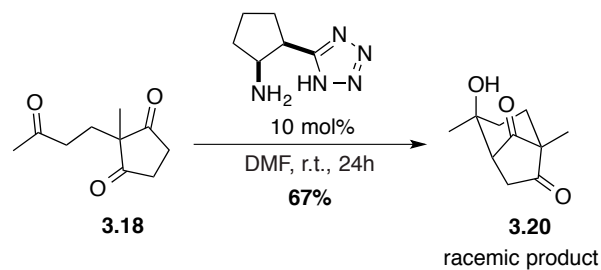


**Figure 73.** Synthesis of **3.20** by Davies and coworkers.

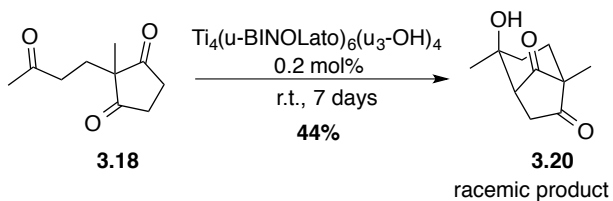


**Figure 74.** Synthesis of **3.20** by Mahrwald and coworkers.

Our previous study of the cyclization of trione **3.18** under Barbier conditions showed that ketol **3.20** was the favored product (Figure 50, Chapter 3, section 3-1-2), and possibly formed *via* a magnesium-chelated transition state (Figure 64, Chapter 3, section 3-3). We envisioned that using a suitable base and chelating additives (e.g. magnesium salts), ketol **3.20** could be generated from **3.18** selectively and efficiently, eventually in an asymmetric or catalytic version.

## 4-2 Results

### 4-2-1 Screening of reaction conditions for the synthesis of $\beta$ -ketol **3.20**

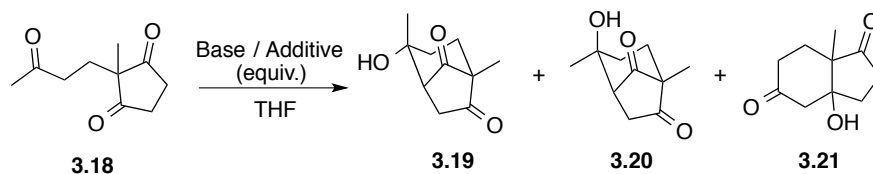
#### 4-2-1-1 Temperature and catalysts loading

As described in our hypothesis, a suitable base was needed to promote the cyclization. We chose 1,8-diazabicyclo[5.4.0]undec-7-ene (DBU), due to its non-nucleophilicity and relatively strong basicity (pKa 16.8 in THF).<sup>43</sup> Triketone **3.18** was treated with DBU (1 equiv.) at room temperature, and converted to all three  $\beta$ -ketol products after 24 h (Table 5, entry 1). Decreasing the temperature to -40 °C, the reaction did not reach completion in 24 h, and **3.19**, **3.20** and **3.21** were generated in equal proportion (Table 5, entry 2). Next, we surmised that introducing an additive would aid in the forming of a chelated transition state, as proposed in Figure 64 (Chapter 3, section 3-3), and lead to  $\beta$ -ketol **3.20** as the major product. Lithium bromide is a mild and neutral inorganic salt. The small size of the lithium cation could benefit the required chelate model in this intramolecular reaction.<sup>44</sup> In the presence of LiBr (1 equiv.) and DBU (1 equiv.), the reaction rate was significantly accelerated at -40 °C, and ketol **3.20** was obtained as the major product as expected (Table 5, entry 3). In further tests using a catalytic amount of DBU and LiBr (5 mol % of each), the reaction proceeded selectively affording **3.20** in 88 % isolated yield (Table 5, entry 4). Under the same catalytic conditions, lowering the temperature to -78 °C, slowed the reaction rate, and only 6 % of **3.20** was observed by <sup>1</sup>H NMR spectroscopy of the reaction mixture (Table 5, entry 5). At room temperature, the same conditions gave **3.20** as the major product, but less selectively compared to at -40 °C (Table 2, entry 6). Employment of DBU or LiBr used alone yielded only a trace amounts of **3.20** (Table 5, entries 7 and 8). The combination of 5 mol% DBU and



LiBr in THF at -40 °C promoted the catalytic reaction to give  $\beta$ -ketol **3.20** in high yield and excellent selectivity (Table 5, entry 4).

**Table 5.** Screening of temperature and catalysts loading.



Entry	Base / Additive (equiv.)	Temperature (°C)	3.18 (%) <sup>a</sup>	3.19	3.20	3.21
				Yield (%) <sup>a</sup>	Yield (%) <sup>a</sup>	Yield (%) <sup>a</sup>
1	DBU (1)	r.t.	4	36	38	22
2	DBU (1)	- 40	69	9	11	11
3	DBU (1), LiBr (1)	- 40	2	21	62	15
4	DBU (0.05), LiBr (0.05)	- 40	-	-	89(88) <sup>b</sup>	11
5	DBU (0.05), LiBr (0.05)	- 78	85	-	6	9
6	DBU (0.05), LiBr (0.05)	r.t.	6	13	68	13
7	DBU (0.05)	- 40	94	2	2	2
8	LiBr (0.05)	- 40	93	1	1	5

Reactions were run with 0.14 mmol triketone in 1 mL THF for 24 h. <sup>a</sup> Calculated from the <sup>1</sup>H NMR spectra of crude reaction material. <sup>b</sup> Isolated yield.

#### 4-2-1-2 Solvents

Intrigued by the catalytic effect of DBU and LiBr, a series of solvents were tested in the reaction of **3.18** (Table 6). Aprotic solvents (Table 6, entries 1 - 5), favored ketol **3.20**; THF was the preferred solvent. The reaction in DMF was also selective, and led to **3.20** in 76 % isolated yield. Protic solvents favored formation of  $\beta$ -ketol **3.19** (72 % isolated yield using MeOH) (Table 6, entry 6).

**Table 6.** Screening of solvents.

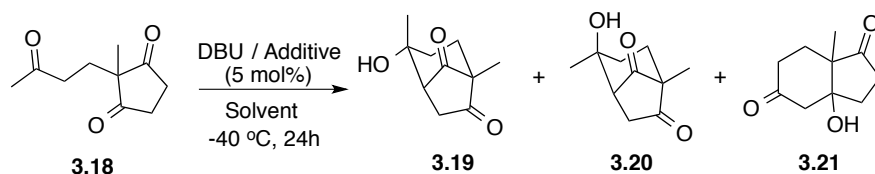
Reaction scheme showing the conversion of triketone **3.18** to products **3.19**, **3.20**, and **3.21** using DBU, LiBr (5 mol%), and a solvent at -40 °C for 24 hours.

Entry	Solvent	<b>3.18</b> (%) <sup>a</sup>	<b>3.19</b> Yield (%) <sup>a</sup>	<b>3.20</b> Yield (%) <sup>a</sup>	<b>3.21</b> Yield (%) <sup>a</sup>
1	THF	-	-	89 (88) <sup>b</sup>	11
2	Et <sub>2</sub> O	11	24	53	12
3	CH <sub>2</sub> Cl <sub>2</sub>	27	20	43	10
4	EtOAc	10	8	73	9
5	DMF	8	3	82 (76) <sup>b</sup>	7
6	MeOH	5	76 (72) <sup>b</sup>	5	14

The reactions were run with 0.14 mmol triketone in 1 mL THF for 24 h. <sup>a</sup> Calculated from <sup>1</sup>H NMR spectra of crude reaction mixture. <sup>b</sup> Isolated yield.

#### 4-2-1-3 Additives

Based on the success of LiBr as an additive, other inorganic salts were tested as chelates. Similar to LiBr, 5 mol % LiCl and DBU gave ketol product **3.20** in 86 % isolated yield (Table 7, entry 4). The anion of the lithium salts had little effect on the reaction. Switching to magnesium salts, neither MgBr<sub>2</sub> nor MgBr<sub>2</sub>·Et<sub>2</sub>O with DBU in THF resulted in the formation of ketol **3.20** (Table 7, entry 6 and 8). Changing solvent to DMF, which should give better solubility for magnesium salts, led to trace amounts of **3.20**. Lithium cation appeared crucial for catalyzing formation of ketol **3.20** from triketone **3.18**.

**Table 7.** Screening of additives.

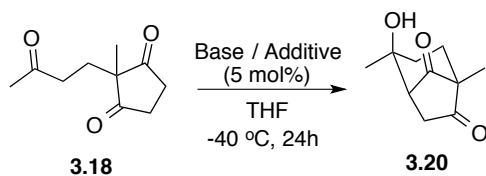
Entry	Base / Additive (5 %)	Solvent	<b>3.18</b> (%) <sup>a</sup>	<b>3.19</b> Yield (%) <sup>a</sup>	<b>3.20</b> Yield (%) <sup>a</sup>	<b>3.21</b> Yield (%) <sup>a</sup>
1	LiBr	THF	93	1	1	5
2	DBU, LiBr	THF	-	-	89 (88) <sup>b</sup>	11
3	LiCl	THF	98	-	-	2
4	DBU, LiCl	THF	-	-	84 (86) <sup>b</sup>	16
5	MgBr <sub>2</sub>	THF	92	-	-	8
6	DBU, MgBr <sub>2</sub>	THF	92	-	-	8
7	MgBr <sub>2</sub> · Et <sub>2</sub> O	THF	93	-	-	7
8	DBU, MgBr <sub>2</sub> · Et <sub>2</sub> O	THF	93	-	-	7
9	MgBr <sub>2</sub>	DMF	95	-	1	4
10	DBU, MgBr <sub>2</sub>	DMF	92	-	5	3

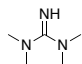
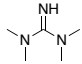
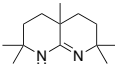
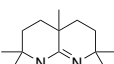
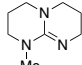
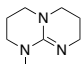
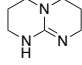
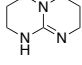
The reactions were run with 0.14 mmol triketone in 1 mL THF for 24 h. <sup>a</sup> Calculated from <sup>1</sup>H NMR spectra of crude reaction mixture. <sup>b</sup> Isolated yield.

#### 4-2-1-4 Achiral bases

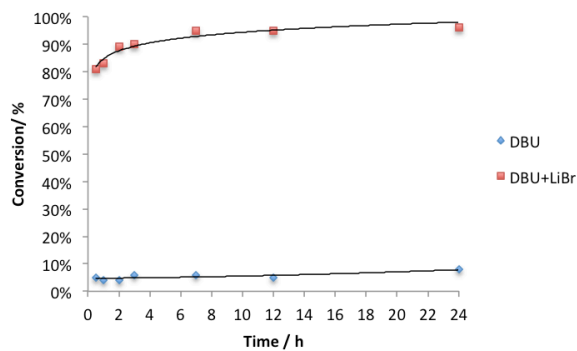
With the optimized catalyst loading (5 mol %), temperature (-40 °C), solvent (THF), and additive (LiBr), we studied a series of bases as catalyst for this reaction (Table 8). Using relatively weaker bases (Et<sub>3</sub>N, TMEDA and pyrrolidine) with and without LiBr, little β-ketol **3.20** was generated (Table 8, entries 1-6). Switching to piperidine, and stronger bases, with 5 % LiBr gave ketol **3.20** in excellent yield (Table 8, entries 8, 10, 12, 14 and 16). The presence of 5 mol % of 3,3,6,9,9-pentamethyl-2,10-diazabicyclo[4.4.0]dec-1-ene (Eschenmoser's amidine) (Table 8, entries 11)<sup>45</sup> gave selectively ketol **3.20** in 35 % yield based on <sup>1</sup>H NMR spectroscopy of the reaction mixture. Tests with 5 mol% of 1,5,7-triazabicyclo[4.4.0]dec-5-ene (TBD) (Table 8, entries 15) generated **3.20** in 89 % yield, indicating that TBD alone was an efficient catalyst to generate β-ketol **3.20** in high yield and selectivity. Employment of 5 mol % of TBD with LiBr also led to **3.20** in excellent yield (Table 8, entries 16). The reaction

rates were also studied over a 24 h period with DBU, the bicyclic Eschenmoser's amidine and TBD (Figure 75-77). It was clear that LiBr accelerated the reaction with DBU and Eschenmoser's amidine in the formation of **3.20**.

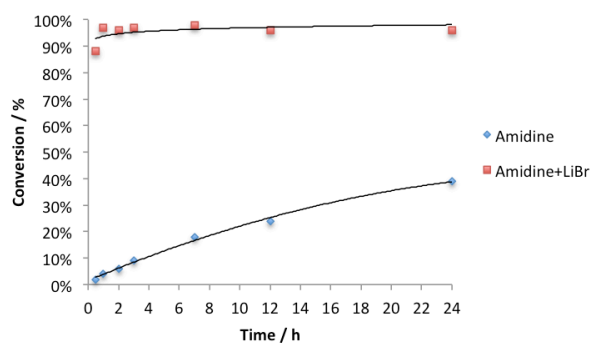
**Table 8.** Screening of bases.

Entry	Base / Additive (5%)	<b>3.20</b> Yield (%) <sup>a</sup>	pKa (in THF) <sup>a</sup>
1	Et <sub>3</sub> N	1	12.5
2	Et <sub>3</sub> N, LiBr	1	
3	TMEDA	n.r.	12.8
4	TMEDA, LiBr	3	
5	Pyrrolidine	1	13.5
6	Pyrrolidine, LiBr	4	
7	Piperidine	n.r.	14.3
8	Piperidine, LiBr	91 (86) <sup>b</sup>	
9		4	15.5
10	 LiBr	87 (86) <sup>b</sup>	
11		35	-
12	 LiBr	89 (87) <sup>b</sup>	
13		5	17.9
14	 LiBr	92 (88) <sup>b</sup>	
15		90 (89) <sup>b</sup>	21.0
16	 LiBr	92 (90) <sup>b</sup>	

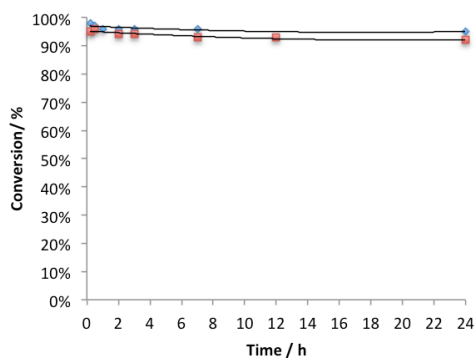
The reactions were run with 0.14 mmol triketone in 1 mL THF for 24 h. <sup>a</sup> Calculated from <sup>1</sup>H NMR spectra of crude reaction mixture. <sup>b</sup> Isolated yield. pKa values were taken from references 43 and 46.



**Figure 75.** Kinetic profiles of DBU, with and without LiBr-catalyzed aldol reaction of **3.18** and the formation of **3.20**.

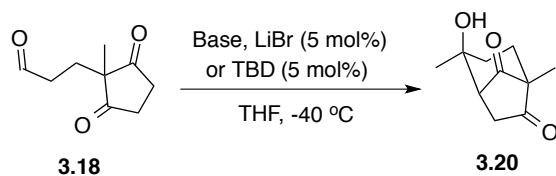


**Figure 76.** Kinetic profiles of Eschenmoser amidine, with and without LiBr-catalyzed aldol reaction of **3.18** and the formation of **3.20**.



**Figure 77.** Kinetic profiles of TBD, with and without LiBr catalyzed aldol reaction of **3.18** and the formation of **3.20**.

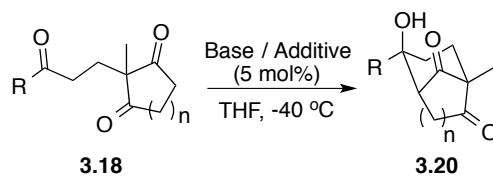
Thus, we have developed two types of catalysts to synthesize  $\beta$ -ketol **3.20** from triketone **3.18** (Figure 78).  $\beta$ -Ketol **3.20** can be selectively generated either by using DBU and LiBr, or 5 mol % TBD (Table 8).

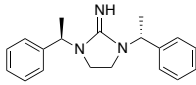
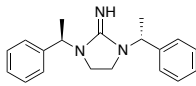
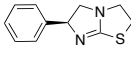
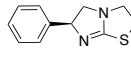
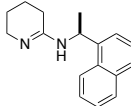
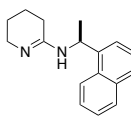


**Figure 78.** Catalytic synthesis of  $\beta$ -ketol **3.20** from triketone **3.18**

#### 4-2-2 Studies toward an enantioselective synthesis of **3.20**

Encouraged by the catalytic effect of bases with and without LiBr in the synthesis of ketol **3.20** (Table 8), we tested chiral bases for the asymmetric synthesis of **3.20** (Table 9). Inspired by the use of sparteine in enantioselective deprotonation,<sup>47</sup> we used (-)-sparteine as chiral base, with and without LiBr, but no cyclization was observed (Table 9, entries 1 and 2). Employing (-)-sparteine as a ligand to generate a chiral lithium complex by mixing it the DBU and LiBr conditions had no influence on the stereoselectivity of **3.20** (Table 9, entries 3 and 4). Treatment of **3.18** with a chiral cyclic guanidine **4.1**<sup>48</sup> and LiBr gave only 20 % of **3.20** without enantioselectivity (Table 9, entries 5 and 6). Reactions with the thioamidine catalyst, (-)-tetramisole (**4.2**) excluded also enantioselectivity (Table 9, entries 7 and 8).<sup>49</sup> Chiral amidine **4.3**<sup>50</sup> with LiBr generated **3.20** successfully as the racemate (Table 9, entries 10).

**Table 9.** Chiral bases with and without LiBr.

Entry	Base / Additive (5%)	<b>3.20</b> Yield (%) <sup>a</sup>
1	(-)-sparteine	n.r.
2	(-)-sparteine, LiBr	n.r.
3	(-)-sparteine, LiBr, DBU	92 (88) <sup>b, c</sup>
4	(-)-sparteine, LiBr, DBU	90 (88) <sup>b, c</sup>
5	 (4.1)	n.r.
6	 LiBr	20 <sup>b, c</sup>
7	 (4.2)	n.r.
8	 LiBr	trace
9	 (4.3)	7
10	 LiBr	85 (74) <sup>b, c</sup>

Entries 1-4, the reactions were run with 0.14 mmol triketone in 1 mL THF at - 40 °C for 24 h. Entry 4, starting material, sparteine and LiBr were stirred at - 40 °C for 0.5h, then DBU was added. Entry 5, DBU, sparteine and LiBr were stirred at - 40 °C for 0.5h, then starting material was added. Entries 5-10, the reactions were run with 0.14 mmol triketone in 1 mL THF at - 40 °C for 72 h. <sup>a</sup> Calculated from <sup>1</sup>H NMR spectra of crude reaction mixture. <sup>b</sup> Isolated yield. <sup>c</sup> Racemic compounds, determined by SFC of **3.20** or GC-MS of the acetate of **3.20**.



## 4-3 Discussion

### 4-3-1 Proposed mechanisms for catalytic synthesis of 3.20

#### 4-3-1-1 Mechanism involving LiBr

In the reaction catalyzed by a base DBU and LiBr, we hypothesized that LiBr pre-organized the conformation of triketone **3.18** to place the carbonyl of the side-chain and the ketone from cyclopentanedione in a parallel orientation, due to bidentate coordination with LiBr (Figure 79). After being activated by LiBr, the most acidic proton at the  $\alpha$ - position of ketone on the ring was abstracted by DBU to give a lithium enolate, which was readily cyclized through an intramolecular aldol reaction with attack of the carbonyl of the side-chain. The resulting alkoxide would then abstract a proton from the conjugated base (DBU-H<sup>+</sup>) to give the  $\beta$ -ketol product **3.20**, and regenerate the base (DBU) and lithium salt being regenerated at the same time.

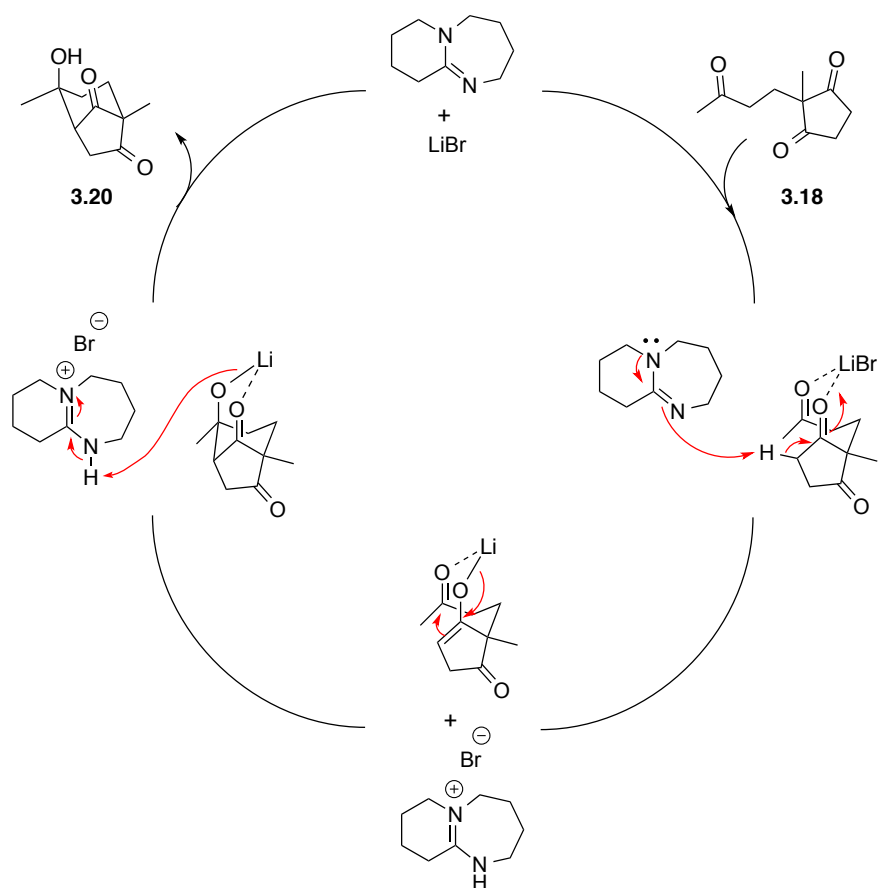
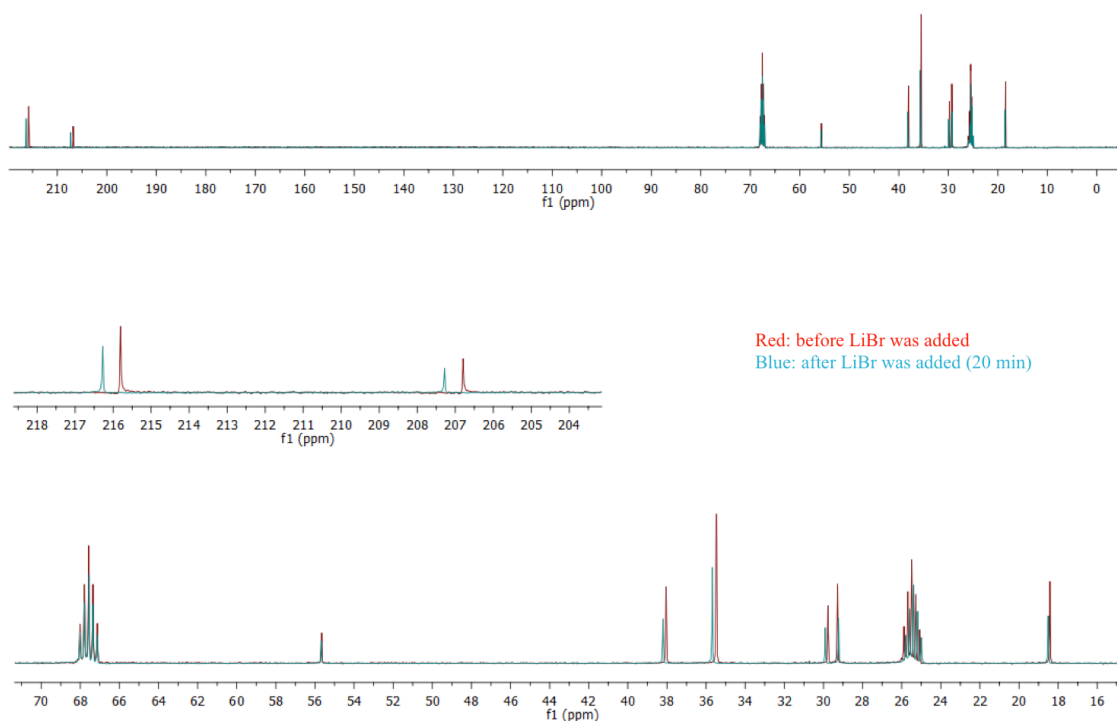


**Figure 79.** Proposed catalytic cycle in the LiBr pre-coordination model.

In support of lithium chelating pre-organization (Figure 79), indirect evidence was provided by study of **3.18** using  $^{13}\text{C}$  NMR spectroscopy. In the presence of LiBr in  $d_8$ -THF, the carbonyl peaks of **3.18** were clearly shifted to lower field (Figure 80). Although this does not necessarily prove the formation of chelated **3.18**-LiBr complex as in Figure 79, the role of LiBr for chelating and activation may be inferred from the reaction of **3.18** with catalytic (5 mol %) DBU alone at  $-40\text{ }^\circ\text{C}$ ; without LiBr, only a trace amount of **3.20** was observed (Table 5, entry 7). Notably, THF as solvent was important, probably due to coordination of  $\text{Li}^+$  by THF in the lithium chelating complexes (Figure 79). In MeOH, the major product was ketol **3.19** (with the equatorial hydroxyl group), presumably due to solvation of triketone **3.18** by MeOH, preventing coordination with LiBr (Table 6, entries 6).



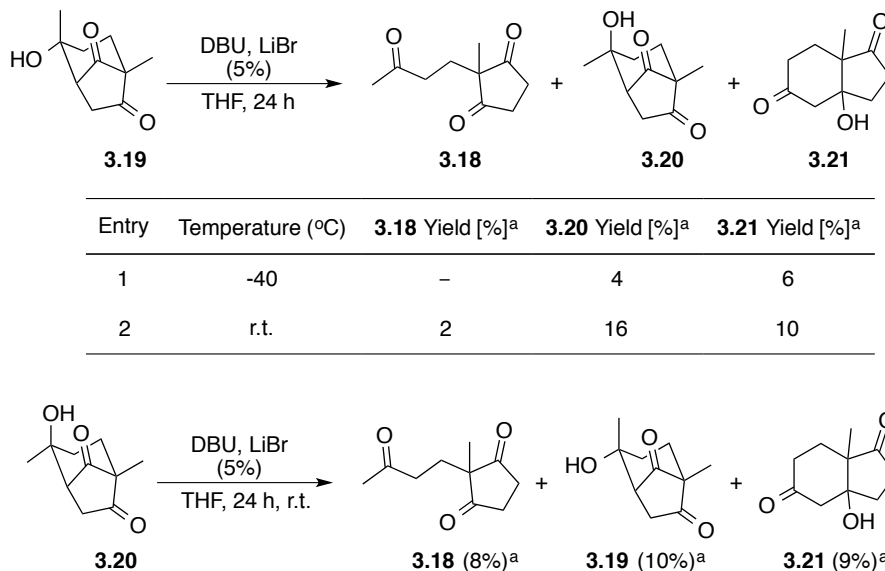
Trione **3.18** (51mg, 0.28 mmol) with LiBr (24 mg, 0.28 mmol) in deuterated THF (0.5 mL)

**Figure 80.**  $^{13}\text{C}$  NMR spectra study of **3.18**.

Hajos and Parrish demonstrated that ketol **3.19** was the kinetic product, and ketol **3.20**, generated from **3.19**, was the thermodynamic product (Scheme 59).<sup>28</sup> Thus, it could be argued that in our catalytic synthesis, ketol product **3.20** could also be generated from **3.19** by a retro-

aldol reaction. To prove that **3.20** was directly formed from triketone **3.18** via the proposed lithium-chelating model (Figure 79), kinetic product **3.19** was treated under the same conditions (5 mol % DBU and LiBr, at -40 °C for 24 h), only 4 % of ketol **3.20** and 6 % of **3.21** were observed from crude <sup>1</sup>H NMR spectra (Table 10, entry 1). This indicated that ketol **3.20** is generated directly from starting triketone **3.19**. Warming the reaction to room temperature, more ketol products **3.20** and **3.21** were obtained due to the faster equilibrium (retro-aldol and aldol) in the reaction (Table 10, entry 2). The equilibrium of ketol **3.20** was also tested at room temperature (Table 10). After 24h, **3.20** was transformed to starting triketone **3.18**, and ketol products **3.19** and **3.21** (Table 10). This confirmed the observation that a lower yield of **3.20** was obtained from **3.18** at room temperature compared to the one at -40 °C (Compare Table 2, entries 4 and 6). Thus, -40 °C temperature is crucial for this catalytic reaction to produce β-ketol **3.20** as the major product.

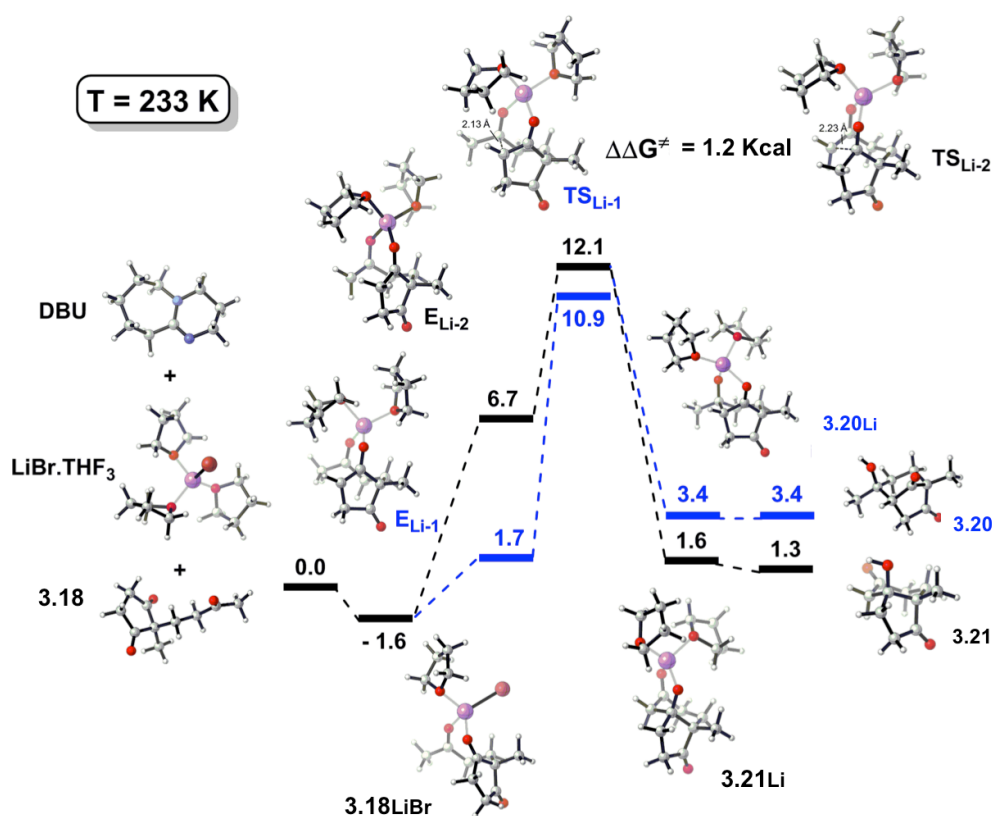
**Table 10.** Equilibration reactions between **3.19** and **3.20**.



The reactions were run with 0.14 mmol ketol in 1 mL THF for 24 h. <sup>a</sup> Calculated from <sup>1</sup>H NMR spectra of crude reaction mixture.

To further analyze the proposed LiBr pre-coordination model, a DFT calculation was conducted by Dr. Gilles Berger (Figure 81). Theoretical calculations demonstrated that the formation of a complex between triketone **3.18** and LiBr (**3.18**<sub>LiBr</sub>) was associated with a

decrease in the free energy of about  $1.6 \text{ kcal}\cdot\text{mol}^{-1}$ , thus favoring LiBr pre-organization of **3.18** (Figure 81). In the presence of a base (DBU), the  $\alpha$ -proton of the ketone is abstracted, followed by generation of the corresponding enolate. Calculation results indicated the enolization is highly favored ( $5 \text{ kcal mol}^{-1}$ ) for the methylene ketone on the ring ( $E_{\text{Li-1}}$ ) compared to the methyl ketone on the side-chain ( $E_{\text{Li-2}}$ ). For the transition states leading to ketol products **3.20** and **3.21** respectively, both of the free energies are around  $10 \text{ kcal}\cdot\text{mol}^{-1}$  higher than the starting triketone **3.18**, and with a  $\Delta\Delta G^\ddagger$  of  $1.2 \text{ kcal}\cdot\text{mol}^{-1}$  favoring the formation of **3.20**. Also in the more stable transition state ( $\text{TS}_{\text{Li-1}}$ ), the length of the forming C-C bond is significantly shorter ( $2.13 \text{ \AA}$  versus  $2.23 \text{ \AA}$ ). Compared to the starting triketone **3.18**, the cyclized ketol products **3.20** and **3.21** are less stable in calculated energy, which is consistent with our observation in the equilibration experiment (Table 10) (ketol **3.20** could give back **3.18** through a retro-aldol reaction), and in accordance with previous DFT studies.<sup>51,52</sup>



Reaction pathway: enolization of ketone on the 5-membered ring is represented in blue, while the enolization occurring on the side-chain is drawn in black.

**Figure 81.** Free energy profile of the DBU & LiBr-catalyzed reaction in THF at 233 K.

### 4-3-1-2 Bifunctional H-bonded mechanism

In addition to using LiBr and catalytic base, we found that the reaction of **3.18** can be catalyzed by Eschenmoser's amidine alone (Table 8, entry 11), and more efficiently by TBD (Table 8, entry 15). A different mechanism was proposed (Figure 82), in which the ketone on ring of triketone **3.18** was enolized by 5 mol % TBD, leading to a H-bonded transition state with the enol and side chain carbonyl group aligned by a bridging TBD (Figure 82A). Intramolecular aldol reaction generated  $\beta$ -ketol **3.20** with recovery of catalytic TBD. A similar mechanism could operate in the presence of the Eschenmoser's amidine (Figure 82B).<sup>53</sup>

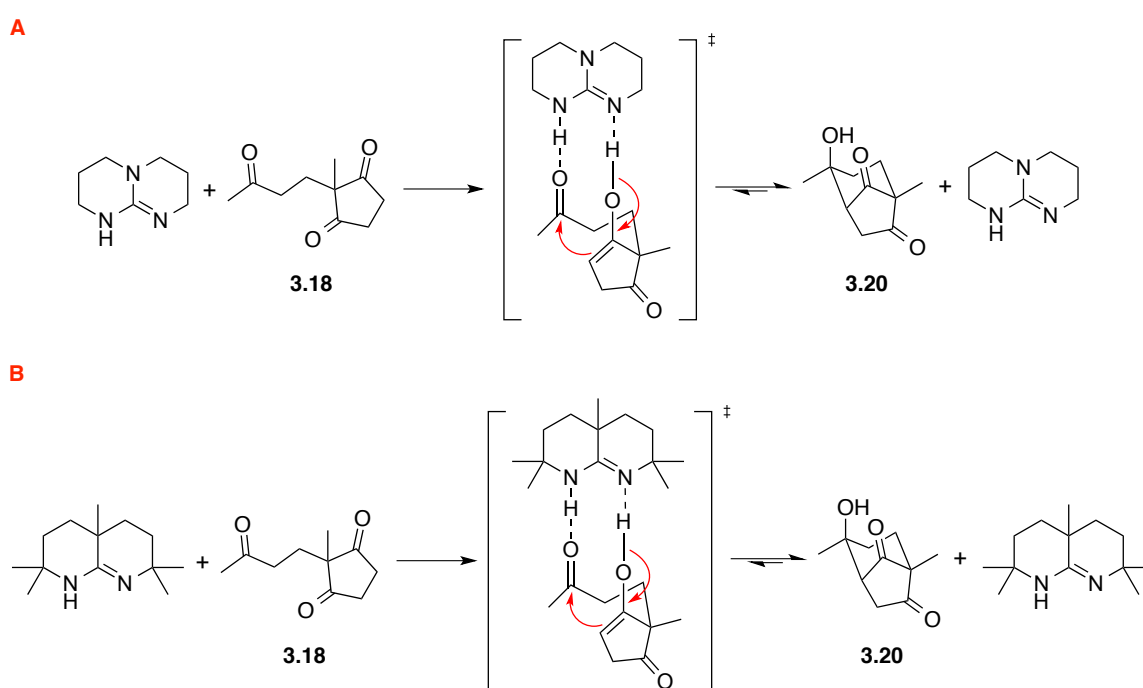


**Figure 82.** Proposed bifunctional H-bonded mechanism.

Baati, Himo and coworkers<sup>52,54</sup> have reported a DFT study of TBD catalyzed intramolecular aldol reactions of acyclic ketoaldehydes. They proposed a proton shuffling general base mechanism, in which TBD acts as a bifunctional catalyst, acting as a proton donor and acceptor, aiding proton transfer from enol to the aldehyde during C-C bond formation (Figure 83). A similar mechanism may be involved in our intramolecular aldol reaction of **3.18**. Computational analysis of the reaction catalyzed by TBD with DFT was conducted by Dr. Gilles Berger (Figure 84). Enolization of **3.18** through a TBD mediated

bifunctional H-bonding structure (H-bond lengths between 1.7 and 2.1 Å) was preferred with enolization of the methene rather than the methyl ketone. Although the activation energy was slightly higher (around 2 kcal mol<sup>-1</sup>) compared to the LiBr-catalyzed reaction (Figure 81), the intracyclic enolate (TS<sub>TBD1</sub>) was favored rather than the side-chain enolate (TS<sub>TBD2</sub>) with a energy difference  $\Delta\Delta G^\ddagger$  about 1.2 kcal mol<sup>-1</sup>. The C-C distance was also shorter in the transition state (TS<sub>TBD1</sub>), which leads to ketol product **3.20**. Thus, ketol **3.20** was favored due to faster enolization and less energetic transition state.

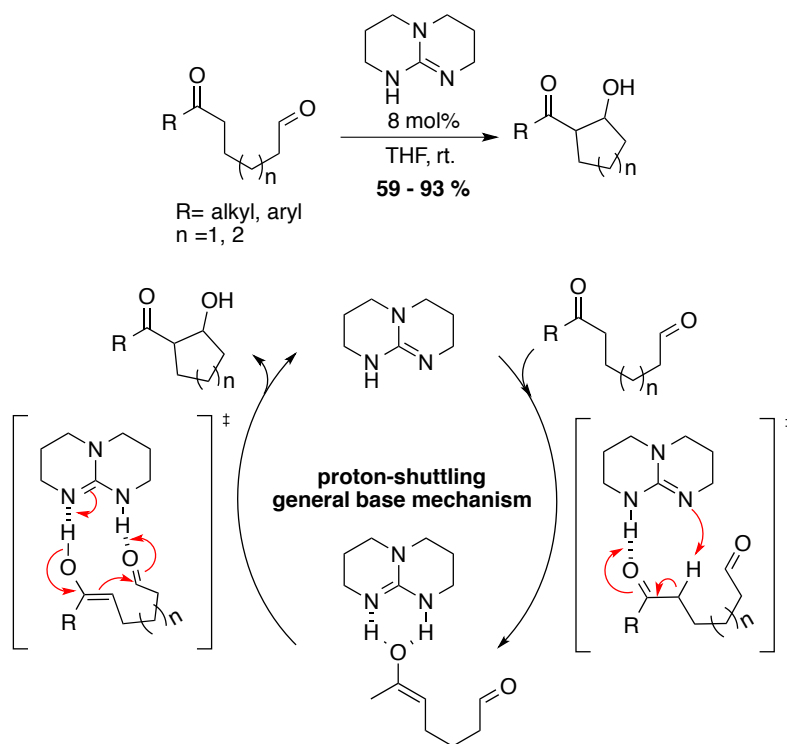
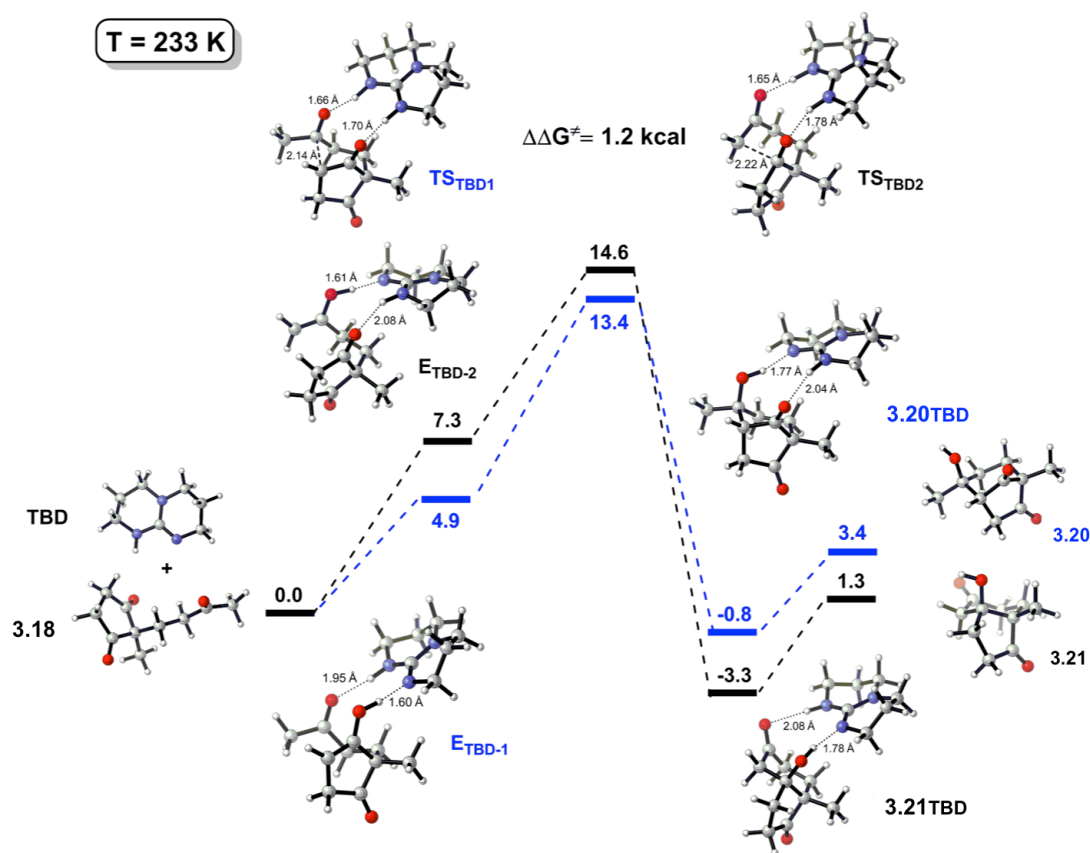


**Figure 83.** Baati's proton shuffling general base mechanism.<sup>52</sup>

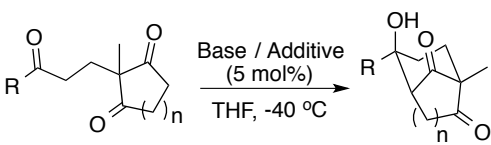


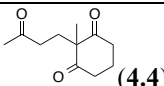
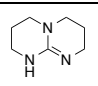
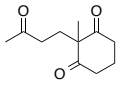
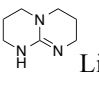
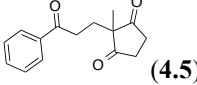
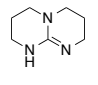
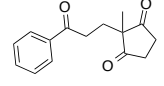
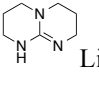
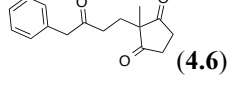
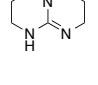
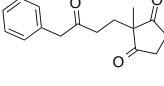
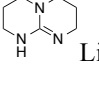
Reaction pathway: enolization of ketone on the 5-membered ring is represented in blue, while the enolization occurring on the side-chain is drawn in black.

**Figure 84.** Free energy profile of the TBD-catalyzed reaction in THF at 233 K.

The catalytic effect of TBD with and without LiBr was also observed in other triketone substrates (Table 11). Excellent yields of the ketol product were obtained from 2-methyl-2-(3-oxobutyl)cyclohexane-1,3-dione (**4.4**) (Table 11, entries 1 and 2). The reaction of phenyl triketone **4.5** and TBD was not completed after 72 h, and gave a modest yield of  $\beta$ -ketol product (Table 11, entries 3). The ketone on the side-chain of **4.5** is stabilized by the phenyl group, and bulkier than **3.18**, which may account for the lower yield. The conversion of phenyl triketone **4.5** was not improved using LiBr (Table 11, entries 4). Switching to benzyl triketone **4.6**, gave the desired axial  $\beta$ -ketol **4.7** in only 30-40 % yield (Table 11, entries 5 and 6). The efficiency of the TBD reaction was thus dependent on ketone substrate.

**Table 11.** Reactions with other triketones catalyzed by TBD with and without LiBr.



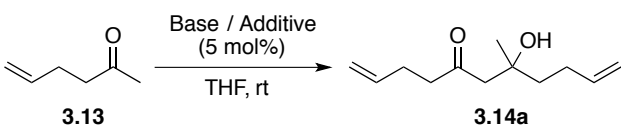
Entry	Substrate	Base / Additive (5%)	Yield (%) <sup>a</sup>
1	 ( <b>4.4</b> )		85
2		 LiBr	86
3	 ( <b>4.5</b> )		50 <sup>b</sup>
4		 LiBr	33 <sup>b</sup>
5	 ( <b>4.6</b> )		33
6		 LiBr	40

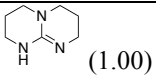
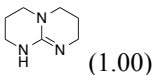
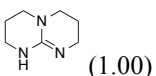
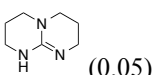
The reactions were run with 0.14 mmol triketone in 1 mL THF at -40 °C. Entries 1-2, 24 h; entries 3-6, 72h. <sup>a</sup> Isolated yield. <sup>b</sup> Calculated from <sup>1</sup>H NMR spectra of crude reaction mixture.

Intermolecular self-aldol reactions were studied using 5-hexen-2-one **3.13** in the presence of 1 equiv. TBD, but no reaction took place (Table 12, entry 1) in the absence and presence of LiBr (1 equiv.) (Table 12, entry 2). Adding stoichiometric amounts of MgBr<sub>2</sub> to the TBD reaction gave the ketol **3.14a** in 48 % yield (Table 12, entry 3), but on decreasing the quantities of TBD and MgBr<sub>2</sub> to catalytic amounts (5 mol %), **3.14a** was no longer observed. With stoichiometric amount of TBD serving as base, the β-ketol **3.14a** may be generated through a magnesium chelated transition state, rather than by a TBD-mediated H-bonding mechanism. An indirect evidence of the magnesium chelate was obtained using (1 equiv.) Et<sub>3</sub>N and MgBr<sub>2</sub>, which gave **3.14a** in 51 % yield.



**Table 12.** Intermolecular Reactions in the presence of TBD with and without additives.

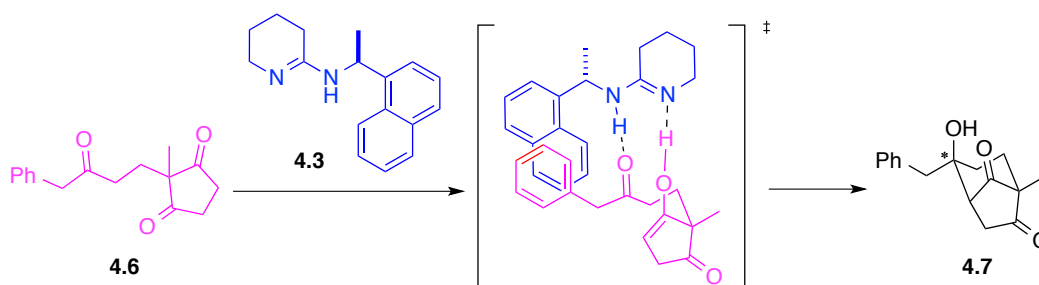


Entry	Base (equiv.)	Additive (equiv.)	Time (h)	Yield (%) <sup>a</sup>
1	 (1.00)	-	24	n.r.
2	 (1.00)	LiBr (1.00)	24	n.r.
3	 (1.00)	MgBr <sub>2</sub> (1.00)	1	48
4	 (0.05)	MgBr <sub>2</sub> (0.05)	24	n.r.
5	Et <sub>3</sub> N (1.00)		24	n.r.
6	Et <sub>3</sub> N (1.00)	LiBr (1.00)	24	n.r.
7	Et <sub>3</sub> N (1.00)	MgBr <sub>2</sub> (1.00)	2	51

The reactions were run with 0.25 mmol methyl ketone **3.13**, in 2 mL THF. <sup>a</sup> Isolated yield.

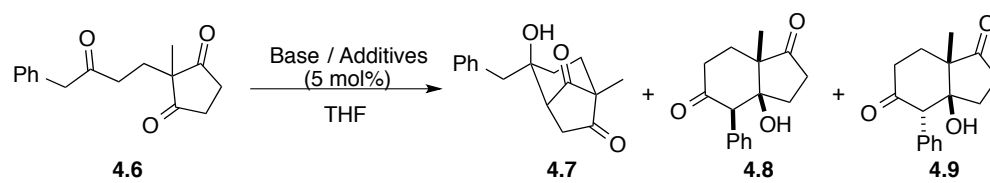
### 4-3-2 Studies toward the symmetric syntheses of $\beta$ -ketols from benzyl triketone **4.6**

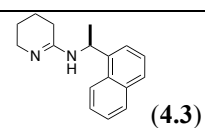
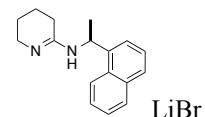
Intrigued by the proposed H-bonded mechanism (Figure 82), we hypothesized that in the reaction of benzyl triketone **4.6**, chiral naphthyl amidine **4.3** may serve as a bifunctional catalyst to generate enantioselectively  $\beta$ -ketol (axial alcohol) **4.7**, by a mechanism featuring  $\pi$ - $\pi$  stacking of the phenyl ring of **4.6** and naphthyl group in **4.3** (Figure 85).

**Figure 85.** Hypothesis for enantioselective synthesis of  $\beta$ -ketol **4.7** from benzyl triketone **4.6**.

Benzyl triketone **4.6** was treated with amidine catalyst **4.3** at - 40 °C for 72 h, but racemic  $\beta$ -ketol **4.7** was obtained in only 4 % yield. The major product, **4.8** was a Hajos-Parrish type of ketol (Table 13, entry 1). Although a modest improvement in yield of ketol **4.7** in the presence of LiBr,  $\beta$ -ketol **4.8** remained the major product, and no enantioselectivity was observed for **4.7** (Table 13, entry 2). Switching to a catalytic amount DBU at - 40 °C led to the formation of diastereomer **4.9** in 83 % yield (Table 13, entry 3). The combination of DBU and LiBr gave the ketol **4.7** in 16 % yield, accompanying with **4.8** in 81 % yield (Table 13, entry 4). Treatment of **4.6** with 5 mol% DBU at - 78 °C produced ketol **4.8** in 82 % yield (Table 13, entry 5). The relative configurations of all three ketol products were confirmed by single crystal X-ray analysis (Figure 86).

**Table 13.** Reactions with benzyl triketone **4.6**.



Entry	Base / Additive (5 mol %)	Temperature (°C)	<b>4.7</b> Yield (%) <sup>a</sup>	<b>4.8</b> Yield (%) <sup>a</sup>	<b>4.9</b> Yield (%) <sup>a</sup>
1	 ( <b>4.3</b> )	- 40	4	85	-
2	 LiBr	- 40	27	65	-
3	DBU	- 40	-	-	83
4	DBU, LiBr	- 40	16	81	-
5	DBU	- 78	-	82	-

The reactions were run with 0.14 mmol triketone in 1 mL THF for 72 h. <sup>a</sup> Isolated yield.



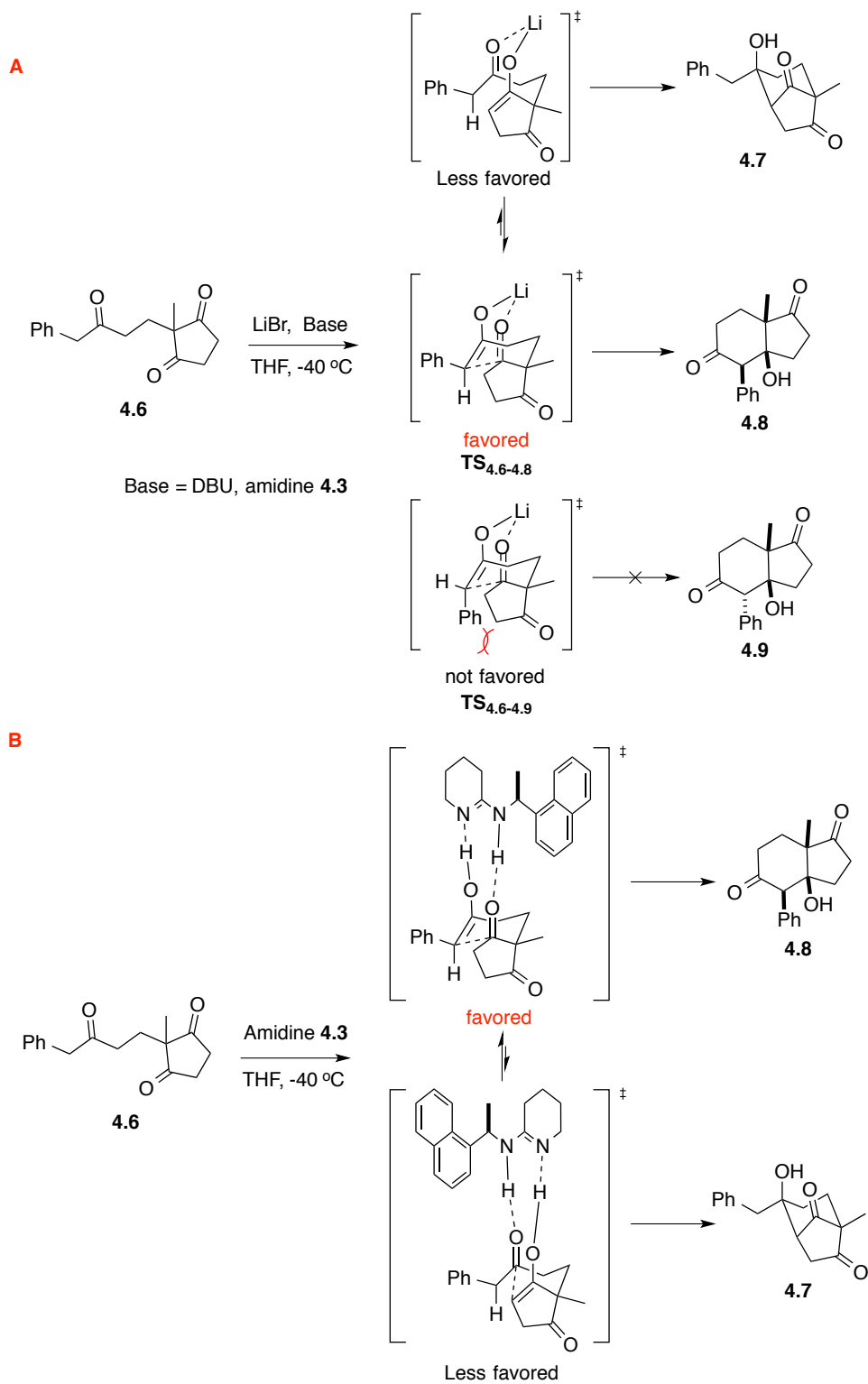


**Figure 87.** Proposed Li-coordinated and bifunctional H-bonding transition states model in the reaction of benzyl triketone **4.6** at - 40 °C.

Temperature was important for the diastereoselective cyclization of **4.6**. Using 5 mol % DBU at -40 °C, a chair conformation may be preferred to give the more stable ketol product **4.9** (Figure 88). At -78 °C, ketol **4.8** was generated as the kinetic product, through another chair transition state (Figure 88). The kinetic property of ketol **4.8** was also confirmed by treating it with 5 % DBU at 0 °C, giving the more stable ketol **4.9** in 39 % yield as calculated from the <sup>1</sup>H NMR spectrum of the crude reaction mixture (Table 14, entry 2). In contrast, treatment of ketol **4.9** under the same condition, only 8 % starting benzyl triketone **4.6** was observed after 12 h, which was generated through a retro-aldol reaction (Table 14).

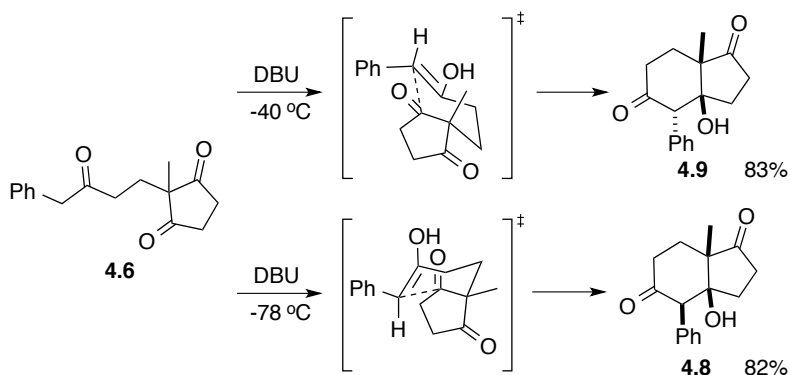
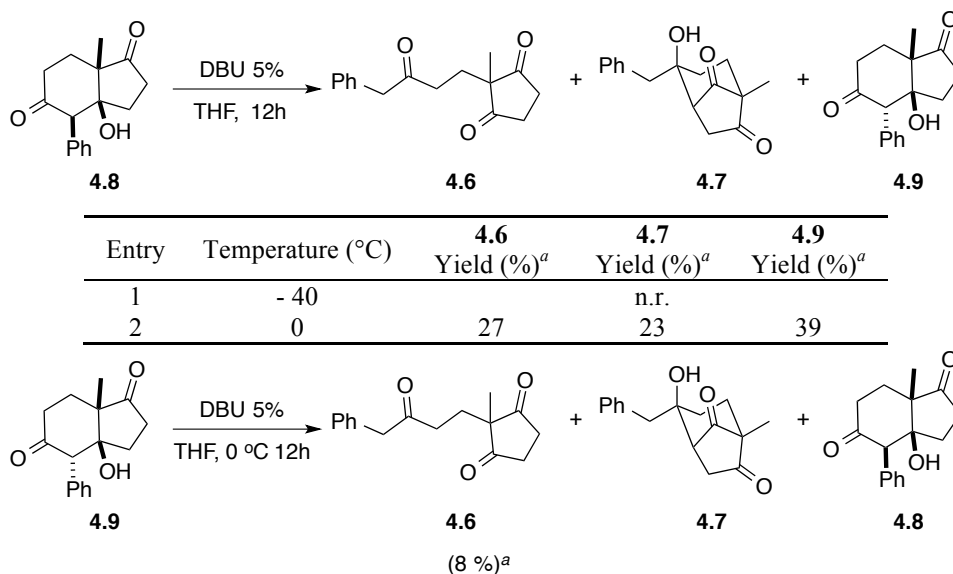


**Figure 88.** Proposed transition state model and effect of the temperature in the reaction of benzyl triketone **4.6** with DBU.

**Table 14.** Equilibrium reactions between ketol **4.8** and **4.9**.

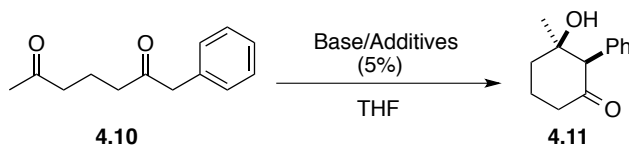


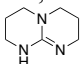
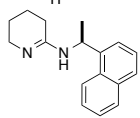
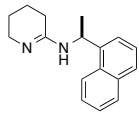
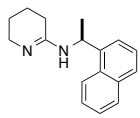
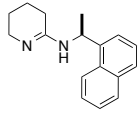
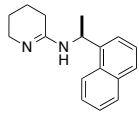
The reactions were run with 0.14 mmol ketol in 1 mL THF for 12 h. <sup>a</sup> Calculated from <sup>1</sup>H NMR spectra of crude reaction mixture.

### 4-3-3 $\beta$ -Ketol formation from a benzyl diketone **4.10**

Based on all the previous observations and mechanistic studies in the  $\beta$ -ketol formation from aldol reactions, we hypothesized that if 1-phenylheptane-2,6-dione (**4.10**) was treated with catalytic amount DBU and LiBr, first, there should be no intermolecular aldol reaction since it requires a stoichiometric amount base and MgBr<sub>2</sub> (Table 12), then in the intramolecular reaction, it should give only one  $\beta$ -ketol diastereomer due to the LiBr pre-organization. The same result would be expected by using catalytic amount TBD. Thus, to prove our hypothesis, benzyl diketone **4.10** was firstly treated with 5 mol% DBU, there was no reaction (Table 15, entry 1). Then, upon addition of 5% LiBr, the reaction gave ketol **4.11** as a single diastereomer in 74 % yield (Table 12, entry 2). The same ketol product was also obtained using 5 mol% TBD as we expected (Table 12, entry 2). The relative configuration of **4.11** was confirmed by single crystal x-ray analysis (Figure 89). Treating **4.10** with chiral amidine **4.3** with and without LiBr, there was no reaction at -40 °C. It is notable that under the same conditions, benzyl triketone **4.6** was enolized (Table 13, entries 1 and 2). At room temperature, with the combination of amidine and LiBr, 23 % ketol product **4.11** was observed from <sup>1</sup>H NMR of the crude mixture (Table 15, entry 7). Extending the reaction time to 72 h, however, no additional ketol **4.11** was obtained (Table 15, entry 8). Therefore, these results confirmed our hypothesis, and supported the proposed lithium pre-organization and bifunctional H-bonded mechanisms (Figure 90).

**Table 15.** Intramolecular aldol reaction of 1-phenylheptane-2,6-dione (**4.10**).



Entry	Base / Additive (5 %)	Temperature (°C)	Time (h)	<b>4.11</b> Yield (%) <sup>a</sup>
1	DBU	- 40	12	n.r.
2	DBU, LiBr	- 40	12	74
3		- 40	12	85
4		- 40	12	n.r.
5	 LiBr	- 40	12	n.r.
6		r.t.	12	n.r.
7	 LiBr	r.t.	12	23 <sup>b</sup>
8	 LiBr	r.t.	72	23 <sup>b</sup>

The reactions were run with 0.14 mmol diketone in 1 mL THF for 12 h. <sup>a</sup> Isolated yield. <sup>b</sup> Calculated from <sup>1</sup>H NMR spectra of crude reaction mixture.

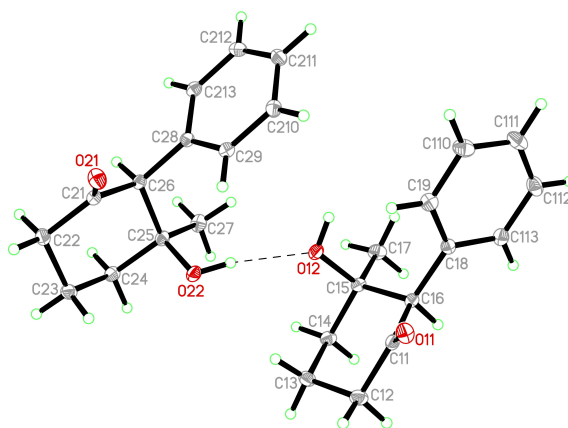


**Figure 89.** X-ray structure of ketol **4.11**.

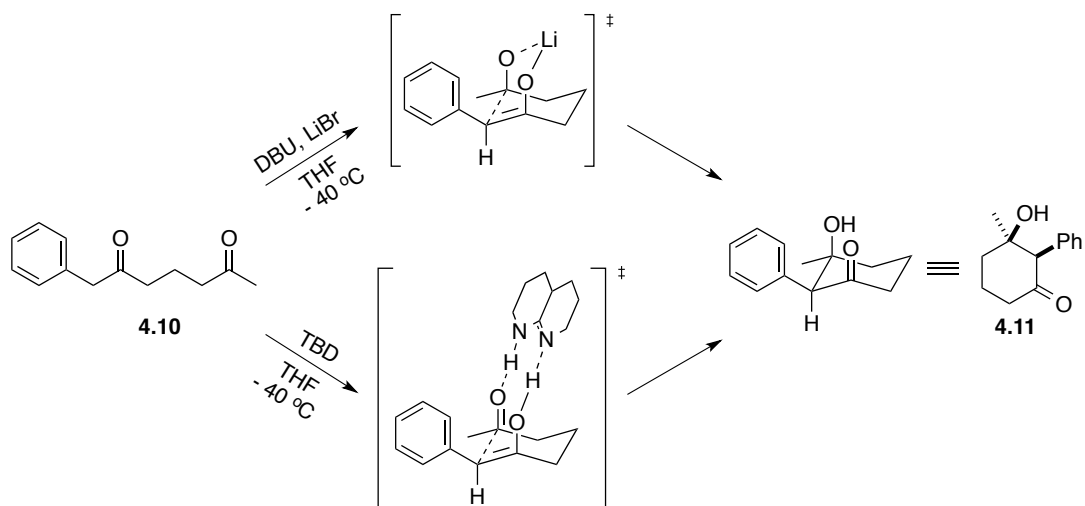


**Figure 90.** Proposed transition state model in the cyclization of diketone **4.10**.

## 4-4 Conclusion

Inspired by the observation of  $\beta$ -ketol product **3.20** from intramolecular cyclization of triketone **3.18**, we screened reaction temperatures, catalyst loadings, additives, as well as chiral and achiral bases. This led to the successful development of a catalytic synthesis of ketol **3.20**, which can be highly efficiently generated either through a lithium pre-organization mechanism, by using a combination of a suitable base (e.g. DBU) and lithium salt (e.g. LiBr) as the catalysts, or *via* a bifunctional H-bonding mechanism, by using TBD as the catalyst. These mechanisms were also supported by DFT computational studies. In addition to triketone **3.18**, Our methods of catalytic synthesis of  $\beta$ -ketol were also applicable to other ketone substrates (e.g. benzyl triketone **4.6** and benzyl diketone **4.10**). While, for intermolecular reactions, it was found that stoichiometric amount of base and  $\text{MgBr}_2$  were essential.

In the efforts of asymmetric synthesis of  $\beta$ -ketol, although so far there was no success with chiral amidines, we have designed a new chiral catalyst **4.12** based on the predictions by DFT calculations (Figure 91). Thus, it is proposed that the  $\pi$ -stacking was not possible due to the shorter connecting chain between the naphthyl group and the amidine motif in **4.3** (Figure 85 and 91). By adding one more carbon to extend the connecting chain, and also changing the substitution on the naphthalene to 2-position rather than 1-position, **4.12** could act as



bifunctional catalyst through a possible  $\pi$ -stacking and H-bonding transition model and the enantioselectivity could be introduced from the chiral methyl group in the catalyst **4.12** (Figure 91). The synthesis of catalyst **4.12** is currently in progress.

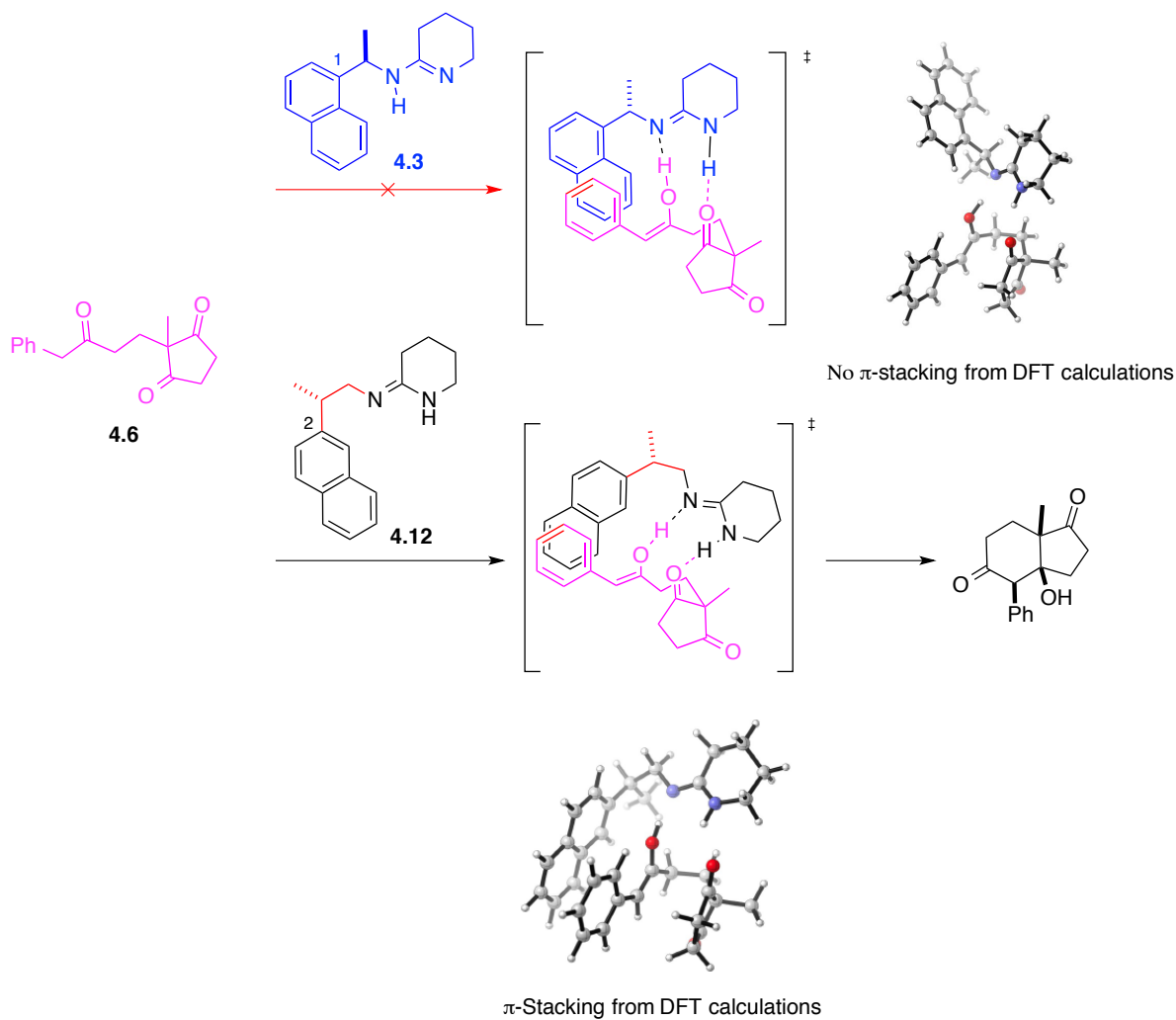


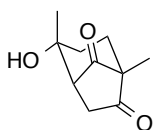
**Figure 91.** Proposed bifunctional chiral amidine catalyst and the transition state model from DFT calculations.

## 4-5 Experimental

General methods are same as described in the experimental section in Chapter 1.

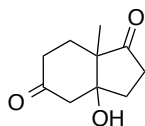
General procedure: ketone substrate was dissolved in solvent in a dried flask. The resulting solution was stirred for 0.5 h, then base or base and additive were added to the solution. The reaction mixture was stirred for 24-72h, quenched with saturated aqueous  $\text{NH}_4\text{Cl}$  and extracted by  $\text{CH}_2\text{Cl}_2$ . The organic phases were combined, washed with brine, dried over  $\text{MgSO}_4$  and filtered. The solvent was removed under reduced pressure and the residue was purified by flash chromatography.

For screening conditions, all the reactions were run with **3.18** (25 mg, 0.14 mmol) in anhydrous solvent (1 mL) for 24 h. Pure reference ketol products **3.19** and **3.21** were synthesized according to reported procedures by Hajos and Parrish.<sup>37</sup> The spectroscopic data were in agreement with the proposed structures and matched those reported in the literature.<sup>37,41</sup>



**3.19**

**(±)-4 $\alpha$ -Hydroxy-1 $\beta$ , 4 $\beta$ -dimethylbicyclo[3.2.1]octane-7,8-dione (3.19).** White solid, yield (70%).  $^1\text{H}$  NMR (400 MHz,  $\text{CDCl}_3$ )  $\delta$  3.05 (d,  $J = 19.4$  Hz, 1H), 2.80 (d,  $J = 7.6$  Hz, 1H), 2.53 (dd,  $J = 19.4, 7.6$  Hz, 1H), 1.92-1.69 (m, 4H), 1.62-1.53 (m, 1H), 1.41-1.40 (m, 3H), 1.07 (s, 3H);  $^{13}\text{C}$  NMR (100 MHz,  $\text{CDCl}_3$ )  $\delta$  213.1, 211.1, 58.5, 58.0, 40.9, 35.5, 32.84, 26.8, 11.5. HRMS (ESI) calcd for  $\text{C}_{10}\text{H}_{14}\text{NaO}_3$  ( $\text{M}+\text{Na}$ )<sup>+</sup> 205.0835, found 205.0835.



**3.21**

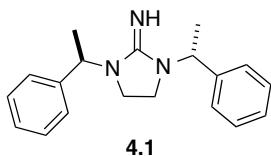
**(±)-3 $\alpha$ ,4,7,7 $\alpha$ -Tetrahydro-3 $\alpha\beta$ -hydroxyl-7 $\alpha\beta$ -methyl-1,5(6*H*)-indandione (3.21).** White solid, yield (56%). <sup>1</sup>H NMR (400 MHz, CDCl<sub>3</sub>)  $\delta$  2.62 (s, 2H), 2.58-2.51 (m, 1H), 2.47-2.39 (m, 2H), 2.38-2.25 (m, 1H), 2.02-1.98 (m, 2H), 1.92 (s, 1H), 1.79-1.74 (m, 1H), 1.72-1.67 (m, 1H), 1.25 (s, 3H); <sup>13</sup>C NMR (100 MHz, CDCl<sub>3</sub>)  $\delta$  218.1, 207.9, 81.5, 52.5, 50.4, 36.5, 33.5, 32.8, 29.7, 13.9; HRMS (ESI) calcd for C<sub>10</sub>H<sub>14</sub>NaO<sub>3</sub> (M+Na)<sup>+</sup> 205.0835, found 205.0839.

Typical procedure of base & additive (e.g. DBU & LiBr) catalyzed reaction of **3.18**: (Table 5, entry 4)

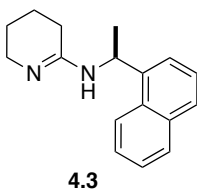
2-Methyl-2-(3-oxobutyl)cyclopentane-1,3-dione (**3.18**) (25 mg, 0.14 mmol) was dissolved in THF (0.8 mL) in a dried flask at – 40 °C. The solution was stirred for 0.5 h, DBU (1.1 mg, 0.007 mmol) as 0.1 mL of a THF solution of DBU (11 mg/mL) and LiBr (0.61 mg, 0.007 mmol) as 0.1 mL of a THF Solution of LiBr (6.1 mg/mL) were added to the solution. The reaction was stirred for 24 h in total, quenched with saturated aqueous NH<sub>4</sub>Cl and extracted with CH<sub>2</sub>Cl<sub>2</sub> (3 $\times$ 10 mL). The organic phases were combined, washed with brine, dried over MgSO<sub>4</sub> and filtered. The volatiles were removed under reduced pressure. The residue was purified by flash chromatography (hexane: EtOAc, 2:1 to 1:1) to give **3.20** (22.0 mg, 88 %) as white solid.

Typical procedure of base (e.g. TBD) catalyzed reaction of **3.18**: (Table 8, entry 15)

2-Methyl-2-(3-oxobutyl)cyclopentane-1,3-dione (**3.18**) (25 mg, 0.14 mmol) was dissolved in THF (0.9 mL) in a dried flask at – 40 °C. The solution was stirred for 0.5 h, TBD (0.97 mg, 0.007 mmol) as 0.1 mL of a THF solution of DBU (9.7 mg/mL) was added to the solution. The reaction was stirred for 24 h in total, quenched with saturated aqueous NH<sub>4</sub>Cl and extracted with CH<sub>2</sub>Cl<sub>2</sub> (3 $\times$ 10 mL). The organic phases were combined, washed with brine, dried over MgSO<sub>4</sub> and filtered. The volatiles were removed under reduced pressure. The residue was purified by flash chromatography (hexane: EtOAc, 2:1 to 1:1) to give **3.20** (22.3 mg, 89 %) as white solid.



**1,3-Bis((*R*)-1-phenylethyl)imidazolidin-2-imine (4.1)** was synthesized according a known procedure.<sup>48a</sup> The spectroscopic data were in agreement with the proposed structures and matched those reported in the literature.<sup>48</sup> Colorless solid, yield (63 %). <sup>1</sup>H NMR (400 MHz, CDCl<sub>3</sub>) δ 8.88 (s, 1H), 7.37-7.35 (m, 2H), 7.32-7.18 (m, 6H), 6.01 (q, *J* = 6.8 Hz, 2H), 3.42-3.20 (m, 2H), 3.15 - 2.95 (m, 2H), 1.49 (d, *J* = 6.9 Hz, 6H). [α]<sub>D</sub> (+) 82.6°, (*c* 1.00, CHCl<sub>3</sub>); HRMS (ESI) calcd for C<sub>19</sub>H<sub>24</sub>N<sub>3</sub> (M+H)<sup>+</sup> 294.1965, found 294.1973.



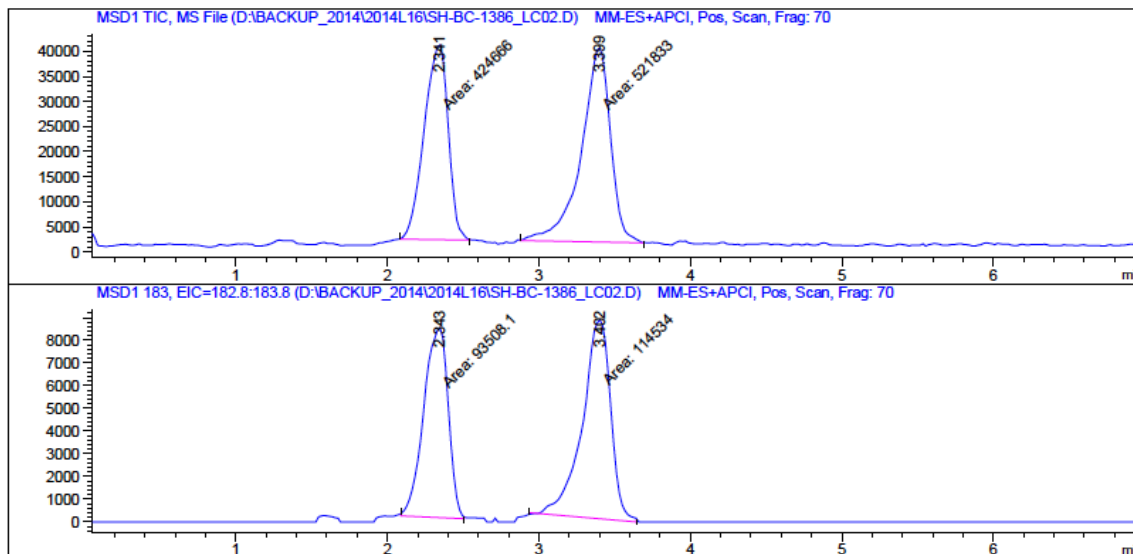
**(*S*)-*N*-(1-(naphthalen-1-yl)ethyl)-3,4,5,6-tetrahydropyridin-2-amine hydrochloride salt** was synthesized according a known procedure from (*S*)-(-)-1-(1-naphthyl)ethylamine.<sup>50</sup> White solid, yield (22%). m.p. 257-259 °C (lit.<sup>50</sup>, m.p. 258-259 °C). <sup>1</sup>H NMR (400 MHz, D<sub>2</sub>O) δ 8.09-8.04 (m, 2H), 8.02-7.94 (m, 1H), 7.72-7.63 (m, 2H), 7.62-7.55 (m, 2H), 5.54 (q, *J* = 6.7 Hz, 1H), 3.36-3.29 (m, 1H), 3.24-3.18 (m, 1H), 2.75 (t, *J* = 6.0 Hz, 2H), 1.86-1.76 (m, 4H), 1.72 (d, *J* = 6.7 Hz, 3H); <sup>13</sup>C NMR (125 MHz, D<sub>2</sub>O) δ 162.7, 135.4, 133.7, 129.8, 129.2, 128.8, 127.0, 126.3, 125.8, 122.6, 122.1, 48.3, 41.8, 26.2, 20.6, 20.3, 17.5; [α]<sub>D</sub> (-) 19.0°, (*c* 0.21, CH<sub>3</sub>OH); FTIR (cm<sup>-1</sup>) (neat) 3033, 2967, 2874, 1654, 1593, 1450, 1414, 1401, 1371, 1356, 1332, 1308, 1263, 1210, 1176, 1141, 1110, 1065, 1017, 1000, 922, 805, 783, 758; HRMS (ESI) calcd for C<sub>17</sub>H<sub>20</sub>N<sub>2</sub> (M+H)<sup>+</sup> 253.1699, found 253.1702.

The free amidine **4.3** was then obtained by washing the hydrochloride salt with one equiv. of 5M NaOH, followed by extracting with CH<sub>2</sub>Cl<sub>2</sub>. The organic phases were combined, washed with brine, dried over MgSO<sub>4</sub> and filtered. The solvent was removed under reduced pressure and left on high vacuum for 2h to give **4.3** as colorless oil.

Table 9, the enantiomeric excess was determined by SFC.

SFC conditions: ChiralPAK@AS-H, 250 x 4.6 mm, particle size 5  $\mu$ m, 10 % MeOH, 150 bar CO<sub>2</sub>, Column temperature: 30 °C, flow rate: 3 mL/min, detection: UV 210 nm, MS.

(Table 9. Entry 3), e.e. = 10.2 %

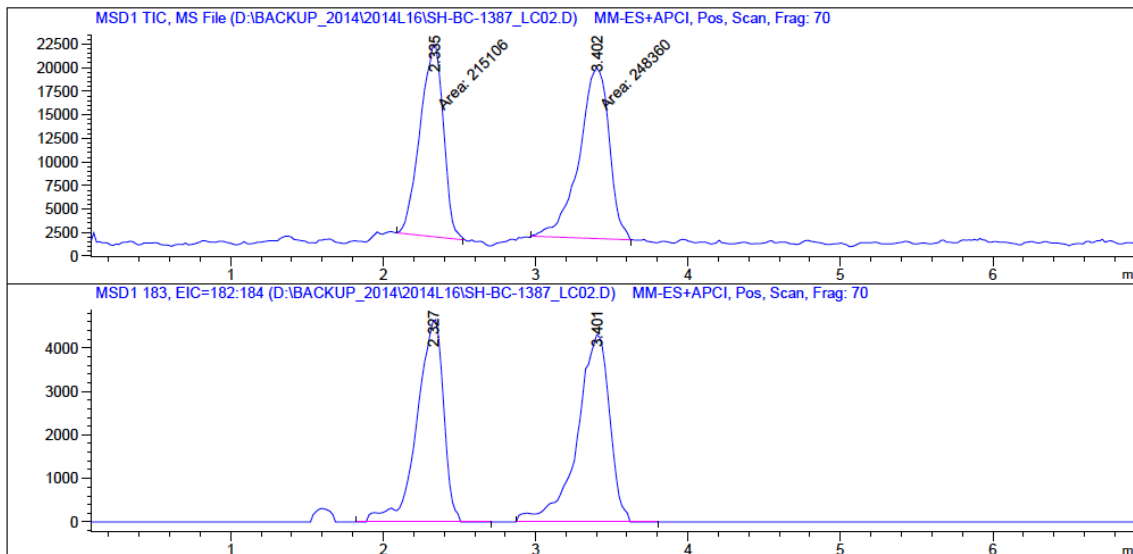


Signal 1: MSD1 TIC, MS File

Signal 2: MSD1 183, EIC=182.8:183.8

Peak #	RetTime [min]	Type	Width [min]	Area	Height	Area %	Peak #	RetTime [min]	Type	Width [min]	Area	Height	Area %
1	2.341	MM	0.1810	4.24666e5	3.91061e4	44.8670	1	2.343	MM	0.1850	9.35081e4	8424.92090	44.9466
2	3.399	MM	0.2236	5.21833e5	3.88959e4	55.1330	2	3.402	MM	0.2172	1.14534e5	8786.87402	55.0534

(Table 9. Entry 4), e.e. = 6.6 %

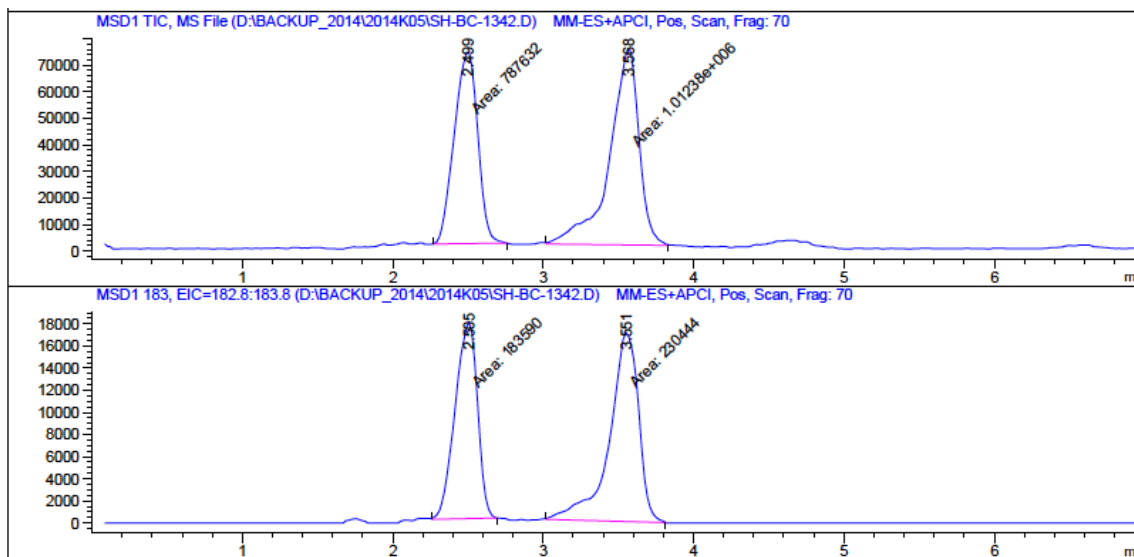


Signal 1: MSD1 TIC, MS File

Signal 2: MSD1 183, EIC=182:184

Peak #	RetTime [min]	Type	Width [min]	Area	Height	Area %	Peak #	RetTime [min]	Type	Width [min]	Area	Height	Area %
1	2.335	MM	0.1737	2.15106e5	2.06403e4	46.4125	1	2.327	VB	0.1960	5.58757e4	4613.03809	46.9423
2	3.402	MM	0.2277	2.48360e5	1.81785e4	53.5875	2	3.401	BB	0.2260	6.31549e4	4300.05713	53.0577

(Table 9. Entry 10), e.e. = 11.9 %

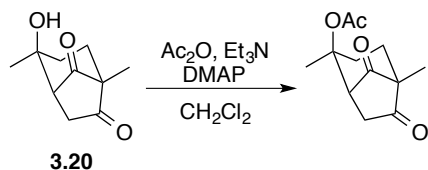


Signal 2: MSD1 TIC, MS File

Signal 3: MSD1 183, EIC=182.8:183.8

Peak #	RetTime [min]	Type	Width [min]	Area	Height	Area %	Peak #	RetTime [min]	Type	Width [min]	Area	Height	Area %
1	2.499	MM	0.1804	7.87632e5	7.27520e4	43.7571	1	2.505	MM	0.1717	1.83590e5	1.78225e4	44.3418
2	3.568	MM	0.2266	1.01238e6	7.44450e4	56.2429	2	3.551	MM	0.2239	2.30444e5	1.71506e4	55.6582

The e.e. of **3.20** (Table 9, entry 6) was determined by chiral GC analysis of the corresponding acetate of **3.20**.

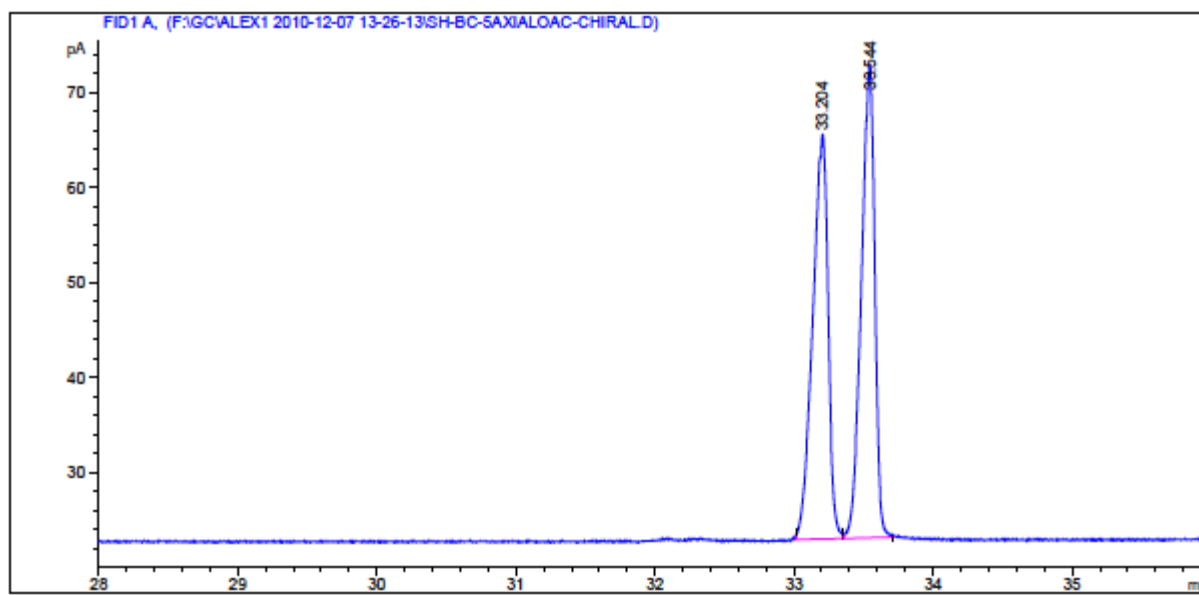


**(1*SR*,2*SR*,5*RS*)-2,5-Dimethyl-6,8-dioxobicyclo[3.2.1]octan-2-yl acetate.** Et<sub>3</sub>N (33 mg, 0.33 mmol, 46  $\mu$ L) was added to a solution of **3.20** (6 mg, 0.033 mmol) in CH<sub>2</sub>Cl<sub>2</sub> (0.5 mL) at 0  $^{\circ}$ C, followed by addition of Ac<sub>2</sub>O (34 mg, 0.33 mmol, 31  $\mu$ L) and DMAP (0.24 mg, 0.002 mmol). The reaction was stirred at r.t. for 24 h, quenched with saturated aqueous NH<sub>4</sub>Cl, and extracted

three time with CH<sub>2</sub>Cl<sub>2</sub> (4 mL). The organic phases were combined, washed with brine, dried over MgSO<sub>4</sub> and filtered. The volatiles were under reduced pressure. The residue was purified by flash chromatography (hexane: EtOAc, 4:1 to 3:1) to give the acetate (5.0 mg, 70 %) as white solid. m.p. 99-100 °C. <sup>1</sup>H NMR (400 MHz, CDCl<sub>3</sub>) δ 3.67-3.66 (m, 1H), 2.71-2.50 (m, 2H), 2.14-2.06 (m 1H), 2.07-1.94 (m, 4H), 1.87-1.82 (m, 1H), 1.76-1.60 (m, 4H), 1.08 (s, 3H); <sup>13</sup>C NMR (100 MHz, CDCl<sub>3</sub>) δ 212.3, 210.5, 170.2, 89.6, 58.2, 52.7, 41.8, 37.9, 31.0, 23.3, 22.0, 11.7; FTIR (cm<sup>-1</sup>) (neat) 2928, 1769, 1729, 1454, 1432, 1407, 1371, 1301, 1245, 1200, 1134, 1065, 1052, 1017, 983, 962, 936, 869, 841, 800; HRMS (ESI) calcd for C<sub>12</sub>H<sub>16</sub>NaO<sub>4</sub> (M+Na)<sup>+</sup> 247.0941, found 247.0939.

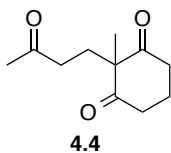
GC conditions: Agilent/HP 6890 GC series with Agilent/HP 7683 automatic liquid sampler, fitted with a β-cyclodextrin 120 column, 145 °C isotherm, 40 min.

(Table 9. Entry 6), e.e. = 0.5 %

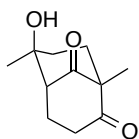


Peak #	RetTime [min]	Type	Width [min]	Area [pA*s]	Height [pA]	Area %
1	33.204	BV	0.1024	326.75326	42.56763	49.76438
2	33.544	VB	0.0863	329.84750	49.66564	50.23562

Table 11:



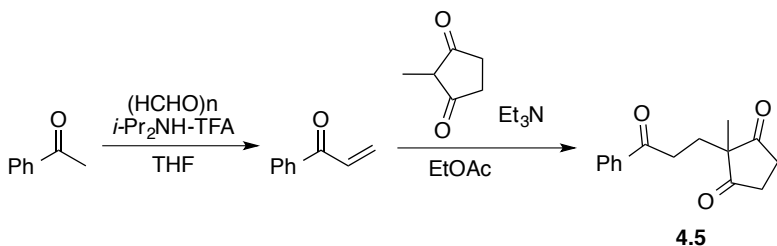
**2-Methyl-2-(3-oxobutyl)cyclohexane-1,3-dione (4.4)** was synthesized according a known procedure.<sup>55</sup> The spectroscopic data were in agreement with the proposed structures and matched those reported in the literature.<sup>56</sup> <sup>1</sup>H NMR (400 MHz, CDCl<sub>3</sub>) δ 2.83-2.56 (m, 4H), 2.34 (t, *J* = 7.4 Hz, 2H), 2.11 (s, 3H), 2.07-1.89 (m, 4H), 1.24 (s, 3H). <sup>13</sup>C NMR (100 MHz, CDCl<sub>3</sub>) δ 210.3, 207.9, 116.2, 64.4, 38.5, 37.8, 30.1, 29.6, 20.2, 17.7; HRMS (ESI) calcd for C<sub>11</sub>H<sub>16</sub>NaO<sub>3</sub> (M+Na)<sup>+</sup> 219.0992, found 219.0992.



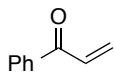
**(1*RS*,5*RS*,6*SR*)-6-Hydroxy-1,6-dimethylbicyclo[3.3.1]nonane-2,9-dione** was obtained from **4.4** based on the typical procedures mentioned before.

White solid. m.p. 110-112 °C. 85 % using TBD, [86 % using TBD & LiBr]. <sup>1</sup>H NMR (400 MHz, CDCl<sub>3</sub>) δ 2.71-2.64 (m, 1H), 2.61-2.53 (m, 1H), 2.46-2.34 (m, 1H), 2.14-2.01 (m, 3H), 1.92 (s, 1H), 1.84-1.72 (m, 2H), 1.72-1.60 (m, 1H), 1.39 (s, 3H), 1.17 (s, 3H); <sup>13</sup>C NMR (100 MHz, CDCl<sub>3</sub>) δ 211.5, 211.3, 78.8, 62.4, 56.9, 38.2, 37.0, 32.4, 27.9, 19.2, 16.4; FTIR (cm<sup>-1</sup>) (neat) 3421, 2973, 2935, 1731, 1693, 1467, 1450, 1405, 1378, 1333, 1310, 1293, 1246, 1232, 1218, 1178, 1150, 1123, 1090, 1066, 1048, 1022, 1009, 945, 924, 876, 815; HRMS (ESI) calcd for C<sub>11</sub>H<sub>16</sub>NaO<sub>3</sub> (M+Na)<sup>+</sup> 219.09917, found 219.09855.

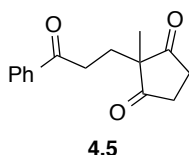
**4.5** was synthesized from acetophenone:





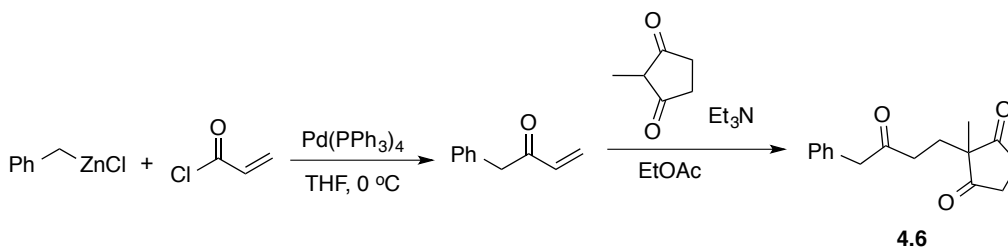


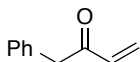
**1-Phenylprop-2-en-1-one** was synthesized according a known procedure.<sup>57</sup> The spectroscopic data were in agreement with the proposed structures and matched those reported in the literature.<sup>57</sup> Yield (680 mg, 52 %). <sup>1</sup>H NMR (400 MHz, CDCl<sub>3</sub>) δ 7.99-7.86 (m, 2H), 7.59-7.49 (m, 1H), 7.49-7.38 (m, 2H), 7.12 (dd, *J* = 17.1, 10.6 Hz, 1H), 6.40 (dd, *J* = 17.1, 1.7 Hz, 1H), 5.88 (dd, *J* = 10.6, 1.7 Hz, 1H); <sup>13</sup>C NMR (100 MHz, CDCl<sub>3</sub>) δ 190.7, 137.1, 132.8, 132.2, 129.9, 128.5, 128.4.



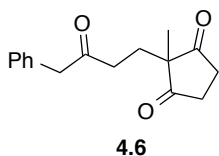
**2-Methyl-2-(3-oxo-3-phenylpropyl)cyclopentane-1,3-dione(4.5).**

1-phenylprop-2-en-1-one (656 mg, 5 mmol) was dissolved in EtOAc (75 mL), followed by addition of Et<sub>3</sub>N (506 mg, 5 mmol, 0.7 mL). The resulting solution was stirred at r.t. for 0.5 h, followed by addition of methyl vinyl ketone (374 mg, 3.3 mmol, 445 μL). After stirring for 6 days, the volatiles were removed under reduced pressure. The residue was purified by flash chromatography (hexane: EtOAc, 3:1 to 2:1) to give the **4.5** (540 mg, 67 %) as white solid. m.p. 77–80 °C (lit.<sup>58</sup>, m.p. 80-82 °C). The spectroscopic data were in agreement with the proposed structures and matched those reported in the literature.<sup>58</sup> <sup>1</sup>H NMR (400 MHz, CDCl<sub>3</sub>) δ 7.98-7.83 (m, 2H), 7.61-7.38 (m, 3H), 3.00 (t, *J* = 7.3 Hz, 2H), 2.97-2.72 (m, 4H), 2.08 (t, *J* = 7.3 Hz, 2H), 1.18 (s, 3H); <sup>13</sup>C NMR (100 MHz, CDCl<sub>3</sub>) δ 215.7, 199.2, 136.4, 133.2, 128.6, 127.9, 55.3, 34.7, 32.5, 28.4, 19.1; HRMS (ESI) calcd for C<sub>15</sub>H<sub>17</sub>O<sub>3</sub> (M+H)<sup>+</sup> 245.1172, found 245.1177.

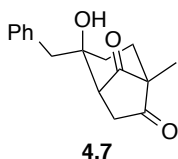




**1-Phenylbut-3-en-2-one** was synthesized according a known procedure from benzyl zinc chloride solution (18.5 mmol) and acryloyl chloride (1.81 g, 20 mmol).<sup>59</sup> Colorless liquid (1.75 g, 65 %). The spectroscopic data were in agreement with the proposed structures and matched those reported in the literature.<sup>59</sup> <sup>1</sup>H NMR (400 MHz, CDCl<sub>3</sub>) δ 7.46-7.16 (m, 5H), 6.44 (dd, *J* = 17.6, 10.2 Hz, 1H), 6.34 (dd, *J* = 17.6, 1.4 Hz, 1H), 5.84 (dd, *J* = 10.2, 1.4 Hz, 1H), 3.90 (s, 2H); <sup>13</sup>C NMR (100 MHz, CDCl<sub>3</sub>) δ 197.4, 135.4, 133.9, 129.3, 128.8, 128.5, 126.8, 46.9.

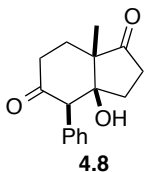


**2-Methyl-2-(3-oxo-4-phenylbutyl)cyclopentane-1,3-dione (4.6)** was synthesized according to the procedure for synthesizing **4.5**. Starting from 1-phenylbut-3-en-2-one (439 mg, 3 mmol) and methyl vinyl ketone (224 mg, 2 mmol, 266 μL). White solid. (450 mg, 87%). m.p. (55-57 °C), <sup>1</sup>H NMR (400 MHz, CDCl<sub>3</sub>) δ 7.43-7.22 (m, 3H), 7.21-7.11 (m, 2H), 3.64 (s, 2H), 2.87-2.65 (m, 4H), 2.47 (t, *J* = 7.1 Hz, 3H), 1.86 (t, *J* = 7.1 Hz, 2H), 1.07 (s, 3H); <sup>13</sup>C NMR (100 MHz, CDCl<sub>3</sub>) δ 215.4, 207.1, 133.5, 129.1, 128.3, 126.7, 54.7, 49.5, 35.6, 34.3, 27.6, 18.5; FTIR (cm<sup>-1</sup>) (neat) 2949, 1754, 1704, 1601, 1493, 1453, 1418, 1406, 1365, 1329, 1307, 1279, 1198, 1171, 1132, 1087, 1072, 1046, 1028, 989, 891, 859, 816, 791, 757, 743, 698, 649; HRMS (ESI) calcd for C<sub>16</sub>H<sub>19</sub>O<sub>3</sub> (M+H)<sup>+</sup> 259.1329, found 259.1330.

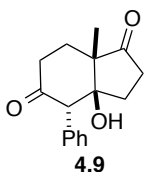


**(1*SR*,2*RS*,5*RS*)-2-Benzyl-2-hydroxy-5-methylbicyclo[3.2.1]octane-6,8-dione (4.7)** was obtained from **4.6** (26 mg, 0.10 mmol) based on the typical procedure described before. White solid (8.7 mg, 33 % using TBD, [10.4 mg, 40 %, using TBD & LiBr]. m.p. 124-129 °C. <sup>1</sup>H NMR (400 MHz, CDCl<sub>3</sub>) δ 7.40-7.29 (m, 3H), 7.18-7.16 (m, 2H), 2.91 (s, 2H), 2.81-2.59 (m,

3H), 2.20-2.06 (m, 1H), 1.94-1.77 (m, 3H), 1.73-1.62 (m, 1H), 1.08 (s, 3H);  $^{13}\text{C}$  NMR (100 MHz,  $\text{CDCl}_3$ )  $\delta$  213.3, 210.8, 134.6, 130.4, 128.8, 127.4, 81.6, 58.6, 54.4, 46.0, 42.1, 38.2, 31.1, 11.8; FTIR ( $\text{cm}^{-1}$ ) (neat) 3490, 2918, 2850, 1762, 1716, 1498, 1448, 1403, 1373, 1354, 1324, 1278, 1252, 1213, 1147, 1125, 1104, 1071, 1048, 1034, 1001, 965, 886, 859, 803, 778, 716, 705, 658; HRMS (ESI) calcd for  $\text{C}_{16}\text{H}_{19}\text{O}_3$  ( $\text{M}+\text{H}$ ) $^+$  259.1329, found 259.1330.



**(3aSR,4RS,7aSR)-3a-Hydroxy-7a-methyl-4-phenylhexahydro-1H-indene-1,5(4H)-dione (4.8)** was obtained from **4.6** (26 mg, 0.10 mmol) based on the typical procedure of the reaction of **3.18**. White solid. 22 mg, 85 % using **4.3**, [16.8 mg, 65 % using **4.3** & LiBr], [81 %, 21.0 mg using DBU], [82 %, 21.4 mg using DBU at  $-78\text{ }^\circ\text{C}$ ]. m.p.  $105\text{-}107\text{ }^\circ\text{C}$ .  $^1\text{H}$  NMR (400 MHz,  $\text{CDCl}_3$ )  $\delta$  7.44-7.35 (m, 3H), 7.28-7.23 (m, 2H), 3.46 (s, 1H), 2.65 (ddd,  $J = 19.7, 10.0, 2.1$  Hz, 1H), 2.54-2.27 (m, 4H), 2.08 (s, 1H), 1.97 - 1.89 (m, 2H), 1.83-1.75 (m, 1H), 1.19 (s, 3H);  $^{13}\text{C}$  NMR (100 MHz,  $\text{CDCl}_3$ )  $\delta$  217.8, 207.2, 132.9, 131.0, 128.5, 127.9, 83.7, 61.0, 53.3, 37.4, 34.6, 31.3, 28.7, 19.3; FTIR ( $\text{cm}^{-1}$ ) (neat) 3505, 2967, 1732, 1716, 1496, 1471, 1450, 1434, 1410, 1379, 1353, 1320, 1301, 1279, 1263, 1213, 1182, 1127, 1096, 1044, 944, 883, 828, 777, 748, 727, 701, 673; HRMS (ESI) calcd for  $\text{C}_{16}\text{H}_{19}\text{O}_3$  ( $\text{M}+\text{H}$ ) $^+$  259.1329, found 259.1331.



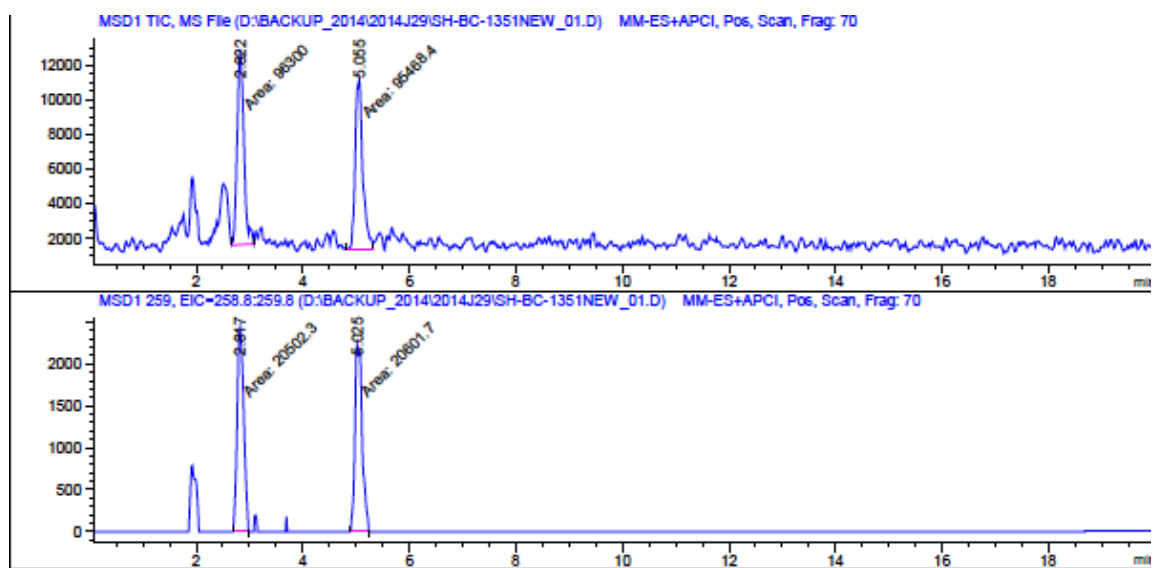
**(3aSR,4SR,7aSR)-3a-hydroxy-7a-methyl-4-phenylhexahydro-1H-indene-1,5(4H)-dione (4.9)** was obtained from **4.6** (26 mg, 0.10 mmol) based on the typical procedure of the reaction of **3.16**. White solid (21.5 mg, 83%). m.p.  $162\text{-}164\text{ }^\circ\text{C}$ ;  $^1\text{H}$  NMR (400 MHz,  $\text{CDCl}_3$ )  $\delta$  7.42-7.34 (m, 3H), 7.30-7.25 (m, 2H), 3.94 (s, 1H), 2.78-2.65 (m, 1H), 2.57-2.27 (m, 4H), 2.17-2.09 (m, 1H), 1.98-1.68 (m, 3H), 1.44 (s, 3H);  $^{13}\text{C}$  NMR (100 MHz,  $\text{CDCl}_3$ )  $\delta$  217.5, 205.4, 131.4, 131.3, 128.4, 128.1, 83.9, 63.2, 53.2, 36.9, 32.7, 31.0, 29.8, 12.5; FTIR ( $\text{cm}^{-1}$ ) (neat)

3480, 2970, 2938, 2874, 1734, 1710, 1499, 1474, 1455, 1418, 1405, 1376, 1345, 1311, 1265, 1231, 1209, 1136, 1060, 1017, 975, 954, 873, 800, 769, 726, 703; HRMS (ESI) calcd for  $C_{16}H_{19}O_3 (M+H)^+$  259.1329, found 259.1328.

Table 13, the enantiomeric excess of **4.7** was determined by SFC.

SFC conditions: ChiralPAK@AS-H, 250 x 4.6 mm, particle size 5  $\mu$ m, 10 % MeOH, 150 bar  $CO_2$ , Column temperature: 30  $^\circ C$ , flow rate: 3 mL/min, detection: UV 210 nm, MS.

(Table 13 entry 1) e.e < 1 %, racemic



Signal 1: MSD1 TIC, MS File

Signal 2: MSD1 259, EIC-258.8:259.8

Peak #	RetTime [min]	Type	Width [min]	Area	Height	Area %	Peak #	RetTime [min]	Type	Width [min]	Area	Height	Area %
1	2.822	MM	0.1413	9.63000e4	1.13623e4	50.2168	1	2.817	MM	0.1395	2.05023e4	2450.16943	49.8792
2	5.055	MM	0.1604	9.54684e4	9920.22266	49.7832	2	5.025	MM	0.1530	2.06017e4	2244.64111	50.1208

(Table 13 entry 2) e.e < 1 %, racemic

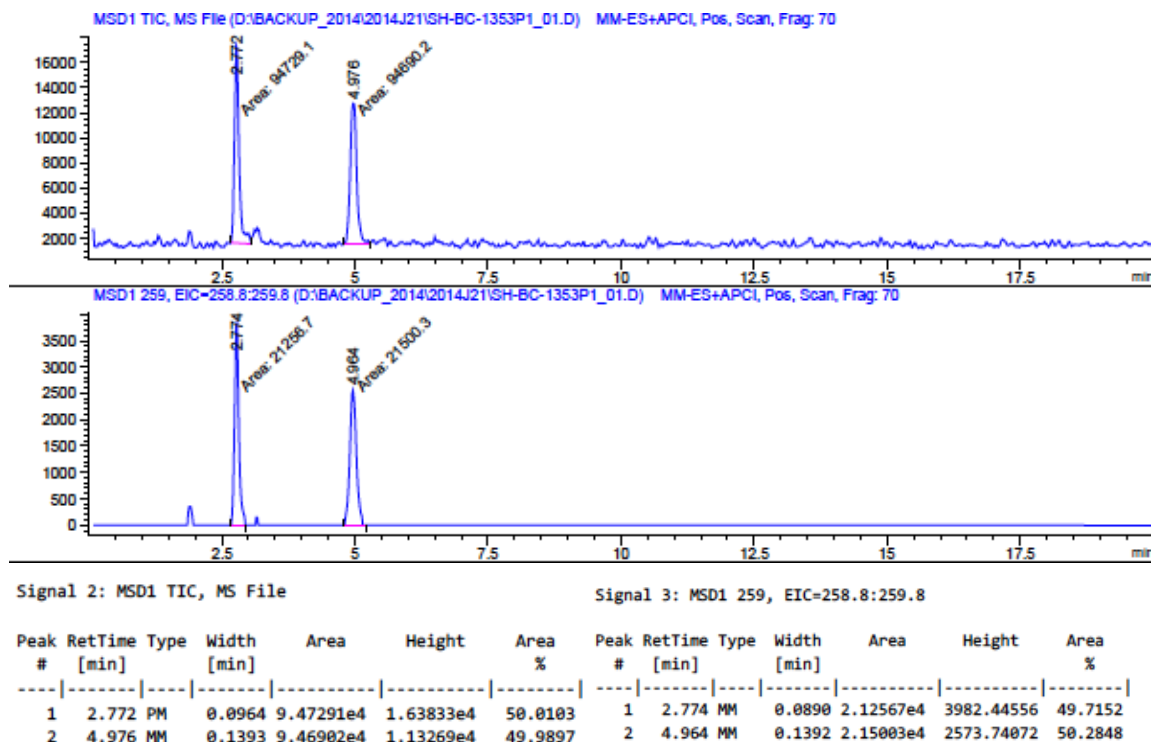
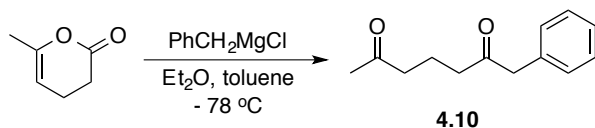
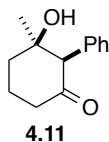


Table 15:



**1-Phenylheptane-2,6-dione (4.10)** was prepared according to a known procedure from benzyl magnesium chloride solution (2.25 mmol) and 3,4-dihydro-6-methyl-2H-pyran -2-one (0.5 g, 4.5 mmol).<sup>60</sup> The spectroscopic data were in agreement with the proposed structures and matched those reported in the literature.<sup>60</sup> Colorless solid, (50 mg, 11 %). <sup>1</sup>H NMR (400 MHz, CDCl<sub>3</sub>) δ 7.37-7.31 (m, 2H), 7.29-7.25 (m, 1H), 7.23-7.19 (m, 2H), 3.67 (s, 2H), 2.49 (t, *J* = 7.0 Hz, 2H), 2.40 (t, *J* = 7.1 Hz, 2H), 2.07 (s, 3H), 1.81 (p, *J* = 7.0 Hz, 2H); <sup>13</sup>C NMR (101 MHz, CDCl<sub>3</sub>) δ 208.3, 207.8, 134.1, 129.3, 128.7, 127.0, 50.1, 42.3, 40.6, 29.8, 17.6; HRMS (ESI) calcd for C<sub>13</sub>H<sub>16</sub>NaO<sub>2</sub> (M+Na)<sup>+</sup> 227.1043, found 227.1045.



**(2RS,3RS)-3-Hydroxy-3-methyl-2-phenylcyclohexan-1-one (4.11)** was obtained from **4.10** (29 mg, 0.14 mmol) based on the typical procedure of the reaction of **3.18**. White solid, 21.0 mg, 72 % using DBU & LiBr, [24.7 mg, 85 % using TBD]. m.p. 109-110 °C. <sup>1</sup>H NMR (400 MHz, CDCl<sub>3</sub>) δ 7.42-7.28 (m, 3H), 7.28-7.22 (m, 2H), 3.59 (s, 1H), 2.60-2.54 (m, 1H), 2.50-2.40 (m, 1H), 2.33-2.15 (m, 1H), 2.11-1.91 (m, 3H), 1.57 (s, 1H), 1.08 (s, 3H); <sup>13</sup>C NMR (100 MHz, CDCl<sub>3</sub>) δ 207.9, 134.2, 130.9, 128.1, 127.3, 76.6, 66.5, 41.1, 39.0, 29.9, 21.3; FTIR (cm<sup>-1</sup>) (neat) 3451, 3028, 2974, 2955, 2912, 1698, 1497, 1445, 1426, 1371, 1353, 1318, 1272, 1244, 1217, 1181, 1143, 1118, 1066, 1038, 998, 960, 943, 930, 912, 888, 868, 853, 801, 785, 743, 700; HRMS (ESI) calcd for C<sub>13</sub>H<sub>17</sub>O<sub>2</sub> (M+H)<sup>+</sup> 205.1223, found 205.1224.

## 4-6 References

1. Wurtz, C. A. *Bull. Soc. Chim. Fr.* **1872**, 17, 436.
2. Wurtz, C. A. *J. Prakt. Chem.* **1872**, 5, 457.
3. For books and reviews of Aldol reactions, see: (a) Denmark, S. E.; Stavenger, R. A. *Acc. Chem. Res.* **2000**, 33, 432. (b) Machajewski, T. D.; Wong, C. H. *Angew. Chem. Int. Ed.* **2000**, 39, 1352. (c) Mahrwald, R. *Modern Aldol Reactions*, Wiley-VCH Verlag GmbH, **2004**. (d) Palomo, C.; Oiarbide, M.; García, J. M. *Chem. Soc. Rev.* **2004**, 33, 65. (e) Mahrwald, R. *Aldol Reactions*, Springer, **2009**. (f) Trost, B. M.; Brindle, C. S. *Chem. Soc. Rev.* **2010**, 39, 1600. (g) Matsuo, J.-i. Murakami, M. *Angew. Chem. Int. Ed.* **2013**, 52, 9109. (h) Mahrwald, R. *Modern Methods in Stereoselective Aldol Reactions*, Wiley-VCH, **2013**.
4. Kino, T.; Hatanaka, H.; Hashimoto, M.; Nishiyama, M.; Goto, T.; Okuhara, M.; Kohsaka, M.; Aoki, H.; Imanaka, H. *J. Antibiot.* **1987**, 40, 1249.
5. Tanaka, H.; Kuroda, A.; Marusawa, H.; Hatanaka, H.; Kino, T.; Goto, T.; Hashimoto, M.; Taga, T. *J. Am. Chem. Soc.* **1987**, 109, 5031.
6. Nakatsuka, M.; Ragan, J. A.; Sammakia, T.; Smith, D. B.; Uehling, D. E.; Schreiber, S. L. *J. Am. Chem. Soc.* **1990**, 112, 5583.

7. Höfle, G.; Bedorf, N.; Reichenbach, H. (GBF), DE-4138042, **1993**; *Chem. Abstr.* **1993**, *120*, 52841.
8. Gerth, K.; Bedorf, N.; Höfle, G.; Irschik, H.; Reichenbach, H. *J. Antibiot.* **1996**, *49*, 560.
9. Höfle, G.; Bedorf, N.; Steinmertz, H.; Schomburg, D.; Gerth, K.; Reichenbach, H. *Angew. Chem. Int. Ed.* **1996**, *35*, 1567.
10. For total synthesis of Epothilone A and B, see: (a) Balog, A.; Meng, D.; Kamenecka, T.; Bertinato, P.; Su, D. S.; Sorensen, E. J.; Danishefsky, S. J. *Angew. Chem. Int. Ed.* **1996**, *35*, 2801. (b) Yang, Z.; He, Y.; Vourloumis, D.; Vallberg, H.; Nicolaou, K. C. *Angew. Chem. Int. Ed.* **1997**, *36*, 166. (c) Schinzer, D.; Limberg, A.; Bauer, A.; Böhm, O. M.; Cordes, M. *Angew. Chem. Int. Ed.* **1997**, *36*, 523. (d) Su, D. S.; Meng, D.; Bertinato, P.; Balog, D. M.; Sorensen, E. J.; Danishefsky, S. J.; Zheng, Y. H.; Chou, T. C.; He, L.; Horwitz, S. B. *Angew. Chem. Int. Ed.* **1997**, *36*, 757. (e) Nicolaou, K. C.; Ninkovic, S.; Sarabia, F.; Vourloumis, D.; He, Y.; Vallberg, H.; Finlay, M.R.V.; Yang, Z.; *J. Am. Chem. Soc.* **1997**, *119*, 7974. (f) Mulzer, J.; Mantoulidis, A.; Öhler, E. *J. Org. Chem.* **2000**, *65*, 745. (g) Bode, J. W.; Carreira, E. M. *J. Am. Chem. Soc.* **2001**, *123*, 3611.
11. Wani, M. C.; Taylor, H. L.; Wall, M. E.; Coggon, P.; McPhail, A. T. *J. Am. Chem. Soc.* **1971**, *93*, 2325.
12. For total synthesis of Taxol, see: (a) Holton, R. A.; Somoza, C.; Kim, H. B.; Liang, F.; Biediger, R. J.; Boatman, P. D.; Shindo, M.; Smith, C. C.; Kim, S.; Nadizadeh, H.; Suzuki, Y.; Tao, C. L.; Vu, P.; Tang, S. H.; Zhang, P. S.; Murthi, K. K.; Gentile, L. N.; Liu, J. H. *J. Am. Chem. Soc.* **1994**, *116*, 1597. (b) Holton, R. A.; Kim, H. B.; Somoza, C.; Liang, F.; Biediger, R. J.; Boatman, P. D.; Shindo, M.; Smith, C. C.; Kim, S.; Nadizadeh, H.; Suzuki, Y.; Tao, C. L.; Vu, P.; Tang, S. H.; Zhang, P. S.; Murthi, K. K.; Gentile, L. N.; Liu, J. H. *J. Am. Chem. Soc.* **1994**, *116*, 1599. (c) Nicolaou, K. C.; Yang, Z.; Liu, J. J.; Ueno, H.; Nantermet, P. G.; Guy, R. K.; Claiborne, C. F.; Renaud, J.; Couladouros, E. A.; Paulvannan, K.; Sorenson, E. J. *Nature*, **1994**, *367*, 630. (d) Danishefsky, S. J.; Masters, J. J.; Young, W. B.; Link, J. T.; Snyder, L. B.; Magee, T. V.; Jung, D. K.; Isaacs, R. C. A.; Bornmann, W. G.; Alaimo, C. A.; Coburn, C. A.; Grandi, M. J. D. *J. Am. Chem. Soc.* **1996**, *118*, 2843. (e) Wender, P. A.; Badham, N. F.; Conway, S. P.; Floreancig, P. E.; Glass, T. E.; Gränicher, C.; Houze, J. B.; Jänichen, J.; Lee, D.; Marquess, D. G.; McGrane, P. L.; Meng,

- W.; Mucciario, T. P.; Mühlebach, M.; Natchus, M. G.; Paulsen, H.; Rawlins, D. B.; Satkofsky, J.; Shuker, A. J.; Sutton, J. C.; Taylor, R. E.; Tomooka, K. *J. Am. Chem. Soc.* **1997**, *119*, 2755. (f) Wender, P. A.; Badham, N. F.; Conway, S. P.; Floreancig, P. E.; Glass, T. E.; Houze, J. B.; Krauss, N. E.; Lee, D.; Marquess, D. G.; McGrane, P. L.; Meng, W.; Natchus, M. G.; Shuker, A. J.; Sutton, J. C.; Taylor, R. E. *J. Am. Chem. Soc.* **1997**, *119*, 2757. (g) Morihira, K.; Hara, R.; Kawahara, S.; Nishimori, T.; Nakamura, N.; Kusama, H.; Kuwajima, I. *J. Am. Chem. Soc.* **1998**, *120*, 12980. (h) Shiina, I.; Iwadare, H.; Sakoh, H.; Hasegawa, M.; Tani, Y.; Mukaiyama, T. *Chem. Lett.* **1998**, *27*, 1. (i) Shiina, I.; Saitoh, K.; Frécharde-Ortuno, I.; Mukaiyama, T. *Chem. Lett.* **1998**, *27*, 3. (j) Mukaiyama, T.; Shiina, I.; Iwadare, H.; Saitoh, M.; Nishimura, T.; Ohkawa, N.; Sakoh, H.; Nishimura, K.; Tani, Y.; Hasegawa, M.; Yamada, K.; Saitoh, K. *Chem. Eur. J.* **1999**, *5*, 121. (k) Kusama, H.; Hara, R.; Kawahara, S.; Nishimori, T.; Kashima, H.; Nakamura, N.; Morihira, K.; Kuwajima, I. *J. Am. Chem. Soc.* **2000**, *122*, 3811. (l) Doi, T.; Fuse, S.; Miyamoto, S.; Nakai, K.; Sasuga, D.; Takahashi, T. *Chem. Asian J.* **2006**, *1*, 370. (m) Hirai, S.; Utsugi, M.; Iwamoto, M.; Nakada, M. *Chem. Eur. J.* **2015**, *21*, 355.
13. Evans, D. A.; Bartroli, J.; Shih, T. L. *J. Am. Chem. Soc.* **1981**, *103*, 2127.
  14. Walker, M. A.; Heathcock, C. H. *J. Org. Chem.* **1991**, *56*, 5747.
  15. Crimmins, M. T.; King, B. W.; Tabet, E. A.; Chaudhary, L. *J. Org. Chem.* **2001**, *66*, 894.
  16. Evans, D. A.; Ng, H. P.; Clark, J. S.; Rieger, D. L. *Tetrahedron.* **1992**, *48*, 2127.
  17. Evans, D. A.; Clark, J. S.; Metternich, R.; Sheppard, G. S. *J. Am. Chem. Soc.* **1990**, *112*, 866.
  18. Evans, D. A.; Tedrow, J. S.; Shaw, J. T.; Downey, C. W. *J. Am. Chem. Soc.* **2002**, *134*, 392.
  19. Evans, D. A.; Downey, C. W.; Shaw, J. T.; Tedrow, J. S. *Org. Lett.* **2002**, *4*, 1127.
  20. Mukaiyama, T.; Narasaka, K.; Banno, K. *Chem. Lett.* **1973**, 1011.
  21. Kobayashi, S.; Uchiro, H.; Fujishita, Y.; Shiina, I.; Mukaiyama, T. *J. Am. Chem. Soc.* **1991**, *113*, 4247.
  22. Corey, E. J.; Cywin, C. L.; Roper, T. D. *Tetrahedron Lett.* **1992**, *33*, 6907.
  23. Carreira, E. M.; Singer, R. A.; Lee, W. *J. Am. Chem. Soc.* **1994**, *116*, 8837.
  24. Evans, D. A.; Kozlowski, M. C.; Murry, J. A.; Burgey, C. S.; Campos, K. R.; Connell, B. T.; Staples, R. J., *J. Am. Chem. Soc.* **1999**, *121*, 669.
  25. Denmark, S. E.; Stavenger, R. A.; Wong, K. T.; Su, X. P. *J. Am. Chem. Soc.* **1999**, *121*,



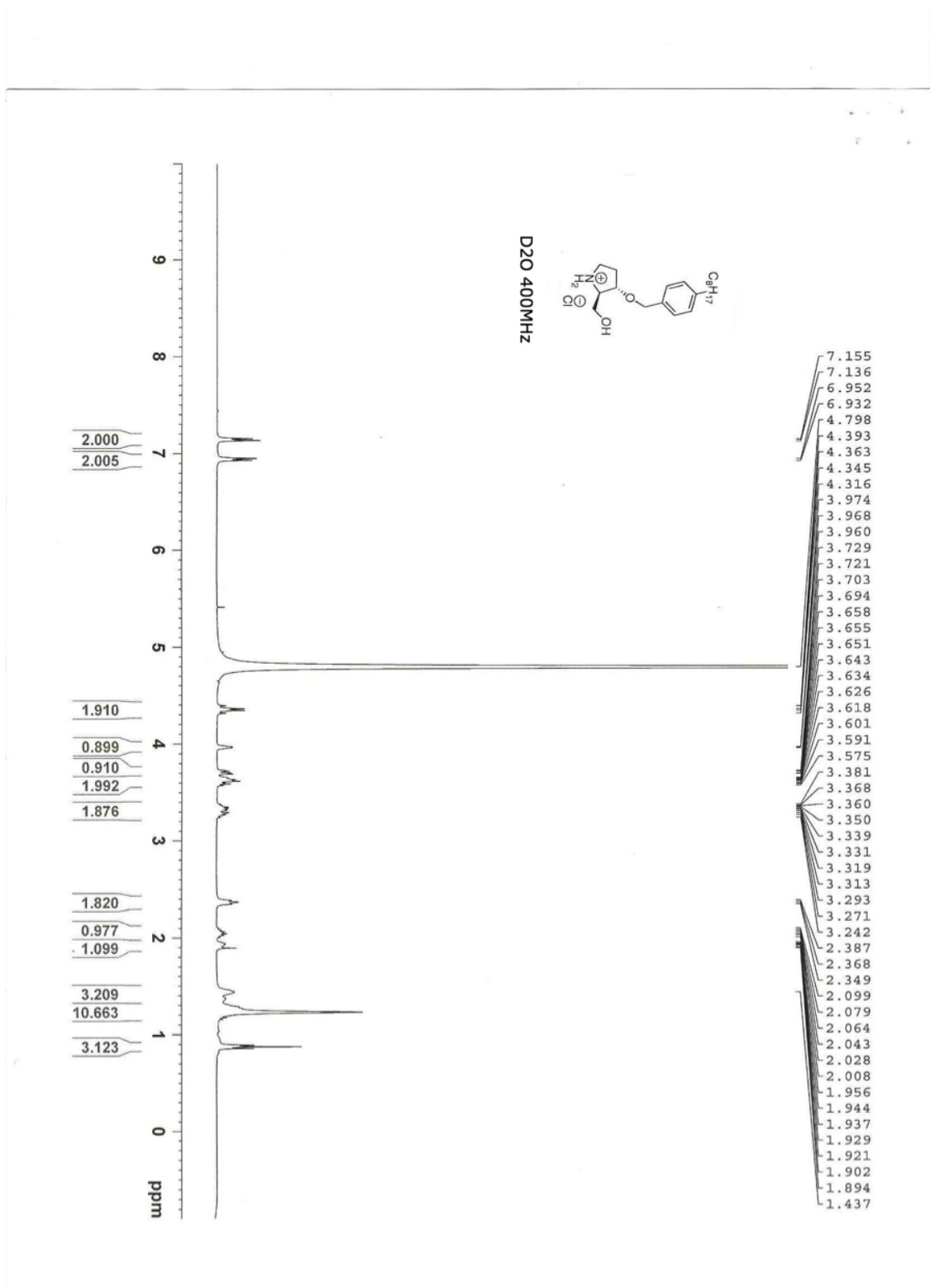
4982.

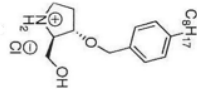
26. Wadamoto, M.; Ozasa, N.; Yanagisawa, A.; Yamamoto, H. *J. Org. Chem.* **2003**, *68*, 5593.
27. Heravi, M. M.; Asadi, S. *Tetrahedron: Asymmetry*, **2012**, *23*, 1431.
28. Hajos, Z. G.; Parrish, D. R. *J. Org. Chem.*, **1974**, *39*, 1615.
29. List, B.; Lerner, R. A.; Barbas III, C. F. *J. Am. Chem. Soc.* **2000**, *122*, 2395.
30. Sakthivel, K.; Notz, W.; Bui, T.; Barbas III, C. F. *J. Am. Chem. Soc.* **2001**, *123*, 5260.
31. Northrup, A. B.; MacMillan, D. W. C. *J. Am. Chem. Soc.* **2002**, *124*, 6798.
32. Hartikka, A.; Arvidsson, P. I. *Tetrahedron: Asymmetry*, *15*, 1831.
33. Berkessel, A.; Koch, B.; Lex, J. *Adv. Synth. Catal.* **2004**, *346*, 1141
34. Tang, Z.; Yang, Z. H.; Chen, X. H.; Cun, L. F.; Mi, A. Q.; Jiang, Y. Z.; Gong, L. *J. Am. Chem. Soc.* **2005**, *127*, 9285.
35. Subba Reddy, B. V.; Bhavani, K.; Raju, A.; Yadav, J. S. *Tetrahedron: Asymmetry* **2011**, *22*, 881.
36. Cheong, P. H. Y.; Houk, K. N.; Warrier, J. S.; Hanessian, S. *Adv. Synth. Catal.* **2004**, *346*, 1111.
37. Hajos, Z. G.; Parrish, D. R. *J. Org. Chem.*, **1974**, *39*, 1612.
38. (a) Brown, K. L.; Damm, L.; Dunitz, J. D.; Eschenmoser, A.; Hobi, R.; Kratky, C. *Helv. Chim. Acta* **1978**, *61*, 3108. (b) Agami, C.; Meynier, F.; Puchot, C.; Guilhem, J.; Pascard, C. *Tetrahedron*, **1984**, *40*, 1031. (c) Agami, C.; Sevestre, H. *J. Chem. Soc. Chem. Commun.* **1984**, 1385; (d) Bahmanyar, S.; Houk, K. N. *J. Am. Chem. Soc.* **2001**; *123*, 12911. (e) Bahmanyar, S.; Houk, K. N. *J. Am. Chem. Soc.* **2001**; *123*, 11273.
39. Dauben, W. G.; Bunce, R. A. *J. Org. Chem.* **1983**, *48*, 4642.
40. Sasai, H.; Szuki, T.; Arai, S.; Arai, T.; Shibasaki, M. *J. Am. Chem. Soc.* **1992**, *114*, 4418.
41. Davies, S. G.; Russell, A. J.; Sheppard, R. L.; Smith, A. D.; Thomson, J. E. *Org. Biomol. Chem.* **2007**, *5*, 3190.
42. Schetter, B.; Ziemer, B.; Schnakenburg, G.; Mahrwald, R. *J. Org. Chem.*, **2008**, *73*, 813.
43. Kaljurand, I.; Rodima, T.; Pihl, A.; Mäemets, V.; Leito, I.; Koppel, Ilmar. A. Mishima, M. *J. Org. Chem.* **2003**, *68*, 9988.
44. For the chelation effect of LiBr: see (a) Seebach, D.; Thaler, A.; Beck, A. K. *Helv. Chim. Acta.* **1989**, *72*, 857. (b) Fuchs, J. R.; Mitchell, M. L.; Shabangi, M.; Flowers II, R. A.

- Tetrahedron Lett.* **1997**, *38*, 8157. (c) Chakraborti, A. K.; Rudrawar, S.; Kondaskar, A. *Eur. J. Org. Chem.* **2004**, 3597. (d) Mojtahedi, M. M.; Akbarzadeh, E.; Sharifi, R.; Abaee, M. S. *Org. Lett.* **2007**, *9*, 2791.
45. Heinzer, F.; Soukup, M.; Eschenmoser, A. *Helv. Chim. Acta.* **1978**, *61*, 2851.
46. Rõõm, E. I.; Kütt, A.; Kaljurand, I.; Koppel, I.; Leito, I.; Koppel, Ilmar A.; Mishima, M.; Goto, K.; Miyahara, Y. *Chem. Eur. J.* **2007**, *13*, 7631.
47. For review of lithium/(-)-sparteine catalysis, see Hoppe, D.; Hense, T. *Angew. Chem. Int. Ed.* **1997**, *36*, 2282.
48. (a) Ma, D. W.; Cheng, K. J. *Tetrahedron: Asymmetry.* **1999**, *10*, 713; (b) Lovick, H. M.; Michael, F. E. *Tetrahedron Lett.* **2009**, *50*, 1016.
49. (a) Birman, V. B.; Li, X. *Org. Lett.* **2006**, *8*, 1351. (b) Leverett, C. A.; Purohit, V. C.; Romo, D. *Angew. Chem. Int. Ed.* **2010**, *122*, 9669.
50. Roberts, E. M.; Grisar, J. M.; MacKenzie, R. D.; Claxton, G. P.; Blohm, T. R. *J. Med. Chem.* **1972**, *15*, 1270.
51. Clemente, F. R.; Houk, K. N. *Angew. Chem. Int. Ed.* **2004**, *43*, 5766.
52. Hammar, P.; Ghobril, C.; Antheaume, C.; Wagner, A.; Baati, R.; Himo, F. *J. Org. Chem.* **2010**, *75*, 4728.
53. For recent reviews on bifunctional H-bonded catalysis, see (a) Doyle, A. G.; Jacobsen, E. N. *Chem. Rev.* **2007**, *107*, 5713. (b) Palomo, C.; Oiarbide, M.; López, R. *Chem. Soc. Rev.* **2009**, *38*, 632. (c) Ting, A.; Goss, J. M.; McDougal, N. T.; Schaus, S. E. *Top. Curr. Chem.* **2010**, *291*, 145. (d) Marcelli, T.; Hiemstra, H. *Synthesis*, **2010**, 1229. (e) Marqués-López, E.; Herrera, R. P. *Hydrogen Bonds as an Alternative Activation*, in *New Strategies in Chemical Synthesis and Catalysis* (ed B. Pignataro), **2012**, Wiley-VCH Verlag GmbH & Co. KGaA, Weinheim, Germany.
54. (a) Ghobril, C.; Sabot, C.; Mioskowski, C.; Baati, R. *Eur. J. Org. Chem.* **2008**, 4104. (b) Ghobril, C.; Hammar, P.; Kodepelly, S.; Spiess, B.; Wagner, A.; Himo, F.; Baati, R. *Chem. Cat. Chem.* **2010**, *2*, 1573.
55. Harada, N.; Sugioka, T.; Uda, H.; Kuriki, T. *Synthesis*, **1990**, 53.
56. Lacoste, E.; Vaique, E.; Berlande, M.; Pianet, I.; Vincent, J. M.; Landais, Y. *Eur. J. Org. Chem.* **2007**, 167.

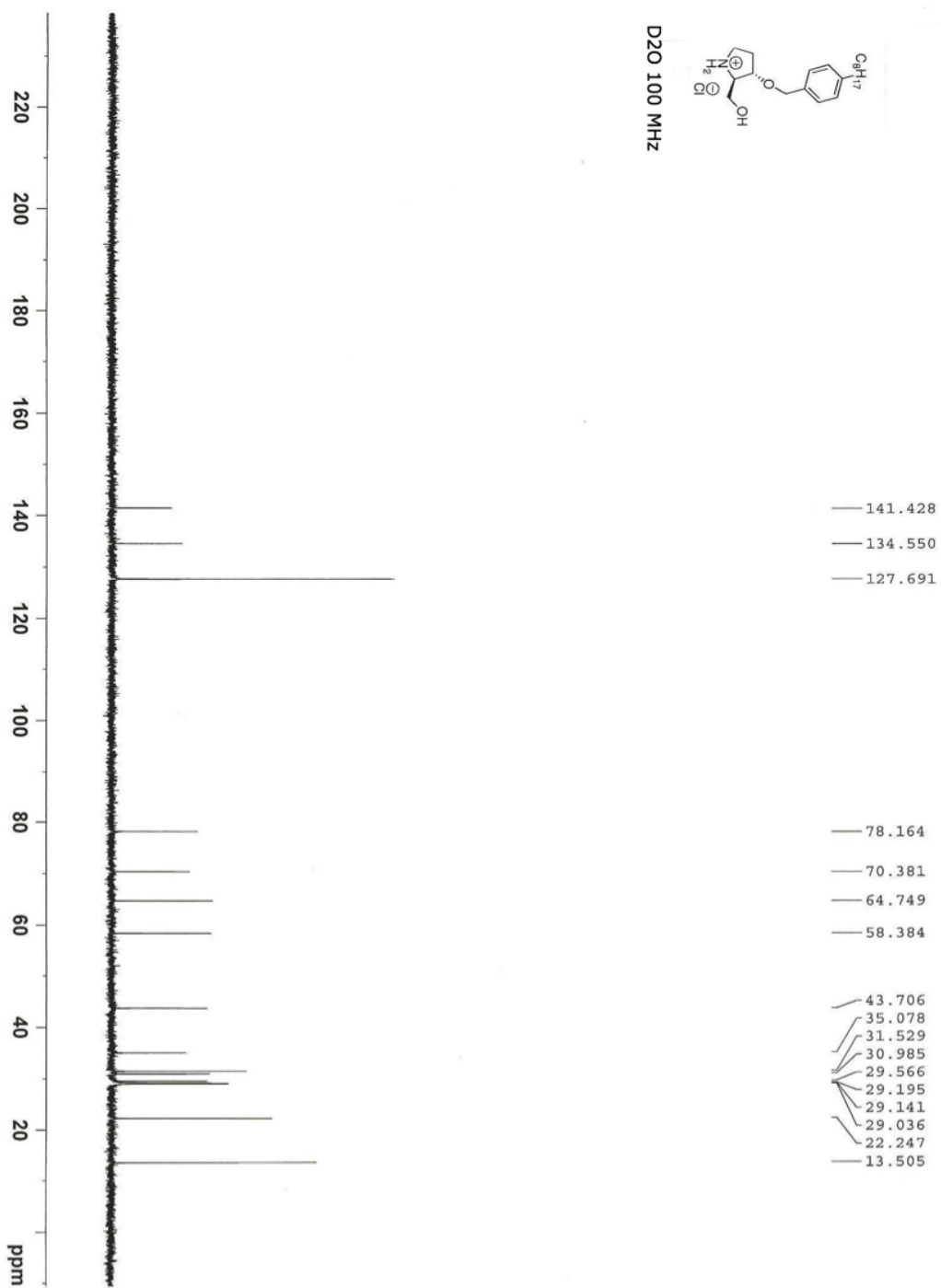
57. Bugarin, A.; Jonesa, K. D.; Connell, B. T. *Chem. Commun.* **2010**, 46, 1715.
58. Rao, H. S. P.; Poonguzhali E.; Senthilkumar, S. *Synth. Commun.* **2008**, 38, 937.
59. Ogasawara, M.; Ge, Y. H.; Uetake, K.; Takahashi, T. *Org. Lett.* **2005**, 7, 5697.
60. Zhou, J.; List, B. *J. Am. Chem. Soc.* **2007**, 129, 7498.

# Annex 1: $^1\text{H}$ and $^{13}\text{C}$ NMR Spectra of Compound 1.32

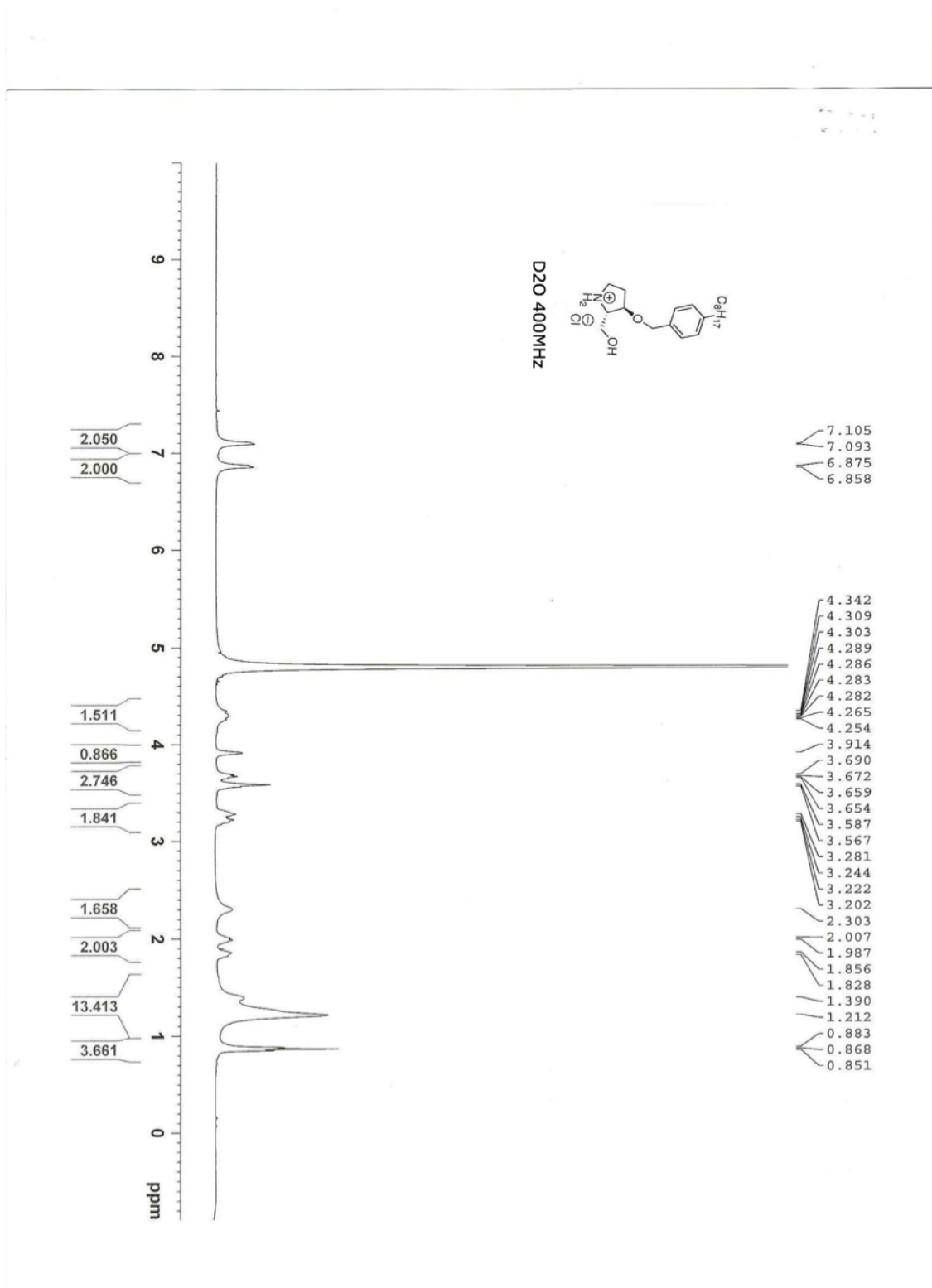


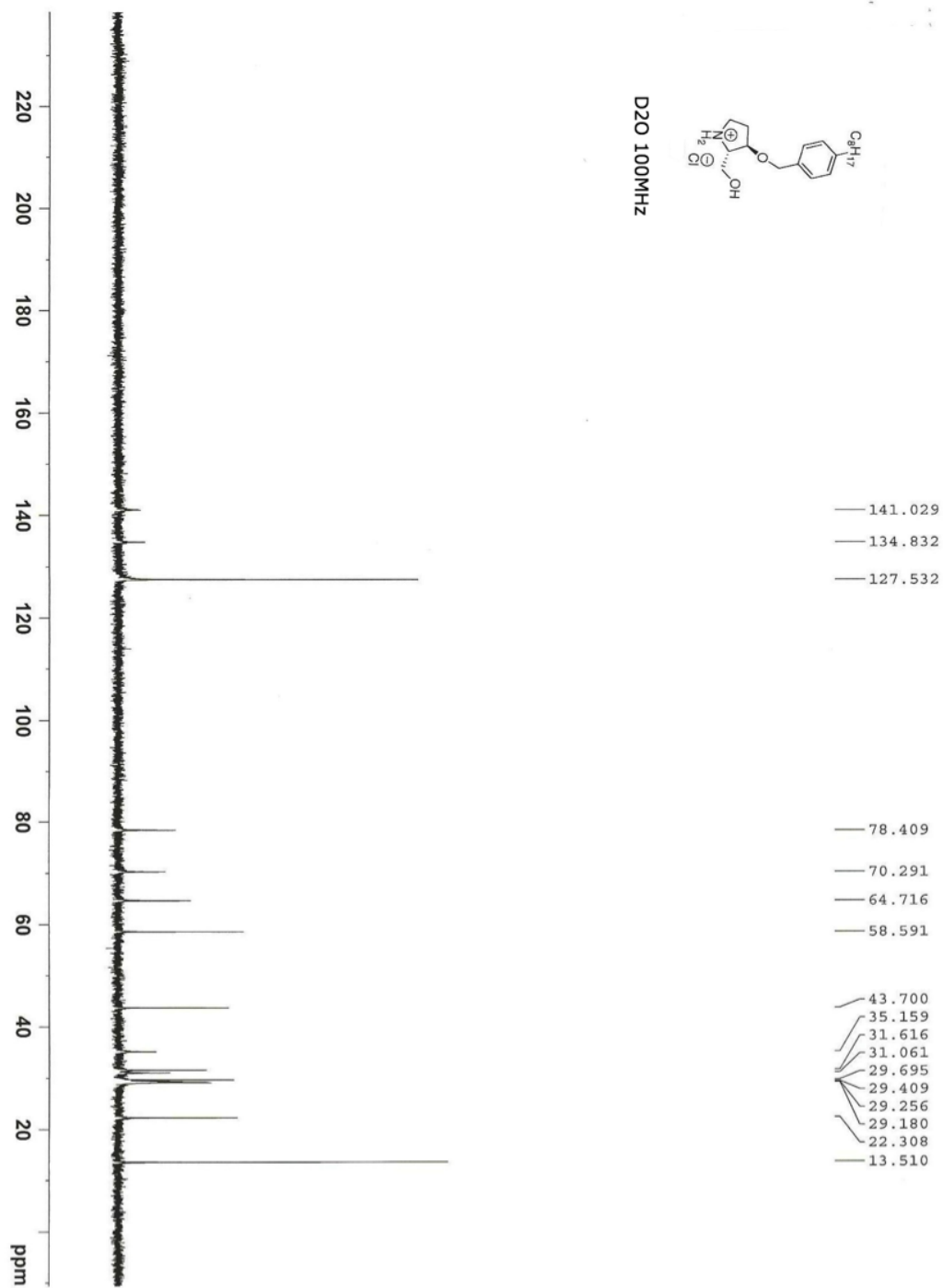


D2O 100 MHz

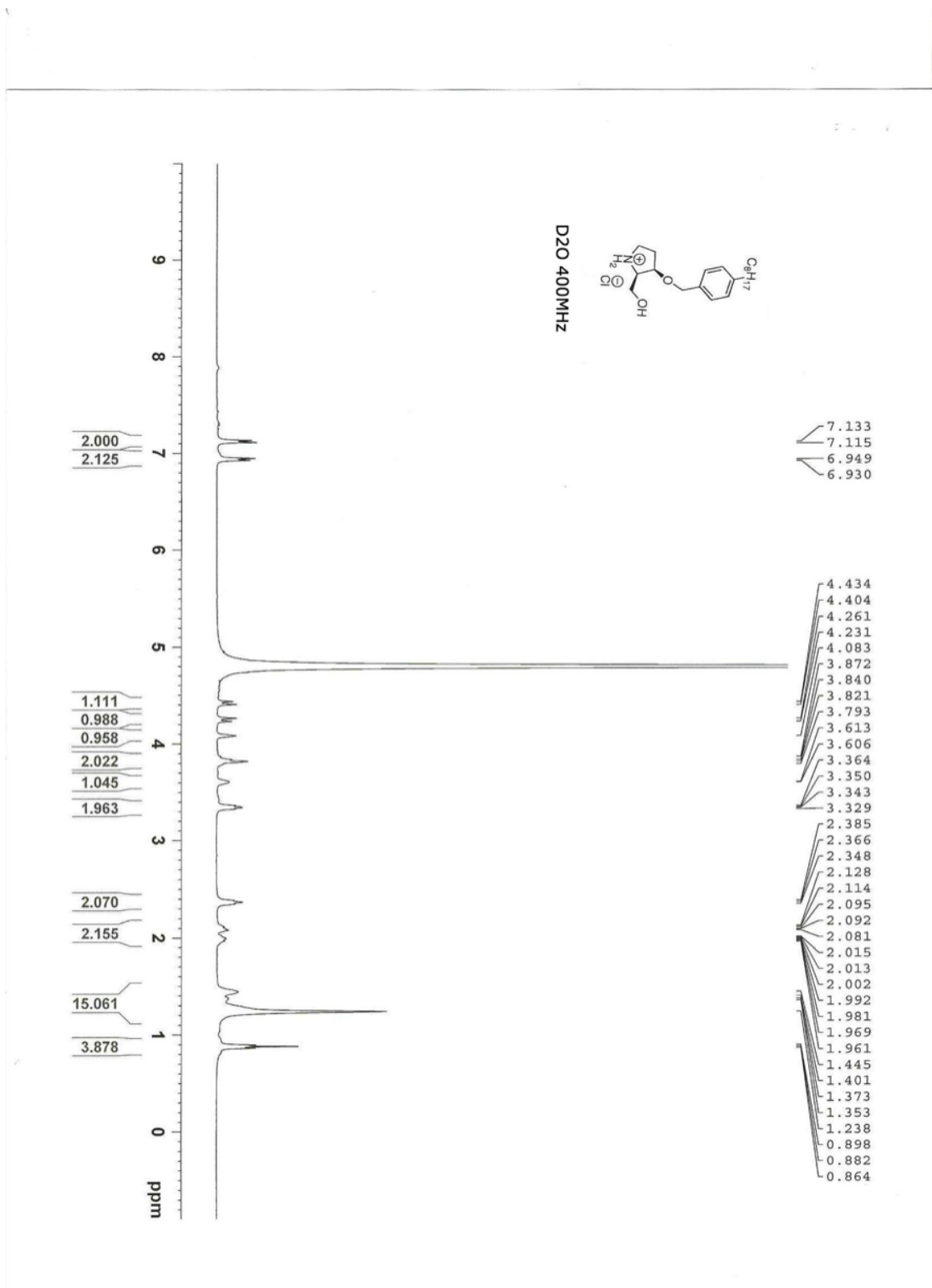


# Annex 2: $^1\text{H}$ and $^{13}\text{C}$ NMR Spectra of Compound 1.39

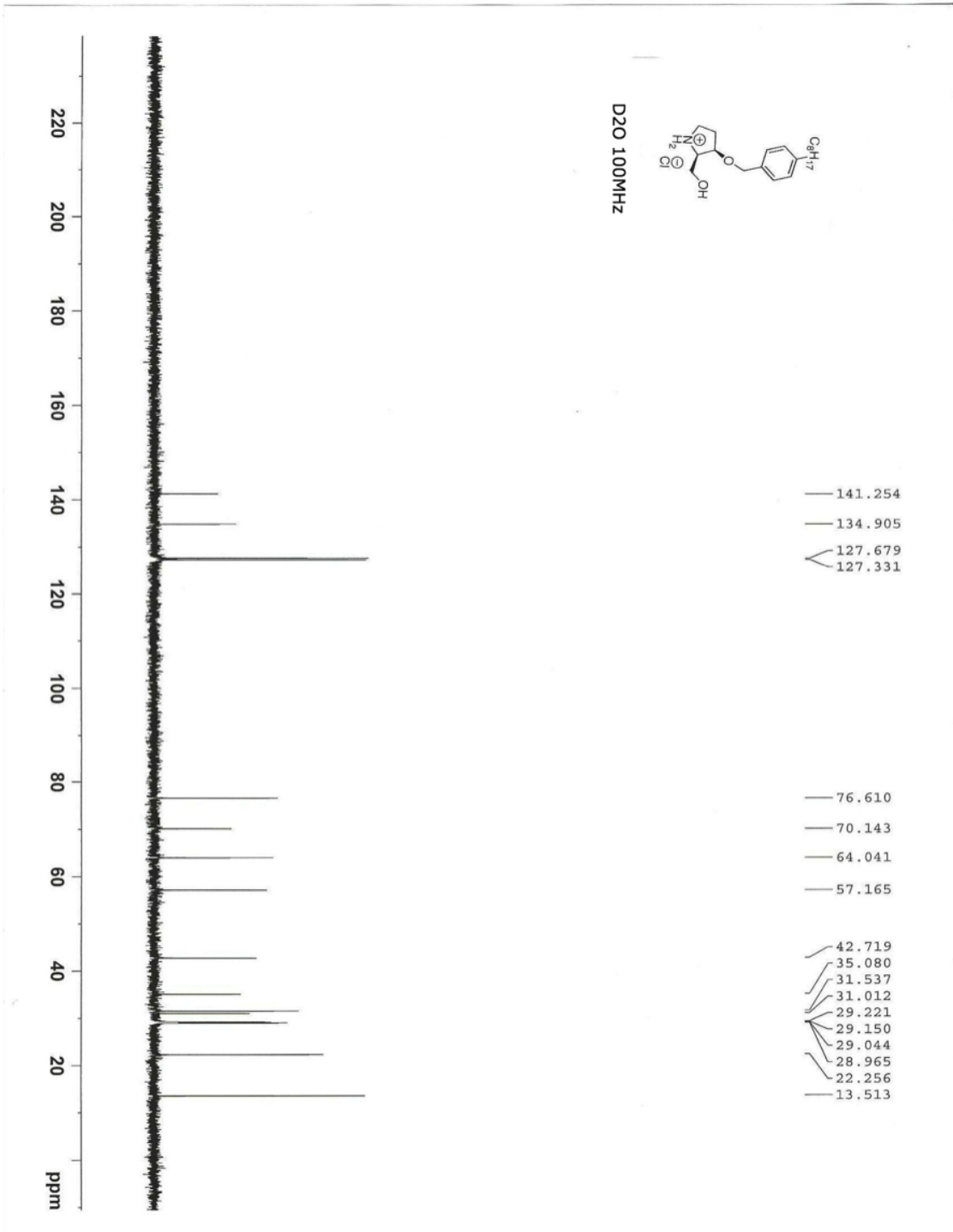




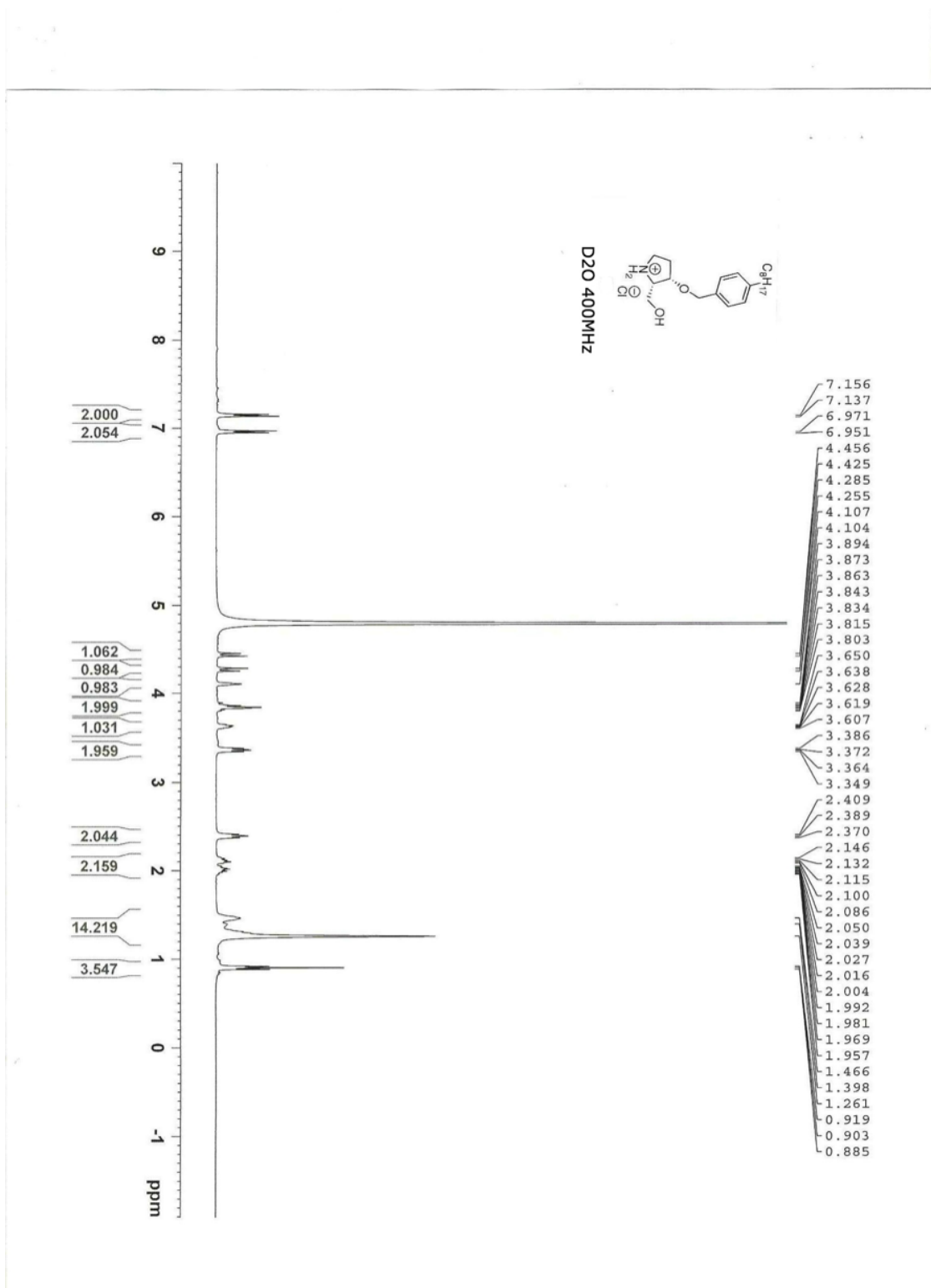
# Annex 3: $^1\text{H}$ and $^{13}\text{C}$ NMR Spectra of Compound 1.44

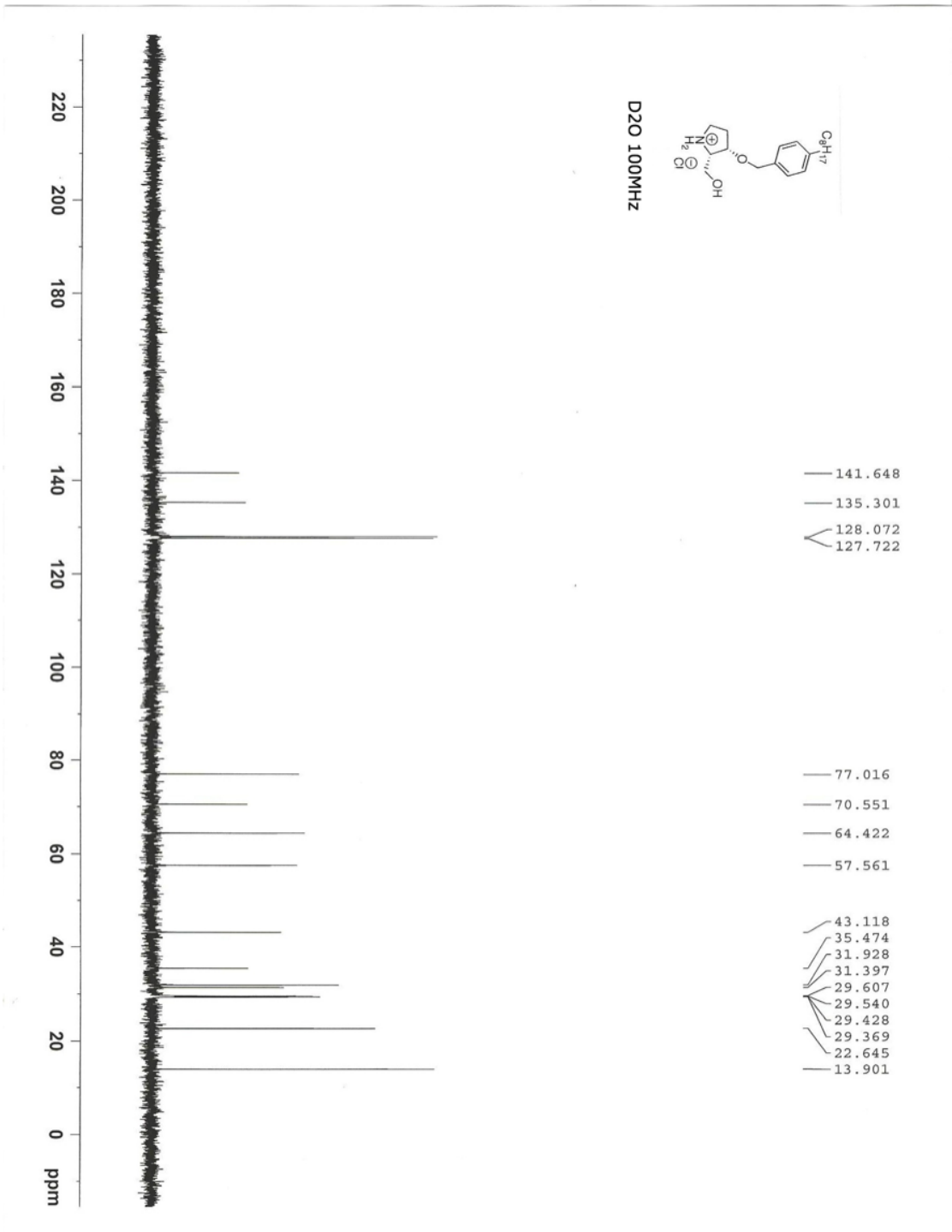




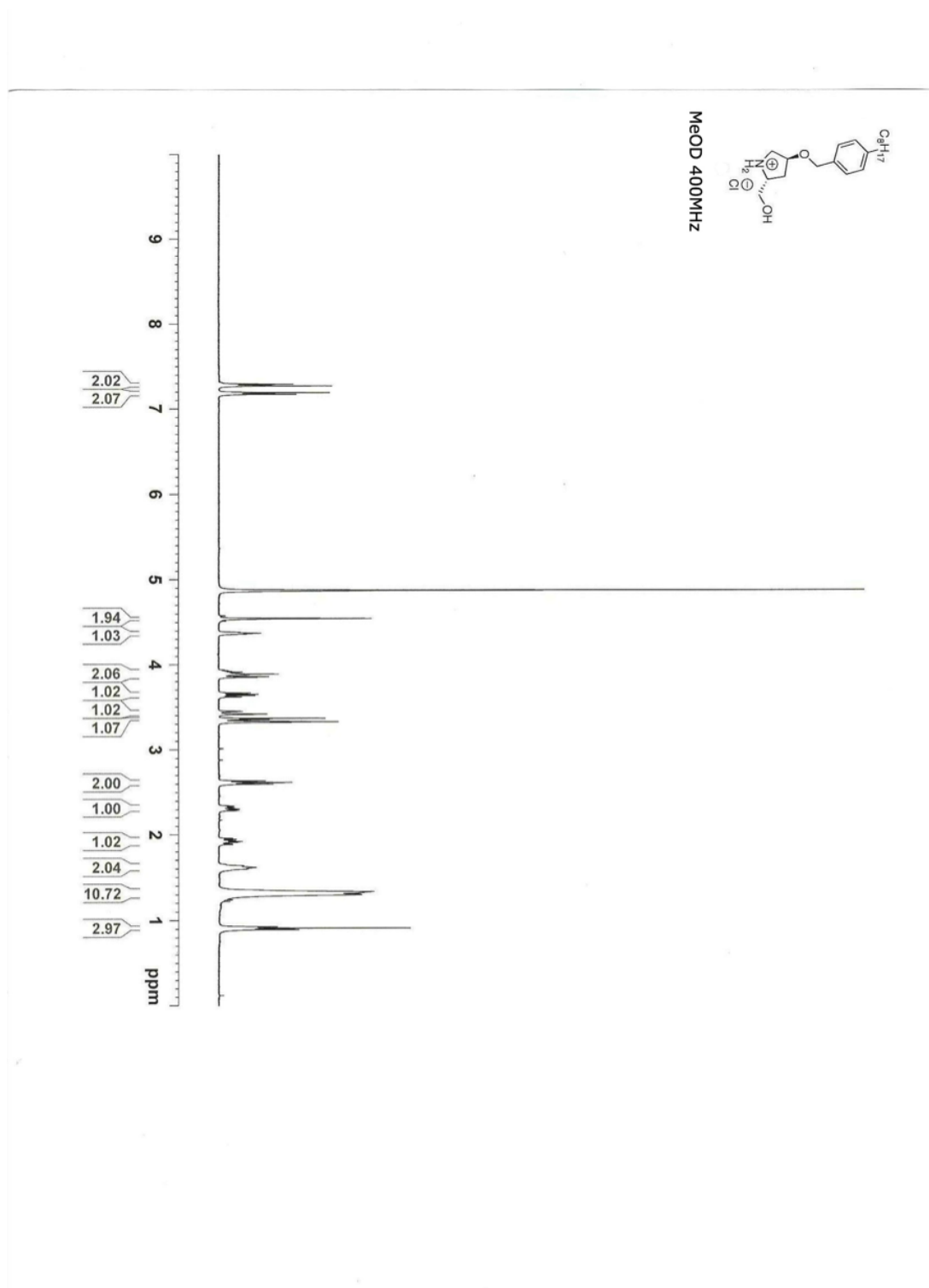


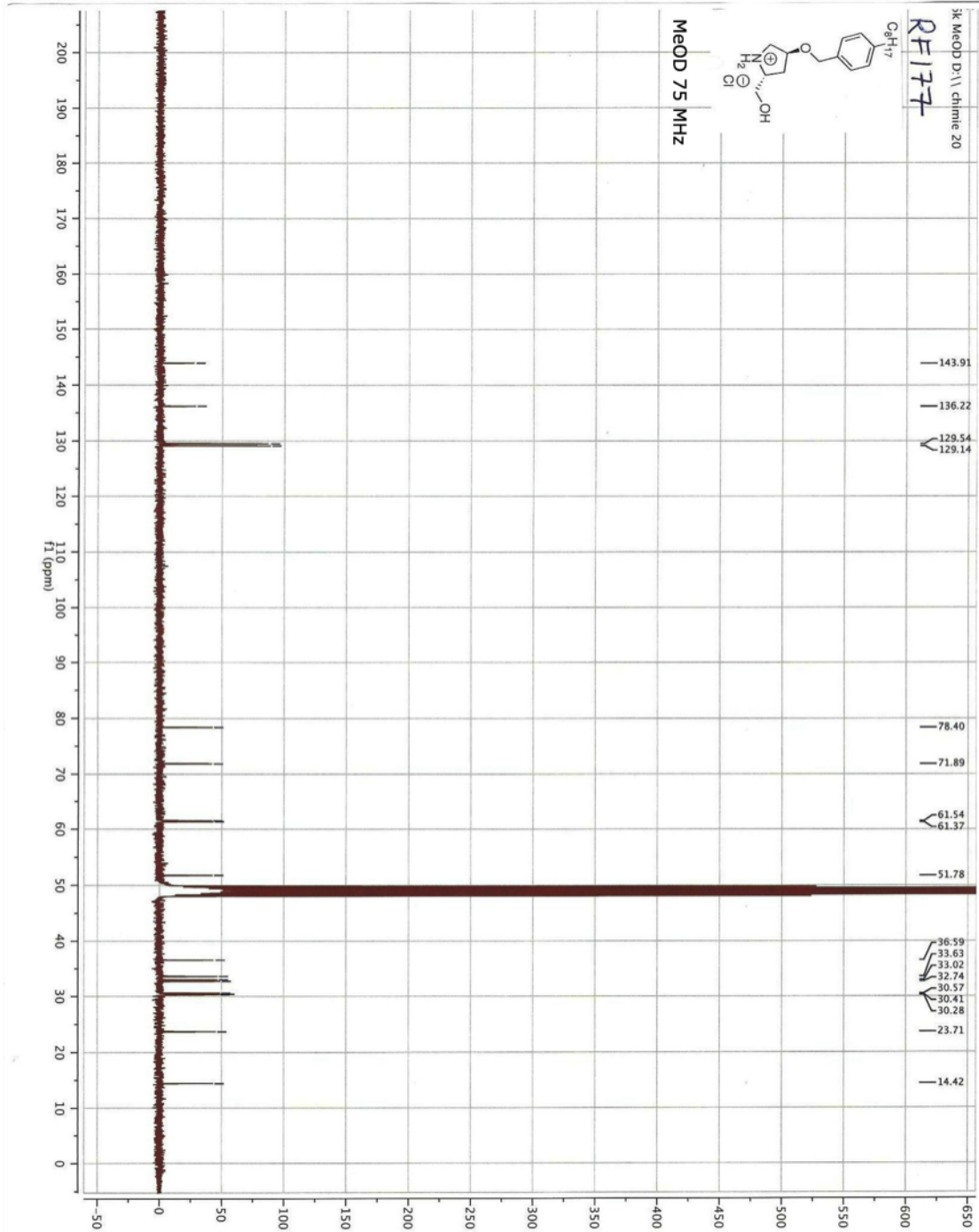
# Annex 4: $^1\text{H}$ and $^{13}\text{C}$ NMR Spectra of Compound 1.49



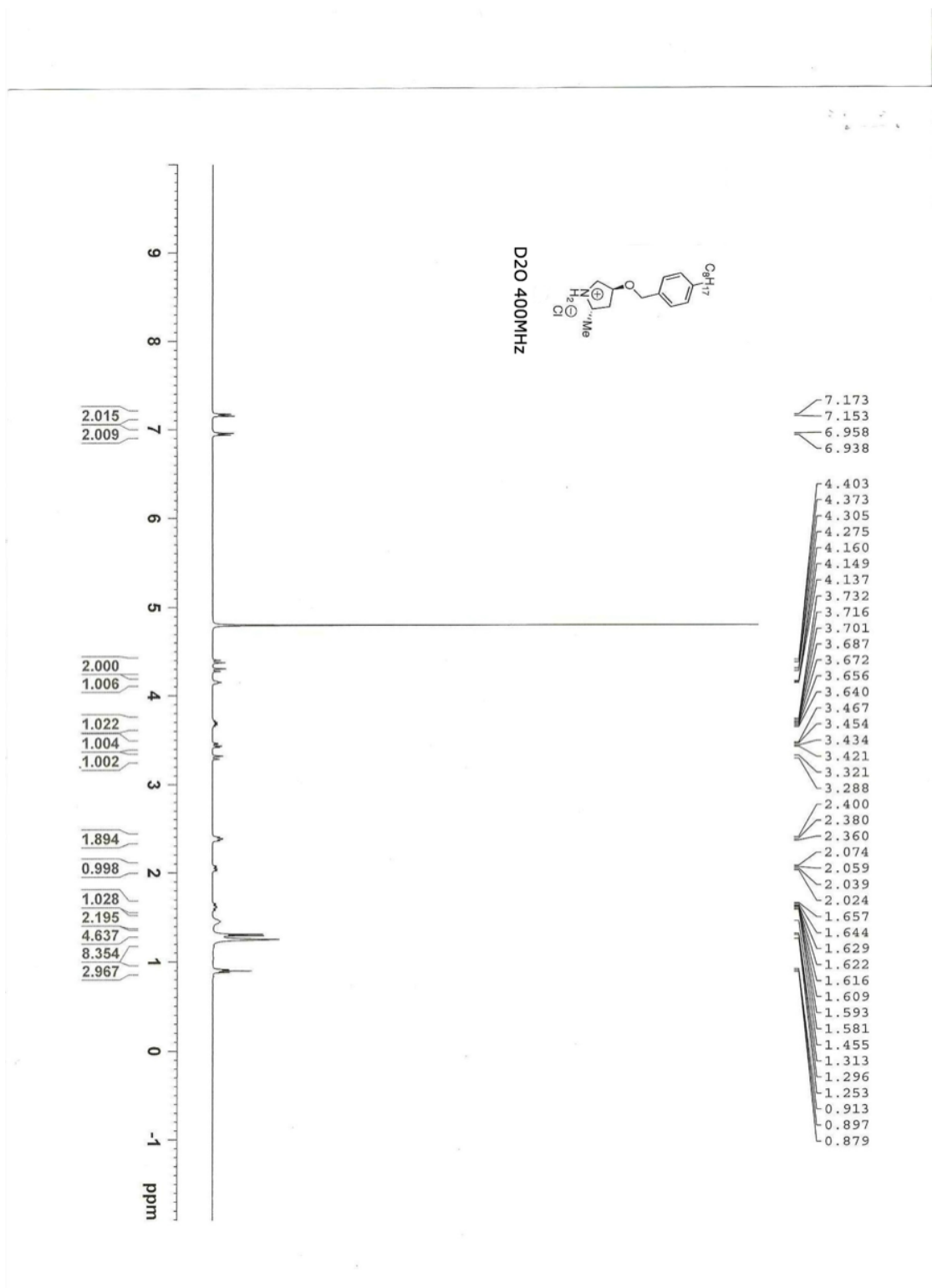


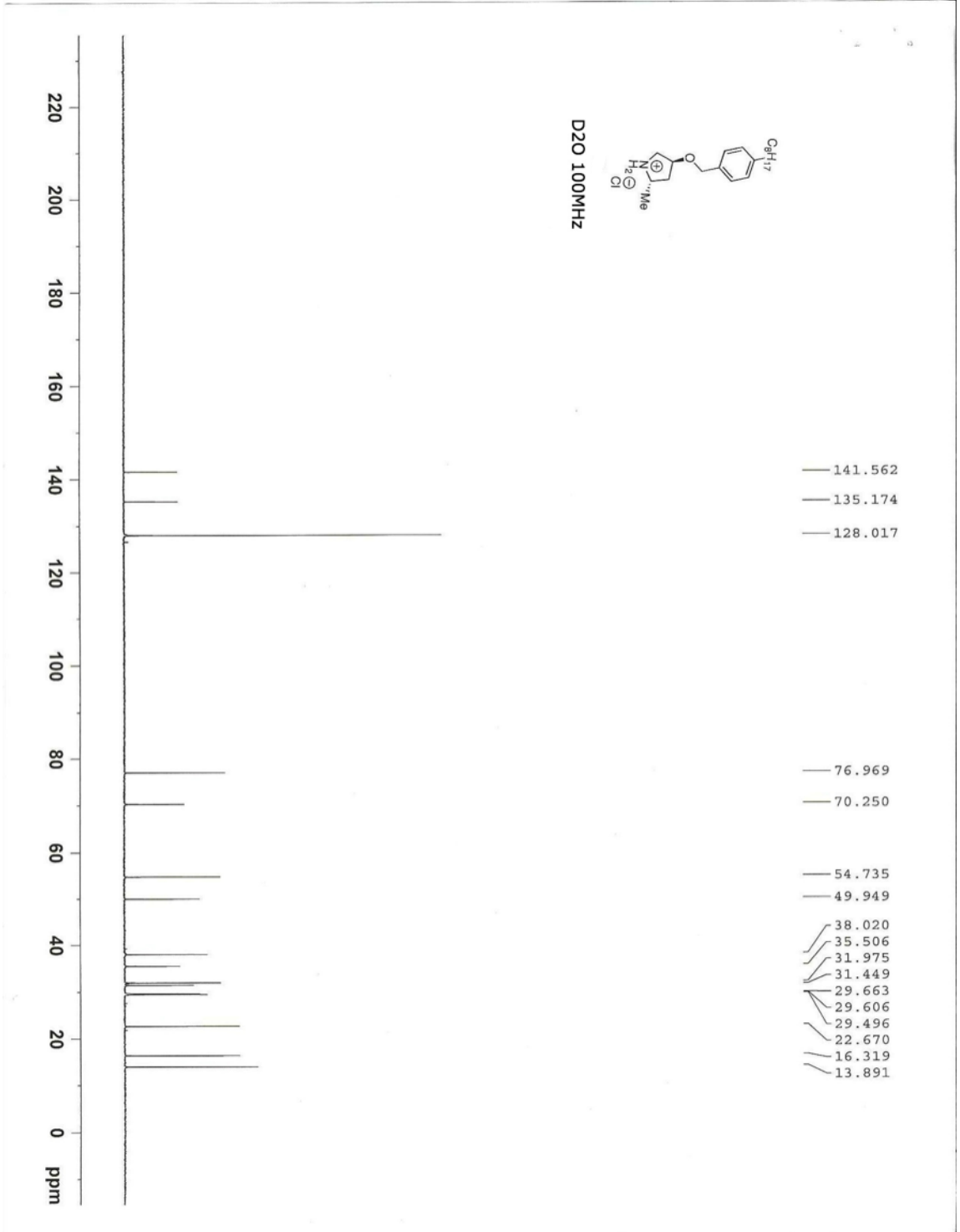
## Annex 5: $^1\text{H}$ and $^{13}\text{C}$ NMR Spectra of Compound 1.65





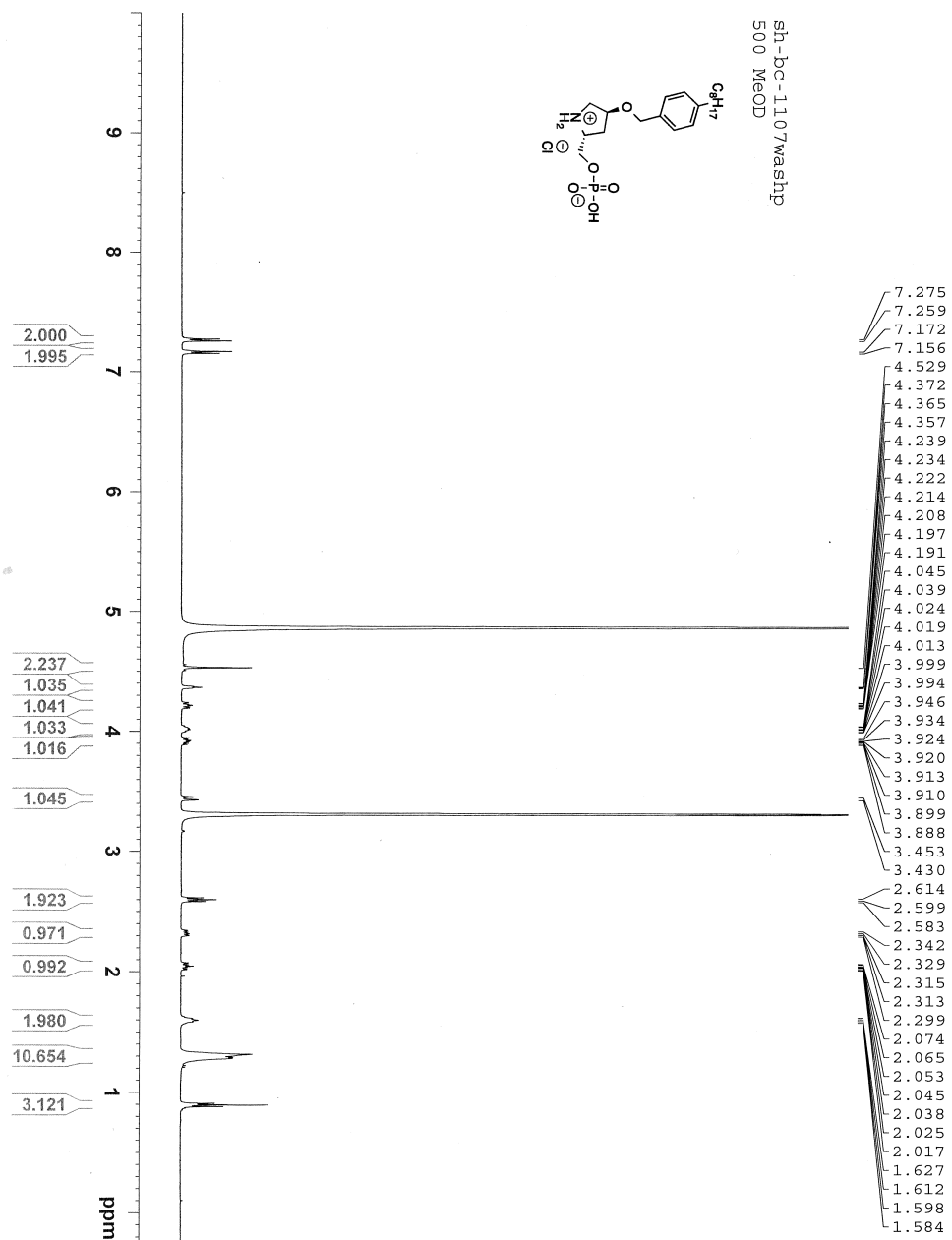
# Annex 6: $^1\text{H}$ and $^{13}\text{C}$ NMR Spectra of Compound 1.70





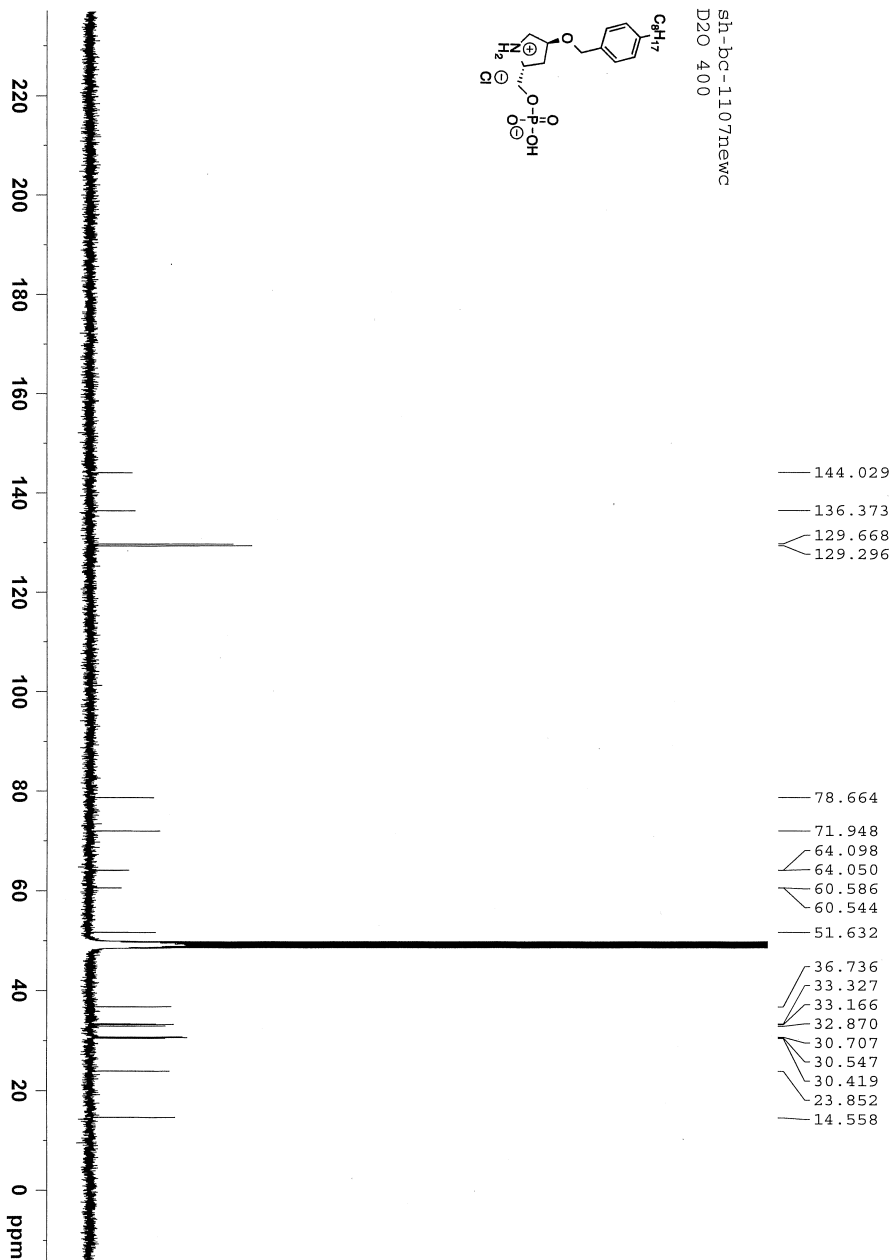
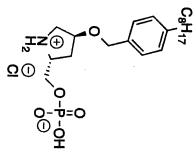
# Annex 7: $^1\text{H}$ , $^{13}\text{C}$ and $^{31}\text{P}$ NMR Spectra of Compound

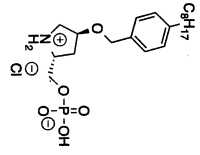
## 1.77



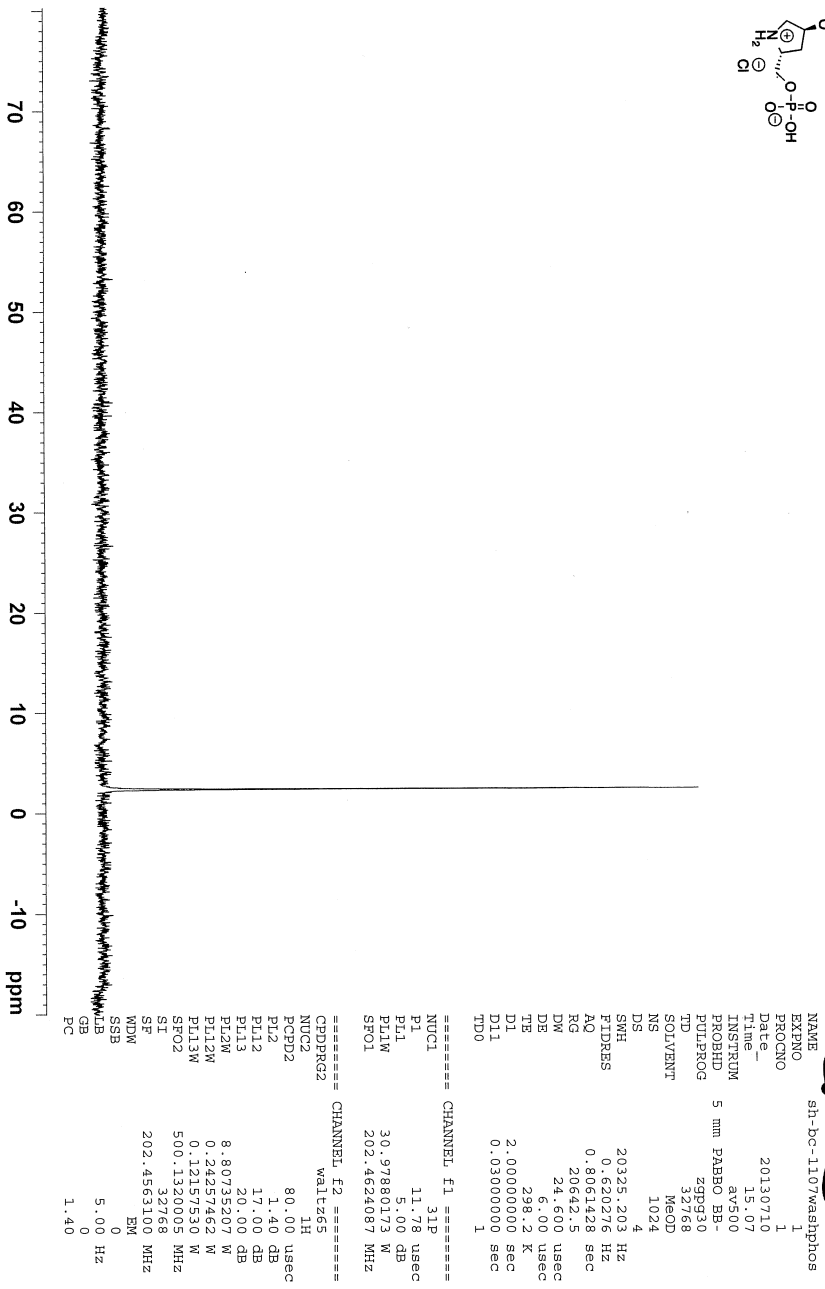


sh-bc-1107newc  
D2O 400





— 2.363



```

NAME sh-bc-1107/washphos
EXPNO 1
PROCNO 1
Date_ 20130710
Time 15.07
INSTRUM av500
PROBHD zpp930
PULPROG 5 mm PABBO BB-
TD 32768
SOLVENT MeOD
NS 1024
DS 4
SWH 20325.203 Hz
FIDRES 0.620276 Hz
AQ 0.8061428 sec
RG 20642.5
DW 24.600 usec
DE 6.00 usec
TE 298.2 K
D1 2.00000000 sec
D11 0.03000000 sec
TDO 1
  
```

```

===== CHANNEL f1 =====
NUC1 31P
P1 11.78 usec
PL1 5.00 dB
PL1W 30.97880173 W
SFO1 202.4624087 MHz
  
```

```

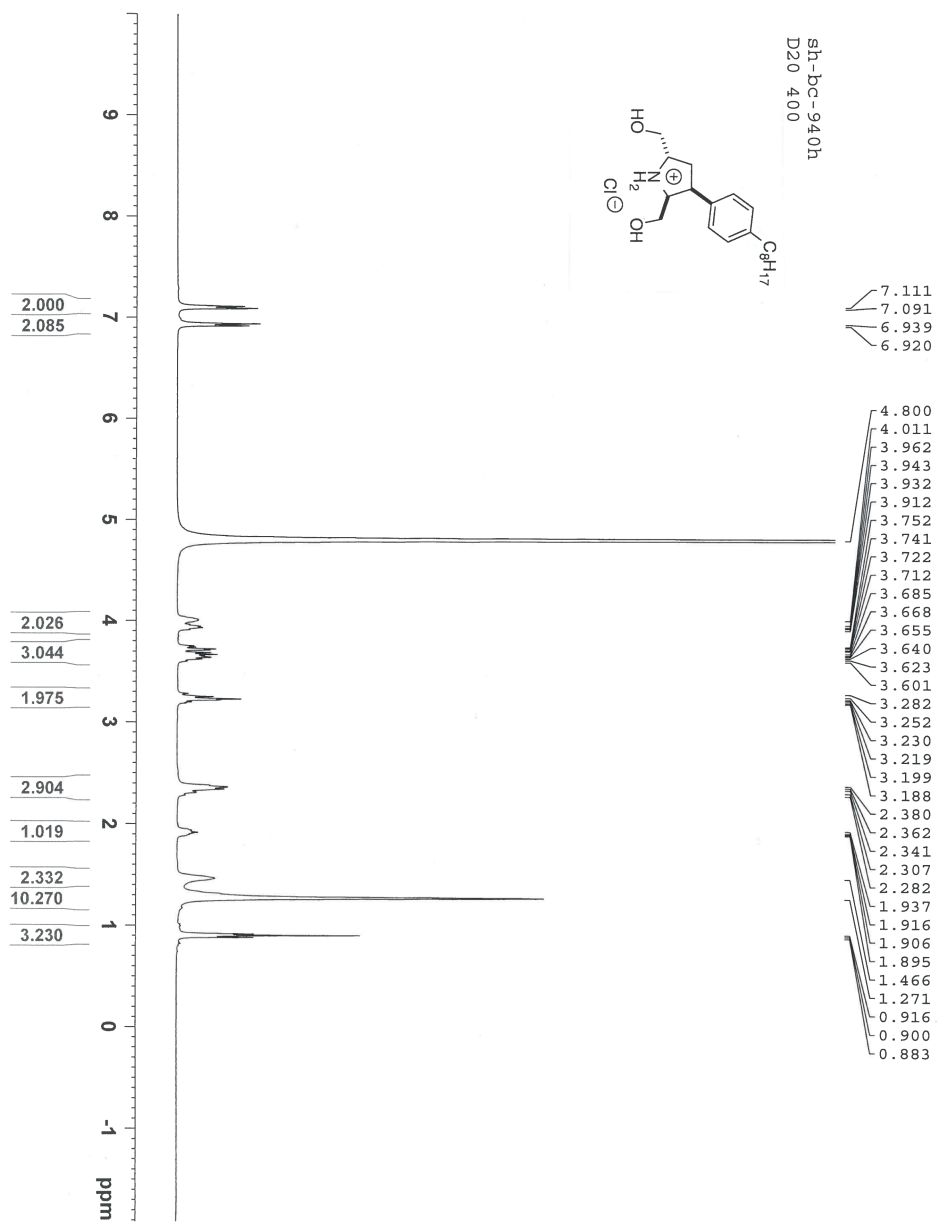
===== CHANNEL f2 =====
CPDPRG2 waltz65
NUC2 1H
PCPD2 80.00 usec
PL2 1.40 dB
PL12 17.00 dB
PL13 20.00 dB
PL1W 8.80735207 W
PL2W 0.24257462 W
PL13W 0.12157530 W
SFO2 500.1320005 MHz
SI 32768
SF 202.4563100 MHz
WDW EM
SSB 0
GB 5.00 Hz
PC 0
  
```

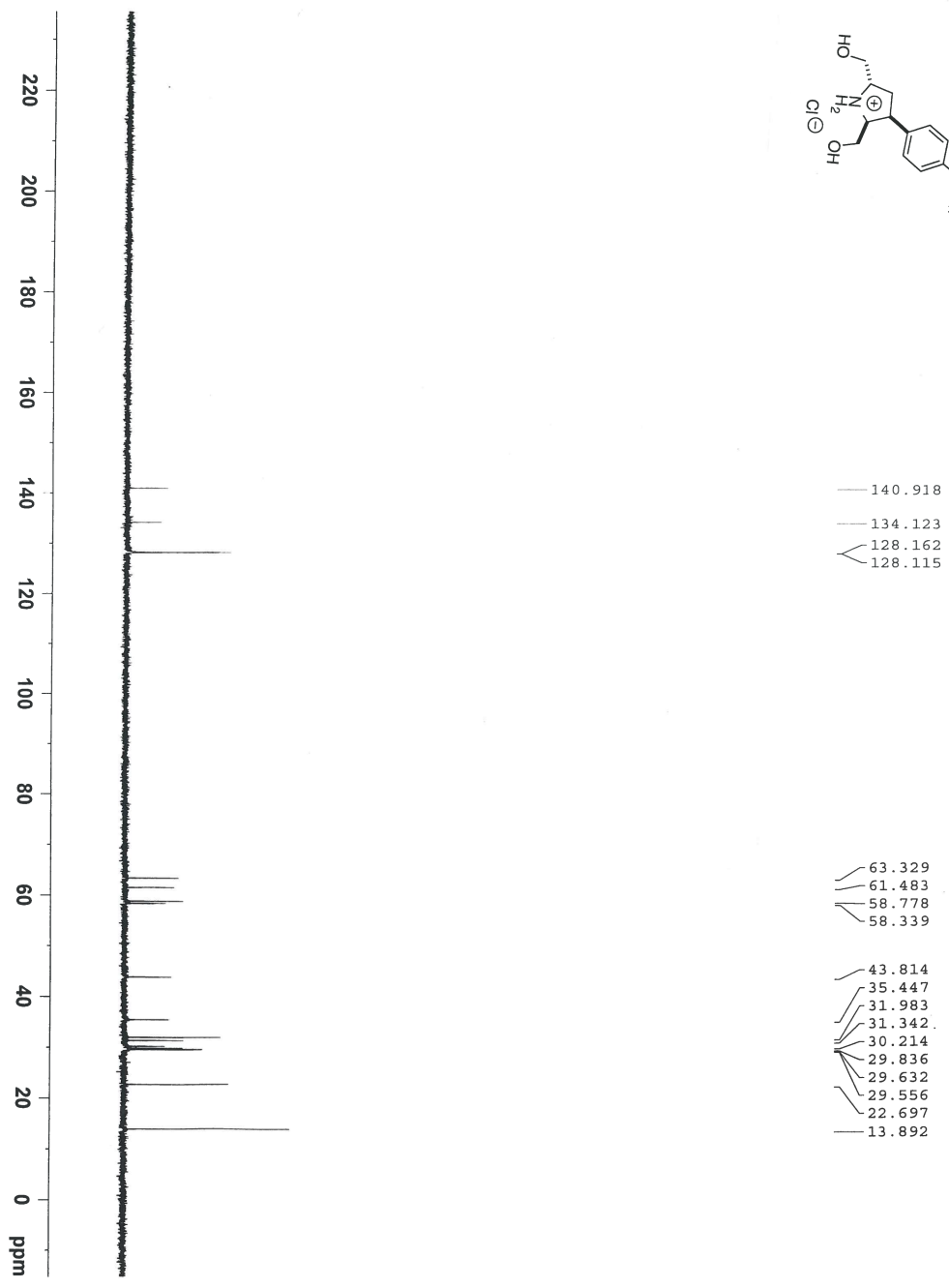
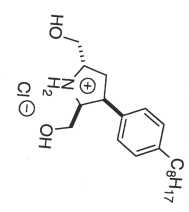
```

===== CHANNEL f3 =====
PC 1.40
  
```

# Annex 8: $^1\text{H}$ and $^{13}\text{C}$ NMR Spectra of Compound

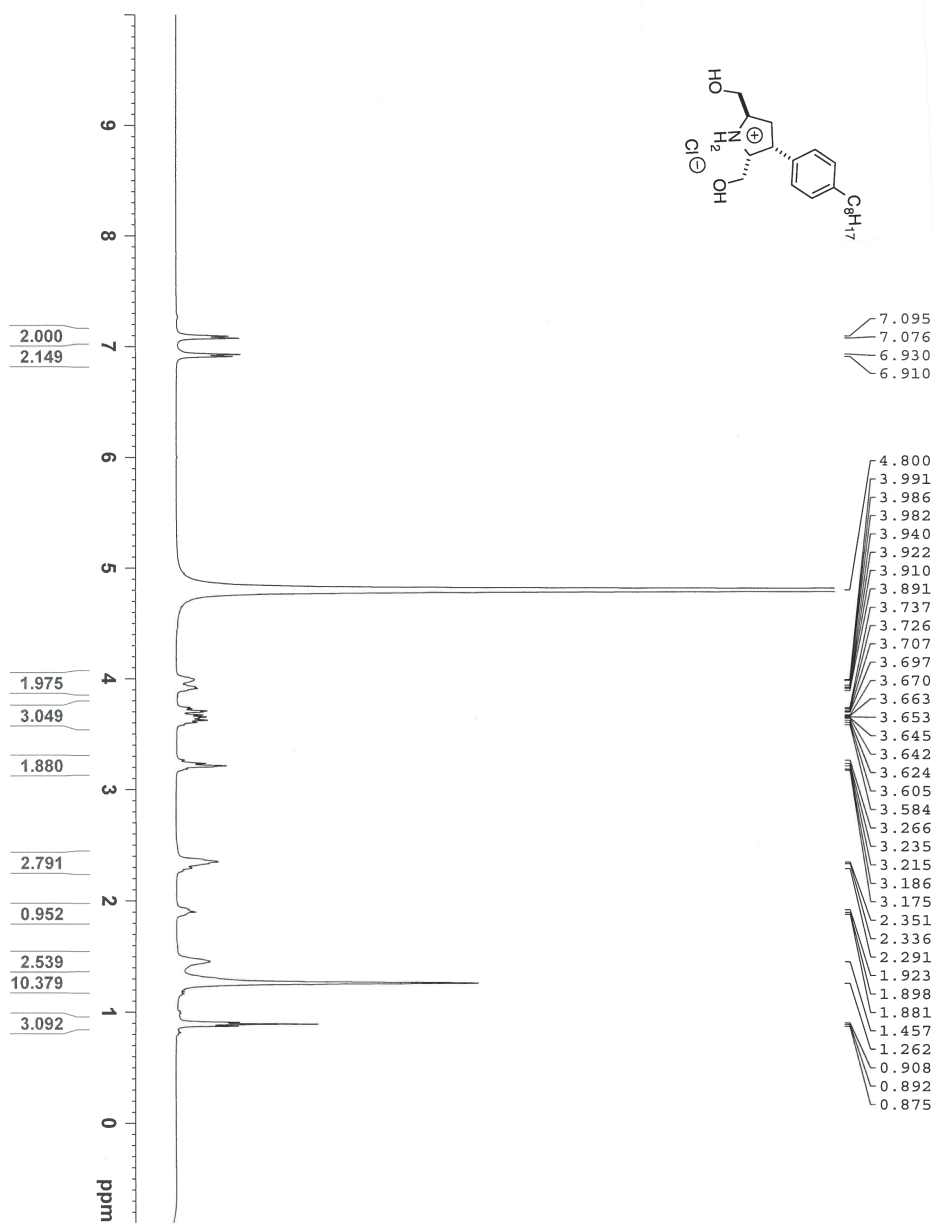
## 1.100

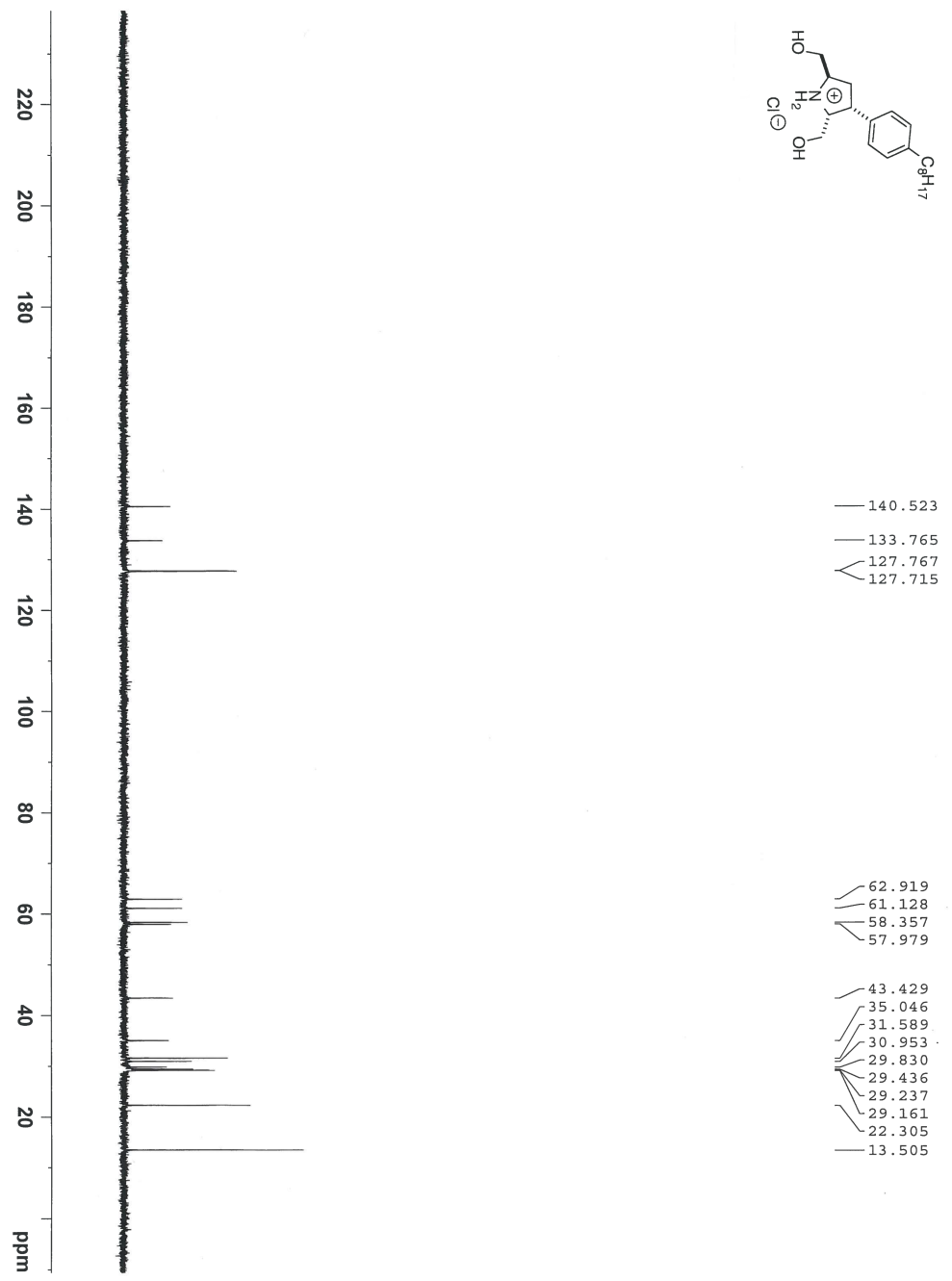
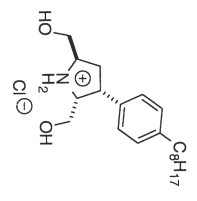




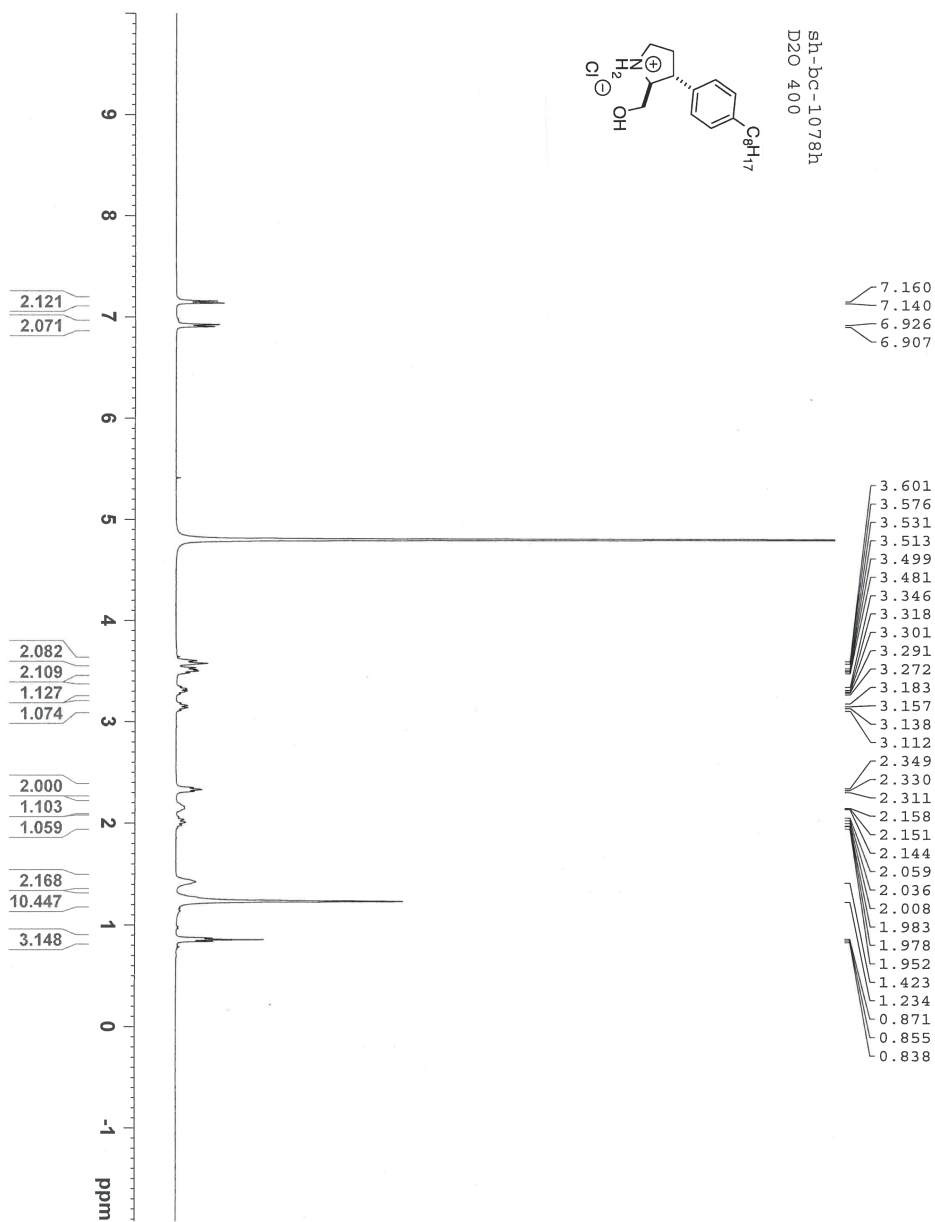
# Annex 9: $^1\text{H}$ and $^{13}\text{C}$ NMR Spectra of Compound

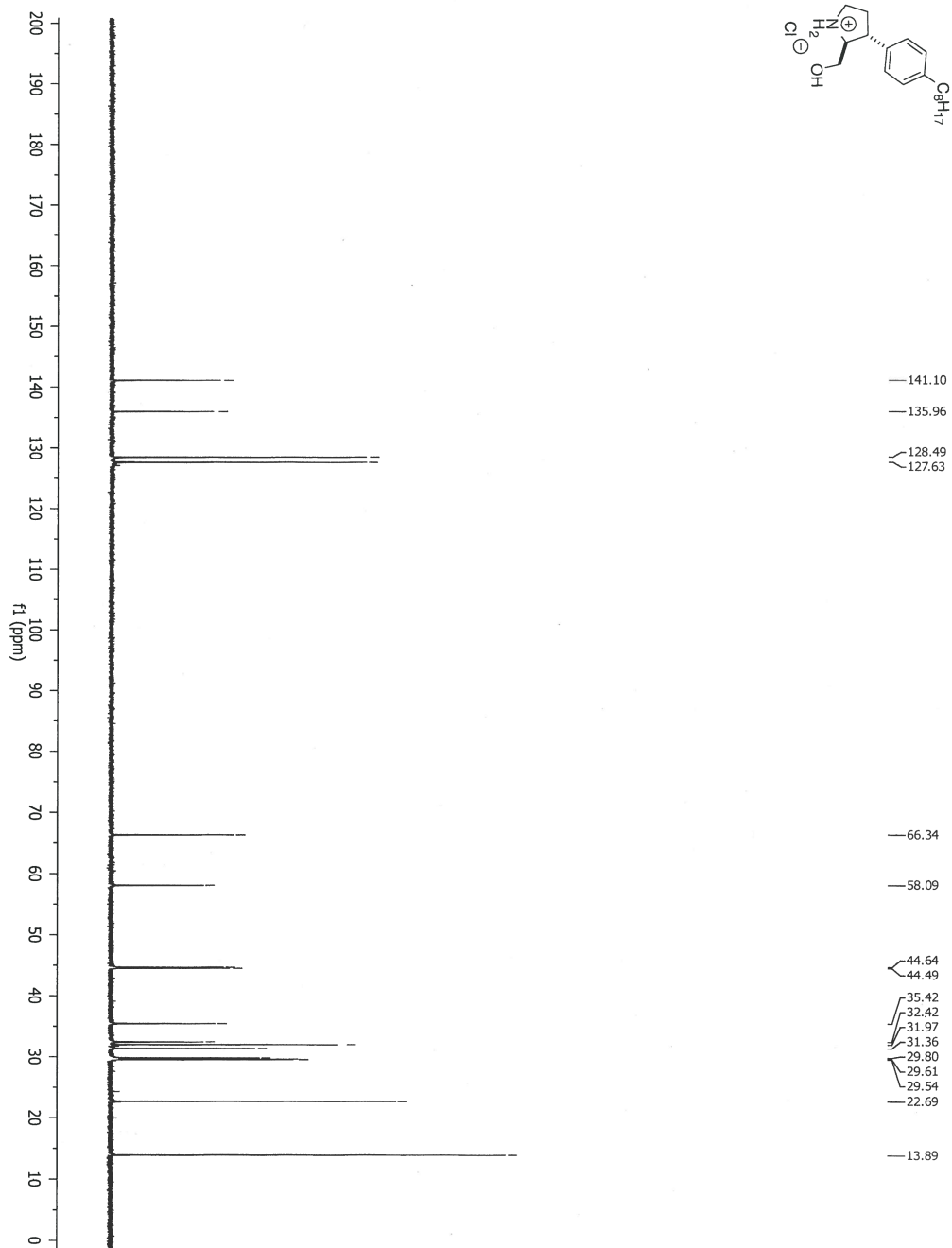
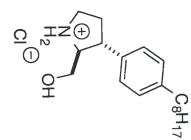
## 1.101





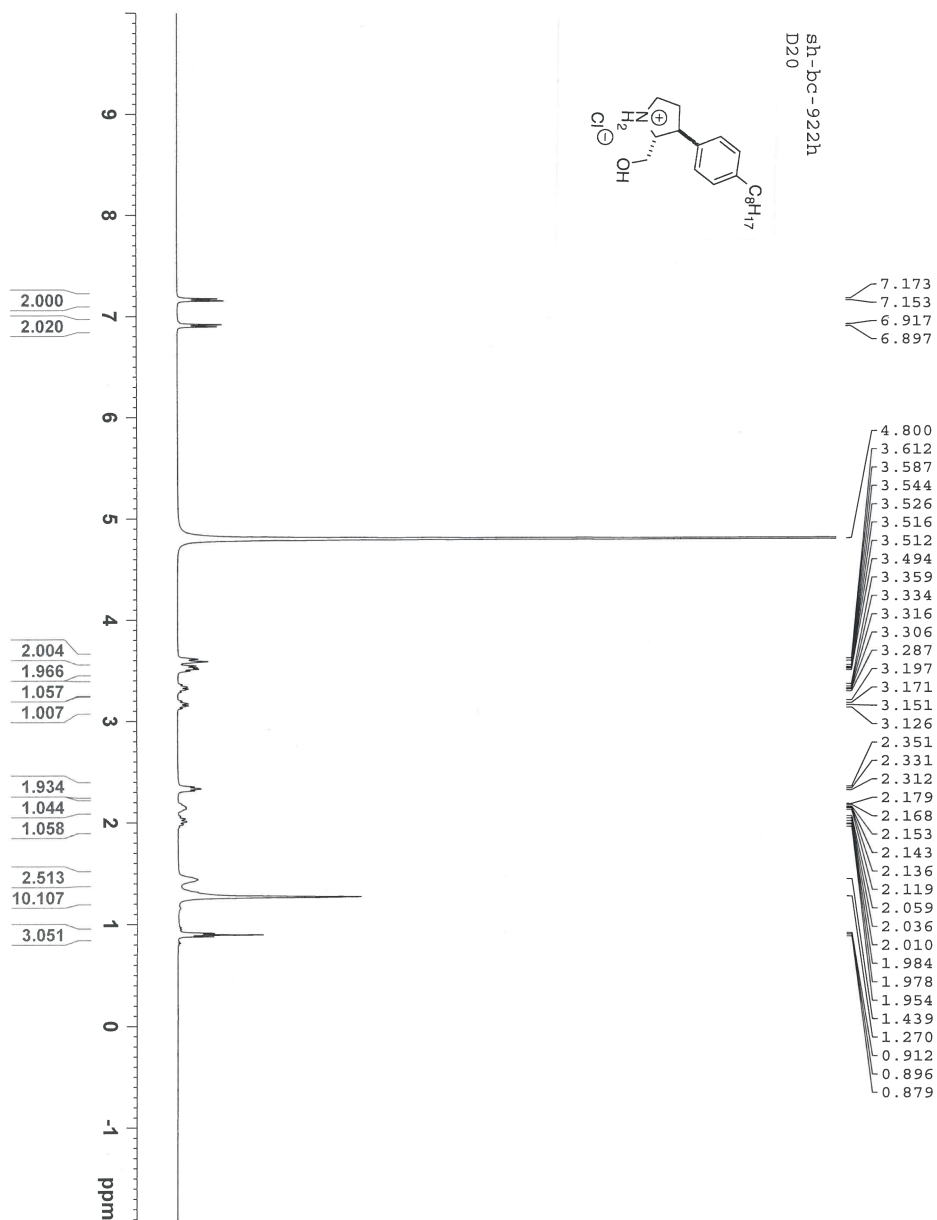
# Annex 10: $^1\text{H}$ and $^{13}\text{C}$ NMR Spectra of Compound 1.114



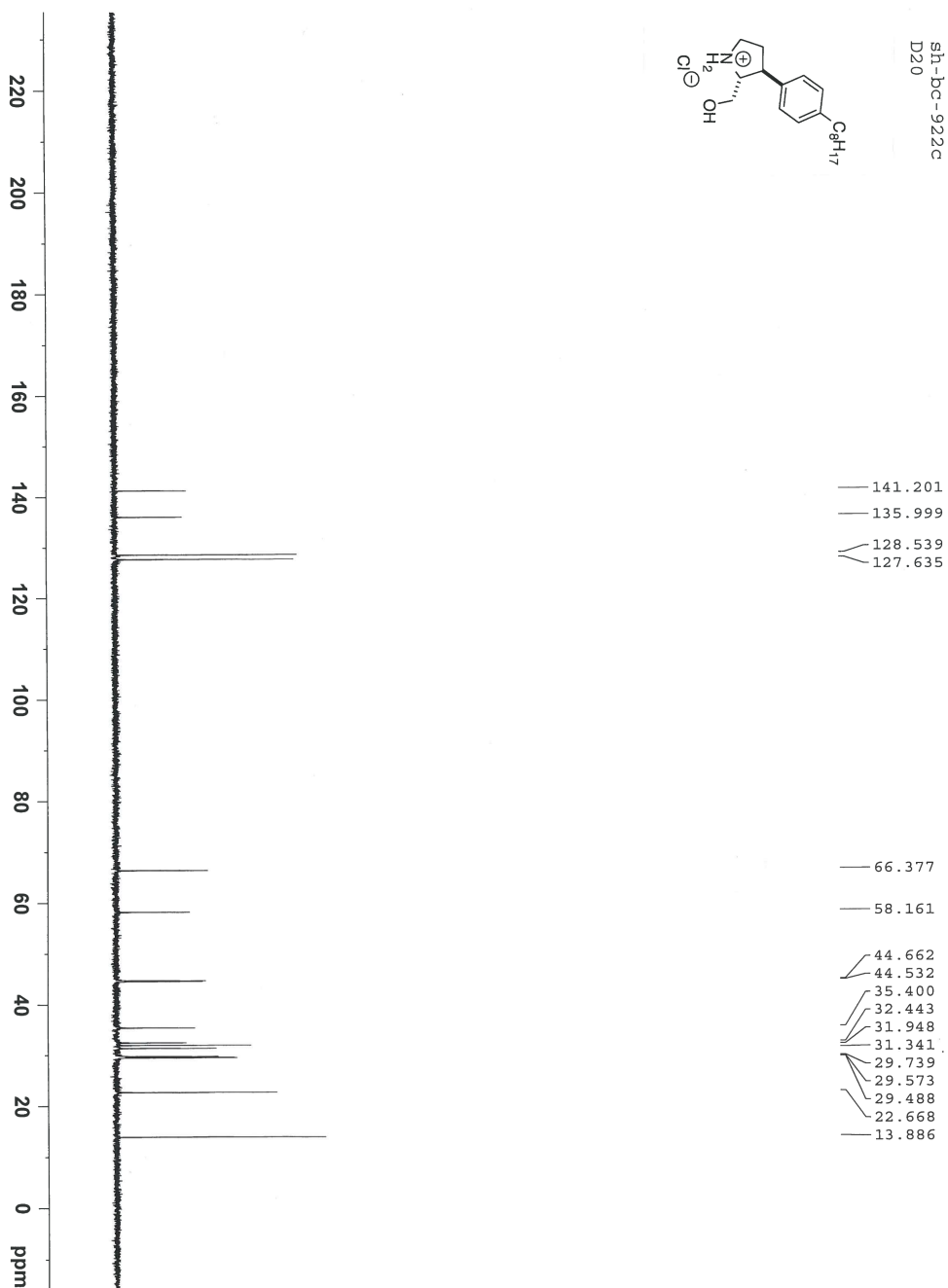
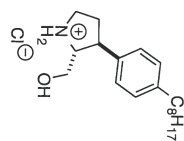




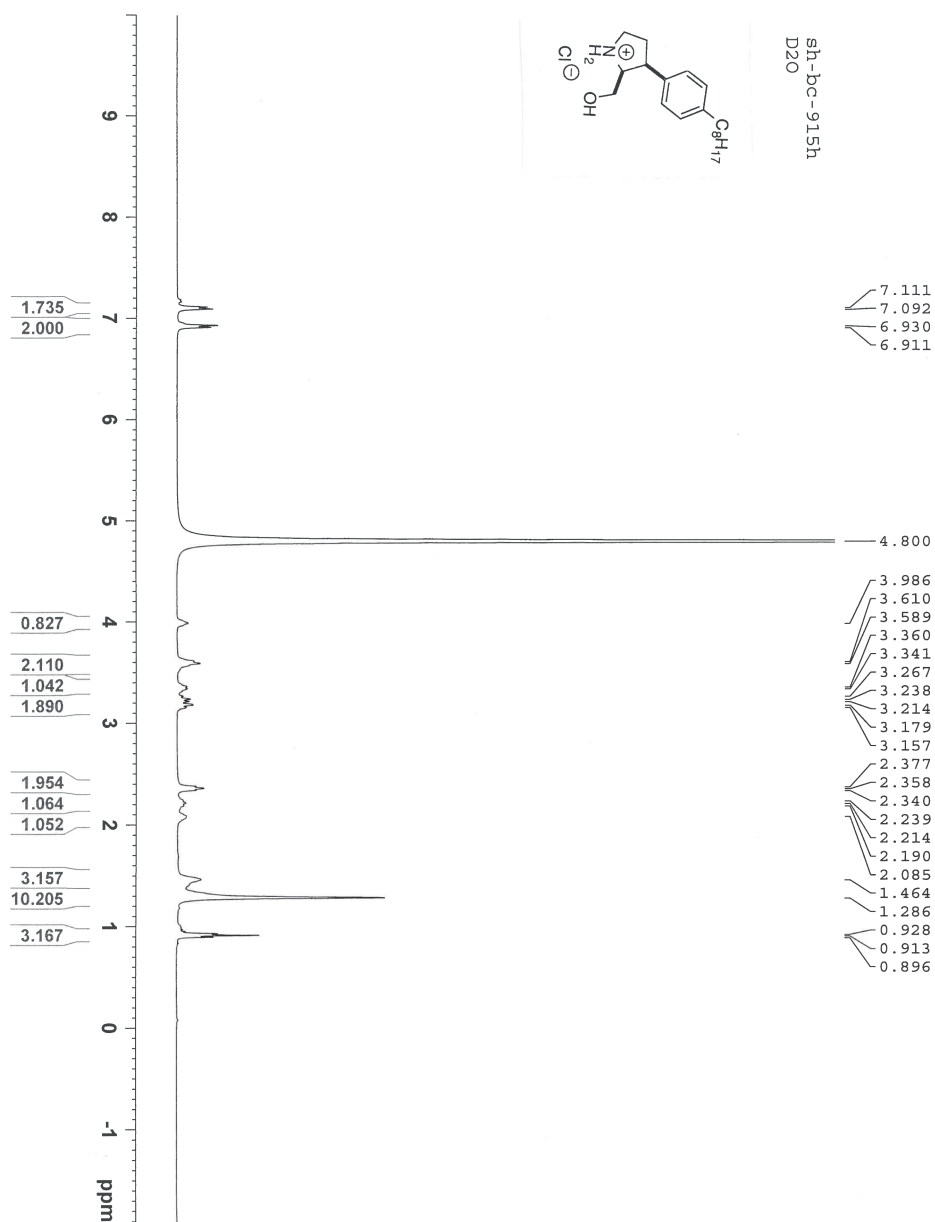
# Annex 11: $^1\text{H}$ and $^{13}\text{C}$ NMR Spectra of Compound 1.117



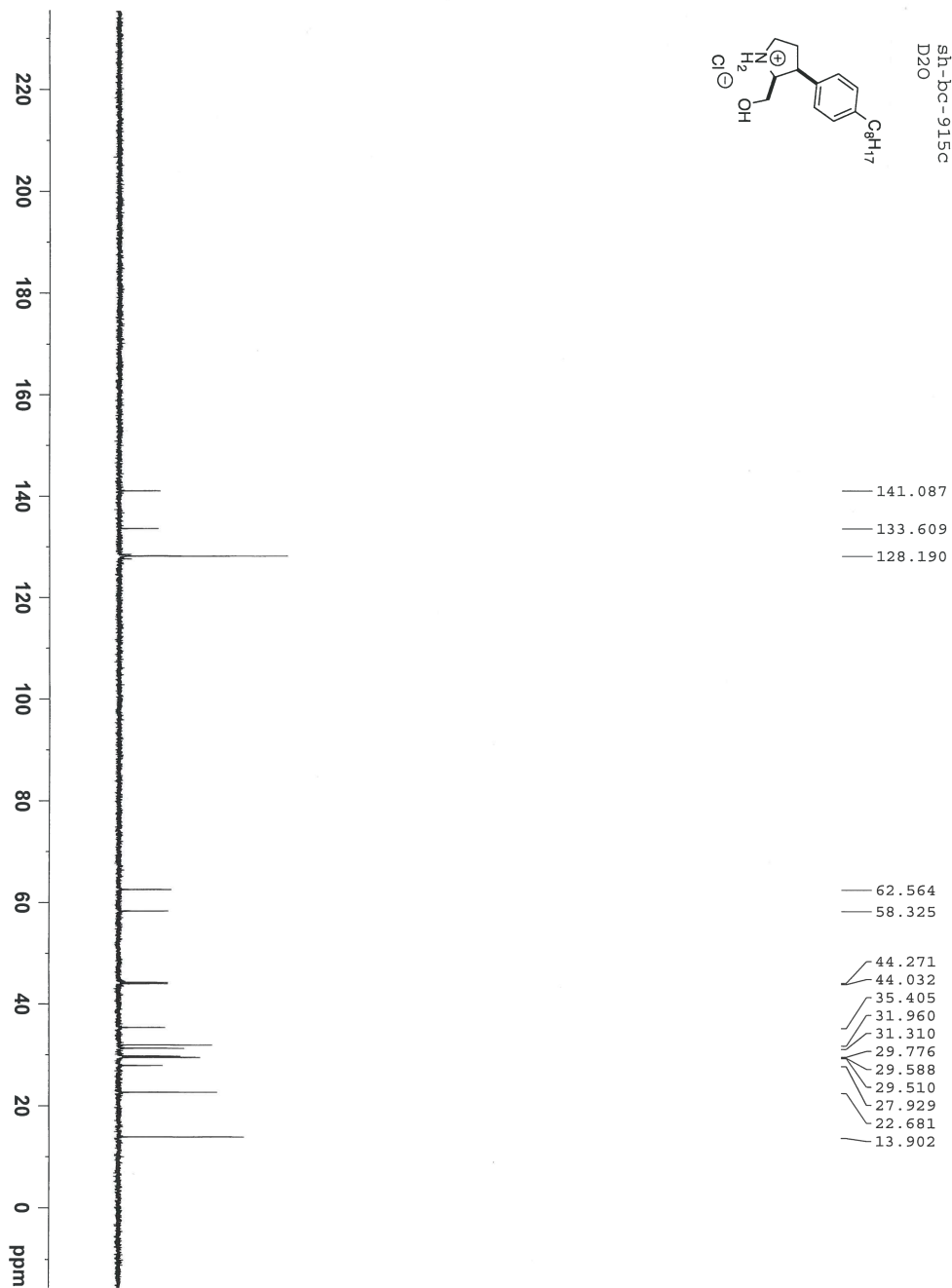
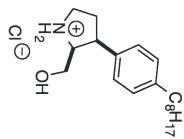
sh-bc-922c  
D2O



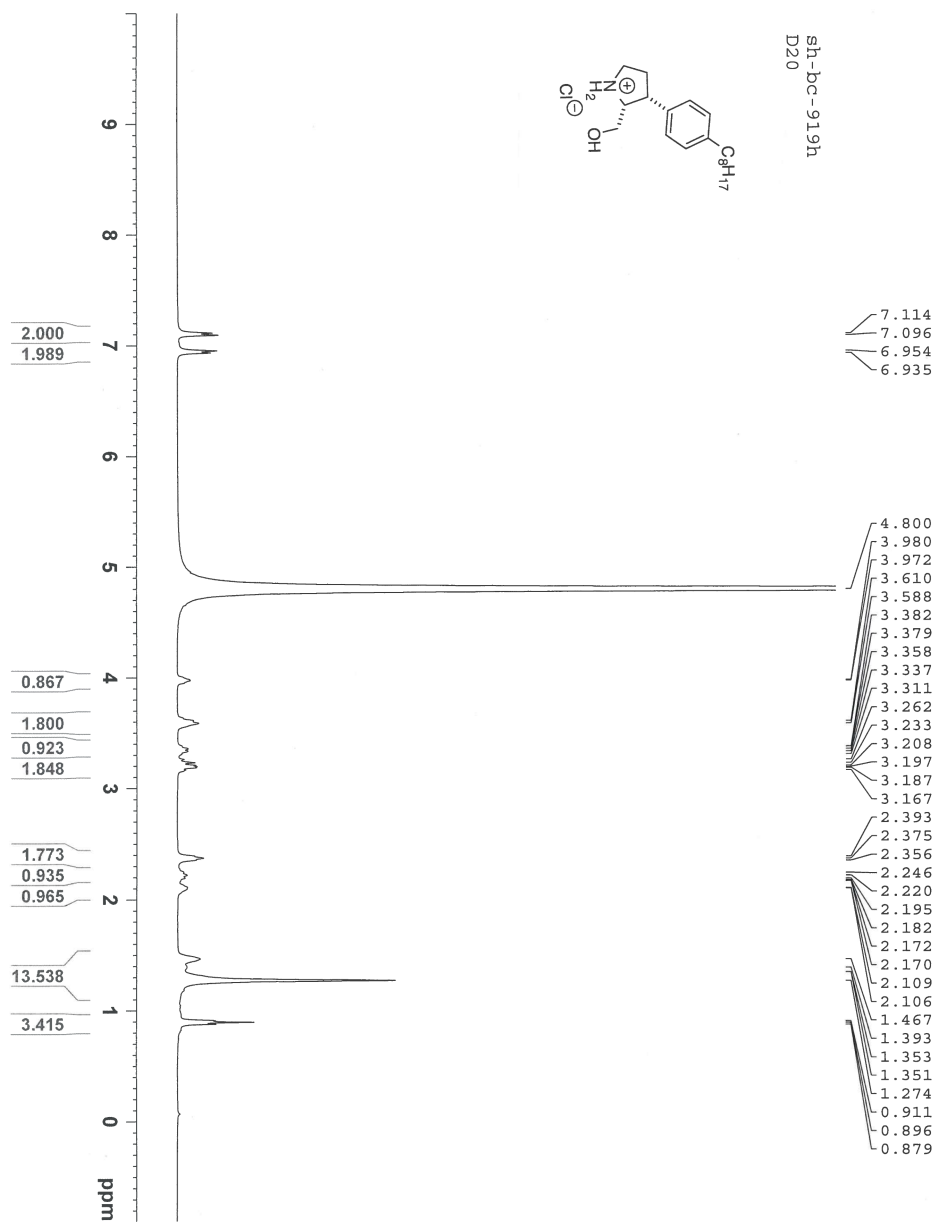
# Annex 12: $^1\text{H}$ and $^{13}\text{C}$ NMR Spectra of Compound 1.120



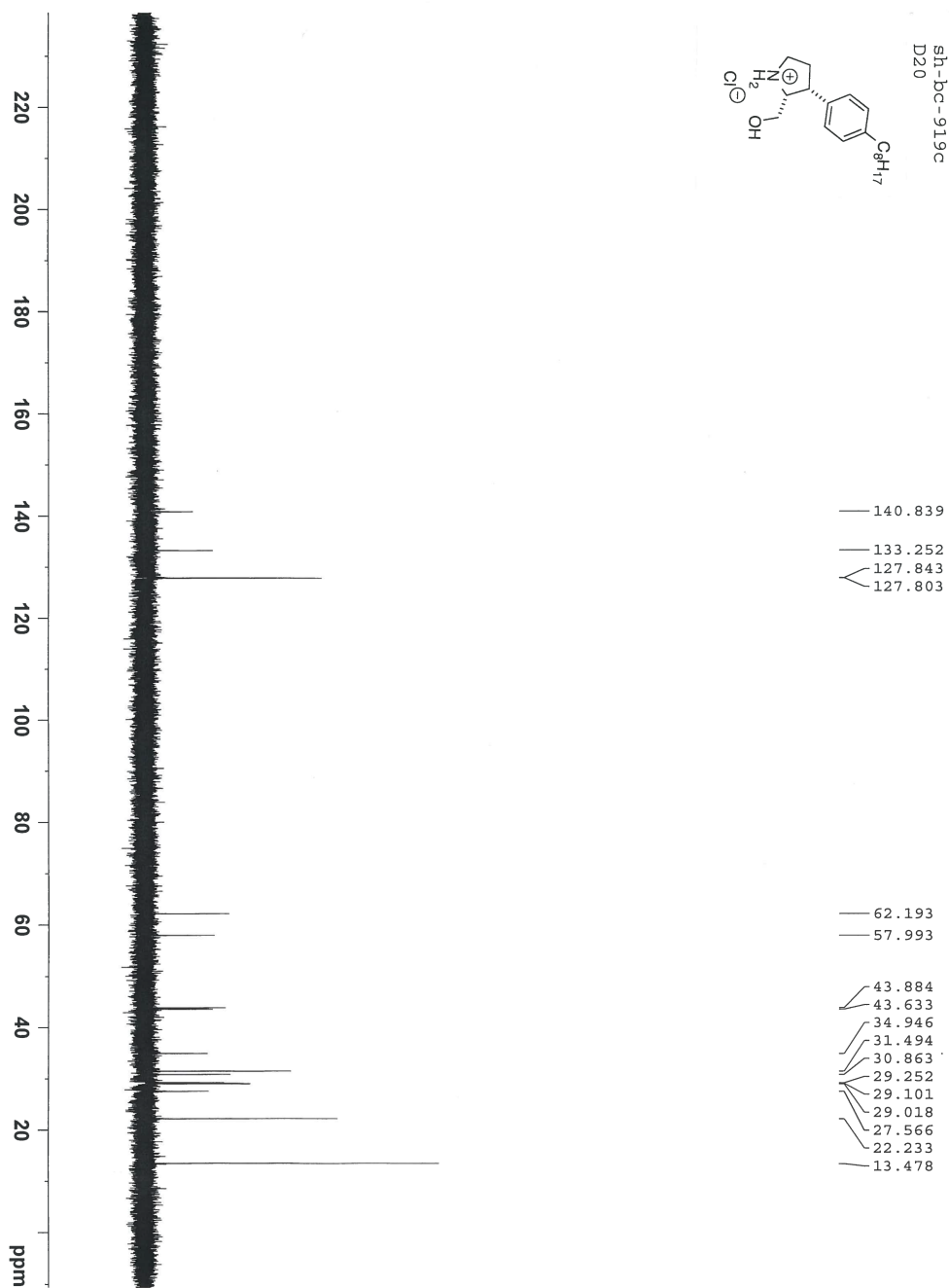
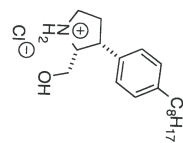
sh-pc-915c  
D2O



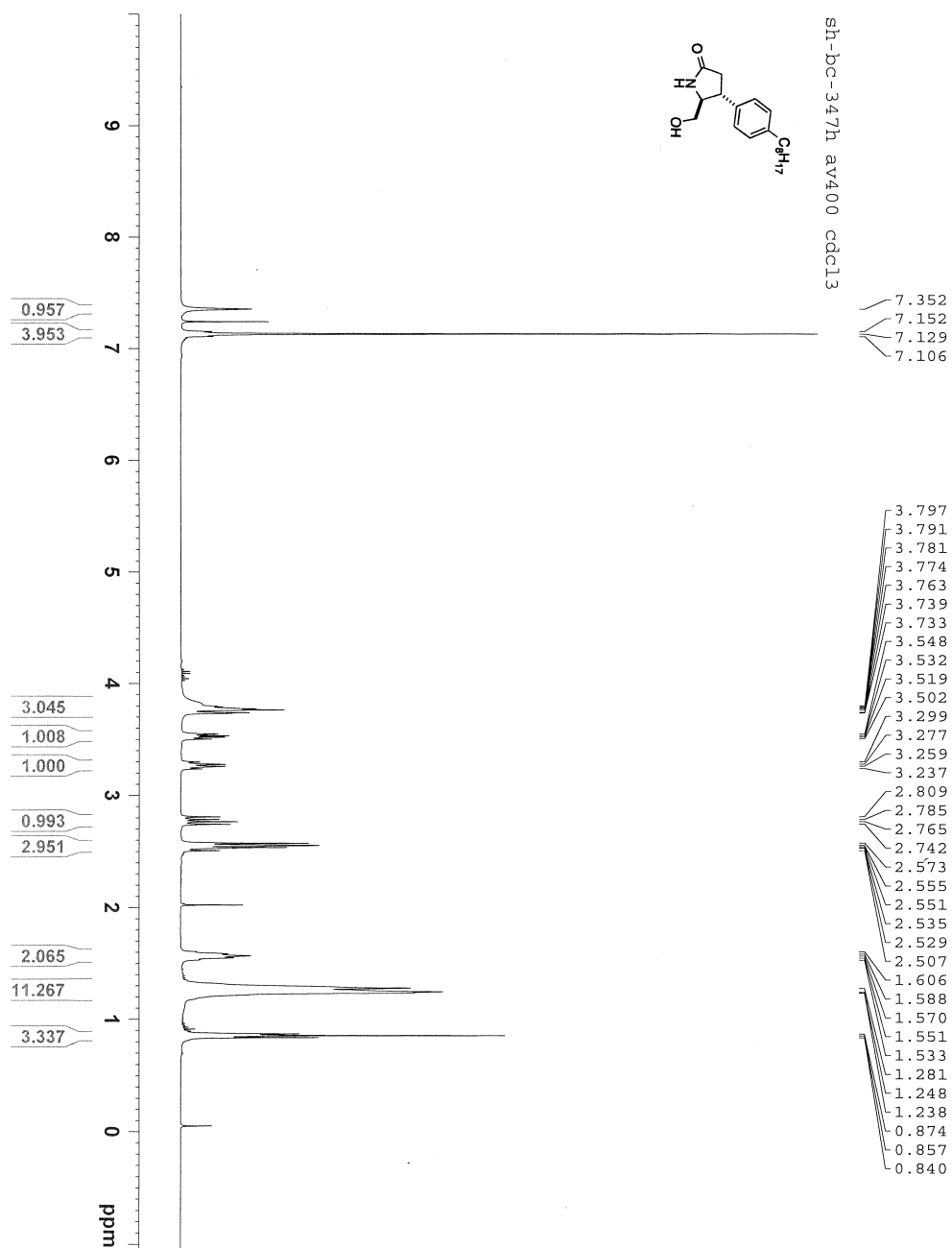
# Annex 13: $^1\text{H}$ and $^{13}\text{C}$ NMR Spectra of Compound 1.123

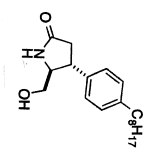
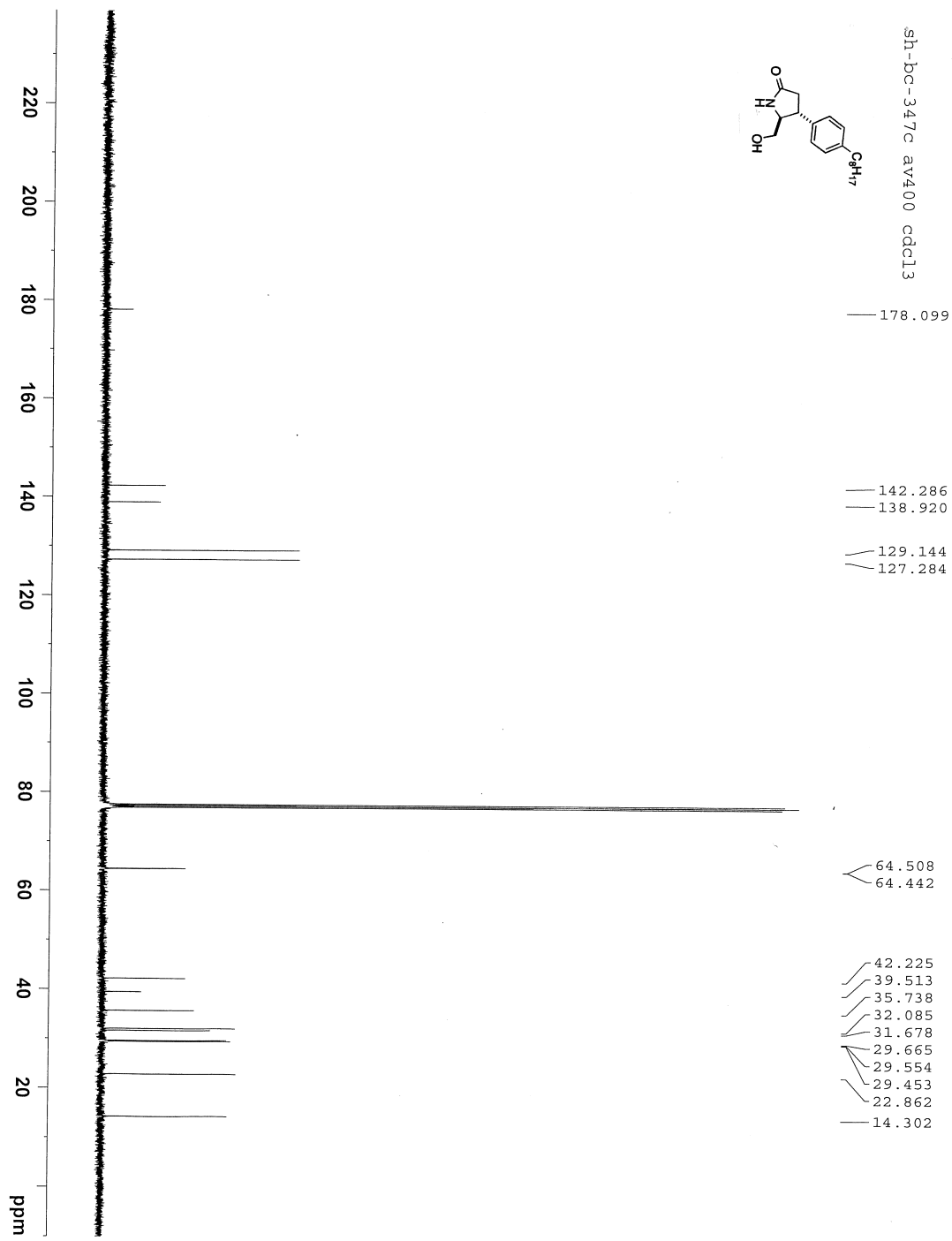


sh-bc-919c  
D2O



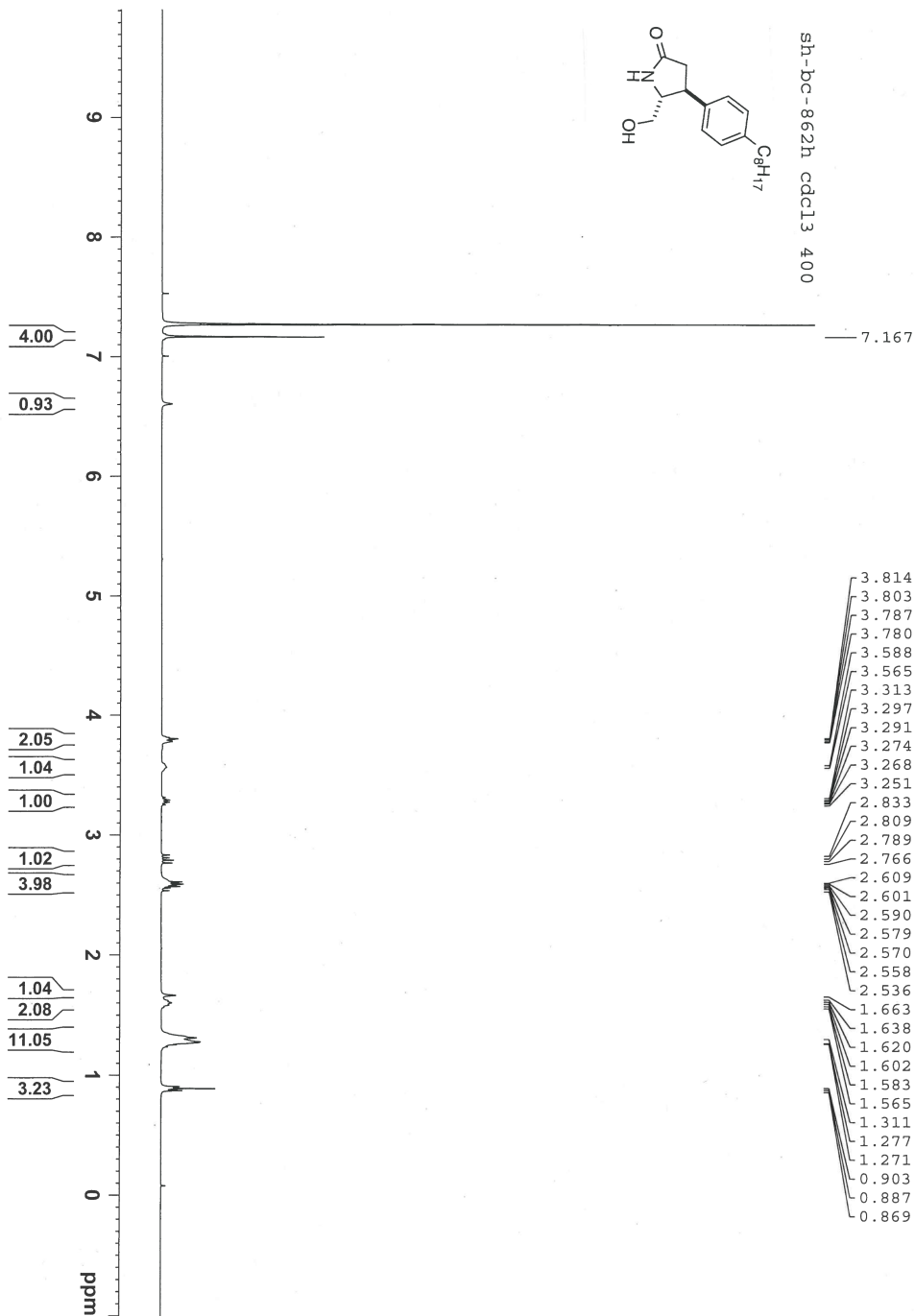
# Annex 14: $^1\text{H}$ and $^{13}\text{C}$ NMR Spectra of Compound 1.124



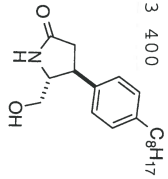




# Annex 15: <sup>1</sup>H and <sup>13</sup>C NMR Spectra of Compound 1.125



200 190 180 170 160 150 140 130 120 110 100 90 80 70 60 50 40 30 20 10 ppm



sh-bc-862c cdcl3 400

177.2

142.1

138.6

128.9

127.1

64.6

63.7

42.2

39.1

35.5

31.9

31.5

29.4

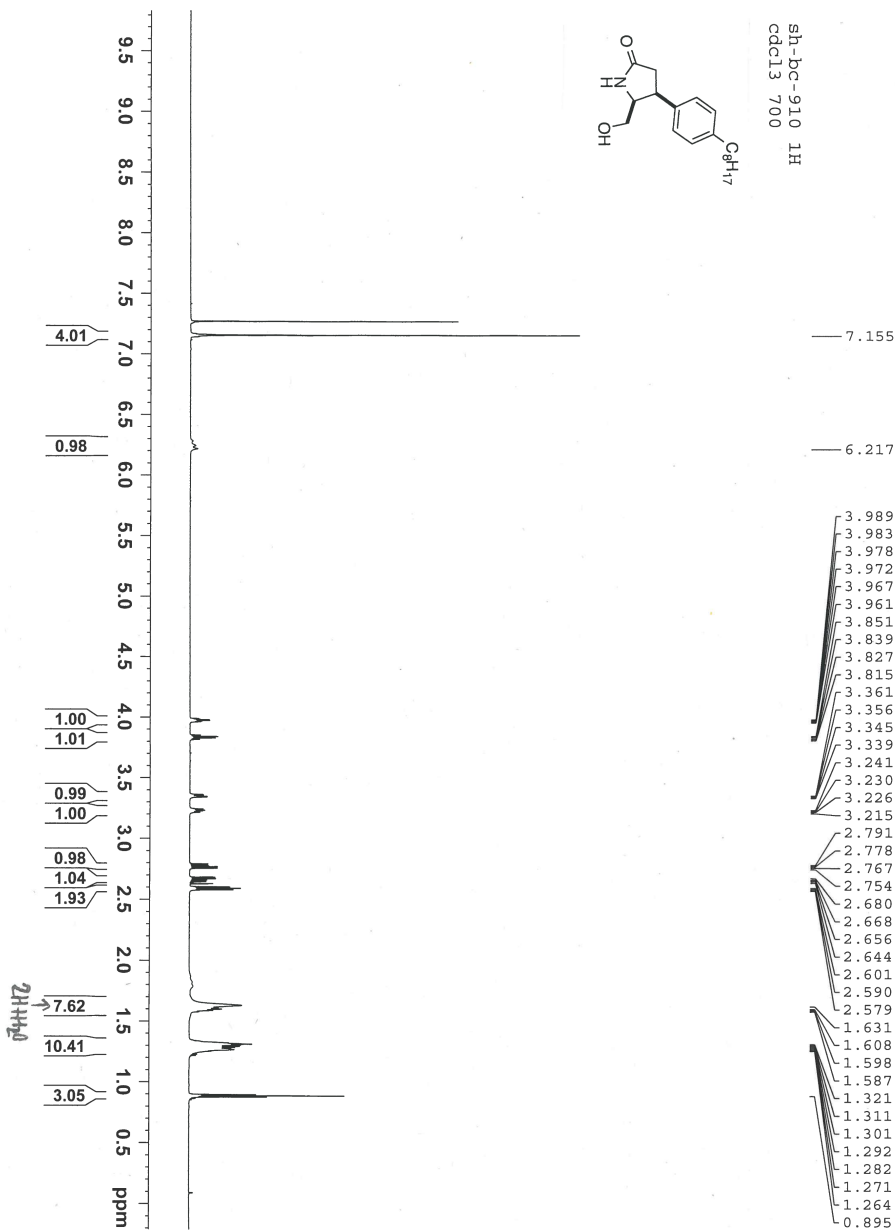
29.3

29.2

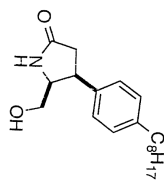
22.6

14.1

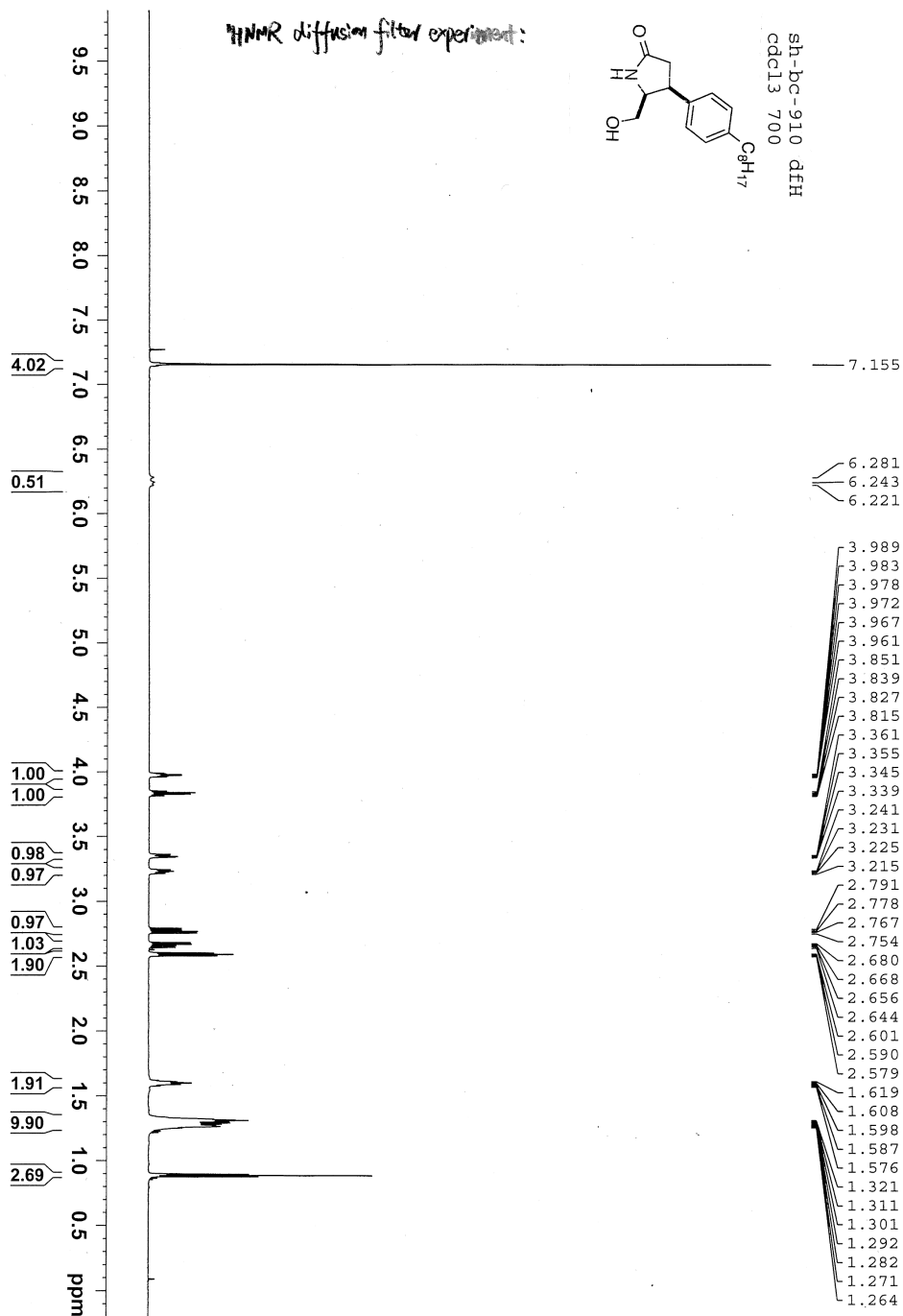
# Annex 16: $^1\text{H}$ and $^{13}\text{C}$ NMR Spectra of Compound 1.126

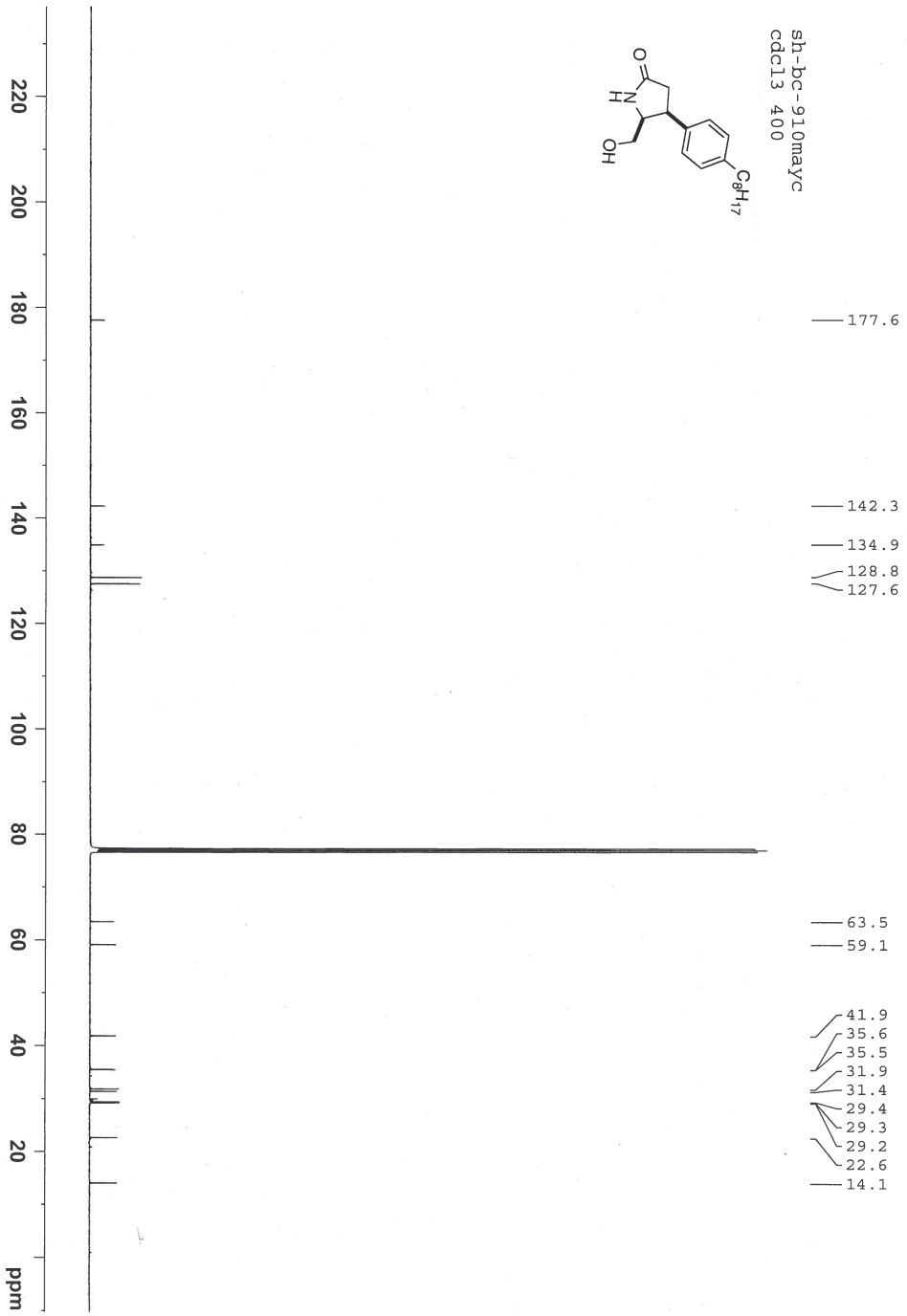


*1H*NMR diffusion filter experiment:

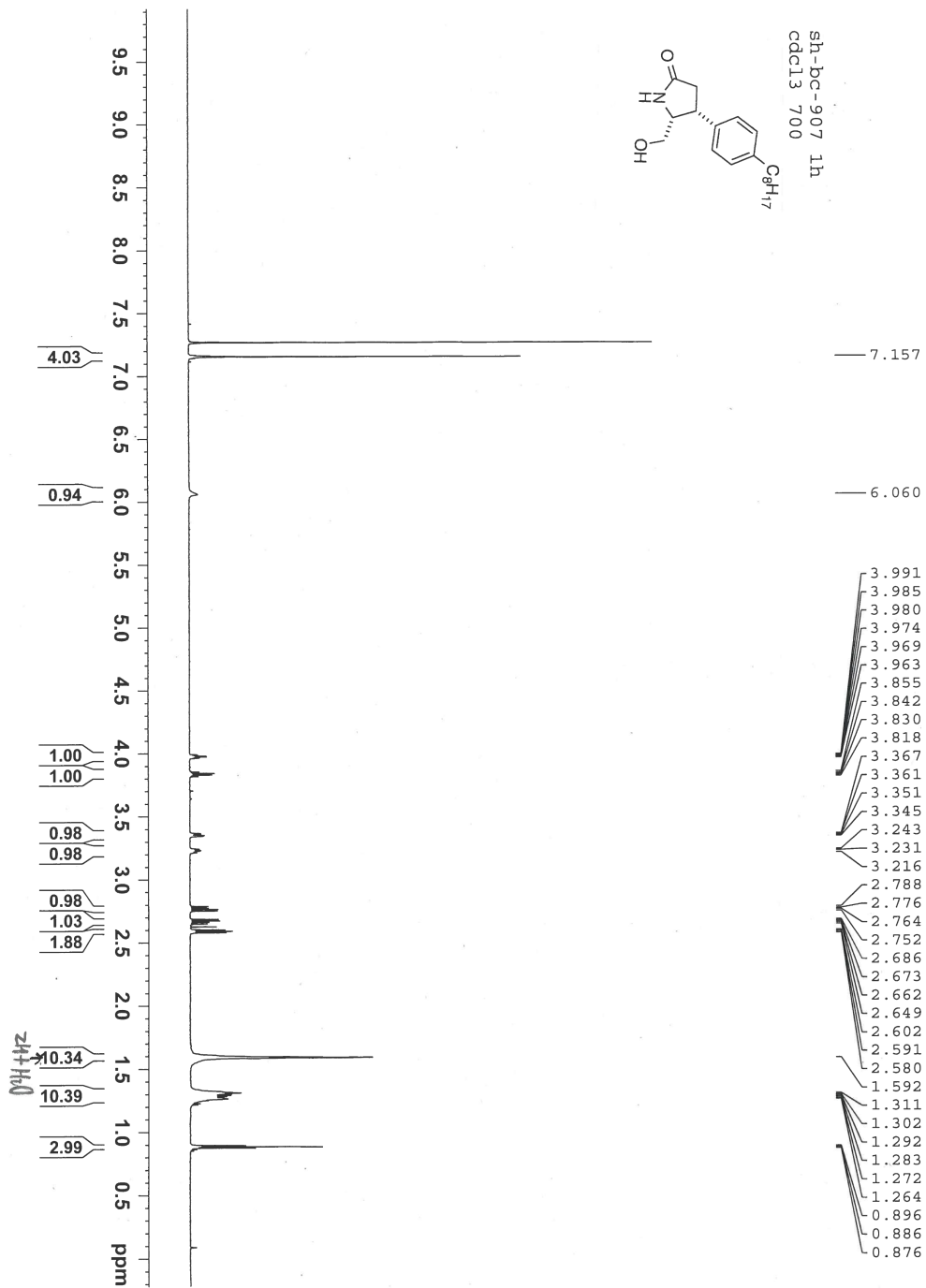


sh-bc-910 dFH  
cdcl3 700

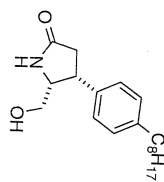




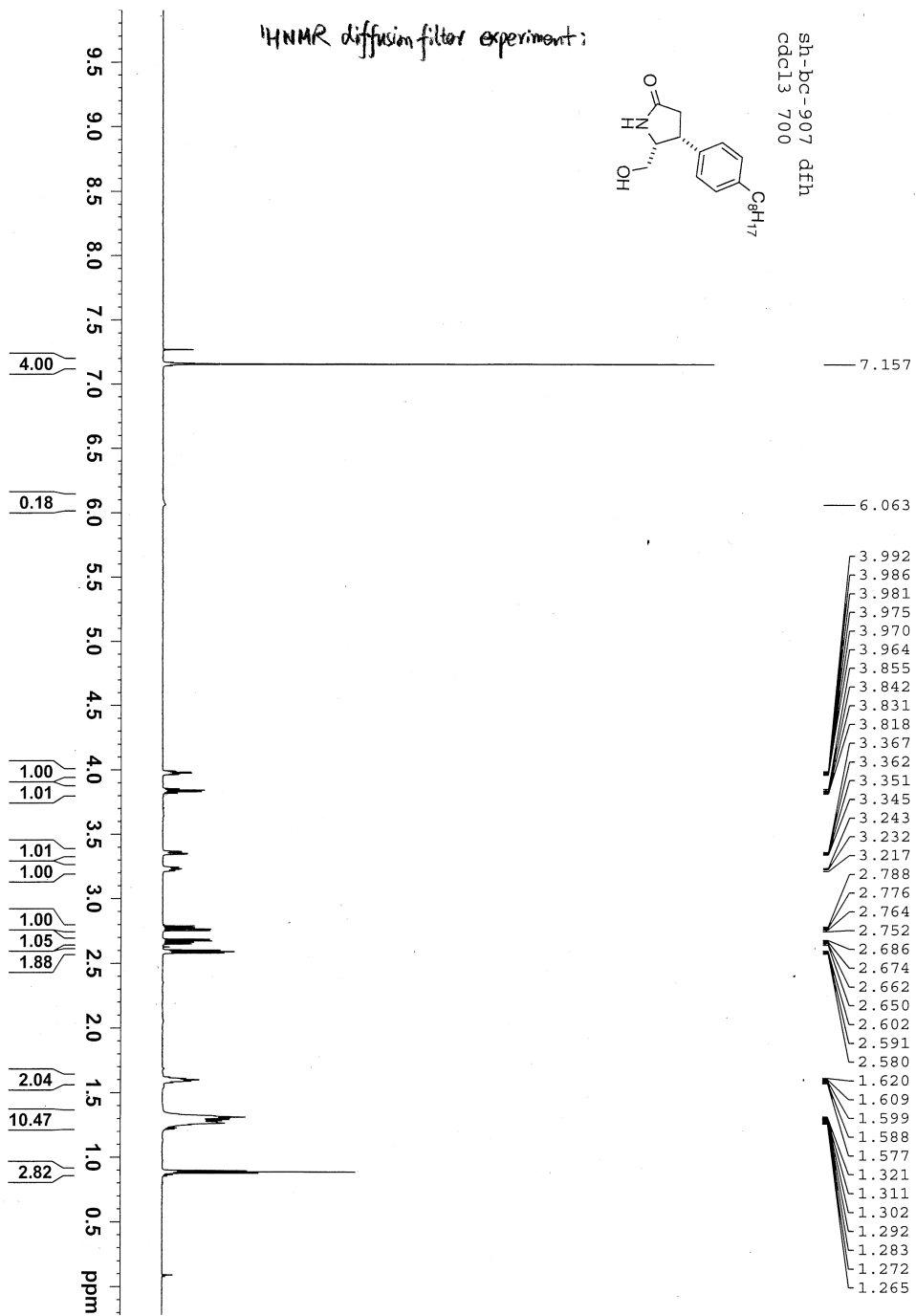
# Annex 17: $^1\text{H}$ and $^{13}\text{C}$ NMR Spectra of Compound 1.127

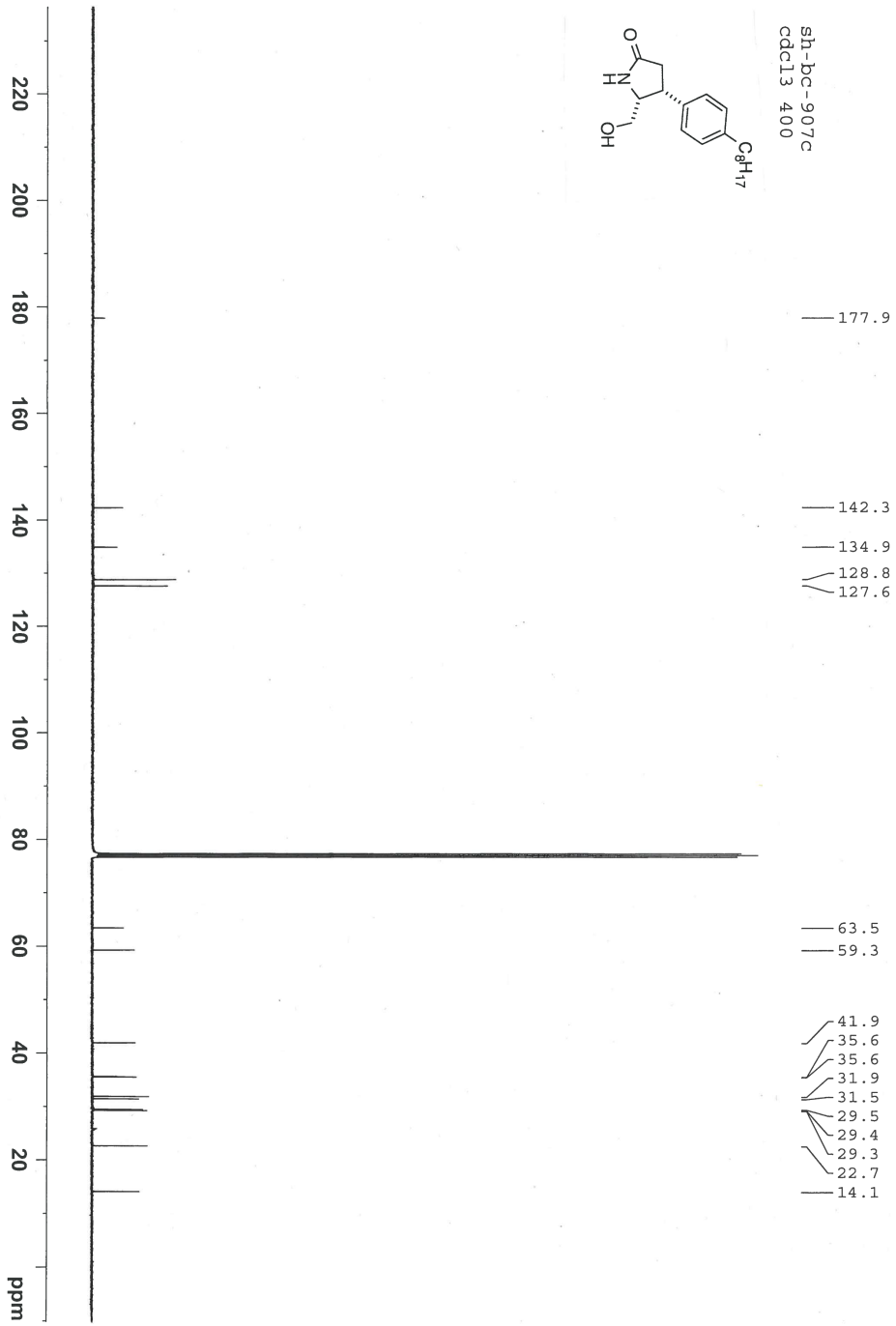


<sup>1</sup>H NMR diffusion filter experiment;



sh-bc-907 dfh  
cdcl<sub>3</sub> 700

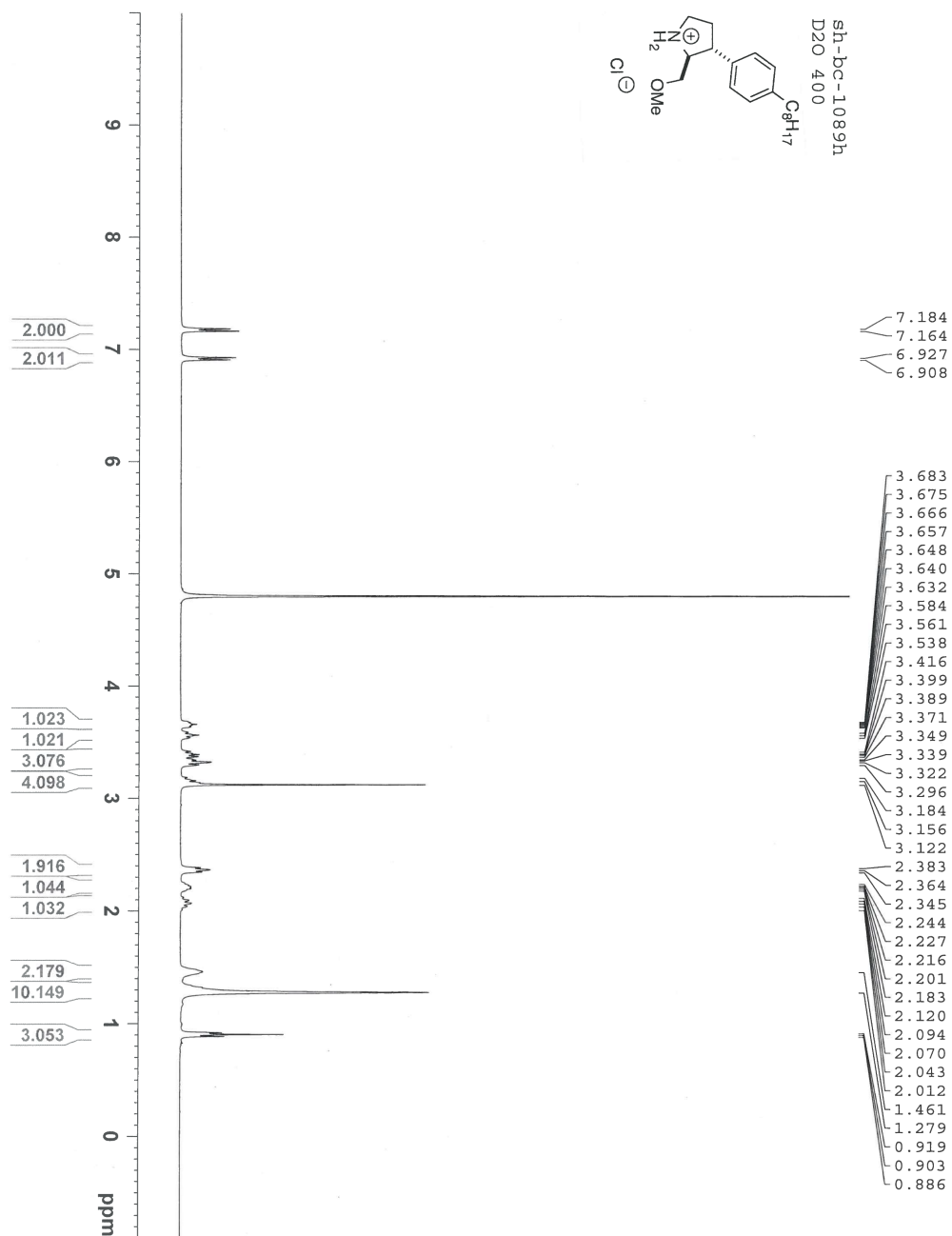




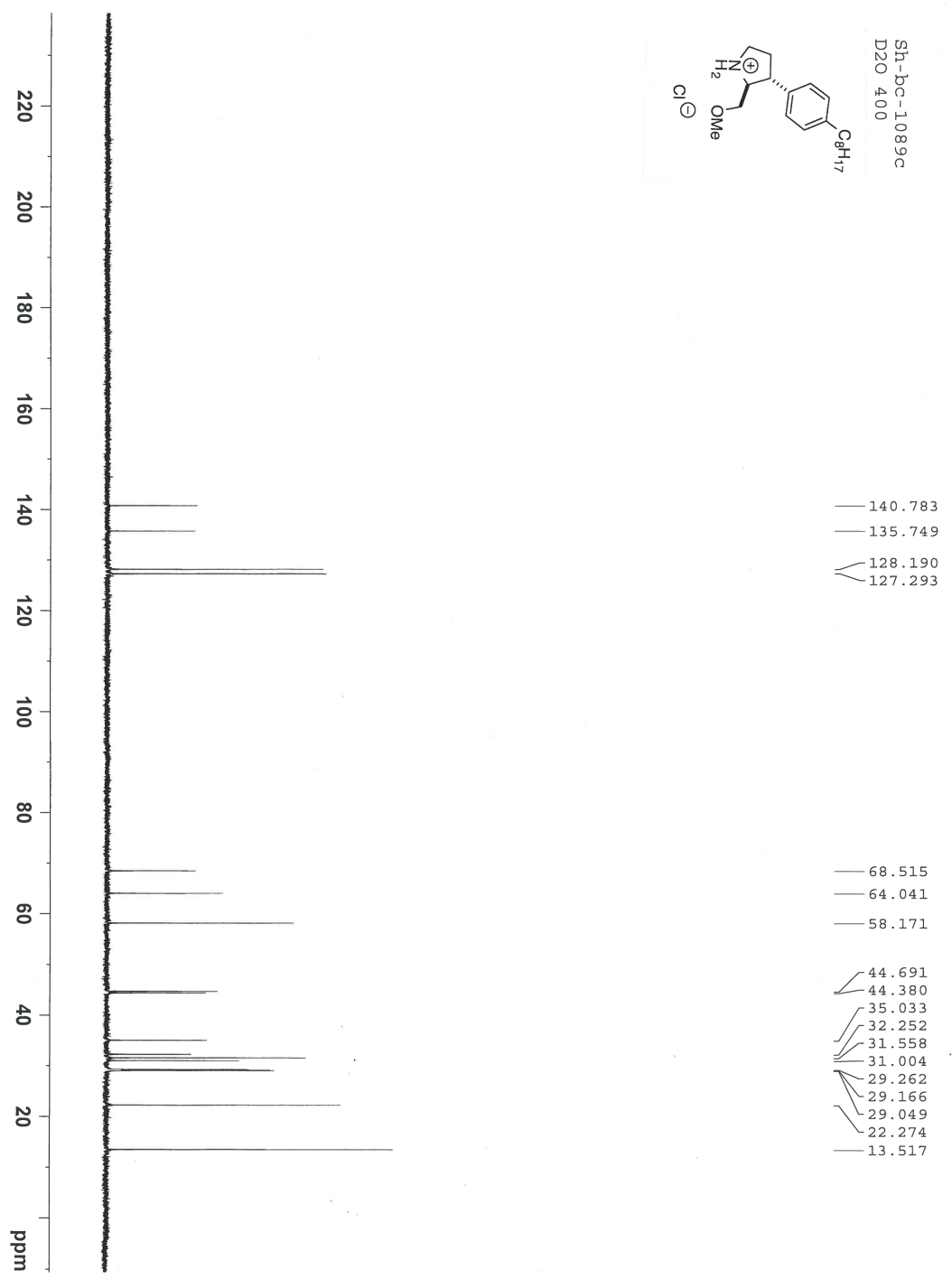
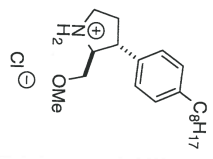


# Annex 18: $^1\text{H}$ and $^{13}\text{C}$ NMR Spectra of Compound

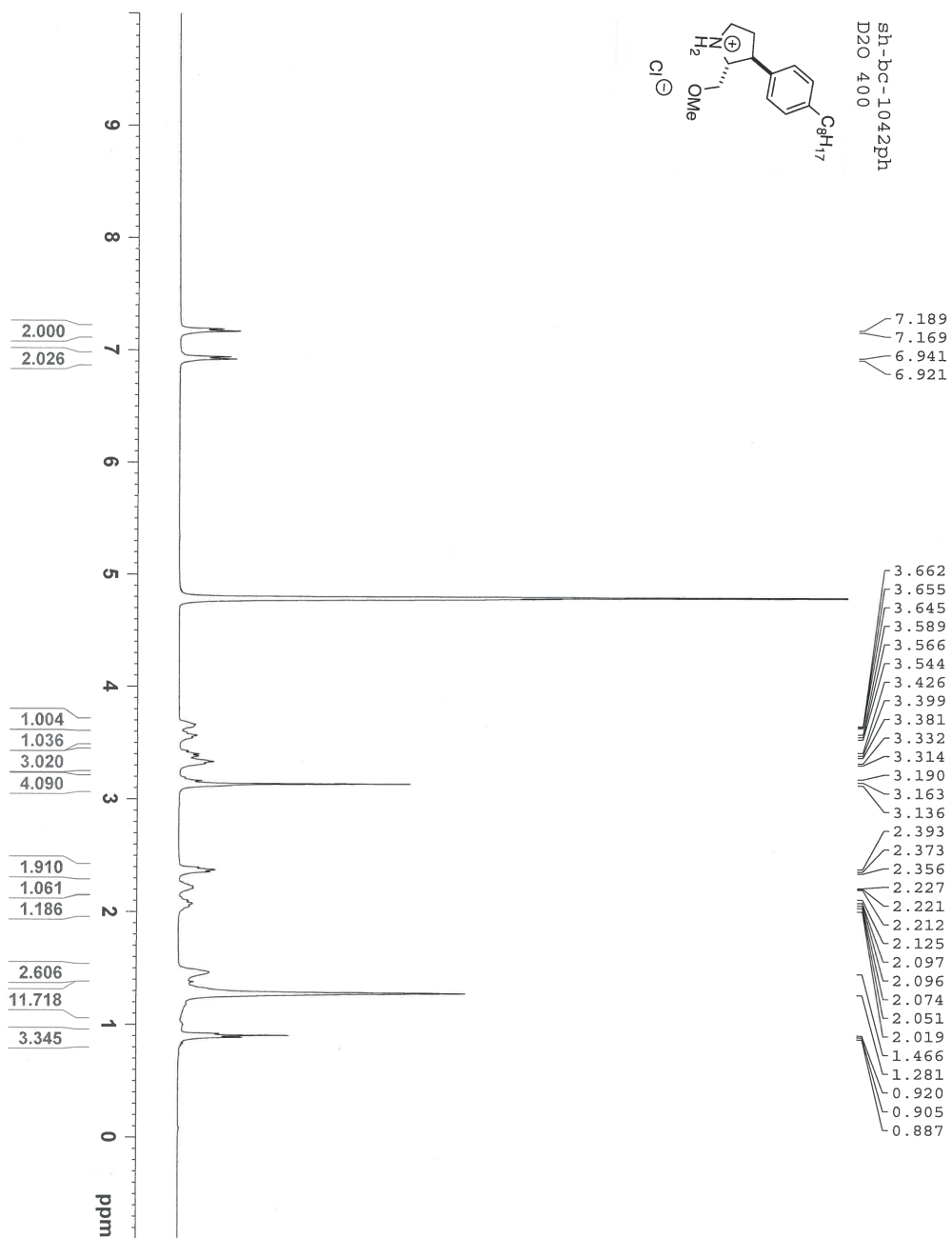
## 1.129

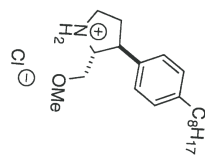


Sh-Dc-1089c  
D2O 400

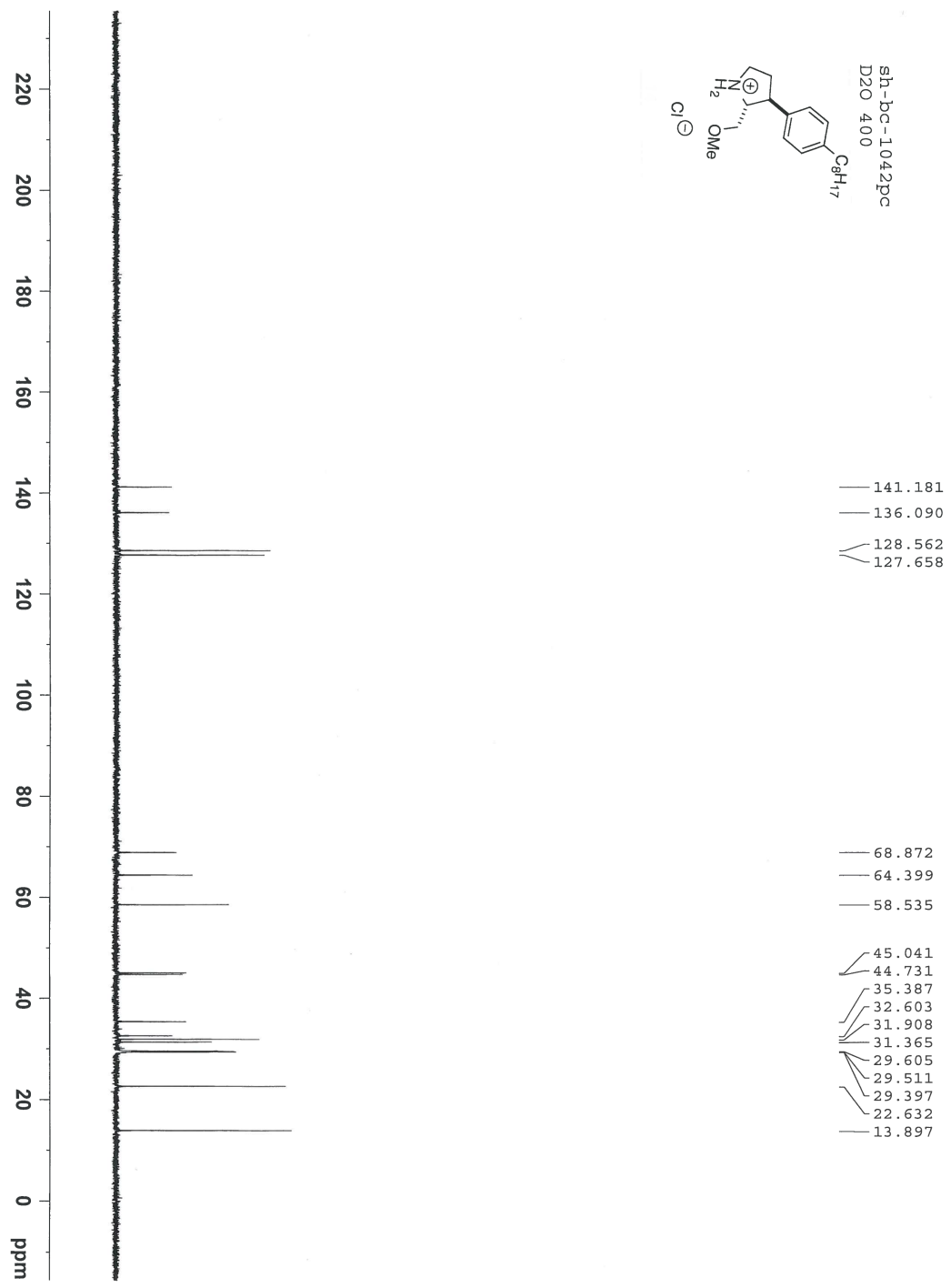


# Annex 19: $^1\text{H}$ and $^{13}\text{C}$ NMR Spectra of Compound 1.131

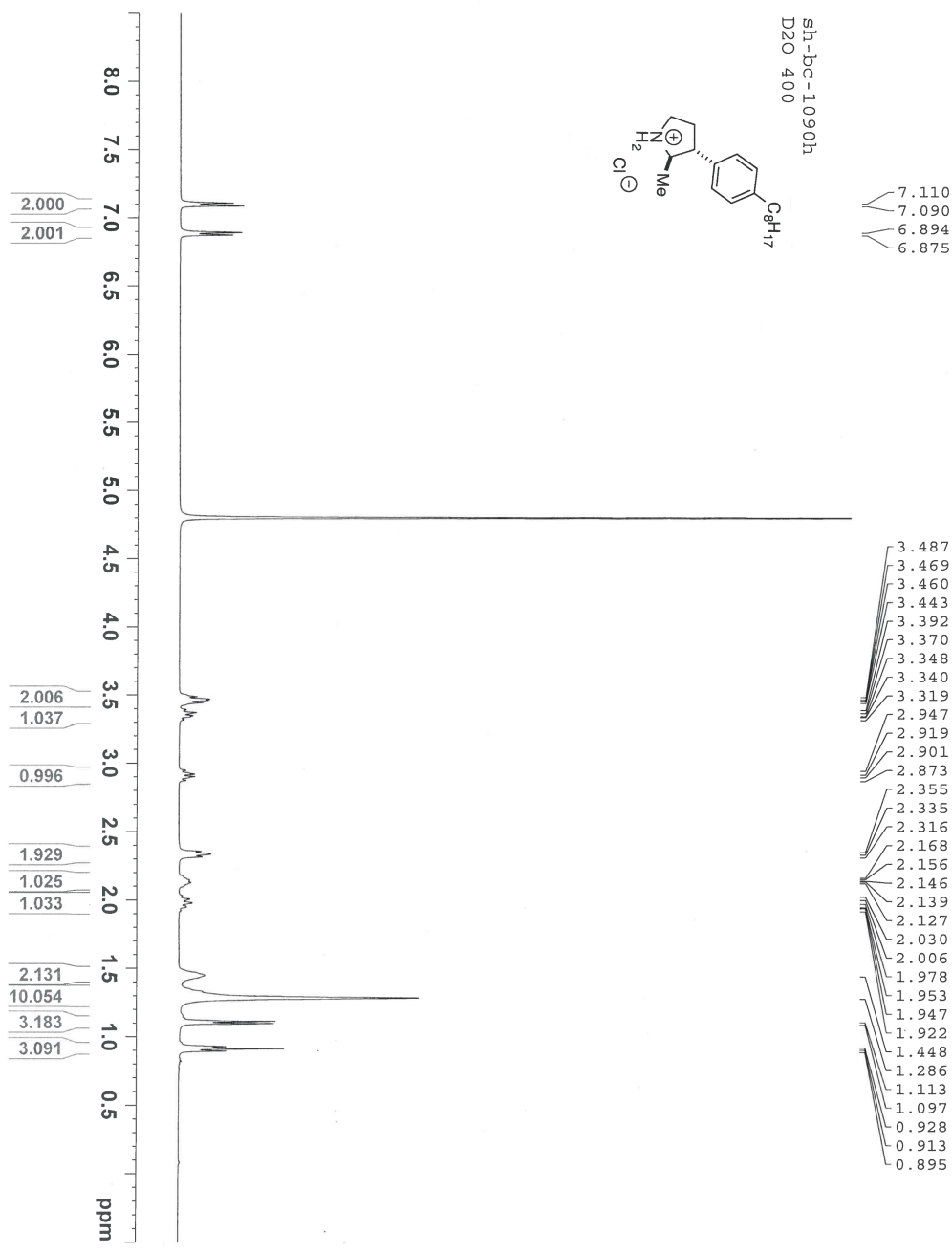


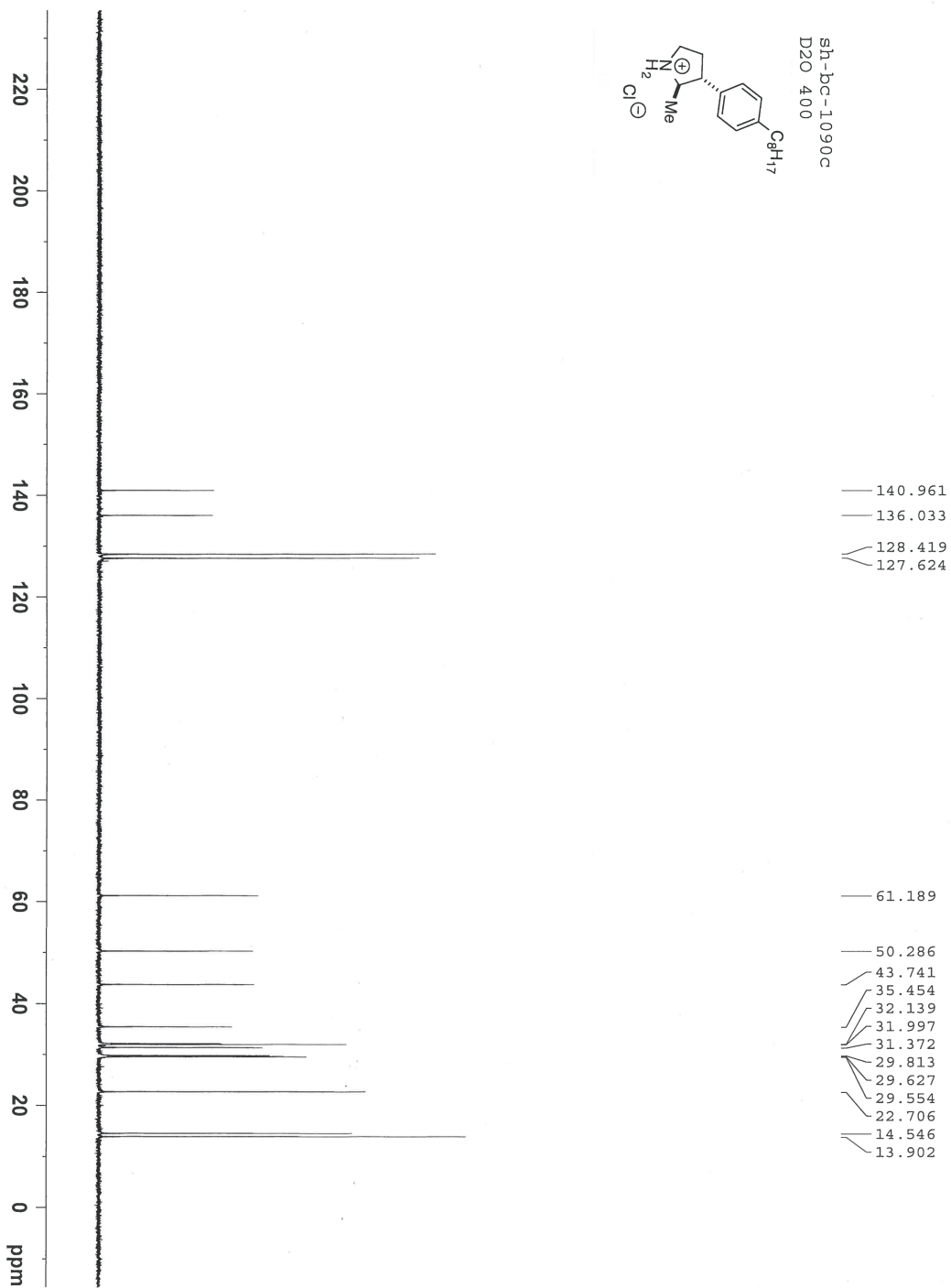
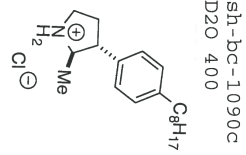


slh-bc-1042pc  
D2O 400



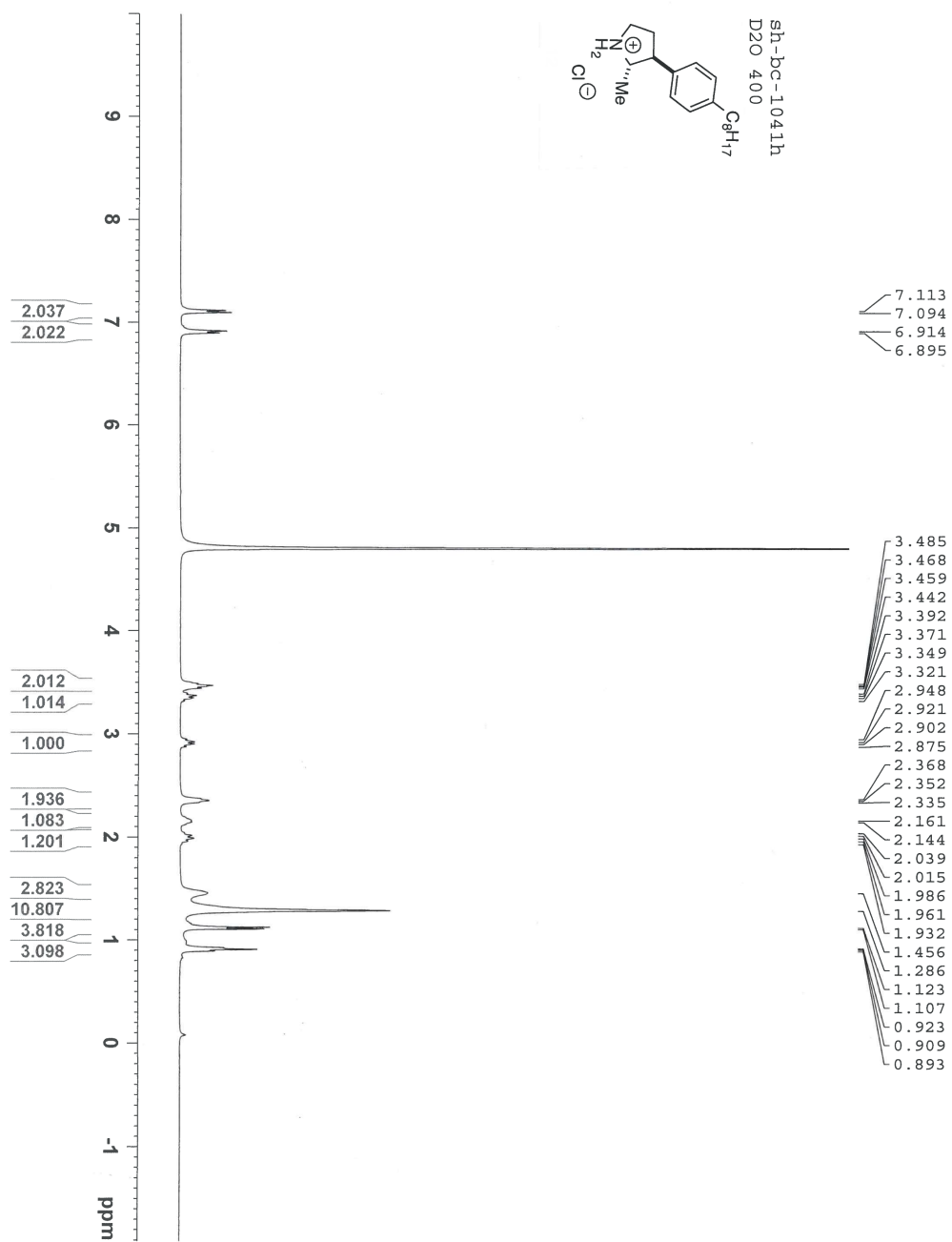
# Annex 20: $^1\text{H}$ and $^{13}\text{C}$ NMR Spectra of Compound 1.134

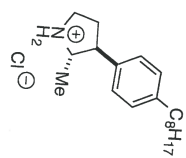




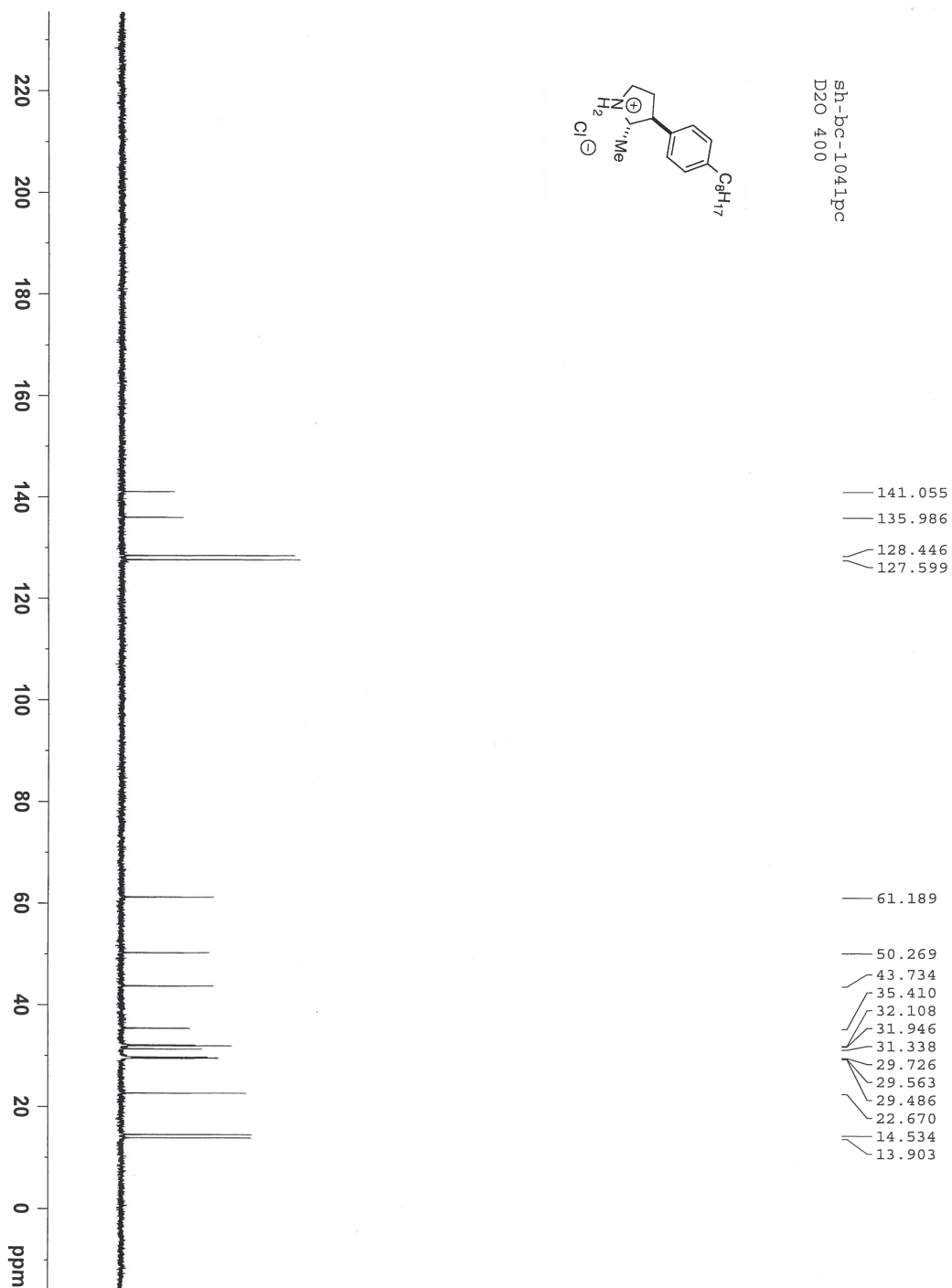
# Annex 21: $^1\text{H}$ and $^{13}\text{C}$ NMR Spectra of Compound

## 1.137



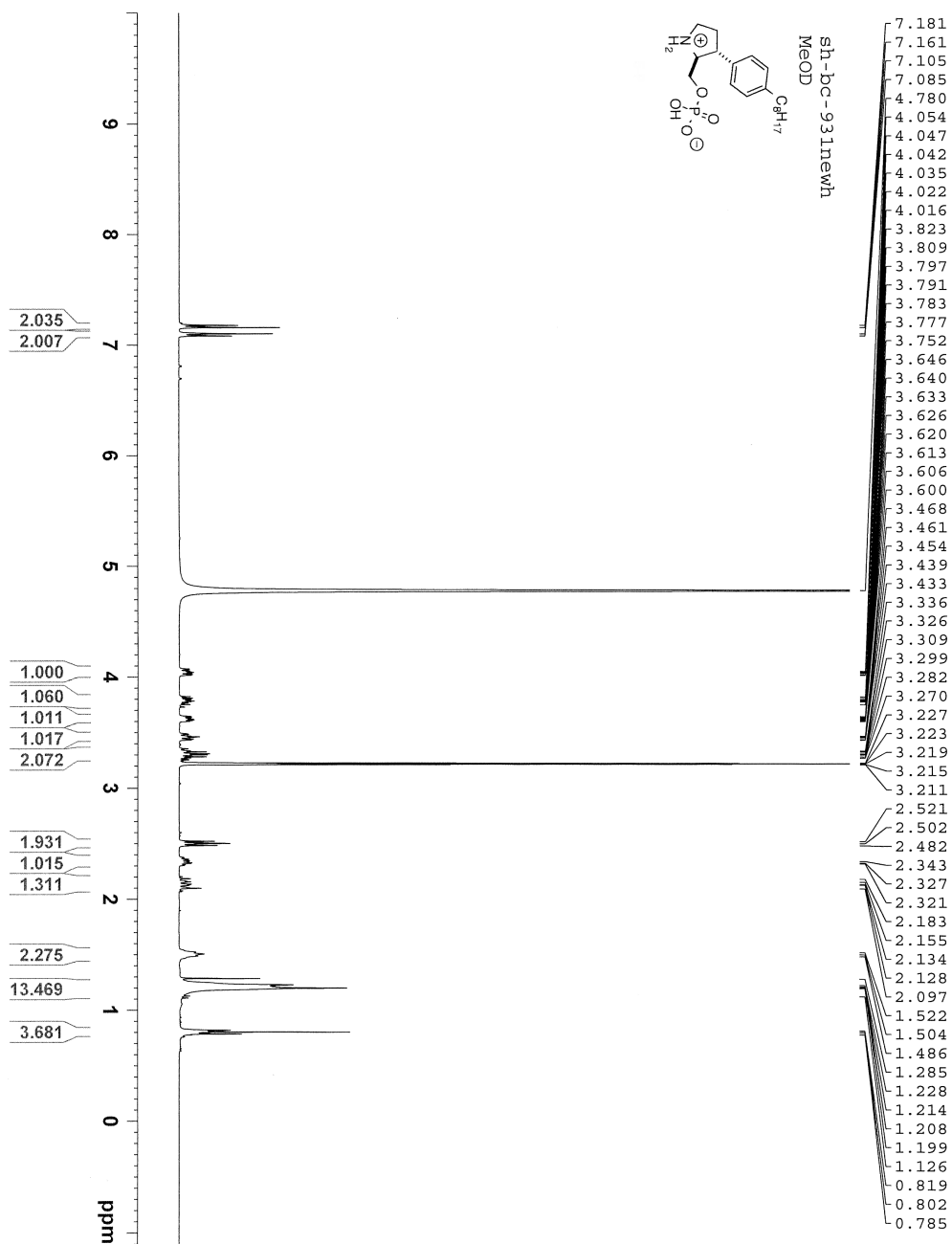


sh-bc-1041pc  
D2O 400

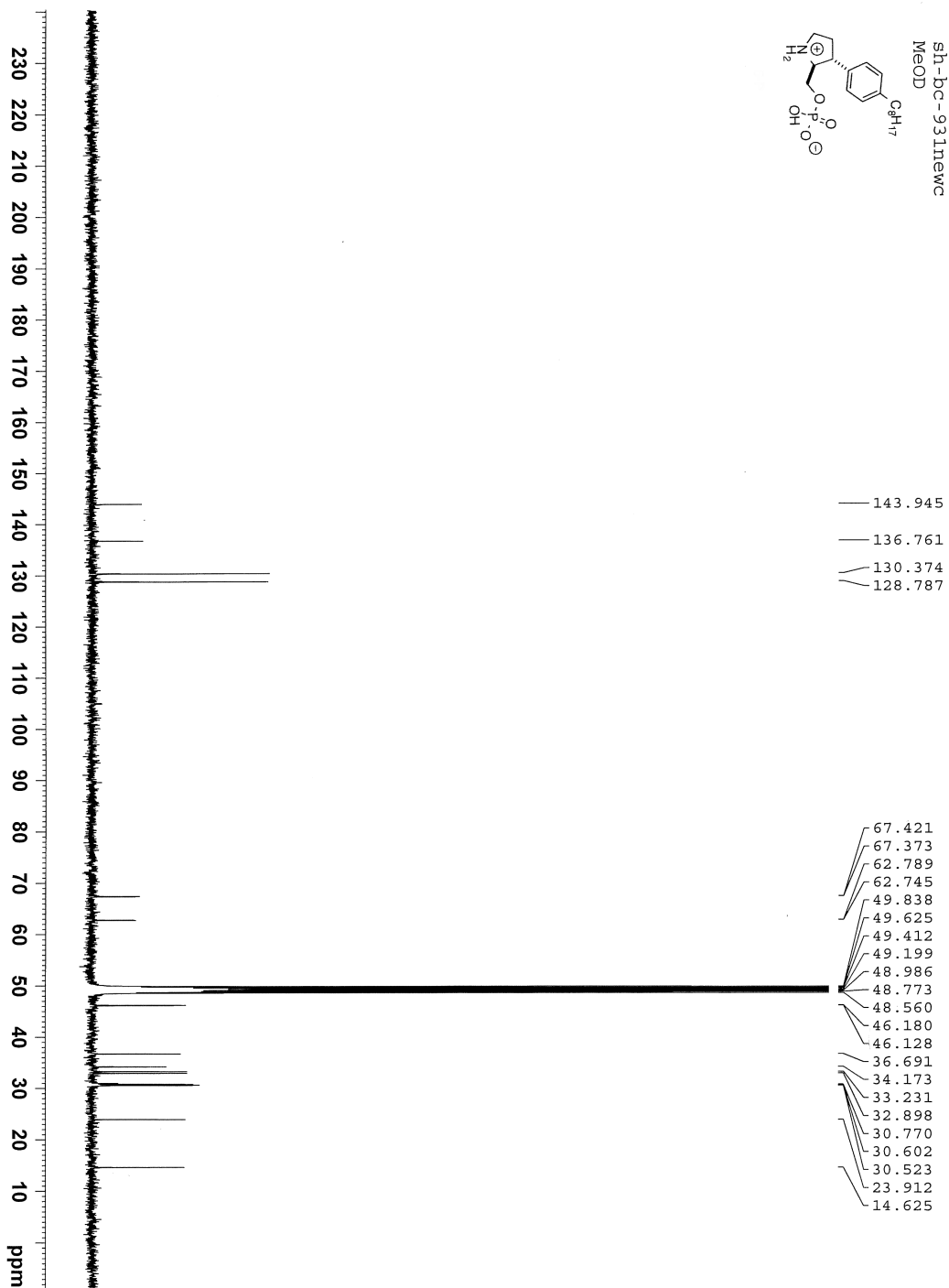
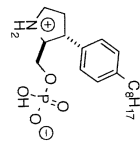


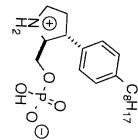


# Annex 22: $^1\text{H}$ , $^{13}\text{C}$ and $^{31}\text{P}$ NMR Spectra of Compound 1.139



sh-bc-931newc  
MeOD

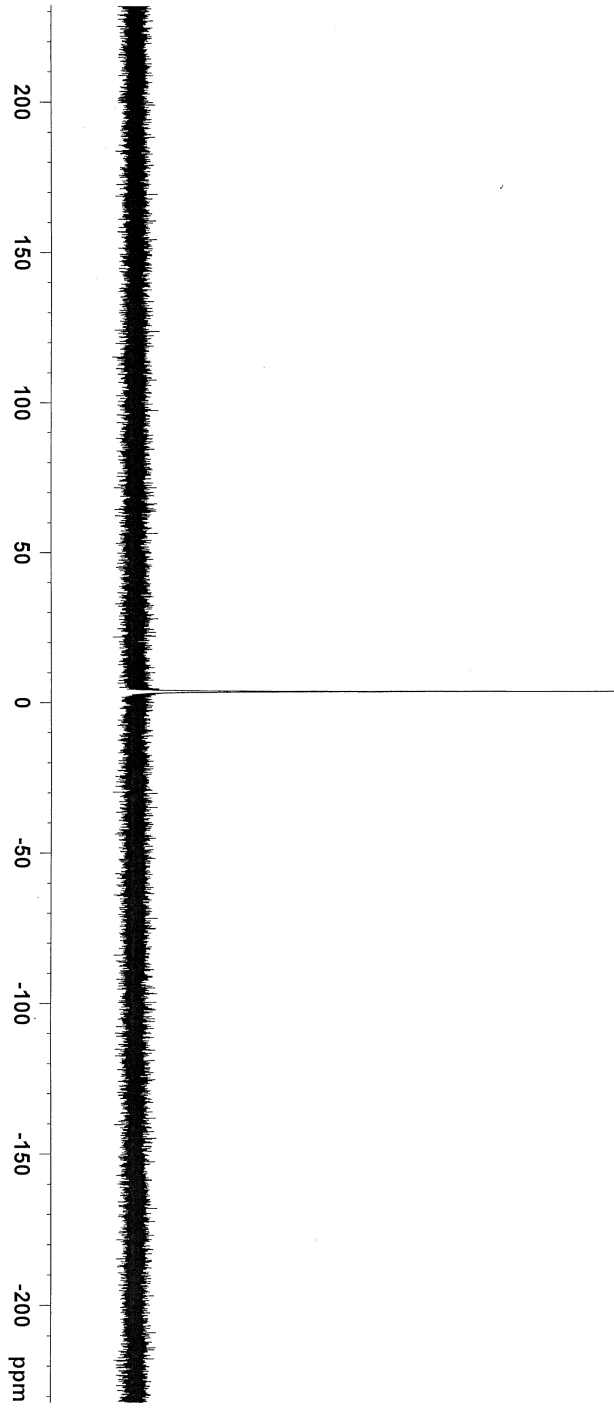




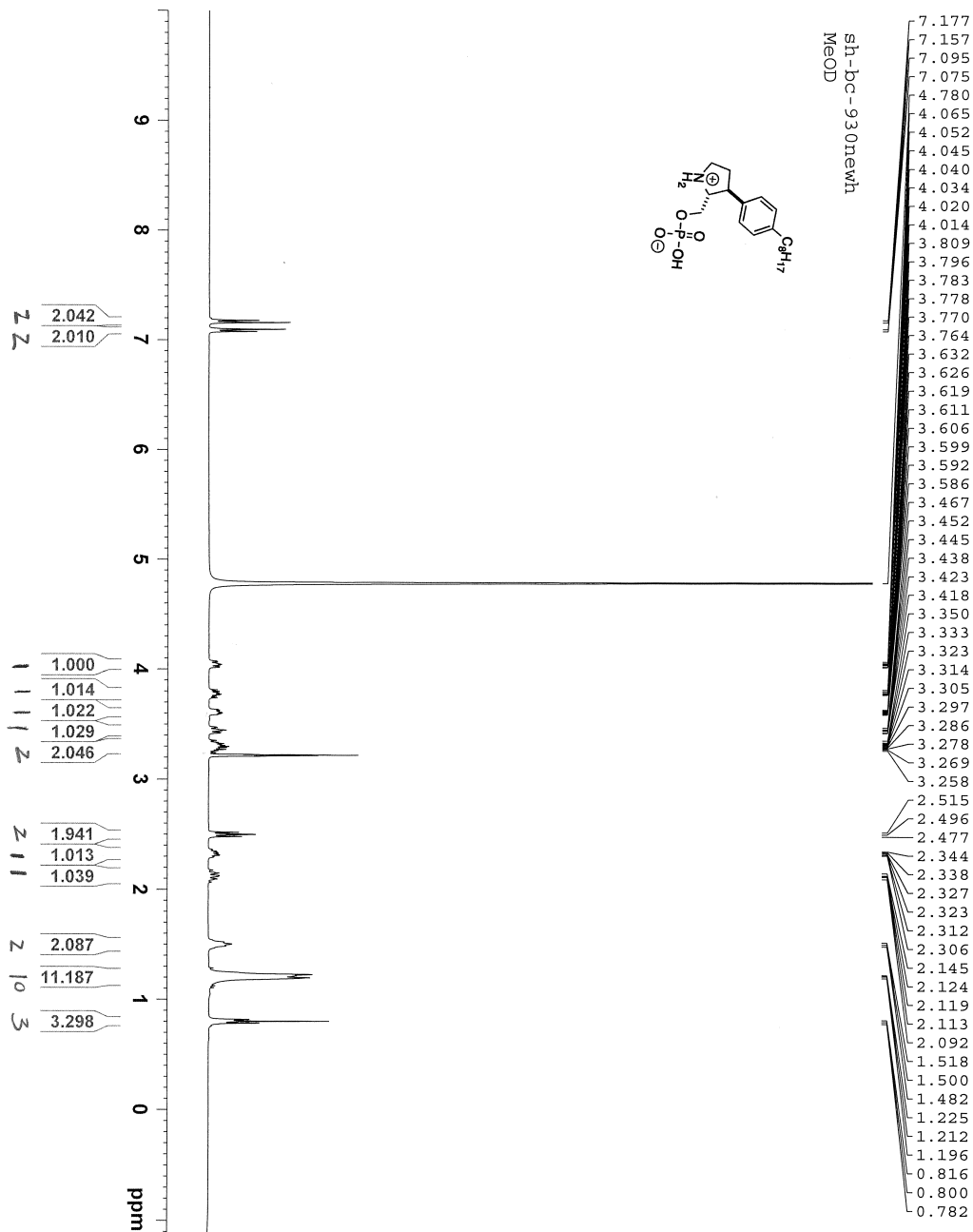
MeOD 400

phos

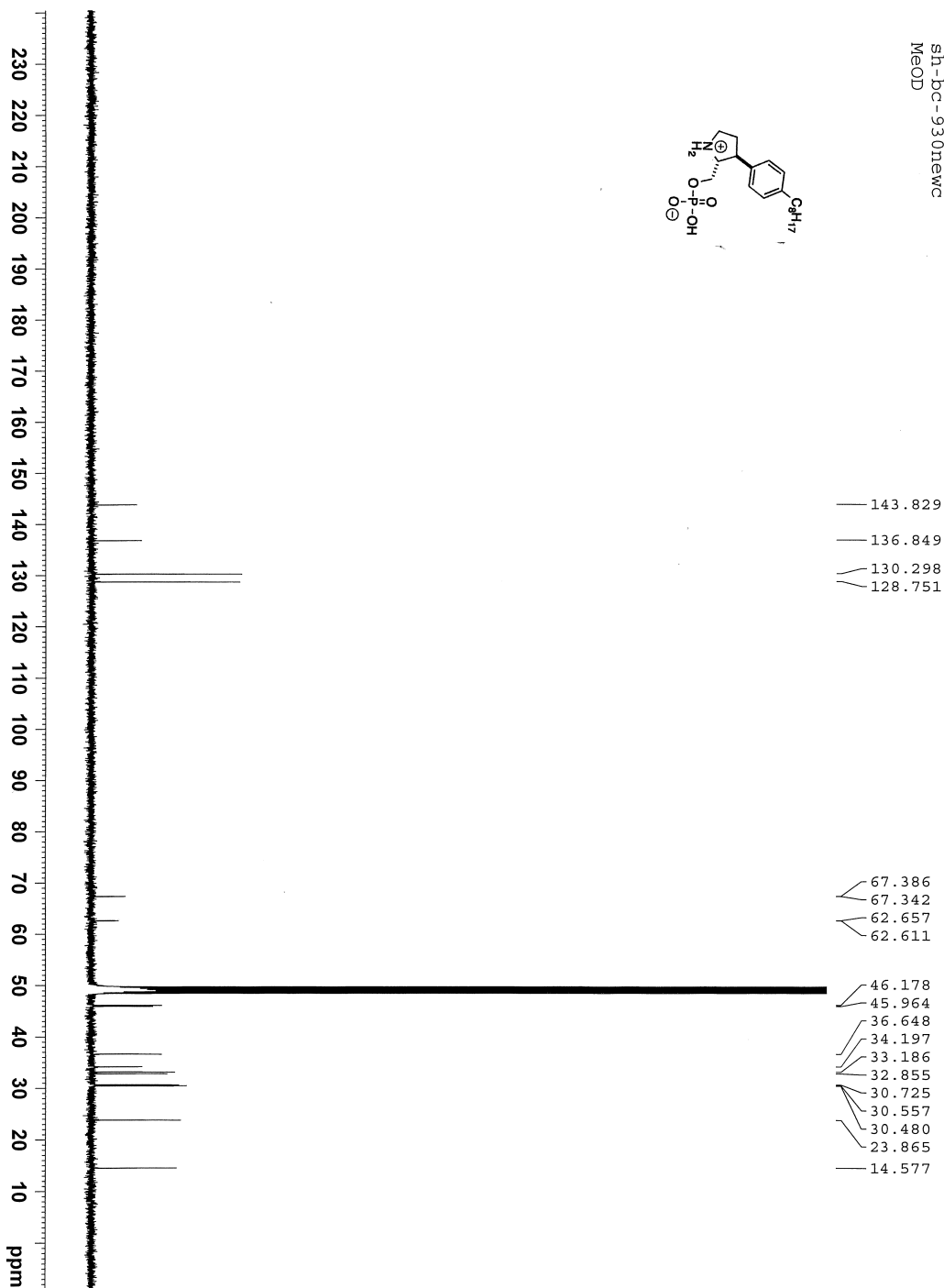
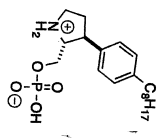
3.648

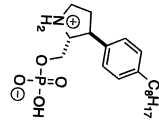


# Annex 23: $^1\text{H}$ , $^{13}\text{C}$ and $^{31}\text{P}$ NMR Spectra of Compound 1.141

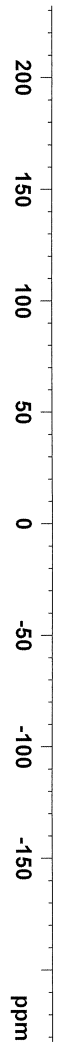


sh-bc-930newc  
MeOD





2.98



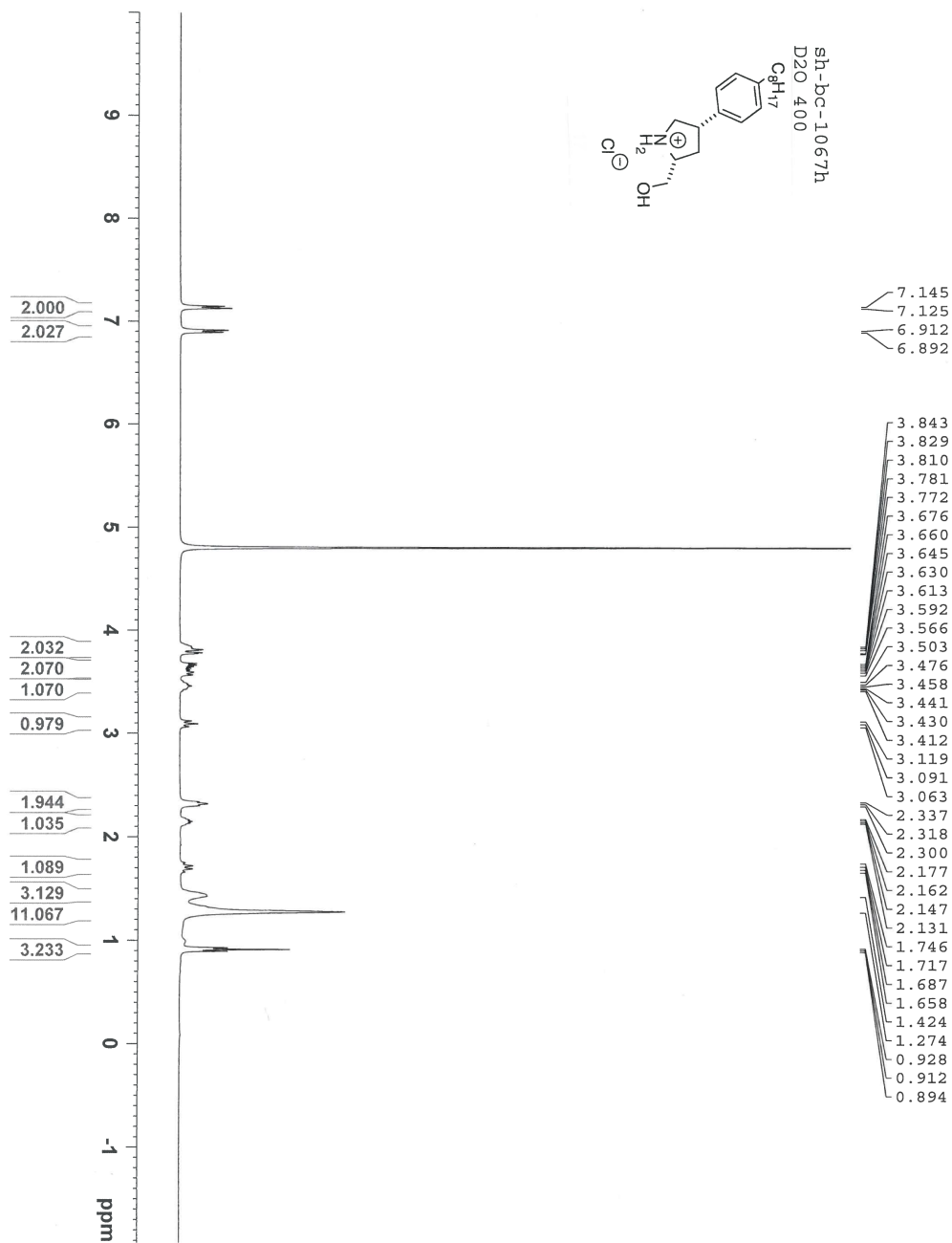
```

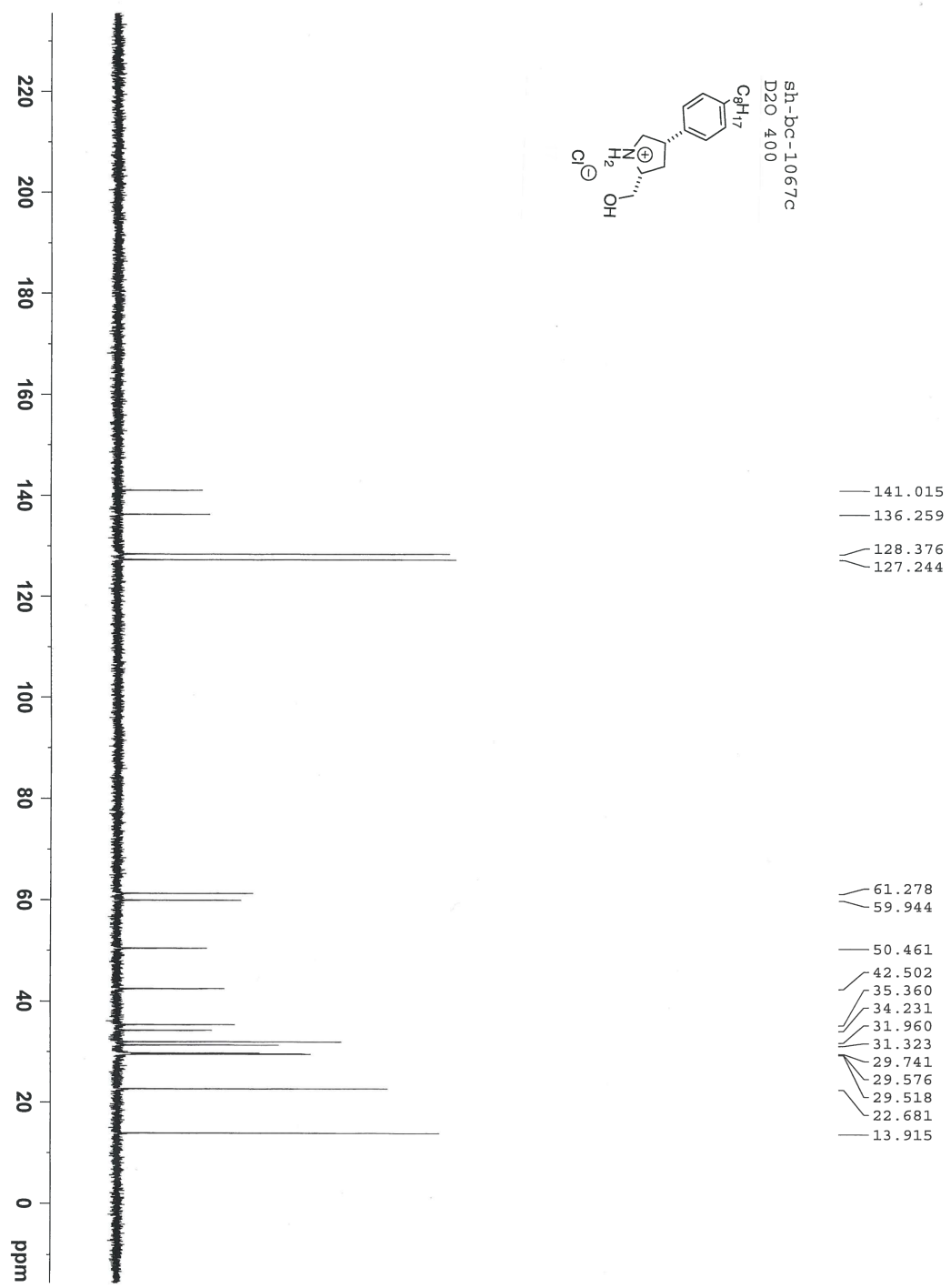
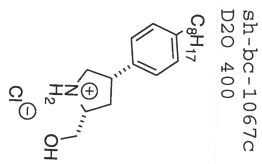
NAME sh-bc-930newp31
EXPNO 1
PROCNO 1
Date_ 20120710
Time_ 20.17
INSTRUM spect
PROBHD 5 mm PABBO BB-
PULPROG zgpg30
TD 102400
SOLVENT MeOD
NS 354
DS 2
SMH 75187.969 Hz
FIDRES 0.734258 Hz
AQ 0.6810100 sec
RG 2580.3
DM 6.650 usec
DE 9.50 usec
TE 284.2 K
D1 3.00000000 sec
D11 0.03000000 sec
TDO 1

===== CHANNEL f1 =====
NUC1 31P
P1 16.10 usec
PL1 0.00 dB
PL1W 36.92473221 W
SFO1 161.9754752 MHz

===== CHANNEL f2 =====
CPDPRG2 waltz65
NUC2 1H
PCPD2 96.00 usec
PL2 -3.00 dB
PL12 16.00 dB
PL13 120.00 dB
PL1W 23.05461311 W
PL2W 0.29024038 W
PL13W 0.00000000 W
SFO2 400.1316000 MHz
SI 131072
SF 161.9754749 MHz
WDW no
SSB 0
LB 0.00 Hz
GB 0
PC 1.40
  
```

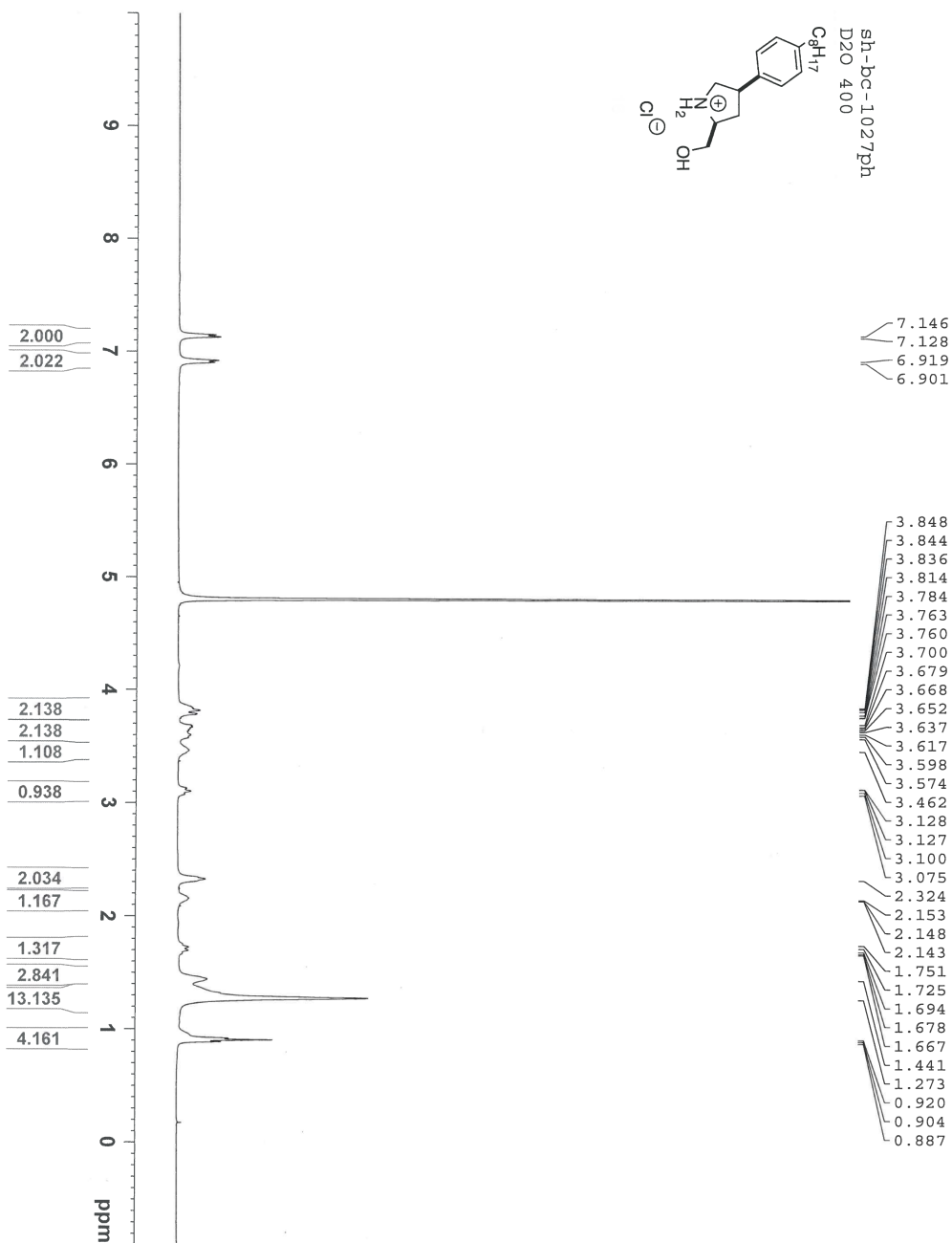
# Annex 24: $^1\text{H}$ and $^{13}\text{C}$ NMR Spectra of Compound 1.150

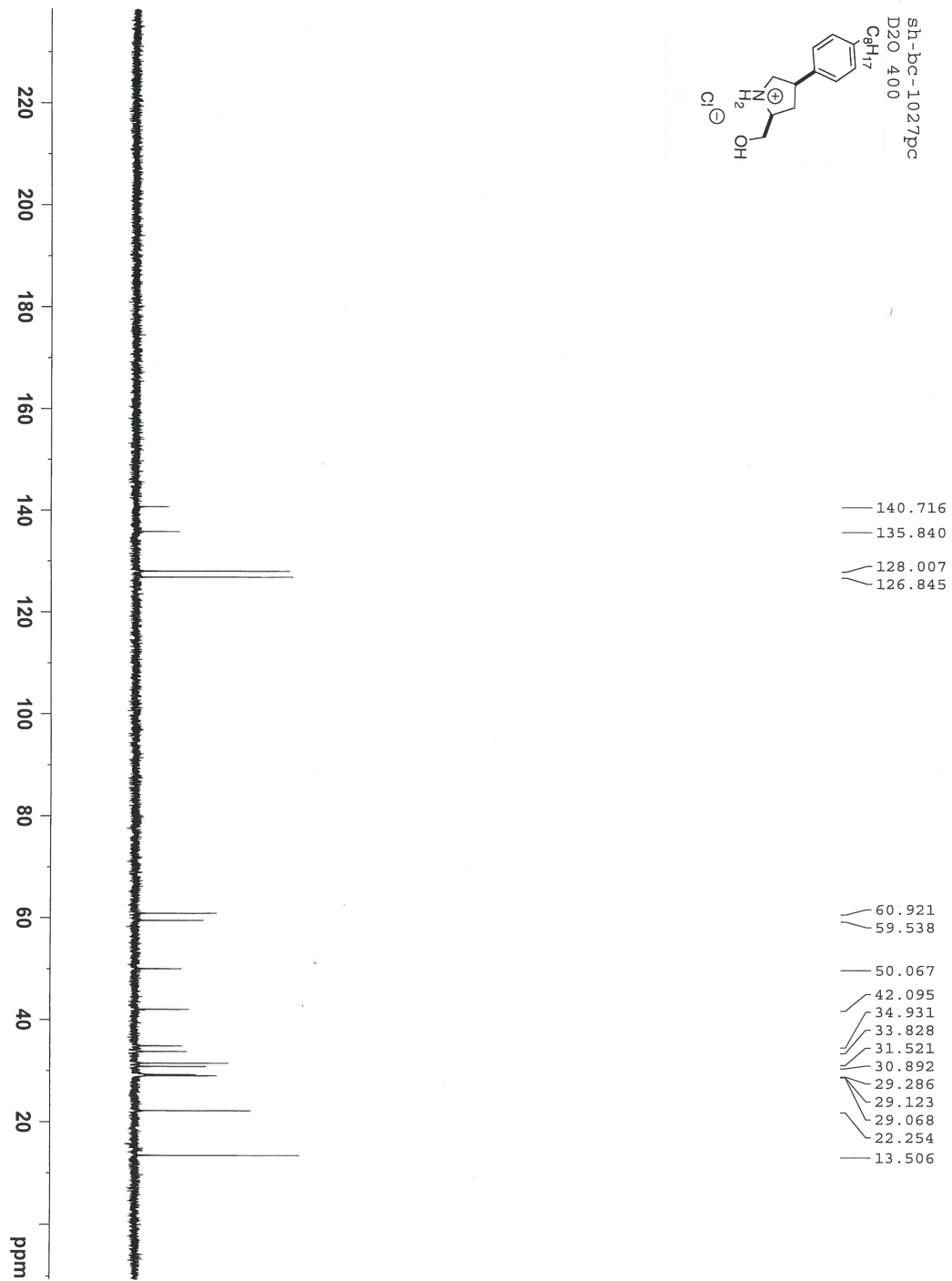
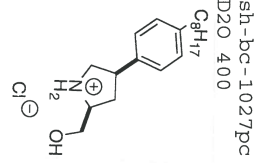




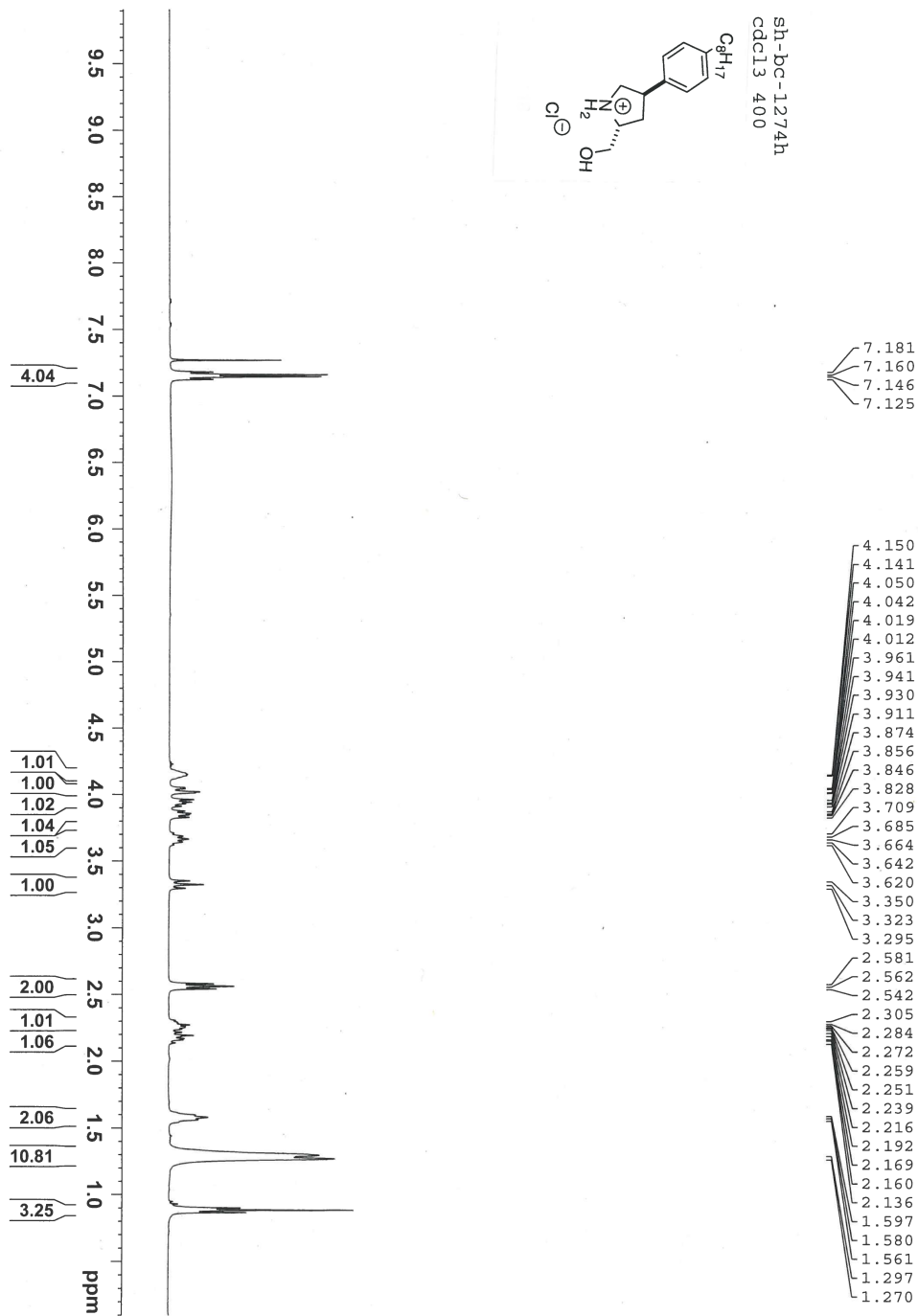


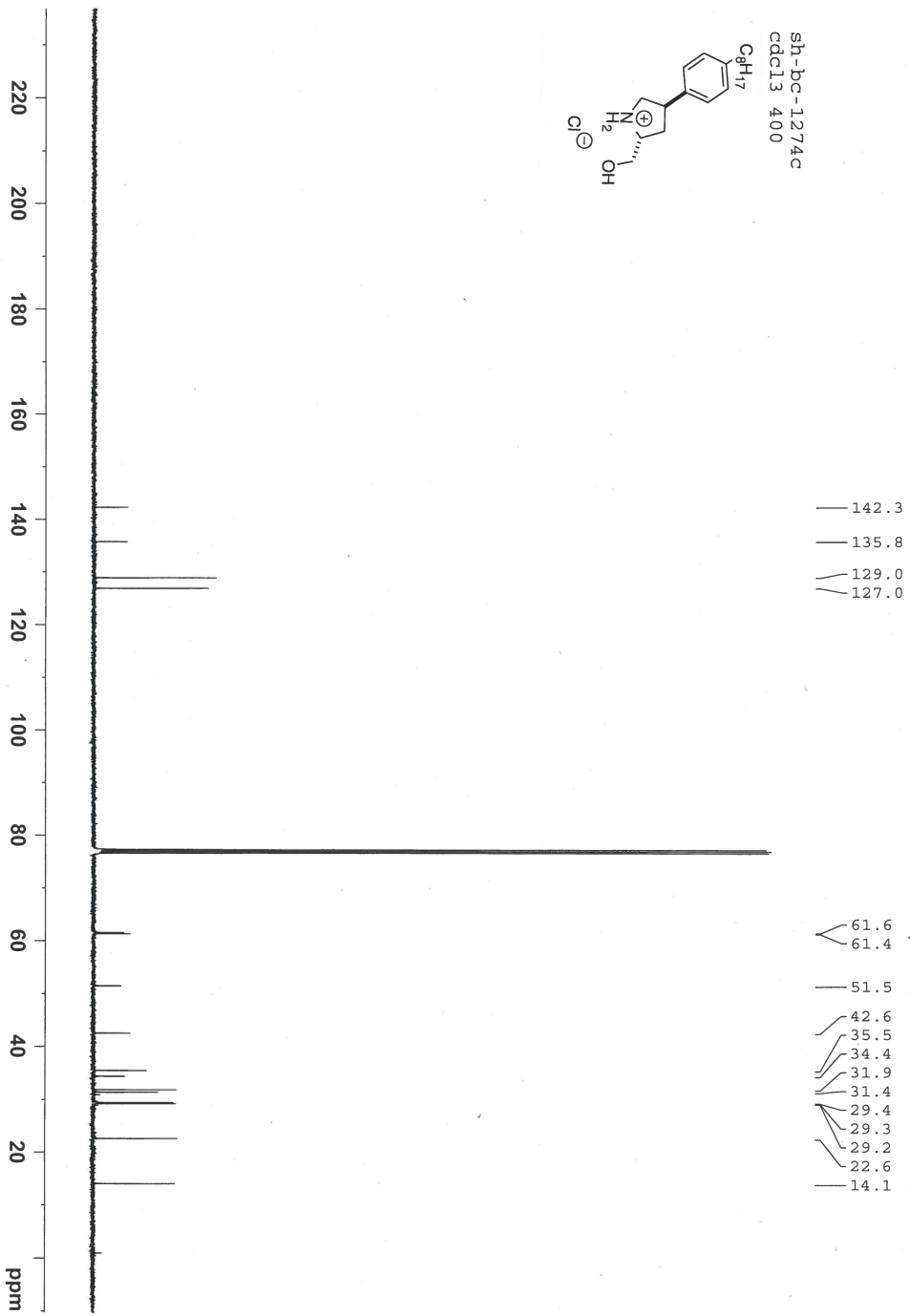
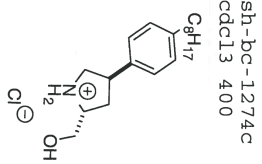
# Annex 25: $^1\text{H}$ and $^{13}\text{C}$ NMR Spectra of Compound 1.157



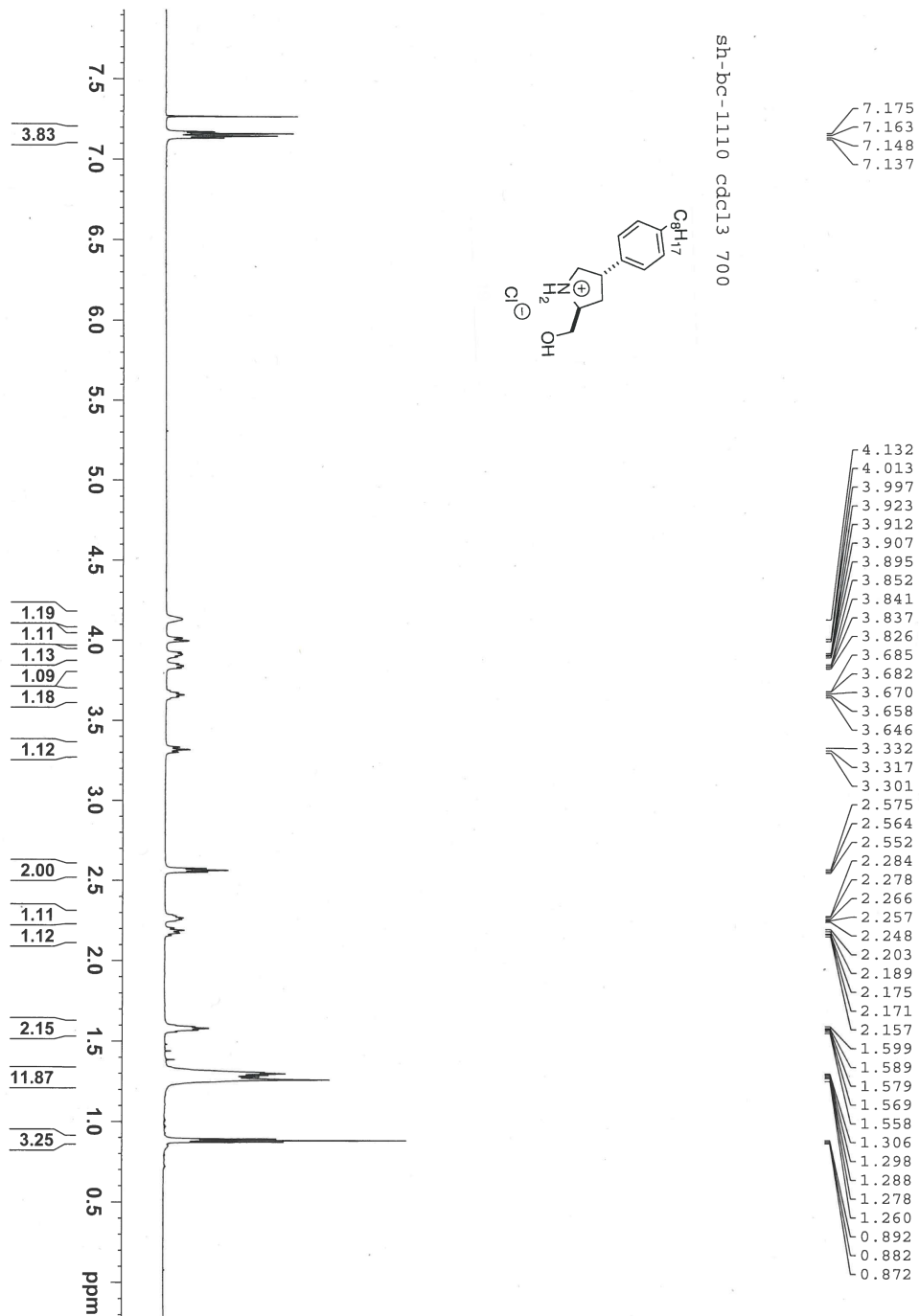


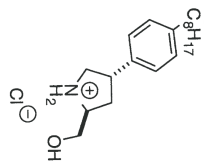
# Annex 26: $^1\text{H}$ and $^{13}\text{C}$ NMR Spectra of Compound 1.161



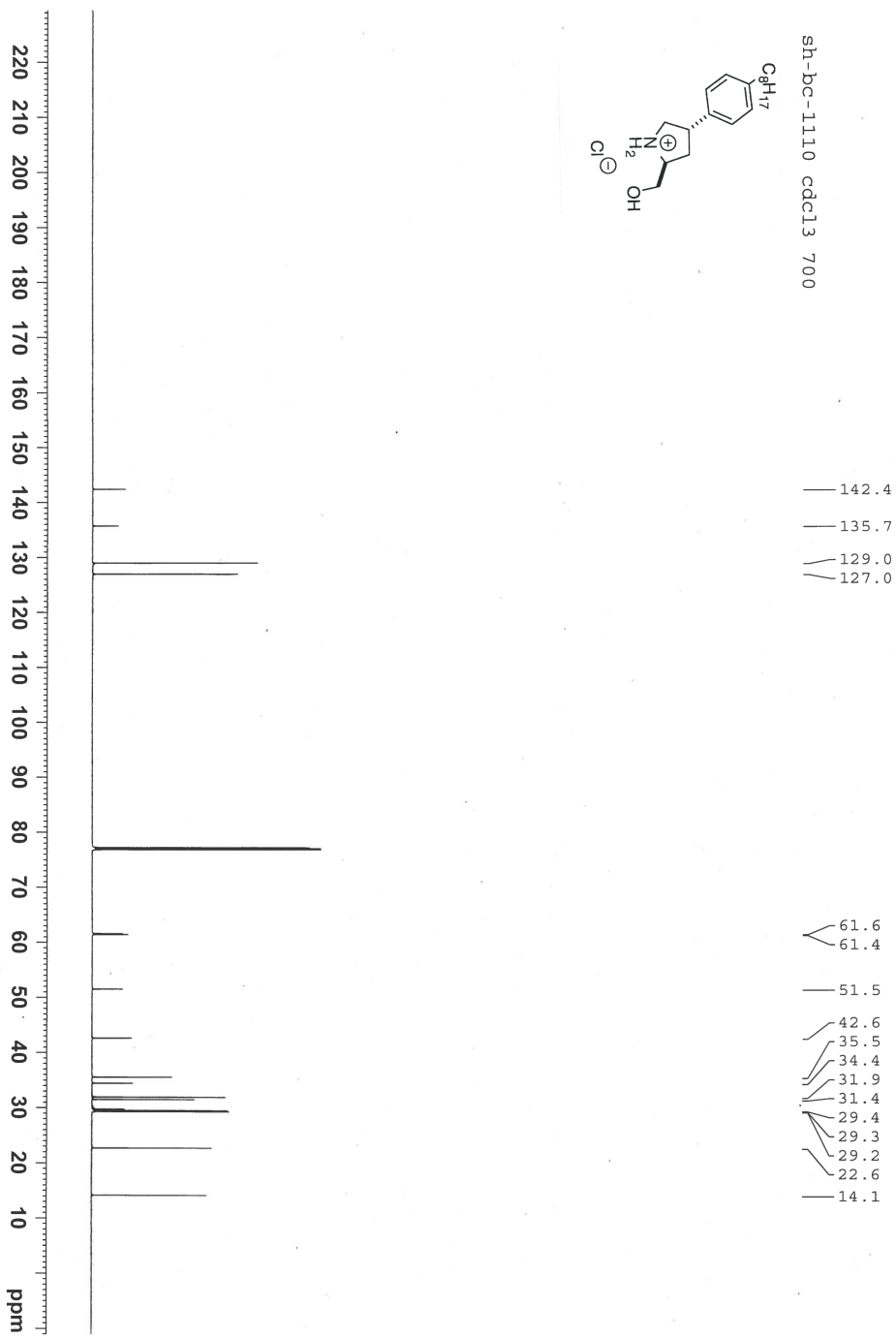


# Annex 27: $^1\text{H}$ and $^{13}\text{C}$ NMR Spectra of Compound 1.164

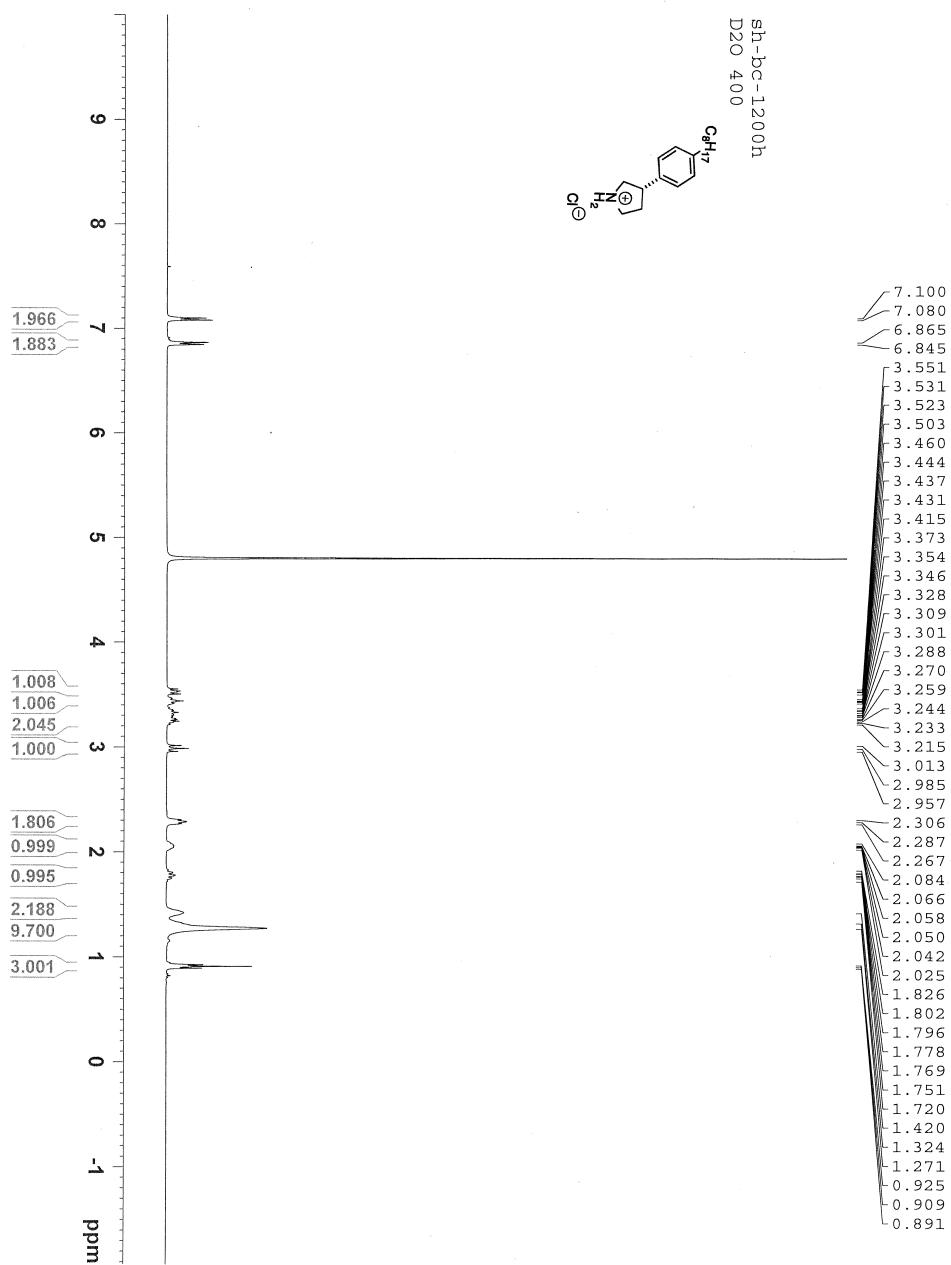




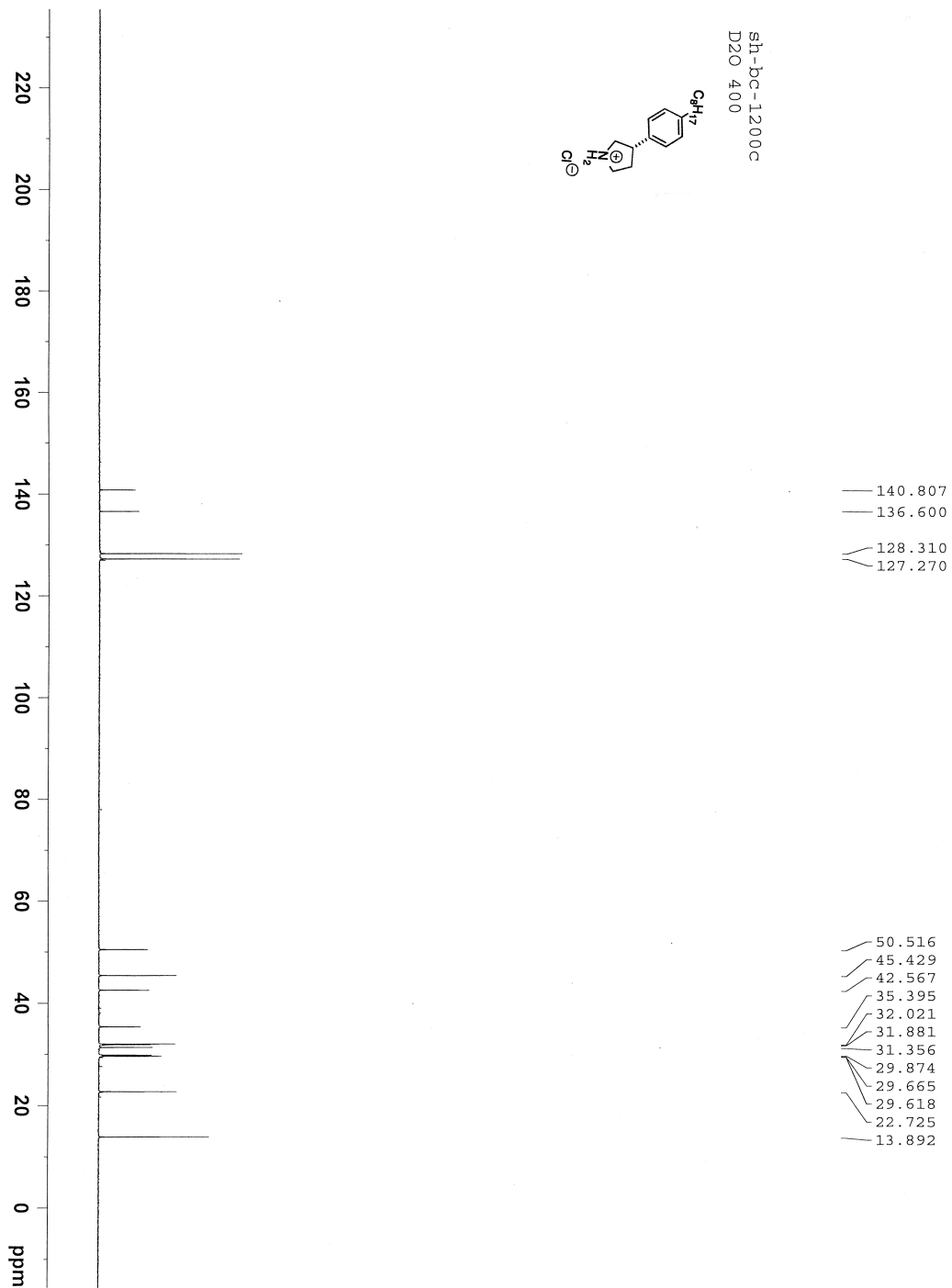
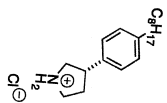
sh-bc-1110 cdcl3 700



# Annex 28: $^1\text{H}$ and $^{13}\text{C}$ NMR Spectra of Compound 1.170



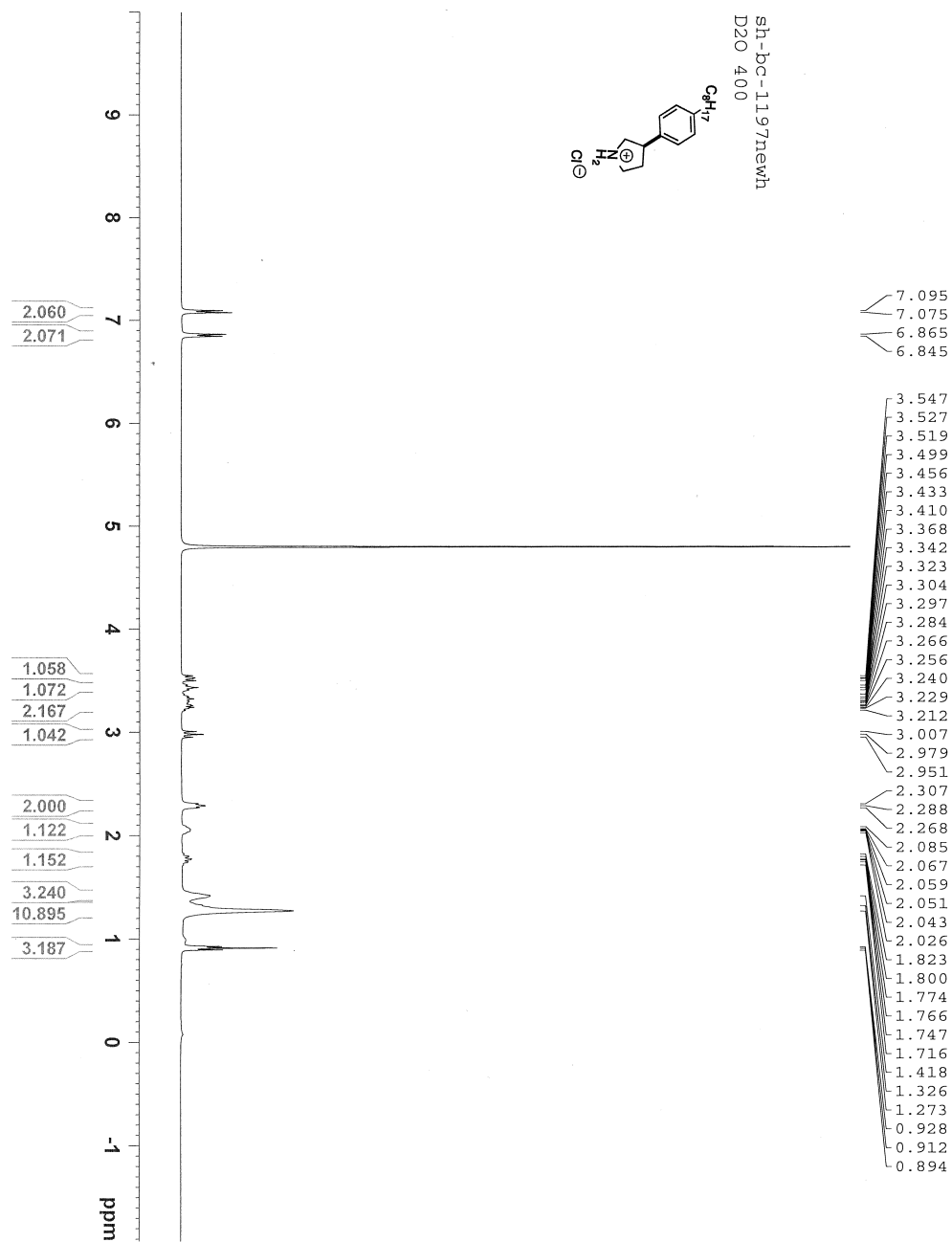
sh-bc-1200c  
D2O 400

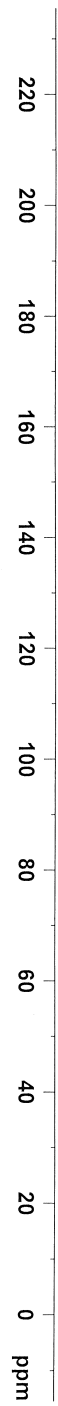
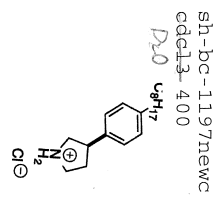




# Annex 29: $^1\text{H}$ and $^{13}\text{C}$ NMR Spectra of Compound

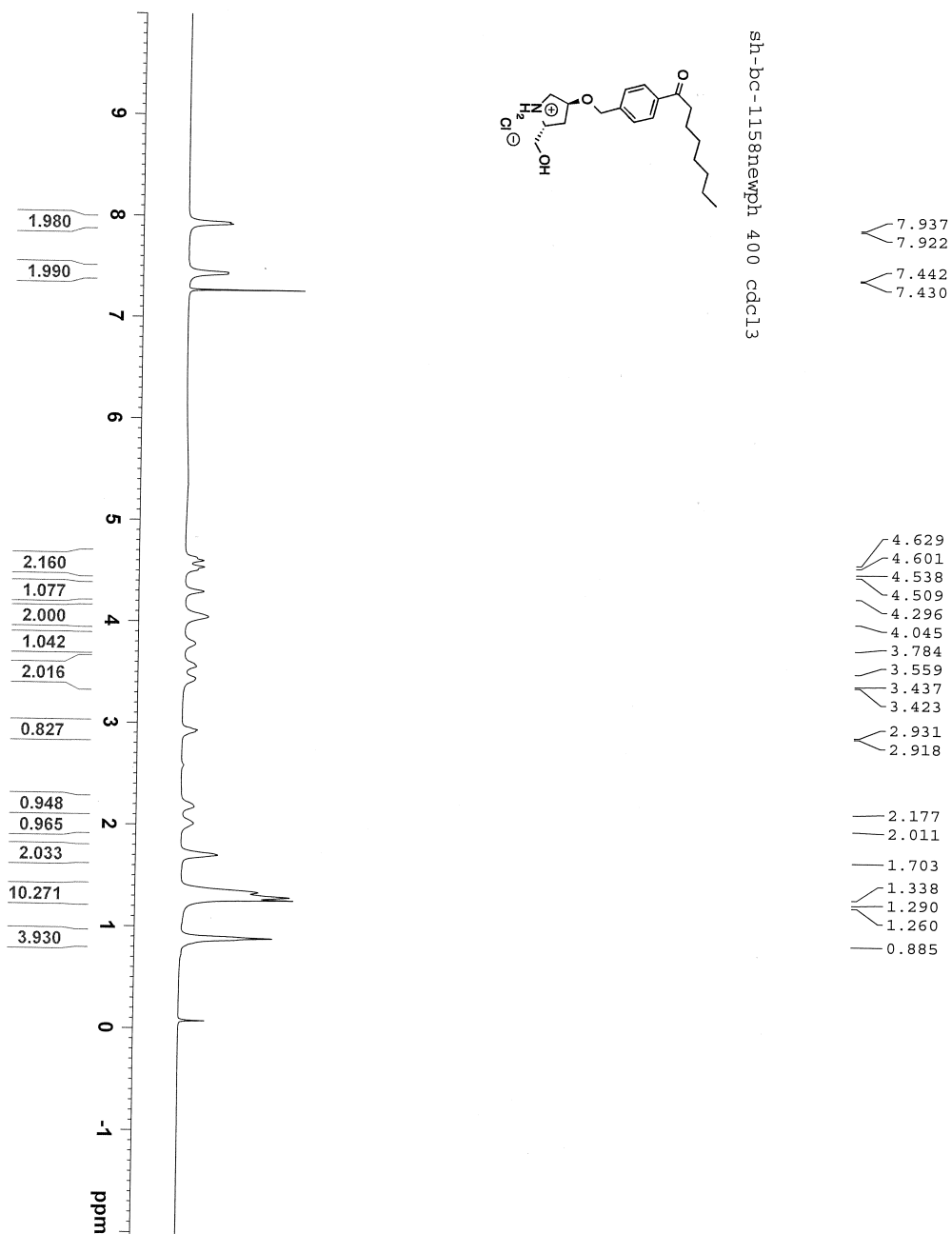
## 1.175

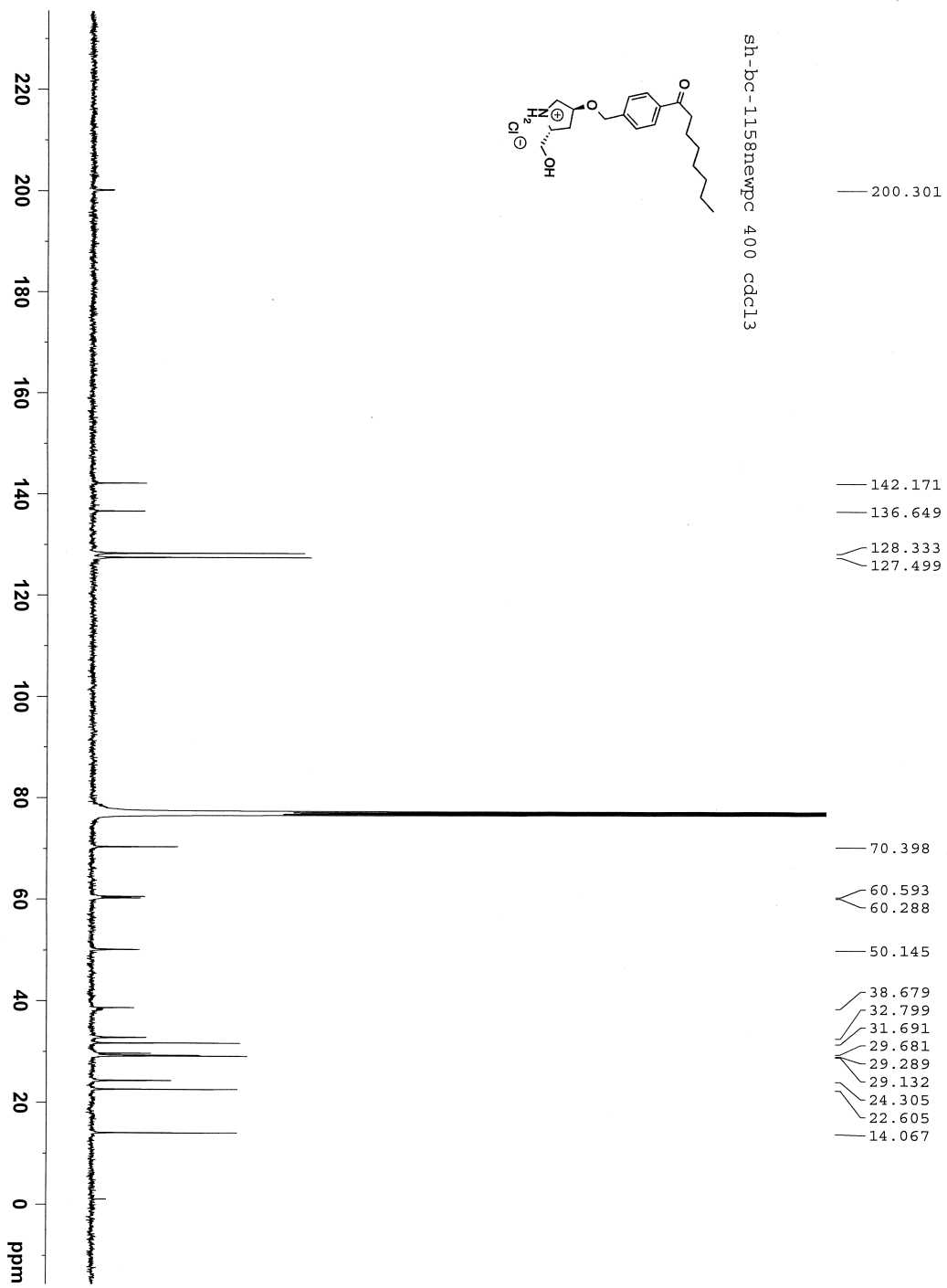




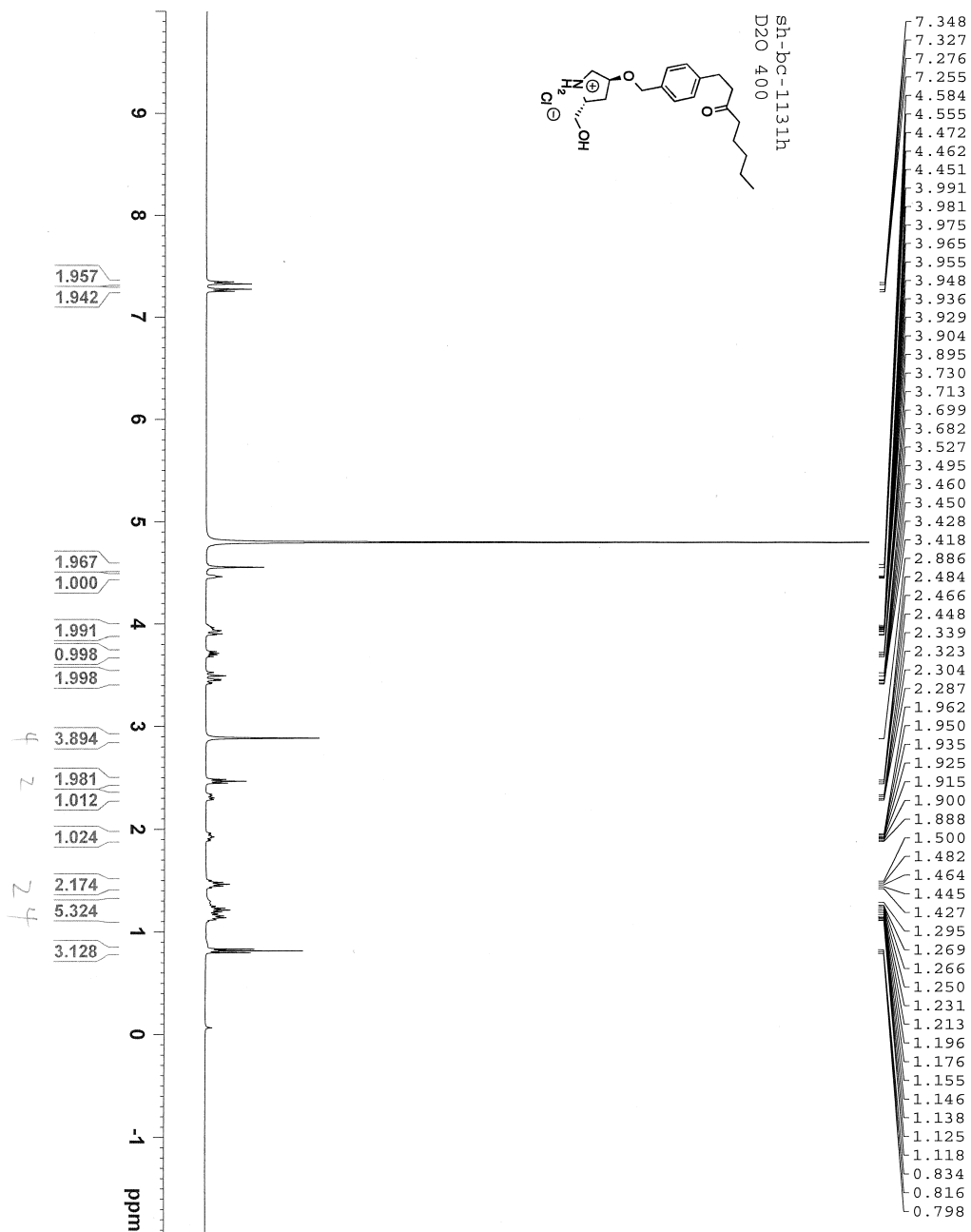
- 140.814
- 136.625
- 128.310
- 127.259
  
- 50.523
- 45.431
- 42.558
- 35.376
- 32.009
- 31.870
- 31.334
- 29.843
- 29.640
- 29.600
- 22.721
- 13.925

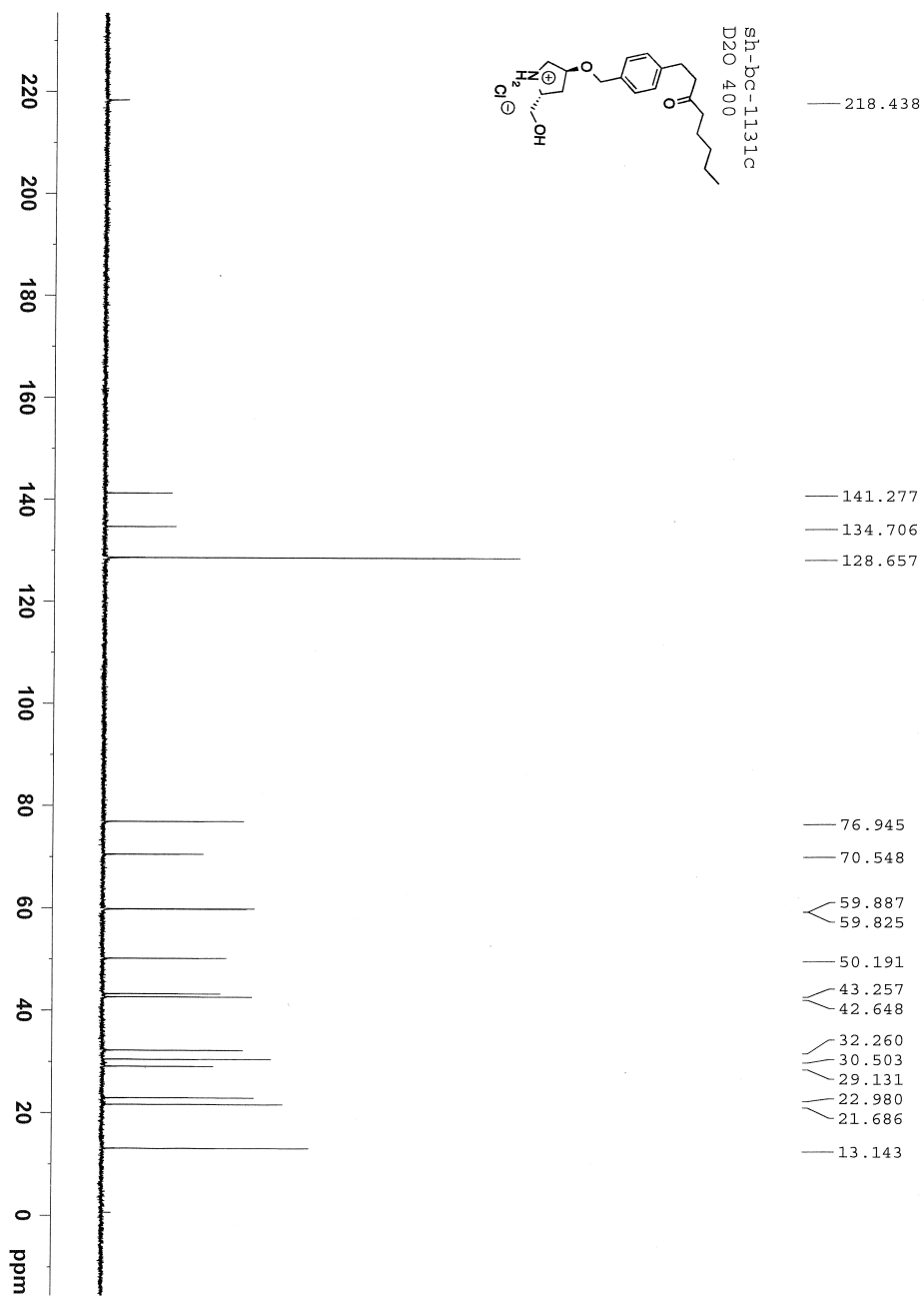
# Annex 30: $^1\text{H}$ and $^{13}\text{C}$ NMR Spectra of Compound 2.1



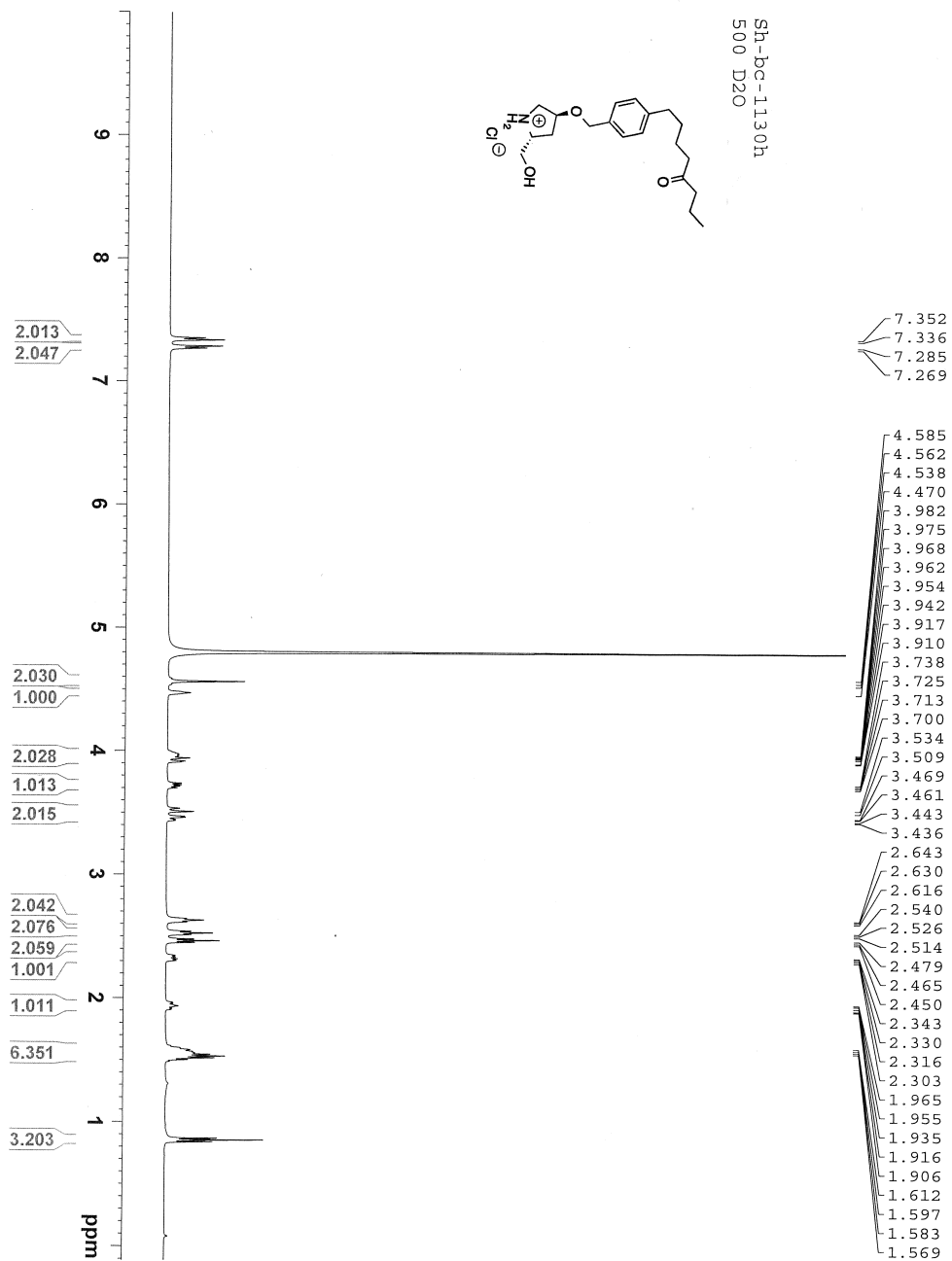


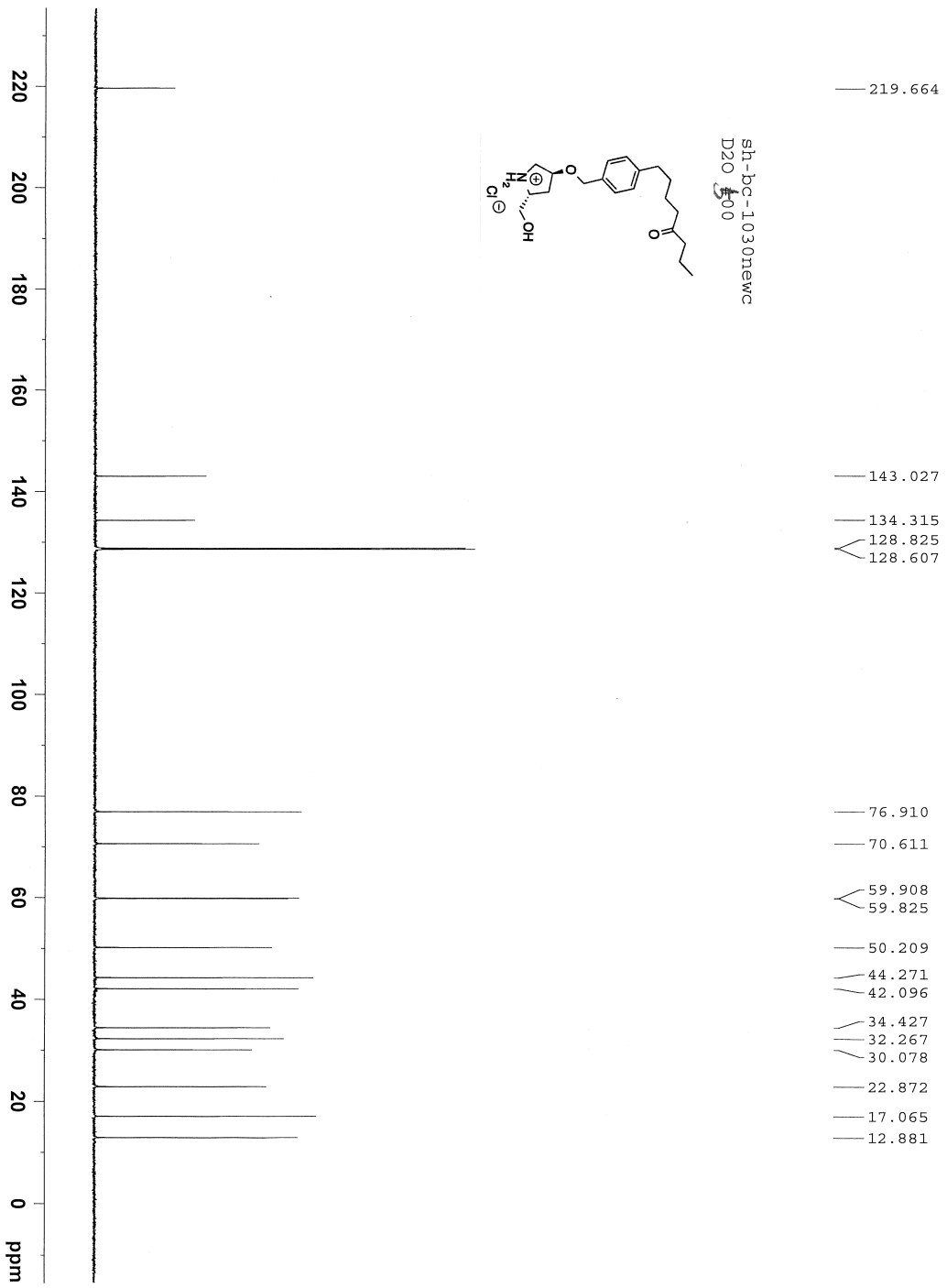
# Annex 31: $^1\text{H}$ and $^{13}\text{C}$ NMR Spectra of Compound 2.2





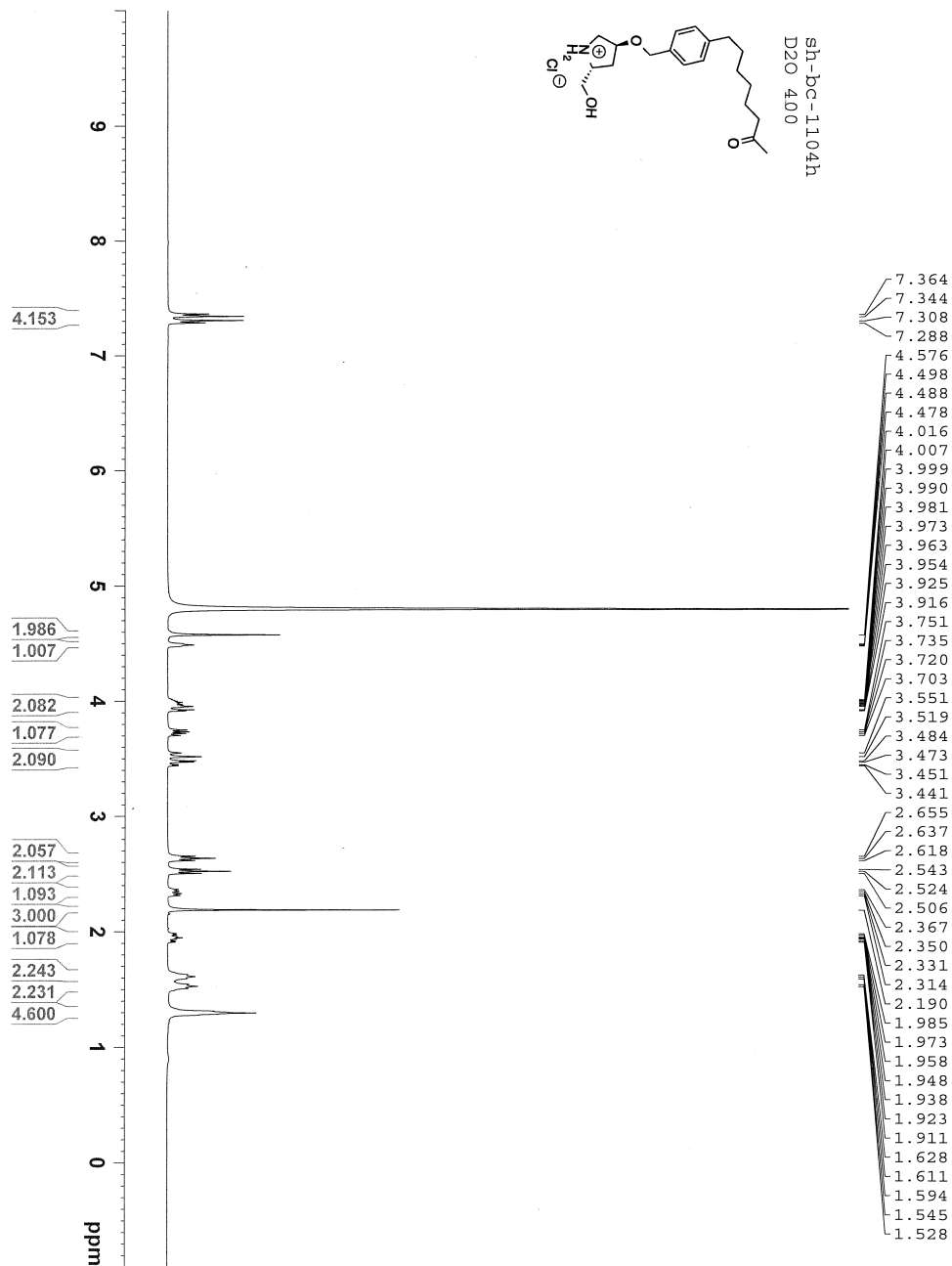
# Annex 32: $^1\text{H}$ and $^{13}\text{C}$ NMR Spectra of Compound 2.3

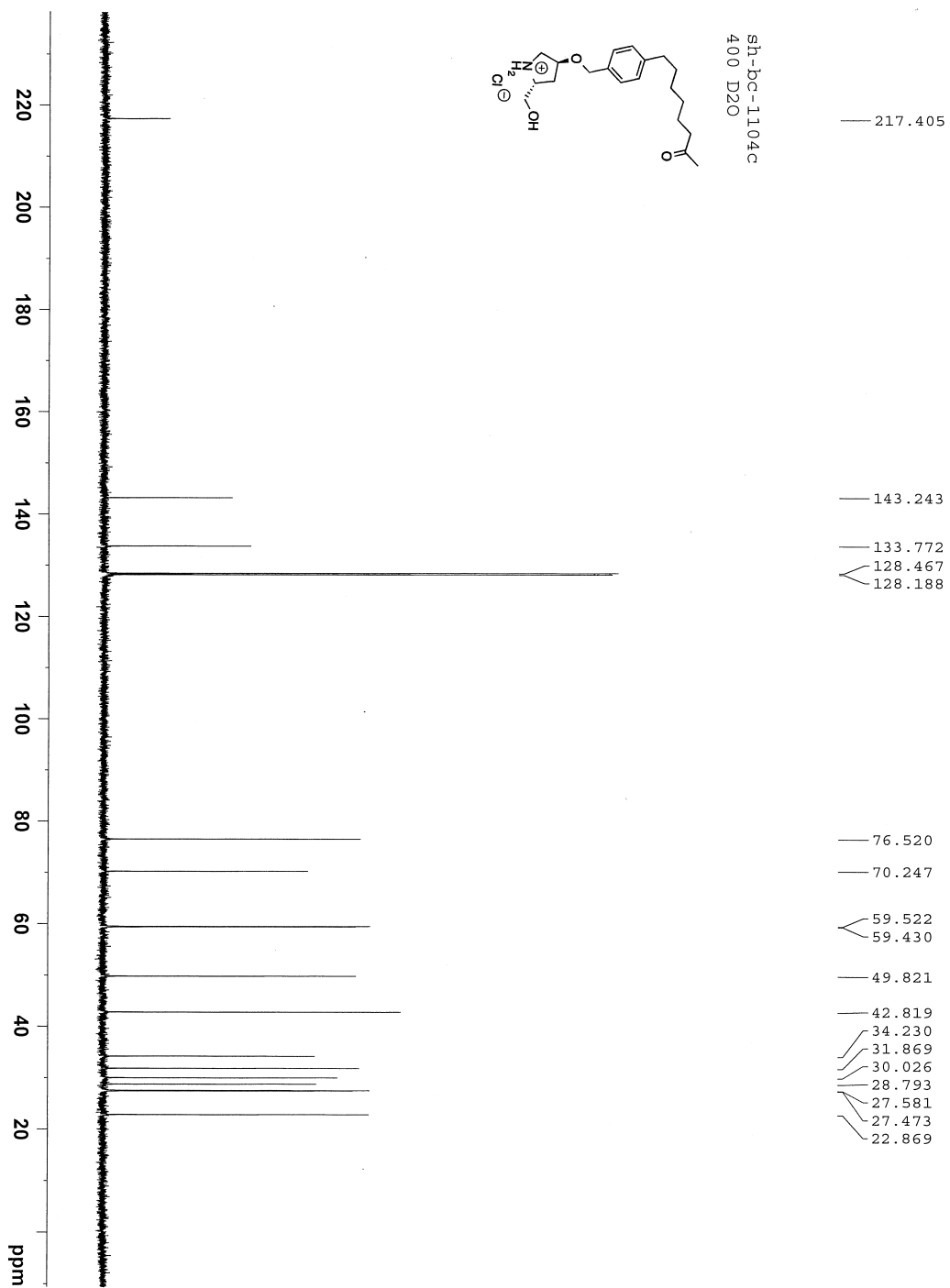




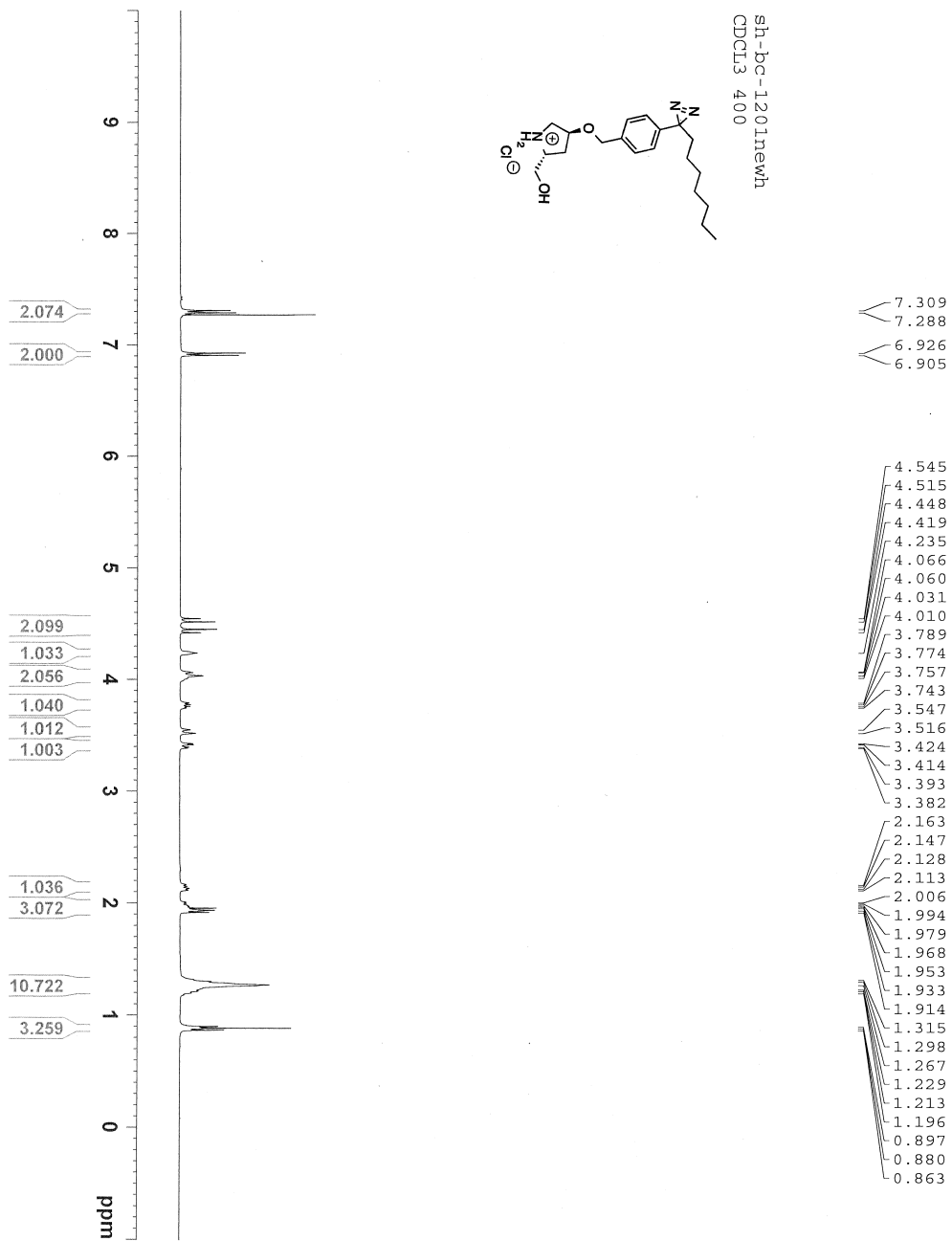


# Annex 33: $^1\text{H}$ and $^{13}\text{C}$ NMR Spectra of Compound 2.4

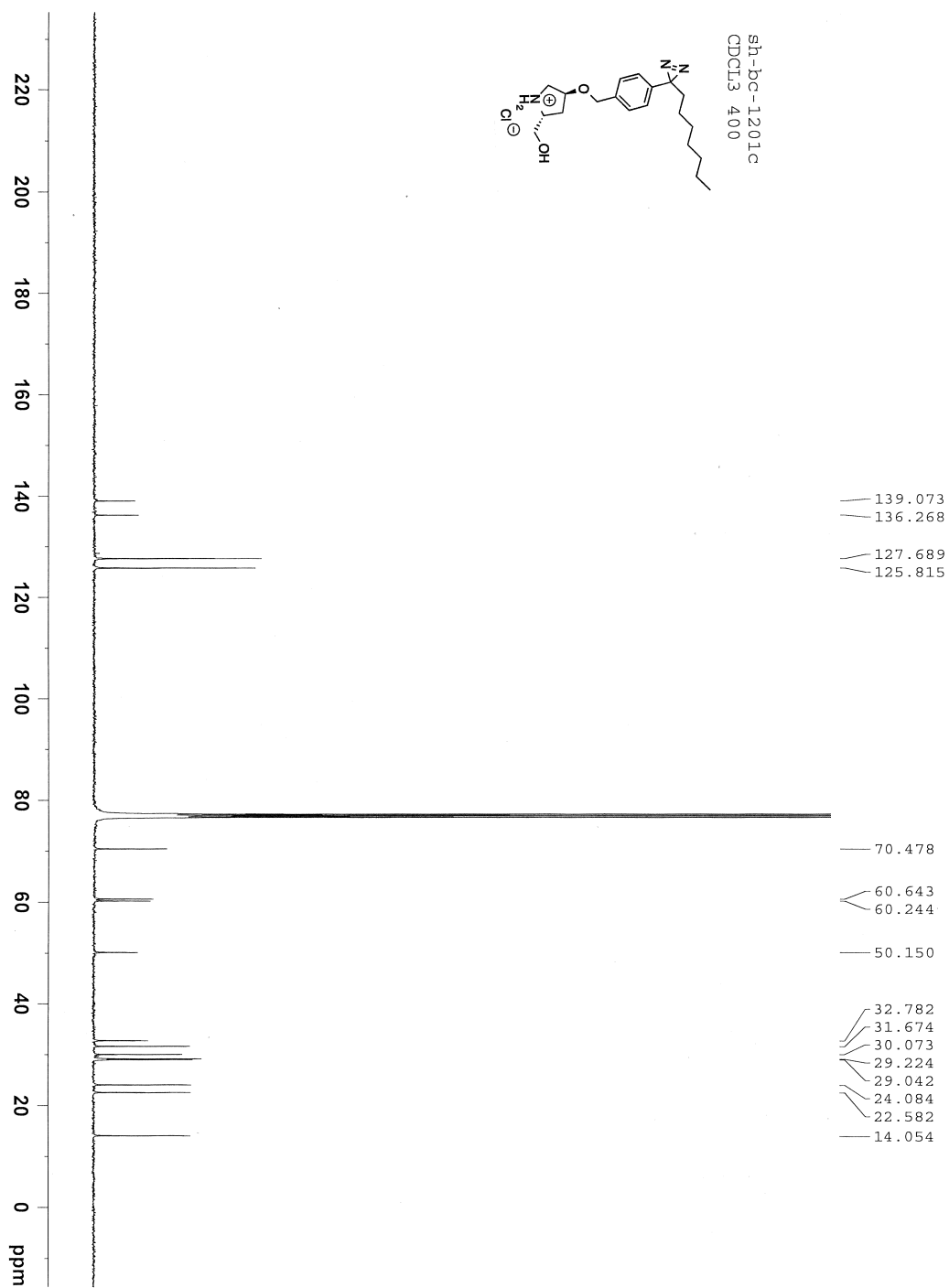
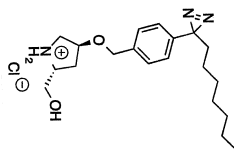




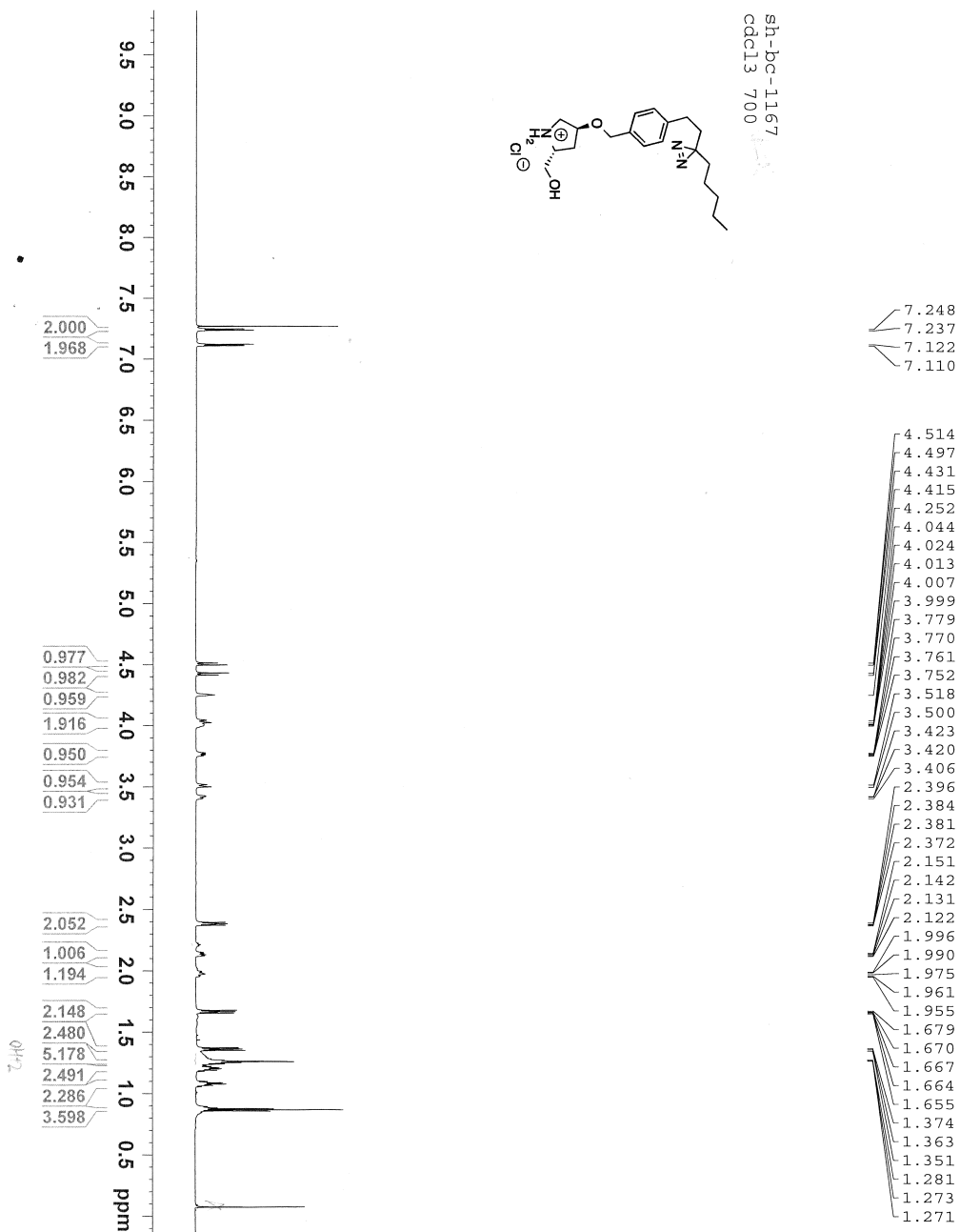
# Annex 35: $^1\text{H}$ and $^{13}\text{C}$ NMR Spectra of Compound 2.21



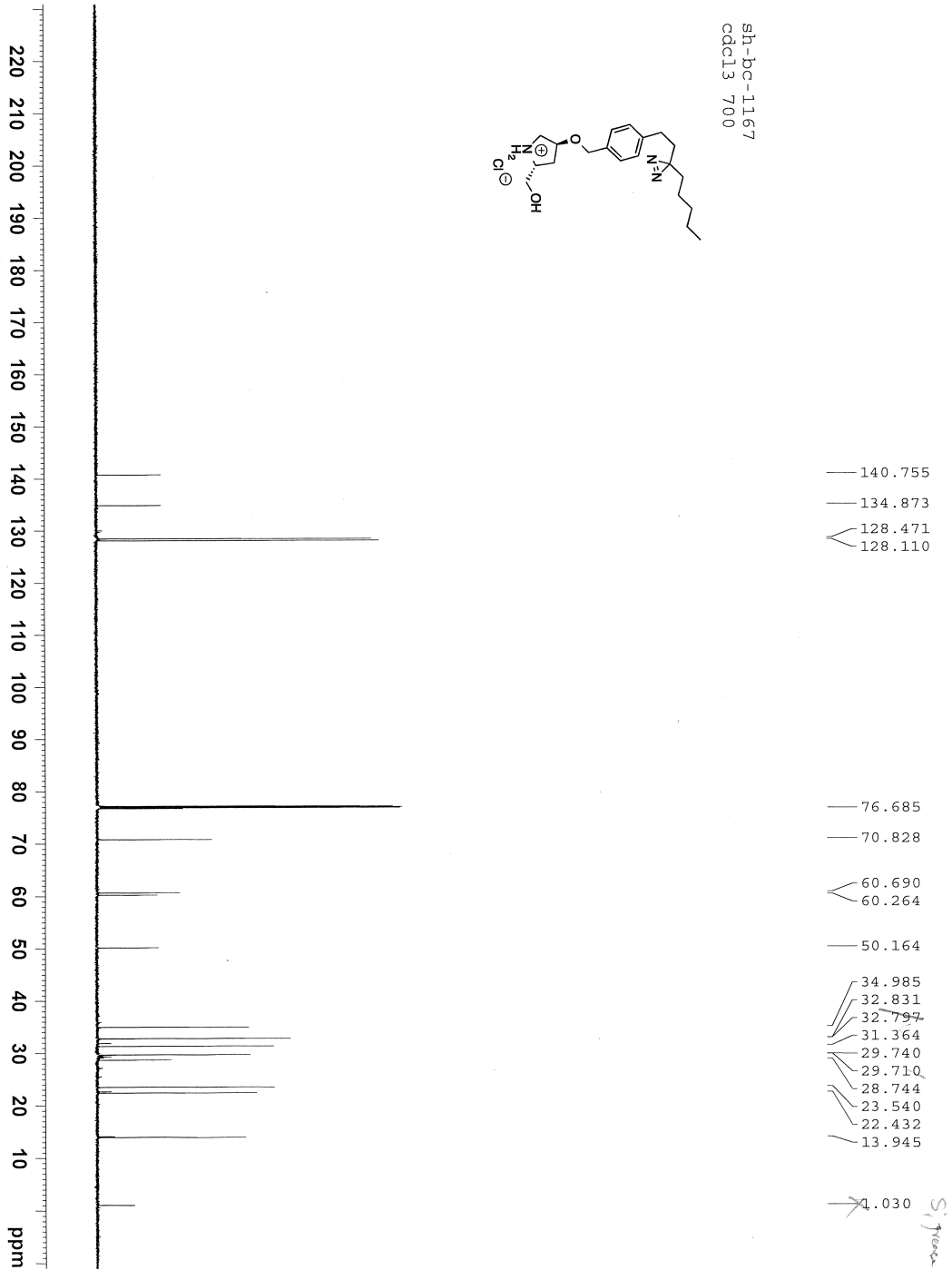
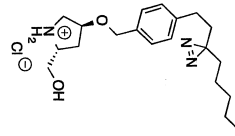
sh-bc-1201c  
CDCl3 400



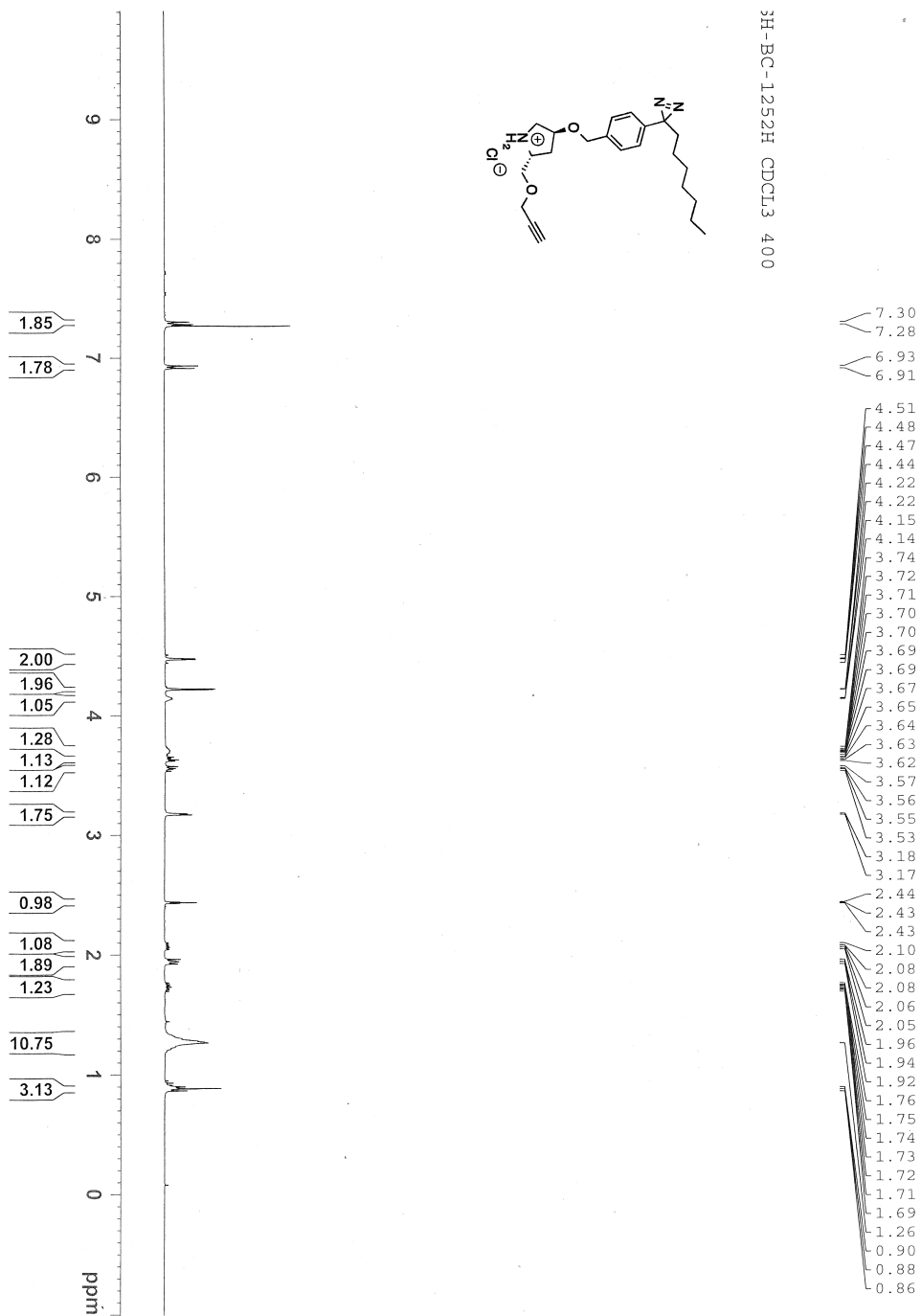
# Annex 36: $^1\text{H}$ and $^{13}\text{C}$ NMR Spectra of Compound 2.22



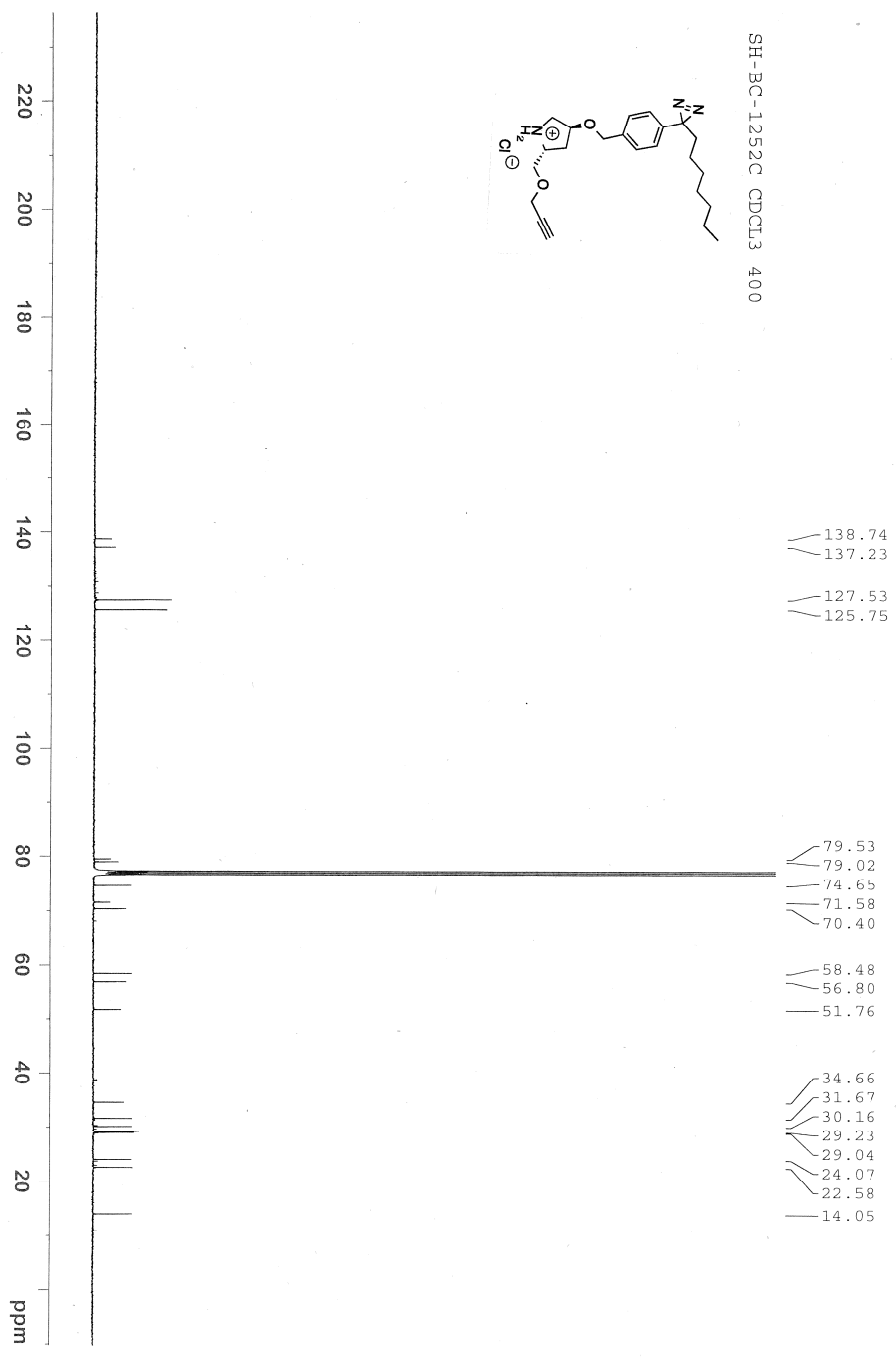
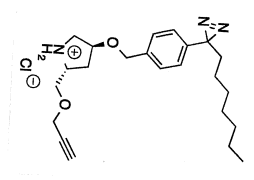
sh-bc-1167  
cdcl3 700



# Annex 37: $^1\text{H}$ and $^{13}\text{C}$ NMR Spectra of Compound 2.30

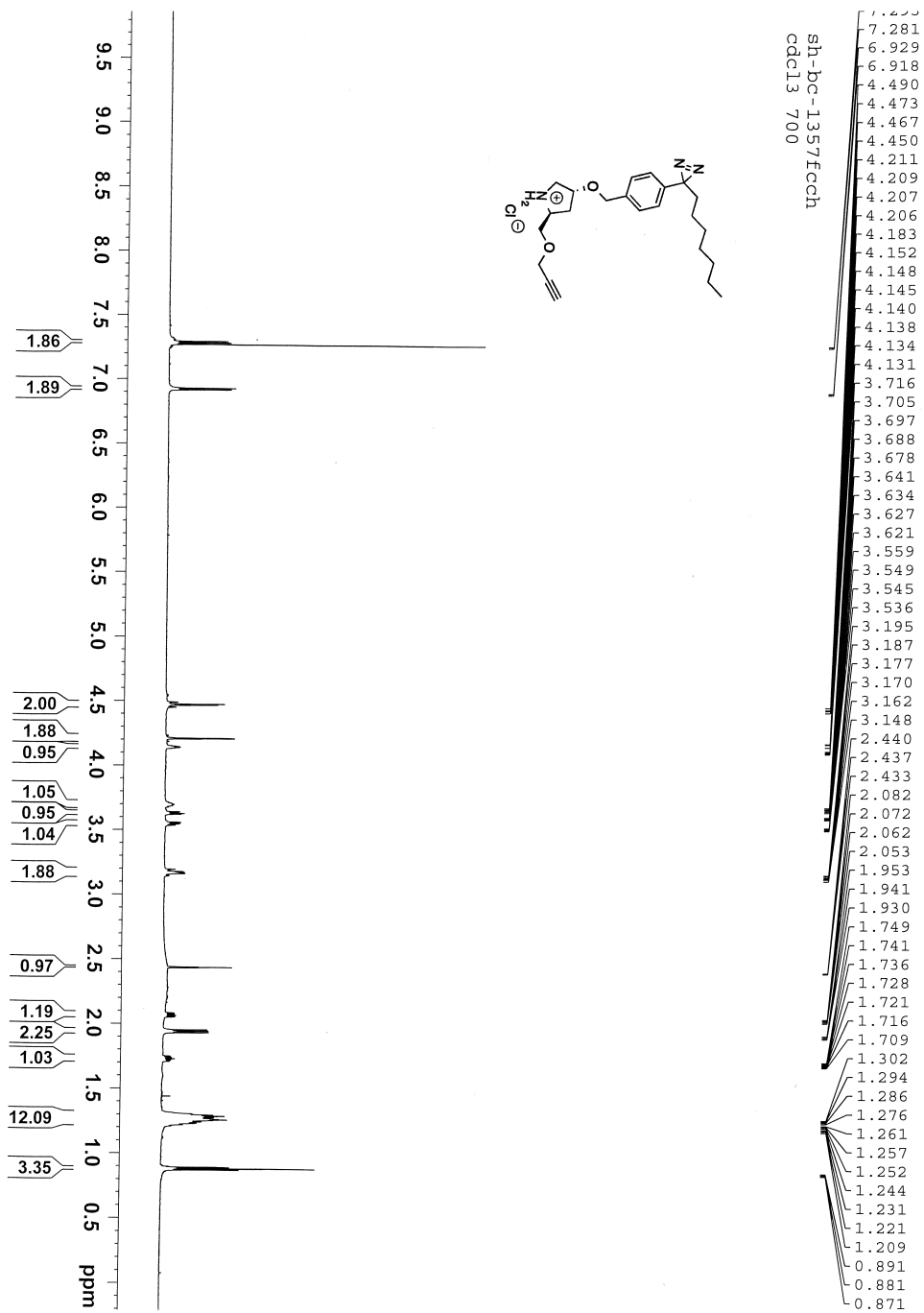


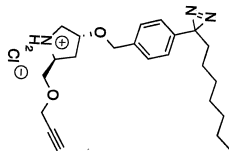
SH-BC-1252C CDCl3 400



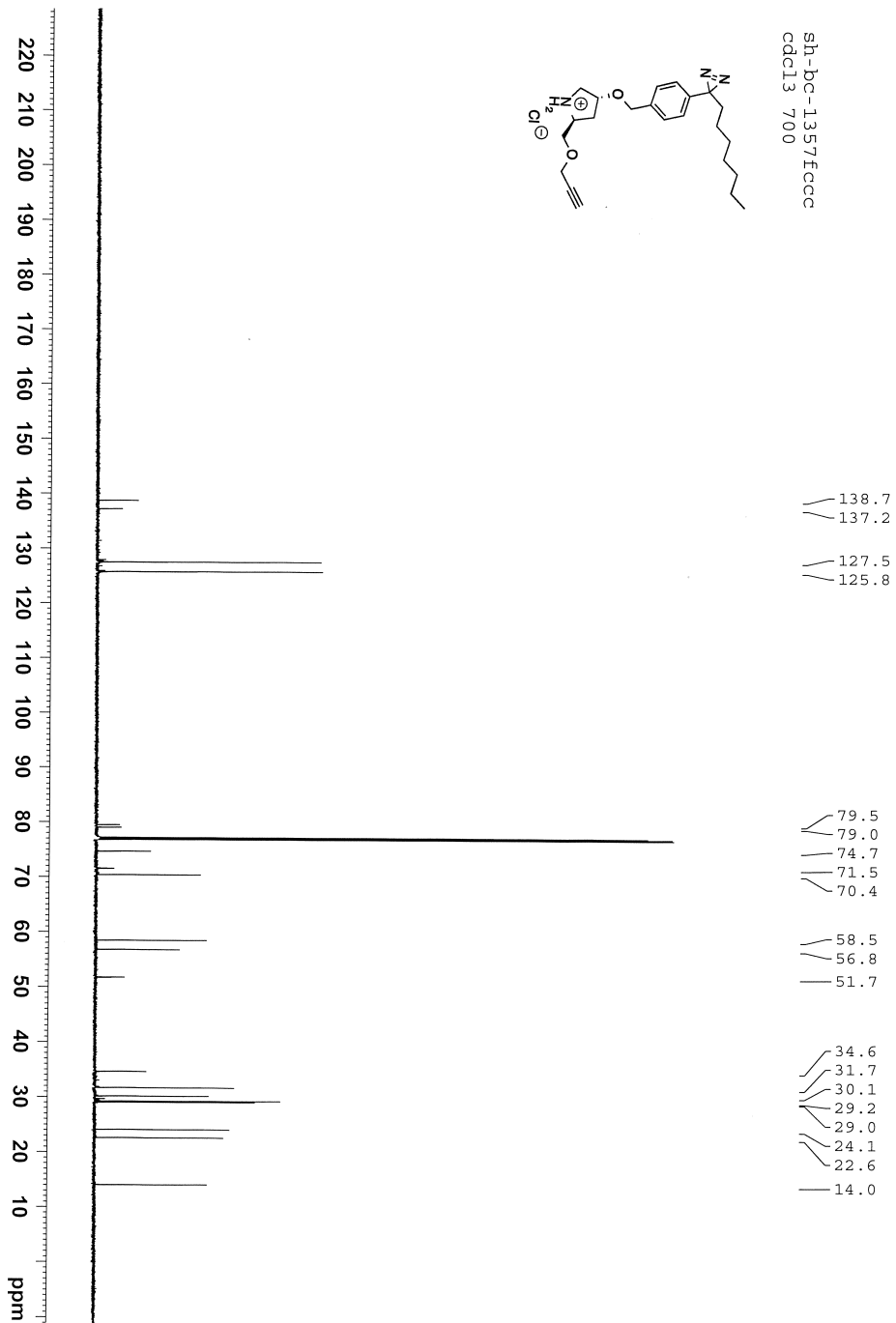


# Annex 38: <sup>1</sup>H and <sup>13</sup>C NMR Spectra of Compound 2.38



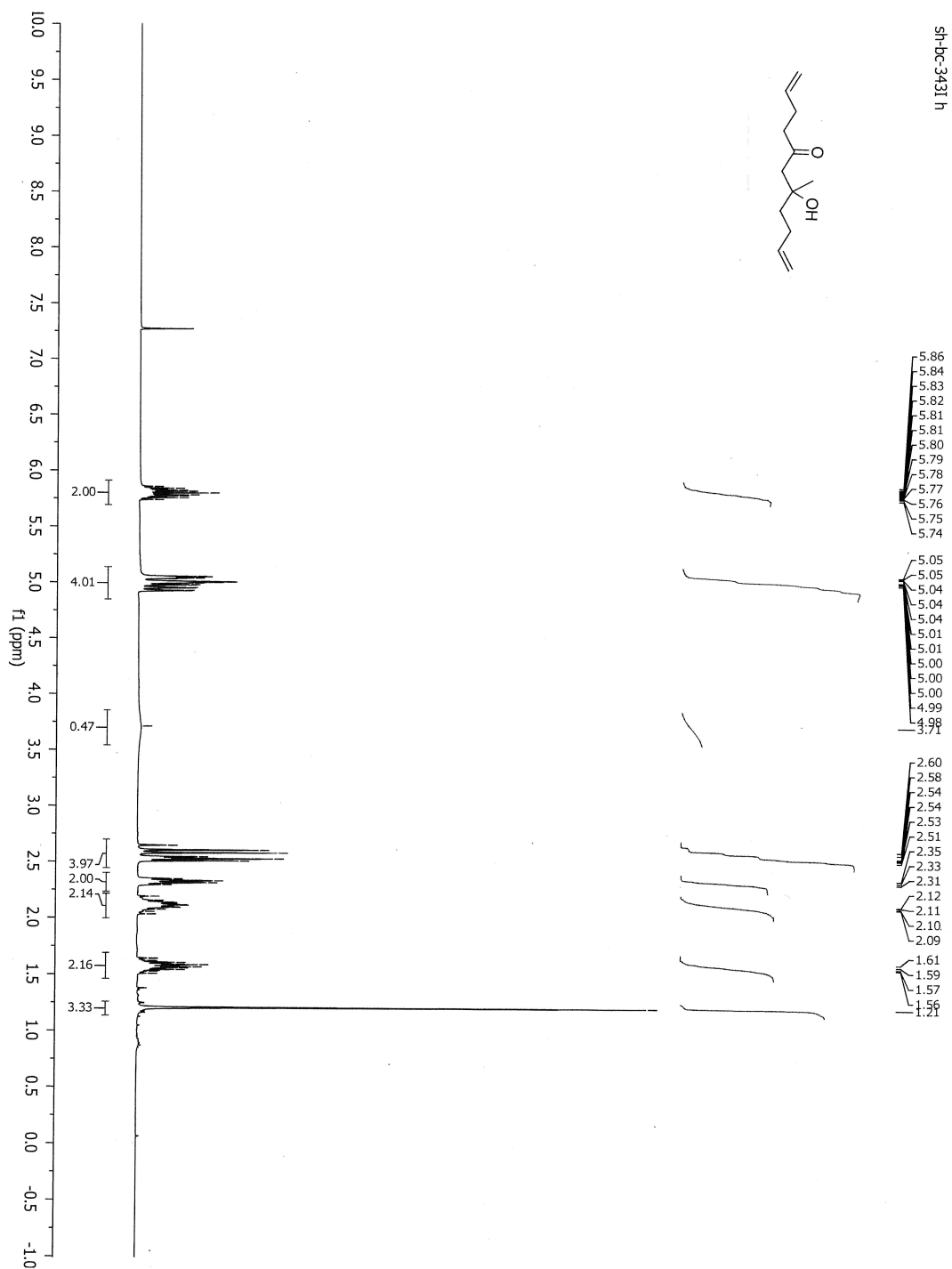


sh-bc-1357fccc  
cdcl3 700



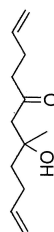
# Annex 39: $^1\text{H}$ and $^{13}\text{C}$ NMR Spectra of Compound

## 3.14a



SIH-DC-3431 c

212.27



138.59  
136.60

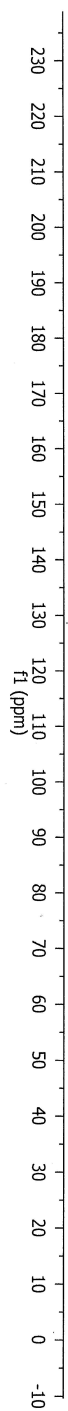
115.48  
114.42

77.32  
77.00  
76.68  
71.48

51.58

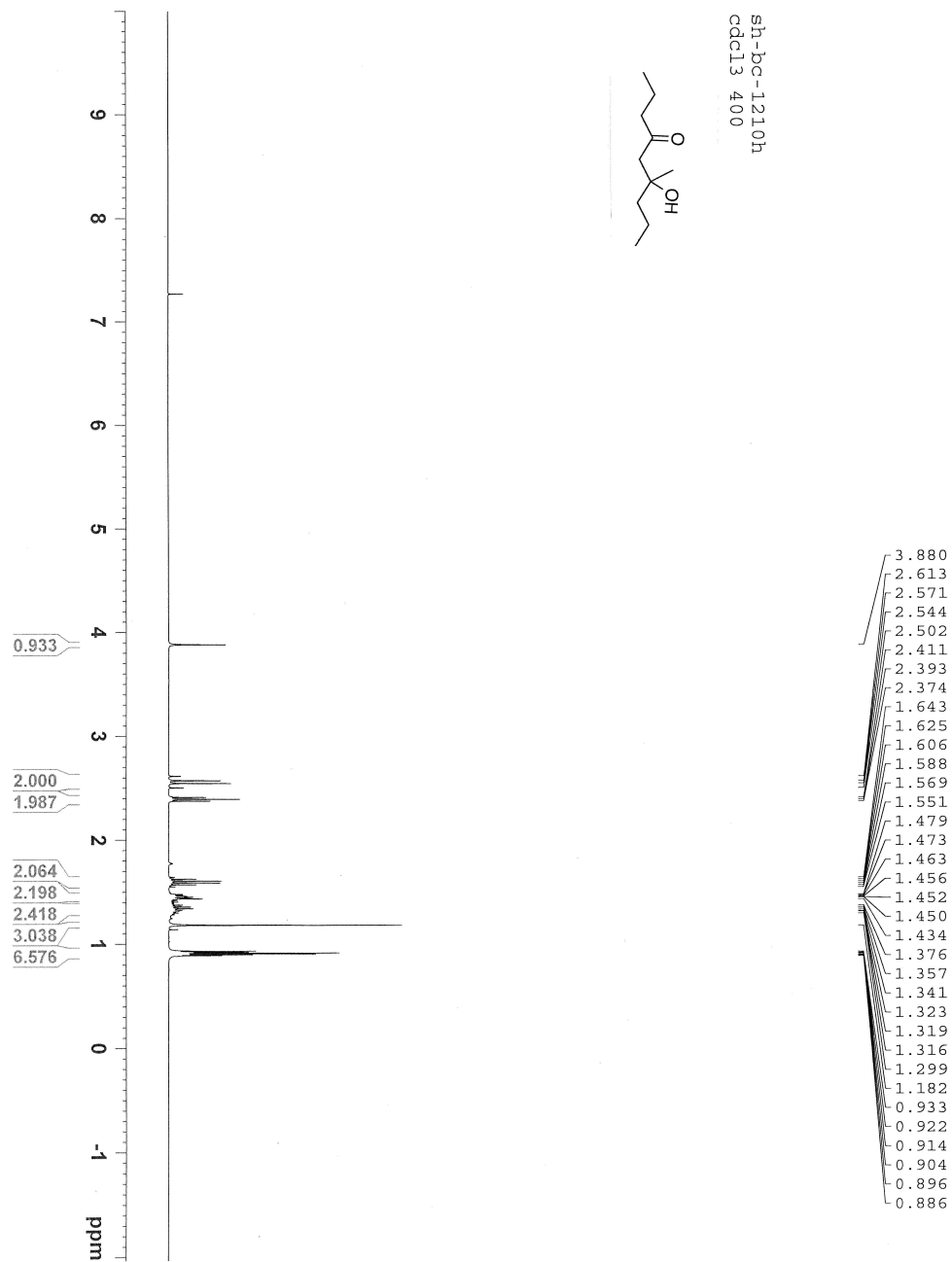
43.54  
41.07

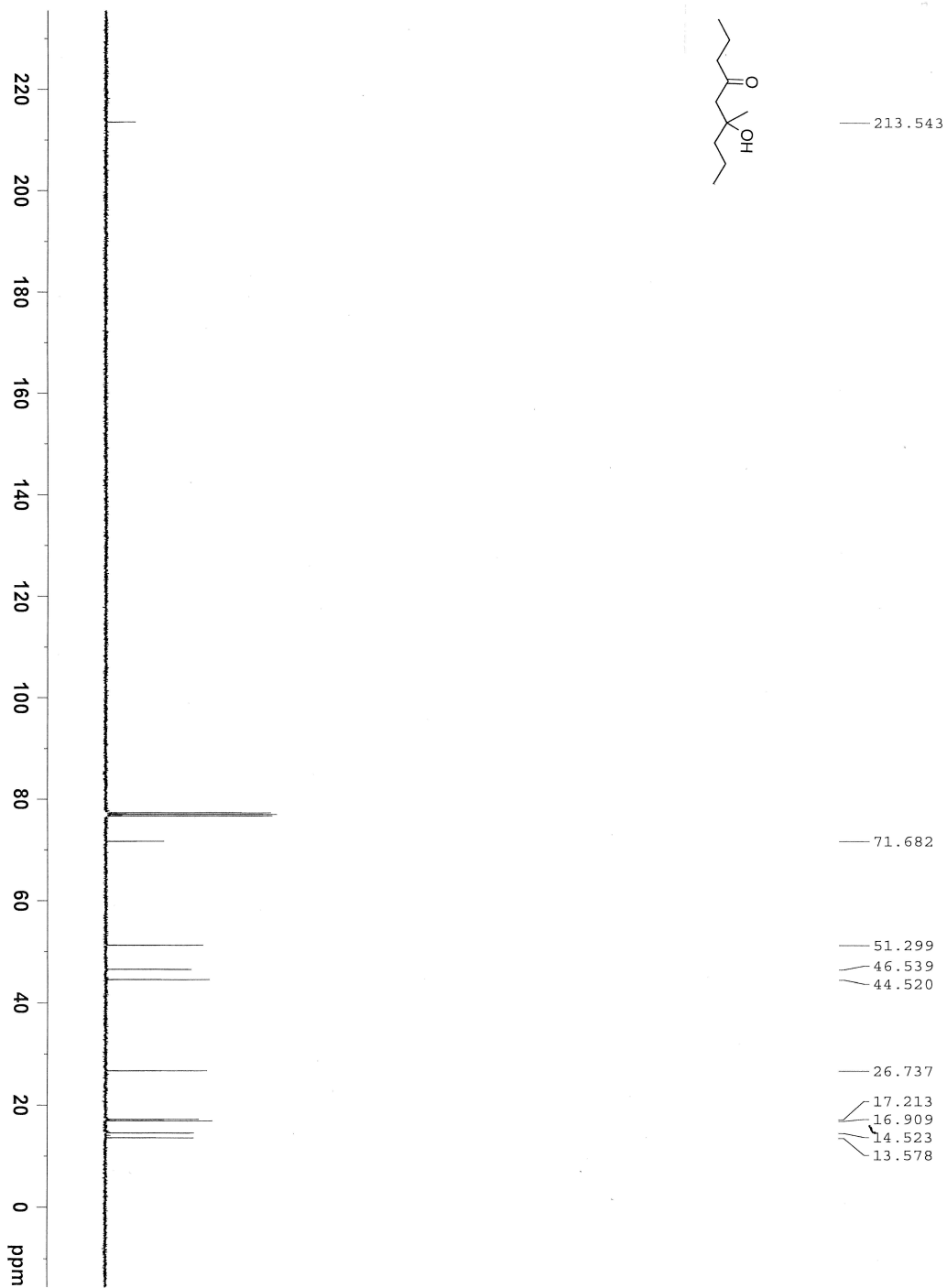
28.19  
27.31  
26.70



# Annex 40: $^1\text{H}$ and $^{13}\text{C}$ NMR Spectra of Compound

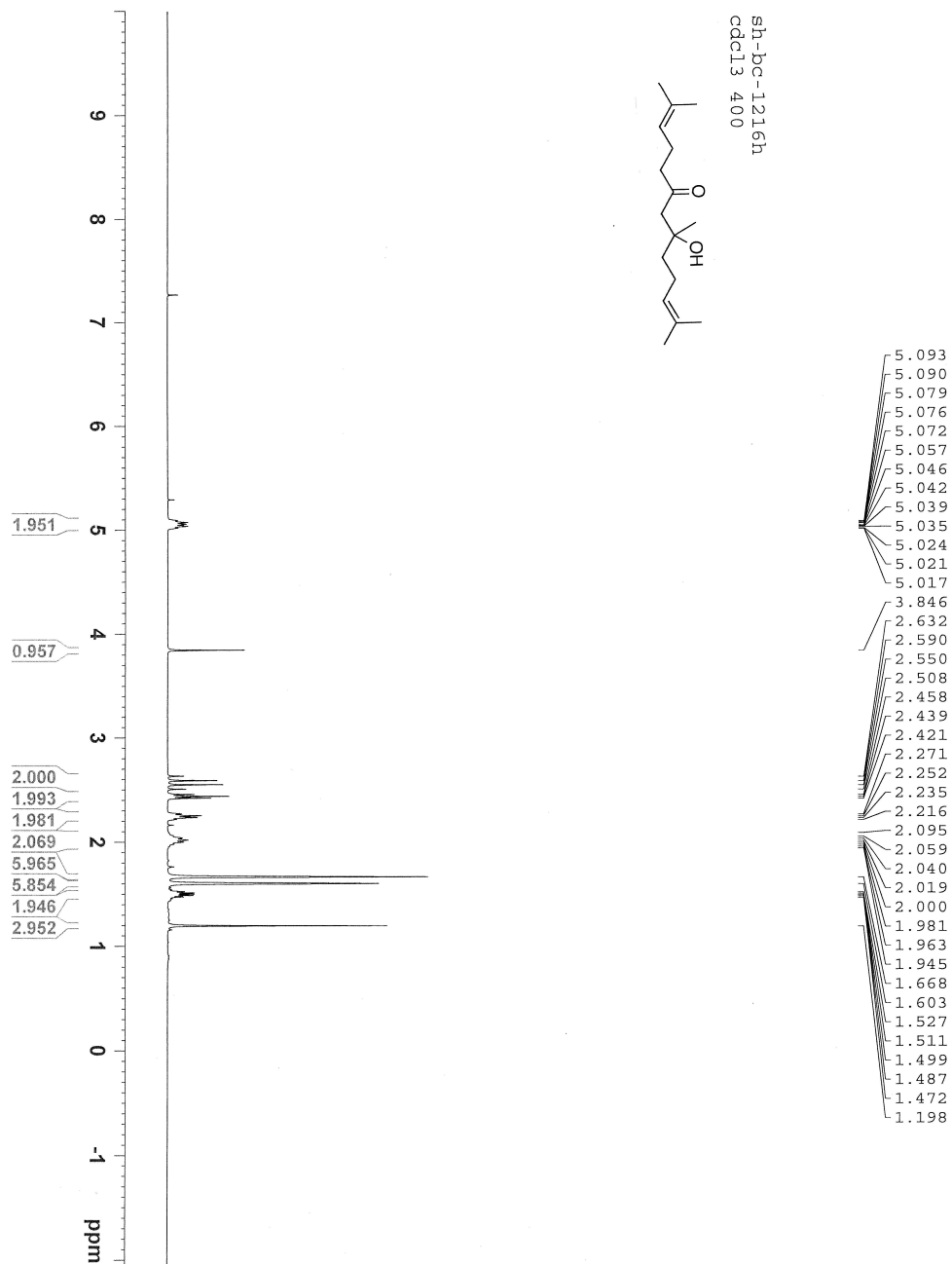
## 3.14b

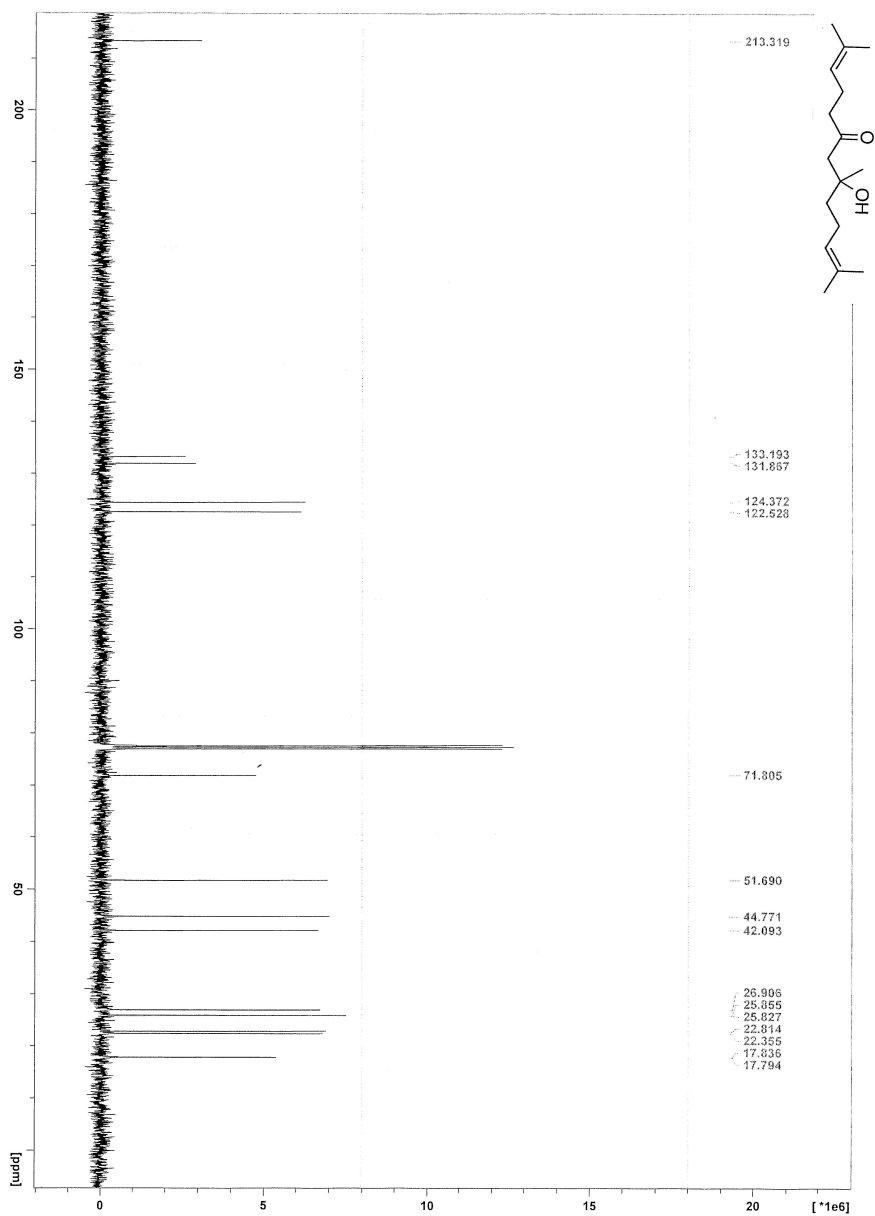




# Annex 41: $^1\text{H}$ and $^{13}\text{C}$ NMR Spectra of Compound

## 3.14c

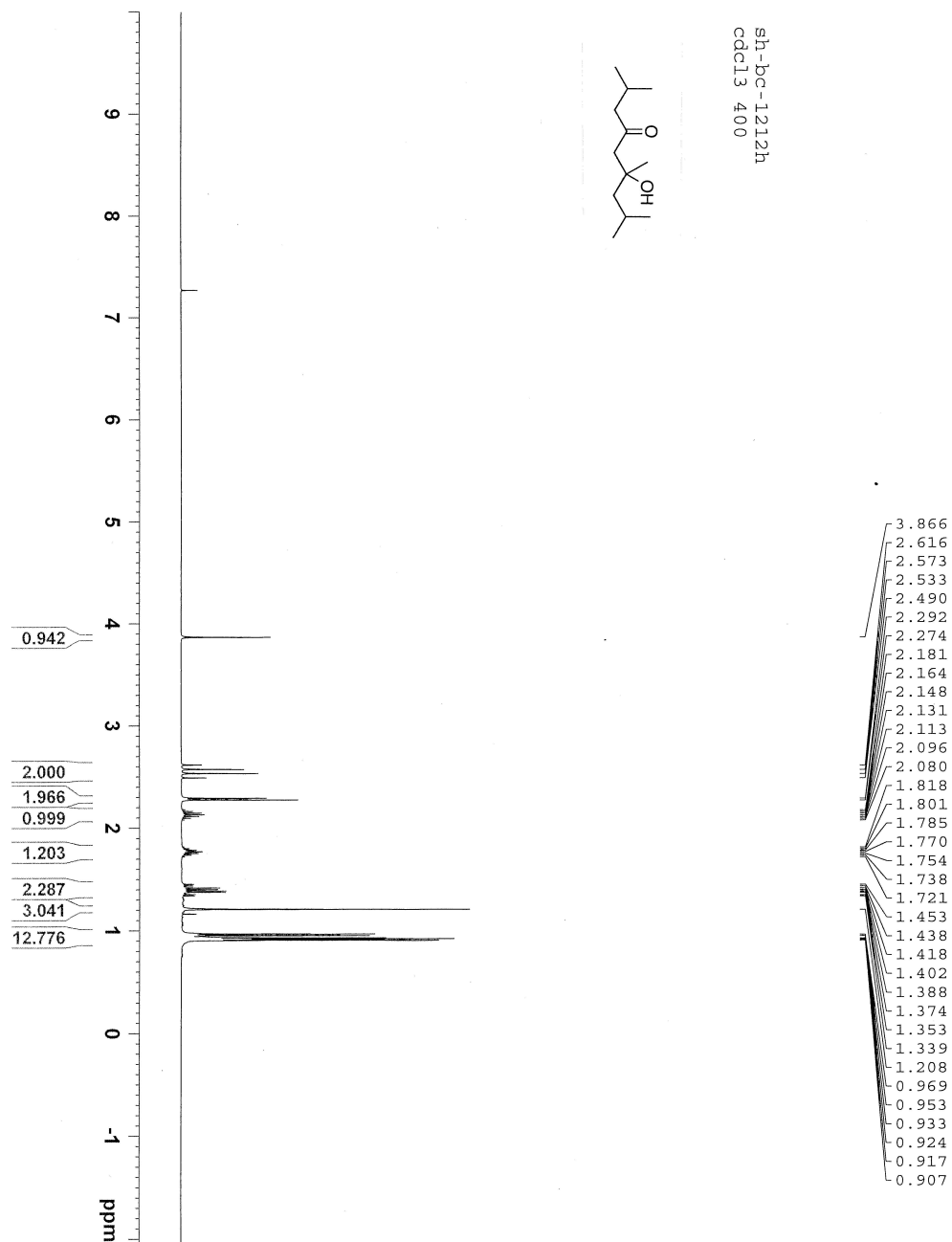


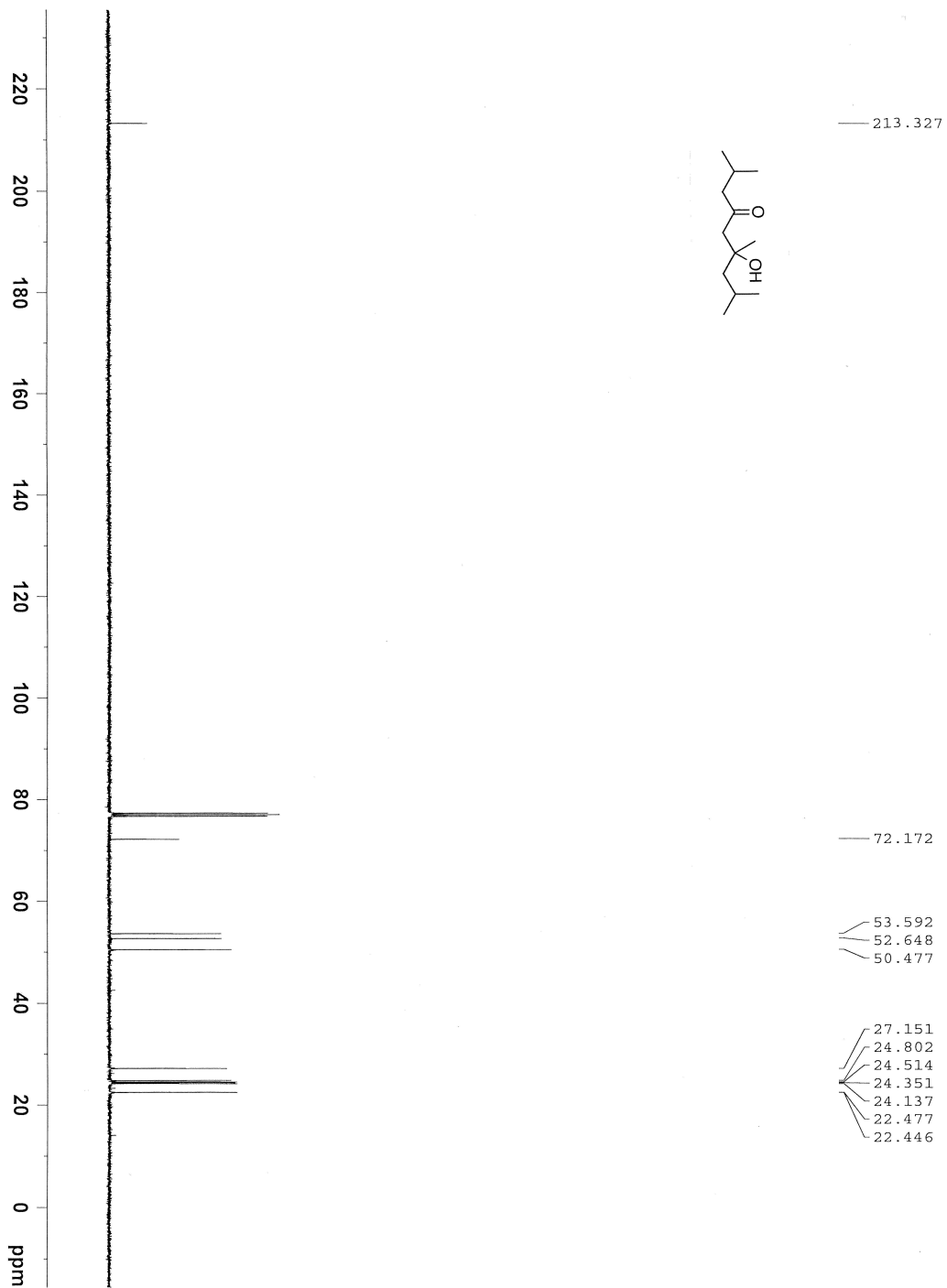




# Annex 42: $^1\text{H}$ and $^{13}\text{C}$ NMR Spectra of Compound

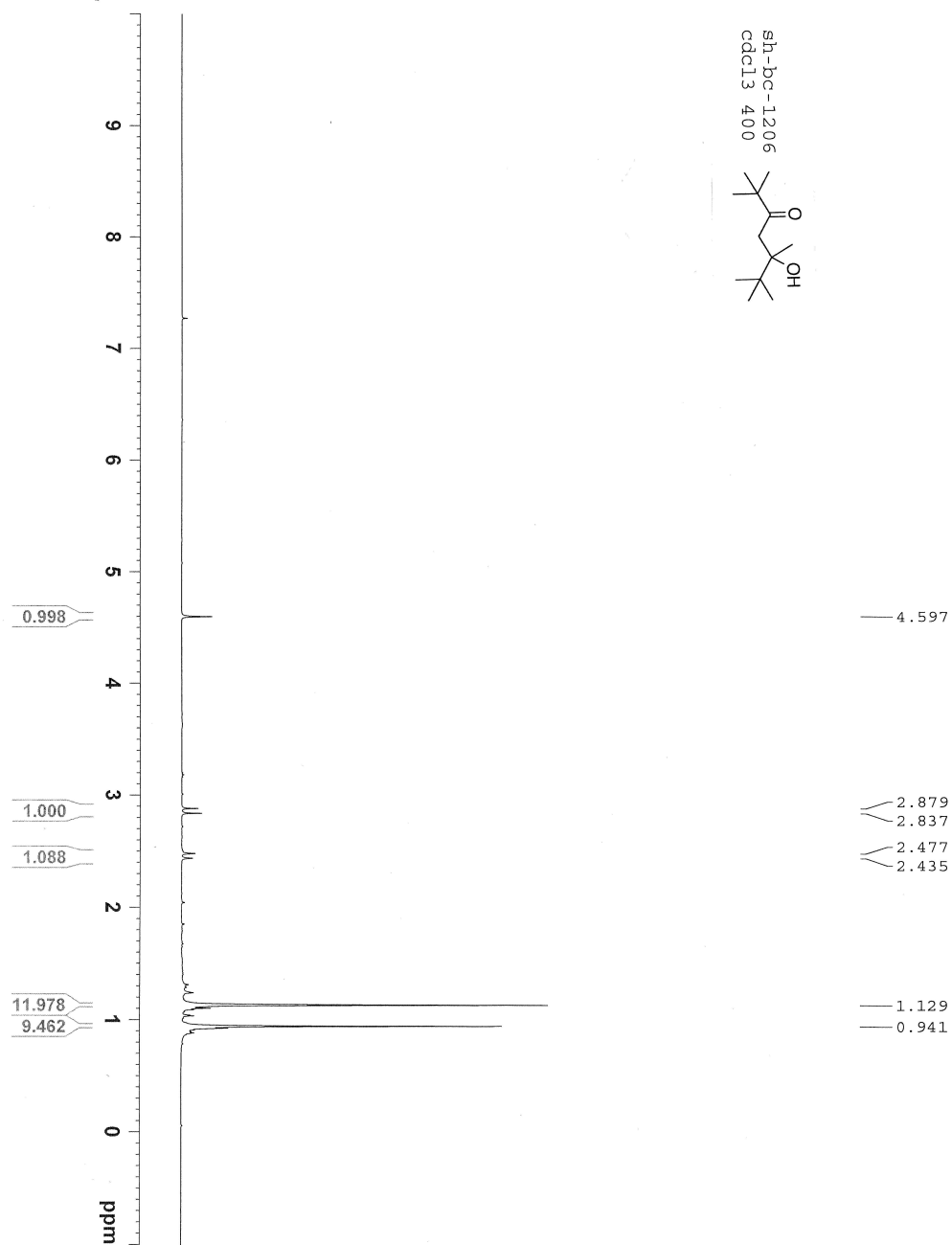
## 3.14d

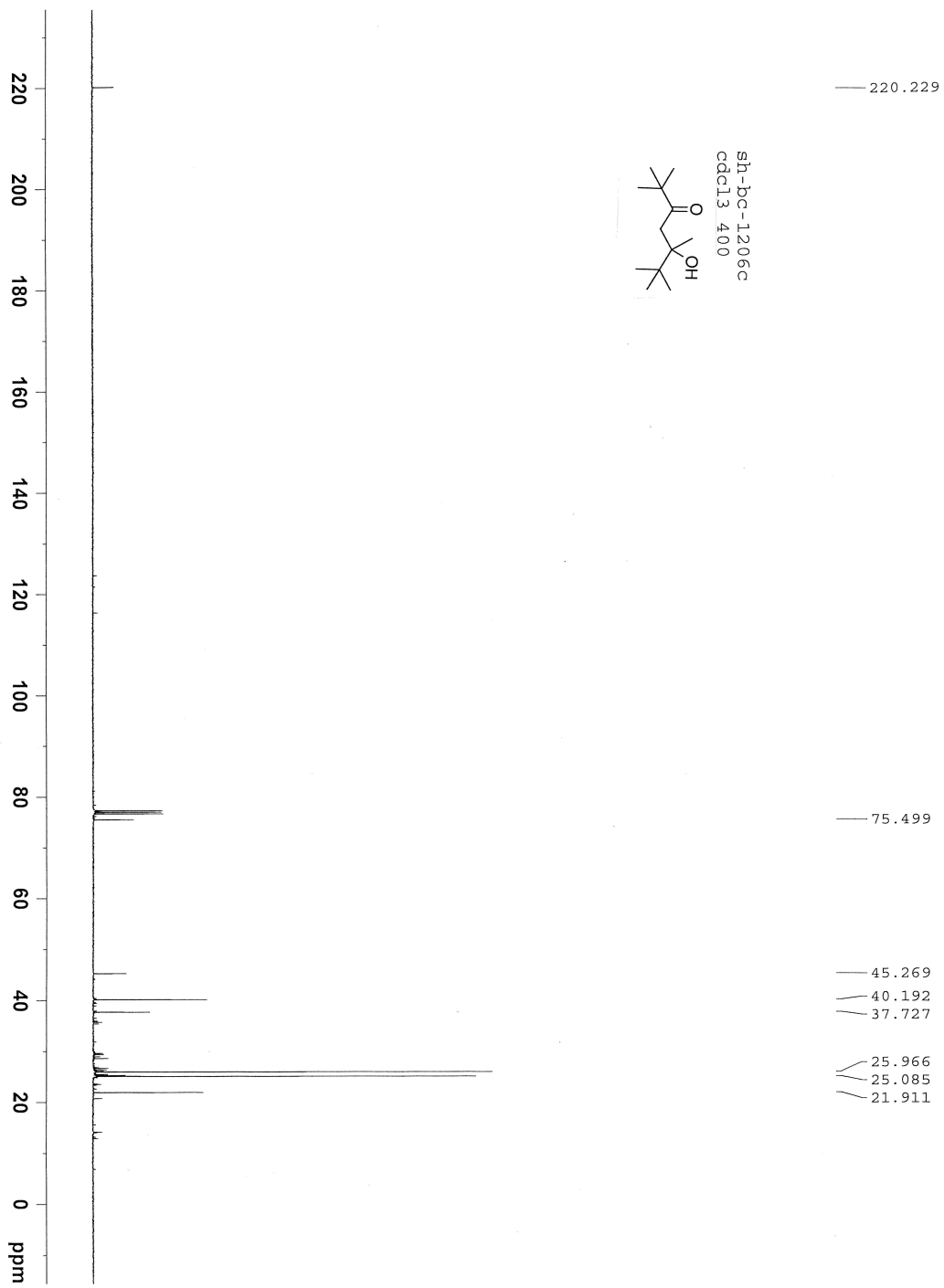




# Annex 43: $^1\text{H}$ and $^{13}\text{C}$ NMR Spectra of Compound

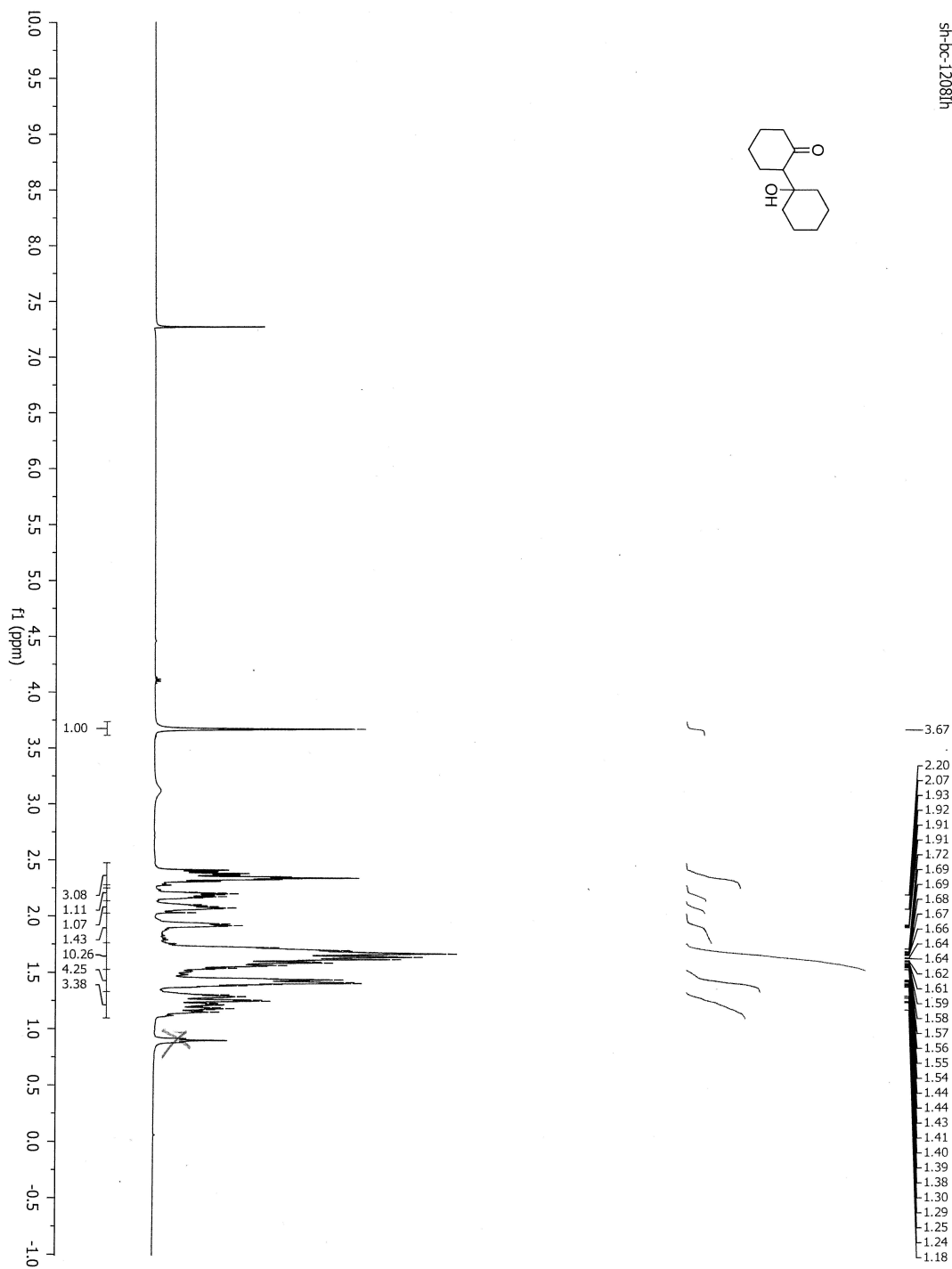
## 3.14e



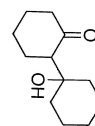


# Annex 44: $^1\text{H}$ and $^{13}\text{C}$ NMR Spectra of Compound

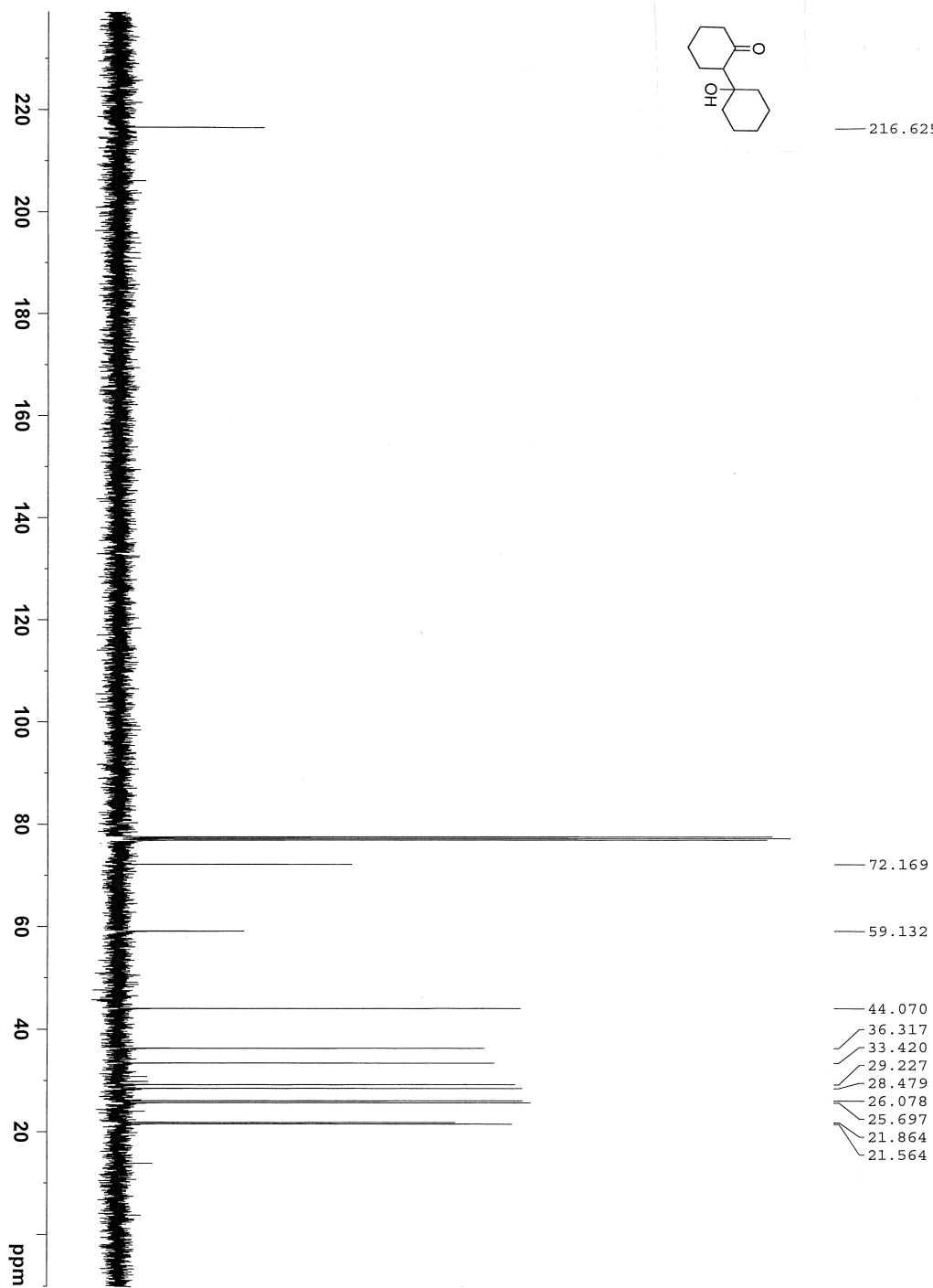
## 3.14f



sh-bc-405111c av400 cdcl3

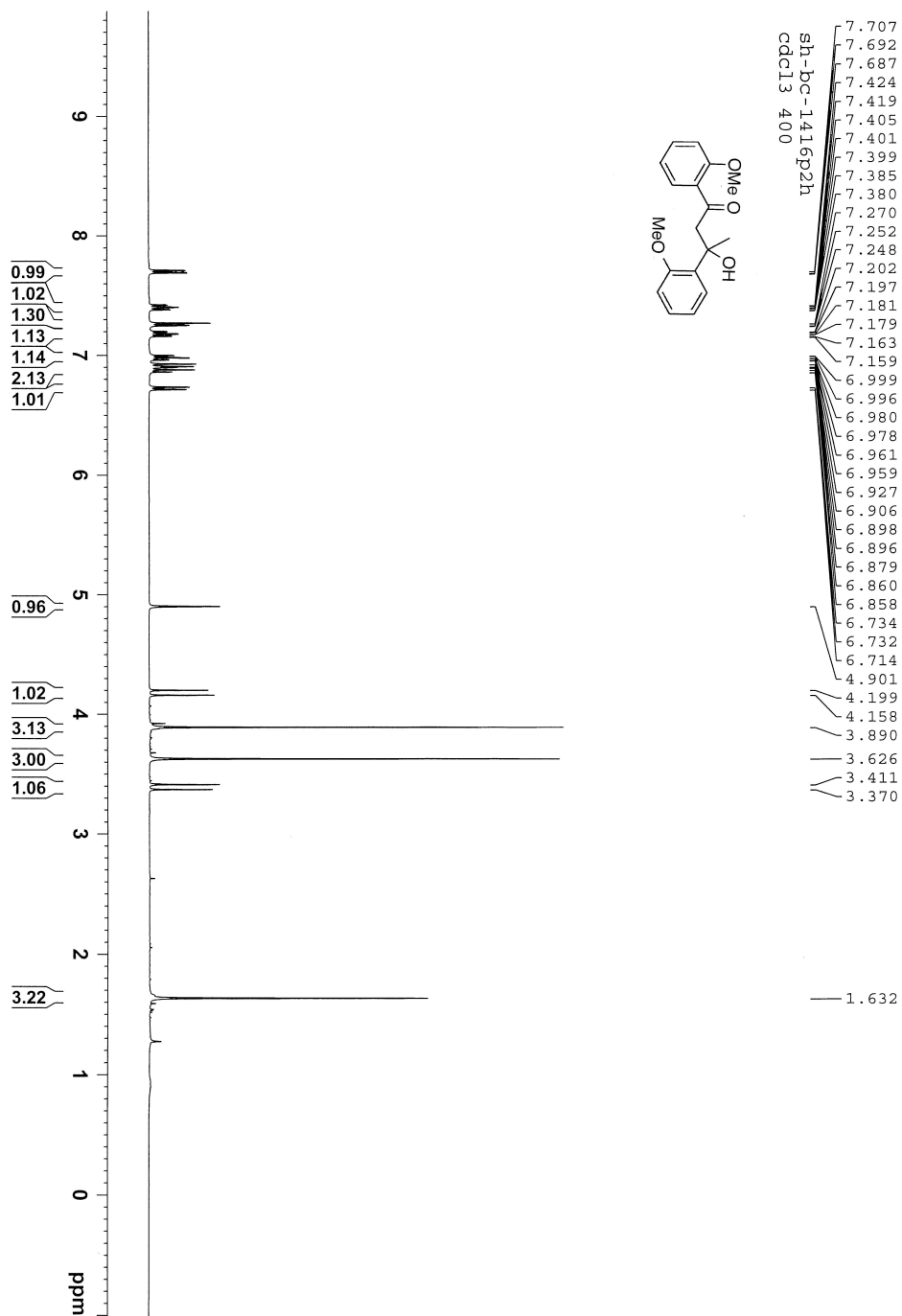


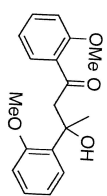
216.625



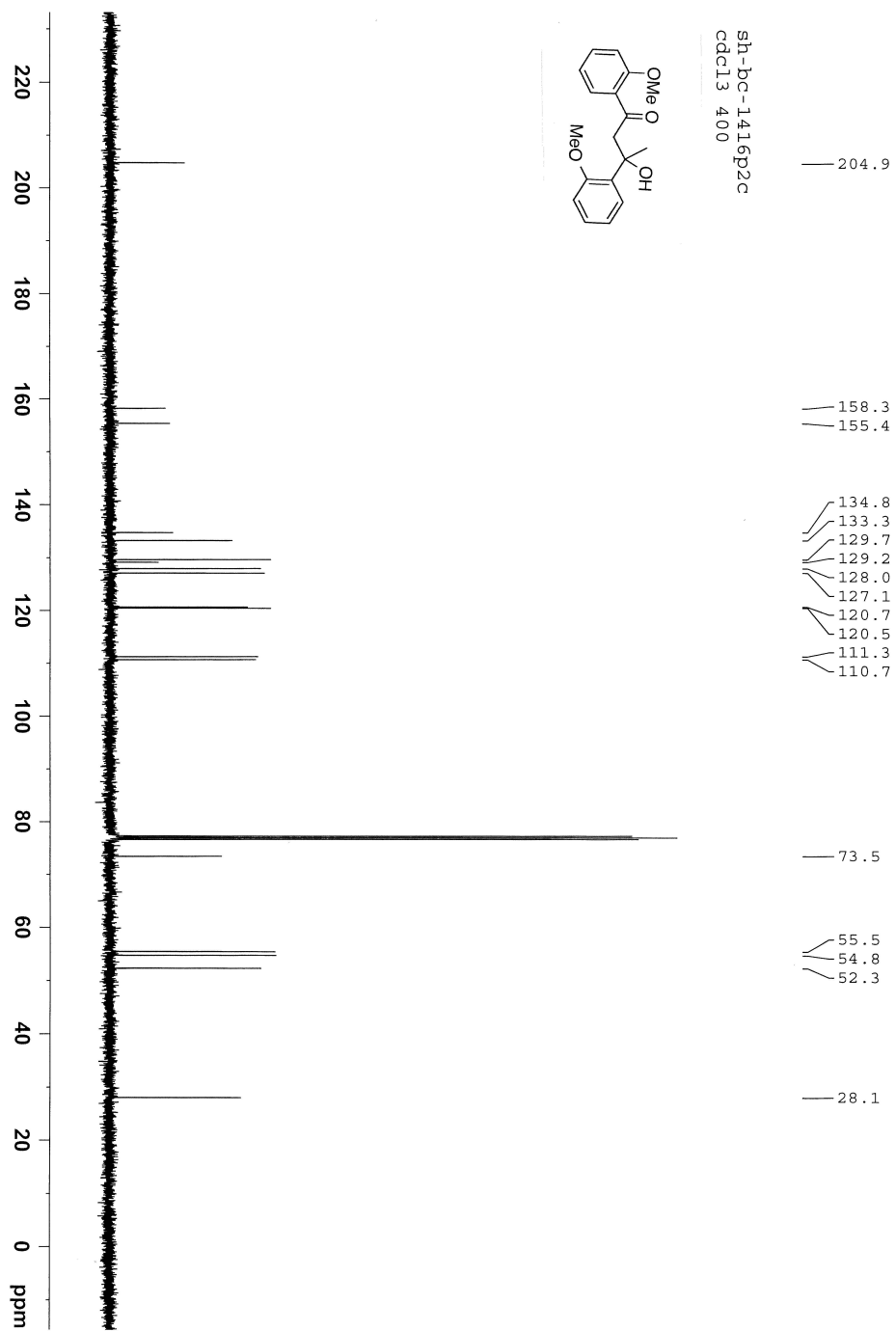
# Annex 45: $^1\text{H}$ and $^{13}\text{C}$ NMR Spectra of Compound

## 3.14g





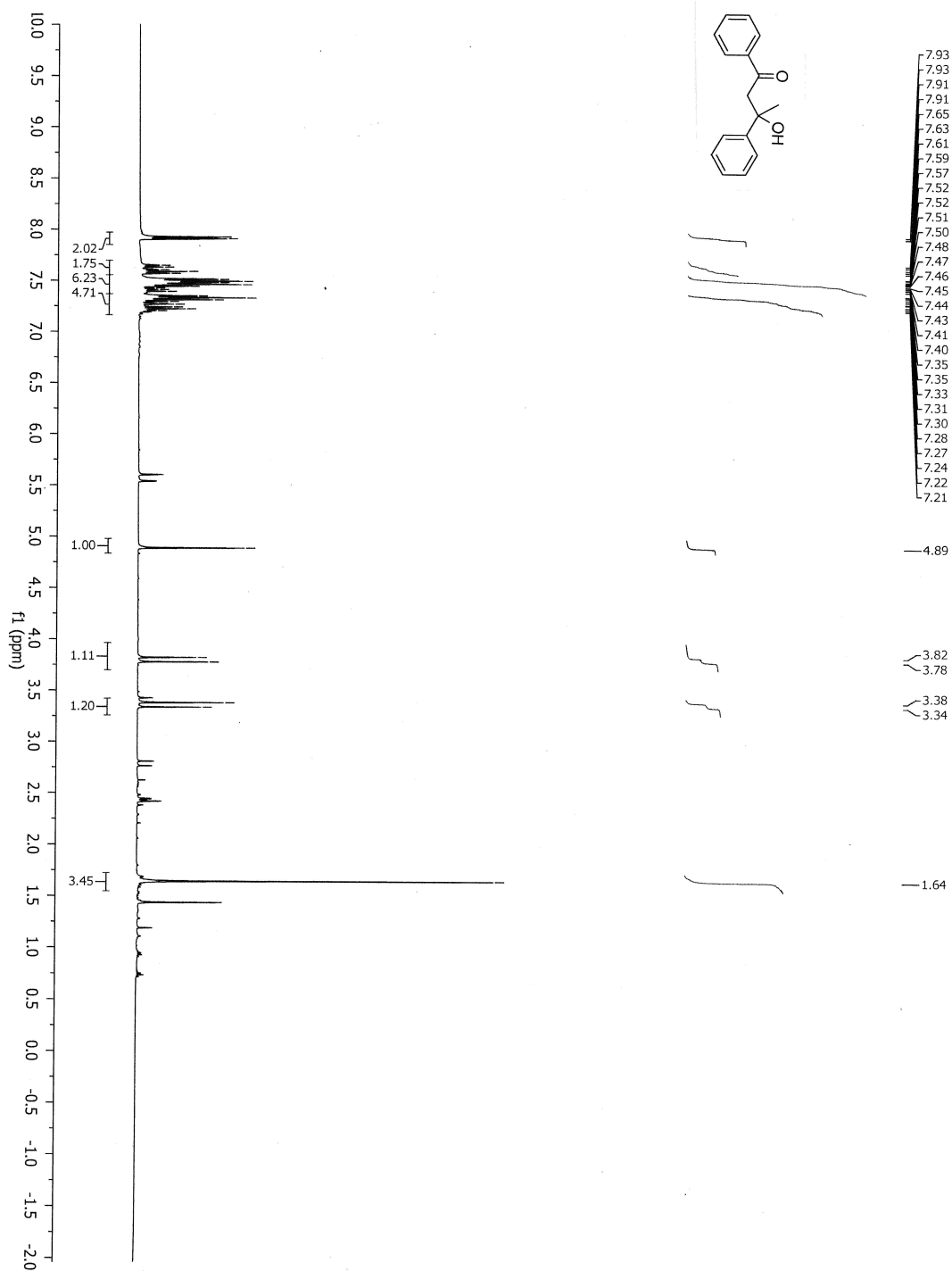
sh-bc-1416p2c  
cdcl3 400

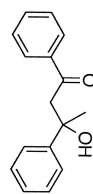




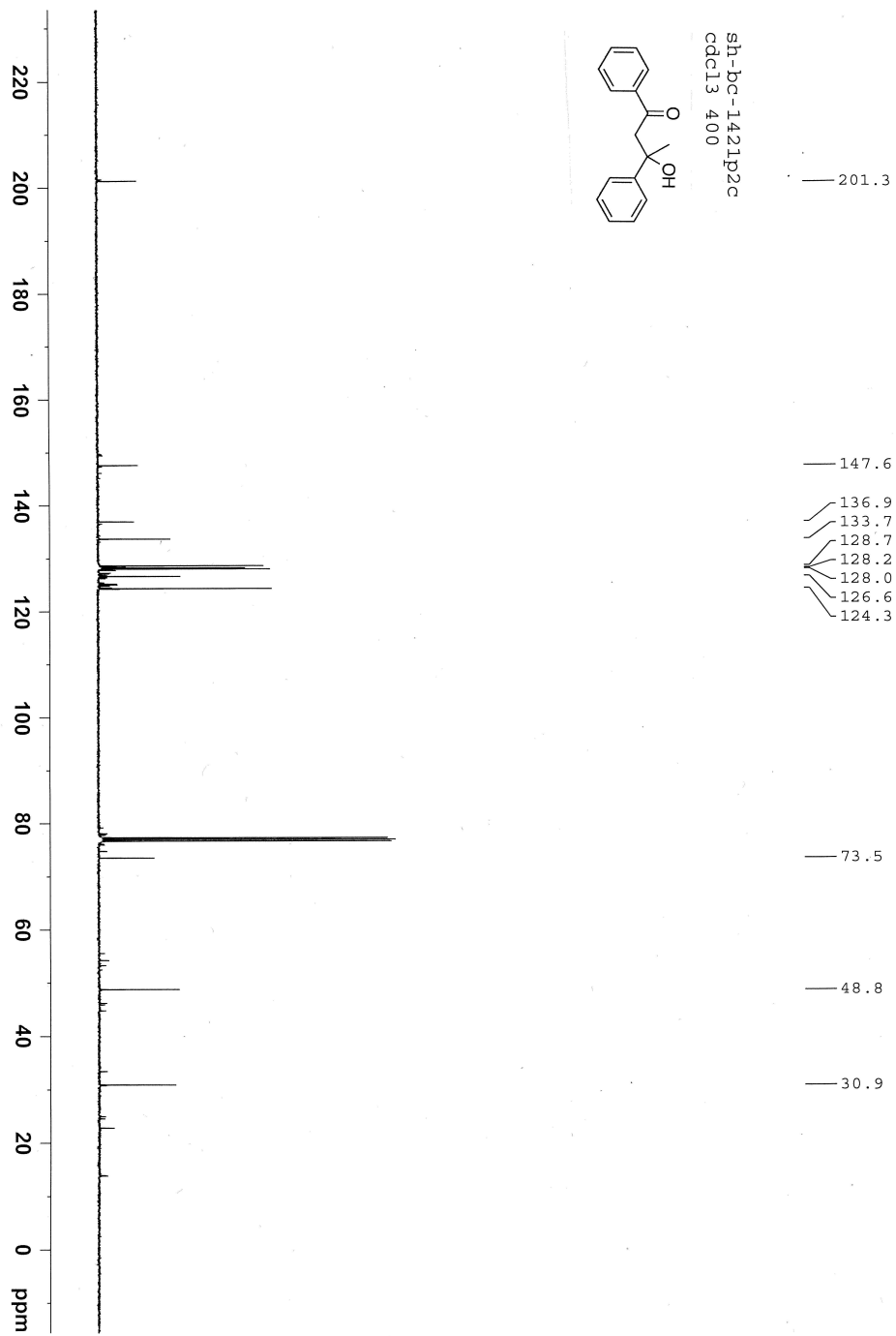
# Annex 46: $^1\text{H}$ and $^{13}\text{C}$ NMR Spectra of Compound

## 3.14h

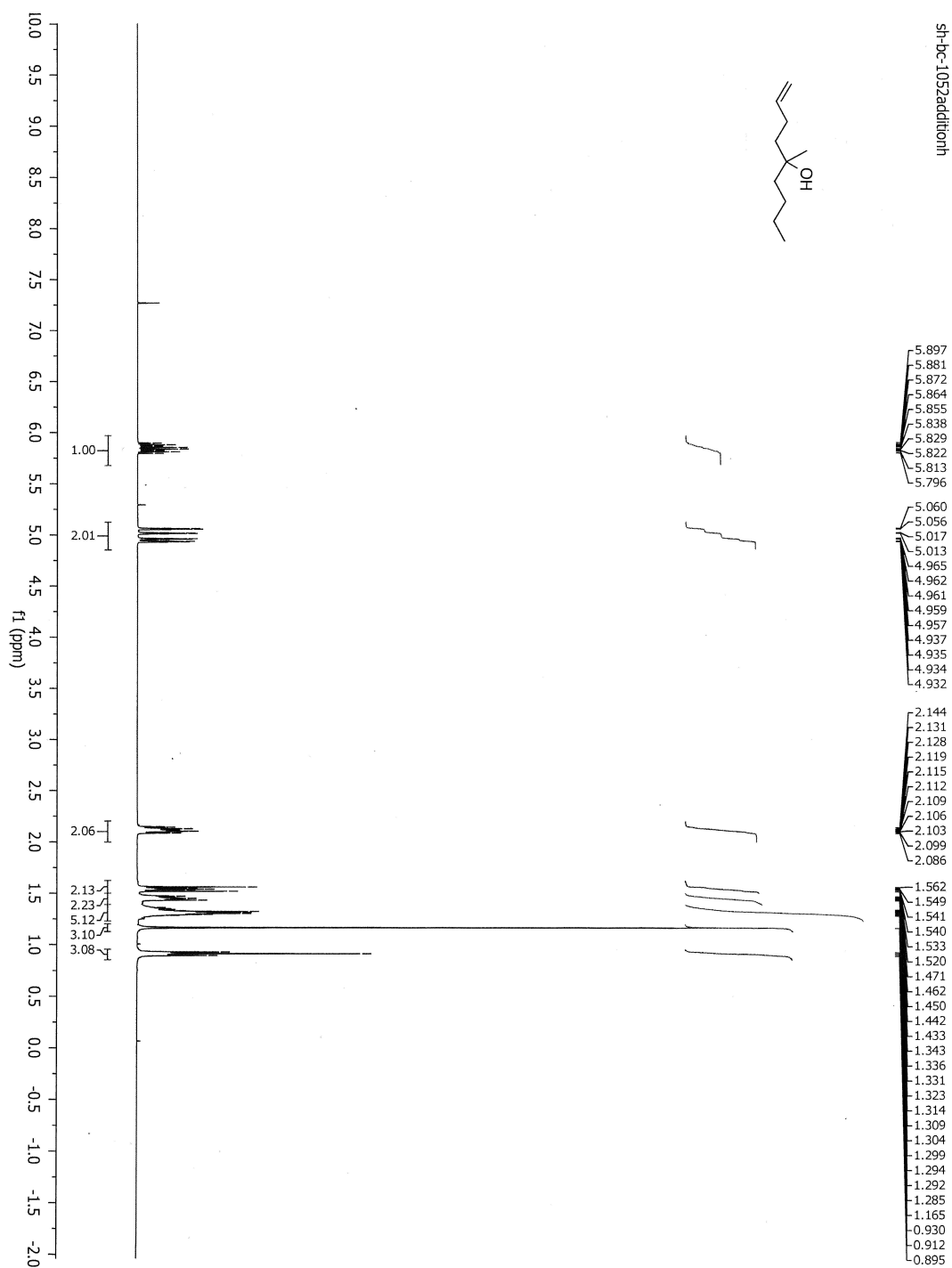


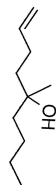


sh-bc-1421p2c  
cdcl3 400

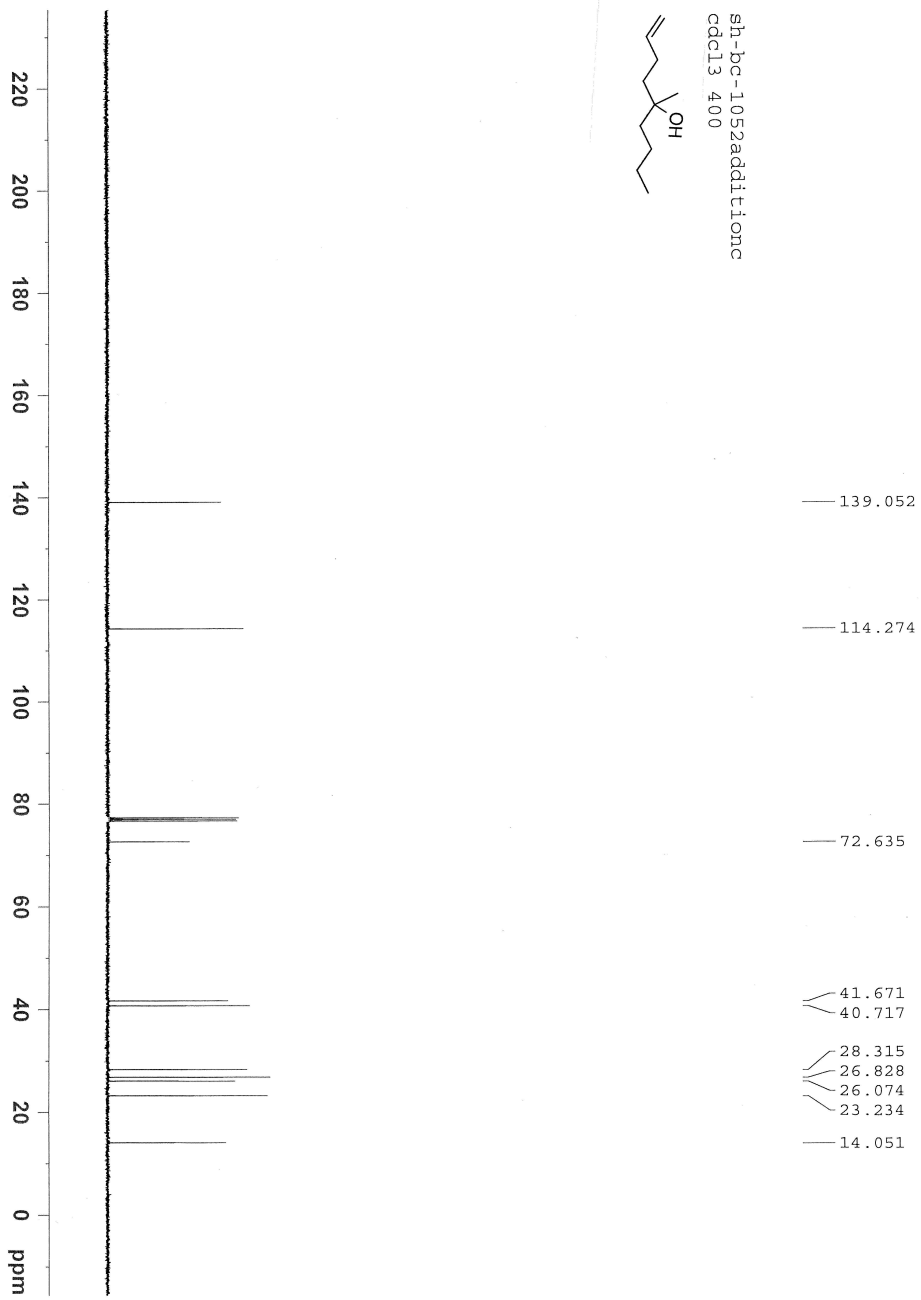


# Annex 47: $^1\text{H}$ and $^{13}\text{C}$ NMR Spectra of Compound 3.15

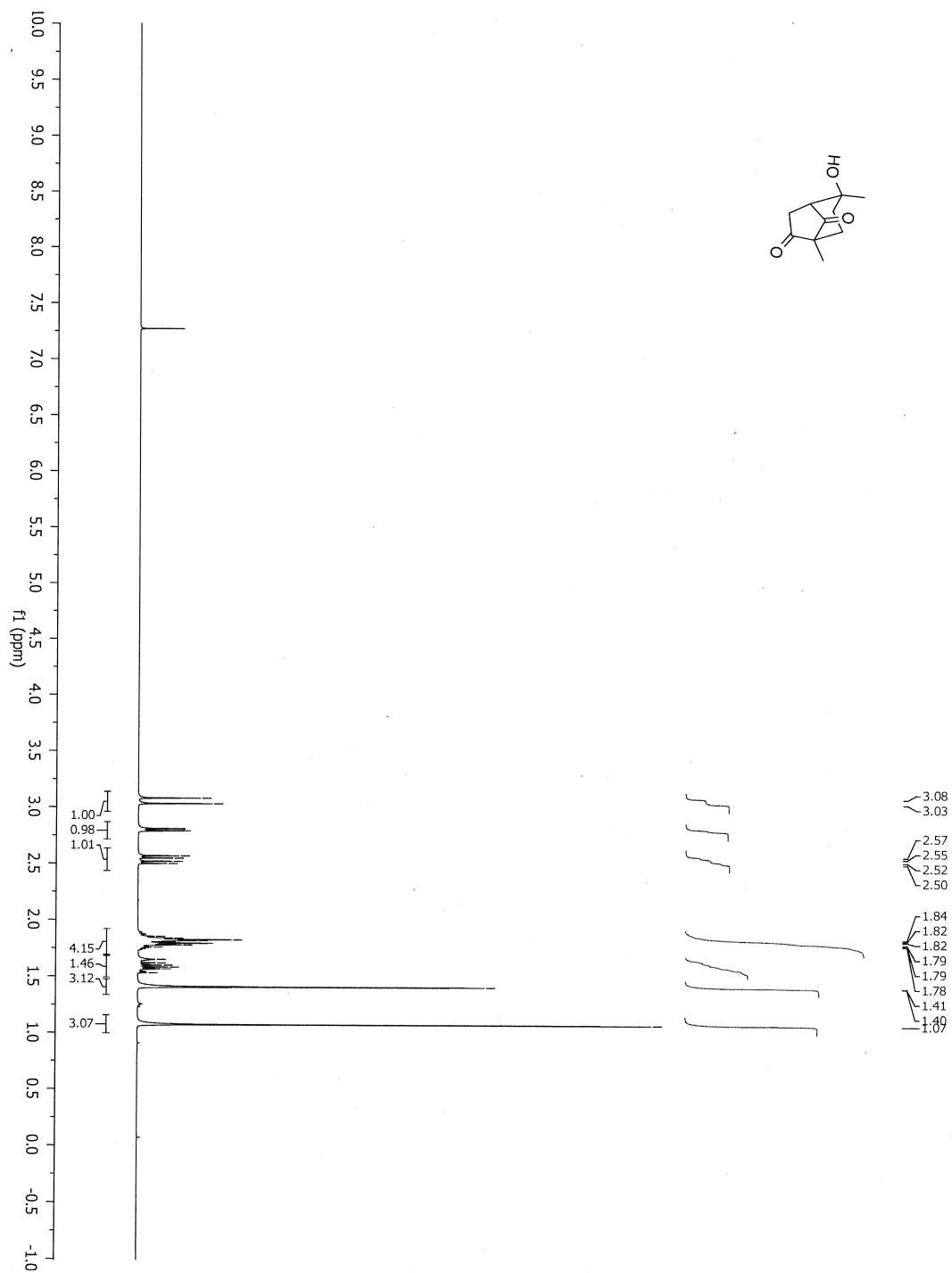


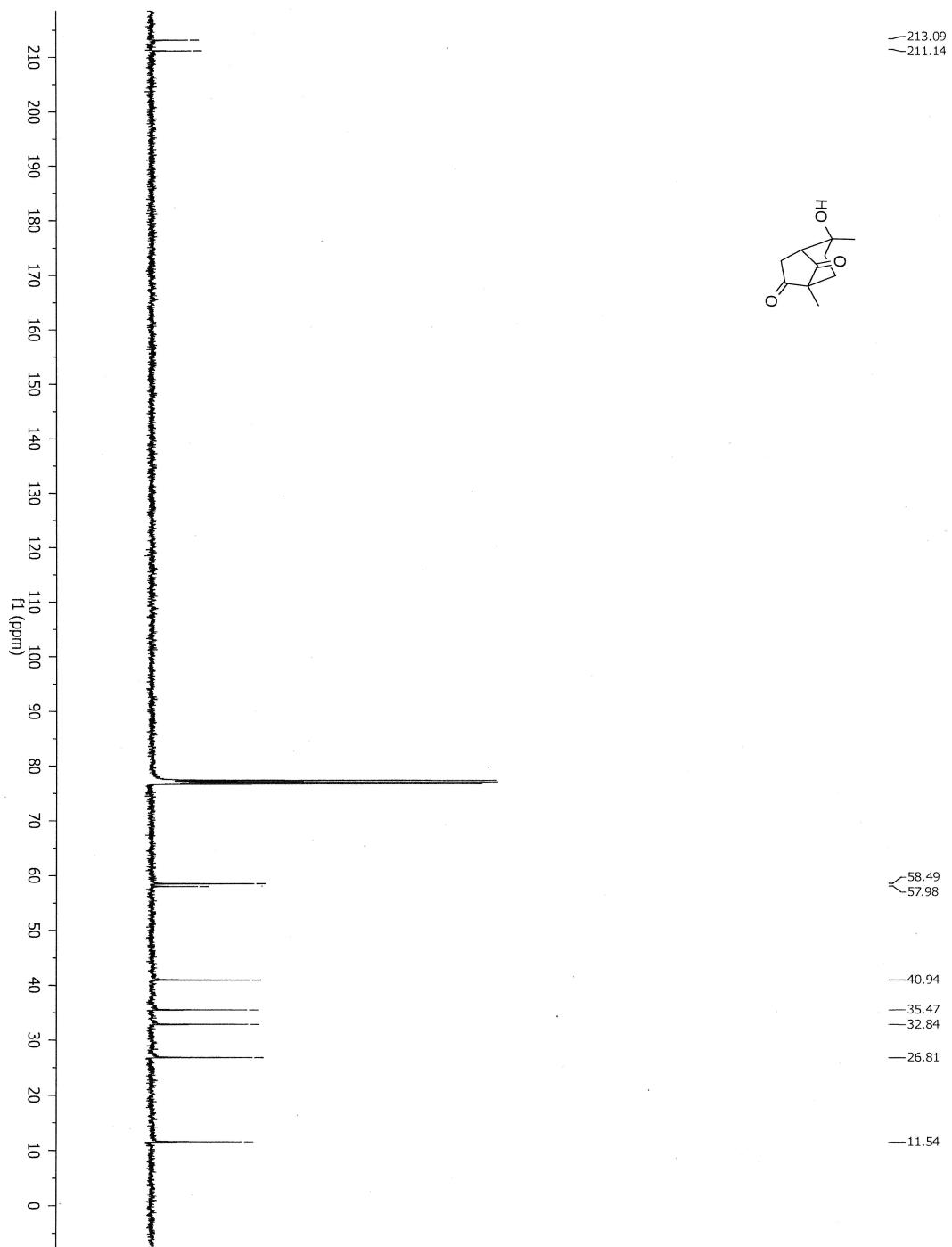


sh-bc-1052additionc  
cdcl3 400

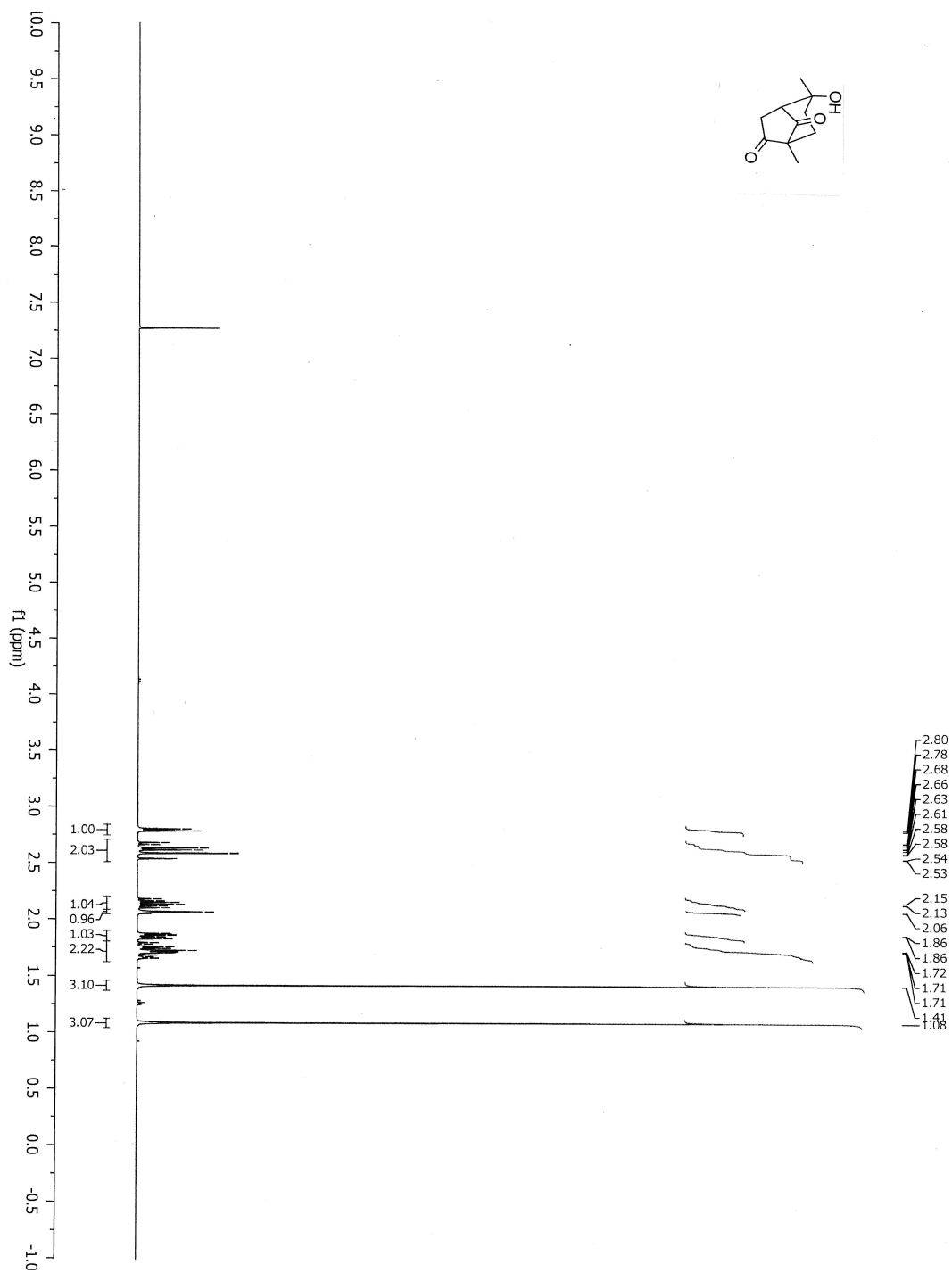


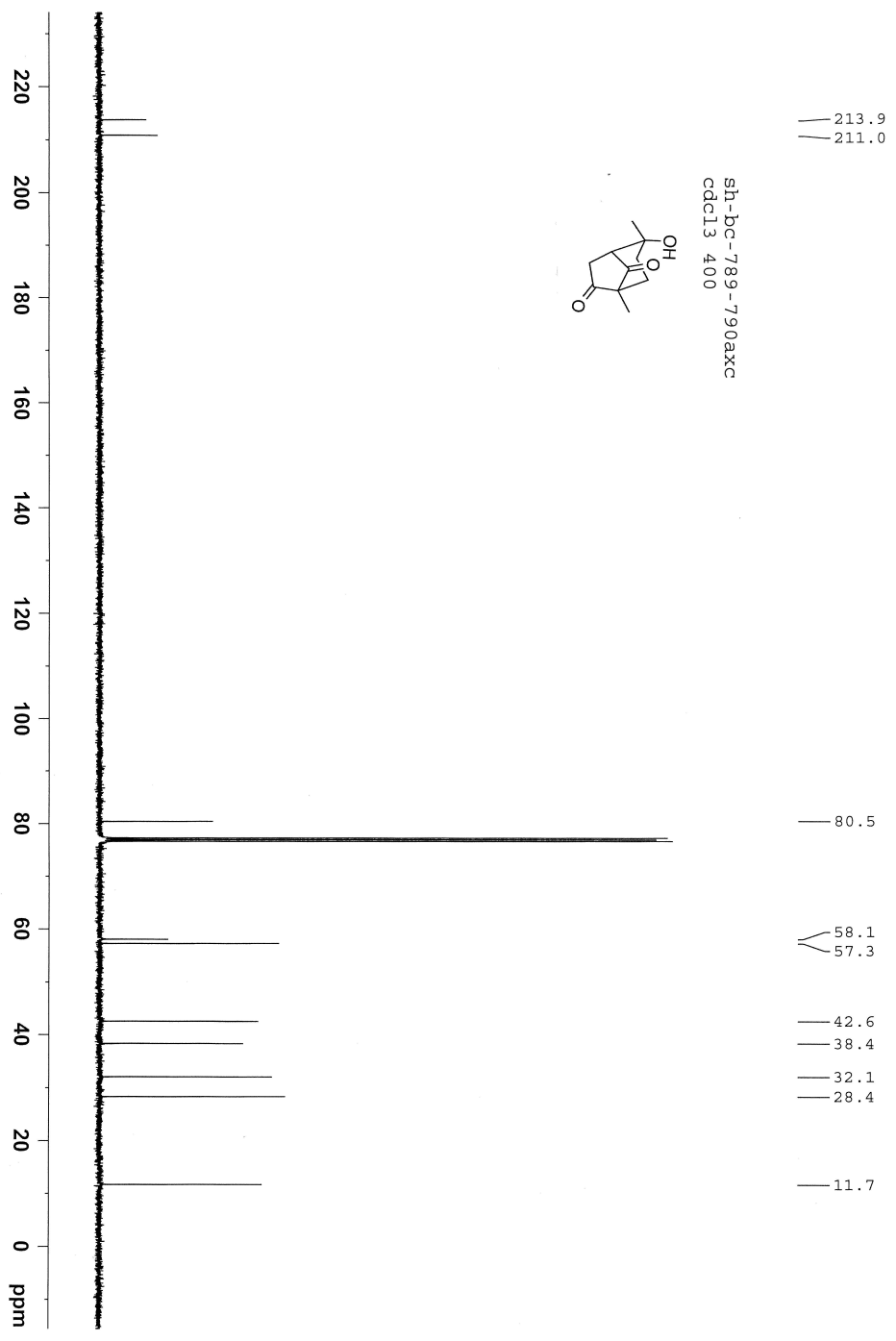
# Annex 48: $^1\text{H}$ and $^{13}\text{C}$ NMR Spectra of Compound 3.19





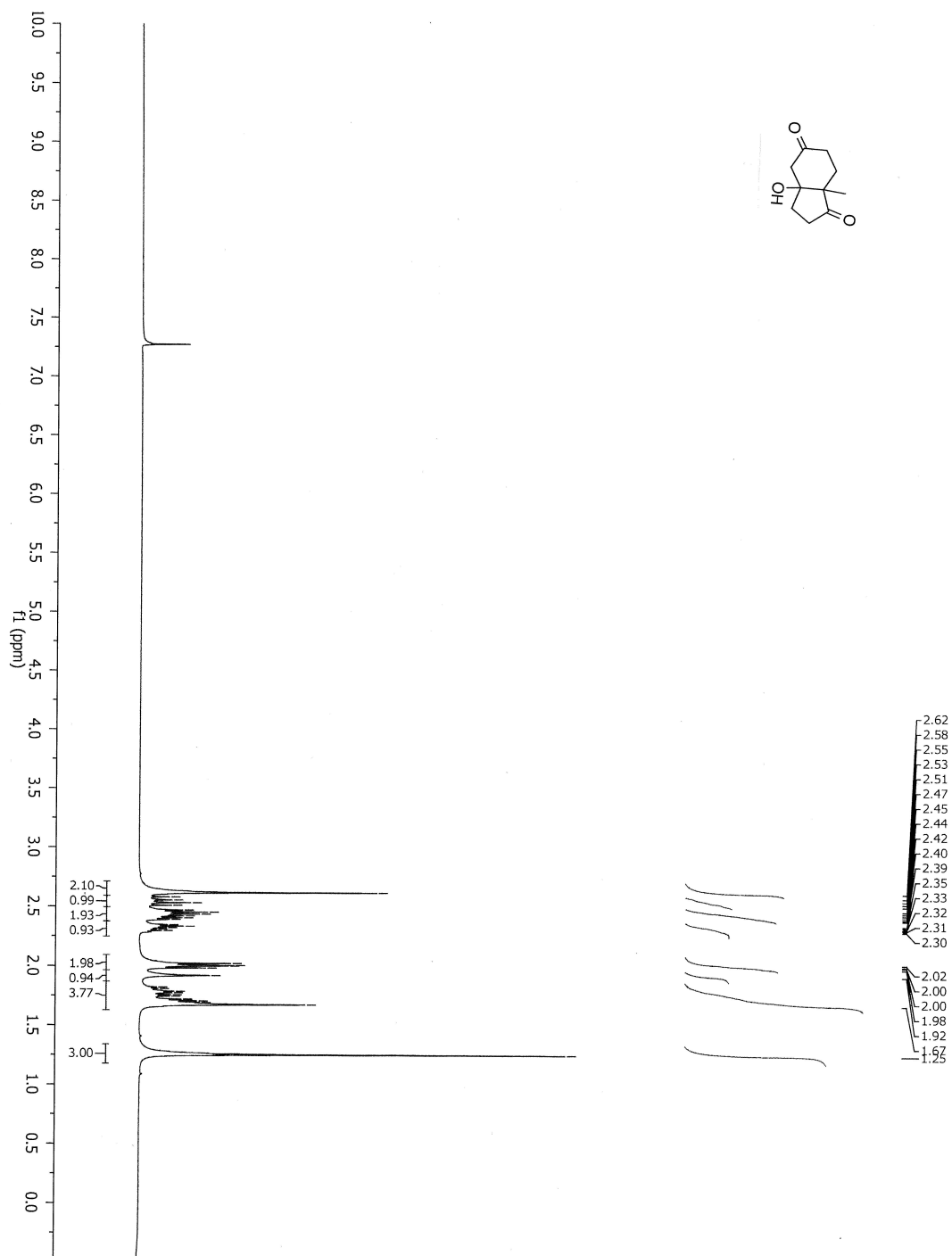
# Annex 49: $^1\text{H}$ and $^{13}\text{C}$ NMR Spectra of Compound 3.20

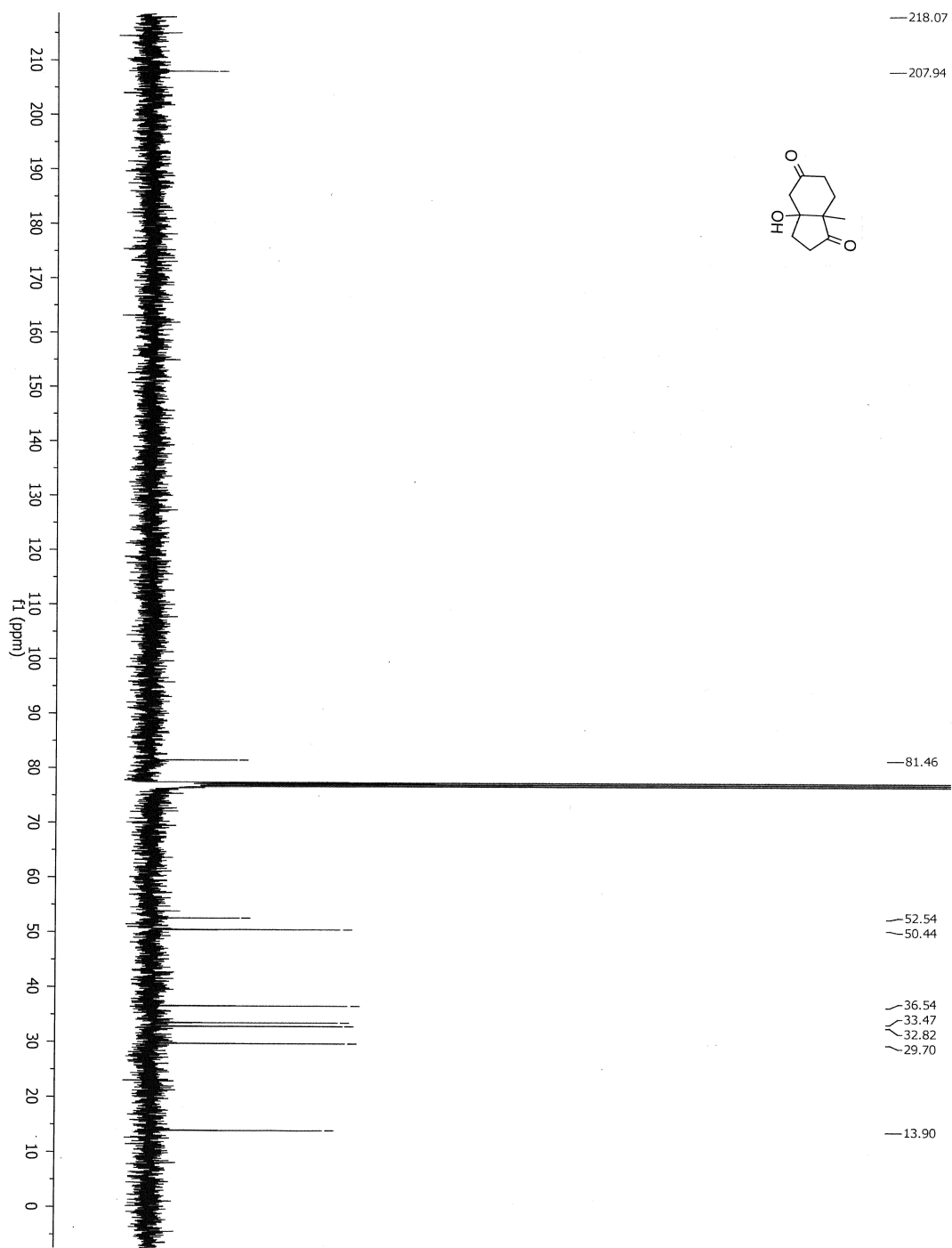




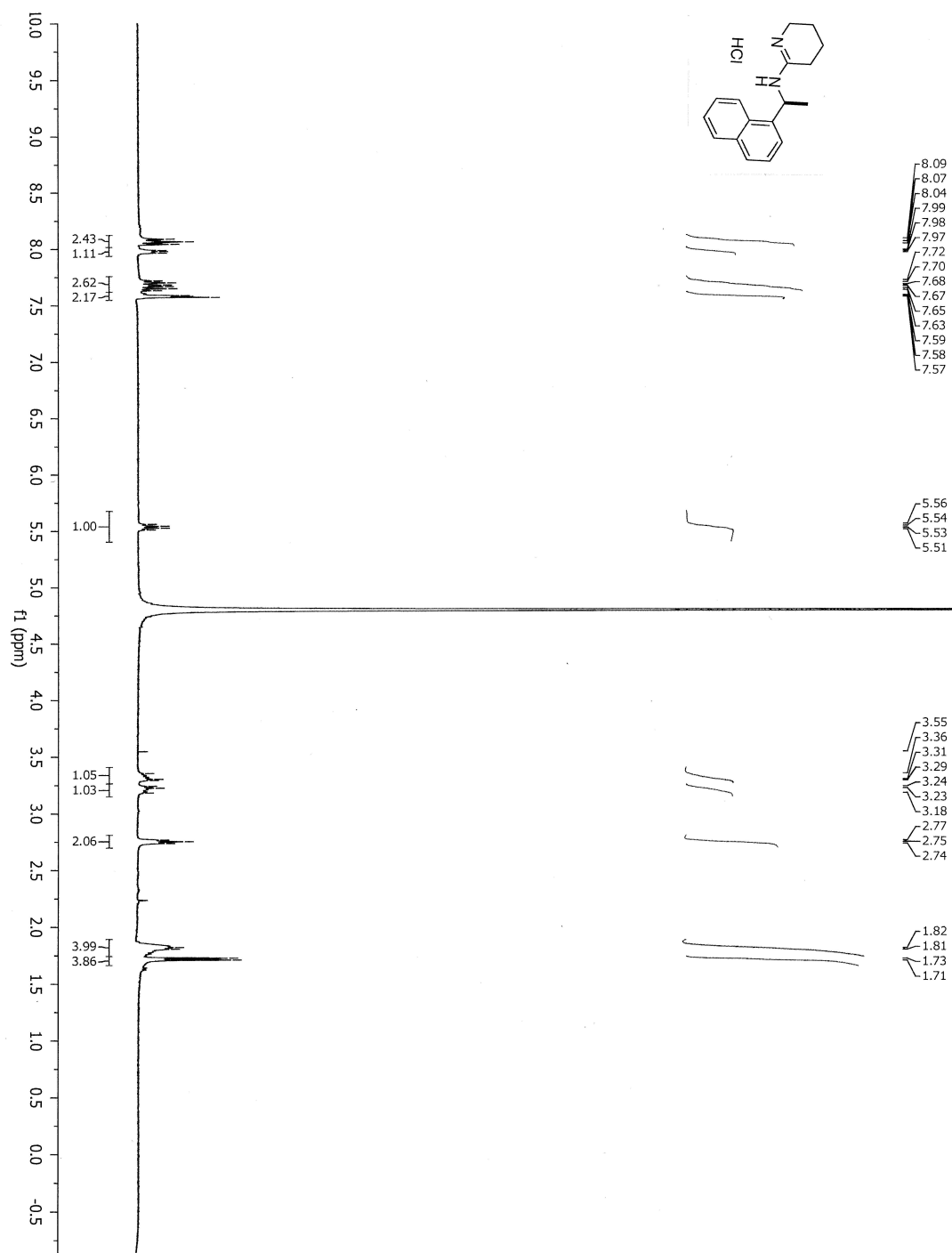


# Annex 50: $^1\text{H}$ and $^{13}\text{C}$ NMR Spectra of Compound 3.21

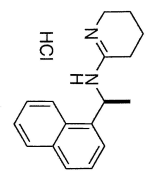
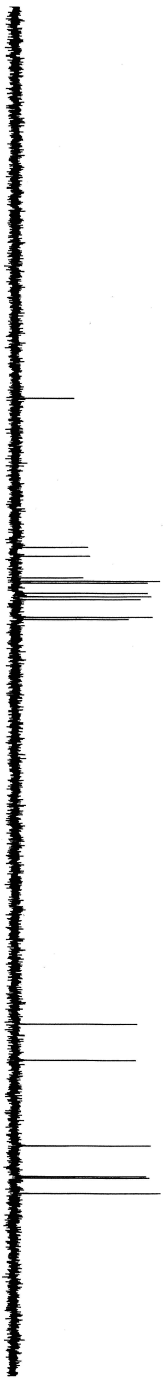




# Annex 51: $^1\text{H}$ and $^{13}\text{C}$ NMR Spectra of Compound 4.3



220  
200  
180  
160  
140  
120  
100  
80  
60  
40  
20  
0  
ppm



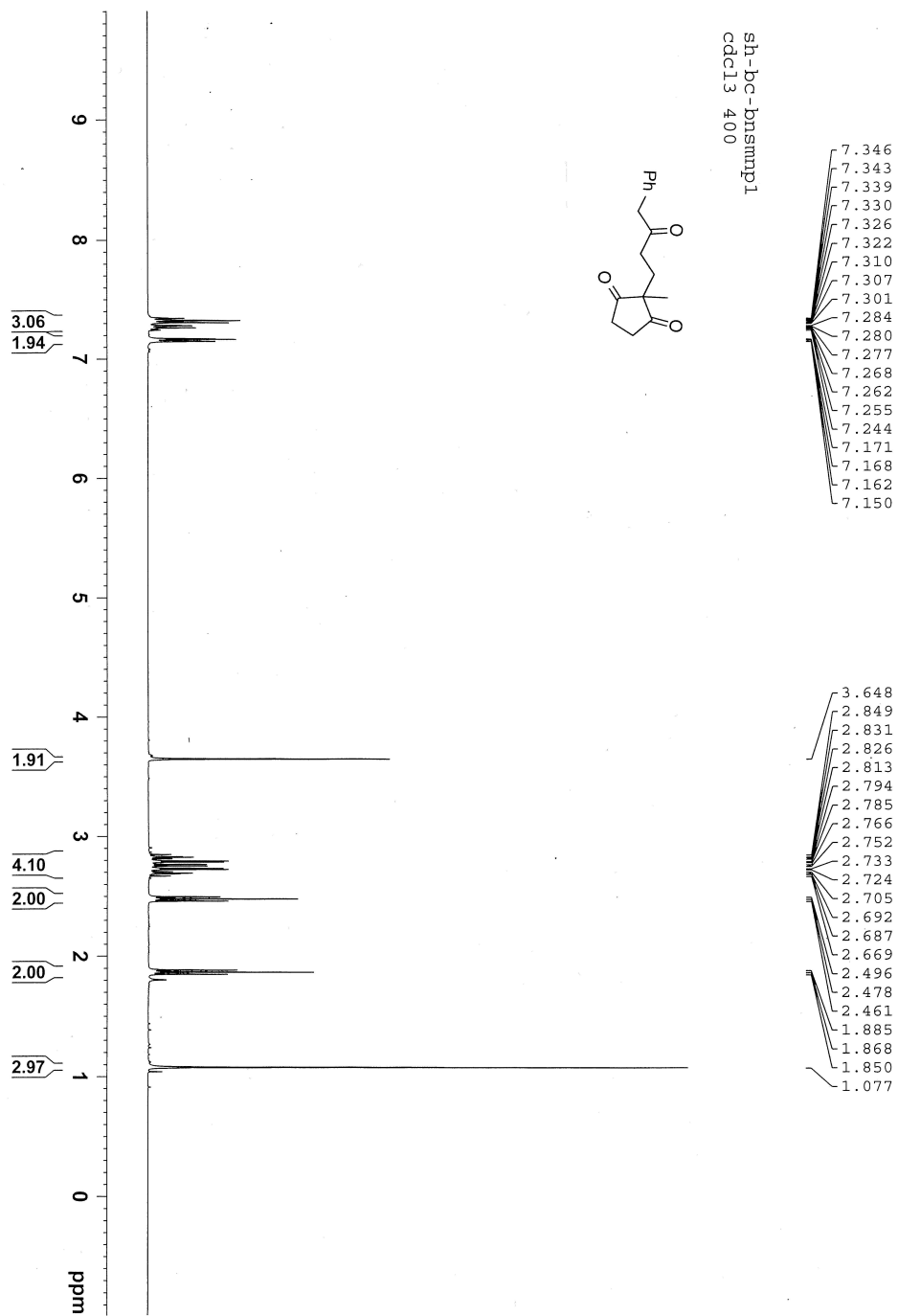
162.6

135.4  
133.7  
129.8  
129.2  
128.8  
127.0  
126.3  
125.8  
122.5  
122.1

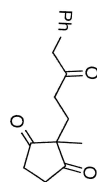
48.3  
41.8

26.2  
20.6  
20.3  
17.5

# Annex 52: $^1\text{H}$ and $^{13}\text{C}$ NMR Spectra of Compound 4.6



sh-bc-column-c cdcl3



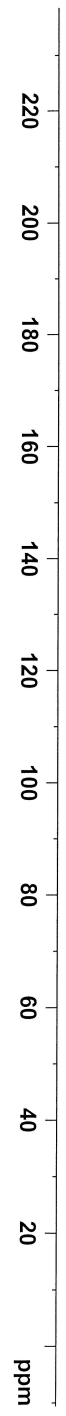
— 215.421  
— 207.111

— 133.543  
— 129.126  
— 128.336  
— 126.710

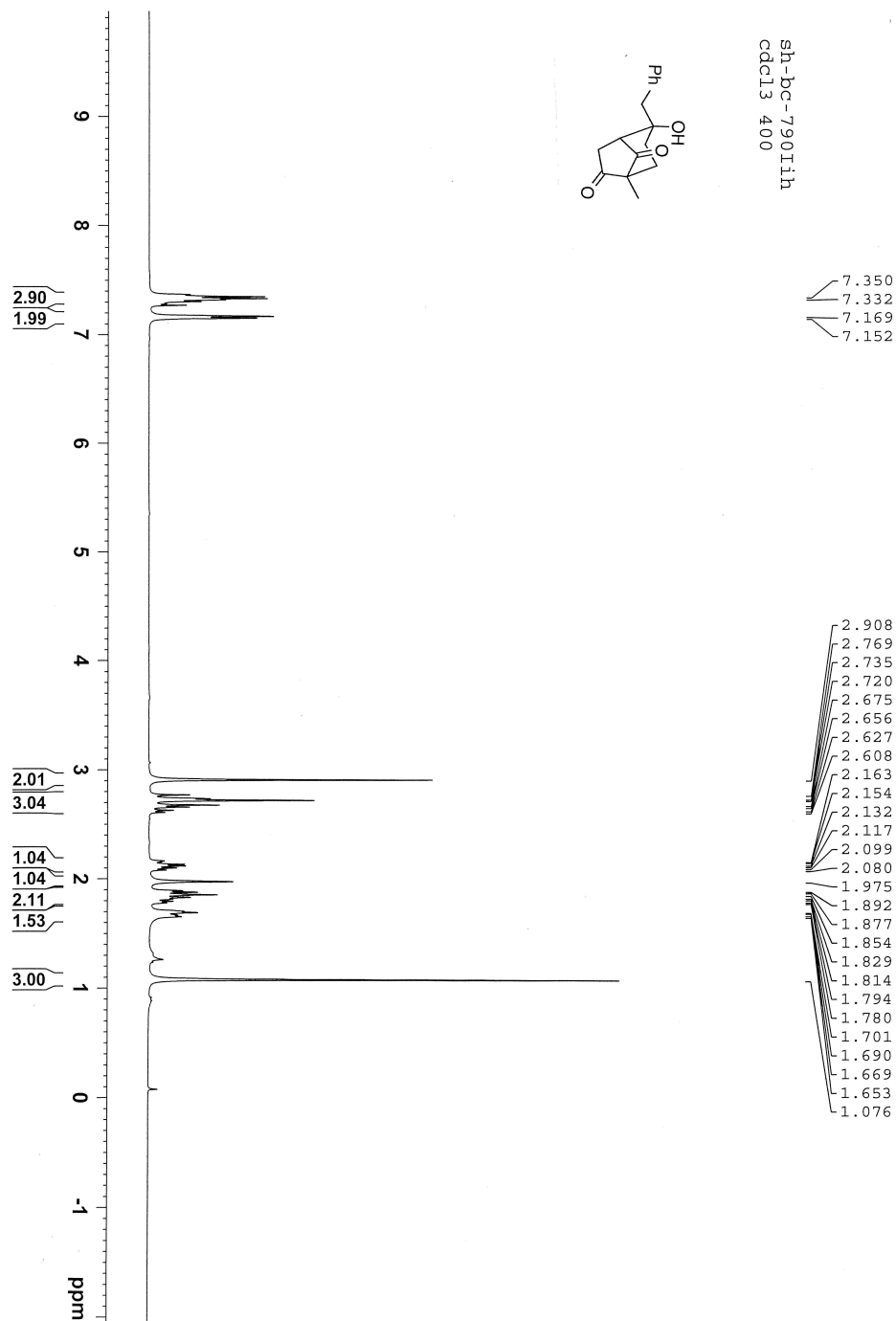
— 54.718  
— 49.548

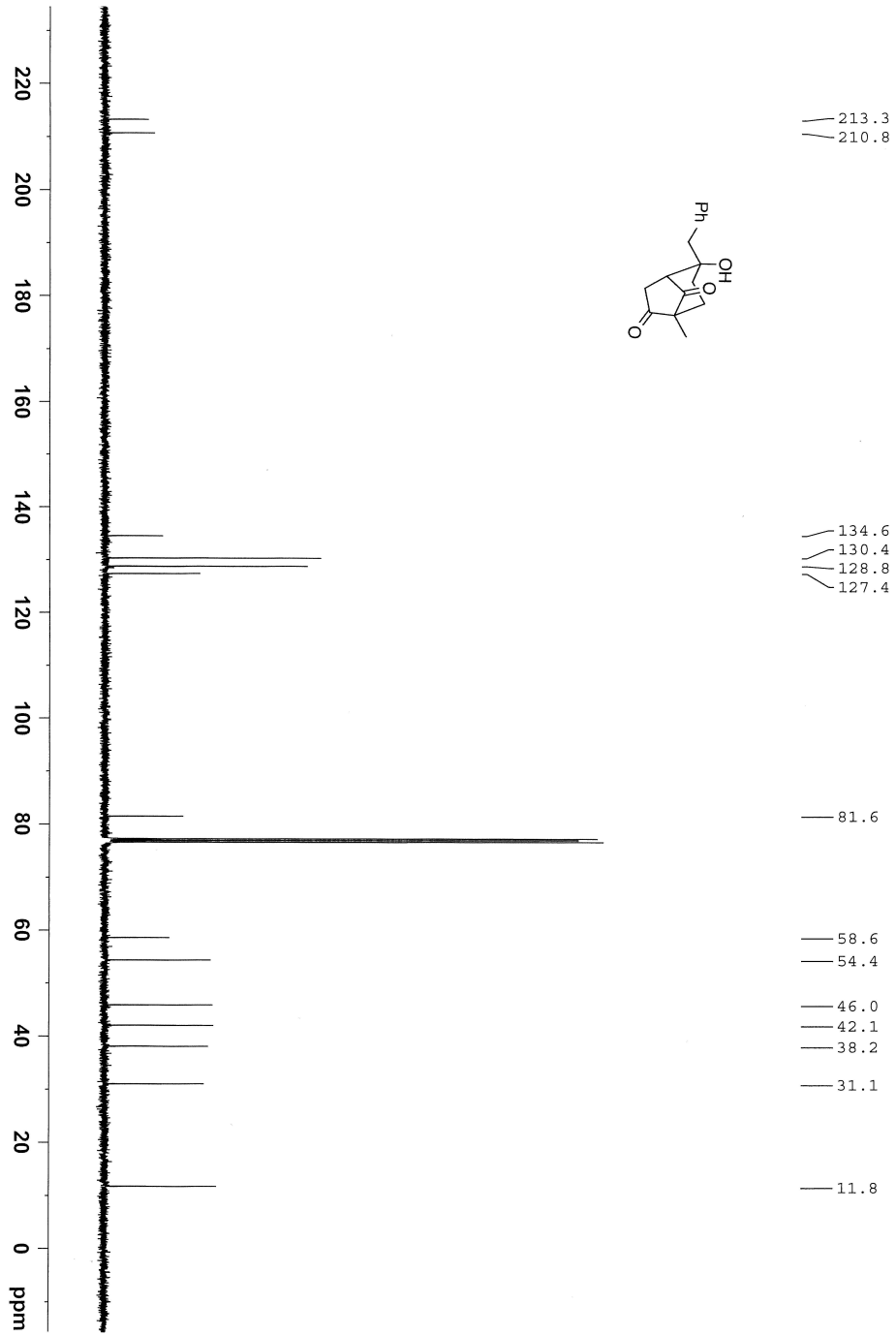
— 35.571  
— 34.339  
— 27.625

— 18.520



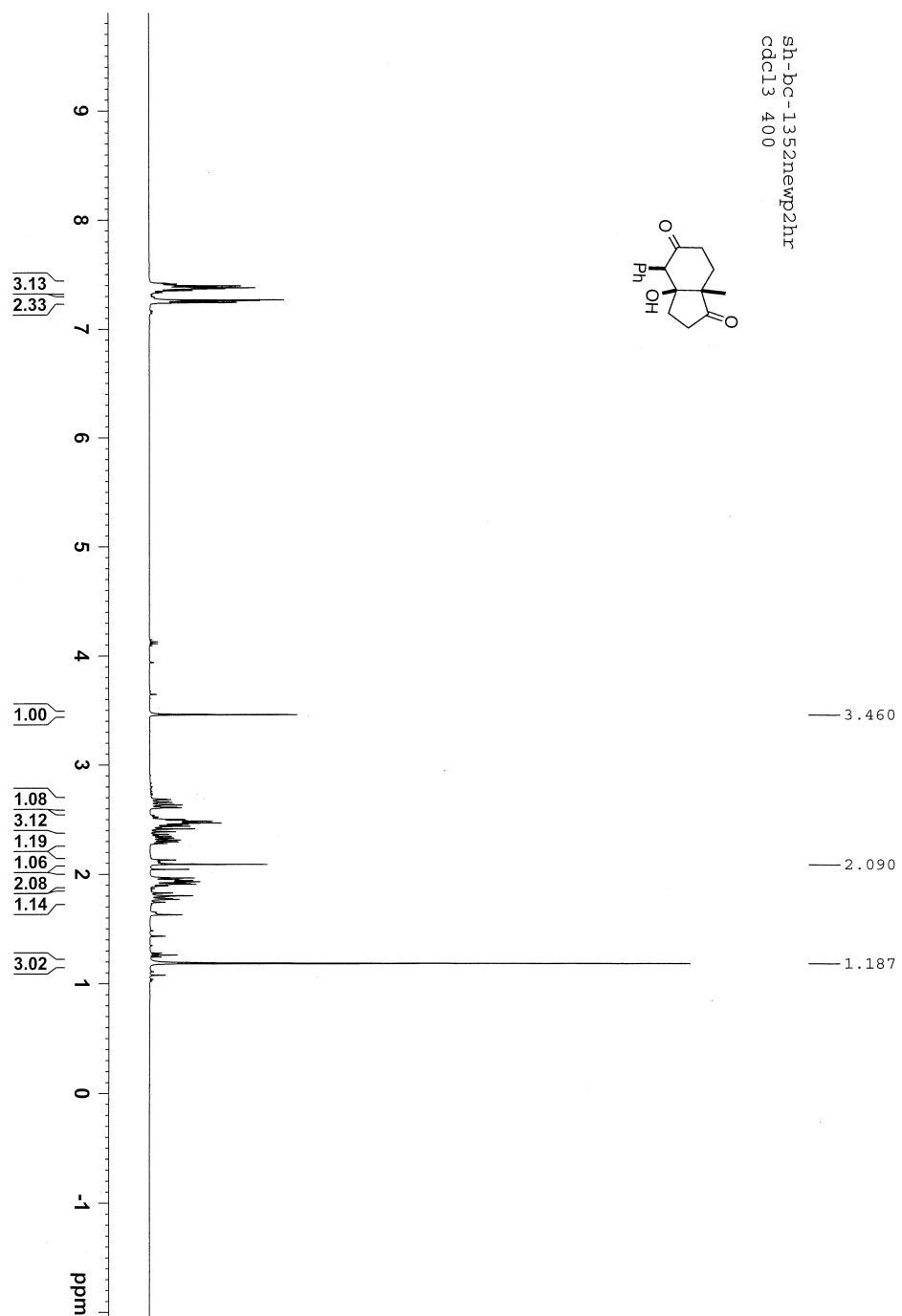
# Annex 53: $^1\text{H}$ and $^{13}\text{C}$ NMR Spectra of Compound 4.7

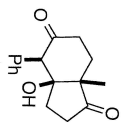




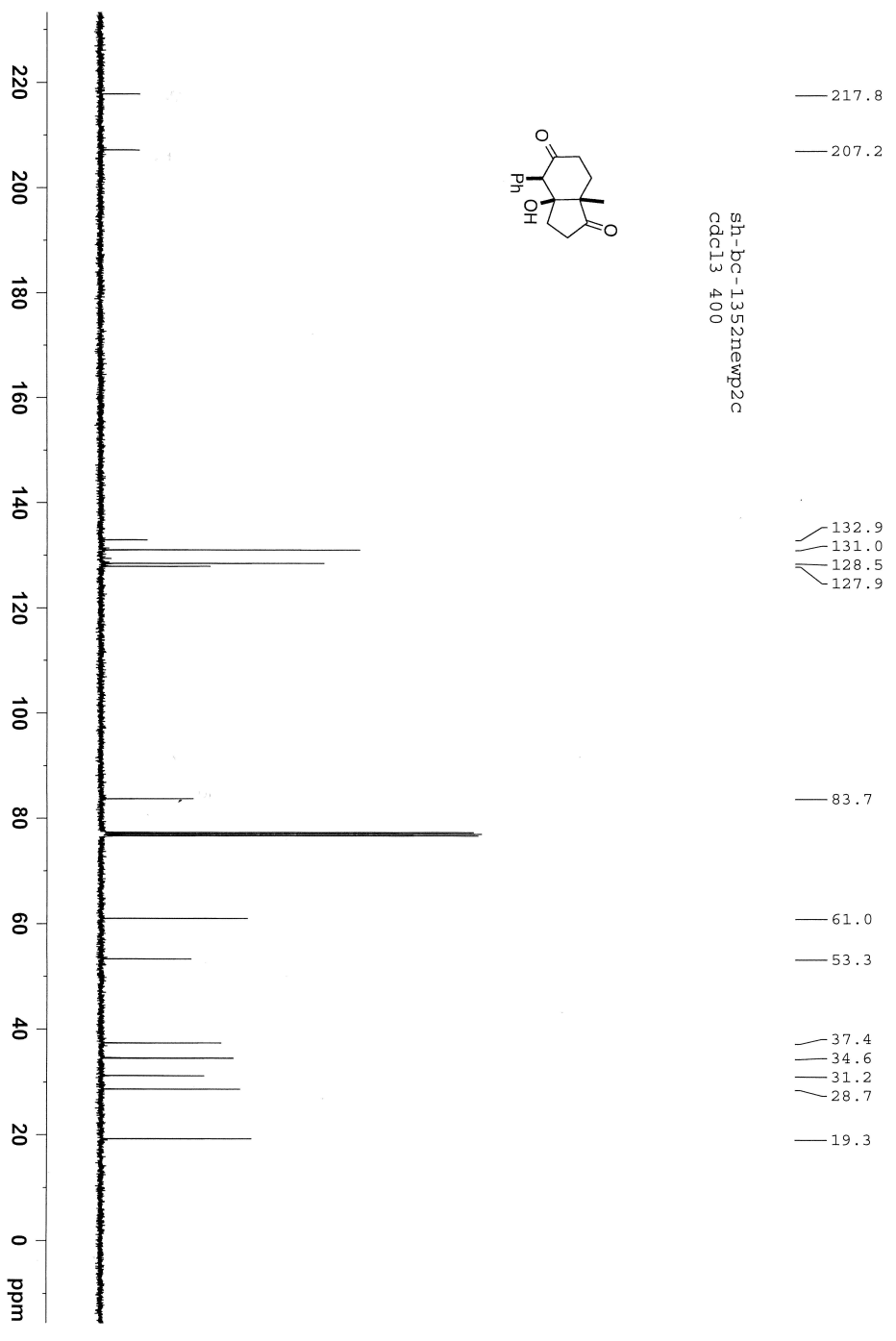


# Annex 54: $^1\text{H}$ and $^{13}\text{C}$ NMR Spectra of Compound 4.8

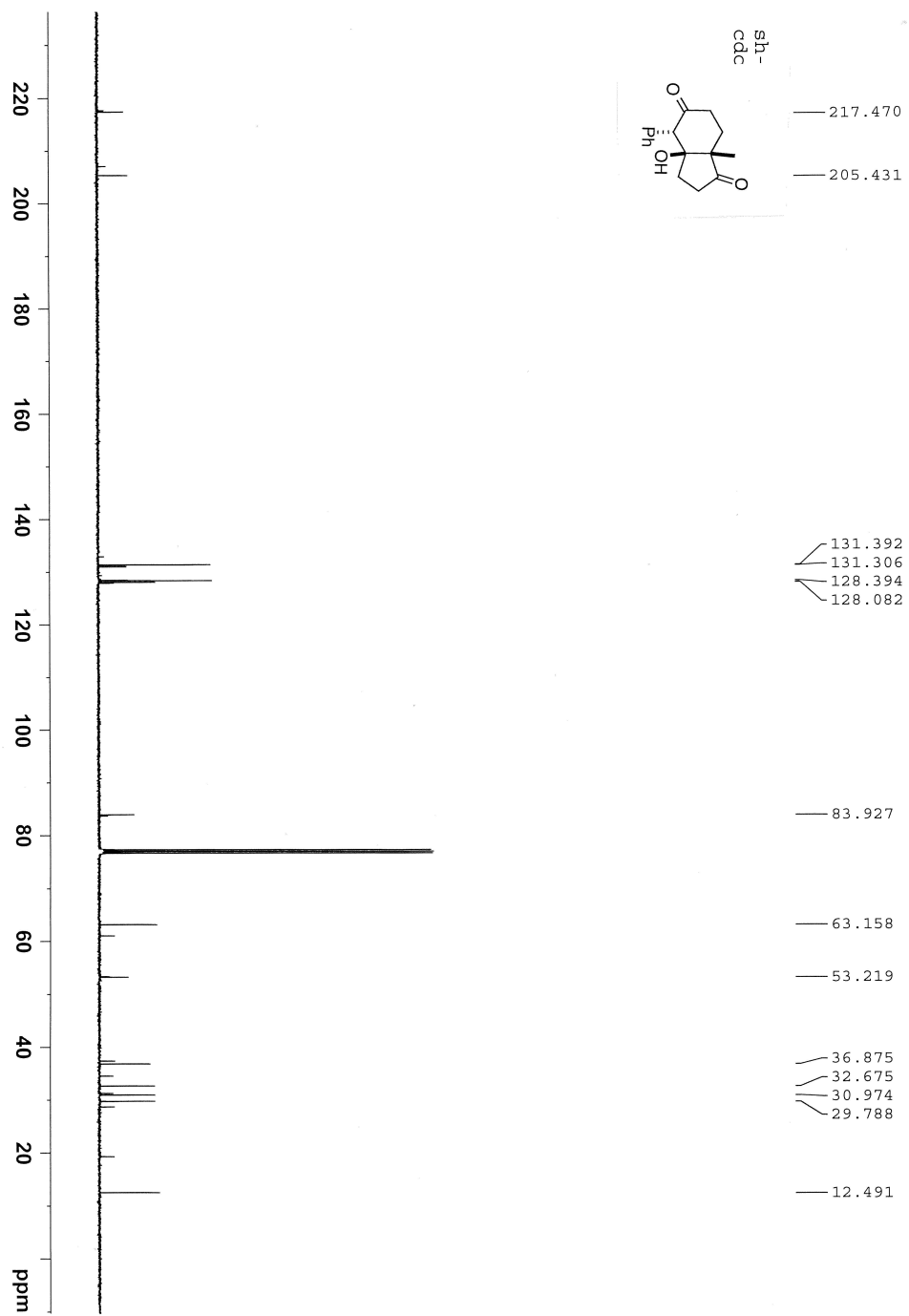




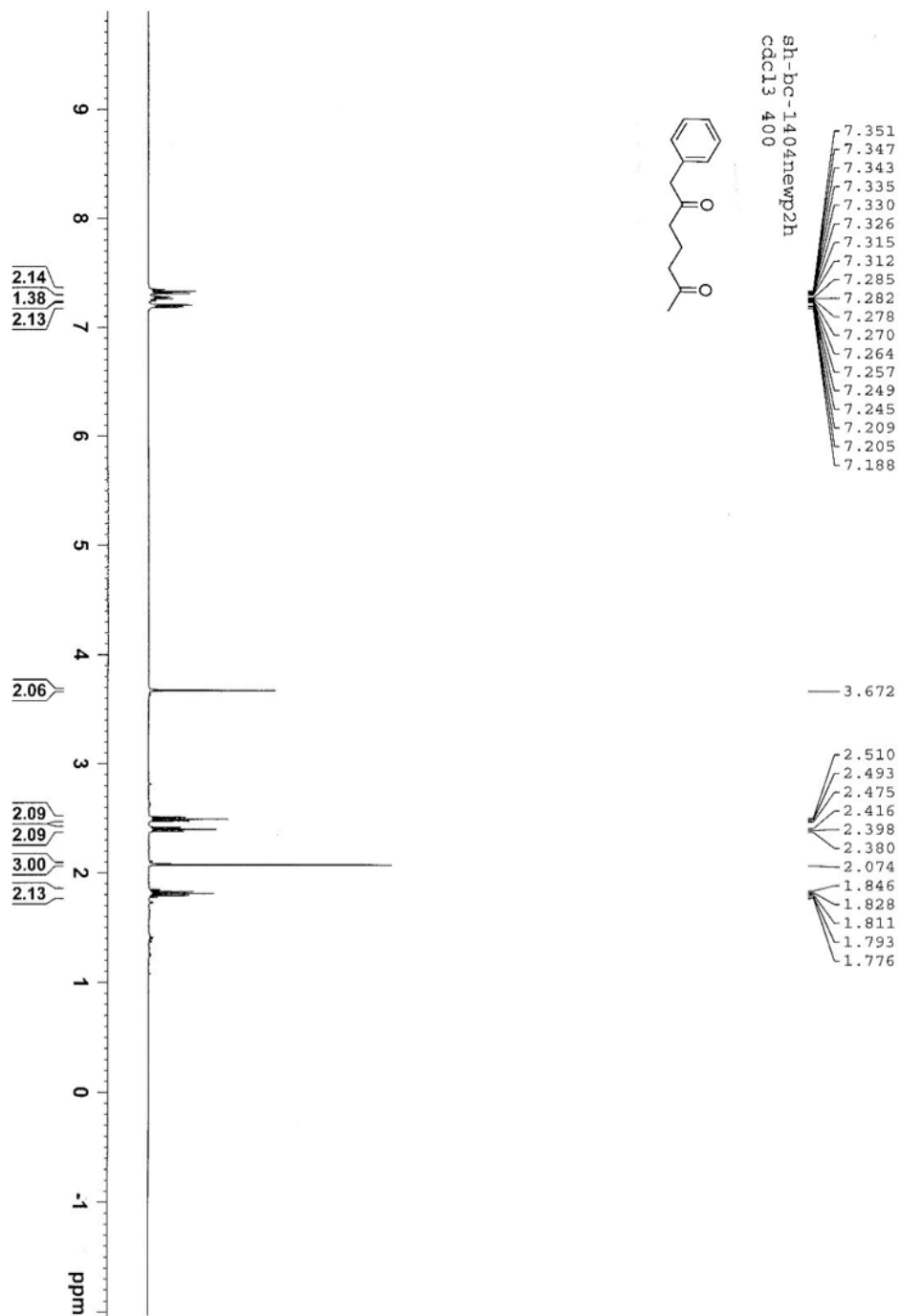
sh-bc-1352newp2c  
cdcl3 400

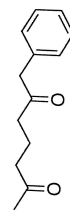






# Annex 56: $^1\text{H}$ and $^{13}\text{C}$ NMR Spectra of Compound 4.10





sh-bc-1404newp2c  
cdcl3 400

208.295  
207.792

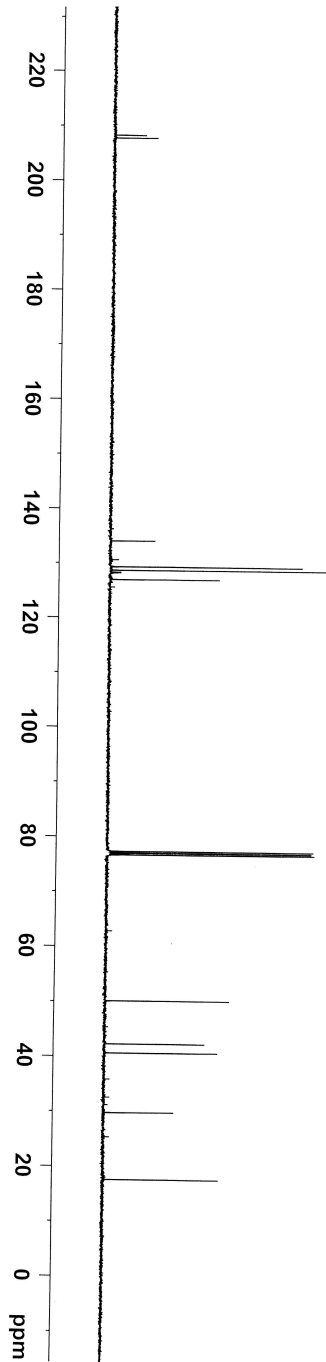
134.058  
129.321  
128.688  
126.985

50.096

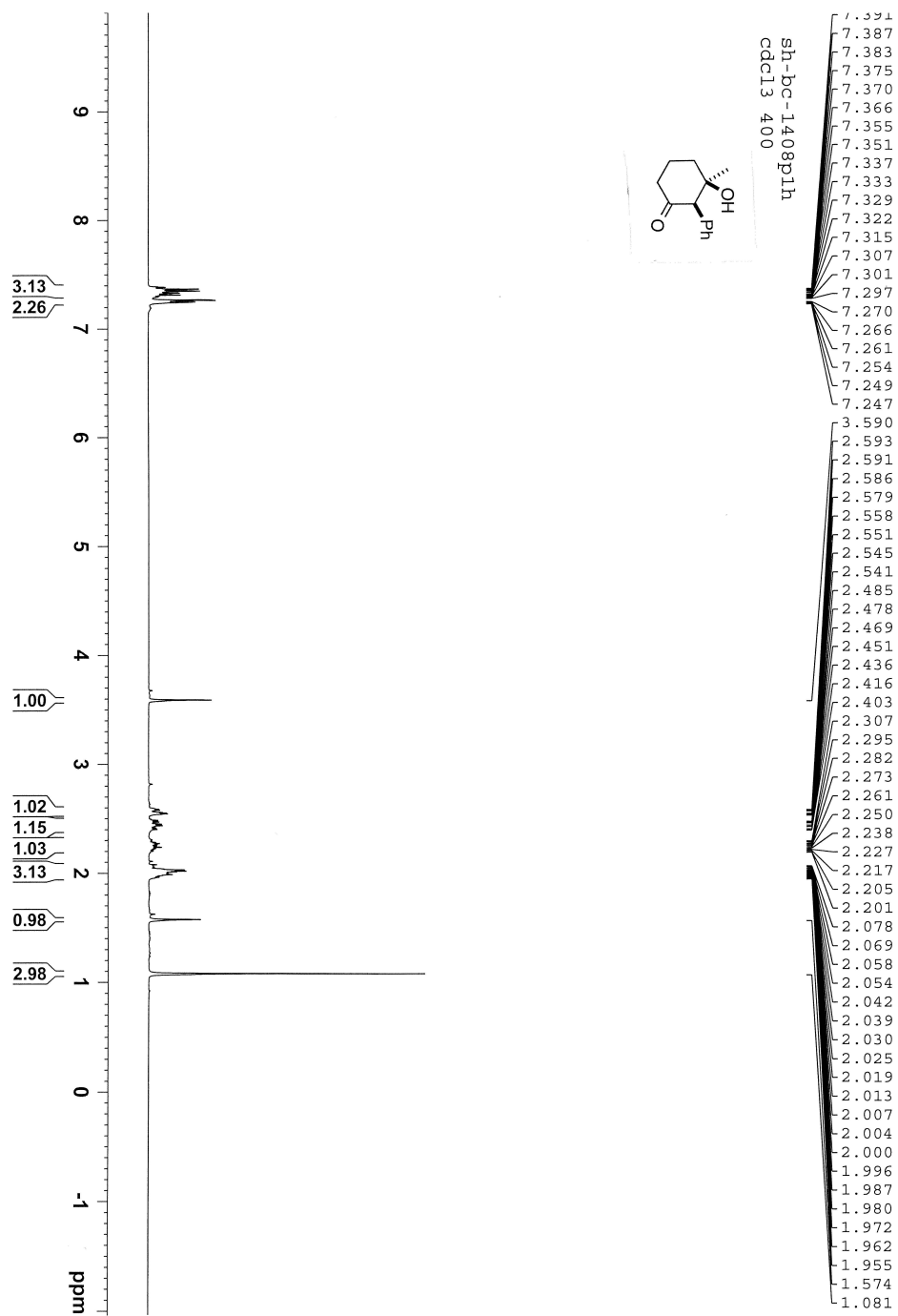
42.253  
40.587

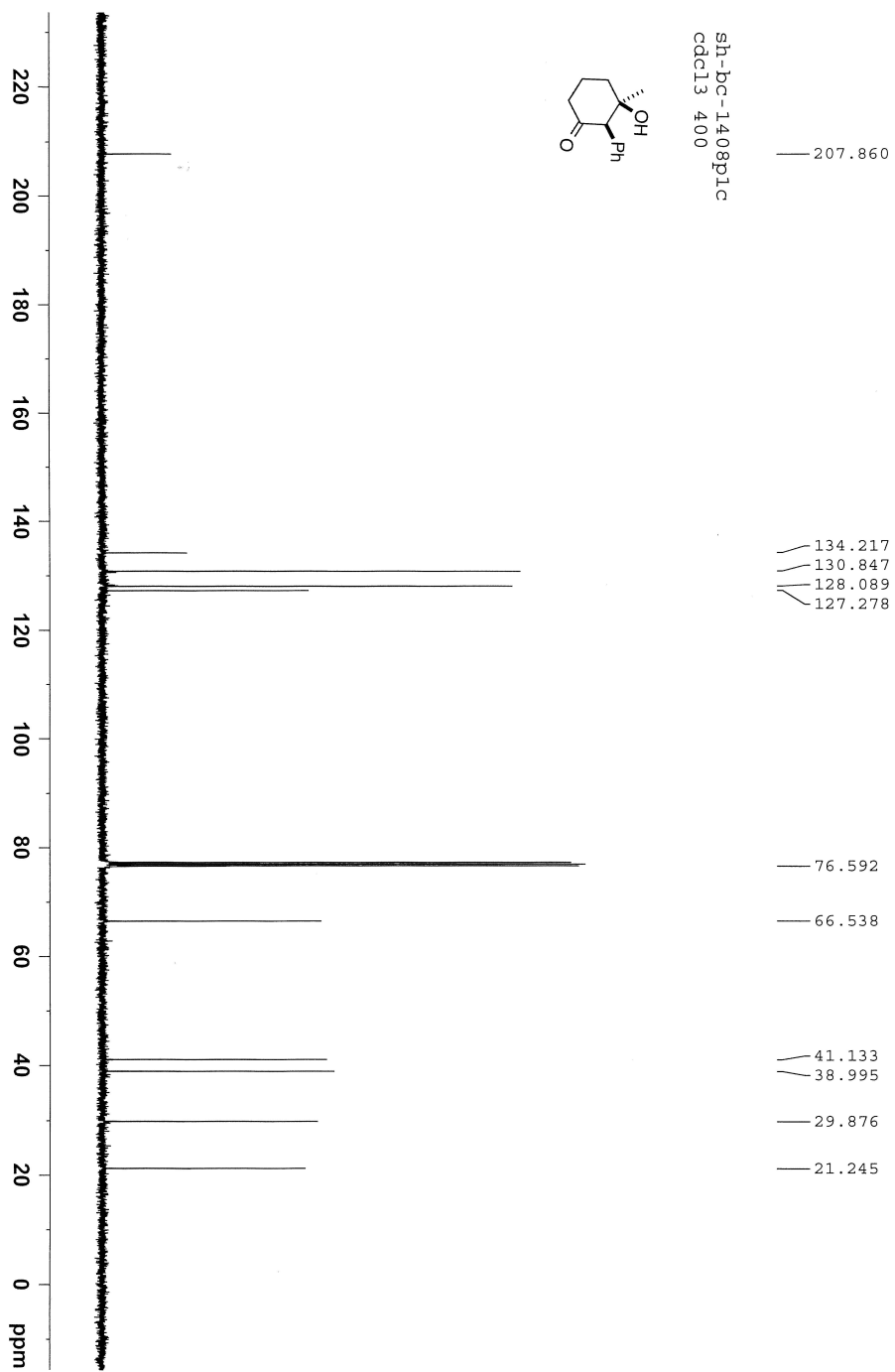
29.783

17.550



# Annex 57: $^1\text{H}$ and $^{13}\text{C}$ NMR Spectra of Compound 4.11







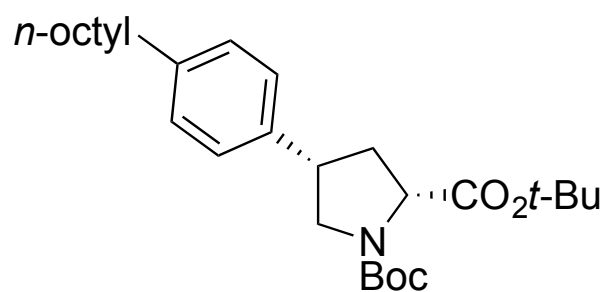
## **Annex 58: X-Ray Data for Compound 1.148**

CRYSTAL AND MOLECULAR STRUCTURE OF  
C<sub>28</sub> H<sub>45</sub> N<sub>1</sub> O<sub>4</sub> COMPOUND (ROBE26)

Equipe Hanessian

Département de chimie, Université de Montréal,

C.P. 6128, Succ. Centre-Ville, Montréal, Québec, H3C 3J7 (Canada)



Structure solved and refined in the laboratory of X-ray diffraction Université de Montréal by Robert D. Giacometti.

**Table 1.** Crystal data and structure refinement for C<sub>28</sub> H<sub>45</sub> N<sub>1</sub> O<sub>4</sub>.

Identification code	robe26
Empirical formula	C <sub>28</sub> H <sub>45</sub> NO <sub>4</sub>
Formula weight	459.65
Temperature/K	100.15
Crystal system	monoclinic
Space group	C2
a/Å	26.5372 (15)
b/Å	5.5899 (4)
c/Å	20.8906 (12)
α/°	90
β/°	118.206 (3)
γ/°	90
Volume/Å <sup>3</sup>	2730.9 (3)
Z	4
ρ <sub>calc</sub> /cm <sup>3</sup>	1.118
μ/mm <sup>-1</sup>	0.576
F(000)	1008.0
Crystal size/mm <sup>3</sup>	0.23 × 0.06 × 0.04
Radiation	CuKα (λ = 1.54178)
2θ range for data collection/°	4.8 to 142.454
Index ranges	-31 ≤ h ≤ 32, -6 ≤ k ≤ 6, -24 ≤ l ≤ 25
Reflections collected	10895
Independent reflections	4622 [R <sub>int</sub> = 0.0436, R <sub>sigma</sub> = 0.0563]
Data/restraints/parameters	4622/29/325
Goodness-of-fit on F <sup>2</sup>	1.005
Final R indexes [I ≥ 2σ (I)]	R <sub>1</sub> = 0.0635, wR <sub>2</sub> = 0.1578
Final R indexes [all data]	R <sub>1</sub> = 0.0714, wR <sub>2</sub> = 0.1628
Largest diff. peak/hole / e Å <sup>-3</sup>	0.31/-0.37
Flack parameter	0.0 (2)

**Table 2.** Fractional atomic coordinates ( $\times 10^4$ ) and equivalent isotropic displacement parameters ( $\text{\AA}^2 \times 10^3$ ) for C28 H45 N1 O4.

$U_{eq}$  is defined as one third of the trace of the orthogonalized  $U_{ij}$  tensor.

Atom	<i>x</i>	<i>y</i>	<i>z</i>	<i>U</i> (eq)
C1	830.1(15)	3805(8)	3470.3(19)	24.1(8)
C2	1122.4(15)	2867(9)	4259.9(19)	27.7(8)
C3	643.3(15)	2748(8)	4476.4(19)	25.0(8)
C4	269.9(14)	4883(8)	4064.6(19)	24.9(8)
C5	-88.3(15)	5962(8)	2787.4(19)	24.5(8)
C6	-282.4(16)	6974(8)	1550(2)	27.1(9)
C7	-904.0(16)	6218(9)	1166(2)	34.9(10)
C8	-204.3(19)	9626(10)	1696(2)	37.7(10)
C9	23.7(17)	6194(9)	1121(2)	32.9(10)
C10	1200.8(15)	5745(8)	3396.1(19)	25.2(8)
C11	2141.1(16)	6155(9)	3443(2)	34.2(10)
C12	2571(2)	4271(11)	3508(3)	54.5(15)
C13	2377.2(18)	7730(12)	4112(2)	44.3(12)
C14	1942.7(19)	7564(11)	2746(2)	40(1)
C15	851.5(15)	2740(8)	5284.7(19)	25.2(8)
C16	732.1(15)	807(8)	5615(2)	26.4(8)
C17	915.6(15)	771(8)	6360(2)	26.4(8)
C18	1229.0(15)	2651(8)	6799.1(19)	26.5(8)
C19	1360.6(15)	4581(8)	6475(2)	26.8(8)
C20	1169.6(15)	4617(8)	5731(2)	25.9(8)
C21	1431.4(17)	2601(9)	7605(2)	31.7(9)
C22	1828.6(16)	488(9)	7996(2)	30.9(9)
C23	2087.4(17)	631(9)	8816(2)	33.8(9)
C24	2450.5(18)	-1500(9)	9225(2)	35.4(10)
C25	2937.2(19)	-2073(12)	9049(2)	44.0(12)
C26	3344.4(18)	-3972(11)	9538(2)	41.9(11)
C27A	3736(2)	-5069(11)	9261(3)	37.1(14)
C27B	3927(9)	-3600(80)	9537(17)	44(6)
C28A	4134(3)	-3207(14)	9214(5)	64(2)
C28B	3870(20)	-3850(100)	8770(20)	66(7)
N1	291.0(12)	4812(7)	3380.0(16)	25.5(7)
O1	-491.0(11)	7126(6)	2749.8(15)	30.2(7)
O2	32.3(10)	5628(5)	2228.8(13)	25.9(6)
O3	1118.4(12)	7856(6)	3382.2(16)	34.1(7)
O4	1658.8(11)	4685(6)	3396.1(15)	30.9(6)

**Table 3.** Hydrogen atom coordinates ( $\times 10^4$ ) and isotropic displacement parameters ( $\text{\AA}^2 \times 10^3$ ) for C28 H45 N1 O4.

$U_{eq}$  is defined as one third of the trace of the orthogonalized  $U_{ij}$  tensor.

Atom	<i>x</i>	<i>y</i>	<i>z</i>	<i>U</i> (eq)
H1	760	2476	3117	29
H2A	1290	1263	4287	33
H2B	1429	3969	4584	33
H3	419	1251	4268	30
H4A	-126	4688	3985	30
H4B	429	6400	4327	30
H7A	-928	4471	1124	52
H7B	-1094	6931	680	52
H7C	-1093	6763	1446	52
H8A	-403	10118	1969	57
H8B	-364	10494	1234	57
H8C	204	9990	1980	57
H9A	429	6623	1393	49
H9B	-149	7000	649	49
H9C	-13	4458	1048	49
H12A	2701	3402	3967	82
H12B	2899	5040	3498	82
H12C	2393	3148	3101	82
H13A	2106	9023	4040	66
H13B	2743	8414	4195	66
H13C	2435	6772	4534	66
H14A	1768	6474	2330	60
H14B	2271	8369	2746	60
H14C	1661	8760	2710	60
H16	521	-511	5325	32
H17	825	-561	6569	32
H19	1583	5875	6767	32
H20	1258	5955	5522	31
H21A	1094	2523	7688	38
H21B	1636	4112	7821	38
H22A	1610	-1020	7826	37
H22B	2141	444	7864	37
H23A	2326	2090	8985	41
H23B	1774	805	8943	41
H24A	2200	-2922	9112	43
H24B	2617	-1191	9753	43
H25A	2770	-2618	8539	53
H25B	3156	-590	9095	53
H26A	3118	-5270	9601	50
H26B	3586	-3259	10022	50
H26C	3191	-5587	9354	50
H26D	3396	-3813	10037	50
H27A	3965	-6369	9592	45
H27B	3498	-5774	8774	45
H27C	4077	-1988	9729	53
H27D	4207	-4793	9862	53
H28A	3908	-1966	8864	97
H28B	4388	-3973	9055	97
H28C	4363	-2481	9693	97
H28D	3756	-2306	8523	99
H28E	3573	-5046	8499	99
H28F	4233	-4360	8810	99

**Table 4.** Anisotropic displacement parameters ( $\text{\AA}^2 \times 10^3$ ) for C28 H45 N1 O4.

The anisotropic displacement factor exponent takes the form:

$$-2\pi^2 [h^2 a^{*2} U_{11} + \dots + 2hka^* b^* U_{12}]$$

Atom	$U_{11}$	$U_{22}$	$U_{33}$	$U_{23}$	$U_{13}$	$U_{12}$
C1	20.0 (15)	34 (2)	23.9 (17)	0.7 (16)	14.7 (13)	3.6 (16)
C2	20.9 (15)	42 (2)	24.5 (17)	2.1 (18)	14.4 (14)	5.3 (19)
C3	22.7 (16)	32 (2)	24.7 (17)	-1.9 (17)	15.0 (14)	-1.0 (18)
C4	23.1 (16)	32 (2)	23.7 (17)	0.0 (17)	14.8 (14)	-2.4 (18)
C5	26.5 (17)	30 (2)	21.5 (16)	-0.1 (17)	15.0 (14)	-1.7 (18)
C6	27.6 (17)	36 (2)	22.8 (16)	2.6 (18)	15.9 (14)	3.9 (18)
C7	31.1 (19)	46 (3)	28.0 (18)	3.9 (19)	14.6 (16)	2 (2)
C8	46 (2)	37 (2)	36 (2)	4 (2)	24.6 (19)	-1 (2)
C9	39 (2)	43 (3)	26.8 (18)	2.3 (19)	23.3 (16)	3 (2)
C10	22.0 (16)	32 (2)	24.6 (16)	2.6 (17)	13.7 (13)	6.1 (18)
C11	24.6 (18)	41 (3)	46 (2)	1 (2)	23.8 (17)	-6 (2)
C12	39 (2)	55 (3)	91 (4)	13 (3)	48 (3)	0 (3)
C13	29.2 (19)	66 (3)	40 (2)	0 (3)	17.9 (17)	-11 (2)
C14	36 (2)	51 (3)	42 (2)	-1 (2)	25.8 (18)	-8 (2)
C15	22.0 (16)	33 (2)	24.3 (17)	2.9 (18)	13.8 (14)	6.0 (18)
C16	24.7 (16)	31 (2)	28.6 (18)	-3.1 (18)	17.0 (14)	-0.6 (18)
C17	26.4 (17)	31 (2)	28.4 (18)	5.7 (18)	18.8 (15)	5.4 (18)
C18	24.8 (16)	35 (2)	25.3 (18)	2.4 (17)	16.4 (14)	9.3 (18)
C19	24.8 (16)	32 (2)	27.0 (18)	-1.7 (18)	14.9 (14)	3.5 (18)
C20	24.3 (16)	31 (2)	28.5 (18)	5.0 (18)	17.4 (14)	3.5 (18)
C21	38 (2)	38 (2)	25.9 (18)	1.4 (19)	20.8 (16)	5 (2)
C22	30.7 (18)	41 (2)	26.2 (18)	3.5 (18)	18.1 (15)	7.1 (19)
C23	34.7 (19)	45 (3)	25.9 (19)	0 (2)	17.7 (16)	2 (2)
C24	32 (2)	51 (3)	28.4 (19)	2.7 (19)	18.2 (16)	2 (2)
C25	36 (2)	69 (3)	34 (2)	9 (2)	22.2 (18)	8 (3)
C26	34 (2)	62 (3)	36 (2)	7 (2)	21.1 (17)	8 (2)
C27A	40 (3)	38 (3)	38 (3)	-2 (3)	22 (2)	3 (3)
C27B	47 (11)	45 (12)	41 (11)	-1 (10)	21 (9)	0 (11)
C28A	57 (4)	57 (4)	110 (6)	0 (5)	65 (5)	-1 (4)
C28B	63 (12)	59 (12)	98 (13)	-1 (11)	55 (10)	5 (11)
N1	23.6 (14)	34.7 (18)	24.3 (15)	-0.6 (15)	16.3 (12)	3.5 (16)
O1	27.2 (12)	38.7 (17)	31.4 (13)	4.4 (13)	19.2 (11)	9.1 (13)
O2	26.4 (11)	35.7 (15)	22.0 (12)	2.1 (12)	16.6 (10)	5.4 (13)
O3	29.4 (14)	34.5 (16)	43.5 (16)	-1.1 (15)	21.4 (12)	0.7 (14)
O4	23.8 (12)	36.1 (16)	42.7 (15)	1.6 (15)	24.0 (11)	1.0 (14)

**Table 5.** Bond lengths [Å] for C28 H45 N1 O4.

Atom	Atom	Length/Å	Atom	Atom	Length/Å
C1	C2	1.545 (5)	C11	C14	1.515 (6)
C1	C10	1.520 (5)	C11	O4	1.484 (4)
C1	N1	1.464 (4)	C15	C16	1.396 (6)
C2	C3	1.539 (4)	C15	C20	1.393 (6)
C3	C4	1.530 (6)	C16	C17	1.394 (5)
C3	C15	1.508 (5)	C17	C18	1.385 (6)
C4	N1	1.458 (4)	C18	C19	1.403 (6)
C5	N1	1.335 (5)	C18	C21	1.507 (5)
C5	O1	1.221 (5)	C19	C20	1.387 (5)
C5	O2	1.361 (4)	C21	C22	1.536 (6)
C6	C7	1.514 (5)	C22	C23	1.517 (5)
C6	C8	1.508 (7)	C23	C24	1.516 (7)
C6	C9	1.529 (5)	C24	C25	1.534 (5)
C6	O2	1.469 (5)	C25	C26	1.514 (7)
C10	O3	1.198 (6)	C26	C27A	1.536 (6)
C10	O4	1.352 (4)	C26	C27B	1.562 (13)
C11	C12	1.511 (7)	C27A	C28A	1.519 (8)
C11	C13	1.514 (7)	C27B	C28B	1.53 (2)

**Table 6.** Bond angles [°] for C28 H45 N1 O4.

Atom	Atom	Atom	Angle/°	Atom	Atom	Atom	Angle/°
C10	C1	C2	109.2 (3)	O4	C11	C14	109.1 (3)
N1	C1	C2	103.6 (3)	C16	C15	C3	120.4 (4)
N1	C1	C10	110.7 (3)	C20	C15	C3	122.2 (4)
C3	C2	C1	105.1 (3)	C20	C15	C16	117.3 (3)
C4	C3	C2	101.9 (3)	C17	C16	C15	121.4 (4)
C15	C3	C2	114.4 (3)	C18	C17	C16	120.8 (4)
C15	C3	C4	115.4 (3)	C17	C18	C19	118.1 (3)
N1	C4	C3	102.4 (3)	C17	C18	C21	120.8 (4)
N1	C5	O2	110.5 (3)	C19	C18	C21	121.0 (4)
O1	C5	N1	124.7 (3)	C20	C19	C18	120.6 (4)
O1	C5	O2	124.8 (3)	C19	C20	C15	121.6 (4)
C7	C6	C9	111.0 (3)	C18	C21	C22	113.7 (3)
C8	C6	C7	113.1 (4)	C23	C22	C21	113.0 (3)
C8	C6	C9	109.8 (3)	C24	C23	C22	115.0 (4)
O2	C6	C7	110.4 (3)	C23	C24	C25	114.3 (4)
O2	C6	C8	110.3 (3)	C26	C25	C24	113.5 (4)
O2	C6	C9	101.7 (3)	C25	C26	C27A	114.8 (4)
O3	C10	C1	125.8 (3)	C25	C26	C27B	107.3 (15)
O3	C10	O4	125.8 (4)	C28A	C27A	C26	111.4 (5)
O4	C10	C1	108.2 (4)	C28B	C27B	C26	112 (2)
C12	C11	C13	110.9 (4)	C4	N1	C1	111.8 (3)
C12	C11	C14	110.6 (4)	C5	N1	C1	124.6 (3)
C13	C11	C14	112.9 (4)	C5	N1	C4	122.3 (3)
O4	C11	C12	102.2 (4)	C5	O2	C6	120.1 (3)
O4	C11	C13	110.6 (3)	C10	O4	C11	120.3 (3)

**Table 7.** Torsion angles [ $^{\circ}$ ] for C28 H45 N1 O4.

<b>A</b>	<b>B</b>	<b>C</b>	<b>D</b>	<b>Angle/<math>^{\circ}</math></b>	<b>A</b>	<b>B</b>	<b>C</b>	<b>D</b>	<b>Angle/<math>^{\circ}</math></b>
C1	C2	C3	C4	-33.9(4)	C16	C17	C18	C19	-0.6(5)
C1	C2	C3	C15	-159.2(4)	C16	C17	C18	C21	-179.5(3)
C1	C10	O4	C11	-170.7(3)	C17	C18	C19	C20	1.4(5)
C2	C1	C10	O3	-102.2(4)	C17	C18	C21	C22	60.3(5)
C2	C1	C10	O4	73.9(4)	C18	C19	C20	C15	-1.1(5)
C2	C1	N1	C4	8.3(4)	C18	C21	C22	C23	172.8(3)
C2	C1	N1	C5	175.8(4)	C19	C18	C21	C22	-118.6(4)
C2	C3	C4	N1	38.1(4)	C20	C15	C16	C17	1.0(5)
C2	C3	C15	C16	-119.1(4)	C21	C18	C19	C20	-179.6(3)
C2	C3	C15	C20	60.5(5)	C21	C22	C23	C24	176.0(4)
C3	C4	N1	C1	-29.8(4)	C22	C23	C24	C25	55.1(5)
C3	C4	N1	C5	162.4(4)	C23	C24	C25	C26	171.8(4)
C3	C15	C16	C17	-179.4(3)	C24	C25	C26	C27A	164.5(5)
C3	C15	C20	C19	-179.7(3)	C24	C25	C26	C27B	-156.1(15)
C4	C3	C15	C16	123.2(4)	C25	C26	C27A	C28A	63.2(7)
C4	C3	C15	C20	-57.3(4)	C25	C26	C27B	C28B	-60(4)
C7	C6	O2	C5	-66.7(4)	C27A	C26	C27B	C28B	48(3)
C8	C6	O2	C5	59.1(4)	C27B	C26	C27A	C28A	-23(2)
C9	C6	O2	C5	175.5(3)	N1	C1	C2	C3	16.6(4)
C10	C1	C2	C3	134.5(3)	N1	C1	C10	O3	11.2(5)
C10	C1	N1	C4	-108.5(4)	N1	C1	C10	O4	-172.7(3)
C10	C1	N1	C5	58.9(5)	N1	C5	O2	C6	-172.1(3)
C12	C11	O4	C10	174.1(4)	O1	C5	N1	C1	-167.8(4)
C13	C11	O4	C10	56.0(5)	O1	C5	N1	C4	-1.7(6)
C14	C11	O4	C10	-68.7(5)	O1	C5	O2	C6	8.7(6)
C15	C3	C4	N1	162.7(3)	O2	C5	N1	C1	13.0(6)
C15	C16	C17	C18	-0.7(5)	O2	C5	N1	C4	179.2(3)
C16	C15	C20	C19	-0.1(5)	O3	C10	O4	C11	5.4(6)

**Table 8.** Atomic occupancy for C28 H45 N1 O4.

<b>Atom</b>	<b>Occupancy</b>	<b>Atom</b>	<b>Occupancy</b>	<b>Atom</b>	<b>Occupancy</b>
H26A	0.859(10)	H26B	0.859(10)	H26C	0.141(10)
H26D	0.141(10)	C27A	0.859(10)	H27A	0.859(10)
H27B	0.859(10)	C27B	0.141(10)	H27C	0.141(10)
H27D	0.141(10)	C28A	0.859(10)	H28A	0.859(10)
H28B	0.859(10)	H28C	0.859(10)	C28B	0.141(10)
H28D	0.141(10)	H28E	0.141(10)	H28F	0.141(10)



## Experimental

Single crystals of  $C_{28}H_{45}NO_4$  [robe26] were prepared by slow recrystallized from chloroform-hexanes. A suitable crystal was selected and mounted on a loop fiber on a 'Bruker APEX-II CCD' diffractometer. The crystal was kept at 100.15 K during data collection. Using Olex2 [1], the structure was solved with the olex2.solve [2] structure solution program using Charge Flipping and refined with the ShelXL [3] refinement package using Least Squares minimization.

1. Dolomanov, O.V., Bourhis, L.J., Gildea, R.J., Howard, J.A.K. & Puschmann, H. (2009), *J. Appl. Cryst.* 42, 339-341.
2. Bourhis, L.J., Dolomanov, O.V., Gildea, R.J., Howard, J.A.K., Puschmann, H. (2013). in preparation.
3. Sheldrick, G.M. (2008). *Acta Cryst.* A64, 112-122.
4. APEX2 (2008), Bruker AXS Inc., Madison, WI 53719-1173.
5. SAINT (2009) V7.60A, Bruker AXS Inc., Madison, WI 53719-1173.
6. XPREP (2013); X-ray data Preparation and Reciprocal space Exploration Program. Bruker AXS Inc., Madison, WI 53719-1173.

## Crystal structure determination of ROBE26:

**Crystal Data** for  $C_{28}H_{45}NO_4$  ( $M = 459.65$  g/mol): monoclinic, space group C2 (no. 5),  $a = 26.5372(15)$  Å,  $b = 5.5899(4)$  Å,  $c = 20.8906(12)$  Å,  $\beta = 118.206(3)^\circ$ ,  $V = 2730.9(3)$  Å<sup>3</sup>,  $Z = 4$ ,  $T = 100.15$  K,  $\mu(\text{CuK}\alpha) = 0.576$  mm<sup>-1</sup>,  $D_{\text{calc}} = 1.118$  g/cm<sup>3</sup>, 10895 reflections measured ( $4.8^\circ \leq 2\theta \leq 142.454^\circ$ ), 4622 unique ( $R_{\text{int}} = 0.0436$ ,  $R_{\text{sigma}} = 0.0563$ ) which were used in all calculations. The final  $R_1$  was 0.0635 ( $I > 2\sigma(I)$ ) and  $wR_2$  was 0.1628 (all data).

## Refinement model description

Number of restraints - 29, number of constraints - unknown.

Details:

### 1. Fixed Uiso

At 1.2 times of:

All C(H) groups, All C(H,H) groups, All C(H,H,H,H) groups

At 1.5 times of:

All C(H,H,H) groups

### 2. Restrained distances

C27A-C28A

1.54 with sigma of 0.02

C26-C27A

1.54 with sigma of 0.02

C27B-C28B

1.54 with sigma of 0.02

C26-C27B

1.54 with sigma of 0.01

### 3. Uiso/Uanis restraints and constraints

C27A  $\approx$  C27B: within 1.7Å with sigma of 0.01 and sigma for terminal atoms of 0.01

C28A  $\approx$  C28B: within 1.7Å with sigma of 0.01 and sigma for terminal atoms of 0.01

Uanis(C28A)  $\approx$  Ueq, Uanis(C28B)  $\approx$  Ueq: with sigma of 0.005 and sigma for terminal atoms of 0.02

### 4. Others

Sof(H26C)=Sof(H26D)=Sof(C27B)=Sof(H27C)=Sof(H27D)=Sof(C28B)=Sof(H28D)=  
Sof(H28E)=Sof(H28F)=1-FVAR(1)

Sof(H26A)=Sof(H26B)=Sof(C27A)=Sof(H27A)=Sof(H27B)=Sof(C28A)=Sof(H28A)=  
Sof(H28B)=Sof(H28C)=FVAR(1)

### 5.a Ternary CH refined with riding coordinates:

C1(H1), C3(H3)

### 5.b Secondary CH2 refined with riding coordinates:

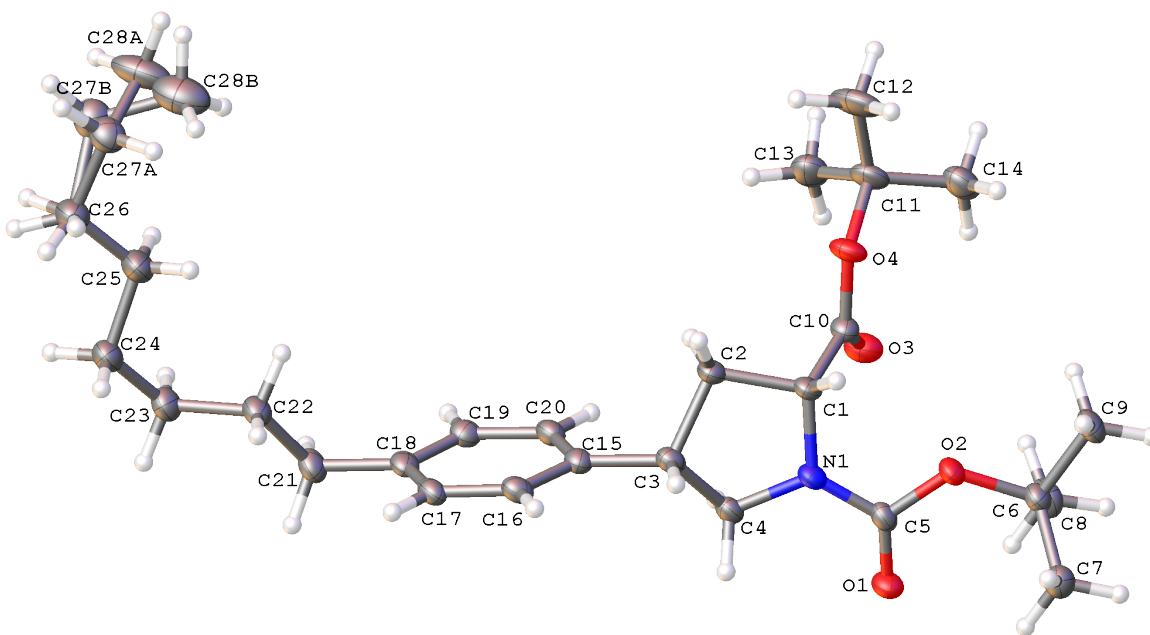
C2(H2A,H2B), C4(H4A,H4B), C21(H21A,H21B), C22(H22A,H22B), C23(H23A,H23B),  
C24(H24A,H24B), C25(H25A,H25B), C26(H26A,H26B), C26(H26C,H26D), C27A(H27A,  
H27B), C27B(H27C,H27D)

5.c Aromatic/amide H refined with riding coordinates:

C16(H16), C17(H17), C19(H19), C20(H20)

5.d Idealised Me refined as rotating group:

C7(H7A,H7B,H7C), C8(H8A,H8B,H8C), C9(H9A,H9B,H9C), C12(H12A,H12B,H12C),  
C13(H13A,H13B,H13C), C14(H14A,H14B,H14C), C28A(H28A,H28B,H28C),  
C28B(H28D,H28E,H28F)



ORTEP view of the C<sub>28</sub> H<sub>45</sub> N<sub>1</sub> O<sub>4</sub> compound with the numbering scheme adopted. Ellipsoids are drawn at the 50% probability level. Hydrogen atoms are represented by spheres of arbitrary size.

## **Annex 59: X-Ray Data for Compound 3.20**

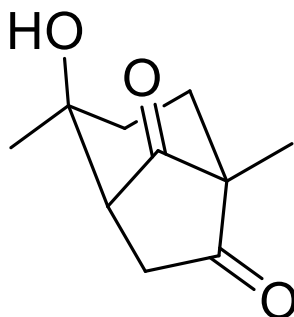
CRYSTAL AND MOLECULAR STRUCTURE OF

C<sub>10</sub> H<sub>14</sub> O<sub>3</sub> COMPOUND (bent63)

Equipe Hanessian

Département de chimie, Université de Montréal,

C.P. 6128, Succ. Centre-Ville, Montréal, Québec, H3C 3J7 (Canada)



**Racemic**

Structure solved and refined in the laboratory of X-ray diffraction Université de Montréal by Benoît Deschênes Simard.

**Table 1.** Crystal data and structure refinement for C10 H14 O3.

Identification code	bent63
Empirical formula	C10 H14 O3
Formula weight	182.21
Temperature	200K
Wavelength	1.54178 Å
Crystal system	Orthorhombic
Space group	Pna21
Unit cell dimensions	a = 12.0380(3) Å $\alpha = 90^\circ$ b = 10.6966(2) Å $\beta = 90^\circ$ c = 7.1306(2) Å $\gamma = 90^\circ$
Volume	918.18(4) Å <sup>3</sup>
Z	4
Density (calculated)	1.318 g/cm <sup>3</sup>
Absorption coefficient	0.793 mm <sup>-1</sup>
F(000)	392
Crystal size	0.18 x 0.11 x 0.09 mm
Theta range for data collection	5.53 to 72.28°
Index ranges	-14 ≤ h ≤ 14, -12 ≤ k ≤ 13, -8 ≤ l ≤ 8
Reflections collected	12321
Independent reflections	1774 [R <sub>int</sub> = 0.031]
Absorption correction	Semi-empirical from equivalents
Max. and min. transmission	0.9311 and 0.8101
Refinement method	Full-matrix least-squares on F <sup>2</sup>
Data / restraints / parameters	1774 / 1 / 122
Goodness-of-fit on F <sup>2</sup>	1.091
Final R indices [I > 2σ(I)]	R <sub>1</sub> = 0.0303, wR <sub>2</sub> = 0.0788
R indices (all data)	R <sub>1</sub> = 0.0307, wR <sub>2</sub> = 0.0795
Absolute structure parameter	0.03(17)

Extinction coefficient                    0.0107(9)  
Largest diff. peak and hole            0.151 and -0.225 e/Å<sup>3</sup>

**Table 2.** Atomic coordinates ( $\times 10^4$ ) and equivalent isotropic displacement parameters ( $\text{Å}^2 \times 10^3$ ) for C10 H14 O3.

$U_{eq}$  is defined as one third of the trace of the orthogonalized  $U_{ij}$  tensor.

	x	y	z	$U_{eq}$
O(1)	3821(1)	4490(1)	4720(2)	39(1)
O(2)	3328(1)	8720(1)	5183(2)	33(1)
O(3)	868(1)	8131(1)	6169(1)	28(1)
C(1)	3441(1)	5482(1)	5263(2)	27(1)
C(2)	3156(1)	6582(1)	4010(2)	26(1)
C(3)	3076(1)	7636(1)	5432(2)	24(1)
C(4)	2562(1)	7066(1)	7177(2)	23(1)
C(5)	1292(1)	6932(1)	6741(2)	24(1)
C(6)	1147(1)	6066(1)	5048(2)	29(1)
C(7)	1912(1)	6386(1)	3402(2)	30(1)
C(8)	3165(1)	5795(1)	7286(2)	27(1)
C(9)	3920(1)	6795(2)	2351(2)	38(1)
C(10)	652(1)	6470(1)	8448(2)	31(1)

**Table 3.** Hydrogen coordinates ( $\times 10^4$ ) and isotropic displacement parameters ( $\text{\AA}^2 \times 10^3$ ) for C10 H14 O3.

	x	y	z	U <sub>eq</sub>
H(3)	952	8648	7044	42
H(4)	2700	7589	8316	28
H(6A)	1293	5195	5446	35
H(6B)	366	6111	4617	35
H(7A)	1640	7158	2790	36
H(7B)	1877	5703	2467	36
H(8A)	3849	5862	8051	32
H(8B)	2676	5149	7842	32
H(9A)	3847	6099	1466	57
H(9B)	4691	6846	2789	57
H(9C)	3718	7578	1724	57
H(10A)	-128	6340	8108	47
H(10B)	700	7093	9452	47
H(10C)	972	5679	8882	47

**Table 4.** Anisotropic parameters ( $\text{\AA}^2 \times 10^3$ ) for C10 H14 O3.

The anisotropic displacement factor exponent takes the form:

$$-2 \pi^2 [ h^2 a^{*2} U_{11} + \dots + 2 h k a^* b^* U_{12} ]$$

	U11	U22	U33	U23	U13	U12
O(1)	46(1)	31(1)	41(1)	-10(1)	-3(1)	11(1)
O(2)	32(1)	24(1)	42(1)	4(1)	1(1)	-4(1)
O(3)	31(1)	23(1)	30(1)	-1(1)	-2(1)	3(1)
C(1)	25(1)	26(1)	29(1)	-3(1)	-2(1)	-1(1)
C(2)	28(1)	29(1)	22(1)	-2(1)	-2(1)	2(1)
C(3)	21(1)	25(1)	26(1)	0(1)	-3(1)	0(1)
C(4)	25(1)	22(1)	22(1)	-1(1)	-1(1)	-2(1)
C(5)	23(1)	22(1)	28(1)	1(1)	0(1)	0(1)
C(6)	26(1)	27(1)	36(1)	-7(1)	-5(1)	-2(1)
C(7)	31(1)	34(1)	27(1)	-8(1)	-7(1)	2(1)
C(8)	27(1)	28(1)	25(1)	3(1)	-1(1)	2(1)
C(9)	39(1)	50(1)	25(1)	1(1)	7(1)	0(1)
C(10)	29(1)	29(1)	35(1)	6(1)	5(1)	1(1)



**Table 5.** Bond lengths [Å] and angles [°] for C10 H14 O3

---

O(1)-C(1)	1.2185(15)	C(1)-C(2)-C(3)	101.37(10)
O(2)-C(3)	1.2119(15)	C(9)-C(2)-C(7)	112.49(11)
O(3)-C(5)	1.4394(13)	C(1)-C(2)-C(7)	105.92(10)
C(1)-C(2)	1.5171(17)	C(3)-C(2)-C(7)	102.86(9)
C(1)-C(8)	1.5186(18)	O(2)-C(3)-C(4)	127.38(12)
C(2)-C(9)	1.5160(19)	O(2)-C(3)-C(2)	126.59(12)
C(2)-C(3)	1.5194(17)	C(4)-C(3)-C(2)	105.96(10)
C(2)-C(7)	1.5728(16)	C(3)-C(4)-C(8)	101.78(9)
C(3)-C(4)	1.5170(17)	C(3)-C(4)-C(5)	105.79(10)
C(4)-C(8)	1.5425(17)	C(8)-C(4)-C(5)	112.86(9)
C(4)-C(5)	1.5667(17)	O(3)-C(5)-C(10)	109.66(10)
C(5)-C(10)	1.5229(18)	O(3)-C(5)-C(6)	105.95(10)
C(5)-C(6)	1.5321(18)	C(10)-C(5)-C(6)	112.07(10)
C(6)-C(7)	1.5313(19)	O(3)-C(5)-C(4)	108.72(9)
		C(10)-C(5)-C(4)	111.41(10)
O(1)-C(1)-C(2)	125.00(12)	C(6)-C(5)-C(4)	108.84(10)
O(1)-C(1)-C(8)	125.22(12)	C(7)-C(6)-C(5)	113.59(10)
C(2)-C(1)-C(8)	109.78(10)	C(6)-C(7)-C(2)	113.05(11)
C(9)-C(2)-C(1)	116.02(11)	C(1)-C(8)-C(4)	104.45(10)
C(9)-C(2)-C(3)	116.62(11)		

---

**Table 6.** Torsion angles [°] for C10 H14 O3.

---

O(1)-C(1)-C(2)-C(9)	-35.89(18)	C(8)-C(4)-C(5)-O(3)	-164.63(10)
C(8)-C(1)-C(2)-C(9)	145.06(12)	C(3)-C(4)-C(5)-C(10)	-175.14(9)
O(1)-C(1)-C(2)-C(3)	-163.25(12)	C(8)-C(4)-C(5)-C(10)	74.41(13)
C(8)-C(1)-C(2)-C(3)	17.71(12)	C(3)-C(4)-C(5)-C(6)	60.80(12)
O(1)-C(1)-C(2)-C(7)	89.69(15)	C(8)-C(4)-C(5)-C(6)	-49.66(13)
C(8)-C(1)-C(2)-C(7)	-89.36(11)	O(3)-C(5)-C(6)-C(7)	69.20(12)
C(9)-C(2)-C(3)-O(2)	19.28(18)	C(10)-C(5)-C(6)-C(7)	-171.23(10)
C(1)-C(2)-C(3)-O(2)	146.25(12)	C(4)-C(5)-C(6)-C(7)	-47.56(14)
C(7)-C(2)-C(3)-O(2)	-104.31(13)	C(5)-C(6)-C(7)-C(2)	48.06(14)
C(9)-C(2)-C(3)-C(4)	-163.58(11)	C(9)-C(2)-C(7)-C(6)	175.40(11)
C(1)-C(2)-C(3)-C(4)	-36.62(11)	C(1)-C(2)-C(7)-C(6)	47.68(13)
C(7)-C(2)-C(3)-C(4)	72.83(11)	C(3)-C(2)-C(7)-C(6)	-58.31(13)
O(2)-C(3)-C(4)-C(8)	-141.48(12)	O(1)-C(1)-C(8)-C(4)	-172.07(12)
C(2)-C(3)-C(4)-C(8)	41.41(11)	C(2)-C(1)-C(8)-C(4)	6.97(12)
O(2)-C(3)-C(4)-C(5)	100.40(13)	C(3)-C(4)-C(8)-C(1)	-28.79(11)
C(2)-C(3)-C(4)-C(5)	-76.71(11)	C(5)-C(4)-C(8)-C(1)	84.13(12)
C(3)-C(4)-C(5)-O(3)	-54.18(12)		

---

**Table 7.** Bond lengths [Å] and angles [°] related to the hydrogen bonding for C10 H14 O3.

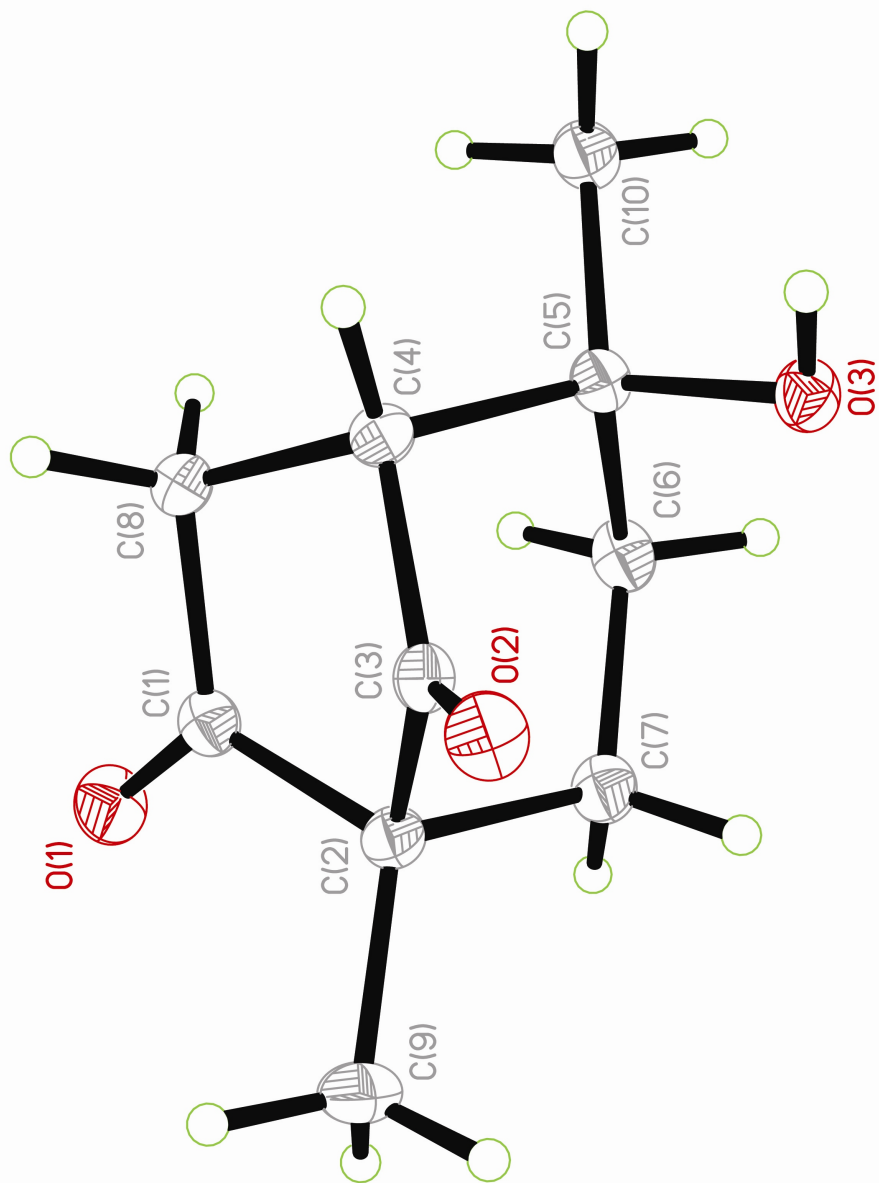
---

D-H	..A	d(D-H)	d(H..A)	d(D..A)	<DHA
O(3)-H(3)	O(1)#1	0.84	2.13	2.9433(14)	163.8

---

Symmetry transformations used to generate equivalent atoms:

#1  $-x+1/2, y+1/2, z+1/2$



ORTEP view of the C<sub>10</sub> H<sub>14</sub> O<sub>3</sub> compound with the numbering scheme adopted. Ellipsoids drawn at 30% probability level. Hydrogen atoms are represented by sphere of arbitrary size.

## REFERENCES

Flack, H.D. (1983). *Acta Cryst.* A39, 876-881.

Flack, H.D. and Schwarzenbach, D. (1988). *Acta Cryst.* A44, 499-506.

SAINT (2006) Release 7.34A; Integration Software for Single Crystal Data. Bruker AXS Inc., Madison, WI 53719-1173.

Sheldrick, G.M. (2004 ). SADABS, Bruker Area Detector Absorption Corrections. Bruker AXS Inc., Madison, WI 53719-1173.

Sheldrick, G.M. (2008). *Acta Cryst.* A64, 112-122.

SHELXTL (2001) version 6.12; Bruker Analytical X-ray Systems Inc., Madison, WI 53719-1173.

APEX2 (2008) ; Bruker Molecular Analysis Research Tool. Bruker AXS Inc., Madison, WI 53719-1173.

Spek, A.L. (2008). PLATON, A Multipurpose Crystallographic Tool, Utrecht University, Utrecht, The Netherlands.

Maris, T. (2004). UdmX, University of Montréal, Montréal, QC, Canada.

XPREP (2008) Version 2008/2; X-ray data Preparation and Reciprocal space Exploration Program. Bruker AXS Inc., Madison, WI 53719-1173.

## **Annex 60: X-Ray Data for Compound 4.7**

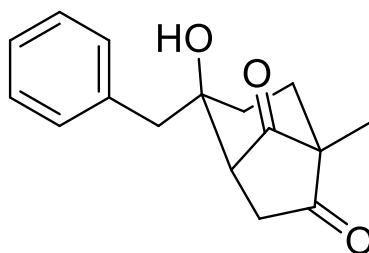
CRYSTAL AND MOLECULAR STRUCTURE OF

C<sub>16</sub> H<sub>18</sub> O<sub>3</sub> COMPOUND (bent93)

Equipe Hanessian

Département de chimie, Université de Montréal,

C.P. 6128, Succ. Centre-Ville, Montréal, Québec, H3C 3J7 (Canada)



Structure solved and refined in the laboratory of X-ray diffraction Université de Montréal by Benoît Deschênes Simard.

**Table 1.** Crystal data and structure refinement for C16 H18 O3.

Identification code	bent93
Empirical formula	C16 H18 O3
Formula weight	258.30
Temperature	100K
Wavelength	1.54178 Å
Crystal system	Orthorhombic
Space group	P212121
Unit cell dimensions	a = 11.8790(2) Å $\alpha = 90^\circ$ b = 12.1705(2) Å $\beta = 90^\circ$ c = 37.5309(8) Å $\gamma = 90^\circ$
Volume	5425.97(17) Å <sup>3</sup>
Z	16
Density (calculated)	1.265 g/cm <sup>3</sup>
Absorption coefficient	0.697 mm <sup>-1</sup>
F(000)	2208
Crystal size	0.10 x 0.06 x 0.04 mm
Theta range for data collection	2.35 to 70.91°
Index ranges	-14 ≤ h ≤ 14, -14 ≤ k ≤ 14, -45 ≤ l ≤ 45
Reflections collected	80689
Independent reflections	10395 [R <sub>int</sub> = 0.041]
Absorption correction	Semi-empirical from equivalents
Max. and min. transmission	0.9725 and 0.9124
Refinement method	Full-matrix least-squares on F <sup>2</sup>
Data / restraints / parameters	10395 / 1 / 694
Goodness-of-fit on F <sup>2</sup>	0.939
Final R indices [I > 2σ(I)]	R <sub>1</sub> = 0.0300, wR <sub>2</sub> = 0.0663
R indices (all data)	R <sub>1</sub> = 0.0362, wR <sub>2</sub> = 0.0677

Absolute structure parameter	0.00(9)
Extinction coefficient	0.00017(2)
Largest diff. peak and hole	0.156 and -0.165 e/Å <sup>3</sup>



**Table 2.** Atomic coordinates ( $\times 10^4$ ) and equivalent isotropic displacement parameters ( $\text{\AA}^2 \times 10^3$ ) for C16 H18 O3.

$U_{eq}$  is defined as one third of the trace of the orthogonalized  $U_{ij}$  tensor.

	x	y	z	$U_{eq}$
O(11)	1935(1)	4998(1)	7963(1)	31(1)
O(12)	5655(1)	5294(1)	7710(1)	28(1)
O(13)	2177(1)	7424(1)	8285(1)	25(1)
C(11)	2798(1)	5526(1)	7934(1)	22(1)
C(12)	3956(1)	5209(1)	8070(1)	22(1)
C(13)	4697(1)	5580(1)	7762(1)	22(1)
C(14)	4045(1)	6396(1)	7535(1)	24(1)
C(15)	2951(1)	6614(1)	7746(1)	22(1)
C(16)	3099(1)	7502(1)	8040(1)	21(1)
C(17)	4151(1)	7246(1)	8260(1)	21(1)
C(18)	4196(1)	6044(1)	8379(1)	24(1)
C(19)	4098(1)	4032(1)	8193(1)	31(1)
C(110)	3136(1)	8636(1)	7862(1)	24(1)
C(111)	3313(1)	9602(1)	8107(1)	24(1)
C(112)	4391(1)	9978(1)	8184(1)	29(1)
C(113)	4552(2)	10879(1)	8404(1)	34(1)
C(114)	3642(2)	11414(1)	8550(1)	36(1)
C(115)	2572(2)	11063(1)	8472(1)	36(1)
C(116)	2404(1)	10165(1)	8252(1)	30(1)
O(21)	10115(1)	8483(1)	7975(1)	36(1)
O(22)	6409(1)	8415(1)	7697(1)	33(1)
O(23)	9878(1)	6047(1)	8209(1)	28(1)
C(21)	9241(1)	8009(1)	7920(1)	27(1)
C(22)	8089(1)	8304(1)	8064(1)	27(1)
C(23)	7339(1)	8047(1)	7746(1)	26(1)
C(24)	7954(1)	7252(1)	7501(1)	27(1)
C(25)	9068(1)	6986(1)	7698(1)	25(1)
C(26)	8941(1)	6025(1)	7970(1)	23(1)
C(27)	7903(1)	6228(1)	8202(1)	24(1)
C(28)	7856(1)	7398(1)	8351(1)	29(1)
C(29)	7968(2)	9449(1)	8214(1)	39(1)
C(210)	8893(1)	4939(1)	7763(1)	25(1)
C(211)	8702(1)	3927(1)	7985(1)	22(1)
C(212)	7611(1)	3583(1)	8066(1)	25(1)
C(213)	7430(1)	2672(1)	8278(1)	30(1)
C(214)	8325(2)	2084(1)	8412(1)	33(1)
C(215)	9406(2)	2399(1)	8326(1)	35(1)
C(216)	9596(1)	3312(1)	8116(1)	29(1)
O(31)	7681(1)	5566(1)	9578(1)	33(1)
O(32)	7262(1)	1894(1)	9775(1)	37(1)
O(33)	5267(1)	5416(1)	9243(1)	28(1)
C(31)	7135(1)	4729(1)	9600(1)	25(1)
C(32)	7434(1)	3615(1)	9450(1)	26(1)
C(33)	7009(1)	2853(1)	9742(1)	28(1)
C(34)	6183(1)	3477(1)	9976(1)	29(1)
C(35)	6010(1)	4576(1)	9783(1)	25(1)
C(36)	5117(1)	4502(1)	9478(1)	23(1)

---

	x	y	z	Ueq
C(37)	5351(1)	3499(1)	9249(1)	26(1)
C(38)	6589(1)	3435(1)	9134(1)	29(1)
C(39)	8645(1)	3449(1)	9333(1)	35(1)
C(310)	3939(1)	4505(1)	9644(1)	26(1)
C(311)	2974(1)	4423(1)	9383(1)	24(1)
C(312)	2459(1)	3421(1)	9312(1)	29(1)
C(313)	1569(1)	3360(2)	9072(1)	36(1)
C(314)	1198(1)	4281(2)	8897(1)	36(1)
C(315)	1703(1)	5277(2)	8962(1)	35(1)
C(316)	2576(1)	5354(1)	9207(1)	30(1)
O(41)	4142(1)	7274(1)	9674(1)	45(1)
O(42)	3978(1)	11005(1)	9784(1)	41(1)
O(43)	6460(1)	7592(1)	9347(1)	35(1)
C(41)	4538(1)	8188(1)	9686(1)	31(1)
C(42)	4067(1)	9201(1)	9511(1)	32(1)
C(43)	4392(1)	10096(1)	9773(1)	29(1)
C(44)	5324(1)	9670(1)	10012(1)	30(1)
C(45)	5628(1)	8538(1)	9855(1)	27(1)
C(46)	6494(1)	8603(1)	9540(1)	25(1)
C(47)	6099(1)	9476(1)	9278(1)	29(1)
C(48)	4850(1)	9351(2)	9180(1)	37(1)
C(49)	2835(1)	9166(2)	9404(1)	49(1)
C(410)	7657(1)	8824(1)	9693(1)	32(1)
C(411)	8606(1)	8934(1)	9427(1)	27(1)
C(412)	9147(1)	8016(1)	9292(1)	36(1)
C(413)	10016(1)	8123(2)	9049(1)	45(1)
C(414)	10372(1)	9151(2)	8942(1)	44(1)
C(415)	9848(2)	10069(2)	9079(1)	44(1)
C(416)	8974(1)	9961(1)	9318(1)	35(1)

---

**Table 3.** Hydrogen coordinates ( $\times 10^4$ ) and isotropic displacement parameters ( $\text{\AA}^2 \times 10^3$ ) for C16 H18 O3.

	x	y	z	U <sub>eq</sub>
H(13)	1580	7615	8182	38
H(14A)	3874	6081	7297	29
H(14B)	4478	7084	7502	29
H(15)	2304	6785	7585	26
H(17A)	4166	7727	8472	25
H(17B)	4827	7412	8115	25
H(18A)	3635	5930	8571	29
H(18B)	4949	5890	8480	29
H(19A)	3927	3532	7995	46
H(19B)	3584	3885	8391	46
H(19C)	4876	3915	8271	46
H(11A)	3749	8632	7683	29
H(11B)	2420	8747	7732	29
H(112)	5024	9612	8085	34
H(113)	5293	11128	8453	41
H(114)	3754	12023	8704	43
H(115)	1942	11440	8569	43
H(116)	1659	9930	8200	36
H(23)	10452	5801	8105	42
H(24A)	8107	7597	7267	32
H(24B)	7504	6577	7463	32
H(25)	9705	6860	7529	30
H(27A)	7905	5700	8402	29
H(27B)	7218	6091	8058	29
H(28A)	8419	7468	8544	35
H(28B)	7103	7525	8456	35
H(29A)	8468	9534	8420	58
H(29B)	7187	9569	8288	58
H(29C)	8171	9988	8031	58
H(21A)	8282	4990	7584	30
H(21B)	9610	4849	7631	30
H(212)	6986	3980	7974	30
H(213)	6683	2448	8331	36
H(214)	8199	1469	8562	40
H(215)	10026	1985	8412	41
H(216)	10346	3521	8060	35
H(33)	5165	6004	9355	43
H(34A)	6498	3595	10217	35
H(34B)	5463	3073	9997	35
H(35)	5841	5187	9953	29
H(37A)	4867	3525	9034	31
H(37B)	5154	2829	9385	31
H(38A)	6730	3999	8949	35
H(38B)	6731	2706	9026	35
H(39A)	8842	4002	9154	52
H(39B)	8729	2713	9230	52
H(39C)	9144	3523	9539	52
H(31A)	3887	3881	9813	31
H(31B)	3849	5189	9784	31
H(312)	2718	2774	9427	35

---

	x	y	z	U <sub>eq</sub>
H(313)	1214	2673	9029	43
H(314)	594	4231	8731	43
H(315)	1455	5915	8839	42
H(316)	2906	6049	9255	36
H(43)	6849	7119	9454	52
H(44A)	5058	9599	10260	36
H(44B)	5982	10169	10006	36
H(45)	5877	8011	10044	33
H(47A)	6559	9429	9059	35
H(47B)	6221	10211	9385	35
H(48A)	4763	8707	9021	45
H(48B)	4606	10010	9046	45
H(49A)	2719	8579	9229	73
H(49B)	2620	9873	9298	73
H(49C)	2371	9024	9614	73
H(41A)	7621	9510	9835	38
H(41B)	7846	8219	9859	38
H(412)	8919	7305	9367	44
H(413)	10371	7485	8956	54
H(414)	10969	9225	8775	52
H(415)	10092	10780	9009	53
H(416)	8618	10600	9410	42

---

**Table 4.** Anisotropic parameters ( $\text{\AA}^2 \times 10^3$ ) for C16 H18 O3.

The anisotropic displacement factor exponent takes the form:

$$-2 \pi^2 [ h^2 a^{*2} U_{11} + \dots + 2 h k a^* b^* U_{12} ]$$

	U11	U22	U33	U23	U13	U12
O(11)	20(1)	25(1)	47(1)	-3(1)	1(1)	-4(1)
O(12)	19(1)	32(1)	34(1)	-7(1)	-1(1)	3(1)
O(13)	18(1)	27(1)	30(1)	2(1)	5(1)	2(1)
C(11)	20(1)	22(1)	24(1)	-5(1)	2(1)	1(1)
C(12)	19(1)	19(1)	28(1)	1(1)	-1(1)	1(1)
C(13)	20(1)	20(1)	25(1)	-7(1)	-4(1)	-1(1)
C(14)	24(1)	25(1)	24(1)	-1(1)	1(1)	2(1)
C(15)	17(1)	24(1)	25(1)	0(1)	-5(1)	2(1)
C(16)	18(1)	22(1)	24(1)	2(1)	2(1)	1(1)
C(17)	19(1)	23(1)	22(1)	0(1)	-1(1)	-2(1)
C(18)	22(1)	26(1)	24(1)	3(1)	-3(1)	2(1)
C(19)	30(1)	24(1)	39(1)	4(1)	-4(1)	2(1)
C(110)	26(1)	23(1)	24(1)	4(1)	-1(1)	3(1)
C(111)	30(1)	18(1)	23(1)	8(1)	2(1)	-1(1)
C(112)	31(1)	26(1)	29(1)	5(1)	9(1)	-4(1)
C(113)	38(1)	29(1)	35(1)	5(1)	0(1)	-15(1)
C(114)	57(1)	17(1)	35(1)	1(1)	2(1)	-3(1)
C(115)	42(1)	27(1)	39(1)	-2(1)	4(1)	10(1)
C(116)	30(1)	26(1)	34(1)	4(1)	-2(1)	3(1)
O(21)	23(1)	26(1)	58(1)	2(1)	-8(1)	-4(1)
O(22)	22(1)	38(1)	40(1)	-2(1)	-5(1)	7(1)
O(23)	19(1)	28(1)	37(1)	-5(1)	-6(1)	3(1)
C(21)	22(1)	21(1)	39(1)	6(1)	-5(1)	-1(1)
C(22)	22(1)	21(1)	39(1)	-6(1)	-5(1)	0(1)
C(23)	23(1)	23(1)	34(1)	2(1)	0(1)	-3(1)
C(24)	24(1)	26(1)	29(1)	1(1)	1(1)	0(1)
C(25)	20(1)	23(1)	31(1)	1(1)	3(1)	-1(1)
C(26)	17(1)	22(1)	28(1)	-3(1)	-3(1)	0(1)
C(27)	20(1)	26(1)	26(1)	-2(1)	-1(1)	-2(1)
C(28)	23(1)	32(1)	32(1)	-7(1)	-2(1)	3(1)
C(29)	35(1)	28(1)	52(1)	-12(1)	-10(1)	6(1)
C(210)	25(1)	24(1)	26(1)	-3(1)	2(1)	-2(1)
C(211)	25(1)	19(1)	23(1)	-7(1)	-2(1)	0(1)
C(212)	24(1)	25(1)	26(1)	-3(1)	-3(1)	1(1)
C(213)	33(1)	27(1)	30(1)	-3(1)	2(1)	-7(1)
C(214)	51(1)	19(1)	30(1)	-1(1)	-1(1)	-2(1)
C(215)	37(1)	24(1)	42(1)	-4(1)	-11(1)	9(1)
C(216)	25(1)	26(1)	38(1)	-9(1)	-1(1)	1(1)
O(31)	26(1)	26(1)	48(1)	1(1)	-2(1)	-3(1)
O(32)	39(1)	25(1)	46(1)	-1(1)	-5(1)	6(1)
O(33)	29(1)	25(1)	31(1)	2(1)	1(1)	0(1)
C(31)	23(1)	25(1)	26(1)	2(1)	-4(1)	2(1)
C(32)	21(1)	28(1)	28(1)	-3(1)	0(1)	2(1)
C(33)	26(1)	26(1)	32(1)	-4(1)	-6(1)	0(1)
C(34)	31(1)	30(1)	26(1)	1(1)	1(1)	2(1)
C(35)	25(1)	22(1)	26(1)	-6(1)	1(1)	0(1)
C(36)	22(1)	23(1)	25(1)	1(1)	0(1)	1(1)

---

	U11	U22	U33	U23	U13	U12
C(37)	25(1)	28(1)	23(1)	-3(1)	-1(1)	-2(1)
C(38)	28(1)	32(1)	27(1)	-7(1)	4(1)	3(1)
C(39)	24(1)	39(1)	42(1)	-7(1)	3(1)	5(1)
C(310)	23(1)	29(1)	26(1)	-2(1)	4(1)	2(1)
C(311)	18(1)	29(1)	25(1)	-3(1)	7(1)	-1(1)
C(312)	25(1)	29(1)	34(1)	0(1)	8(1)	-2(1)
C(313)	27(1)	39(1)	42(1)	-12(1)	8(1)	-12(1)
C(314)	20(1)	57(1)	31(1)	-7(1)	1(1)	-2(1)
C(315)	24(1)	44(1)	37(1)	7(1)	3(1)	7(1)
C(316)	25(1)	28(1)	38(1)	-4(1)	5(1)	-1(1)
O(41)	38(1)	32(1)	67(1)	-7(1)	13(1)	-12(1)
O(42)	42(1)	33(1)	48(1)	-2(1)	4(1)	12(1)
O(43)	29(1)	27(1)	48(1)	-8(1)	-3(1)	1(1)
C(41)	27(1)	28(1)	36(1)	-3(1)	7(1)	-5(1)
C(42)	24(1)	38(1)	33(1)	-4(1)	-5(1)	2(1)
C(43)	26(1)	29(1)	31(1)	3(1)	3(1)	-1(1)
C(44)	28(1)	34(1)	27(1)	-2(1)	0(1)	-2(1)
C(45)	29(1)	25(1)	28(1)	7(1)	-1(1)	-1(1)
C(46)	24(1)	24(1)	27(1)	-1(1)	-3(1)	-2(1)
C(47)	31(1)	33(1)	25(1)	3(1)	2(1)	2(1)
C(48)	36(1)	49(1)	27(1)	1(1)	-6(1)	10(1)
C(49)	27(1)	65(1)	54(1)	-13(1)	-10(1)	7(1)
C(410)	27(1)	38(1)	30(1)	0(1)	-6(1)	-2(1)
C(411)	21(1)	28(1)	32(1)	-2(1)	-8(1)	-1(1)
C(412)	26(1)	28(1)	55(1)	-2(1)	-8(1)	-1(1)
C(413)	23(1)	57(1)	55(1)	-20(1)	-5(1)	6(1)
C(414)	21(1)	75(2)	35(1)	3(1)	-1(1)	-5(1)
C(415)	31(1)	46(1)	54(1)	16(1)	-5(1)	-8(1)
C(416)	28(1)	30(1)	48(1)	-3(1)	-5(1)	1(1)

---

**Table 5.** Bond lengths [Å] and angles [°] for C16 H18 O3

---

O(11)-C(11)	1.2143(17)	C(36)-C(310)	1.533(2)
O(12)-C(13)	1.2058(16)	C(37)-C(38)	1.535(2)
O(13)-C(16)	1.4314(16)	C(310)-C(311)	1.512(2)
C(11)-C(15)	1.511(2)	C(311)-C(312)	1.391(2)
C(11)-C(12)	1.5177(19)	C(311)-C(316)	1.393(2)
C(12)-C(19)	1.515(2)	C(312)-C(313)	1.390(2)
C(12)-C(13)	1.522(2)	C(313)-C(314)	1.373(2)
C(12)-C(18)	1.569(2)	C(314)-C(315)	1.374(2)
C(13)-C(14)	1.520(2)	C(315)-C(316)	1.390(2)
C(14)-C(15)	1.5447(19)	O(41)-C(41)	1.2089(18)
C(15)-C(16)	1.556(2)	O(42)-C(43)	1.2115(18)
C(16)-C(17)	1.5284(19)	O(43)-C(46)	1.4272(18)
C(16)-C(110)	1.5341(19)	C(41)-C(42)	1.505(2)
C(17)-C(18)	1.531(2)	C(41)-C(45)	1.505(2)
C(110)-C(111)	1.507(2)	C(42)-C(43)	1.517(2)
C(111)-C(112)	1.390(2)	C(42)-C(49)	1.518(2)
C(111)-C(116)	1.391(2)	C(42)-C(48)	1.561(2)
C(112)-C(113)	1.385(2)	C(43)-C(44)	1.516(2)
C(113)-C(114)	1.376(2)	C(44)-C(45)	1.540(2)
C(114)-C(115)	1.373(2)	C(45)-C(46)	1.571(2)
C(115)-C(116)	1.384(2)	C(46)-C(47)	1.519(2)
O(21)-C(21)	1.2062(17)	C(46)-C(410)	1.522(2)
O(22)-C(23)	1.2065(17)	C(47)-C(48)	1.537(2)
O(23)-C(26)	1.4301(16)	C(410)-C(411)	1.513(2)
C(21)-C(25)	1.511(2)	C(411)-C(412)	1.384(2)
C(21)-C(22)	1.514(2)	C(411)-C(416)	1.385(2)
C(22)-C(29)	1.510(2)	C(412)-C(413)	1.383(3)
C(22)-C(23)	1.520(2)	C(413)-C(414)	1.381(3)
C(22)-C(28)	1.566(2)	C(414)-C(415)	1.378(3)
C(23)-C(24)	1.522(2)	C(415)-C(416)	1.379(2)
C(24)-C(25)	1.551(2)		
C(25)-C(26)	1.559(2)	O(11)-C(11)-C(15)	127.39(13)
C(26)-C(27)	1.5297(19)	O(11)-C(11)-C(12)	126.89(14)
C(26)-C(210)	1.534(2)	C(15)-C(11)-C(12)	105.70(12)
C(27)-C(28)	1.531(2)	C(19)-C(12)-C(11)	116.36(12)
C(210)-C(211)	1.504(2)	C(19)-C(12)-C(13)	116.59(13)
C(211)-C(216)	1.389(2)	C(11)-C(12)-C(13)	101.06(12)
C(211)-C(212)	1.395(2)	C(19)-C(12)-C(18)	111.59(12)
C(212)-C(213)	1.381(2)	C(11)-C(12)-C(18)	104.43(11)
C(213)-C(214)	1.377(2)	C(13)-C(12)-C(18)	105.39(11)
C(214)-C(215)	1.378(2)	O(12)-C(13)-C(14)	125.48(14)
C(215)-C(216)	1.382(2)	O(12)-C(13)-C(12)	125.51(14)
O(31)-C(31)	1.2110(17)	C(14)-C(13)-C(12)	108.99(11)
O(32)-C(33)	1.2120(18)	C(13)-C(14)-C(15)	104.65(12)
O(33)-C(36)	1.4316(17)	C(11)-C(15)-C(14)	100.96(11)
C(31)-C(32)	1.510(2)	C(11)-C(15)-C(16)	106.96(12)
C(31)-C(35)	1.515(2)	C(14)-C(15)-C(16)	112.90(12)
C(32)-C(39)	1.516(2)	O(13)-C(16)-C(17)	105.51(11)
C(32)-C(33)	1.522(2)	O(13)-C(16)-C(110)	111.20(11)
C(32)-C(38)	1.570(2)	C(17)-C(16)-C(110)	113.29(12)
C(33)-C(34)	1.521(2)	O(13)-C(16)-C(15)	108.83(11)
C(34)-C(35)	1.534(2)	C(17)-C(16)-C(15)	109.40(11)
C(35)-C(36)	1.564(2)	C(110)-C(16)-C(15)	108.51(12)
C(36)-C(37)	1.517(2)	C(16)-C(17)-C(18)	112.41(12)

C(17)-C(18)-C(12)	113.32(12)	O(33)-C(36)-C(37)	104.71(12)
C(111)-C(110)-C(16)	116.03(12)	O(33)-C(36)-C(310)	111.27(12)
C(112)-C(111)-C(116)	118.16(14)	C(37)-C(36)-C(310)	113.54(13)
C(112)-C(111)-C(110)	120.84(13)	O(33)-C(36)-C(35)	108.82(12)
C(116)-C(111)-C(110)	120.97(14)	C(37)-C(36)-C(35)	109.71(12)
C(113)-C(112)-C(111)	120.79(15)	C(310)-C(36)-C(35)	108.66(12)
C(114)-C(113)-C(112)	120.25(16)	C(36)-C(37)-C(38)	112.04(13)
C(115)-C(114)-C(113)	119.64(16)	C(37)-C(38)-C(32)	113.16(12)
C(114)-C(115)-C(116)	120.44(16)	C(311)-C(310)-C(36)	115.30(12)
C(115)-C(116)-C(111)	120.69(16)	C(312)-C(311)-C(316)	118.23(14)
O(21)-C(21)-C(25)	127.23(15)	C(312)-C(311)-C(310)	121.01(14)
O(21)-C(21)-C(22)	127.15(15)	C(316)-C(311)-C(310)	120.76(14)
C(25)-C(21)-C(22)	105.61(12)	C(313)-C(312)-C(311)	120.36(16)
C(29)-C(22)-C(21)	115.97(13)	C(314)-C(313)-C(312)	120.74(16)
C(29)-C(22)-C(23)	115.24(13)	C(313)-C(314)-C(315)	119.64(16)
C(21)-C(22)-C(23)	101.60(13)	C(314)-C(315)-C(316)	120.20(16)
C(29)-C(22)-C(28)	112.13(14)	C(315)-C(316)-C(311)	120.81(15)
C(21)-C(22)-C(28)	103.74(12)	O(41)-C(41)-C(42)	126.36(16)
C(23)-C(22)-C(28)	106.92(12)	O(41)-C(41)-C(45)	127.68(16)
O(22)-C(23)-C(22)	125.48(15)	C(42)-C(41)-C(45)	105.85(13)
O(22)-C(23)-C(24)	125.60(15)	C(41)-C(42)-C(43)	102.17(13)
C(22)-C(23)-C(24)	108.93(12)	C(41)-C(42)-C(49)	116.82(15)
C(23)-C(24)-C(25)	104.64(12)	C(43)-C(42)-C(49)	115.89(14)
C(21)-C(25)-C(24)	101.94(12)	C(41)-C(42)-C(48)	102.80(13)
C(21)-C(25)-C(26)	105.75(12)	C(43)-C(42)-C(48)	106.20(14)
C(24)-C(25)-C(26)	112.75(12)	C(49)-C(42)-C(48)	111.53(14)
O(23)-C(26)-C(27)	105.50(12)	O(42)-C(43)-C(44)	125.97(15)
O(23)-C(26)-C(210)	111.30(12)	O(42)-C(43)-C(42)	125.17(15)
C(27)-C(26)-C(210)	113.45(12)	C(44)-C(43)-C(42)	108.86(13)
O(23)-C(26)-C(25)	108.71(11)	C(43)-C(44)-C(45)	104.62(13)
C(27)-C(26)-C(25)	109.16(12)	C(41)-C(45)-C(44)	102.23(12)
C(210)-C(26)-C(25)	108.60(12)	C(41)-C(45)-C(46)	104.95(13)
C(26)-C(27)-C(28)	112.83(12)	C(44)-C(45)-C(46)	113.30(12)
C(27)-C(28)-C(22)	113.37(13)	O(43)-C(46)-C(47)	105.52(12)
C(211)-C(210)-C(26)	115.45(12)	O(43)-C(46)-C(410)	111.72(13)
C(216)-C(211)-C(212)	118.09(14)	C(47)-C(46)-C(410)	113.65(13)
C(216)-C(211)-C(210)	121.43(14)	O(43)-C(46)-C(45)	108.68(12)
C(212)-C(211)-C(210)	120.48(13)	C(47)-C(46)-C(45)	108.68(12)
C(213)-C(212)-C(211)	120.75(14)	C(410)-C(46)-C(45)	108.45(12)
C(214)-C(213)-C(212)	120.52(15)	C(46)-C(47)-C(48)	112.55(13)
C(213)-C(214)-C(215)	119.26(16)	C(47)-C(48)-C(42)	113.34(13)
C(214)-C(215)-C(216)	120.64(15)	C(411)-C(410)-C(46)	116.14(13)
C(215)-C(216)-C(211)	120.70(15)	C(412)-C(411)-C(416)	118.27(15)
O(31)-C(31)-C(32)	127.14(14)	C(412)-C(411)-C(410)	121.09(15)
O(31)-C(31)-C(35)	127.41(14)	C(416)-C(411)-C(410)	120.62(15)
C(32)-C(31)-C(35)	105.45(12)	C(413)-C(412)-C(411)	120.77(17)
C(31)-C(32)-C(39)	116.78(13)	C(414)-C(413)-C(412)	120.40(18)
C(31)-C(32)-C(33)	101.56(12)	C(415)-C(414)-C(413)	119.11(17)
C(39)-C(32)-C(33)	116.22(13)	C(414)-C(415)-C(416)	120.42(17)
C(31)-C(32)-C(38)	104.86(12)	C(415)-C(416)-C(411)	121.01(17)
C(39)-C(32)-C(38)	111.68(13)		
C(33)-C(32)-C(38)	104.25(12)		
O(32)-C(33)-C(34)	125.57(15)		
O(32)-C(33)-C(32)	125.38(15)		
C(34)-C(33)-C(32)	109.01(12)		
C(33)-C(34)-C(35)	104.42(12)		
C(31)-C(35)-C(34)	101.71(12)		
C(31)-C(35)-C(36)	105.86(12)		
C(34)-C(35)-C(36)	112.73(12)		



**Table 6.** Torsion angles [ $^{\circ}$ ] for C16 H18 O3.

---

O(11)-C(11)-C(12)-C(19)	12.3(2)	C(21)-C(22)-C(23)-O(22)	-158.85(16)
C(15)-C(11)-C(12)-C(19)	-166.12(13)	C(28)-C(22)-C(23)-O(22)	92.73(18)
O(11)-C(11)-C(12)-C(13)	139.61(15)	C(29)-C(22)-C(23)-C(24)	147.21(14)
C(15)-C(11)-C(12)-C(13)	-38.82(14)	C(21)-C(22)-C(23)-C(24)	20.99(16)
O(11)-C(11)-C(12)-C(18)	-111.15(16)	C(28)-C(22)-C(23)-C(24)	-87.43(14)
C(15)-C(11)-C(12)-C(18)	70.41(14)	O(22)-C(23)-C(24)-C(25)	-176.46(15)
C(19)-C(12)-C(13)-O(12)	-35.8(2)	C(22)-C(23)-C(24)-C(25)	3.70(16)
C(11)-C(12)-C(13)-O(12)	-162.95(14)	O(21)-C(21)-C(25)-C(24)	-139.39(17)
C(18)-C(12)-C(13)-O(12)	88.55(17)	C(22)-C(21)-C(25)-C(24)	41.48(15)
C(19)-C(12)-C(13)-C(14)	145.81(13)	O(21)-C(21)-C(25)-C(26)	102.55(18)
C(11)-C(12)-C(13)-C(14)	18.67(14)	C(22)-C(21)-C(25)-C(26)	-76.58(14)
C(18)-C(12)-C(13)-C(14)	-89.83(13)	C(23)-C(24)-C(25)-C(21)	-26.97(15)
O(12)-C(13)-C(14)-C(15)	-171.12(14)	C(23)-C(24)-C(25)-C(26)	85.96(15)
C(12)-C(13)-C(14)-C(15)	7.26(15)	C(21)-C(25)-C(26)-O(23)	-52.57(14)
O(11)-C(11)-C(15)-C(14)	-134.79(16)	C(24)-C(25)-C(26)-O(23)	-163.15(11)
C(12)-C(11)-C(15)-C(14)	43.63(14)	C(21)-C(25)-C(26)-C(27)	62.03(14)
O(11)-C(11)-C(15)-C(16)	106.95(17)	C(24)-C(25)-C(26)-C(27)	-48.54(16)
C(12)-C(11)-C(15)-C(16)	-74.63(13)	C(21)-C(25)-C(26)-C(210)	-173.81(12)
C(13)-C(14)-C(15)-C(11)	-30.28(14)	C(24)-C(25)-C(26)-C(210)	75.61(15)
C(13)-C(14)-C(15)-C(16)	83.57(14)	O(23)-C(26)-C(27)-C(28)	68.70(15)
C(11)-C(15)-C(16)-O(13)	-53.14(14)	C(210)-C(26)-C(27)-C(28)	-169.22(13)
C(14)-C(15)-C(16)-O(13)	-163.31(11)	C(25)-C(26)-C(27)-C(28)	-47.97(16)
C(11)-C(15)-C(16)-C(17)	61.67(14)	C(26)-C(27)-C(28)-C(22)	47.31(17)
C(14)-C(15)-C(16)-C(17)	-48.49(16)	C(29)-C(22)-C(28)-C(27)	176.55(13)
C(11)-C(15)-C(16)-C(110)	-174.28(11)	C(21)-C(22)-C(28)-C(27)	-57.58(16)
C(14)-C(15)-C(16)-C(110)	75.56(15)	C(23)-C(22)-C(28)-C(27)	49.33(16)
O(13)-C(16)-C(17)-C(18)	68.48(15)	O(23)-C(26)-C(210)-C(211)	63.86(16)
C(110)-C(16)-C(17)-C(18)	-169.65(12)	C(27)-C(26)-C(210)-C(211)	-54.94(17)
C(15)-C(16)-C(17)-C(18)	-48.45(16)	C(25)-C(26)-C(210)-C(211)	-176.51(12)
C(16)-C(17)-C(18)-C(12)	48.30(17)	C(26)-C(210)-C(211)-C(216)	-92.43(17)
C(19)-C(12)-C(18)-C(17)	175.52(12)	C(26)-C(210)-C(211)-C(212)	87.41(17)
C(11)-C(12)-C(18)-C(17)	-57.97(15)	C(216)-C(211)-C(212)-C(213)	1.6(2)
C(13)-C(12)-C(18)-C(17)	48.07(15)	C(210)-C(211)-C(212)-C(213)	-178.29(13)
O(13)-C(16)-C(110)-C(111)	62.21(16)	C(211)-C(212)-C(213)-C(214)	-0.1(2)
C(17)-C(16)-C(110)-C(111)	-56.43(17)	C(212)-C(213)-C(214)-C(215)	-1.6(2)
C(15)-C(16)-C(110)-C(111)	-178.13(12)	C(213)-C(214)-C(215)-C(216)	1.8(2)
C(16)-C(110)-C(111)-C(112)	90.45(17)	C(214)-C(215)-C(216)-C(211)	-0.3(2)
C(16)-C(110)-C(111)-C(116)	-91.73(17)	C(212)-C(211)-C(216)-C(215)	-1.3(2)
C(116)-C(111)-C(112)-C(113)	0.9(2)	C(210)-C(211)-C(216)-C(215)	178.51(14)
C(110)-C(111)-C(112)-C(113)	178.76(14)	O(31)-C(31)-C(32)-C(39)	15.1(2)
C(111)-C(112)-C(113)-C(114)	0.2(2)	C(35)-C(31)-C(32)-C(39)	-165.08(13)
C(112)-C(113)-C(114)-C(115)	-1.3(2)	O(31)-C(31)-C(32)-C(33)	142.54(16)
C(113)-C(114)-C(115)-C(116)	1.2(3)	C(35)-C(31)-C(32)-C(33)	-37.61(14)
C(114)-C(115)-C(116)-C(111)	0.0(2)	O(31)-C(31)-C(32)-C(38)	-109.14(17)
C(112)-C(111)-C(116)-C(115)	-1.0(2)	C(35)-C(31)-C(32)-C(38)	70.71(14)
C(110)-C(111)-C(116)-C(115)	-178.86(14)	C(31)-C(32)-C(33)-O(32)	-164.12(15)
O(21)-C(21)-C(22)-C(29)	16.3(3)	C(39)-C(32)-C(33)-O(32)	-36.3(2)
C(25)-C(21)-C(22)-C(29)	-164.59(14)	C(38)-C(32)-C(33)-O(32)	87.09(18)
O(21)-C(21)-C(22)-C(23)	142.03(17)	C(31)-C(32)-C(33)-C(34)	17.96(15)
C(25)-C(21)-C(22)-C(23)	-38.84(15)	C(39)-C(32)-C(33)-C(34)	145.79(14)
O(21)-C(21)-C(22)-C(28)	-107.11(18)	C(38)-C(32)-C(33)-C(34)	-90.84(14)
C(25)-C(21)-C(22)-C(28)	72.01(14)	O(32)-C(33)-C(34)-C(35)	-170.26(15)
C(29)-C(22)-C(23)-O(22)	-32.6(2)	C(32)-C(33)-C(34)-C(35)	7.66(16)

O(31)-C(31)-C(35)-C(34) -137.27(16)  
C(32)-C(31)-C(35)-C(34) 42.88(14)  
O(31)-C(31)-C(35)-C(36) 104.76(18)  
C(32)-C(31)-C(35)-C(36) -75.09(14)  
C(33)-C(34)-C(35)-C(31) -30.07(15)  
C(33)-C(34)-C(35)-C(36) 82.85(15)  
C(31)-C(35)-C(36)-O(33) -51.02(15)  
C(34)-C(35)-C(36)-O(33) -161.38(12)  
C(31)-C(35)-C(36)-C(37) 63.00(15)  
C(34)-C(35)-C(36)-C(37) -47.36(16)  
C(31)-C(35)-C(36)-C(310) -172.34(12)  
C(34)-C(35)-C(36)-C(310) 77.31(15)  
O(33)-C(36)-C(37)-C(38) 67.15(15)  
C(310)-C(36)-C(37)-C(38) -171.28(13)  
C(35)-C(36)-C(37)-C(38) -49.49(17)  
C(36)-C(37)-C(38)-C(32) 47.99(18)  
C(31)-C(32)-C(38)-C(37) -57.54(17)  
C(39)-C(32)-C(38)-C(37) 175.08(14)  
C(33)-C(32)-C(38)-C(37) 48.80(17)  
O(33)-C(36)-C(310)-C(311) 60.87(17)  
C(37)-C(36)-C(310)-C(311) -56.96(18)  
C(35)-C(36)-C(310)-C(311) -179.34(13)  
C(36)-C(310)-C(311)-C(312) 97.48(17)  
C(36)-C(310)-C(311)-C(316) -82.60(18)  
C(316)-C(311)-C(312)-C(313) -0.3(2)  
C(310)-C(311)-C(312)-C(313) 179.65(14)  
C(311)-C(312)-C(313)-C(314) 1.3(2)  
C(312)-C(313)-C(314)-C(315) -0.7(2)  
C(313)-C(314)-C(315)-C(316) -0.8(2)  
C(314)-C(315)-C(316)-C(311) 1.8(2)  
C(312)-C(311)-C(316)-C(315) -1.3(2)  
C(310)-C(311)-C(316)-C(315) 178.83(14)  
O(41)-C(41)-C(42)-C(43) 146.93(17)  
C(45)-C(41)-C(42)-C(43) -36.73(16)  
O(41)-C(41)-C(42)-C(49) 19.4(3)  
C(45)-C(41)-C(42)-C(49) -164.28(15)  
O(41)-C(41)-C(42)-C(48) -103.09(19)  
C(45)-C(41)-C(42)-C(48) 73.26(15)  
C(41)-C(42)-C(43)-O(42) -162.36(16)  
C(49)-C(42)-C(43)-O(42) -34.2(2)  
C(48)-C(42)-C(43)-O(42) 90.26(19)  
C(41)-C(42)-C(43)-C(44) 18.32(17)  
C(49)-C(42)-C(43)-C(44) 146.48(16)  
C(48)-C(42)-C(43)-C(44) -89.06(15)  
O(42)-C(43)-C(44)-C(45) -173.30(16)  
C(42)-C(43)-C(44)-C(45) 6.01(16)  
O(41)-C(41)-C(45)-C(44) -142.93(17)  
C(42)-C(41)-C(45)-C(44) 40.79(15)  
O(41)-C(41)-C(45)-C(46) 98.60(19)  
C(42)-C(41)-C(45)-C(46) -77.68(15)  
C(43)-C(44)-C(45)-C(41) -27.93(15)  
C(43)-C(44)-C(45)-C(46) 84.45(15)  
C(41)-C(45)-C(46)-O(43) -51.89(15)  
C(44)-C(45)-C(46)-O(43) -162.61(12)  
C(41)-C(45)-C(46)-C(47) 62.46(15)  
C(44)-C(45)-C(46)-C(47) -48.25(16)  
C(41)-C(45)-C(46)-C(410) -173.54(13)  
C(44)-C(45)-C(46)-C(410) 75.75(16)  
O(43)-C(46)-C(47)-C(48) 67.79(16)  
C(410)-C(46)-C(47)-C(48) -169.47(14)  
C(45)-C(46)-C(47)-C(48) -48.62(17)  
C(46)-C(47)-C(48)-C(42) 48.44(19)  
C(41)-C(42)-C(48)-C(47) -58.29(18)  
C(43)-C(42)-C(48)-C(47) 48.64(18)  
C(49)-C(42)-C(48)-C(47) 175.76(15)  
O(43)-C(46)-C(410)-C(411) 61.26(18)  
C(47)-C(46)-C(410)-C(411) -58.01(19)  
C(45)-C(46)-C(410)-C(411) -178.98(13)  
C(46)-C(410)-C(411)-C(412) -83.53(19)  
C(46)-C(410)-C(411)-C(416) 98.19(18)  
C(416)-C(411)-C(412)-C(413) -1.4(2)  
C(410)-C(411)-C(412)-C(413) -179.76(15)  
C(411)-C(412)-C(413)-C(414) 1.2(3)  
C(412)-C(413)-C(414)-C(415) -0.1(3)  
C(413)-C(414)-C(415)-C(416) -0.7(3)  
C(414)-C(415)-C(416)-C(411) 0.3(3)  
C(412)-C(411)-C(416)-C(415) 0.7(2)  
C(410)-C(411)-C(416)-C(415) 179.02(15)

**Table 7.** Bond lengths [ $\text{\AA}$ ] and angles [ $^\circ$ ] related to the hydrogen bonding for C16 H18 O3.

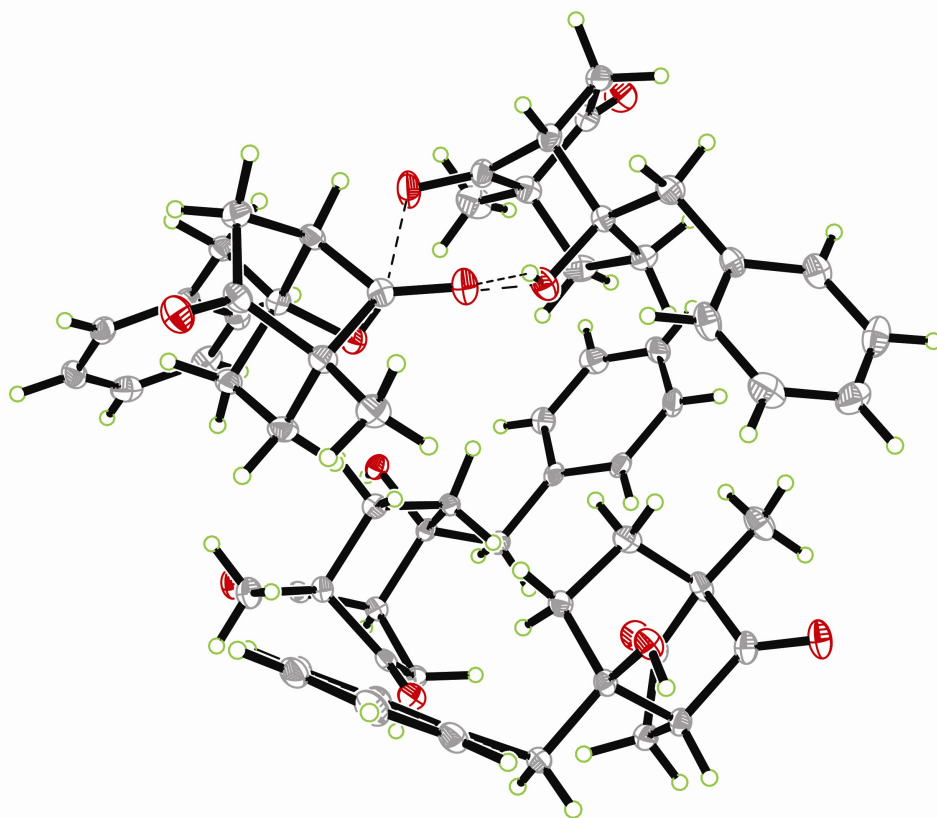
---

D-H	..A	d(D-H)	d(H..A)	d(D..A)	<DHA
O(13)-H(13)	O(21)#1	0.84	2.18	3.0019(14)	166.4
O(23)-H(23)	O(11)#2	0.84	2.08	2.9078(15)	166.3
O(33)-H(33)	O(41)	0.84	2.3	3.0841(16)	155.5
O(33)-H(33)	O(43)	0.84	2.47	3.0288(15)	124.7
O(43)-H(43)	O(31)	0.84	2.18	2.9885(15)	160.7

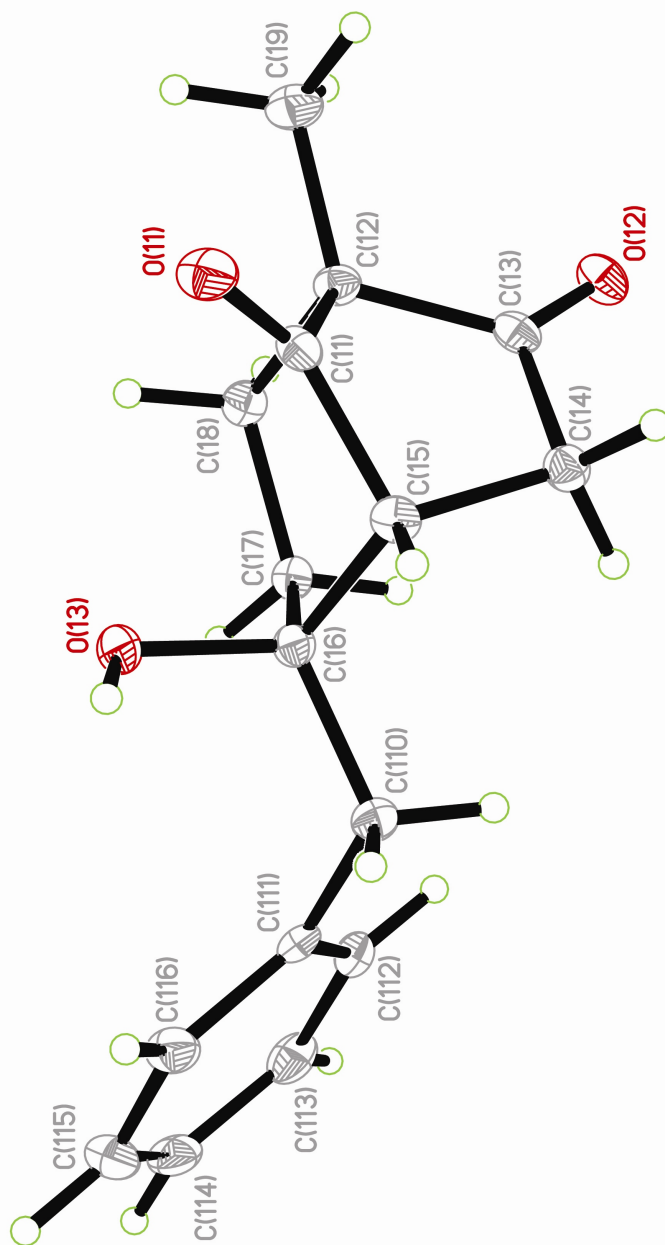
---

Symmetry transformations used to generate equivalent atoms:

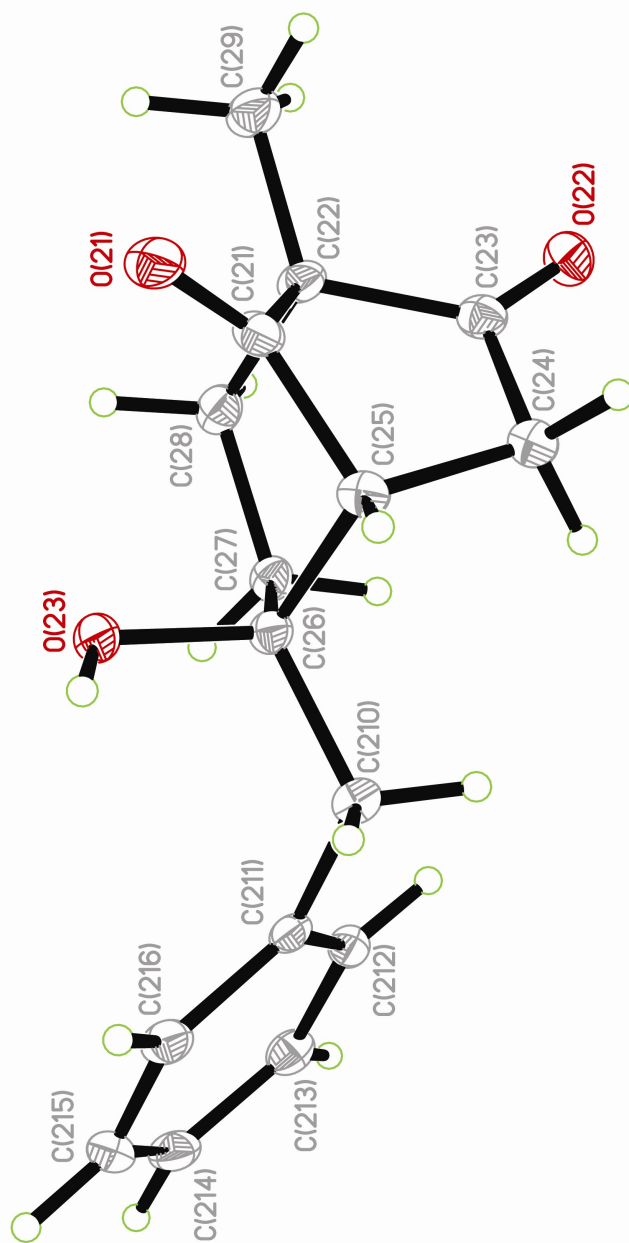
#1  $x-1, y, z$     #2  $x+1, y, z$



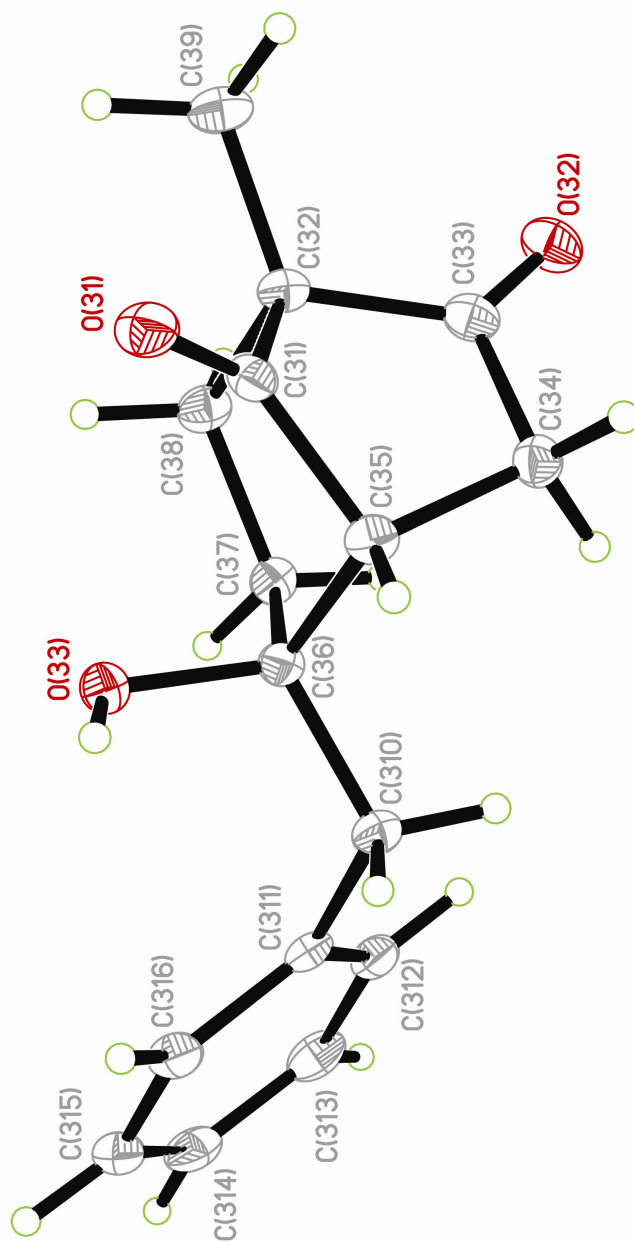
ORTEP (Asymmetric unit) view of the C<sub>16</sub> H<sub>18</sub> O<sub>3</sub> compound with the numbering scheme adopted. Ellipsoids drawn at 30% probability level. Hydrogen atoms are represented by sphere of arbitrary size.



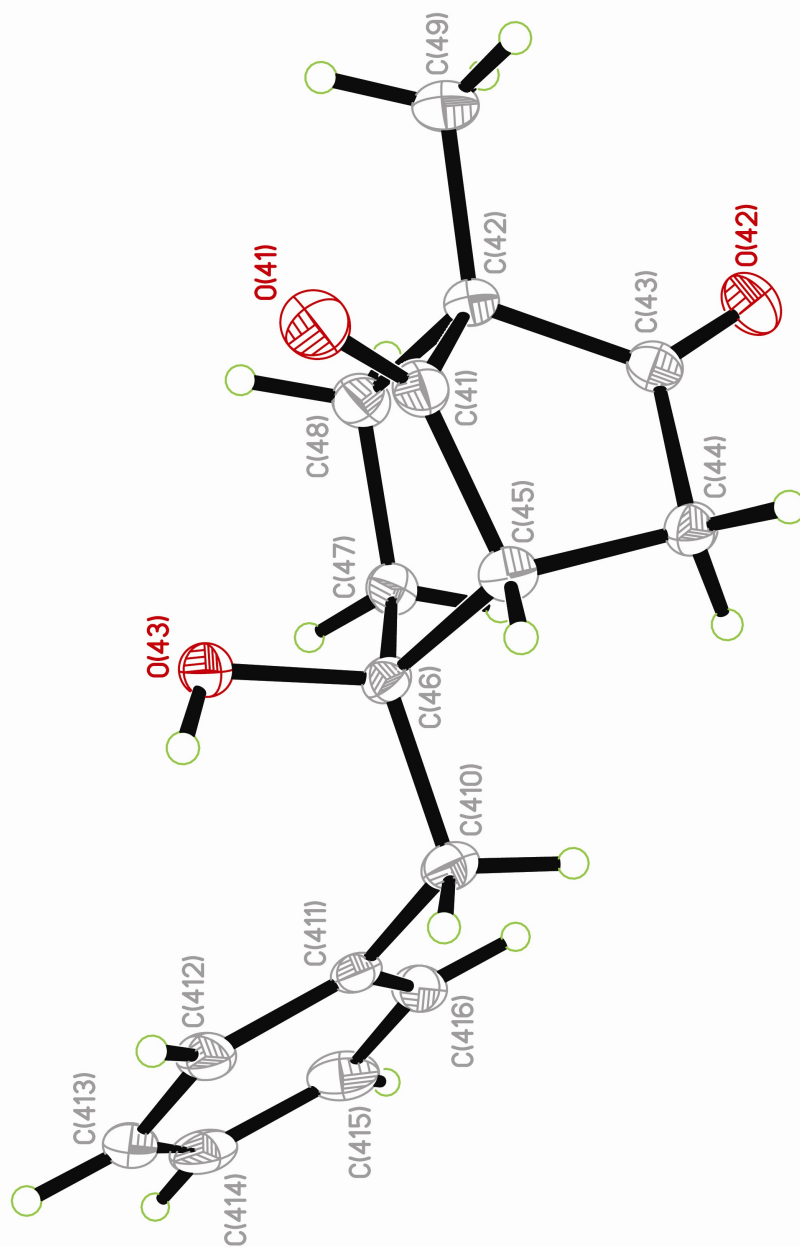
ORTEP 1 view of the C<sub>16</sub> H<sub>18</sub> O<sub>3</sub> compound with the numbering scheme adopted. Ellipsoids drawn at 30% probability level. Hydrogen atoms are represented by sphere of arbitrary size.



ORTEP 2 view of the C<sub>16</sub> H<sub>18</sub> O<sub>3</sub> compound with the numbering scheme adopted. Ellipsoids drawn at 30% probability level. Hydrogen atoms are represented by sphere of arbitrary size.



ORTEP 3 view of the C<sub>16</sub> H<sub>18</sub> O<sub>3</sub> compound with the numbering scheme adopted. Ellipsoids drawn at 30% probability level. Hydrogen atoms are represented by sphere of arbitrary size.



ORTEP 4 view of the C<sub>16</sub> H<sub>18</sub> O<sub>3</sub> compound with the numbering scheme adopted. Ellipsoids drawn at 30% probability level. Hydrogen atoms are represented by sphere of arbitrary size.



## REFERENCES

Flack, H.D. (1983). *Acta Cryst.* A39, 876-881.

Flack, H.D. and Schwarzenbach, D. (1988). *Acta Cryst.* A44, 499-506.

SAINT (2006) Release 7.34A; Integration Software for Single Crystal Data. Bruker AXS Inc., Madison, WI 53719-1173.

Sheldrick, G.M. (1996). SADABS, Bruker Area Detector Absorption Corrections. Bruker AXS Inc., Madison, WI 53719-1173.

Sheldrick, G.M. (2008). *Acta Cryst.* A64, 112-122.

SHELXTL (2001) version 6.12; Bruker Analytical X-ray Systems Inc., Madison, WI 53719-1173.

APEX2 (2008) ; Bruker Molecular Analysis Research Tool. Bruker AXS Inc., Madison, WI 53719-1173.

Spek, A.L. (2008). PLATON, A Multipurpose Crystallographic Tool, Utrecht University, Utrecht, The Netherlands.

Maris, T. (2004). UdmX, University of Montréal, Montréal, QC, Canada.

XPREP (2008) Version 2008/2; X-ray data Preparation and Reciprocal space Exploration Program. Bruker AXS Inc., Madison, WI 53719-1173.

## Annex 61: X-Ray Data for Compound 4.8

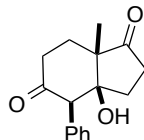


**Table 1 Crystal data and structure refinement for han470.**

Identification code	han470
Empirical formula	C <sub>16</sub> H <sub>18</sub> O <sub>3</sub>
Formula weight	258.30
Temperature/K	100
Crystal system	orthorhombic
Space group	Pna2 <sub>1</sub>
a/Å	13.0120 (7)
b/Å	6.5847 (3)
c/Å	15.4360 (8)
α/°	90
β/°	90
γ/°	90
Volume/Å <sup>3</sup>	1322.56 (12)
Z	4
ρ <sub>calc</sub> /cm <sup>3</sup>	1.297
μ/mm <sup>-1</sup>	0.459
F(000)	552.0
Crystal size/mm <sup>3</sup>	0.24 × 0.16 × 0.12
Radiation	GaKα (λ = 1.34139)
2θ range for data collection/°	12.846 to 121.428
Index ranges	-16 ≤ h ≤ 16, -8 ≤ k ≤ 8, -20 ≤ l ≤ 20
Reflections collected	56212
Independent reflections	3007 [R <sub>int</sub> = 0.0263, R <sub>sigma</sub> = 0.0150]
Data/restraints/parameters	3007/1/177
Goodness-of-fit on F <sup>2</sup>	1.143
Final R indexes [I>=2σ (I)]	R <sub>1</sub> = 0.0278, wR <sub>2</sub> = 0.0769
Final R indexes [all data]	R <sub>1</sub> = 0.0291, wR <sub>2</sub> = 0.0848
Largest diff. peak/hole / e Å <sup>-3</sup>	0.28/-0.21
Flack parameter	0.02 (2)

**Table 2 Fractional Atomic Coordinates ( $\times 10^4$ ) and Equivalent Isotropic Displacement Parameters ( $\text{\AA}^2 \times 10^3$ ) for han470.  $U_{\text{eq}}$  is defined as 1/3 of the trace of the orthogonalised  $U_{\text{IJ}}$  tensor.**

Atom	x	y	z	U(eq)
C1	5829.8(11)	8757(2)	5952.0(9)	18.8(3)
C2	4884.9(12)	10090(2)	5828.6(13)	23.8(3)
C3	3968.1(11)	8622(2)	5793.1(10)	20.0(3)
C4	4454.8(11)	6547(2)	5584.6(9)	16.0(3)
C5	4705.1(11)	6443(2)	4584.7(9)	16.9(3)
C6	5381.6(12)	4586(2)	4429.3(10)	19.7(3)
C7	6411.6(12)	4731(2)	4875.6(11)	23.4(3)
C8	6254.6(11)	4960(2)	5857.1(11)	19.5(3)
C9	5477.1(11)	6582(2)	6103.5(10)	17.2(3)
C10	5271.6(13)	6450(3)	7087.7(10)	24.7(3)
C11	3772.4(11)	6607(2)	4002.8(10)	18.6(3)
C12	3019.2(13)	5089(2)	3963.0(11)	22.7(3)
C13	2167.4(13)	5307(3)	3424.2(12)	27.8(3)
C14	2064.3(13)	7025(3)	2908.2(12)	30.5(4)
C15	2806.2(14)	8539(3)	2935.7(11)	28.9(4)
C16	3653.7(13)	8330(2)	3482.4(11)	23.6(3)
O1	6711.2(8)	9345.1(19)	5934.0(8)	26.1(3)
O4	3857.2(8)	4851.8(16)	5834.9(8)	19.7(2)
O6	5108.5(9)	3117.6(17)	4018.5(8)	25.3(3)

**Table 3 Anisotropic Displacement Parameters ( $\text{\AA}^2 \times 10^3$ ) for han470. The Anisotropic displacement factor exponent takes the form:  $-2\pi^2 [h^2 a^{*2} U_{11} + 2hka^* b^* U_{12} + \dots]$ .**

Atom	$U_{11}$	$U_{22}$	$U_{33}$	$U_{23}$	$U_{13}$	$U_{12}$
C1	17.4(6)	23.4(6)	15.6(6)	-2.7(5)	0.4(5)	-1.7(5)
C2	20.2(7)	20.6(6)	30.6(8)	-3.3(6)	0.0(7)	0.1(5)
C3	15.2(6)	23.0(6)	22.0(7)	-1.5(6)	0.8(5)	2.1(5)
C4	11.9(6)	19.5(6)	16.6(7)	0.9(5)	-0.2(5)	-1.5(5)
C5	13.1(6)	20.8(6)	16.7(7)	0.4(5)	-0.2(5)	-1.4(5)
C6	18.2(7)	25.3(7)	15.7(6)	0.4(5)	2.1(5)	2.0(5)
C7	15.9(7)	30.6(7)	23.7(8)	-5.1(6)	0.5(6)	4.8(6)
C8	13.2(6)	22.3(6)	23.1(7)	1.2(5)	-2.9(6)	1.0(5)
C9	12.8(6)	22.4(6)	16.6(6)	1.0(5)	-0.6(5)	-1.1(5)
C10	20.8(7)	36.3(8)	17.0(7)	1.5(6)	-1.4(6)	-1.8(6)
C11	15.4(6)	25.2(7)	15.3(6)	-0.5(5)	-0.5(5)	0.4(5)
C12	20.5(7)	26.7(7)	20.8(7)	-0.1(6)	-1.0(6)	-2.9(5)
C13	20.2(7)	37.5(8)	25.8(8)	-4.4(7)	-3.1(6)	-3.8(6)
C14	23.7(8)	47.1(10)	20.6(7)	-1.0(7)	-7.1(6)	5.1(7)
C15	29.4(8)	37.8(8)	19.6(7)	5.4(6)	-1.1(7)	5.2(7)
C16	22.1(7)	27.5(7)	21.1(7)	3.2(6)	1.0(6)	0.7(5)
O1	17.5(5)	30.6(6)	30.3(6)	-4.9(5)	1.2(5)	-6.3(4)
O4	12.6(5)	23.5(5)	22.9(5)	4.1(4)	1.2(4)	-3.2(4)
O6	28.5(6)	26.8(6)	20.7(5)	-4.5(4)	-3.3(5)	3.6(4)

**Table 4 Bond Lengths for han470.**

Atom	Atom	Length/Å	Atom	Atom	Length/Å
C1	C2	1.522 (2)	C6	O6	1.209 (2)
C1	C9	1.522 (2)	C7	C8	1.536 (2)
C1	O1	1.2109 (19)	C8	C9	1.520 (2)
C2	C3	1.536 (2)	C9	C10	1.545 (2)
C3	C4	1.5402 (19)	C11	C12	1.401 (2)
C4	C5	1.579 (2)	C11	C16	1.398 (2)
C4	C9	1.5529 (18)	C12	C13	1.393 (2)
C4	O4	1.4141 (16)	C13	C14	1.390 (3)
C5	C6	1.526 (2)	C14	C15	1.388 (3)
C5	C11	1.5137 (19)	C15	C16	1.395 (2)
C6	C7	1.510 (2)			

**Table 5 Bond Angles for han470.**

Atom	Atom	Atom	Angle/°	Atom	Atom	Atom	Angle/°
C9	C1	C2	108.55 (12)	C6	C7	C8	109.77 (12)
O1	C1	C2	125.29 (14)	C9	C8	C7	113.86 (13)
O1	C1	C9	126.16 (14)	C1	C9	C4	101.14 (11)
C1	C2	C3	105.60 (12)	C1	C9	C10	104.86 (12)
C2	C3	C4	104.26 (11)	C8	C9	C1	114.97 (12)
C3	C4	C5	109.11 (12)	C8	C9	C4	115.51 (12)
C3	C4	C9	103.36 (11)	C8	C9	C10	108.76 (13)
C9	C4	C5	109.16 (11)	C10	C9	C4	110.98 (12)
O4	C4	C3	114.65 (11)	C12	C11	C5	122.41 (14)
O4	C4	C5	110.26 (11)	C16	C11	C5	119.16 (13)
O4	C4	C9	110.00 (11)	C16	C11	C12	118.43 (14)
C6	C5	C4	107.90 (11)	C13	C12	C11	120.62 (15)
C11	C5	C4	114.31 (12)	C14	C13	C12	120.16 (15)
C11	C5	C6	115.24 (12)	C15	C14	C13	120.00 (15)
C7	C6	C5	112.93 (13)	C14	C15	C16	119.80 (16)
O6	C6	C5	123.62 (14)	C15	C16	C11	120.99 (15)
O6	C6	C7	123.41 (14)				

**Table 6 Hydrogen Bonds for han470.**

D	H	A	d(D-H) / Å	d(H-A) / Å	d(D-A) / Å	D-H-A / °
O4	H4	O1 <sup>1</sup>	0.80 (3)	2.05 (3)	2.8461 (15)	172 (2)

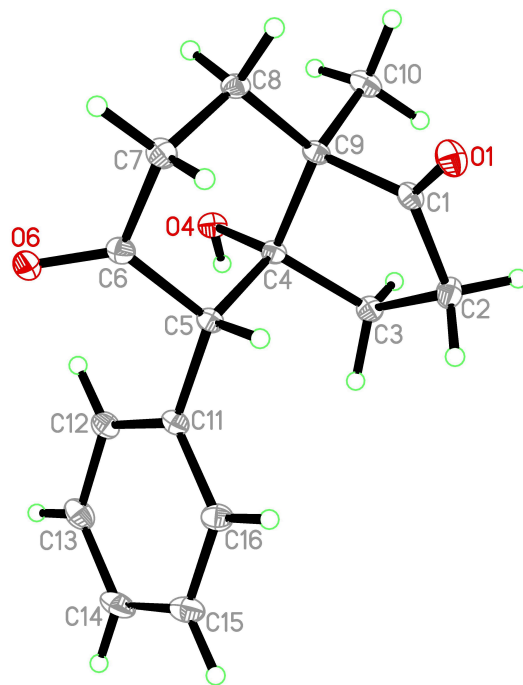
<sup>1</sup>-1/2+x, 3/2-y, +z

**Table 7 Torsion Angles for han470.**

<b>A</b>	<b>B</b>	<b>C</b>	<b>D</b>	<b>Angle/°</b>	<b>A</b>	<b>B</b>	<b>C</b>	<b>D</b>	<b>Angle/°</b>
C1	C2	C3	C4	-18.82 (16)	C7	C8	C9	C1	-71.01 (16)
C2	C1	C9	C4	29.57 (14)	C7	C8	C9	C4	46.27 (17)
C2	C1	C9	C8	154.73 (14)	C7	C8	C9	C10	171.80 (12)
C2	C1	C9	C10	-85.89 (15)	C9	C1	C2	C3	-7.07 (17)
C2	C3	C4	C5	-78.75 (14)	C9	C4	C5	C6	56.06 (14)
C2	C3	C4	C9	37.32 (15)	C9	C4	C5	C11	-174.33 (12)
C2	C3	C4	O4	157.04 (13)	C11	C5	C6	C7	167.00 (13)
C3	C4	C5	C6	168.35 (12)	C11	C5	C6	O6	-15.6 (2)
C3	C4	C5	C11	-62.04 (15)	C11	C12	C13	C14	1.0 (3)
C3	C4	C9	C1	-40.72 (13)	C12	C11	C16	C15	0.0 (2)
C3	C4	C9	C8	-165.52 (13)	C12	C13	C14	C15	-0.7 (3)
C3	C4	C9	C10	70.10 (14)	C13	C14	C15	C16	0.0 (3)
C4	C5	C6	C7	-63.91 (15)	C14	C15	C16	C11	0.3 (3)
C4	C5	C6	O6	113.53 (16)	C16	C11	C12	C13	-0.7 (2)
C4	C5	C11	C12	-67.76 (19)	O1	C1	C2	C3	173.13 (14)
C4	C5	C11	C16	112.38 (15)	O1	C1	C9	C4	-150.63 (14)
C5	C4	C9	C1	75.31 (13)	O1	C1	C9	C8	-25.5 (2)
C5	C4	C9	C8	-49.49 (16)	O1	C1	C9	C10	93.91 (16)
C5	C4	C9	C10	-173.87 (12)	O4	C4	C5	C6	-64.88 (14)
C5	C6	C7	C8	59.31 (17)	O4	C4	C5	C11	64.73 (15)
C5	C11	C12	C13	179.44 (14)	O4	C4	C9	C1	-163.59 (11)
C5	C11	C16	C15	179.89 (15)	O4	C4	C9	C8	71.61 (15)
C6	C5	C11	C12	58.09 (19)	O4	C4	C9	C10	-52.77 (15)
C6	C5	C11	C16	-121.76 (15)	O6	C6	C7	C8	-118.14 (16)
C6	C7	C8	C9	-48.60 (17)					

**Table 8 Hydrogen Atom Coordinates ( $\text{\AA}\times 10^4$ ) and Isotropic Displacement Parameters ( $\text{\AA}^2\times 10^3$ ) for han470.**

<b>Atom</b>	<b>x</b>	<b>y</b>	<b>z</b>	<b>U (eq)</b>
H2A	4937	10876	5284	29
H2B	4810	11050	6318	29
H3A	3477	9029	5335	24
H3B	3604	8583	6356	24
H5	5142	7654	4454	20
H7A	6796	5915	4649	28
H7B	6819	3492	4755	28
H8A	6025	3641	6097	23
H8B	6923	5296	6128	23
H10A	4857	7616	7270	37
H10B	5927	6458	7400	37
H10C	4900	5191	7217	37
H12	3090	3901	4307	27
H13	1656	4278	3409	33
H14	1486	7163	2537	37
H15	2737	9714	2583	35
H16	4158	9373	3501	28
H4	3260 (20)	5180 (30)	5834 (18)	29 (6)



## Experimental

Single crystals of  $C_{16}H_{18}O_3$  [han470] were slow recrystallized from chloroform-hexanes. A suitable crystal was selected and mounted on a loop fiber on a Bruker Venture Metaljet diffractometer. The crystal was kept at 100 K during data collection. Using Olex2 [1], the structure was solved with the XT [2] structure solution program using Direct Methods and refined with the XL [3] refinement package using Least Squares minimisation.

1. Dolomanov, O.V., Bourhis, L.J., Gildea, R.J., Howard, J.A.K. & Puschmann, H. (2009), *J. Appl. Cryst.* 42, 339-341.
2. Bourhis, L.J., Dolomanov, O.V., Gildea, R.J., Howard, J.A.K., Puschmann, H. (2013). in preparation.
3. Sheldrick, G.M. (2008). *Acta Cryst.* A64, 112-122.
4. APEX2 (2008), Bruker AXS Inc., Madison, WI 53719-1173.
5. SAINT (2009) V7.60A, Bruker AXS Inc., Madison, WI 53719-1173.
6. XPREP (2013); X-ray data Preparation and Reciprocal space Exploration Program. Bruker AXS Inc., Madison, WI 53719-1173.

## Crystal structure determination of [han470]

**Crystal Data** for  $C_{16}H_{18}O_3$  ( $M = 258.30$  g/mol): orthorhombic, space group  $Pna_2_1$  (no. 33),  $a = 13.0120(7)$  Å,  $b = 6.5847(3)$  Å,  $c = 15.4360(8)$  Å,  $V = 1322.56(12)$  Å<sup>3</sup>,  $Z = 4$ ,  $T = 100$  K,  $\mu(\text{GaK}\alpha) = 0.459$  mm<sup>-1</sup>,  $D_{\text{calc}} = 1.297$  g/cm<sup>3</sup>, 56212 reflections measured ( $12.846^\circ \leq 2\theta \leq 121.428^\circ$ ), 3007 unique ( $R_{\text{int}} = 0.0263$ ,  $R_{\text{sigma}} = 0.0150$ ) which were used in all calculations. The final  $R_1$  was 0.0278 ( $I > 2\sigma(I)$ ) and  $wR_2$  was 0.0848 (all data).

## Refinement model description

Number of restraints - 1, number of constraints - unknown.

Details:

1. Fixed Uiso

At 1.2 times of:

All C(H) groups, All C(H,H) groups

At 1.5 times of:

All C(H,H,H) groups

2.a Ternary CH refined with riding coordinates:

C5(H5)

2.b Secondary CH2 refined with riding coordinates:

C2(H2A,H2B), C3(H3A,H3B), C7(H7A,H7B), C8(H8A,H8B)

2.c Aromatic/amide H refined with riding coordinates:

C12(H12), C13(H13), C14(H14), C15(H15), C16(H16)

2.d Idealised Me refined as rotating group:

C10(H10A,H10B,H10C)



## Annex 62: X-Ray Data for Compound 4.9

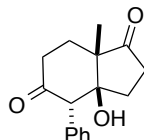


**Table 1 Crystal data and structure refinement for han477.**

Identification code	han477
Empirical formula	C <sub>16</sub> H <sub>18</sub> O <sub>3</sub>
Formula weight	258.30
Temperature/K	110
Crystal system	orthorhombic
Space group	Pca2 <sub>1</sub>
a/Å	20.6653 (5)
b/Å	6.1757 (2)
c/Å	10.3155 (3)
α/°	90
β/°	90
γ/°	90
Volume/Å <sup>3</sup>	1316.49 (7)
Z	4
ρ <sub>calc</sub> /cm <sup>3</sup>	1.303
μ/mm <sup>-1</sup>	0.461
F(000)	552.0
Crystal size/mm <sup>3</sup>	0.22 × 0.16 × 0.08
Radiation	GaKα (λ = 1.34139)
2θ range for data collection/°	7.444 to 121.25
Index ranges	-26 ≤ h ≤ 26, -8 ≤ k ≤ 8, -13 ≤ l ≤ 13
Reflections collected	45195
Independent reflections	2986 [R <sub>int</sub> = 0.0229, R <sub>sigma</sub> = 0.0145]
Data/restraints/parameters	2986/1/174
Goodness-of-fit on F <sup>2</sup>	1.058
Final R indexes [I ≥ 2σ (I)]	R <sub>1</sub> = 0.0285, wR <sub>2</sub> = 0.0746
Final R indexes [all data]	R <sub>1</sub> = 0.0286, wR <sub>2</sub> = 0.0748
Largest diff. peak/hole / e Å <sup>-3</sup>	0.27/-0.14
Flack parameter	0.06 (2)

**Table 2 Fractional Atomic Coordinates ( $\times 10^4$ ) and Equivalent Isotropic Displacement Parameters ( $\text{\AA}^2 \times 10^3$ ) for han477.  $U_{eq}$  is defined as 1/3 of the trace of the orthogonalised  $U_{IJ}$  tensor.**

Atom	x	y	z	$U(eq)$
C1	4972.0 (7)	7559 (2)	2508.1 (15)	20.6 (3)
C2	4755.0 (7)	8318 (3)	3840.9 (15)	27.1 (3)
C3	5363.6 (7)	8204 (3)	4694.1 (14)	21.8 (3)
C4	5821.1 (6)	6646 (2)	3968.3 (13)	17.1 (3)
C5	6543.8 (6)	6818 (2)	4375.0 (14)	18.7 (3)
C6	6863.7 (7)	8900 (2)	3884.5 (15)	22.5 (3)
C7	6733.4 (8)	9438 (3)	2476.7 (17)	32.7 (4)
C8	6006.4 (8)	9384 (3)	2169.7 (16)	25.1 (3)
C9	5702.6 (7)	7172 (2)	2519.4 (13)	18.4 (3)
C10	5906.1 (8)	5416 (3)	1570.1 (15)	25.9 (3)
C11	6648.1 (6)	6413 (2)	5810.6 (14)	18.8 (3)
C12	6879.1 (7)	4396 (2)	6212.1 (16)	22.2 (3)
C13	6965.4 (7)	3945 (3)	7526.7 (17)	26.2 (3)
C14	6831.5 (7)	5517 (3)	8448.8 (15)	26.8 (3)
C15	6604.2 (8)	7531 (3)	8058.9 (16)	25.4 (3)
C16	6512.2 (7)	7987 (2)	6750.7 (15)	21.8 (3)
O1	4622.5 (6)	7331.0 (19)	1581.3 (11)	26.6 (3)
O4	5600.4 (6)	4466.9 (16)	4117.8 (10)	22.5 (2)
O6	7220.4 (6)	9982.1 (18)	4546.7 (12)	27.5 (3)

**Table 3 Anisotropic Displacement Parameters ( $\text{\AA}^2 \times 10^3$ ) for han477. The Anisotropic displacement factor exponent takes the form:  $-2\pi^2 [h^2 a^{*2} U_{11} + 2hka^* b^* U_{12} + \dots]$ .**

Atom	$U_{11}$	$U_{22}$	$U_{33}$	$U_{23}$	$U_{13}$	$U_{12}$
C1	23.6 (7)	18.1 (6)	19.9 (7)	1.6 (5)	-0.8 (6)	-1.7 (5)
C2	21.3 (6)	39.4 (9)	20.7 (7)	-3.9 (6)	-1.7 (6)	6.0 (6)
C3	19.6 (6)	27.8 (7)	18.0 (6)	-4.2 (6)	-0.4 (5)	4.1 (5)
C4	19.5 (6)	16.7 (6)	15.1 (6)	-0.3 (5)	0.4 (5)	-1.1 (5)
C5	18.5 (6)	19.2 (6)	18.3 (6)	-1.1 (5)	0.3 (5)	0.4 (5)
C6	19.0 (6)	23.4 (6)	25.3 (7)	0.2 (6)	2.7 (5)	-0.2 (5)
C7	28.6 (8)	40.0 (9)	29.6 (8)	12.2 (7)	-1.0 (7)	-12.6 (7)
C8	28.4 (7)	22.9 (7)	24.0 (7)	7.4 (6)	-2.5 (6)	-4.4 (6)
C9	22.1 (6)	17.9 (6)	15.1 (6)	0.9 (5)	0.0 (5)	0.0 (5)
C10	32.9 (8)	27.3 (7)	17.5 (7)	-3.2 (6)	0.4 (6)	5.3 (6)
C11	15.7 (6)	21.8 (7)	18.7 (6)	-0.2 (5)	-1.3 (5)	-0.6 (5)
C12	18.9 (6)	21.4 (7)	26.2 (7)	-0.2 (6)	-0.3 (5)	1.4 (5)
C13	20.3 (6)	28.2 (7)	30.1 (8)	6.8 (7)	-1.7 (6)	2.3 (6)
C14	18.9 (6)	42.1 (9)	19.4 (7)	3.9 (6)	-0.9 (5)	1.8 (6)
C15	18.8 (7)	36.2 (8)	21.2 (7)	-6.2 (6)	-0.4 (5)	2.4 (6)

C16	18.2 (6)	23.2 (7)	24.0 (7)	-2.6 (6)	-2.1 (6)	2.7 (5)
O1	27.9 (5)	30.5 (6)	21.5 (5)	-0.4 (4)	-6.3 (4)	-1.1 (4)
O4	31.0 (5)	19.6 (5)	17.1 (5)	2.7 (4)	-2.0 (4)	-6.1 (4)
O6	25.9 (5)	26.2 (5)	30.4 (6)	-5.3 (5)	3.5 (4)	-5.9 (4)

**Table 4 Bond Lengths for han477.**

Atom	Atom	Length/Å	Atom	Atom	Length/Å
C1	C2	1.520 (2)	C6	O6	1.2069 (19)
C1	C9	1.5287 (19)	C7	C8	1.536 (2)
C1	O1	1.2063 (19)	C8	C9	1.546 (2)
C2	C3	1.537 (2)	C9	C10	1.520 (2)
C3	C4	1.5428 (19)	C11	C12	1.3971 (19)
C4	C5	1.5549 (18)	C11	C16	1.401 (2)
C4	C9	1.5489 (18)	C12	C13	1.396 (2)
C4	O4	1.4295 (15)	C13	C14	1.387 (2)
C5	C6	1.5320 (19)	C14	C15	1.389 (2)
C5	C11	1.5172 (19)	C15	C16	1.392 (2)
C6	C7	1.514 (2)			

**Table 5 Bond Angles for han477.**

Atom	Atom	Atom	Angle/°	Atom	Atom	Atom	Angle/°
C2	C1	C9	109.42 (12)	C6	C7	C8	111.54 (13)
O1	C1	C2	125.17 (14)	C7	C8	C9	111.60 (13)
O1	C1	C9	125.40 (14)	C1	C9	C4	101.32 (11)
C1	C2	C3	105.21 (12)	C1	C9	C8	105.15 (12)
C2	C3	C4	104.61 (12)	C8	C9	C4	110.25 (12)
C3	C4	C5	114.54 (11)	C10	C9	C1	112.30 (12)
C3	C4	C9	103.93 (11)	C10	C9	C4	115.36 (12)
C9	C4	C5	113.45 (11)	C10	C9	C8	111.57 (13)
O4	C4	C3	109.84 (11)	C12	C11	C5	118.99 (13)
O4	C4	C5	109.95 (11)	C12	C11	C16	118.81 (14)
O4	C4	C9	104.54 (11)	C16	C11	C5	122.20 (13)
C6	C5	C4	112.48 (11)	C13	C12	C11	120.62 (14)
C11	C5	C4	112.87 (11)	C14	C13	C12	120.10 (14)
C11	C5	C6	113.53 (12)	C13	C14	C15	119.70 (15)
C7	C6	C5	115.11 (13)	C14	C15	C16	120.54 (15)
O6	C6	C5	122.78 (14)	C15	C16	C11	120.22 (14)
O6	C6	C7	122.01 (14)				

**Table 6 Hydrogen Bonds for han477.**

D	H	A	d(D-H) / Å	d(H-A) / Å	d(D-A) / Å	D-H-A / °
O4	H4	O1 <sup>1</sup>	0.84	2.00	2.8112 (15)	162.9

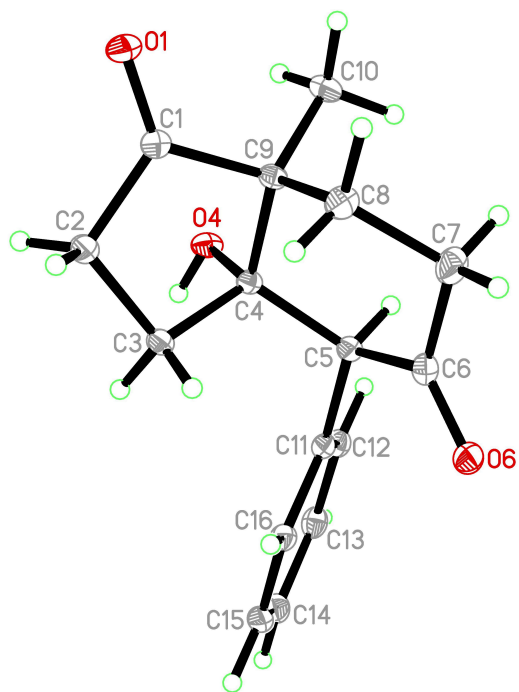
<sup>1</sup>1-X, 1-Y, 1/2+Z

**Table 7 Torsion Angles for han477.**

<b>A</b>	<b>B</b>	<b>C</b>	<b>D</b>	<b>Angle/°</b>	<b>A</b>	<b>B</b>	<b>C</b>	<b>D</b>	<b>Angle/°</b>
C1	C2	C3	C4	-19.85 (16)	C7	C8	C9	C1	165.35 (13)
C2	C1	C9	C4	26.65 (15)	C7	C8	C9	C4	56.89 (17)
C2	C1	C9	C8	-88.18 (14)	C7	C8	C9	C10	-72.66 (17)
C2	C1	C9	C10	150.31 (13)	C9	C1	C2	C3	-4.53 (17)
C2	C3	C4	C5	161.10 (12)	C9	C4	C5	C6	46.95 (15)
C2	C3	C4	C9	36.77 (15)	C9	C4	C5	C11	177.00 (11)
C2	C3	C4	O4	-74.60 (15)	C11	C5	C6	C7	-176.11 (13)
C3	C4	C5	C6	-72.16 (15)	C11	C5	C6	O6	7.5 (2)
C3	C4	C5	C11	57.89 (16)	C11	C12	C13	C14	-1.0 (2)
C3	C4	C9	C1	-38.37 (13)	C12	C11	C16	C15	-0.3 (2)
C3	C4	C9	C8	72.60 (14)	C12	C13	C14	C15	0.7 (2)
C3	C4	C9	C10	-159.92 (12)	C13	C14	C15	C16	-0.2 (2)
C4	C5	C6	C7	-46.39 (17)	C14	C15	C16	C11	0.0 (2)
C4	C5	C6	O6	137.19 (14)	C16	C11	C12	C13	0.8 (2)
C4	C5	C11	C12	101.39 (14)	O1	C1	C2	C3	176.58 (15)
C4	C5	C11	C16	-77.72 (17)	O1	C1	C9	C4	-154.46 (14)
C5	C4	C9	C1	-163.40 (11)	O1	C1	C9	C8	90.71 (17)
C5	C4	C9	C8	-52.43 (15)	O1	C1	C9	C10	-30.8 (2)
C5	C4	C9	C10	75.05 (16)	O4	C4	C5	C6	163.61 (11)
C5	C6	C7	C8	51.19 (19)	O4	C4	C5	C11	-66.34 (15)
C5	C11	C12	C13	-178.37 (13)	O4	C4	C9	C1	76.81 (12)
C5	C11	C16	C15	178.82 (14)	O4	C4	C9	C8	-172.22 (11)
C6	C5	C11	C12	-129.10 (14)	O4	C4	C9	C10	-44.74 (15)
C6	C5	C11	C16	51.80 (18)	O6	C6	C7	C8	-132.37 (16)
C6	C7	C8	C9	-56.2 (2)					

**Table 8 Hydrogen Atom Coordinates ( $\text{\AA} \times 10^4$ ) and Isotropic Displacement Parameters ( $\text{\AA}^2 \times 10^3$ ) for han477.**

<b>Atom</b>	<b>x</b>	<b>y</b>	<b>z</b>	<b>U (eq)</b>
H2A	4411	7363	4187	33
H2B	4587	9819	3800	33
H3A	5258	7636	5566	26
H3B	5563	9653	4788	26
H5	6770	5606	3918	22
H7A	6961	8383	1917	39
H7B	6906	10897	2281	39
H8A	5941	9672	1235	30
H8B	5785	10542	2663	30
H10A	6373	5168	1645	39
H10B	5803	5876	685	39
H10C	5674	4073	1769	39
H12	6978	3320	5584	27
H13	7116	2560	7790	31
H14	6895	5217	9343	32
H15	6511	8606	8690	30
H16	6357	9370	6494	26
H4	5548	4197	4909	34



## Experimental

Single crystals of  $C_{16}H_{18}O_3$  [han477] were slow recrystallized from chloroform-hexanes. A suitable crystal was selected and mounted on a loop fiber on a Bruker Venture Metaljet diffractometer. The crystal was kept at 110 K during data collection. Using Olex2 [1], the structure was solved with the XT [2] structure solution program using Direct Methods and refined with the XL [3] refinement package using Least Squares minimisation.

1. Dolomanov, O.V., Bourhis, L.J., Gildea, R.J., Howard, J.A.K. & Puschmann, H. (2009), *J. Appl. Cryst.* 42, 339-341.
2. Bourhis, L.J., Dolomanov, O.V., Gildea, R.J., Howard, J.A.K., Puschmann, H. (2013). in preparation.
3. Sheldrick, G.M. (2008). *Acta Cryst.* A64, 112-122.
4. APEX2 (2008), Bruker AXS Inc., Madison, WI 53719-1173.
5. SAINT (2009) V7.60A, Bruker AXS Inc., Madison, WI 53719-1173.
6. XPREP (2013); X-ray data Preparation and Reciprocal space Exploration Program. Bruker AXS Inc., Madison, WI 53719-1173.

## Crystal structure determination of [han477]

**Crystal Data** for  $C_{16}H_{18}O_3$  ( $M = 258.30$  g/mol): orthorhombic, space group  $Pca2_1$  (no. 29),  $a = 20.6653(5)$  Å,  $b = 6.1757(2)$  Å,  $c = 10.3155(3)$  Å,  $V = 1316.49(7)$  Å<sup>3</sup>,  $Z = 4$ ,  $T = 110$  K,  $\mu(\text{GaK}\alpha) = 0.461$  mm<sup>-1</sup>,  $D_{\text{calc}} = 1.303$  g/cm<sup>3</sup>, 45195 reflections measured ( $7.444^\circ \leq 2\theta \leq 121.25^\circ$ ), 2986 unique ( $R_{\text{int}} = 0.0229$ ,  $R_{\text{sigma}} = 0.0145$ ) which were used in all calculations. The final  $R_1$  was 0.0285 ( $I > 2\sigma(I)$ ) and  $wR_2$  was 0.0748 (all data).

## Refinement model description

Number of restraints - 1, number of constraints - unknown.

Details:

### 1. Fixed Uiso

At 1.2 times of:

All C(H) groups, All C(H,H) groups

At 1.5 times of:

All C(H,H,H) groups, All O(H) groups

### 2.a Ternary CH refined with riding coordinates:

C5(H5)

### 2.b Secondary CH2 refined with riding coordinates:

C2(H2A,H2B), C3(H3A,H3B), C7(H7A,H7B), C8(H8A,H8B)

### 2.c Aromatic/amide H refined with riding coordinates:

C12(H12), C13(H13), C14(H14), C15(H15), C16(H16)

### 2.d Idealised Me refined as rotating group:

C10(H10A,H10B,H10C)

### 2.e Idealised tetrahedral OH refined as rotating group:

O4(H4)

## Annex 63: X-Ray Data for Compound 4.11

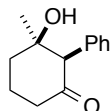


**Table 1 Crystal data and structure refinement for han479.**

Identification code	han479
Empirical formula	C <sub>13</sub> H <sub>16</sub> O <sub>2</sub>
Formula weight	204.26
Temperature/K	110
Crystal system	monoclinic
Space group	P2 <sub>1</sub> /c
a/Å	18.7276 (4)
b/Å	7.4816 (2)
c/Å	15.9354 (4)
α/°	90
β/°	100.5880 (10)
γ/°	90
Volume/Å <sup>3</sup>	2194.73 (9)
Z	8
ρ <sub>calc</sub> /cm <sup>3</sup>	1.236
μ/mm <sup>-1</sup>	0.419
F(000)	880.0
Crystal size/mm <sup>3</sup>	0.2 × 0.12 × 0.04
Radiation	GaKα (λ = 1.34139)
2θ range for data collection/°	8.358 to 121.324
Index ranges	-24 ≤ h ≤ 24, -9 ≤ k ≤ 9, -20 ≤ l ≤ 20
Reflections collected	35407
Independent reflections	5040 [R <sub>int</sub> = 0.0238, R <sub>sigma</sub> = 0.0164]
Data/restraints/parameters	5040/0/281
Goodness-of-fit on F <sup>2</sup>	1.035
Final R indexes [I ≥ 2σ (I)]	R <sub>1</sub> = 0.0357, wR <sub>2</sub> = 0.0919
Final R indexes [all data]	R <sub>1</sub> = 0.0382, wR <sub>2</sub> = 0.0944
Largest diff. peak/hole / e Å <sup>-3</sup>	0.37/-0.16



**Table 2 Fractional Atomic Coordinates ( $\times 10^4$ ) and Equivalent Isotropic Displacement Parameters ( $\text{\AA}^2 \times 10^3$ ) for han479.  $U_{\text{eq}}$  is defined as 1/3 of of the trace of the orthogonalised  $U_{\text{IJ}}$  tensor.**

Atom	<i>x</i>	<i>y</i>	<i>z</i>	<i>U</i> (eq)
C11	4386.0 (5)	5968.9 (13)	2998.2 (6)	20.09 (19)
C12	4706.0 (6)	4955.8 (14)	3800.6 (6)	25.7 (2)
C13	4188.1 (5)	3490.1 (14)	3996.6 (6)	24.8 (2)
C14	3953.1 (5)	2291.8 (13)	3223.1 (6)	22.7 (2)
C15	3616.1 (5)	3317.8 (12)	2419.1 (6)	19.36 (18)
C16	4146.7 (5)	4800.5 (12)	2215.3 (5)	17.87 (18)
C17	3414.9 (6)	2037.0 (14)	1672.5 (7)	27.6 (2)
C18	3861.7 (5)	5803.7 (12)	1398.2 (6)	19.22 (18)
C19	3293.2 (5)	7038.1 (13)	1324.7 (6)	24.2 (2)
C110	3013.7 (6)	7822.5 (14)	540.9 (7)	30.3 (2)
C111	3307.7 (7)	7417.5 (14)	-175.1 (7)	31.4 (2)
C112	3881.9 (6)	6228.0 (15)	-108.1 (6)	29.0 (2)
C113	4154.1 (5)	5425.7 (14)	671.6 (6)	23.6 (2)
O11	4346.9 (4)	7588.8 (9)	2980.4 (4)	25.85 (16)
O12	2969.9 (4)	4154.9 (10)	2613.6 (5)	24.49 (16)
C21	917.5 (5)	4909.7 (13)	4387.9 (6)	20.31 (19)
C22	916.9 (5)	3996.7 (14)	5233.6 (6)	23.8 (2)
C23	1594.9 (5)	2826.7 (14)	5474.8 (6)	24.1 (2)
C24	1659.3 (5)	1509.1 (13)	4765.1 (6)	23.5 (2)
C25	1679.8 (5)	2442.4 (13)	3913.8 (6)	20.38 (19)
C26	985.1 (5)	3637.5 (12)	3657.4 (6)	18.56 (18)
C27	1726.5 (6)	1056.4 (14)	3224.8 (7)	27.0 (2)
C28	928.8 (5)	4564.9 (12)	2804.8 (6)	18.71 (18)
C29	1384.6 (5)	5986.3 (13)	2683.5 (6)	20.39 (19)
C210	1325.8 (5)	6791.7 (13)	1885.3 (6)	22.9 (2)
C211	807.4 (6)	6202.9 (13)	1199.8 (6)	24.0 (2)
C212	346.0 (5)	4813.8 (13)	1318.7 (6)	23.7 (2)
C213	405.5 (5)	3998.6 (13)	2114.0 (6)	20.93 (19)
O21	859.8 (4)	6517.1 (10)	4301.6 (5)	28.34 (17)
O22	2312.1 (4)	3559.6 (10)	4059.7 (5)	23.38 (15)

**Table 3 Anisotropic Displacement Parameters ( $\text{\AA}^2 \times 10^3$ ) for han479.**  
**The Anisotropic displacement factor exponent takes the form: -**  
 **$2\pi^2 [h^2 a^2 U_{11} + 2hka^* b^* U_{12} + \dots]$ .**

Atom	$U_{11}$	$U_{22}$	$U_{33}$	$U_{23}$	$U_{13}$	$U_{12}$
C11	17.2(4)	22.7(5)	21.0(4)	-1.7(3)	5.3(3)	-4.2(3)
C12	26.1(5)	26.3(5)	22.3(4)	-0.5(4)	-1.7(4)	-4.6(4)
C13	26.1(5)	25.7(5)	21.4(4)	3.9(4)	1.0(4)	-1.7(4)
C14	21.5(4)	19.3(4)	26.1(5)	3.2(4)	0.8(3)	-0.6(3)
C15	16.8(4)	18.2(4)	22.7(4)	0.2(3)	2.5(3)	0.1(3)
C16	16.3(4)	18.1(4)	19.3(4)	-1.2(3)	3.6(3)	0.0(3)
C17	29.4(5)	22.4(5)	28.4(5)	-3.4(4)	-2.0(4)	-4.5(4)
C18	20.2(4)	17.6(4)	19.8(4)	-1.4(3)	3.4(3)	-2.8(3)
C19	27.2(5)	20.1(4)	25.6(5)	-0.8(4)	5.6(4)	2.1(4)
C110	34.0(5)	21.0(5)	33.4(5)	2.7(4)	-0.1(4)	4.2(4)
C111	43.5(6)	24.8(5)	22.7(5)	4.3(4)	-2.1(4)	-6.5(4)
C112	37.9(6)	29.4(5)	20.4(4)	-2.6(4)	7.1(4)	-8.4(4)
C113	25.3(5)	23.4(5)	22.9(4)	-3.7(4)	6.5(4)	-2.5(4)
O11	32.4(4)	20.4(3)	25.5(3)	-2.8(3)	7.2(3)	-5.7(3)
O12	17.3(3)	28.6(4)	28.4(4)	7.0(3)	6.4(3)	3.1(3)
C21	16.4(4)	23.7(5)	21.0(4)	0.7(4)	3.9(3)	0.7(3)
C22	25.8(5)	26.3(5)	20.2(4)	1.0(4)	6.7(3)	0.0(4)
C23	21.6(4)	27.0(5)	22.6(4)	5.5(4)	1.8(3)	-3.5(4)
C24	21.2(4)	21.9(5)	27.7(5)	6.1(4)	4.8(4)	0.5(4)
C25	18.1(4)	18.6(4)	24.8(4)	1.4(3)	5.1(3)	-0.8(3)
C26	16.7(4)	19.0(4)	20.3(4)	0.3(3)	4.2(3)	-2.4(3)
C27	29.5(5)	21.1(5)	32.1(5)	-1.6(4)	10.0(4)	1.4(4)
C28	17.9(4)	19.1(4)	19.5(4)	-0.6(3)	4.3(3)	2.1(3)
C29	18.9(4)	20.6(4)	21.5(4)	-0.2(3)	3.2(3)	0.6(3)
C210	24.4(4)	20.0(4)	25.8(5)	2.4(4)	8.7(4)	2.3(4)
C211	29.8(5)	23.3(5)	19.6(4)	1.7(4)	6.1(4)	8.8(4)
C212	24.8(4)	24.3(5)	20.4(4)	-5.0(4)	0.2(3)	6.4(4)
C213	19.2(4)	19.6(4)	24.0(4)	-3.1(3)	3.9(3)	0.8(3)
O21	37.6(4)	22.9(4)	26.1(3)	0.2(3)	9.8(3)	5.1(3)
O22	17.0(3)	26.7(4)	26.9(3)	2.9(3)	5.5(3)	-3.1(3)

**Table 4 Bond Lengths for han479.**

Atom	Atom	Length/Å	Atom	Atom	Length/Å
C11	C12	1.5123 (13)	C21	C22	1.5111 (13)
C11	C16	1.5218 (12)	C21	C26	1.5268 (13)
C11	O11	1.2141 (12)	C21	O21	1.2129 (12)
C12	C13	1.5337 (14)	C22	C23	1.5319 (14)
C13	C14	1.5224 (13)	C23	C24	1.5217 (14)
C14	C15	1.5269 (12)	C24	C25	1.5325 (13)
C15	C16	1.5627 (12)	C25	C26	1.5697 (13)
C15	C17	1.5203 (13)	C25	C27	1.5244 (13)
C15	O12	1.4459 (11)	C25	O22	1.4331 (11)
C16	C18	1.5126 (12)	C26	C28	1.5119 (12)
C18	C19	1.3980 (13)	C28	C29	1.3991 (13)
C18	C113	1.3977 (13)	C28	C213	1.3982 (13)
C19	C110	1.3921 (14)	C29	C210	1.3934 (13)
C110	C111	1.3884 (16)	C210	C211	1.3928 (14)
C111	C112	1.3848 (17)	C211	C212	1.3867 (15)
C112	C113	1.3896 (14)	C212	C213	1.3924 (13)

**Table 5 Bond Angles for han479.**

Atom	Atom	Atom	Angle/°	Atom	Atom	Atom	Angle/°
C12	C11	C16	114.61 (8)	C22	C21	C26	114.32 (8)
O11	C11	C12	122.20 (9)	O21	C21	C22	122.32 (9)
O11	C11	C16	123.15 (8)	O21	C21	C26	123.36 (8)
C11	C12	C13	111.31 (8)	C21	C22	C23	110.23 (8)
C14	C13	C12	110.83 (8)	C24	C23	C22	111.03 (8)
C13	C14	C15	113.38 (8)	C23	C24	C25	112.40 (8)
C14	C15	C16	110.53 (7)	C24	C25	C26	109.60 (7)
C17	C15	C14	110.16 (8)	C27	C25	C24	109.98 (8)
C17	C15	C16	111.12 (8)	C27	C25	C26	110.76 (8)
O12	C15	C14	105.73 (7)	O22	C25	C24	106.05 (7)
O12	C15	C16	109.04 (7)	O22	C25	C26	109.31 (7)
O12	C15	C17	110.11 (8)	O22	C25	C27	111.02 (7)
C11	C16	C15	109.87 (7)	C21	C26	C25	109.72 (7)
C18	C16	C11	115.14 (8)	C28	C26	C21	113.40 (8)
C18	C16	C15	113.20 (7)	C28	C26	C25	114.39 (7)
C19	C18	C16	122.87 (8)	C29	C28	C26	121.96 (8)
C113	C18	C16	118.86 (8)	C213	C28	C26	119.43 (8)
C113	C18	C19	118.20 (9)	C213	C28	C29	118.60 (8)
C110	C19	C18	120.58 (9)	C210	C29	C28	120.46 (9)
C111	C110	C19	120.31 (10)	C211	C210	C29	120.39 (9)
C112	C111	C110	119.77 (9)	C212	C211	C210	119.47 (9)
C111	C112	C113	119.91 (9)	C211	C212	C213	120.33 (9)
C112	C113	C18	121.20 (9)				

**Table 6 Hydrogen Bonds for han479.**

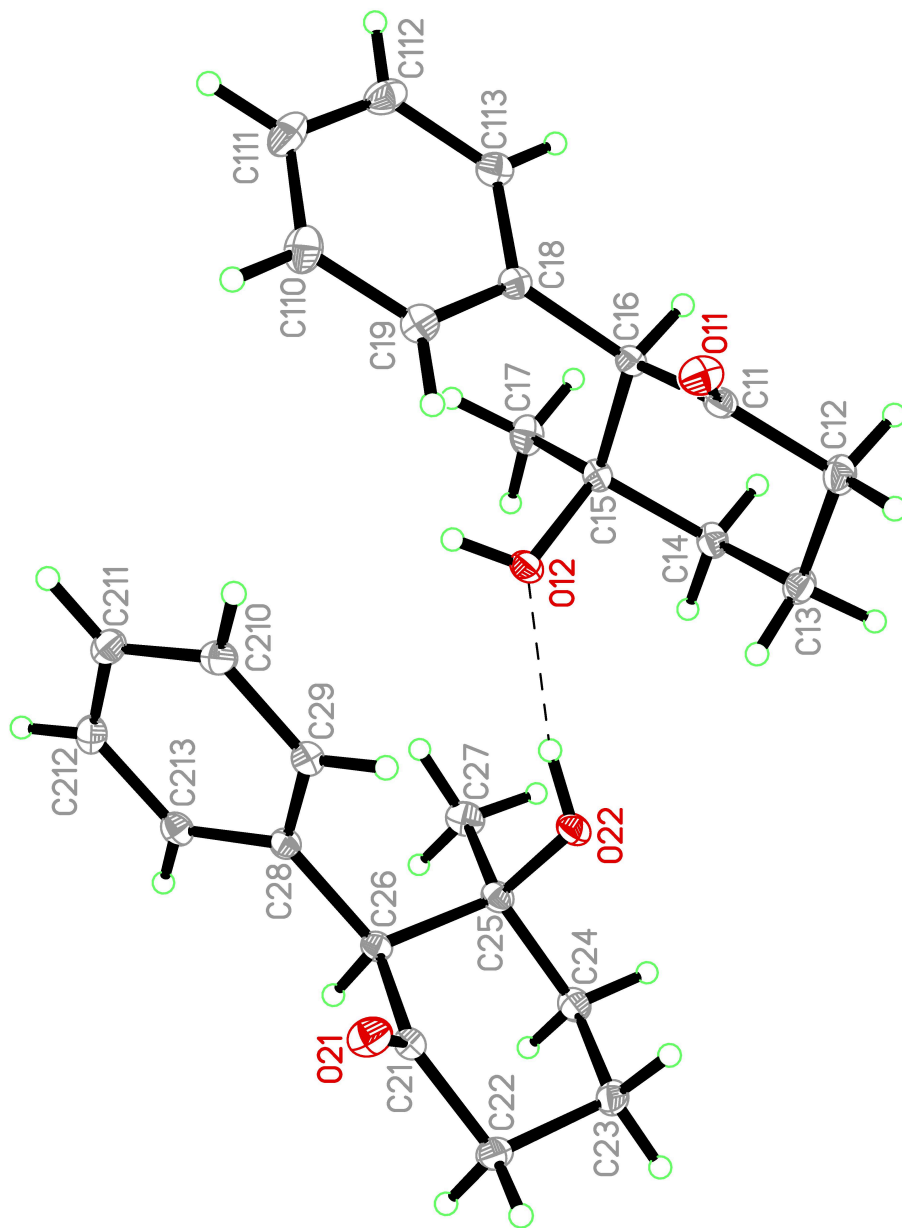
D	H	A	d(D-H)/Å	d(H-A)/Å	d(D-A)/Å	D-H-A/°
O22	H22	O12	0.875 (16)	1.975 (16)	2.8407 (10)	170.0 (14)

**Table 7 Torsion Angles for han479.**

A	B	C	D	Angle/°	A	B	C	D	Angle/°
C11	C12	C13	C14	52.56 (11)	C21	C22	C23	C24	-54.61 (10)
C11	C16	C18	C19	-54.97 (12)	C21	C26	C28	C29	55.53 (11)
C11	C16	C18	C113	128.09 (9)	C21	C26	C28	C213	-124.24 (9)
C12	C11	C16	C15	53.81 (10)	C22	C21	C26	C25	-54.98 (10)
C12	C11	C16	C18	-176.97 (8)	C22	C21	C26	C28	175.74 (7)
C12	C13	C14	C15	-55.01 (11)	C22	C23	C24	C25	57.41 (10)
C13	C14	C15	C16	55.33 (10)	C23	C24	C25	C26	-56.67 (10)
C13	C14	C15	C17	178.52 (8)	C23	C24	C25	C27	-178.67 (8)
C13	C14	C15	O12	-62.54 (10)	C23	C24	C25	O22	61.22 (10)
C14	C15	C16	C11	-52.81 (10)	C24	C25	C26	C21	53.85 (10)
C14	C15	C16	C18	176.92 (7)	C24	C25	C26	C28	-177.41 (8)
C15	C16	C18	C19	72.59 (11)	C25	C26	C28	C29	-71.33 (11)
C15	C16	C18	C113	-104.34 (10)	C25	C26	C28	C213	108.90 (9)
C16	C11	C12	C13	-54.07 (11)	C26	C21	C22	C23	55.18 (10)
C16	C18	C19	C110	-174.99 (9)	C26	C28	C29	C210	178.94 (8)
C16	C18	C113	C112	176.03 (9)	C26	C28	C213	C212	-179.29 (8)
C17	C15	C16	C11	-175.44 (8)	C27	C25	C26	C21	175.38 (8)
C17	C15	C16	C18	54.29 (10)	C27	C25	C26	C28	-55.89 (10)
C18	C19	C110	C111	-1.46 (16)	C28	C29	C210	C211	0.64 (14)
C19	C18	C113	C112	-1.05 (14)	C29	C28	C213	C212	0.93 (14)
C19	C110	C111	C112	-0.02 (16)	C29	C210	C211	C212	0.40 (14)
C110	C111	C112	C113	0.94 (16)	C210	C211	C212	C213	-0.76 (14)
C111	C112	C113	C18	-0.39 (15)	C211	C212	C213	C28	0.09 (14)
C113	C18	C19	C110	1.96 (14)	C213	C28	C29	C210	-1.29 (13)
O11	C11	C12	C13	128.16 (10)	O21	C21	C22	C23	-125.69 (10)
O11	C11	C16	C15	-128.44 (9)	O21	C21	C26	C25	125.90 (10)
O11	C11	C16	C18	0.77 (13)	O21	C21	C26	C28	-3.38 (13)
O12	C15	C16	C11	63.01 (9)	O22	C25	C26	C21	-61.99 (9)
O12	C15	C16	C18	-67.26 (9)	O22	C25	C26	C28	66.75 (10)

**Table 8 Hydrogen Atom Coordinates ( $\text{\AA}\times 10^4$ ) and Isotropic Displacement Parameters ( $\text{\AA}^2\times 10^3$ ) for han479.**

<b>Atom</b>	<b>x</b>	<b>y</b>	<b>z</b>	<b>U (eq)</b>
H12A	4806	5798	4287	31
H12B	5172	4408	3729	31
H13A	4434	2761	4483	30
H13B	3755	4047	4161	30
H14A	3596	1411	3357	27
H14B	4381	1622	3109	27
H16	4593	4161	2117	21
H17A	3856	1469	1549	41
H17B	3174	2699	1169	41
H17C	3085	1118	1818	41
H19	3096	7344	1814	29
H110	2620	8639	496	36
H111	3116	7955	-709	38
H112	4089	5961	-594	35
H113	4546	4605	711	28
H12	2716 (9)	4560 (20)	2158 (10)	50 (4)
H22A	476	3248	5194	29
H22B	908	4908	5682	29
H23A	2032	3596	5585	29
H23B	1569	2162	6006	29
H24A	1241	678	4690	28
H24B	2108	795	4933	28
H26	560	2810	3600	22
H27A	2158	312	3401	41
H27B	1759	1664	2689	41
H27C	1291	302	3141	41
H29	1737	6405	3149	24
H210	1641	7748	1808	27
H211	770	6749	655	29
H212	-12	4416	855	28
H213	87	3047	2188	25
H22	2464 (8)	3710 (20)	3577 (10)	45 (4)



## Experimental

Single crystals of  $C_{13}H_{16}O_2$  [han479] were slow recrystallized from ethyl acetate-hexanes. A suitable crystal was selected and mounted on a loop fiber on a Bruker Venture Metaljet diffractometer. The crystal was kept at 110 K during data collection. Using Olex2 [1], the structure was solved with the XT [2] structure solution program using Direct Methods and refined with the XL [3] refinement package using Least Squares minimisation.

1. Dolomanov, O.V., Bourhis, L.J., Gildea, R.J., Howard, J.A.K. & Puschmann, H. (2009), *J. Appl. Cryst.* 42, 339-341.
2. Bourhis, L.J., Dolomanov, O.V., Gildea, R.J., Howard, J.A.K., Puschmann, H. (2013). in preparation.
3. Sheldrick, G.M. (2008). *Acta Cryst.* A64, 112-122.
4. APEX2 (2008), Bruker AXS Inc., Madison, WI 53719-1173.
5. SAINT (2009) V7.60A, Bruker AXS Inc., Madison, WI 53719-1173.
6. XPREP (2013); X-ray data Preparation and Reciprocal space Exploration Program. Bruker AXS Inc., Madison, WI 53719-1173.

## Crystal structure determination of [han479]

**Crystal Data** for  $C_{13}H_{16}O_2$  ( $M = 204.26$  g/mol): monoclinic, space group  $P2_1/c$  (no. 14),  $a = 18.7276(4)$  Å,  $b = 7.4816(2)$  Å,  $c = 15.9354(4)$  Å,  $\beta = 100.5880(10)^\circ$ ,  $V = 2194.73(9)$  Å<sup>3</sup>,  $Z = 8$ ,  $T = 110$  K,  $\mu(\text{GaK}\alpha) = 0.419$  mm<sup>-1</sup>,  $D_{\text{calc}} = 1.236$  g/cm<sup>3</sup>, 35407 reflections measured ( $8.358^\circ \leq 2\theta \leq 121.324^\circ$ ), 5040 unique ( $R_{\text{int}} = 0.0238$ ,  $R_{\text{sigma}} = 0.0164$ ) which were used in all calculations. The final  $R_1$  was 0.0357 ( $I > 2\sigma(I)$ ) and  $wR_2$  was 0.0944 (all data).

## Refinement model description

Number of restraints - 0, number of constraints - unknown.

Details:

### 1. Fixed Uiso

At 1.2 times of:

All C(H) groups, All C(H,H) groups

At 1.5 times of:

All C(H,H,H) groups

### 2.a Ternary CH refined with riding coordinates:

C16(H16), C26(H26)

### 2.b Secondary CH2 refined with riding coordinates:

C12(H12A,H12B), C13(H13A,H13B), C14(H14A,H14B), C22(H22A,H22B), C23(H23A,H23B), C24(H24A,H24B)

### 2.c Aromatic/amide H refined with riding coordinates:

C19(H19), C110(H110), C111(H111), C112(H112), C113(H113), C29(H29), C210(H210), C211(H211), C212(H212), C213(H213)

### 2.d Idealised Me refined as rotating group:

C17(H17A,H17B,H17C), C27(H27A,H27B,H27C)